

CONFERENCE PROCEEDINGS 7  
REFERENCE COPY  
FOR LIBRARY USE ONLY

# Fourth International Bridge Engineering Conference

Volume 1



TRANSPORTATION  
RESEARCH  
BOARD

NATIONAL  
RESEARCH  
COUNCIL

**TRANSPORTATION RESEARCH BOARD  
1995 EXECUTIVE COMMITTEE**

---

**Chairman:** Lillian C. Borrone, Director, Port Department, The Port Authority of New York and New Jersey, New York City

**Vice Chairman:** James W. van Loben Sels, Director, California Department of Transportation, Sacramento

**Executive Director:** Robert E. Skinner, Jr., Transportation Research Board

---

Edward H. Arnold, Chairman and President, Arnold Industries, Lebanon, Pennsylvania

Sharon D. Banks, General Manager, AC Transit, Oakland, California

Brian J. L. Berry, Lloyd Viel Berkner Regental Professor and Chair, Bruton Center for Development Studies, University of Texas at Dallas

Dwight M. Bower, Director, Idaho Transportation Department, Boise

John E. Breen, The Nasser I. Al-Rashid Chair in Civil Engineering, Department of Civil Engineering, The University of Texas at Austin

William F. Bundy, Director, Rhode Island Department of Transportation, Providence

David Burwell, President, Rails-to-Trails Conservancy, Washington, D.C.

A. Ray Chamberlain, Vice President, Freight Policy, American Trucking Associations, Alexandria, Virginia (Past Chairman, 1993)

Ray W. Clough (Nishkian Professor of Structural Engineering, Emeritus, University of California, Berkeley), Structures Consultant, Sunriver, Oregon

James C. DeLong, Director of Aviation, Denver International Airport, Colorado

James N. Denn, Commissioner, Minnesota Department of Transportation, St. Paul, Minnesota

Dennis J. Fitzgerald, Executive Director, Capital District Transportation Authority, Albany, New York

James A. Hagen, Chairman of the Board, Conrail Inc., Philadelphia, Pennsylvania

Delon Hampton, Chairman and CEO, Delon Hampton & Associates, Chartered, Washington, D.C.

Lester A. Hoel, Hamilton Professor, Department of Civil Engineering, University of Virginia, Charlottesville

Don C. Kelly, Secretary, Kentucky Transportation Cabinet, Frankfort

Robert Kochanowski, Executive Director, Southwestern Pennsylvania Regional Planning Commission, Pittsburgh

James L. Lammie, President and CEO, Parsons Brinckerhoff, Inc., New York City

Charles P. O'Leary, Jr., Commissioner, New Hampshire Department of Transportation, Concord

Jude W. P. Patin (Brig. Gen., U.S. Army, retired), Secretary, Louisiana Department of Transportation and Development, Baton Rouge

Craig E. Philip, President, Ingram Barge Company, Nashville, Tennessee

Darrel Rensink, Director, Iowa Department of Transportation, Ames

Joseph M. Sussman, JR East Professor and Professor of Civil and Environmental Engineering, Massachusetts Institute of Technology, Cambridge (Past Chairman, 1994)

Martin Wachs, Director, Institute of Transportation Studies, School of Public Policy and Social Research, University of California, Los Angeles

David N. Wormley, Dean of Engineering, Pennsylvania State University, University Park

Howard Yerusalem, Vice President, KCI Technologies, Inc., Hunt Valley, Maryland

Mike Acott, President, National Asphalt Pavement Association, Lanham, Maryland (ex officio)

Roy A. Allen, Vice President, Research and Test Department, Association of American Railroads, Washington, D.C. (ex officio)

Andrew H. Card, Jr., President and CEO, American Automobile Manufacturers Association, Washington, D.C. (ex officio)

Thomas J. Donohue, President and CEO, American Trucking Associations, Inc., Alexandria, Virginia (ex officio)

Francis B. Francois, Executive Director, American Association of State Highway and Transportation Officials, Washington, D.C. (ex officio)

Jack R. Gilstrap, Executive Vice President, American Public Transit Association, Washington, D.C. (ex officio)

Albert J. Herberger (Vice Adm., U.S. Navy, retired), Administrator, Maritime Administration, U.S. Department of Transportation (ex officio)

David R. Hinson, Administrator, Federal Aviation Administration, U.S. Department of Transportation (ex officio)

T. R. Lakshmanan, Director, Bureau of Transportation Statistics, U.S. Department of Transportation (ex officio)

Gordon J. Linton, Administrator, Federal Transit Administration, U.S. Department of Transportation (ex officio)

Ricardo Martinez, Administrator, National Highway Traffic Safety Administration, U.S. Department of Transportation (ex officio)

Jolene M. Molitoris, Administrator, Federal Railroad Administration, U.S. Department of Transportation (ex officio)

Dharmendra K. Sharma, Administrator, Research and Special Programs Administration, U.S. Department of Transportation (ex officio)

Rodney E. Slater, Administrator, Federal Highway Administration, U.S. Department of Transportation (ex officio)

Arthur E. Williams (Lt. Gen., U.S. Army), Chief of Engineers and Commander, U.S. Army Corps of Engineers, Washington, D.C. (ex officio)



# Fourth International Bridge Engineering Conference

Volume 1

San Francisco, California  
August 28–30, 1995

*Sponsored by*

Transportation Research Board  
Federal Highway Administration  
Federal Railroad Administration  
American Association of State Highway and Transportation Officials  
California Department of Transportation

TRANSPORTATION  
RESEARCH  
BOARD

NATIONAL  
RESEARCH  
COUNCIL

NATIONAL ACADEMY PRESS  
WASHINGTON, D.C. 1995

Conference Proceedings 7  
ISSN 1073-1652  
ISBN 0-309-06109-1

Subscriber Category  
IIC bridges, other structures, and hydraulics and hydrology

Transportation Research Board publications are available by ordering individual publications directly from the TRB Business Office or by annual subscription through organizational or individual affiliation with TRB. Affiliates and library subscribers are eligible for substantial discounts. For further information or to obtain a catalog of TRB publications in print, write to Transportation Research Board, Business Office, National Research Council, 2101 Constitution Avenue, N.W., Washington, D.C. 20418 (telephone 202-334-3214).

Printed in the United States of America

NOTICE: The conference that is the subject of this report was approved by the Governing Board of the National Research Council, whose members are drawn from the councils of the National Academy of Sciences, the National Academy of Engineering, and the Institute of Medicine. The members of the committee responsible for the report were chosen for their special competence and with regard for appropriate balance.

The papers in this report have been reviewed by a group other than the authors according to procedures approved by the Governing Board of the National Research Council. The views expressed are those of the authors and do not necessarily reflect the views of the Transportation Research Board, the National Research Council, or the sponsors of the conference.

The conference was sponsored by the Federal Highway Administration and the Federal Railroad Administration of the U.S. Department of Transportation, the American Association of State Highway and Transportation Officials, and the California Department of Transportation.

## Steering Committee for the Fourth International Bridge Engineering Conference

*Chairman*, David B. Beal, New York State Department of Transportation

Craig A. Ballinger, Craig Ballinger & Associates  
Protasio Ferreira e Castro, Fluminense Federal University, Brazil  
Thomas J. Collins, Collins Engineers, Inc.  
Bruce M. Douglas, Center for Civil Engineering Earthquake Research, University of Nevada  
Donald J. Flemming, Minnesota Department of Transportation  
Robert J. Heywood, Queensland University of Technology, Australia  
Robert N. Kamp, Albany, New York  
Ramankutty Kannankutty, City of Minneapolis  
Chitoshi Miki, Tokyo Institute of Technology, Japan  
A.P. Moser, Utah State University  
Andrzej S. Nowak, University of Michigan  
Wojciech Radomski, Warsaw University of Technology, Poland  
James E. Roberts, California Department of Transportation  
Charles W. Roeder, University of Washington, Seattle  
Arunprakash M. Shirole, New York State Department of Transportation  
Robert A. P. Sweeney, Canadian National Railways  
Paul Zia, North Carolina State University

### Liaison Representatives

Scott A. Sabol, Transportation Research Board  
Louis N. Triandafilou, Federal Highway Administration

### Transportation Research Board Staff

Robert E. Spicher, Director, Technical Activities  
Daniel W. (Bill) Dearasaugh, Jr., Engineer of Design  
Nancy A. Ackerman, Director, Reports and Editorial Services  
Naomi Kassabian, Editor



# Contents

---

INTRODUCTION .....	xi
--------------------	----

## VOLUME 1

### BRIDGE MANAGEMENT SYSTEMS, PART 1

Managing Minnesota's Bridges .....	3
<i>Paul M. Kivisto and Donald J. Flemming</i>	
Bridge Management System: Computer-Aided Planning Decision System for Polish Road Administration .....	16
<i>Andrzej Legosz, Adam Wysokowski, and Aleksandra Hutnik</i>	
Development of Hungarian Bridge Management System .....	25
<i>Gyula Kolozsi, László Gáspár, Jr., Ernő Tóth, and Árpád Csorba</i>	
Condition Rating and Maintenance System for Railway Bridges in Poland .....	32
<i>Maciej Sawicki and Jan Bień</i>	
Innovative Stand-Alone Financing for Mid-Bay Bridge Across Choctawhatchee Bay .....	38
<i>Eugene C. Figg, Jr., and Linda F. McCallister</i>	

### BRIDGE AESTHETICS

Innovation and Aesthetics .....	47
<i>Frederick Gottemoeller and Alicia Buchwalter</i>	
Bridge Architecture: The Good, the Bad, and the Ugly .....	57
<i>R. Ralph Mays</i>	
Humane Urban Aesthetic: US-183 Elevated Project in Austin, Texas .....	60
<i>Dean Van Landuyt</i>	
Discovery Bridge .....	68
<i>Ronald K. Mattox</i>	
Alsea Bay Bridge Replacement .....	80
<i>Maurice D. Miller</i>	

## BRIDGE PERFORMANCE

<b>British Practice in Arch Bridge Assessment .....</b>	<b>91</b>
<i>W. J. Harvey and F.W. Smith</i>	
<b>Case Study of Concrete Deck Behavior Without Top Reinforcing Bars .....</b>	<b>100</b>
<i>Li Cao, P. Benson Shing, John Allen, and Dave Woodham</i>	
<b>Probabilistic Assessment of Prestressed Concrete Bridge .....</b>	<b>110</b>
<i>J. A. Sobrino and J. R. Casas</i>	
<b>Effect of Cross Frames on Behavior of Steel Girder Bridges .....</b>	<b>117</b>
<i>Atorod Azizinamini, Steve Kathol, and Mike Beacham</i>	
<b>On the Use of Measured Vibration for Detecting Bridge Damage .....</b>	<b>125</b>
<i>Sreenivas Alampalli, Gongkang Fu, and Everett W. Dillon</i>	

## BRIDGE CONSTRUCTION

<b>FHWA's Bridge Temporary Works Research Program .....</b>	<b>141</b>
<i>John F. Duntemann and Sheila Rimal Duwadi</i>	
<b>Constructability Reviews: An Opportunity for Partnering .....</b>	<b>151</b>
<i>William J. Schmitz</i>	
<b>High-Performance Concrete for a Floating Bridge .....</b>	<b>155</b>
<i>M. Myint Lwin, Alan W. Bruesch, and Charles F. Evans</i>	
<b>Premature Cracking of Concrete Bridge Decks: Causes and Methods of Prevention .....</b>	<b>163</b>
<i>Ron Purvis, Khossrow Babaei, Nalin Udani, Abid Qanbari, and William Williams</i>	
<b>Design and Construction of North Halawa Valley Viaduct .....</b>	<b>176</b>
<i>Tim J. Ingham, Rafael Manzanarez, and Karen Cormier</i>	

## BRIDGE MANAGEMENT SYSTEMS, PART 2

<b>Development and Implementation of New York State's Comprehensive Bridge Safety Assurance Program .....</b>	<b>187</b>
<i>A. M. Shirolé</i>	
<b>Pontis Version 3: Reaching Out to the Bridge Management Community .....</b>	<b>197</b>
<i>Paul D. Thompson</i>	
<b>Environmental Classification Scheme for Pontis .....</b>	<b>203</b>
<i>Dixie T. Wells</i>	
<b>Development of Life-Cycle Activity Profiles in BRIDGIT Bridge Management System .....</b>	<b>209</b>
<i>Hugh Hawk</i>	



<b>Calibration and Application of Deterioration Models for Highway Bridges .....</b>	<b>220</b>
<i>George Hearn, Dan M. Frangopol, and Milan Chakravorty</i>	

## LONG-SPAN BRIDGES

<b>A Second High-Level Blue Water Bridge .....</b>	<b>233</b>
<i>Sudhakar R. Kulkarni</i>	
<b>Northumberland Strait Crossing, Canada .....</b>	<b>238</b>
<i>Gerard Sauvageot</i>	
<b>Design and Construction of Tsurumi Tsubasa Bridge Superstructure .....</b>	<b>249</b>
<i>Mamoru Enomoto, Hisashi Morikawa, Haruo Takano, Masafumi Ogasawara, Hiroyuku Hayashi, Wataru Takahashi, Nobuo Watanabe, and Masahito Inoue</i>	
<b>Kap Shui Mun Cable-Stayed Bridge .....</b>	<b>259</b>
<i>Steven L. Stroh and Thomas G. Lovett</i>	
<b>Implications of Test Results from Full-Scale Fatigue Tests of Stay Cables Composed of Seven-Wire Prestressing Strand .....</b>	<b>266</b>
<i>Habib Tabatabai, A. T. Ciolko, and T. J. Dickson</i>	

## BRIDGE LOADS AND DYNAMICS

<b>Are Road-Friendly Suspensions Bridge-Friendly? OECD DIVINE .....</b>	<b>281</b>
<i>Robert J. Heywood</i>	
<b>Analysis and Evaluation of Bridge Behavior Under Static Load Testing Leading to Better Design and Judgment Criteria .....</b>	<b>296</b>
<i>Munzer Hassan, Olivier Burdet, and Renaud Favre</i>	
<b>Experimental Verification of Inelastic Design Procedures for Steel Bridges .....</b>	<b>304</b>
<i>Michael G. Barker and Bryan A. Hartnagel</i>	
<b>Load Spectra for Girder Bridges .....</b>	<b>314</b>
<i>Jeffrey A. Laman</i>	
<b>Simplified Numerical Analysis of Suspension Bridges .....</b>	<b>324</b>
<i>Diego Cobo del Arco and Angel C. Aparicio</i>	

## FRP COMPOSITES AND OTHER MATERIALS FOR BRIDGES

<b>Shear Strengthening of Concrete Bridge Girders Using Carbon Fiber-Reinforced Plastic Sheets .....</b>	<b>337</b>
<i>Efrosini Drimoussis and J.J. Roger Cheng</i>	
<b>Advanced Composites for Bridge Infrastructure Renewal .....</b>	<b>348</b>
<i>Frieder Seible, Gilbert A. Hegemier, and Vistasp Karbhari</i>	

<b>Modern Brickwork Highway Structures .....</b>	<b>358</b>
<i>S. W. Garrity</i>	

<b>Large Deformation Cyclic Tests on Stainless Steel Reinforcing Bars for Reinforced-Concrete Structures in Seismic Regions .....</b>	<b>368</b>
<i>Roberto Gori, Enzo Siviero, and Salvatore Russo</i>	

## VOLUME 2

### BRIDGE REHABILITATION

<b>Cracking, Fracture Assessment, and Repairs of Green River Bridge, I-26 .....</b>	<b>3</b>
<i>John W. Fisher, Eric J. Kaufmann, Michael J. Koob, and Gerald White</i>	

<b>Crack Evaluation and Repair of Cantilever Bracket Tie Plates of Edison Bridge .....</b>	<b>15</b>
<i>John W. Fisher, Ben T. Yen, Eric J. Kaufmann, Zuo-Zhang Ma, and Thomas A. Fisher</i>	

<b>Determination of Heat-Straightening Parameters for Repair of Steel Pedestrian Bridge .....</b>	<b>26</b>
<i>Henryk Zobel</i>	

<b>Strengthening of Continuous-Span Composite Steel-Stringer Bridges .....</b>	<b>33</b>
<i>T. J. Wipf, F. W. Klaiber, F. S. Fanous, and H. El-Arabaty</i>	

<b>Controlling Lead-Based Paint Emissions During Rehabilitation of the Williamsburg Bridge: A Partnering Approach .....</b>	<b>45</b>
<i>Ralph D. Csogi</i>	

### SEISMIC RESPONSE OF BRIDGES

<b>Improved Screening Procedure for Seismic Retrofitting of Highway Bridges .....</b>	<b>59</b>
<i>Ian G. Buckle and Ian M. Friedland</i>	

<b>Effectiveness of Hinge Restrainers as Seismic Retrofit Measure .....</b>	<b>71</b>
<i>M. Saiidi and E. Maragakis</i>	

<b>Application of Base Isolation to Single-Span Bridge in a Zone with High Seismicity .....</b>	<b>79</b>
<i>James Kwong, Richard K. Lindsay, Arthur J. Woodworth, David M. Jones, and Richard P. Knight</i>	

<b>Seismic Retrofit of Southern Freeway Viaduct, Route 280 (Single-Level Segment), San Francisco, California .....</b>	<b>88</b>
<i>Roy A. Imbsen, Robert A. Schamber, and A.A. (Frank) Abugattas</i>	



<b>Earthquake Retrofit of California Bridge: Route 242/680 Separation .....</b>	<b>101</b>
<i>Robert C. Fish and George L. Rowe</i>	

## **BRIDGE BEARINGS, JOINTS, AND DETAILS**

<b>Field Measurements of Large Modular Expansion Joint .....</b>	<b>111</b>
<i>Charles W. Roeder, Mark Hildahl, and John A. Van Lund</i>	

<b>Bridge Bearing Replacement .....</b>	<b>122</b>
<i>John A. Van Lund</i>	

<b>Behavior of Bearing Plate Type Bridge Bearings Under Traveling Load .....</b>	<b>130</b>
<i>Toshihiko Naganuma, Koretada Seki, Masanori Iwasaki, and Koichi Tokuda</i>	

<b>Development and Testing of a New Shear Connector for Steel Concrete Composite Bridges .....</b>	<b>137</b>
<i>Wayne S. Roberts and Robert J. Heywood</i>	

<b>Application of Precast, Prestressed Concrete Piles in Integral Abutment Bridges .....</b>	<b>146</b>
<i>Mounir R. Kamel, Joseph V. Benak, Maher K. Tadros, and Mostafa Jamshidi</i>	

## **PRESTRESSED CONCRETE BRIDGES**

<b>Development Length of Prestressing Strand in Bridge Members .....</b>	<b>161</b>
<i>Susan N. Lane</i>	

<b>Applications and Limitations of High-Strength Concrete in Prestressed Bridge Girders .....</b>	<b>169</b>
<i>Henry G. Russell, Jeffery S. Volz, and Robert N. Bruce</i>	

<b>Serviceability Criteria for Prestressed Concrete Bridge Girders .....</b>	<b>181</b>
<i>Andrzej S. Nowak and Hassan H. El-Hor</i>	

<b>Structural Safety of Prestressed Concrete and Composite Steel Highway Bridges .....</b>	<b>188</b>
<i>Sami W. Tabsh</i>	

<b>Bangkok Second-Stage Expressway System Segmental Structures .....</b>	<b>199</b>
<i>Brian Dodson</i>	

## **BRIDGE STRUCTURAL SYSTEMS**

<b>High-Performance Concrete U-Beam Bridge: From Research to Construction .....</b>	<b>207</b>
<i>Mary Lou Ralls</i>	

<b>External Prestressing for Bridge Rehabilitation in Italy .....</b>	<b>213</b>
<i>Mario P. Petrangeli</i>	

<b>Precast Arches as Innovative Alternative to Short-Span Bridges .....</b>	<b>219</b>
<i>Pierre Segrestin and William J. Brockbank</i>	

<b>Impact of Load and Resistance Factor Design Specifications on Short- to Medium-Span Steel Bridges .....</b>	<b>227</b>
<i>Dennis R. Mertz and John M. Kulicki</i>	

## **BRIDGE SUBSTRUCTURES: SCOUR AND SHIP IMPACT**

<b>Florida Department of Transportation Bridge Scour Evaluation Program .....</b>	<b>237</b>
<i>P. F. Lagasse, E. V. Richardson, and K. E. Weldon</i>	

<b>Bridge Scour in the Coastal Regions .....</b>	<b>249</b>
<i>J. R. Richardson, E. V. Richardson, and B. L. Edge</i>	

<b>Alternatives to Riprap as a Scour Countermeasure .....</b>	<b>261</b>
<i>J. Sterling Jones, David Bertoldi, and Stuart Stein</i>	

<b>Bridge Pier Analysis for Ship Impact .....</b>	<b>279</b>
<i>M. I. Hoit, Mike McVay, and Scott E. Breneman</i>	

## **BRIDGE FATIGUE AND REDUNDANCY**

<b>Evaluation of Fatigue-Sensitive Details Used in Moline Viaduct, Illinois .....</b>	<b>291</b>
<i>Richard A. Walther and Michael J. Koob</i>	

<b>Improvement of Fatigue Strength of Steel Girders with Tapered Partial-Length Welded Cover Plates .....</b>	<b>304</b>
<i>Ahmed F. Hassan and Mark D. Bowman</i>	

<b>After-Fracture Redundancy of Two-Girder Bridge: Testing I-40 Bridges Over Rio Grande .....</b>	<b>316</b>
<i>R. L. Idriss, K. R. White, C. B. Woodward, and D. V. Jauregui</i>	

<b>Fatigue Assessment of Cable Systems of Long-Span Cable-Stayed Bridges .....</b>	<b>327</b>
<i>Kazuo Tada, Yuji Fujii, Harukazu Ohashi, and Chitoshi Miki</i>	

<b>Redundancy in Highway Bridge Superstructures .....</b>	<b>338</b>
<i>Michel Ghosn and Fred Moses</i>	

## **WOOD BRIDGES**

<b>Load and Resistance Factor Design Code for Wood Bridges .....</b>	<b>351</b>
<i>Andrzej S. Nowak and Michael A. Ritter</i>	

<b>Design, Construction, and Evaluation of Timber Bridge Constructed of Cottonwood Lumber .....</b>	<b>358</b>
<i>Michael A. Ritter, James P. Wacker, and Everett D. Tice</i>	



---

<b>Experimental Testing of Composite Wood Beams for Use in Timber Bridges .....</b>	<b>371</b>
<i>Michael J. Chajes, Victor N. Kaliakin, Scott D. Holsinger, and Albert J. Meyer, Jr.</i>	
<b>Dynamic Response of Stress-Laminated-Deck Bridges .....</b>	<b>381</b>
<i>M. A. Ritter, D. L. Wood, T. J. Wipf, Chintaka Wijesooriya, and S. R. Duwadi</i>	
<b>Crash-Tested Bridge Railings for Timber Bridges .....</b>	<b>395</b>
<i>Michael A. Ritter, Ronald K. Faller, and Sheila R. Duwadi</i>	
<b>STEERING COMMITTEE BIOGRAPHICAL INFORMATION .....</b>	<b>405</b>

# Introduction

---

Transportation systems of the world represent a huge investment on the part of governments and taxpayers. There is widespread concern over the status of the infrastructure, and despite indications of increased investment, it is clear that the funds available are not likely to meet all the needs of this sector in the long run. More than ever, wise investment decisions concerning roads and bridges will be crucial to the future of transportation.

This conference is the fourth in a series of International Bridge Engineering Conferences. Previous conferences were held in St. Louis, Missouri, in 1978; Minneapolis, Minnesota, in 1984; and Denver, Colorado, in 1991. Those conferences were well attended, and valuable information was presented and published. Much has transpired since the 1991 conference that should be brought to the attention of the user community.

## OBJECTIVE

The objective of the conference is to provide an international forum for the exchange of bridge research results and technical information on planning, design, construction, repair, rehabilitation, replacement, and maintenance of bridges. The focus is on problems and solutions of interest to bridge engineers and administrators of highway, railroad, and transit agencies. Research results emanating from the AASHTO-sponsored NCHRP bridge studies as well as those of federal, state, and international research agencies' programs are being highlighted.

## FORMAT

The conference, conducted over 2½ days, includes an opening session (not included in the Conference Proceedings) followed by concurrent paper sessions on various topics. All papers presented in those sessions are included in these Proceedings.

Conference sessions cover the following topics:

Bridge Management Systems	Seismic Response of Bridges
Bridge Aesthetics	Bridge Bearings, Joints, and Details
Bridge Performance	Prestressed Concrete Bridges
Bridge Construction	Bridge Structural Systems
Long-Span Bridges	Bridge Substructures: Scour and Ship Impact
Bridge Loads and Dynamics	Bridge Fatigue and Redundancy
FRP Composites and Other Materials	Wood Bridges
Bridge Rehabilitation	

## CONFERENCE PROCEEDINGS

The proceedings of the Fourth International Bridge Engineering Conference is being published in two volumes. The two-volume set will be distributed to all conference attendees and is available for purchase through the Transportation Research Board. All papers contained in these proceedings underwent full TRB peer review.

# BRIDGE MANAGEMENT SYSTEMS, PART 1

---

# Managing Minnesota's Bridges

---

Paul M. Kivisto and Donald J. Flemming, *Minnesota Department of Transportation*

The process that is presently used, and that is anticipated to be used in the future, to manage Minnesota's limited bridge resources is explained. Present bridge management history and policies including present inspection methods, computer tools that are available, present priority-ranking methods for bridge replacements, and the relationship between the Minnesota Department of Transportation (Mn/DOT) and local governments are discussed. Future bridge management practices including Pontis bridge management system (BMS) implementation, element-level inspections, the Minnesota case study in moving to the use of Pontis, new funding processes as a result of the Intermodal Surface Transportation Efficiency Act (ISTEA), and how these factors will tie together for managing bridge resources in the 21st century are covered. In 1994 Minnesota began the process of implementing the Pontis BMS. Before that time all bridge inspections were based on National Bridge Inspection Standards and management decisions were guided by a Minnesota priority-ranking system, (FHWA) sufficiency ratings, Minnesota published improvement guidelines, and engineering judgment. Minnesota has used computer software programs extensively to record and store field inventory and inspection data, which has substantially reduced the amount of paperwork required during each inspection. With the advent of the Pontis BMS, inspection coding is changing and new data collection software has been developed. As a result of ISTEA, Minnesota has established area transportation partnerships that develop the statewide transportation improvement program. Outputs from BMS will provide information to be used in the selec-

tion of appropriate bridge projects and bridge maintenance activities. The outputs necessary to plan a bridge preservation and improvement program include overall conditions, estimates of bridge needs, future conditions assuming certain levels of expenditure, and identification of activities with high benefit-cost ratios. This information will best be illustrated through graphs or charts. Bridge management is another tool that can be used to assist in the definition of bridge programs, so even with the introduction of system analysis, engineering judgment will continue to be a part of the process. In the future integration will occur among the various management systems (pavement, safety, etc.). Limited integration exists at this time in Mn/DOT, and preliminary thoughts on extensive integration of these systems and level-of-service goals are described.

A bridge management system (BMS) is required by the 1991 Intermodal Surface Transportation Efficiency Act (ISTEA) and FHWA regulations mandating that states use management systems in an effort to optimize transportation resources. BMS is defined as a rational and systematic approach to organizing and carrying out all of the activities related to providing programs for bridges vital to the transportation infrastructure.

## BRIDGE MANAGEMENT IN MINNESOTA

A simplified BMS has been in place in Minnesota since the late 1960s with the start of the bridge inspection

and inventory system. This system has worked well for identifying bridges that are in need of replacement and rehabilitation and has provided valuable information for preservation activities; however, there has not been a way to compare the relative benefits of proposed actions, nor has there been a way to determine appropriate life-cycle costs or to trace deterioration rates.

Criteria for certain types of maintenance and rehabilitation work are currently provided in the Minnesota Department of Transportation (Mn/DOT) *Bridge Improvement Guidelines* on the basis of condition and level of service. Examples of such criteria are

- Conditions when spot painting and complete repainting are appropriate,
- Conditions when deck replacement is appropriate,
- Conditions when joint replacement is appropriate,
- Conditions when deck overlays are appropriate, and
- Conditions and functionality when railing replacement is appropriate.

Examples of painting guidelines and deck repair/replacement guidelines are shown in Figure 1.

Eligibility for the funding of bridge projects and the determination of project scope varies depending on the types of funds used as well as on the condition and geometrics of the bridge. For example, bridge projects funded through the Highway Bridge Replacement and Rehabilitation Program must meet federal requirements for sufficiency rating, whereas bridge projects funded under the National Highway System or Surface Transportation Program categories do not have such requirements. Determinations of rehabilitation versus replacement are made on the basis of a comparison of the construction cost of rehabilitation versus the cost of a totally new bridge. The policy in Minnesota is to maximize the life of each bridge and improve geometrics and load capacity when they are economically feasible.

The sufficiency rating is used as a guideline for replacement priority even if federal funding is not involved. This FHWA formula is based on geometric, traffic, and condition data relative to each bridge (1). A report listing the bridges on the various road systems (trunk highway, county, township, city) is generated twice each year, listing bridges by increasing sufficiency rating number. Before the development of the FHWA sufficiency rating formula, Minnesota had developed a formula called the Replacement Priority Criteria (RPC), which uses safe load appraisal rating, average daily traffic (ADT), deck geometry appraisal, structural condition appraisal, and approach roadway appraisal as well as a factor for the age of the structure. The RPC rating was used to generate a statewide ranking of bridge replacement projects and to determine eligibility for re-

placement funding before the development of federal sufficiency formulas and current management systems. The RPC is not currently used as a criterion for funding, but it is still generated and is shown on the priority lists described earlier.

### Weaknesses in Procedures Before BMS

The procedures used before the Pontis BMS identified and ranked bridges that were in need of replacement or rehabilitation, but they did not consider the life-cycle costs of bridges, nor did they define cost-effective actions to be taken during the life of the bridge. These procedures did not consider the remaining life of a bridge or compare the expected life with those of other bridges needing replacement or rehabilitation. Additionally, they did not have the ability to forecast the annual investment needed for a defined level of bridge preservation or replacement activities.

### Present Inspection Process

Minnesota state regulations require annual inspections of all structures greater than 10 ft in length. These inspections are performed by several different levels of government. The Mn/DOT district offices are responsible for the inspection and inventory of 4,600 state-owned bridges. Eighty-seven Minnesota counties are responsible for the inspection and inventory of 13,900 bridges owned by the county, township, and cities with populations of less than 5,000. Minnesota cities with populations of greater than 5,000 are responsible for the inspection of 990 bridges. Other agencies in Minnesota such as the National Forest Service, the Bureau of Indian Affairs, and State Forest Roads are responsible for inspection and inventory of 180 bridges. This makes a total of approximately 19,670 bridges in Minnesota of 10 ft or greater in length.

With the advent of the Pontis BMS and the change to element-level inspections, Minnesota began a transition phase. During 1994 all Mn/DOT districts performed element-level inspections, whereas all counties and cities recorded information by National Bridge Inventory (NBI) methods. Local governments have been trained in element-level inspections and will begin element-level inspections in 1995. The element-level inspections and an outline of how Minnesota transitioned to the Pontis BMS are explained in greater detail later in this paper.

### Computer Hardware and Software

The capabilities and affordability of personal computers (PCs) have increased the use of automation in procedures that previously required manual recording. The

### **Guidelines for Deck Repair/Replacement by Contract**

Priority guidelines are based on the premise that:

1. Overlays are placed on basically intact decks as a protective measure, or
2. Deck replacements are deferred until full deck removal and replacement is warranted.

The following general categories and procedures have been established for deck repair projects:

Category	Deck Condition	Procedure
I	0-5% Unsound (Slight Scarify, deterioration)	Spot removal and 2" low slump concrete overlay or 1 1/2 latex modified concrete overlay
II	5-20% Unsound (Moderate)	Scarify, spot removal and 2" low slump concrete overlay
III	20-40% Unsound (Severe) Only non-interstate highways < 10,000 ADT & bottom of slab sound	100% removal of surface down to reinforcing bars and minimal spot removal below reinforcing bars.  Overlay with 3" of low slump concrete
IV	40+ % Unsound (Critical) (20+ % on Interstate of > 10,000 ADT)	Schedule new deck after usable life of inplace deck is expended. May require bituminous overlay to maintain rideability.

### **Guidelines for Bridge Maintenance Painting**

The guidelines for bridge maintenance painting are based primarily on preserving the structural integrity of steel bridges in the most cost effective and practical manner possible:

Paint Condition	Procedure	PRIORITY	
		Contract	Mn/DOT
(% Unsound)			
0% - 5%	Sandblast isolated areas. Apply two prime coats to all areas where paint was removed.	4	1
6% - 20%	Sandblast isolated areas. Clean all structural steel. Apply two prime coats to all sandblasted areas. Apply two finish coats to areas severely exposed, one finish coat to all other areas.	3	2
21% - 40%	Sandblast isolated areas. Clean all structural steel. Place two complete prime coats and two finish coats on all members.	2	3
More than 40%	Remove all inplace paint and rust per SSPC-10, Near White Blast. Repaint with complete zinc-rich paint system.	1	4

FIGURE 1 Bridge repair guidelines.

advent of networking and modems has allowed data sharing and electronic data transfer, both of which provide increased capabilities for bridge personnel. Two PC programs have been developed in Minnesota and are being used to help in the data collection effort: the Minnesota Bridge Inventory PC System (MBIPS) and the Bridge Inspection Program (BIP).

#### ***MBIPS Program***

The MBIPS program was written in 1988 as a means to allow bridge inspectors to electronically record inventory information on all bridges in their jurisdiction,

obtain reports on those data, and electronically transfer the data to the central office for review. The program was written in Basic, and despite other higher-level languages and data bases available today, it has still proven to be a very effective program. Many summary reports are available from this program, both for screen viewing and as hard copy. The most comprehensive of these reports is the Structure Inventory and Appraisal Sheet, which contains 150 data elements. A sample inventory report form is shown in Figure 2. Examples of other summary reports that are available include lists of bridges by sufficiency rating, by inspection date, by con-

1994

## MINNESOTA DEPARTMENT OF TRANSPORTATION - STRUCTURE INVENTORY

## COUNTY JURISDICTION

09-28-1994

* IDENTIFICATION *		* STRUCTURE DATA *		Suff Rating 23.2 S.D. Status	
Br.No. 2157	15 HWY/STREAM				
District 3 Maint Area	Type of Service				
County AITKIN	Type Main Span . . 301	* SUBSTRUCTURE DATA *			
City	STEEL BM SPAN	Abut CONCRETE FTNG/PILE			
Township LIBBY	Type Appr Span . .	Pier Material NON-APPLY Foundat'n			
CSAH 36 MAIN LINE	Fract Critl NON-APL	* WATERWAY DATA *			
Route Number Function	Spec1 Member PROC Date	A08/90 J/92			
Rdwy Type 2 WAY ROAD		UW Insp Scour DF Area			
STREAM		Waterway Opening 126			
Name of Feature Crossed		Navig Cntrl/Prot NO			
0.2 MI NE OF JCT TH 65		Vert Horiz			
Descriptive Location		* APPROACH PANELS *			
		Near ON -			
		Far ON			
		Type Cond Length			
		* PAINT DATA *			
		Yr Pntd			
		Type . .			
		Area			
		% Unsound			
		* EXPANSION *			
		* DEVICE *			
		Type . . NN			
		Condition			
		Yr Instl			
		* CAPACITY RATINGS *			
		Design Load . UNK/OTH			
		Operating . . H 10.0			
		Inventory . . H 07.3			
		Posting . 10 -TON			
		Rating Date . 01/88			
		Need New Rating NO			
		* CONDITION CODES *			
		* APPRAISAL RATINGS *			
		* IMPROVEMENT DATA *			
		Prop Work REPLACE COND			
		Prop Structure BRIDGE			
		Length 51 Width 24			
		Proj ADT 30 Yr 2011			
		Appr Rdwy Work REGRADE			
		Bridge Cost \$ 55,000			
		Appr Cost \$ 11,000			
		Project Cost \$ 66,000			
		Year of Data 1990 (1)			

FIGURE 2 Structure inventory and appraisal sheet.



dition, and by route system and lists of fracture-critical, load-posted, or scour-critical bridges. MBIPS includes six different screens that allow input and editing of 200 data elements. These six screens group common data elements together.

Effort has been made recently to rewrite MBIPS by using expert system logic to enable better edit checks. Expert system logic or artificial intelligence means that technical expertise and experience in reviewing bridge data are coded into formulas to show relationships between data elements. These formulas can identify data inconsistencies that will improve data reliability. Among the benefits to be gained in using the new program will be (a) a data base compatible with Mn/DOT standards for relational data bases, (b) expert logic that eliminates some errors found in data submittals at the present time, and (c) a system compatible with Windows for ease of operation.

### **BIP**

BIP was written in 1988 in an effort to eliminate the repetitious data and comment recording necessary during bridge inspections. Mn/DOT inspection forms contain space for recording inspection data and comments on bridge deficiencies. Bridge inspectors have found that many comments are repeated from year to year. BIP was written to eliminate the need to rewrite comments and as a means to provide summary reports on inspection data.

BIP is divided into three major parts. The first part gives general information about bridge location and type. The second part provides information about the type of elements and the conditions of elements on a bridge. The third part enables the inspector to record detailed information regarding the conditions and locations of defects. An example of an Mn/DOT NBI inspection report form is shown in Figure 3, and a Mn/DOT Pontis BMS element-level report form is shown in Figure 4. The condition portion of the form is automatically updated with the previous year's inspection data, and the inspector has to revise those values that have changed since the previous inspection. This eliminates some of the repetitious data entry previously encountered and also reduces the chance of data entry errors.

Reports available from BIP include the inspection report as well as lists of bridges that meet certain criteria. These criteria can be selected by using ad hoc selection criteria or by selecting certain data elements and the range of values for which outputs are desired.

### **Data Transfer**

One of the largest benefits of automating bridge inspection and inventory data is the ability to transfer data

between programs and between local and central data bases. To provide the ability to transfer data into the Pontis BMS, a file that is compatible with the required Pontis input file is created. With increased use of relational data bases, all data recorded and stored for bridge purposes can be exchanged with other programs.

The Mn/DOT Office of Bridges and Structures is responsible for maintaining a central bridge data base and submitting the data to FHWA. All information stored on district, county, and city computers is transferred electronically to the Office of Bridges and Structures data base. Data transfer from the counties is done via network modems and eliminates the need for the transmission of floppy disks. Data transfer from Mn/DOT districts to the Office of Bridges and Structures is done via statewide optical transmission lines. Program updates are also transferred by these methods.

The main data base remains in a flat file format on a mainframe computer. Data are downloaded to and uploaded from the local agency computers at least once per year. Statewide reports are still run by using the mainframe data base, although many options are available locally on PCs. Mn/DOT is considering moving to a relational data base such as Oracle in an effort to improve data sharing between various transportation users. Data would be stored on a network instead of on a mainframe. This would reduce costs for data storage and report generation and would eliminate the need for double entry for data such as traffic counts and accident locations.

### **Hardware**

Computer hardware requirements change with the advent of more powerful software. With the move toward the Windows operating system, relational data bases, and higher-level programming tools such as the C language, it is recommended that a minimum configuration of an International Business Machines 486 machine with 66 MHz and 8 MB of random access memory be provided in each agency.

Many Minnesota inspectors are using laptop computers for recording field data. Both the MBIPS and BIP data collection programs can be loaded onto the laptop computer and, with the use of Windows, can be accessed simultaneously. The method most often used is to take a hard copy report to the bridge site, mark any changes from the previous inspection onto the sheet, and then enter the changes into the computer while at the bridge site or while in transit to the next bridge location.

One problem with laptop computers is that they are difficult to carry onto the bridge site. One new technology being considered is the use of palm pad- or pen-based computers. It is anticipated that the easier port-

**Mn/DOT OFFICE OF BRIDGES AND STRUCTURES**  
**Bridge No.: 1241      Bridge Inspection Report      Jun 18, 1993      Sheet 1 of 1**

Road System: 03 MNTH	County: 19 DAKOTA	Location: 2.8 MI W OF FARMINGTON
Road Number: 50	Load Posting (Tons): LEGAL	Feature Crossed: DITCH
City:	Reference Point: 06.724	Bridge Type: W104 113 CONC BOX CULV
Township:	Deck Area (Sq.Ft.):	Min. Vert (Und/Und):
Maint. Area / District: 9A	Painted Area (Sq.Ft.):	Min. Vert (Over/Over):
Control Section: 1914	Crew No.: 2	Inspection Classification: A

NO	ITEM	RATINGS	%PCT	QUANT	UNIT	COMMENTS
SUBSTRUCTURE		N N N N				Bridge 1241 Year 93
1	Abutments .....	N N N N				
2	Piers .....	N N N N				(14) 1/4 to 3/4 inch wide cracks in bit need to be sealed.
3	Bridge Seats .....	N N N N				
SUPERSTRUCTURE		N N N N				(20) [1989] Apron washout 18 inch deep, South end, 10 inch deep North end.
4	Trusses .....	N N N N				
5	Girders .....	N N N N				
6	Floor Beams .....	N N N N				(24) [1987] 50 SF spalled floor. Barrel has 1/16 inch vertical crack
7	Stringers or Beams .....	N N N N				in walls and top along C/L of roadway.
8	Bearing Devices .....	N N N N				
9	Arches .....	N N N N				(25) SE wing spalled, broken off at apron. South headwall 12 SF
10	Fascia Beams .....	N N N N				moderate spell. Light scaling on wings and headwalls. 10 SF of 1/16
11	Diaphragms .....	N N N N				inch deep scale. 6 SF of 2 inch spall on top of wingwall at SW corner.
12	Spandrel Columns .....	N N N N				4 SF of 3/4 inch deep spall on South headwall.
DECK		N N N N				
13	Structural Slab .....	N N N N	00	0	sqft	(26/27) [1991] NUMEROUS CRACKS IN BIT ROADWAY.
14	Wearing Surface .....	7 7 7 7				
15	Curb & Walk .....	N N N N				(28) [1988/92] No Type 2 culvert markers.
16	Railing .....	N N N N				
17	Expansion Joints .....	N N N N				(30) 33 FT-2 inch from face to face of plate beam
18	Bridge Deck Drains .....	N N N N				
19	Median .....	N N N N				
AREA UNDER BRIDGE		6 6 6 6				
20	Channel & Protection .....	6 6 6 6				
21	Fenders .....	N N N N				
22	Roadway, Railway, Other .....	N N N N				
23	Slopes & Berms .....	8 8 8 8				
CULVERT & WALL		7 7 7 7				
24	Barrel & Floor .....	7 7 7 7				
25	Apron, Wingwall, Headwall ..	7 7 7 7				
APPROACH ROADWAY		N 7 7 7				
26	Approach Near (S or W) ...	N 7 7 7				
27	Approach Far (N or E) ....	N 7 7 7				
OTHER		7 7 7 7				
28	Signing .....	N N 7 7				
29	Retaining Wall .....	N N N N				
30	Guardrail .....	7 7 7 7				
31	Fence .....	N N N N				
32	Paint .....	N N N N		0	sqft	
33	Plow Straps .....	N N N N				
34	Drainage .....	8 8 8 8				
35	Miscellaneous .....	N N N N				
INSPECTOR		YEAR		REVIEWED BY		
R EDGELL		KRJ 1990		ROGER SCHULTZ 17JAN91		
N GUSTAFSON		JWH 1991		ROGER SCHULTZ 31JAN92		
L KELLER		JLA 1992		ROGER SCHULTZ 20FEB93		
T FLYNN		PAK 1993		ROGER SCHULTZ 07FEB94		

FIGURE 3 NBI inspection data collection form.

# Mn/DOT OFFICE OF BRIDGES AND STRUCTURES

Bridge No.: 6808 Bridge Inspection Report Sep 28, 1994 Sheet 1 of 2

County:50 MOWER  
Control Section:5080  
City:  
Township:008 LANSING  
Maint. Area / District:6B  
Sec: 33 Twp: 103 Rge: 18W  
Bridge Type:501 4 PREST CONC BEAM SPANS

Road System:01 ISTH  
Road Number:90  
Ref. Point :176.585  
Local Bridge Num.:  
Crew Number:  
Inspection Class:A

Crosses:EB OVER TWP RD & TURTLE C  
Location:0.9 MI W OF W JCT TH 218  
Load Posting(Tons):LEGAL  
Length: 243 Width: 44.2  
Deck Area (Sq.Ft.):  
Painted Area (Sq.Ft.):  
Min. Vert. (Under):  
Min. Vert. (Over):

CONDITIONS											
NO	ELEMENT	ENV	QTY	UNT	YR	1	2	3	4	5	COMMENTS
9	Prest Conc Girder	3	2215	LF	93	85%	15%	15%			*Bridge 6808
					94	85%	15%	15%			
41	Rein Conc Pier Cap	3	133	LF	93	95%	5%				41. All pier caps have several transverse cracks beneath them. Some small holes with rust stains, in side faces of pier caps.
					94	90%	10%				
58	Reinf Conc Column	3	9	EA	93	9					
					94	8	1				
62	Rein Conc Abutment	3	88	LF	93	85%	15%				9. Bottom ends of Span 4 girders, over Pier 3, have spalled off concrete. Several Span 2 girders appear to have longitudinal cracks in the bottom of their lower flanges.
					94	80%	20%				
90	Strip Seal Exp Jt	3	82	LF	93	100					
					94	100					
91	Pourable Joint	3	160	LF	93	100					
					94	50%	50%				
92	Compression Joint	1	56	LF	93	100					96. & 98. Some bearing devices getting quite rusty.
					94	100					
95	Elastomeric Brg	1	4	EA	93	4					62. Minor vertical cracks in face of each abut. (7 at east & 5 at west). Leaching cracks in end diaphragms. Utility access hole, west end, has a brick removed.
					94	3	1				
96	Movable Bearing	3	33	EA	93	28	5				9. Concrete diaphragms at Pier 3 are cracked and breaking apart.
					94	28	4	1			
98	Fixed Bearing	1	20	EA	93	20					122. Leaching cracks with efflorescence, beneath deck at Spans 1, 3 and 4. Some rust stains at transverse cracks, beneath the deck. Some patched areas noted beneath the deck. Low slump concrete overlay placed (1980). Numerous random deck cracks have been epoxy sealed (1990). Construction joint over Pier 2 and at each end of deck have been sealed (1990). Small hole through deck was cut out and patched (1993) in the shoulder area (over river) for foundations crew.
					94	20					
100	Conc Appr Panel	3	2	EA	93	2					
					94	2					
102	Concrete Railing	3	486	LF	93	90%	10%				
					94	90%	10%				
122	Conc Deck &RigidOL	3	1	EA	93		1				
					94		1				
OTHER ITEMS		93	94	SMART FLAGS		93	94				
180	Channel & Protection	8	7	108	Scour	N	N				
181	Signing	1	1	109	Traffic Impact	N	N				
182	Guardrail	3	3	156	Fatigue Cracking	N	N				
183	Plowstraps	N	N	157	Pack Rust	N	N				
184	Drainage	1	1	158	Deck Cracking	1	1				
185	Slope Protection	2	2	159	Under Deck	4	4				
186	Curb & Walk	N	N	160	Substruct Movmnt	N	N				
187	Roadway Over	N	N								
188	Miscellaneous	N	N								
INSPECTOR		YEAR		REVIEWED BY							
RCP		1993									
RCP		1994									
											185. Vandals have rearranged rip

FIGURE 4 Pontis inspection data collection form.

ability of the palm pad will allow data entry directly into the computer instead of using the hard copy form. Entry of comments is a potential problem with the pen-based computers, and Mn/DOT is considering using standard comments that would provide a customized line by entering quantities and location. For example, a standard comment for abutment deterioration could be "m<sup>2</sup> of spalls with rebar exposed m from edge of abutment." Standard comments for each type of element would be developed.

### ISTEA AND RELATIONSHIP OF Mn/DOT TO LOCAL GOVERNMENTS

Local governments (cities, counties, and townships) are responsible for the inspection, maintenance, and replacement of all bridges under their jurisdiction. Mn/DOT offers technical assistance to local governments and works with the local agencies to prioritize bridge projects.

The Mn/DOT Division of State Aid for Local Transportation provides oversight and guidance for all state or federally funded bridge projects. By state law 62 percent of state gas tax funds are distributed to Mn/DOT, 29 percent of funds are distributed to counties, and 9 percent of funds are distributed to cities. State and federal funds for bridge replacements are distributed on the basis of a project selection process in which the readiness of project paperwork, past projects funded, availability of funds, and how the project meets deficient status are all considered. Special state bonding funds are available for bridges with spans of 10 to 20 ft that are not eligible for federal funding, as are matching federal funds for bridges longer than 20 ft.

The Office of Bridges and Structures provides a review of bridge plans, assistance in bridge safety inspections, and technical assistance upon request during construction for local bridges. The Bridge Management Unit provides central storage of all inspection and inventory data, checks all data for accuracy, enters data for new bridges into the data base for future updating, and distributes summary reports each year to all agencies on the conditions of bridges, updated sufficiency ratings, and eligibility for funding.

### STIP PROCESS

As a result of ISTEA Minnesota has revised the process used to develop a statewide transportation improvement program (STIP) including bridge repair, rehabilitation, or improvement. The new process is organized around eight regional transportation groups called area transportation partnerships (ATPs). ATP membership

includes representatives from districts, counties, cities, townships, regional development commissions, and metropolitan planning organizations. See Figure 5 for the relationship among these various agencies in the planning process.

Guidelines have been developed to identify transportation investment goals and objectives (2). These statewide investment goals are drawn from statewide planning and policy studies as well as from previous historical funding levels and are used as an aid in determining priorities. The goals are defined by Mn/DOT Modal and Resource Management committees, as shown in the left column of Figure 5. The basic principles for making transportation investment priorities are that the emphases must be on preservation and management of existing systems over capital improvements, with safety being a key criterion involved in all investment priorities. Specific priority goals for the 1995 to 1997 STIP are as follows:

- Priority 1: preservation—maintenance of existing systems at a level that will provide for the safe movement of people and freight. This includes activities such as bridge repair that retain or restore the existing condition without necessarily adding capacity. The goal is 30 to 40 percent of investment.
- Priority 2: management and operations—safely and efficiently manage and operate existing systems, effectively addressing critical safety and operations problems including bridge railings through minor and moderate cost improvements. The goal is 5 to 15 percent of investment.
- Priority 3: replacement—enhance economic development by replacing eligible system pieces or elements and reducing barriers such as weight restrictions, bottlenecks, and system disruptions. Replacement includes traditional categories of bridge replacement and reconstruction. The goal is 25 to 35 percent of investment.
- Priority 4: expansion—attain a competitive advantage for the state by reducing travel times and maintaining mobility. Expansion includes major construction. The goal is 15 to 25 percent of investment.

Target values for regional funding are provided as an estimate of the funding available for the Regional Transportation Improvement Program (RTIP). Targets are a flexible short-range planning estimate that offers some assistance for establishing a level of investment for solutions to transportation needs and problems within the region. Targets are used as beginning points, not the final answers, in establishing a priority list of projects for the development of the RTIP and the STIP. The flexible target funding in Minnesota is based on an economic formula that includes the region's contribution to the highway trust fund and regional income. Each

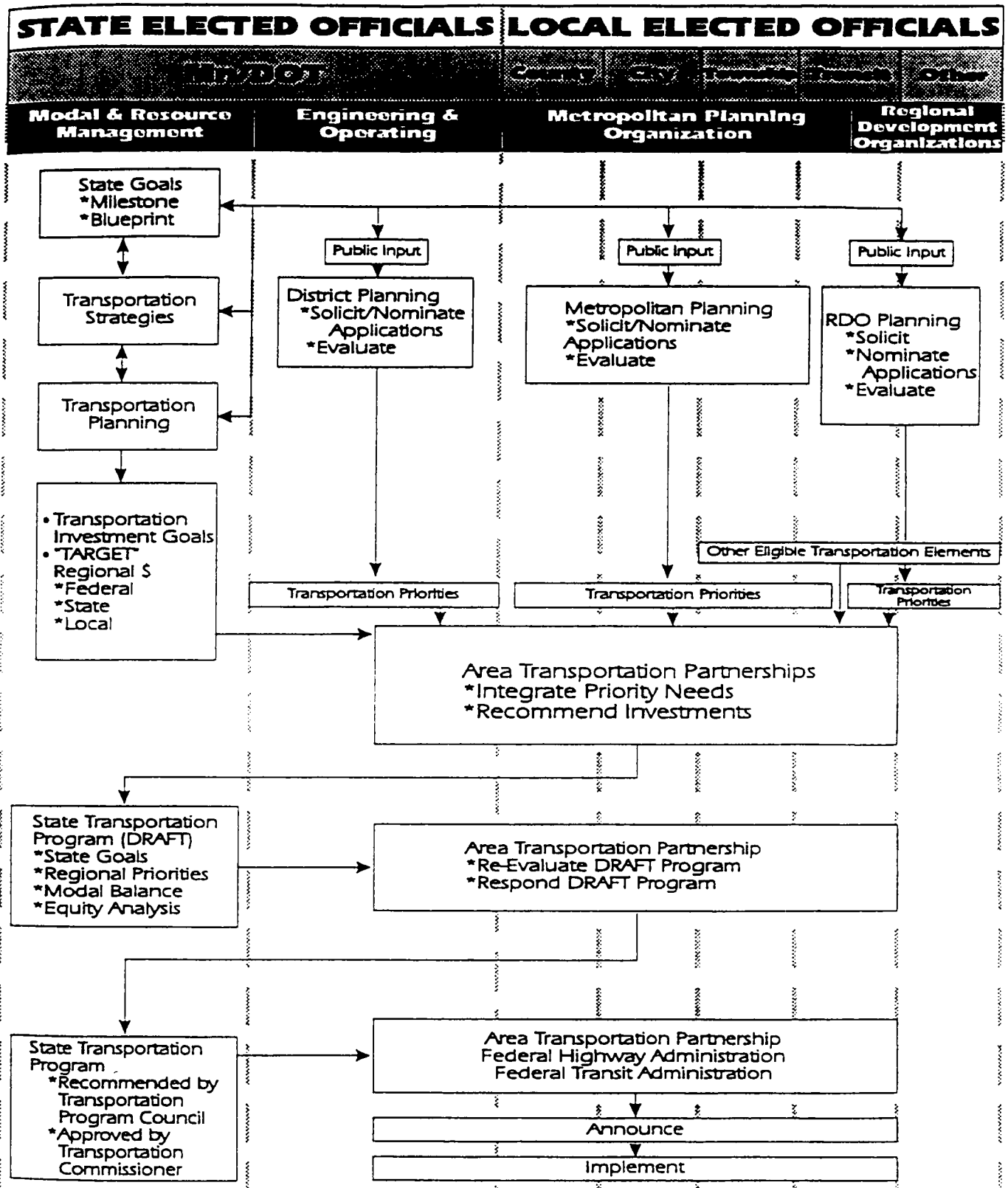


FIGURE 5 Minnesota project selection process.

region must have a target that is no less than 90 percent of the share of its contributions to the trust fund. In the future it is anticipated that the results of Minnesota's BMS and other management systems will affect the target values for the different regions.

Projects are selected on the basis of priority ranking within each RTIP and are combined into the STIP. Each agency in the ATP provides a listing of bridge projects that should be included in the federally funded portion of the STIP. ATP prioritizes the lists along with other transportation projects such as roadway improvements, transit, and safety improvements. At present bridge priority rankings are based largely on the sufficiency rating, and there is no good way to compare the benefits of bridge work to those of other types of highway work. In the future Minnesota expects to use information from the various management systems to allocate funding to the greatest area of need. To help in this process it is important for a BMS to provide accurate and realistic results for bridge improvement and maintenance, repair, and rehabilitation (MR&R) activities.

As the BMS is implemented better results and additional information including well-defined level-of-service goals will become available for determining appropriate regional funding levels and for making informed bridge decisions including needs for MR&R programs as well as the replacement programs used to a large extent today.

## PONTIS BMS

Minnesota has decided to use Pontis as a bridge management tool. Development of Pontis began in 1989 by FHWA and a six-state technical advisory group (3,4). Pontis is a computer software program that uses mathematical models to optimize bridge funding for MR&R as well as for improvements. Both the agency costs and user costs are identified, with the agency costs being limited to the actual costs required to preserve or replace a portion of a bridge. User costs are those costs incurred by the bridge user for detours or accidents due to poor geometrics or clearances on the bridge. The agency costs of various MR&R actions have been estimated by Mn/DOT bridge maintenance personnel and will continue to be updated on an ongoing basis as more accurate costs become known. The deterioration rates of various bridge elements are critical to calculating accurate benefit-cost ratios. These rates were first estimated by Mn/DOT bridge inspectors and will be updated as actual data become available.

## User Costs

User costs are defined as the cost borne by bridge users traveling on or beneath the structure or increased costs

to those who cannot use the bridge because of detours, load posting, or clearance limitations. The costs include travel time, motor vehicle operating costs, and accident costs. These costs will be calculated and updated as needed by Pontis rather than by local agencies. Since user costs can significantly affect the outcomes reported by Pontis, it is important to ensure that these figures accurately reflect the cost to the bridge users.

## Element-Level Inspections

Pontis requires a means of recording bridge inspection information different from that used previously in Minnesota. Bridges have always been categorized into various components, and each one has been rated according to condition severity. Under the Pontis system, bridge elements are defined and ratings will include both severity and extent of deterioration. A condition rating scale between 1 and 5 is used, where a 1 is the best rating for an element and a 3, 4, or 5 is the worst rating, depending on the element (5,6). A sample Pontis inspection form used in Minnesota is shown in Figure 4. This rating system will enable the user to determine the amount of the element that is in either good or poor condition. Since reporting to FHWA of the conditions of the deck, superstructure, and substructure in a standard format is required by all states, a conversion program has been developed by the University of Colorado to translate element-level data to NBI condition data (7). Results obtained from 4,600 conversions indicate that the translated NBI conditions are slightly lower on average than the actual NBI values obtained in the field. Results vary, as shown in Table 1.

The training program for Minnesota bridge inspectors includes an explanation of element-level inspection, an overview of Pontis, a review of terminology, a review of the condition code language for all elements, and a field rating exercise. Since most bridge inspectors have already taken extensive training in bridge inspection techniques, a 1-day class has proven to be sufficient to provide the basics of element-level inspection and data recording. Experienced bridge inspectors are usually comfortable using the new inspection system within 2 to 4 weeks. Many feel that the inspection coding is easier because they are able to break the bridge into elements. Very little additional time is required for element-level coding compared with the time required for NBI coding, and any additional time is mainly due to the initial learning curve of using a new system. Based on the inspection of 4,600 bridges, the increased inspection and recording time the first year ranged from 5 to 20 percent, and that is expected to decrease after inspectors become more familiar with the coding.

TABLE 1 Actual and Translated NBI Condition Values

	-2 point diff.	-1 point diff.	No change	+1 point diff.	+2 point diff.	Errors
Deck	38%	36%	12%	4%	3%	7%
Superstructure	26%	17%	31%	13%	6%	7%
Substructure	16%	41%	29%	5%	2%	7%
Culverts	2%	10%	41%	34%	12%	1%

### Element-Level Reporting

Element-level reporting requires that the inspector record data about each element found on a bridge and the quantity of the element. Because of the computerized inventory data base that Mn/DOT has kept over the past 20 years, a great deal of information about the type of material and the type of elements found on each bridge is available. For example, Minnesota's inventory data base includes information about the type of pier material, the type of pier construction, the type of expansion joints, and the type of deck protection system used. These data enable Mn/DOT to develop formulas to accurately estimate the type of elements on each bridge without checking bridge plans. Quantities are estimated on the basis of typical bridge characteristics such as average beam spacing and on the basis of known dimensions such as deck width and bridge length. Experience to date has shown that approximately 80 to 90 percent of the estimated elements are accurate when these formulas are used, and the estimated quantities are accurate approximately 65 to 75 percent of the time. The estimated elements and quantities are checked by the bridge inspector in the field during the initial element-level inspection. Mn/DOT feels that a great deal of time is saved by using estimated elements as opposed to the alternative of either fully researching plans in the office or entering all elemental data in the field during the initial inspection. On complex bridges, however, the estimated elements and quantities are not accurate, and Mn/DOT finds it beneficial to review plans to determine the elements on bridges longer than 125 m.

### Bridge Management Output

The BMS provides several types of outputs that can be used for three main purposes: (a) to provide information to transportation agencies in developing cost-

effective programs for bridge maintenance, improvements, and replacements; (b) to provide defensible support for target funding requests; and (c) to identify and describe bridge maintenance activities. The outputs needed for transportation agencies include historical conditions and funding levels; anticipated deterioration rates of bridges; the costs of various maintenance, improvement, and replacement activities; present conditions of the system and individual bridges; the overall cost of specific projects; a ranking of proposed projects; a listing of maintenance needs; and the overall budget required to maintain bridges at a selected level of service. Planners will need outputs that show proposed funding levels at the present time and how that level of funding affects future funding needs of the system. Charts and graphs that show proposed funding, optimal funding, and resulting bridge needs are valuable tools for accurately depicting BMS results.

### Bridge Maintenance

Mn/DOT has always spent a reasonable amount of resources on bridge maintenance activities in an effort to preserve this vast infrastructure investment. At present Mn/DOT has 20 bridge maintenance crews stationed in the districts. They perform preventive maintenance, minor bridge rehabilitation, and emergency repair work. In addition to Mn/DOT bridge maintenance crews, contract maintenance is used for larger maintenance projects. A typical priority for maintenance work by Mn/DOT crews or by contract is shown in Figure 1.

Pontis BMS outputs will be used to help plan bridge maintenance activities in the future. The benefit-cost ratio of maintenance activities such as spot painting, deck overlays, and concrete patching will be provided, and suggestions for optimal MR&R activities will also be provided. The comparable value of MR&R activities versus bridge replacement will be shown. The element-level inspections used enable detailed information on



the extent of problems such as deck cracking and deteriorated paint, steel, and concrete conditions to be recorded and summarized. These data can then be used to develop detailed maintenance programs for deck crack sealing, spot painting, and concrete patching.

### Implementation Schedule

Pontis is a new system that requires training of bridge inspection personnel and project programmers. The first Mn/DOT bridge inspectors were trained in element-level inspection techniques during the summer of 1993. Inspections on 1,600 bridges in 1993 produced some minor changes to BIP and training techniques. In 1994 the remainder of Mn/DOT's bridge inspectors were trained. The training consisted of a 1-day class, including general Pontis overview, definition of elements, discussion of condition state language, and a field inspection of one bridge. Approximately 100 Mn/DOT bridge inspectors are now trained in element-level inspection techniques. During 1995 a total of 200 local bridge inspectors have been trained in element-level inspections, and all bridge data in the state will be coded by using element-level criteria by the end of 1996.

### Minnesota Bridge Management Case Study

Minnesota has been involved with the development of BMSs since the inception of FHWA Demonstration Project 71, BMSs, in 1988. Since then Mn/DOT has systematically moved forward until today, when all inspections are being done by using element-level criteria, and the data are being used to help with bridge management decisions. Important milestones along the way are listed below:

- Late 1960s, developed bridge inventory data base and began bridge inspection program.
- Mid to late 1980s, developed PC data collection tools, MBIPS, and BIP.
- 1988 to present, involved with development and guidance of the Pontis BMS.
- 1992, determined initial element deterioration rates and feasible action costs with expert elicitation.
- 1992, involved with testing and implementation of Pontis versions 1.0 and 2.0.
- 1993, developed formulas to approximate elements and estimate quantities for use in Pontis. These estimated elements were used by inspectors in the field during the initial Pontis inspection.
- 1993, began element-level inspections with three pilot districts and inspected 1,600 bridges.

- 1994, began element-level inspection of all Mn/DOT-owned bridges and decided not to collect NBI deck, superstructure, substructure, and culvert data.

- March 1995, BMS results were provided to Mn/DOT districts to assist in developing maintenance and improvement programs and replacement programs.

- 1995, finished training all local bridge inspectors and collected element-level data on all 19,670 bridges in Minnesota.

Critical decisions made during Pontis implementation were (a) to use formulas to estimate elements and quantities in the initial inspection; (b) to first implement the program in three districts, then in the remaining districts, and lastly in local agencies; and (c) to develop a data collection tool that used previous data, especially comments, that were collected during NBI inspections. All of these decisions have proven to be cost-effective and have provided a clean transition from NBI to Pontis inspections.

### HOW WILL MINNESOTA MANAGE BRIDGES IN 2000?

The entire scope of managing transportation resources is changing as a result of ISTEA and other management directives. As we move toward the 21st century there will be a greater emphasis on the results of the management systems used as tools for identifying programs and prioritizing projects. Additional information such as relative health indexes will be determined to assist in overall bridge rankings. Bridges will continue to compete for limited funding, and transportation agencies need to have information that will encourage adequate funding to minimize the impact of pending future bridge needs that are 5 to 10 times the size of today's needs. The construction of a large number of complex bridges in the 1950s, 1960s, and 1970s creates a need for careful management of resources to provide a safe and usable transportation system as this infrastructure system ages.

A comprehensive BMS will provide defensible background information for funding prioritization in the transportation planning process. The funding requests of transportation departments will continue to be balanced against many other needs, and a BMS that shows future needs if funding is delayed may be the tool that can be used to establish the level of funding needed to preserve the infrastructure. A comprehensive BMS will also provide data to show transportation agencies the most cost-beneficial maintenance activities to be performed and to ensure that available funding is used to the optimal benefit.

As the other management systems required in ISTEA are developed there will be a need to integrate the results of all systems into an overall planning tool. Much of the coordination of results will be done through a geographic information system (GIS), which will provide a means of linking data at a common location. Since BMSs are at the forefront of management system development, it is important that a BMS include GIS capabilities. A good GIS tool will allow easier integration of data from all management systems so that the needs of the various transportation system components can be determined and if a variety of needs exist in a certain location. A great deal of work needs to be done to combine bridge, roadway, and safety data into an overall management system that can address a variety of funding issues and needs. For integration to succeed an agency needs to have well-defined level-of-service goals. In a BMS a typical level-of-service goal may include no posted bridges on interstates, no posted bridges on market artery routes, and fewer than 5 percent posted bridges on all collector routes. When combined with level-of-service goals for other transportation sectors, the management systems will be able to identify the level of expenditure necessary to preserve or improve the transportation infrastructure.

## SUMMARY

Minnesota has developed several computer-based programs such as MBIPS and BIP and is implementing BMS tools such as Pontis that provide convenient ways of analyzing bridge data, developing reports on bridge data, and providing information on the most cost-

effective solutions for improving bridge conditions. These data will be used in the planning process to prioritize bridge maintenance activities as well as bridge replacement and rehabilitation projects and provide support for funding requests. Future system improvement efforts will be in the areas of user cost determination, improved data collection, incorporation of GIS capabilities, and overall integration with other management systems.

## REFERENCES

1. *FHWA Recording and Coding Guide for the Structure Inventory and Appraisal of the Nation's Bridges*. FHWA, U.S. Department of Transportation, Dec. 1988.
2. *ISTEA Implementation Guidance for Development of Minnesota's 1996-1998 State Transportation Improvement Program (STIP)*. Minnesota Department of Transportation, Dec. 14, 1994.
3. *Pontis Version 2.0 Technical Manual*. Office of Technology Applications, FHWA, U.S. Department of Transportation, Dec. 1993.
4. *Pontis Version 2.0 Users Manual*. Office of Technology Applications, FHWA, U.S. Department of Transportation, Dec. 1993.
5. *Pontis CoRe Element Report*. Pontis Technical Working Group, FHWA, U.S. Department of Transportation, June 1993.
6. *Commonly Recognized Elements* (preliminary draft). Office of Engineering and Office of Technology Applications, FHWA, U.S. Department of Transportation, April 1994.
7. *BMS NBI Users Manual* (preliminary draft). Colorado Department of Transportation/University of Colorado/FHWA, Jan. 1994.

# Bridge Management System: Computer-Aided Planning Decision System for Polish Road Administration

---

Andrzej Łęgosz and Adam Wysokowski, *Roads and Bridge Research Institute, Poland*

Aleksandra Hutnik, *General Directorate of Public Roads, Poland*

A computer-aided system for the management of bridge structures in the Polish Road Administration is described. The Polish Bridge Management System (BMS), which is still being developed, is grouped in modules containing optimization procedures that support maintenance and management problems. Some of the procedures are based on the method of taxonomic investigation as being optimal for determining the priority for bridges qualified for rehabilitation that forms the basis for a yearly plan at the regional level.

**T**he bridge management process, generally speaking, consists in the selection of an optimal strategy for allocation of budgetary means for the maintenance of bridges on the basis of information collected about their condition. To manage bridges one needs both specialized administration and a practical instrument facilitating data processing and supporting the decision-making process.

The traditional method of bridge management (reporting), which is still in force, produced a vast set of data without using it effectively. The processing of data via reporting made it impossible to utilize fully the col-

lected data base for decision making. The fact that there was no efficient and nationally uniform system of data processing made it impossible to objectively appraise the condition of bridge management in the particular administrative regions so that both financial and material expenditures on bridge maintenance would be used effectively (1).

Therefore, a computer-aided bridge management system, referred to as the Bridge Management System (BMS), was designed. The BMS will serve as a tool in managing bridges for Polish public roads.

## GENERAL DESCRIPTION

The BMS must be compatible with the road management structure. In Poland there is a central road administration that operates on three levels (2):

- Country: general directorate of public roads (GDDP),
- Regional: regional directorates of public roads (DODP), and
- Basic: road management units (ZD).

The Polish BMS is equipped with numerous procedures to aid in planning decisions at each of the three levels of management. Generally, the system consists of the basic module, Inventory (EGM); the program Bridge Data Books (KPOM); and modules Current Maintenance (BUM), Major Repair (RKOM), and so on, which together serve the selected options of the planning function. In addition, the system is aided by the program Central Inventory of Great Bridges (CEDOM), which is a computer inventory of a selected group of large bridges (Figure 1).

The basic task of the BMS is to systematically generate information about the condition of bridges in management units, regions, and countrywide and to allocate funds for maintenance and repairs to regions, management units, and objects. All data, such as inventory and bridge condition, are registered and verified at the lowest level and transmitted to the higher levels.

The particular modules and programs of the BMS can be grouped because, besides collecting or processing appropriate information, they serve the basic data bases of the system that are utilized in the computer-aided process of making planning decisions.

### Location Data Base: Uniform Inventory Number

An indispensable condition for the function of the system is unequivocal location of bridges on roads and

concurrence with road systems. In its original version, the BMS was inseparably configured with the Roads Description Reference System (NET) in which bridges were identified using the code BPS (a description of the spatial location of a bridge on a road management-specific system of coordinates).

A drawback to this solution, apart from the fact that the BMS could not be installed and implemented without the functioning system NET, was the location of bridges by means of the code BPS. Because implementation of a new reference system based on geographical coordinates had begun, a decision was made to make the entire BMS independent of an arbitrary system of road description in this country.

To achieve this, a general assumption was made that each bridge would be identified by a unique, positive, eight-digit integer called a Uniform Inventory Number (JNI) that would not contain any information about location. The method adopted would allow the whole BMS system to be independent of any administrative-organizational changes, and because of the uniform countrywide method of coding, it would be possible to combine the existing location data base (collected in the module Inventory) with any reference system describing the road net (3,4).

Currently, each bridge in the BMS can be located by means of the JNI, geographical coordinates, and the number and kilometers of the road. In future, each

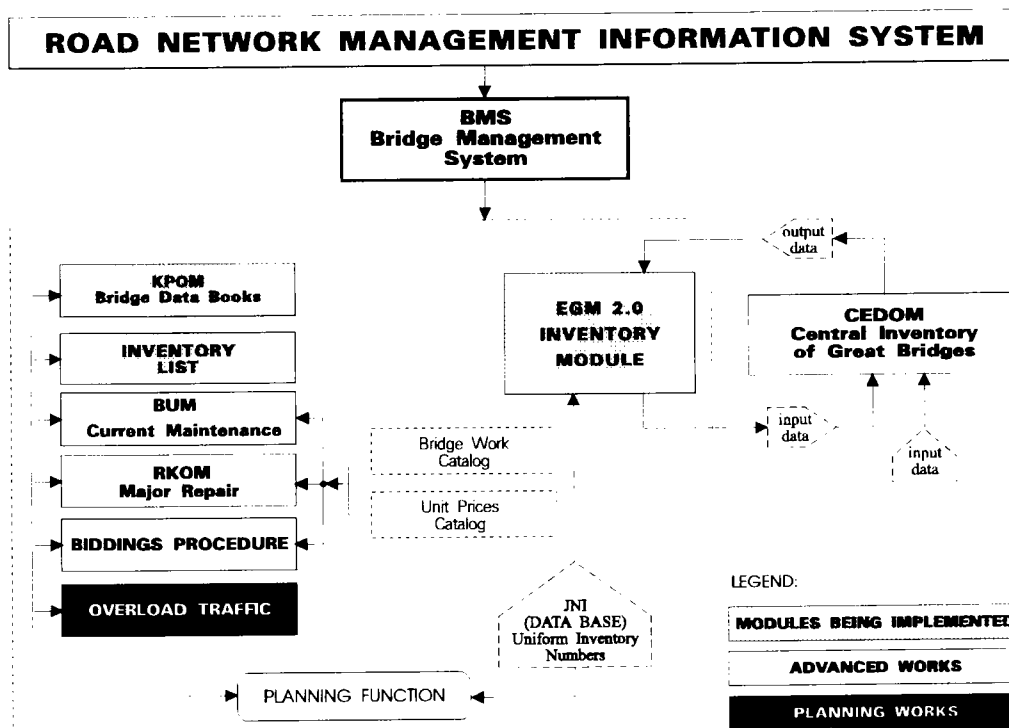


FIGURE 1 Flowchart of Bridge Management System in Poland.

bridge will be assigned through its JNI to a concrete section of a road (the reference section) so that close communication between the BMS and the road reference system will be ensured.

### Inventory Data Base

The BMS software uses the same inventory data base made up of the module EGM and the auxiliary programs KPOM, Inventory List, and CEDOM. Module EGM is the basic component of the BMS and collects location, inventory, technical, and historical data describing individual objects in detail (e.g., bridges, footbridges, floating bridges, missing bridges, ferry crossings, tunnels, underpasses, and culverts). This module in the Polish BMS is a major bridge data base and functions from the basic level (the ZDs) through the regional levels (the DODPs) to the country level (GDDP). The available set of data that describe bridges is formed at the basic level and then transmitted to the higher levels of management (5).

Such data as, for example, the length and width of a bridge, the kind of material, and the technical condition are automatically drawn from the existing inventory data base by program KPOM, which generates all the statistical data used in planning procedures. The program also divides the groups statistical data at each of the management levels (3). The program Inventory List, which on the basis of the necessary data drawn from the inventory data base of module EGM generates exclusively reports mandated by DPA.-16, operates on the same principle (3).

CEDOM's special task is to supplement the inventory data base. This program serves a select group of large bridges on bigger rivers in Poland and allows one to prepare several nonstandard reports about these bridges. It is directly connected to the module Inventory by the JNI. In addition, because of its special structure, CEDOM supplies the Bridge Division of the GDDP, bypassing the regional level, with a full range of country-wide inventory information on large bridges (6).

### Bridge Work Data Base

Another essential data base in the Polish BMS is a bridge work data base, which is a list of work and costs associated with each bridge in a given year. It contains the object's JNI, the date the work is completed, a list of work, and the cost (7).

The basic component of the bridge work data base is the Bridge Work Catalog, which has a special structure and contains a list of all types of bridge work, each coded with three two-digit numbers. The first number

is the type of work, the second refers to the list of this type of work, and the third divides this work into unit sizes and is connected with the Unit Prices Catalog.

All the work done (codes and sizes) and the associated expenditures are registered for each bridge by means of the appropriate JNI, and in the future, the BMS will be able to describe the relationship between the technical condition of a bridge and the expenditures, which is very important for long-term planning.

A source of the data for the bridge work data base is the program Biddings Procedure, which works directly with the program that serves the bridge work data base. Other data, for example, work done with own funds, will be input directly.

### Bridge Ratings Data Base

In the Polish BMS, all information on the technical condition of bridges comes from basic and detailed inspections (8). Therefore one of the first elements needed for the computer-aided planning decision system was a basic inspection data form from which a catalog of typical bridge element damages and principles of bridge technical condition rating could be compiled (9).

The software that is currently used as a base for the ratings is the program Basic Inspection Data Form Editor (KPP), which as one of the procedures of module BUM describes in computer terms the basic inspection. Program KPP operates jointly with the Inventory data base because some parts of this program provide information on the location and structure of bridges. These data are automatically collected by a computer from module EGM and entered into program KPP installed in a bridge inspector's notebook.

During a bridge inspection, the inspector must describe damage to no fewer than 11 elements and rate each of them using a scale from 0 to 5. Codes of damages are included in this program. A list of element and material damages forms the second part of program KPP.

The overall rating of an object is computed as value  $S$  using the following formula:

$$S = \min \left[ \frac{1}{n} \sum_{i=1}^n S_i, S_7, S_8, \frac{1}{2}(S_{12} + S_{15}) \right] \quad (1)$$

where

$S_7, S_8$  = beam and deck rating,  
 $S_{12}, S_{15}$  = piers and abutments rating, and  
 $S_i$  = all elements rating.

$S_i$  is the lowest from the mean ratings of all the elements, the beams, the deck, and the supports.

The next part of program KPP calculates the price of maintenance or repair of the bridge. The task of a bridge inspector is to determine the amount of damage and the kind of bridge work to be done on each element according to the Bridge Work Catalog and the Unit Prices Catalog. The list of the work is edited on the notebook's monitor. The inspector can automatically choose appropriate work for each element and the computer will calculate the costs of repair or maintenance.

Another part of program KPP is associated with the inspector's decisions about work priority made using the rating scale A, 1, 2, 3 (A stands for the failure condition of an element). A list of bridge work with priority ratings, costs of repair, and a bridge condition average constitutes the basis for short-term planning at the regional level.

All damage to elements is grouped by the program Basic Inspection Data Form Analyzer (AKPP) and forms bridge condition statistics such as the frequency and the kind of material and element damage (3).

### **Program Bidding Procedure: Data Base of Contracting Companies**

The Bidding Procedure program was designed to handle awarding of bids for the construction, maintenance, and repair of bridges at the regional or unit level. The program facilitates the preparation of bids by the regional road administration and monitors the awarding of contracts and their realization.

One of the options of this program allows the recording of unit prices from all regional bids, which constitute the basis for unit prices for bridge work for the next year, including unit prices for the whole country. A record of unit prices makes it possible to predict growth rate, which makes these data very important for long-term planning.

Regional directorates hold several rounds of bidding and have the same number of committees. The whole process is secret and only a particular committee knows the password for a particular bid. Information about the winners of awards is released after public announcement of the bidding results.

In addition, a data base of contracting companies was created in the BMS (in the base of program Bidding Procedures). It gathers information about all the companies that take part in various rounds of bid in which each company can be identified in a simple way by its REGON code (7).

### **Overload Traffic Data Base**

The Overload Traffic data base stores information on overload traffic. The source of data acquisition for this base is the module Overload Traffic linked with module

EGM since the latter contains all the data on bridge technical condition, load capacity, clearance, and so on. The module collects the following data: heavy-vehicle weight, pressure on drive axles, number of axles, and distance.

One procedure selects the shortest route and another one checks the passage over the bridges on this route. The main criterion is a bridge condition rating of more than 3 for the beams, the deck, the piers, and the abutments.

The Overload Traffic module incorporates a registering process that makes it possible to monitor the number of all overload vehicles yearly on every bridge and the detection of objects especially exposed to degradation. These factors are particularly important for long-term planning (7).

### **PLANNING FUNCTIONS IN POLISH BMS**

The planning of maintenance work, both current maintenance and repair, is based mainly on results of basic and detailed inspections; thus, input data for planning are already available to a large degree in the system as presented above.

Generally speaking, planning functions in the computer-aided BMS are to ensure a uniform standard of maintenance and technical condition for bridges in the whole country and rational spending of central budget funds (10). In the Polish BMS, these functions are performed by the Current Maintenance (BUM) and Major Repair (RKOM) modules.

The GDDP divides expenditures among 17 regional directorates on the basis of collected data on the condition and the number of bridges administered by the particular regions. The calculated replacement values for all bridges, their average rating of technical condition for a given region (collected from program KPP), and statistical data on, for example, the overall area of bridges in the particular regions (contained in the KPOM program) provide a basis for the allocation of funds.

Assuming a desired average level of bridge condition in this country, the necessary amount of expenditure can be determined or, vice versa, knowing the expenditures allocated from the central budget, the effects in the form of higher bridge condition ratings can be estimated. Following this method, a clear-cut mechanism for controlling the relationships between expenditures and bridge condition at the central level of management can be obtained (11).

Module BUM at the central level distributes the budget for current maintenance and rehabilitation of bridges among regional directorates and allocates funds for concrete modernization and investment tasks.

The purpose of module BUM at the regional level is to match the range and the scope of work in program KPP with a Bridge Work Catalog and a Unit Prices Catalog to determine the amount of expenditure on current bridge maintenance and to allot work within the rehabilitation range. In this way, the regional level has full information about repair needs.

Module RKOM, in turn, operating at the regional level, compiles a list of rehabilitation needs, calculates the capital costs of repairs, and checks if it may be necessary to modernize a bridge. The list of repair needs for rehabilitation at the regional level is then ranked by the taxonomic method. This classification method together with an efficient system of determining the economic effectiveness of ventures gives the road administration of the regional level an objective apparatus for drawing up a yearly plan of maintenance (12).

A bridge modernization plan is a different process. The factor that decides whether modernization is necessary is the exceedance of functional life (insufficient load capacity, lack of clearance), economic life (repair costs exceeding the value determined relative to the replacement costs), or service life (the bridge receives a critically low rating) or the crossing is temporary, so the bridges that have been accepted for modernization form an input basis for a modernization plan.

For all bridge modernization work an internal return rate (IRR) must be calculated. At the national level, funds for bridges are allocated on the basis of which IRR is the highest.

#### ANALYSIS OF ARGUMENTS FOR REPAIR AND THEIR EVALUATION

Repair is based on urgency of the features that need repair. Making a decision about repair is determined by a series of circumstances and events. Therefore, the decision space around each bridge can be described by a set of arguments that, by their description, reveal the importance of these features. An analysis of the arguments, and not personal preference, serves as the basis for a correctly constructed work specification. A certain range of work—the so-called routine current maintenance work—is carried out on bridges and is not subject to ranking by urgency.

The following groups of arguments and diagnostic features can be distinguished (dominant features are underscored):

<i>Group of Arguments</i>	<i>Diagnostic Features</i>
Economic	Capital costs, users' costs, available funds, comparison with cost of building new object

<i>Group of Arguments</i>	<i>Diagnostic Features</i>
Technical	<u>Rating of object's condition</u> , service character
Durability	<u>Estimated percentage of wear and evaluation of degree of bridge's wear</u>
Transportation	<u>Road class</u> , traffic volume, traffic level, defense considerations, fire access road, bridge on border crossing road, international agreements imposed on road's function
Work urgency	Breakdown mode, work under way
Hindrances	Technical, technological

The above groups, taking into account the dominant features, constitute the basis for a description of bridges; by assigning numerical values to the ratings of the arguments, they become arguments of a mathematical method that orders a list of bridges according to the urgency of repair work.

For the evaluation of bridges, the above groups of arguments have been correlated and a grading scale has been assigned to the dominant features. Numerical values have been adopted in reference to the six-grade scale used in the Polish BMS for evaluating the technical condition of bridges (0 = failure condition, 5 = excellent condition). The method described assumes the following diagnostic features as dominant: rating of object's technical condition, road class, and evaluation of durability (degree of wear); it also analyzes the hindrances and the work urgency (13).

#### Bridge Condition

The grading scale is from 0 to 5, in which a grade is generated from program KPP (see the description of the bridge ratings data base).

#### Class of Road

A six-grade scale is imposed to divide Polish roads according to categories and their corresponding weights:

<i>Description</i>	<i>Rating</i>
Roads with one-digit designations	0
Roads with two-digit designations	1
Roads with three-digit designations	2
Roads with four-digit designations	3
Roads with five-digit designations	4
Other roads	5



The grade is lowered by 1 (except for one-digit roads) if the following additional circumstances are imposed on a traffic artery: very large traffic volume, defense considerations, fire access, special importance of the object (e.g., border bridge), international agreements.

### Evaluation of Durability

The six-grade scale imposed to determine degree of wear of a bridge is as follows:

<i>Description</i>	<i>Rating</i>
New object	5
Object in initial service life period	4
Object in normal service life period	3
Object close to exploitation	2
In the end stage of exploitation	1
Exploited	0

### Hindrances

A set of hindrances has been introduced especially for those objects that have features besides the dominant ones (technical condition, transportation importance) that make it difficult or even impossible to bring a contractor in (special circumstances associated with the bridge, its location, or work technology). These features call for special treatment of the task that gives the necessary time for the preparation of the environment or a special work regimen.

A four-grade ranking of hindrances on a scale of 2 to 5 has been adopted. The respective intervals are as follows:

<i>Description</i>	<i>Rating</i>
No hindrances	2
Extraneous equipment present, traffic restrictions, historical bridge or area	3
Environmental aspects (effect on environment)	4
Necessary bypass or temporary crossing	5

### Work Urgency

Work urgency, in the sense of an absolute priority for carrying out work on a bridge, is considered only in the case of a collapse or the continuation of work (value 0). In other cases, its value is neutral and equal to 1.

The effect of ratings of the particular diagnostic features on the acceleration or delay of repairs can be interpreted as follows—the higher the grade, the more the delay:

<i>Description</i>	<i>Rating</i>
Technical condition	0–5 (delaying)
Road's technical class	0–5 (delaying)
Durability	0–5 (accelerating)
Work urgency	0–1 (delaying)
Hindrances	2–5 (delaying)

### TAXONOMIC INVESTIGATION METHOD

Taxonomy is a domain of statistical multivariate analysis that deals with theoretical principles and rules of classification, subordination, grouping, and so on, of multifeature objects. The subject of the classification is a set of objects, bridge objects in this case, described by diagnostic features, or arguments.

The division of diagnostic features into stimulants, destimulants, and nominates is characteristic for each multifeature object studied (14). A *stimulant* is a variable whose high value is advantageous for a studied object, for example, the rating of the technical condition of a bridge. A *destimulant* is a variable whose high value is disadvantageous for a studied object, for example, a hindrance. A *nominate* is a variable whose value is neutral for a studied object, for example, work urgency in cases other than collapse or continuation of work.

It is possible to consider different variants of diagnostic features depending on the aim and the nature of the investigated problem. The algorithm used is fully universal and open-ended. The method used here will consist of inputting a list of bridges described by vectors of numerical data representing diagnostic features, or arguments for doing repairs on these objects. The output will be a list of bridges ordered according to the urgency of repair.

After the primary goals of the study were determined, a set of bridges was created and arguments for repairs to be carried out on each of the studied objects were specified. It should be emphasized that a proper selection of these features allows one to determine the essential characteristics of the investigated phenomenon and to eliminate quantities that carry too incidental or too detailed information.

The next step was the formation of a matrix of information about the studied bridges, that is, a set of features ascribed to these objects, which was then reduced by statistical procedures (coefficient of linear correlation) to a set of diagnostic features. Next the diagnostic features were subjected to standardization; that is, they were made comparable and freed from designation. The standardized features have two properties: their average value is equal to zero and the standard deviation equals 1.

The next stage is the construction of a taxonomic measure of development. It is based on the concept of the so-called *standard of development*, which is an ideal object with standardized coordinates. When this measure is constructed, it is assumed that all diagnostic features are treated as equally important.

A taxonomic measure of development is the extent of the deviation of the considered bridge from the established standard of development. The above measure is interpreted as follows: the smaller the value that it assumes, the better the condition of the considered bridge, that is, the further it is down on the list of repairs to be made.

To fulfill the postulate that a higher value of this measure indicates a better condition of the bridge, the so-called *relative taxonomic measure of development* was constructed. This measure reveals that the less a value differs from 1, the less different is the level of the studied bridge from the standard object, that is, the further it is down the list of repairs to be carried out.

In this case, the stimulants are the rating of the object's technical condition, the category of road, and evaluation of the bridge's degree of wear. Hindrances are destimulants, whereas work urgency, not in the sense of collapse or work continuation, constitutes a nominate.

The algorithm constructed using the method of taxonomic investigation generates a list of bridges ordered according to the urgency of repair work, whereas the amount of funding allocated to a given DODP shows what the possibilities are of doing repairs in this region, which results in a basic plan of maintenance.

#### ALGORITHM OF MODULES BUM AND RKOM AT REGIONAL LEVEL: CONSTRUCTION OF MAINTENANCE PLAN (13)

Bridge maintenance in Poland has only a few sources of funding. Bridges on national highways are financed from the central budget, which is distributed on the national level by the GDDP. This process is supported by module BUM, which on this level divides optimally the financial means for 17 DODPs.

Optimization of funds distribution at the central level is based on the method of linear programming. The important factors in this algorithm are the following: bridges' area, average bridge condition, replacement value, year of bridge construction, kind of material. Every year, the program Bridge Data Books (KPOM) groups all factors separately for every DODP. The task of the DODP is to prepare a proposed maintenance plan for each bridge with a list of all work on all bridges, which is generated by the program Basic

Inspection Data Form Editor (KPP). This list is subject to approval by the GDDP after budget allocation.

The yearly construction of a maintenance work plan by each DODP is facilitated by the optimization procedures contained in modules BUM and RKOM. The algorithm for the operation of these modules at the regional level is presented in Figure 2.

The task of module BUM at this level is, by linking the anticipated range and scope of work (determined during basic and detailed inspections) with a catalog of work and a catalog of prices, to determine the amount of expenditure on current maintenance (routine work) for bridges and to qualify work as repair rehabilitation.

Module RKOM at the regional level compiles a list of bridges needing repairs, orders it according to urgency, and checks if there is a necessity for modernization. Using the catalogs, it calculates the capital costs for repairs and submitted modernizations.

These operating ranges of the two modules require correlation with the Bridge Work Catalog and the Unit Prices Catalog. This is possible through proper notation-coding of the range and scope of work in program KPP conforming to the specifications of the catalogs.

#### List of Needed Repairs

Data from inspections contain a list of work to be done on an object in order to restore the service parameters. Therefore, one can say that the material and financial needs in the area of rehabilitation are specified.

The features that describe an object and are essential for its identification and its placement on the priority list are stored in SGM. From now on, the object will be understood by the procedure as a set of diagnostic features necessary for classification plus a list of work to be done. Thus, a list of objects and a list of needs based on these features are obtained. Such a list of needs is subjected to selection to divide it into current maintenance, rehabilitation, and recommended modernization.

The work assigned in the work catalog passes to the group of current maintenance work. The total financial range of work for all bridges in this group gives the total amount for current maintenance in a region, which in turn, when deducted from the amount of the DODP's budget, gives the amount of expenditures on rehabilitation.

The bridges suggested for modernization that are under the management of regional administrations form a list of modernization needs that is subject to a decision procedure depending on the powers of road administration organs. Some objects that did not qualify for modernization remain in the maintenance group.

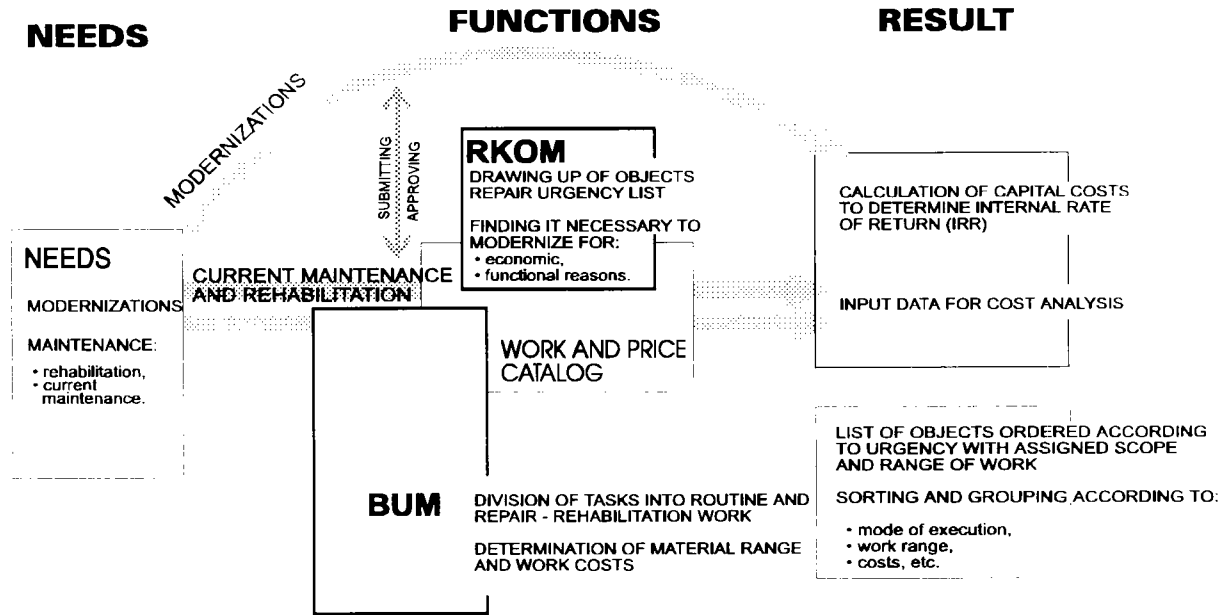


FIGURE 2 Construction of maintenance plan: location of BUM and RKOM procedures.

### List of Priority

The ordering of needs, that is, the drawing up of a list of bridge objects in the order of repair work priority, is done by the taxonomic method. The method's diagnostic features are based on the bridge's technical condition, the class of road, evaluation of the bridge's degree of wear, expected hindrances, and mode of work urgency.

The outcome of this procedure is a list of bridges ordered according to the priority of repair work:

```
Bridge 1_description_identifier_work list_work cost
:           :           :
:           :           :
bridge n_description_identifier_work list_work cost
```

The budget at the disposal of a DODP compared with the generated list presents the possibilities of carrying out rehabilitations in the region and forms a basis for the construction of a yearly plan of maintenance.

### Analysis of List or Maintenance Plan

The indication of bridge priority constitutes valuable information that aids the decision process in the drawing up of yearly plans of maintenance. Since the possession of information that ties the balanced and ordered work with the budget only by regional level administration would be too much of a simplification,

access to the generated list of work has been provided at the level of individual bridges.

The described procedures allows one, to the above extent, to group and order bridges freely according to the range and scope of work and the road's number, as well as making it possible, for example, to select a group of damages that are mostly responsible for the lowering of the technical condition rating of a bridge.

Frequently, the needs exceed the budgetary means. Therefore, the obtained list of bridges ordered according to repair or rehabilitation urgency should be verified and corrected at the Bridges Division of the DODP, where a planner can "manually" control the generated list of work urgency when drawing up a plan of maintenance. In legitimate cases, the position of a bridge on the list may be changed and the scope or the range of the foreseen work widened or narrowed. Each such change will result in automatic generation of a verified list of priority. Finally, the list of bridge work and the appropriate costs must be approved by the General Directorate of Public Roads.

### FINAL REMARKS

The algorithms presented form a basis for handling planning at the regional level. The proposed solutions take into account the prospective directions in which the Bridge Management System in Poland will develop.

The algorithms created include the evaluation of bridge durability and technical condition to the fullest possible extent. Moreover, the optimization procedures

developed use the taxonomic method, the universality of which has been verified in economic practice. In this case, an additional advantage of the application of this method is the possibility of bringing in, depending on the specificity of bridge management in a given region, new evaluation factors that will make possible a more comprehensive analysis of the distribution of funds for bridge maintenance.

Finally, it should be noted that, depending on the object of management (size of fixed assets), the described optimization procedure can be used optionally also at the lower level of management, the road management units (ZDs).

#### REFERENCES

1. Hutnik, A., A. Łęgosz, and A. Wysokowski. Bridge Management System for Polish Road Administration. *Proc., International Bridge Conference*, Warsaw, June 1994, pp. 225–234.
2. Mistewicz, M. *Road Bridges in Poland*. GDDP, Warsaw, 1991.
3. Praca zbiorowa. *Przewodnik po programach EGM, KPOM, Wykaz, KPP i AKPP wraz z instrukcją obsługi użytkownika. Wersja instalacyjna 2.0*. Warsaw, 1994.
4. Cichoń, J., and J. Wierzejewski. Data Basis of the Polish Bridge Management System. *Proc., International Bridge Conference*, Warsaw, June 1994, pp. 195–204.
5. Łęgosz, A., and A. Wysokowski. General Information on Polish Bridge Management System. *Proc., 2nd International Conference on Bridge Management*, University of Surrey, Guildford, April 1993, pp. 870–879.
6. Łęgosz, A., and A. Wysokowski. The Central Record of Great Bridge Objects—CEDOM. *Proc., 4th International Conference on the Safety of Bridge Structures*, Warsaw, Sept. 1992, pp. 307–311.
7. Cichoń, J. *Założenia teoretyczne do rozbudowy Baz Danych SGM*. ProMat, Warsaw, 1994.
8. Mistewicz, M. Bridge Inspection System used by the Polish Road Administration. *Proc., International Bridge Conference*, Warsaw, June 1994, pp. 275–282.
9. Mistewicz, M. *Podstawy teoretyczne funkcji Planowania w SGM oraz założenia dla modernizacji eksploatowanych programów SGM. Zadanie 05-Katalog uszkodzeń i zasady oceny stanu mostów przy przeglądzie podstawowym*. IBDiM, Filia Wrocław, czerwiec 1992.
10. Hutnik, A., M. Ławniczak, E. Misiewicz, and A. Wysokowski. Problems of Long and Short Planning in Polish BMS. *Proc., International Bridge Conference*, Warsaw, June 1994, pp. 235–244.
11. Mistewicz, M. *Optymalizacja podziału budżetu robót mostowych*. Drogownictwo nr 7, 1993, str. 148–154.
12. Hutnik, A., A. Łęgosz, and A. Wysokowski. BMS in Poland: Computer Supported Maintenance. Presented at International Conference, Paris, October 1994.
13. Wysokowski, A., A. Łęgosz, M. Ławniczak, and E. Misiewicz. *System Gospodarki Mostowej. Prace rozwojowe. Koordynacja całości prac przy Systemie - Raport końcowy. Opracowanie algorytmu działania modułów BUM i RKOM na poziomie regionalnym*. IBDiM, Filia Wrocław, maj 1994.
14. Nowak, E. *Metody taksonomiczne w klasyfikacji obiektów społeczno - gospodarczych*. PWE, Warsaw 1990.

# Development of Hungarian Bridge Management System

---

Gyula Kolozsi, *Road Investment Ltd., Hungary*

László Gáspár, Jr., *Institute for Transport Sciences, Ltd., Hungary*

Ernö Tóth, *Road Managing and Coordinating Directorate, Hungary*

Árpád Csorba, *Szolnok Road Directorate, Hungary*

The funds available for bridge maintenance, rehabilitation, and reconstruction are far below the realistic needs in Hungary. That is why the Ministry of Transport, Communication and Water Management has initiated countrywide coordinated efforts to establish the Hungarian bridge management system (BMS). The elements already existing are used, and new relevant research work is in progress. The main elements of the future Hungarian BMS, which are already more or less available, are as follows: computerized bridge data bank, uniform procedure for bridge inspection, countrywide bridge maintenance and construction programs until 2000, methods for the calculation of the gross and net values of bridges, cost-benefit calculation method for bridge rehabilitation and reconstruction, simplified BMS for the ranking of interventions, and a computer program for the selection of appropriate routes for oversized and overweight vehicles. A long-term bridge maintenance strategy has recently been developed.

**B**y the early 1980s several new circumstances that had arisen worldwide required that formerly applied highway operation and maintenance methods be changed. The intensive growth of traffic and, in particular, axle loads increased the demand for roads

and bridges. At the same time, as a consequence of significant network development activities and the corrosion defects during the 1960s, the actual maintenance needs of existing bridges increased sharply. Throughout the world there now are insufficient financial resources for bridge maintenance and operation. The negative effect of postponing or delaying necessary bridge maintenance activities can be observed more often.

The current practice of concentrating financial resources on the construction of new bridges has caused problems in Hungary that are similar to those in west European countries, but on a smaller scale. Even though insufficient funds are available, there is an increased need for funds. This contradiction can be solved only by a well-based prioritization of projects in which their efficiencies are calculated and compared. These kinds of systems require decision arrangement and management activities, and registration and administration elements are worked out gradually in several areas of the Hungarian transport engineering system. After the compilation of the first version of our network-level pavement management system (for highway pavements) the bridge management system (BMS) began to be developed.

Bridge management means that all activities should be concentrated in a uniform system, which is necessary

for the long-term and efficient preservation of the serviceability and longevity of highway bridges. The following activities (intervention types) are included here: bridge operation, bridge protection, bridge inspection, sufficiency rating of bridges, bridge maintenance and rehabilitation, substitution of bridges because of deterioration, and new construction for increasing the serviceability of an insufficient bridge. The main elements of BMS are as follows: bridge condition evaluation, deterioration forecasting, design of improvement in various variants, and optimization. A schematic flow chart of the elements of BMS is provided in Figure 1.

Currently, several countries have already achieved considerable results from the development of their systems, although they are rather different. Because of the different conditions in Hungary, the adaptation of any system in an unchanged form cannot be considered realistic. However, Hungarian experts have carefully studied the major foreign BMSs (1-10).

The Ministry of Transport, Communication and Water Management recently decided that a concentrated effort must be made to develop a working BMS. The accomplishment of this huge task, which requires multiyear, coordinated activities of several Hungarian institutions, should be started by gathering and assessing the results already attained in this field, as well as determining future requirements. The following sections describe the more or less completed elements of the Hungarian BMS.

### BRIDGE DATA REGISTRATION

Since 1965 data for some 5,800 Hungarian highway bridges have been registered and computerized; before that data were registered manually. This computerized registry consisted of the main data for bridges updated annually by using specialized forms. It was a totally centralized system, and costly programs were required for the eventual modification of the data content. The need for modern bridge management mainly justified the development of this system (E. Tóth, unpublished data).

Since 1989 the regional (highway directorate) level rather than the central level of data input and processing have been used. As a part of the Regional Highway Data Bank (TKA) new bridge data were included, for example, the following: sufficiency rating conforming to roadway width and loading capacity, foundation, waterproofing layer joint, bearing, barrier, traffic restriction data, improvement type and time, condition evaluation notes of five aspects (see next section), and data for the connecting road. The system uses International Business Machines-compatible personal computers. The data stored in TKA could be obtained only in the form of fixed tables until 1990. Later a so-called general data inquiry program was developed. Another program was developed. That program made possible the description of data for each bridge on a separate sheet.

The National Highway Data Bank (OKA) is now being developed. It has the following features:

- Wider data stock,
- Faster data processing,
- Up-to-date data inquiry, and
- Drawing programs.

Data storage on the basis of spatial information will be used when it becomes possible.

### BRIDGE INSPECTION

Exact knowledge of the present condition of bridges constitutes a decisive element of bridge management.

Classification of the loading capacities and widths of bridges is of major importance, although the necessary improvements to a bridge can be identified only on the basis of significant knowledge of the present condition of a bridge.

In the 1980s the Institute for Transport Sciences (KTI) in Budapest developed and tested a 12-point evaluation method in which the bridge was classified by using a single condition note (11). The most important

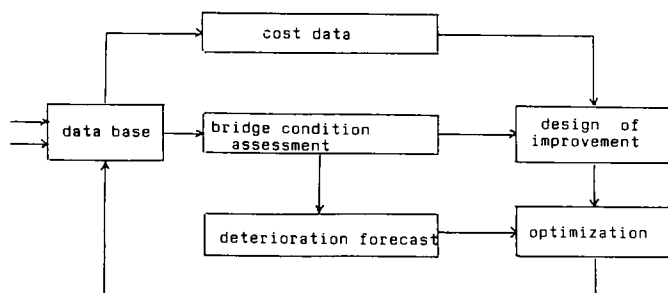


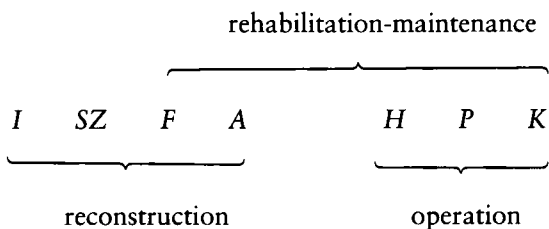
FIGURE 1 Flowchart of Hungarian BMS.

feature of the method was its weighing by geometrical means.

This procedure was developed further, taking into consideration the experiences gained (11–13) by the Ministry of Transport, Communication and Water Management.

The major element of the modification was the use of five main aspects (superstructure, foundation, bridge accessories, deck, and environment) for the final evaluation instead of the former single one. The five main aspects can be determined by using 19 subelements of the bridge elements. Therefore, it can directly reveal the element(s) that needs to be repaired. Another new feature is the application of ratings 1 to 5, as in the case of roads, instead of ratings 0 to 5, which were used previously. According to the final guideline published in 1989 the meanings of the extremes of the ratings are as follows: 1 is perfect condition and 5 indicates severe deficiencies.

The reconstruction needs, as well as maintenance-rehabilitation needs, can be determined on the basis of the load-carrying capacity ( $T$ ) and the roadway width ( $SZ$ ) as well as the five main indicators of the sufficiency rating (superstructure,  $F$ ; foundation,  $A$ ; bridge accessories,  $H$ ; deck,  $P$ ; environment,  $K$ ):



Recently, guidelines have been completed for acquiring the condition and defect size, the *Yearly Bridge Inspection Report* (14). The main objectives of yearly bridge inspections are to update the data for the bridge, which may have changed, and assessment of the urgency for eventual improvement.

### MEDIUM-TERM BRIDGE PROGRAM

On behalf of the Ministry of Transport, Communication and Water Management, the Bridge Department at the Széchenyi István Technical College, Győr, together with the bridge engineers of the highway directorates, completed the report *Bridge Program until 2000* (15). Assessment and a summary of the necessary bridge improvements and priority ranking of bridge projects as the contribution to the creation of a domestic BMS constituted the main goals of the program.

According to the program, a given number of bridges chosen from the viewpoint of their condition, size, or

traffic volume must be assessed through a detailed condition survey consisting of a 19-point condition evaluation and cost needs estimation. The following data are recorded on the bridge inspection report: former and present bridge condition determined visually, measured condition data, and photographs of typical defects. The program is based on the existing bridge data bank. The priority ranking is an open, flexible, multiparameter, and interactive process. The maintenance and development needs of highway bridges can be calculated. In the case of a given project, the cost needs of optimal improvements as well as the extra costs of delayed intervention can also be estimated.

This condition evaluation was carried out on the 1,272 bridges with deck surface areas of more than 70 m<sup>2</sup> [this is 60 percent of the total surface areas of Hungarian bridges; bridge improvements requiring more than 2 million Hungarian forints (HUF; US\$1 = about 120 HUF) were treated separately]. During the survey the actual condition of each structural element was assessed by using notes reflecting the severity of deficiencies, as well as the type, time, and extent of the optimum improvements for bridges with ratings of three to five in an 8-year time period.

It was found that repairs on 45 percent of the bridges on main roads and 60 percent of the bridges on secondary roads were urgent.

The average maintenance and reconstruction costs were taken into account on the basis of 1991 price levels, a forecasted inflation rate was considered, and the quantity of hidden (covered) defects was evaluated to be 10 percent of the visible defects. Five percent of the costs was used for the preparatory work for improvements. Approximate deterioration curves were applied. Table 1 presents the improvement needs for 8 years on the basis of 1991 prices.

A priority ranking of bridge improvements was made, taking into consideration the actual condition, the traffic volume, and the cost needs.

The maintenance priority ranking for 1992 was carried out, using the expert opinions of the regional bridge engineers, by averaging five variants.

### BRIDGE VALUE CALCULATION

For the economic foundation of bridge management, knowledge of the actual net/gross (percent) value ratio is needed.

By 1981 calculation of the gross and net values of the Hungarian highway network had been completed. Approximate mean values for bridges were applied, and linear depreciation rates were considered. During later repeated value estimations, in 1986 and 1990, practically the same technique was used for bridges. Figure 2

TABLE 1 Bridge Funds Needed for Next 8 Years

	Funds (million HUF)	Unit needs (HUF/m <sup>2</sup> /year)	Percentage of gross value
Maintenance funds needed	9882,21	1400	1,00
Development funds needed	7569,42	950	1,33

presents the values that were obtained. Since, among others, the maintenance-rehabilitation funds needed depend on the actual gross value and the net/gross (percent) value ratios, further development of the bridge value calculation procedure became necessary to obtain a more realistic result.

The main steps of this research work (11) are as follows:

- Collection of past available bridge cost data,
- Calculation of mean unit costs for each bridge type and every year,
- Control of these unit costs by using the official indexes of price changes available for main construction materials and activity groups,
- Calculation of a more reliable gross value for all bridges by using the data bank and the unit costs obtained,
- Establishment of typical deterioration curves to determine the net values by using both domestic experience and foreign data,
- Determination of the net value and the net/gross (percent) value ratio of our highway bridge stock by the new procedure, and
- Calculation of the maintenance-rehabilitation needs for various policies as a function of gross value and net/gross (percent) value ratio.

An important task of a realistic value calculation is determination of the necessary yearly maintenance needs. Research work by KTI on this topic (16) has revealed that the general condition preservation of bridges would need some 2.1 times more funds than the average of the funds available in recent years.

### COST-BENEFIT ANALYSIS OF BRIDGE IMPROVEMENT

On the initiation of the World Bank, connected with the loan Transport II given to Hungary, KTI has completed an economic efficiency calculation scheme and its software for bridge improvements.

The cost-benefit analysis (efficiency calculation) covers various types of bridge rehabilitation and reconstruction. The calculation is carried out by using the incurred costs and the resulting economic benefits. The costs and benefits during the investigation period (30 years here) are discounted to the first year (17).

The main input groups of the program are as follows:

- Bridge location and geometric, statistical, value, and operational characteristics;
- Traffic parameters and traffic evolution factors for various vehicle types;
- Characteristics of detour routes;
- Features of bridge improvement;
- Forecasted bridge deterioration data; and
- Forecasted net value of bridge.

The following bridge improvement types can be investigated:

- Load-bearing capacity increase,
- Widening,

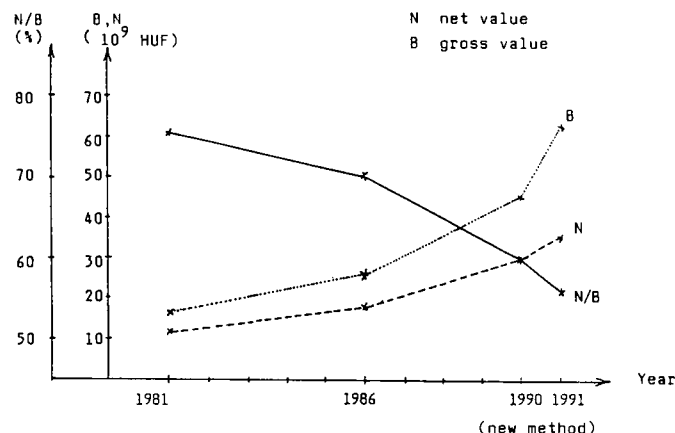


FIGURE 2 Asset values of Hungarian bridge stock between 1981 and 1991.



- Substance preservation (e.g., replacement of bridge pavement with eventual repair of waterproofing layer),
- Total in situ reconstruction,
- Replacement of a pontoon bridge or a ferry by permanent bridges, and
- Reconstruction together with correction of the connecting road.

The following economic benefit types are considered:

- Lower vehicle operating costs because of better bridge geometry,
- Fewer time costs because of the elimination of the detour route,
- Lower time costs because of the end of narrowing of the bridge pavement to a single lane of traffic,
- Lower accident costs because of improvements to the geometric features of the bridge,
- Higher net value as a consequence of pavement condition improvement,
- Lower vehicle operating costs because of better pavement condition,
- Lower time costs because of better pavement condition,
- Lower vehicle operating costs because of the more favorable geometric features of the road leading to the bridge, and
- Lower vehicle operating costs because of the elimination of the detour of a motorway's total traffic volume to one of the carriageways.

The outputs of the variants investigated are as follows: internal rate of return, first year's return.

### FIRST PHASE OF SIMPLIFIED HUNGARIAN BMS

The first phase of the simplified Hungarian BMS (HGR) was established by 1991 (18).

The algorithms of four improvement subsystems (maintenance, reconstruction, rehabilitation, and operation) as well as the program for the operational subsystem have been completed. The latter collects estimates in quantity and sums the operational improvement types for each bridge in pieces, in length (in meters), deck surface area (in square meters) and value (in thousands of HUF).

Algorithms for priority ranking and estimation of economic efficiency are also available.

In a given priority class, the ranking of necessary improvements is carried out as a function of their efficiency levels by a yearly schedule.

The urgency priority is as follows:

- Improvement types that cannot be delayed,
- Improvement types that can be delayed for the short term and that can be financed, and

- Improvement types that can definitely be delayed and that can be financed.

The software is also applicable for managing a rather deteriorated bridge stock.

The data base and the improvement module of HGR were developed further in 1992 so that the following features have been attained: the necessary data for the double—former and present—reference system; more technical bridge data; 22 condition elements instead of the former 19; 60 typical improvement types instead of the earlier 22; and an extended cost module that considers the new requirements of the Road Fund.

Optimum criteria were suggested for the management of a bridge stock in a crisis situation (19). The main questions to be answered by the bridge operator are as follows:

- What technically necessary improvements are needed?
- Which improvements can be considered urgent?
- Which improvements can increase most significantly the service offered by the bridges?
- What is the yearly improvement schedule permitted by the available funds?
- Is the quantity of bridge improvement projects increased or decreased by a given funds/cost ratio?

Software and a data base have been developed for network-level bridge management purposes. The data base covers the bridge stock of a county highway department. Its further development is planned in order to deal with the national bridge stock.

The present system can analyze the bridge stock or any part of it by using a 26-parameter screening. It also possesses a statistical data processing module and a module that calculates the funds needed.

The software can process about 100 data items for the bridge from the data bank, as well as 300 other data items on bridge management (such as condition, sufficiency rating, intervention quantity, price, cost, funds, and form of financing).

The maintenance module of the system is capable of processing some 400 data items for the whole bridge stock of a highway department. It stores the time series of condition and sufficiency data.

Seventy-three different intervention types (9 operational, 50 maintenance, and 14 rehabilitation options) can be calculated by the system. Their parameters refer to bridge sections (expressed in pieces, meters, square meters, or thousands of HUF).

The statistical and management modules are able to solve 30 different engineering-management tasks.

The statistical screening module produces lists and tables, enabling the aggregation of bridge sections with different condition scores.

The intervention module can perform several network-level management tasks, such as the following:

- Calculation of intervention needs,
- Determination of the realistic threshold values of intervention strategies and tactics,
- Calculation of cost needs and funds split ratios,
- Network-level economic analysis for finding the optimum action,
- Technical-economic decision support, and
- Planning and documentation of the design.

The main role of the system is to help the bridge managers at the highway departments before the completion of the first Hungarian BMS.

### FÖMTERV BRIDGE MANAGEMENT MODEL

The Hungarian design firm FÖMTERV recently initiated the elaboration of a system with the following features (A. Horváth, unpublished paper):

- The input data come from a detailed survey of sample bridges selected from the whole stock according to strict sampling rules and from visual inspection of the rest of the stock,
- The measured data are extended to each element of all bridges by using the mathematical similarity theory and Pólya heuristics,
- With the help of the mathematical similarity theory all of the bridges can be compared (their absolute order is given by their differences from the ideal bridge),
- Any structural elements of the bridges can be compared, and
- The eventual urgent improvement needs of any element of any bridge can be identified.

### LONG-TERM BRIDGE MAINTENANCE STRATEGY

Recently, a long-term (10-year) maintenance strategy was compiled for the whole state highway network (20). An important part of this strategy was the bridge maintenance strategy covering nearly 5,900 structures. Based on the actual condition of the bridge asset, three strategy variants (optimum, condition preservation, minimum) were investigated.

The major results obtained by using this strategy were as follows:

- More funds are needed for bridge condition evaluation, cleaning of bridges and culverts, maintenance of bridge drainage systems, and removal of plants that are traffic safety hazards and that impair the capacities of

structures (to prevent severe deterioration, which would require major high-cost maintenance or rehabilitation);

- The average age of bridges of the state highway network is 41 years; nearly 400 bridges are older than 80 years;
- About 30 percent of the bridges have insufficient load-bearing capacities or deck widths;
- Twenty-seven percent of the asset is below the optimum, whereas 9 percent is below the critical level (these quality levels have been determined separately for the main bridge elements and major road types by using expert estimation);
- If the minimum strategy is used, the ratio of the bridge asset below this critical level will triple during the next 10 years;
- The following shares of the whole bridge stock should be improved for various structural elements in order to obtain the general optimum condition after 10 years: substructure, 20 percent; superstructure, 27 percent; bridge deck, 38 percent; and bridge accessories, 38 percent;
- The savings in road user costs are, on average, about 10 times higher than the additional bridge maintenance or rehabilitation costs, so these latter interventions are extremely cost-effective (it is especially true if the investigation is carried out for a longer period, e.g., 30 to 50 years);
- Efforts should be made to reach the overall optimum bridge condition as quickly as possible (e.g., in 10 years) since this is the best way of reducing the total costs; and
- The development of a working BMS that can be applied both on the network and the project level is an important and urgent task.

### REFERENCES

1. Andersen, N. H. *DANBRO Multi-Purpose Bridge Management System*. Road Directorate, Copenhagen, 1989.
2. Andrews, P. *BRAINS (Bridge Record, Assessment and Inspection System). Construction Repairs and Maintenance*, Vol. 11, 1986.
3. Bridge Management. Presented at First International Conference on Bridge Management, Surrey, United Kingdom 1990.
4. *Bridge Management*. Organization for Economic Cooperation and Development, Paris, 1992.
5. *Bridge Management System*. Finnish National Road Administration, 1992.
6. *Bridge Needs and Investment Process: Technical Documentation and User's Guide*. Office of Environment and Planning, FHWA, U.S. Department of Transportation, 1991.
7. Demarre, M. *Basic Concept of Bridge Management*.

- Guidelines*. Report INU-28. Planning and Research Department, World Bank, 1991.
8. EDUARD, *Bridge Management System of SETRA* (in French). Collective of SETRA, Paris, 1990.
  9. Golabi, K., P. Thompson, and W. A. Hyman. *A Network Optimization System for Bridge Improvements and Maintenance*. Pontis Technical Manual. FHWA, U.S. Department of Transportation, 1992.
  10. O'Connor, D. S., and W. A. Hyman. *Bridge Management Systems*. Report FHWA-DP-71-01R. FHWA, U.S. Department of Transportation, 1989.
  11. Galló, L. The Sufficiency of Highway Bridges (in Hungarian). *Civil Engineering Review*, Vol. 7, 1987.
  12. Apáthy, Á., and E. Tóth. Evaluation of the Highway Bridge Sufficiency (in Hungarian). *Transport Construction and Civil Engineering Review*, Vol. 9, 1990.
  13. Tóth, E. A Contribution to the Paper of L. Galló: The Sufficiency of Highway Bridges (in Hungarian). *Civil Engineering Review*, Vol. 10, 1987.
  14. *Guidelines for Filling in the Condition and Quantity Evaluation of Yearly Bridge Inspection Report* (in Hungarian). Road Management and Coordination Administration, Hungary, 1992.
  15. *Bridge Program until 2000* (in Hungarian). Bridge Department, Construction Division, Széchenyi István Technical College, Győr, Hungary, 1991.
  16. Gáspár, L., Jr. *Determination Method and Actual Calculation of Maintenance Needs as a Function of Road and Bridge Asset Values* (in Hungarian). Research Report 243-055-1-2. Institute for Transport Sciences, Budapest, Hungary, 1992.
  17. *Calculation Method of the Efficiency of Bridge Improvements* (in Hungarian). Institute for Transport Sciences, Budapest, Hungary, 1993.
  18. Csorba, Á. *Simplified Bridge Management System and High-Benefit Bridge Management System* (in Hungarian). Szolnok Road Directorate, Hungary, 1992.
  19. Csorba, Á. *Optimum Criteria of a Bridge Stock in Crisis* (in Hungarian). Szolnok Road Directorate, Hungary, 1992.
  20. Long-Term State Highway Maintenance Strategy (in Hungarian). 1994.

# Condition Rating and Maintenance System for Railway Bridges in Poland

---

Maciej Sawicki, *Polish State Railways*

Jan Bień, *Warsaw Technical University, Poland*

Changes in the national economies in Central Europe stimulate changes in bridge maintenance systems. The SMOK railway bridge management system was designed and developed at Wrocław Technical University for Polish State Railways. The main idea of the new system is to combine the new maintenance unit organization with a new inspection system and to implement a computer system to support the collection and processing of data for bridges. The huge amount of fresh and modern knowledge and technology will fill all elements of the management system; among these also will be expert computer systems and economical optimization for supporting the decision-making process.

**P**olish State Railways (PKP) is a state company, the general director of which reports directly to the Minister of Transport and Maritime Economy. PKP is the third largest railway in Europe, after those of Germany and France, and has more than 23 000 km of lines and almost 48 000 km of tracks.

The total number of civil structures is almost 35,000, among which there are almost 10,000 bridges with spans of more than 3 m (Figures 1 and 2). The 64 percent civil structures that are part of Poland's railways were built before the beginning of the World War I in 1914, and only 20 percent of bridges are younger than

50 years (Figure 3). It shows how big a bridge maintenance problem PKP management has.

After changes in the Polish economy in 1990, the Permanent Way Head Management, which is part of the general management of PKP, noticed that the traditional way of bridge maintenance failed and started working to prepare a new system. In 1993, in cooperation with the Technical University in Wrocław, PKP stated new technical, organizational, formal, and economic rules of railway civil structure management. Implementation of the system (Figure 4) was started in 1994 by developing the training system and a computer-supported information system and by setting up new organizational units: bridge divisions (Figure 5).

## INSPECTION SYSTEM

The heart of the maintenance system is new rules of inspection executed by a staff of 200 inspectors who are selected and specially educated for this purpose. There are five types of railway civil structure inspections (Tables 1 to 3):

1. General overview: executed by the track inspector during everyday track inspection; no equipment or procedure is used; the inspector makes notes in an inspection book if any imperfections are found.

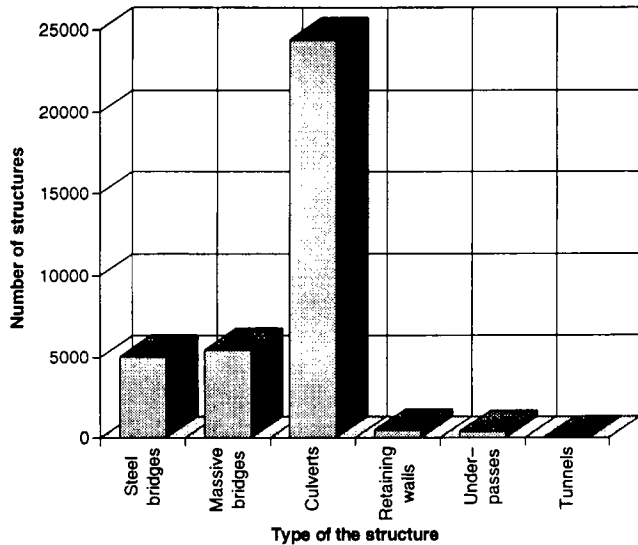


FIGURE 1 Total number of civil structures owned by Polish Railways.

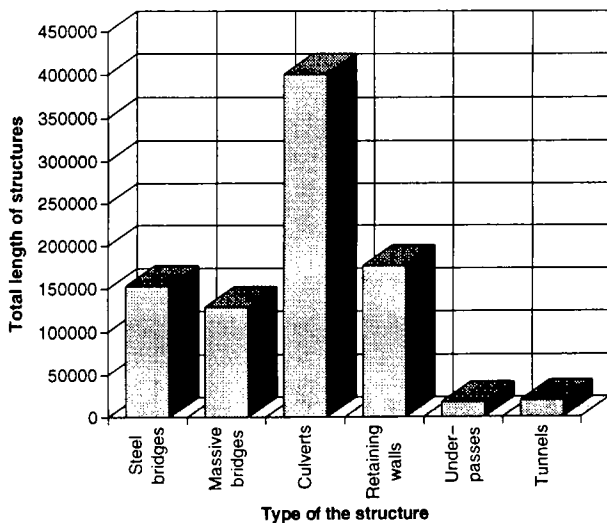


FIGURE 2 Total length of civil structures owned by Polish Railways.

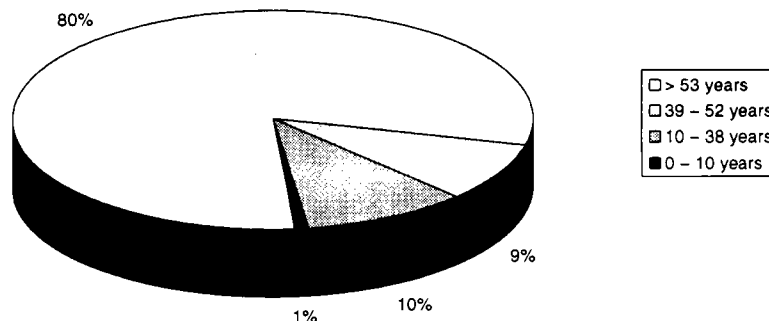


FIGURE 3 Ages of PKP civil structures.

2. Current inspection: executed by the bridge inspector or bridgmaster at least once every 3 months with the use of binoculars; comparison of the condition described in the report of the last basic or more professional inspection is done, and the bridge inspector makes notes in an inspection book if any imperfections are found.

3. Basic inspection: executed by the bridge inspector with the help of the bridgmaster at least once every 1 or 2 years, depending on the condition of the structure, using a set of tools for measuring and simple testing, making photographs, and filling in a special report form, gathering data on bridge condition, serviceability, main deficiencies, and maintenance and repair work needs (Figures 6 to 8).

4. Detailed inspection: executed by the division inspector accompanied by the bridge inspector and the bridgmaster; it is executed at least once every 5 years, depending on the bridge's structural condition, using a wide range of equipment, which allows all necessary measurements to be made and some not very difficult tests to be performed; it always verifies the information in the report from the basic inspection and solutions to problems pointed out by the bridge inspector but that are too complicated to be solved by the bridge inspector; it describes precisely the scope and rough costs of general repairs.

5. Special inspection: executed by consultants, scientists, and testing companies accompanied by division and bridge inspectors, and is ordered by the division inspector in case of problems that need high professional expertise; the result is an opinion that should identify the problem and the requirements for further use of the bridge or a description of the work that must be done.

## BASIC INSPECTION AND MAINTENANCE PLANNING

The most important inspection from the point of view of bridge management is the basic inspection, which gives 95 percent of the information about structures and is therefore the base for maintenance work plan-

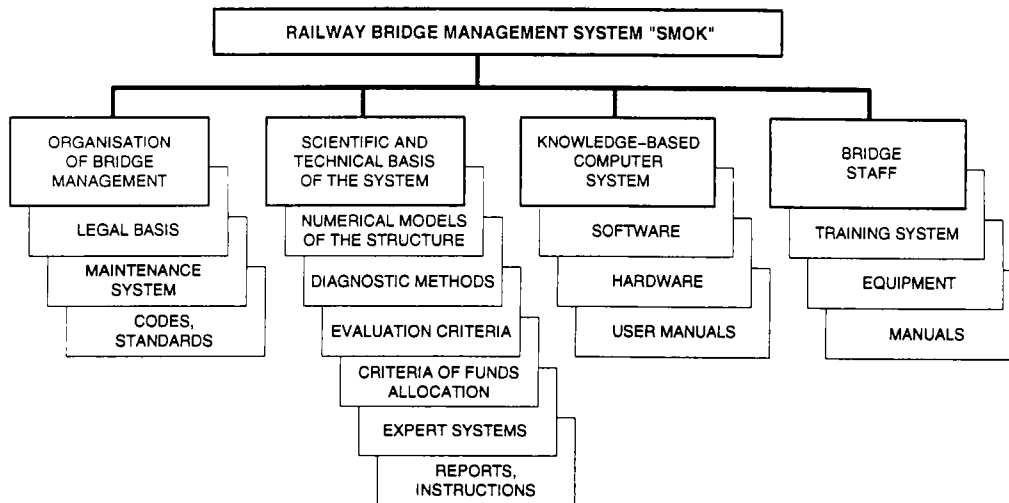


FIGURE 4 Main components of the SMOK railway bridge management system.

ning and selecting structures for repairs. Basic inspection allows observation every year of changes in construction condition and serviceability, selects bridges for conservation and preventive work, and indicates the structures that need inspections by more experienced inspectors.

Such a system saves the time of division inspectors with higher levels of education and more experience and directs them to structures with really serious problems. It also provides a chance for the true owners of bridges to take full responsibility for them.

### SMOK COMPUTER SYSTEM

Execution of each inspection is supported by a computer system for collecting the data derived during inspections, both inventory and a description of the conditions of structures. There also is a place for notes about the need for maintenance work and use restrictions.

During or after basic inspections data from the report form are put into the information system. Condition notes and work cost estimations will be the basis



FIGURE 5 Geographical locations of PKP bridge divisions.

TABLE 1 Structural Elements for Condition Rating

TYPE OF THE STRUCTURE	
<b>BRIDGES, VIADUCTS, PEDESTRIAN OVERPASSES</b>	
0 :	whole structure
1 :	abutments
2 :	piers
3 :	main girders
4 :	deck
5 :	bearings
6 :	water proofing
7 :	drainage
8 :	accessories
9 :	non-bridge installations
10 :	approaches/stairs
11 :	underpass
<b>TUNNELS, UNDERTRACK PASSES</b>	
0 :	whole structure
1 :	construction
2 :	entrance walls/stairs
3 :	water proofing and drainage
4 :	accessories
<b>CULVERTS</b>	
0 :	whole structure
1 :	construction
2 :	entrance walls and slopes
3 :	underpass
<b>RETAINING WALLS</b>	
0 :	whole structure
1 :	construction
2 :	slopes

TABLE 2 Scale of Condition Rating

5	no problems, no repair is needed in next 10 years, in the following year only conservation works
4	small dysfunctions which do not need repair in following 3 years; in the following year only conservation works
3	defects which must be repaired in following 2 years; in the following year possible conservation works
2	reasonable defects which are not dangerous for bridge safety, but need repair in the following year
1	serious damage which may be dangerous for bridge safety and needs major repairs in the following year
0	very serious (dangerous) damage which is very dangerous for bridge safety and needs emergency repair

TABLE 3 Scale of Serviceability Rating

5	operation without restrictions - full serviceability
4	operation without restrictions - small dysfunctions like restricted clearance under the bridge, noise, ugly appearance
3	operation with restrictions of the clearance on the bridge (or in the tunnel)
2	operation with the lowered speed of the trains on the structure (or in the tunnel)
1	operation with reduced loads on the structure
0	structure out of use

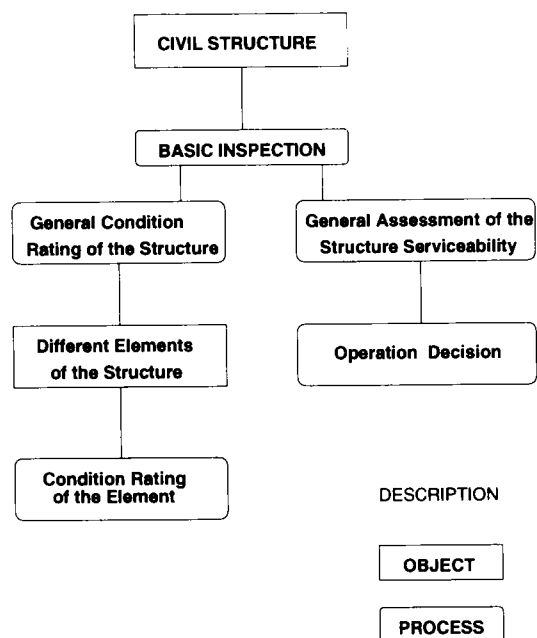


FIGURE 6 Evaluation of bridge structures during basic inspection.

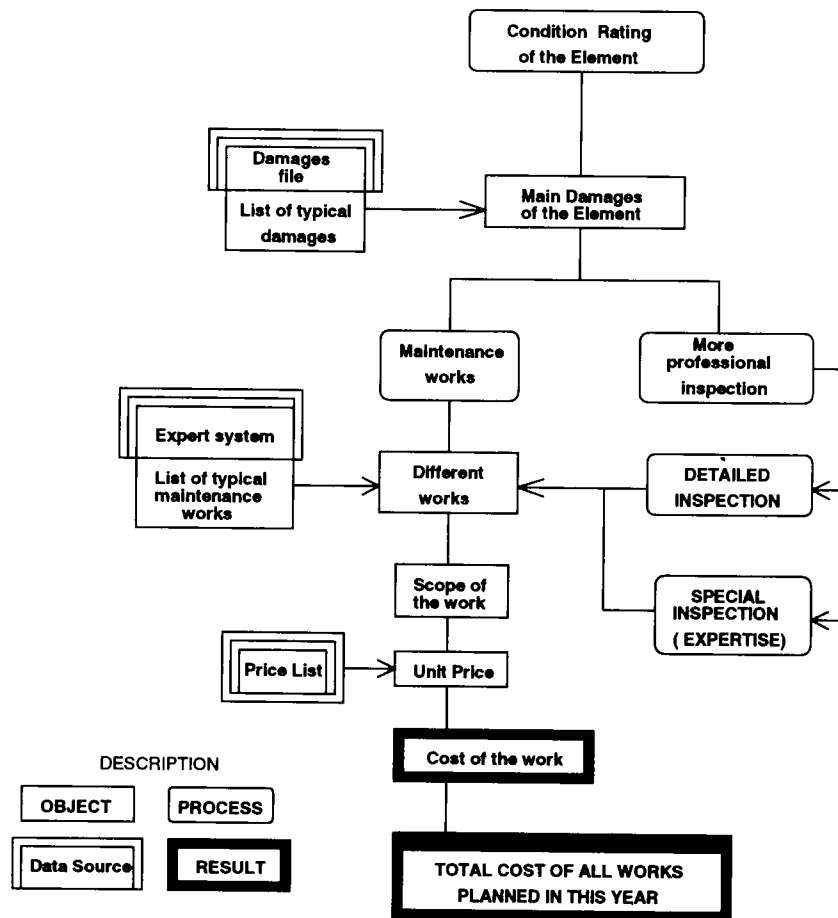


FIGURE 7 Basic inspection: results of condition rating.

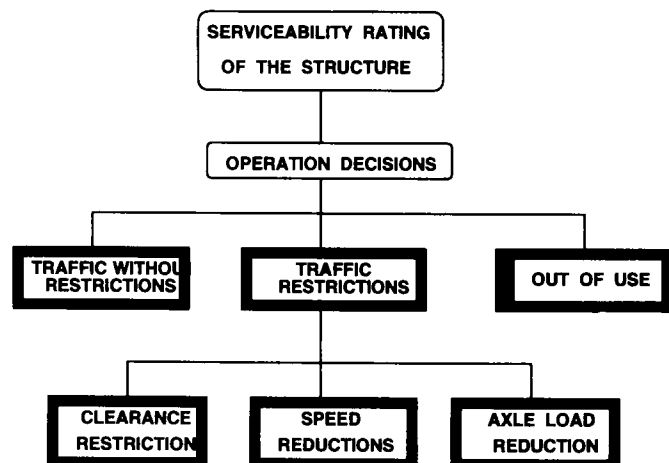


FIGURE 8 Basic inspection: results of serviceability rating.



for preparing priority ranking lists and for determining long-term financial needs.

Detailed inspections verify the data from the basic inspections and add the results of all tests and measurements made during those inspections. Very important is information about the needs for repairs and other maintenance work combined with cost estimates. These data will be created as three different strategies for every structure treated. The information created during the detailed inspection will be the formal base for making financial plans for the following year. These data will be also used to optimize funds allocations among bridges technically selected for repairs.

The computer system supporting bridge maintenance will allow the following:

- Collection of different kinds of data,
- Transfer of data to higher management levels,
- Translation of numerical condition assessments to economic parameters of procedures that support decision making, and
- Application of some expert procedures useful for bridge managers at all levels of the PKP organization.

The computer system consists of bridge inspector terminals (far terminals), division terminals operated by division inspectors, computers in the offices of regional bridge managers, and the computer in the Civil Structures Department of General Management.

In the first organizational step, computers will work as isolated terminals; information will be transferred only by diskettes or telephone modems. After imple-

mentation of the Polish Railway Computer Net KOLPAK in 1995 and getting access to it, the computers of the SMOK system (but not the far terminals) will become terminals of KOLPAK. The bridge data bases will be located in bridge divisions, and inspector terminals will become subterminals of KOLPAK by connection only with division terminals. All of the computer software for bridge management was originally prepared for PKP by the Technical University in Wroclaw.

## CONCLUSIONS

Permanent Way Head Management assumes that 15 to 20 percent of today's spending for railway bridge maintenance is not used properly because of inadequate directing of finances and improper work execution. This is mainly caused by the lack of reliable information about the numbers of and conditions of the bridges and by financial needs estimates, which are not always made by professionals.

Preparing educated staff and setting modern inspection procedures, supporting data collection and transfer of data by a computer system, preparing priority rankings, and using economical procedures for decision-making assistance should allow PKP to spend money in a more efficient way. PKP expects that former losses in bridge maintenance expenditures should be reduced to 5 percent.

The total cost of preparing and implementing the new bridge management system will be covered by better allocation of spending and use of funds during 1 year of repair and maintenance work.

# Innovative Stand-Alone Financing for Mid-Bay Bridge Across Choctawhatchee Bay

---

Eugene C. Figg, Jr., and Linda F. McCallister, *Figg Engineering Group*

Innovative stand-alone financing in the form of an \$81 million unrated, revenue bond project was a first of a kind for transportation and resulted in the successful completion of a 5876-m (19,265-ft) bridge for a Florida coastal community. The development of this project incorporates part of the suggestions of the Intramodal Surface Transportation Efficiency Act. The bridge is owned by a special authority and is being financed completely through the use of tolls backed by 5,000 vehicles a day. There is no full faith and credit backing of any state, federal, or local government. Partnerships were developed, with loan monies received from the Florida Toll Facilities Revolving Trust Fund, the Florida Department of Transportation, and the county. Partnering was done with property owners and the community. This major bridge was accomplished from conception through construction in 6 years. The bonds were unrated and were supported with a special unique insurance. They sold in less than 10 min, and offers were made for twice the amount needed, resulting in lower interest rates. The partnership approach, design, and financing contributed to the project speed and resulted in many unique features: A world record for span-by-span construction was set. Seven spans were completed in 7 days (952 ft of completed bridge in 1 week). A simplified post-tensioning design resulted in greater speed of construction. The bridge was built in 25 months, 5 months ahead of schedule, and opened on June 26, 1993. The bridge cost \$44/ft<sup>2</sup>. The project was selected as the top bridge project for 1993 by the Florida Department of Transportation.

The award was given by the Florida Transportation Builders Association.

To meet today's transportation needs communities are often required to look for innovative funding solutions because state and federal funds are not sufficient to create all of the major facilities that are needed. An example of how one community achieved its 25-year dream for a 5876-m (19,265-ft) bridge without state or federal funding but by using innovative funding solutions is the story of the Mid-Bay Bridge across Choctawhatchee Bay in west Florida.

This major transportation facility was begun before the Intramodal Surface Transportation Efficiency Act (ISTEA) was put into place in 1990. However, it embraces some of the concepts and ideals developed in ISTEA and serves as a model of how communities can better take advantage of ISTEA for their future transportation needs.

## MID-BAY BRIDGE AUTHORITY

The community decided that it could accomplish this major bridge project by making it a local toll facility. In order to accomplish that they asked the Florida Legislature to create a special bridge authority. In 1986 the state of Florida Legislature created the Mid-Bay Bridge

Authority for the purpose of planning, constructing, operating, and maintaining a bridge crossing the Choctawhatchee Bay in Okaloosa County. The expanding local population, the travel demand generated by this expansion, and the need to establish an adequate hurricane evacuation route all contributed to the critical need for this facility. On October 13, 1986, five Okaloosa County citizens appointed by the governor were installed as authority members, and the authority held its first meeting to elect officers and begin this important project.

The membership of the authority included people from the community with many different backgrounds, and through the course of the project 15 people served as members with various terms of office. For example, members included an engineer, an attorney, a sheriff, a banker, a developer, a retired general, a hardware store owner, a fisherman/environmentalist, and other businessmen. All project decisions by the authority were in the best interest of the local community.

#### PROJECT DEVELOPMENT INCLUDING SEED MONEY

The project included the creation of a 5876-m (19,265-ft) bridge, 4572 m (15,000 ft) of connecting roadway to State Road 20 and US-98 from Niceville to Destin, and a toll facility, as seen in the location map of Figure 1. The most important first step was to locate the project and determine the financial and engineering feasibility for implementation of this project with bonds.

Engineering and financial analysis work had to be done, and seed money was needed to get the project started. A loan was obtained from a special trust fund administered by the Florida Department of Transportation (FDOT). The state of Florida created the Florida Toll Facilities Revolving Trust Fund to provide seed money to authorities, cities, counties, or any municipality creating a transportation facility that will be supported by a dedicated revenue stream such as toll revenues (or we could call these user fees). The maximum amount for which an applicant can apply is \$500,000 per year without a special legislative appropriation. With a special legislative appropriation this amount can be in the multimillions of dollars.

This loan money is required to be repaid to the Revolving Trust Fund within 7 to 12 years after it is borrowed. A 1993 change to the rules no longer requires funds to be repaid with interest; only the amount borrowed must be repaid.

The state of Florida has been very progressive in helping to advance transportation through seed money loans. Since the fund started 15 authorities and one county have used loans. Since 1986, \$89.6 million in

seed money has been used to create approximately \$1 billion in toll transportation facilities.

The authority applied for and received a \$500,000 loan enabling it to begin the project by hiring an engineering consultant and a traffic and revenue consultant. Feasibility studies were completed in 6 months, resulting in the establishment of an alignment, a draft environmental document, preliminary construction costs, and a financial analysis and workshop that included the authority and the public.

Only 5,000 vehicles per day could be counted on to pay a toll, and the bond size to finance this project would be in the magnitude of \$80 million. With this traffic volume, the facility would initially have two lanes (with shoulders) and could be expanded to four lanes once the traffic volumes warranted the expansion. The greatest challenge was to support the project on toll revenues only. There would need to be pioneering in bond financing, and multiple partnerships would need to be involved to make this a stand-alone success.

#### CREATING PARTNERSHIPS FOR INNOVATIVE FINANCING

For the project to be successful some additional loans were needed, resulting in a team partnership approach. FDOT agreed to sign a lease-purchase agreement, making it a project partner. FDOT agreed to handle toll operations and maintenance while providing loan funds for these operations in the early years of revenue shortfalls. The early years of operation are primarily the most challenging for a start-up facility because the project is just coming out of the construction period, when there have been no revenues for several years. As the revenues increase with time, operations and maintenance are funded by the toll revenues and FDOT is repaid for the loans.

Next, in order to sell the bonds coverages are required. In this case revenue bonds including both senior bonds and junior bonds would be sold, with coverage as follows:

- Senior bonds: 1.50 coverage, and
- Junior bonds: 1.10 coverage.

The early years of the financing showed a potential shortfall in meeting the full coverage amounts. For instance, in the senior bonds the 1.50 coverage meant that 50 percent more annual revenue was needed than was actually necessary to repay the bond debt. To help with coverage requirements in the early years the county became a partner. The county agreed to set aside a portion of its local-option gas tax as a loan to help achieve the required coverage levels. This was approximately

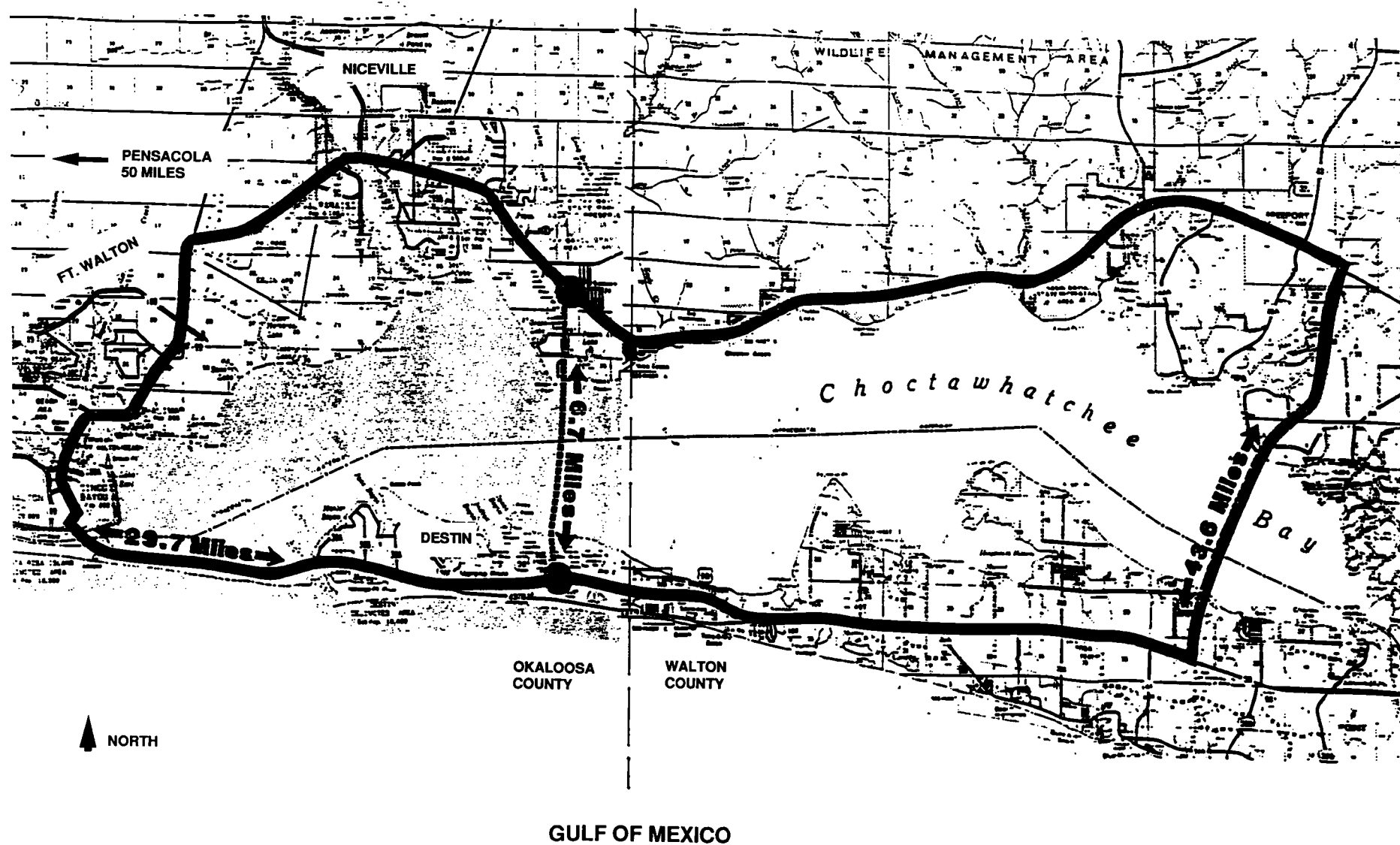


FIGURE 1 Mid-Bay Bridge Project location map (project alignment versus alternate routing).

\$1 million initially, and in each year for several years this amount is reduced as the coverage gets stronger. This was a loan and would not be spent unless the project needed to use the total coverage amount to help repay the debt.

It was also determined that this would be a revenue bond issue without full faith and credit obligation and backing by any government entity (state, federal, or county). Since government monies were obligated to other project needs and the state was already backing its own bonds, it was unrealistic to get government backing of the bond revenues.

Instead, these revenue bonds were created by using a force majeure insurance policy with Lloyds of London that would guarantee the completion of construction. The partnerships and special insurance were instrumental in putting together a financial scenario that could go to market.

These financial aspects were developed over time concurrently with the final design activities, permitting

right-of-way acquisition and other activities to bring the project to construction bids before selling the bonds and beginning construction.

#### IMPLEMENTATION OF DESIGN AND FINANCING

To implement the project following the feasibility studies and the development of a conceptual financing plan the authority obtained two additional loans from the trust fund, each for \$500,000. This brought the total amount borrowed from the trust fund to \$1.5 million. More was needed to get the project to construction, and the timing was not ideal for going to the state legislature for a trust fund appropriation greater than \$500,000. Therefore, the authority obtained a loan of \$800,000 from the county to be repaid with the bond sale. The right-of-way needed was secured in advance with the property owners, but the actual purchase was not made until the bond money was available. Throughout the

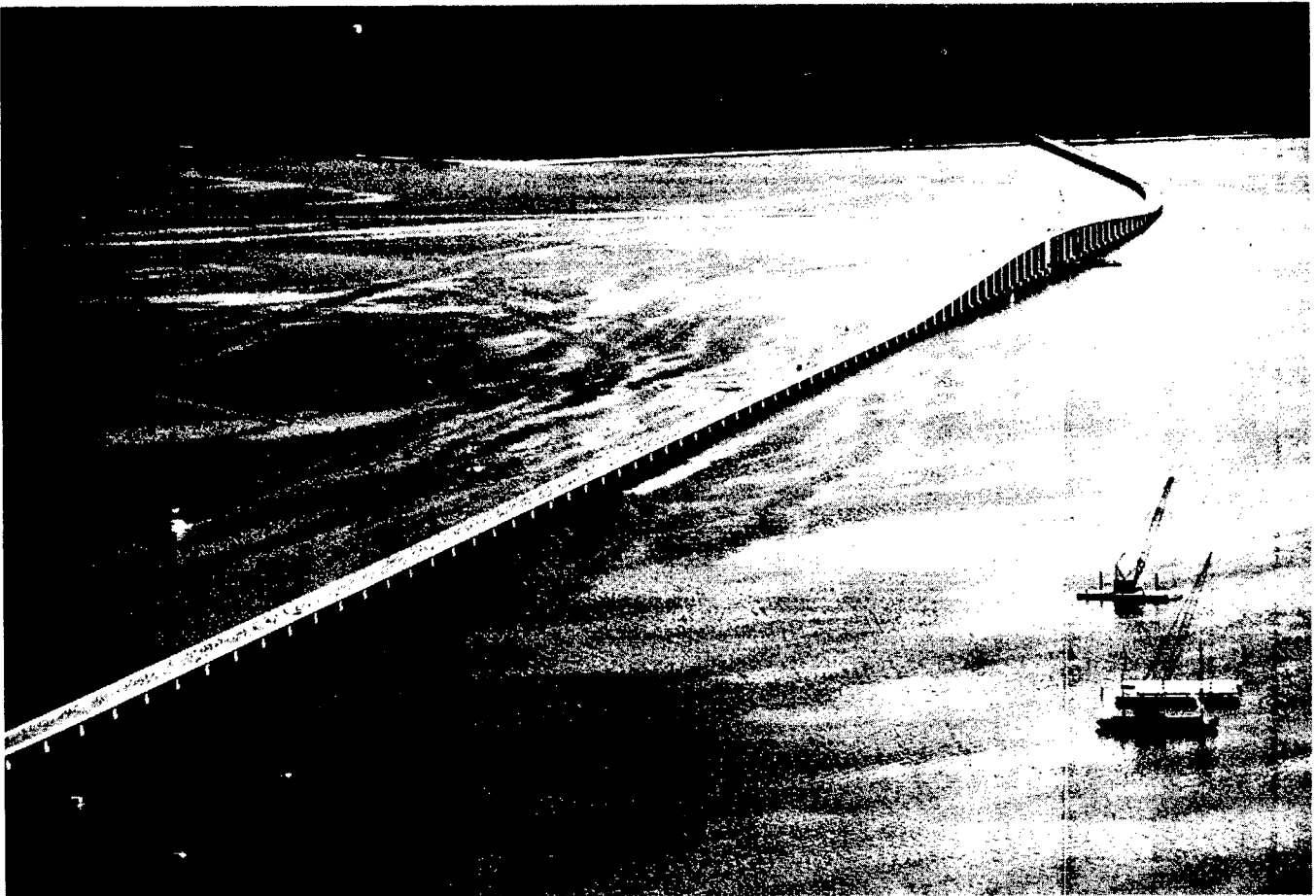


FIGURE 2 The 5876-m (19,265-ft) bridge was dedicated and opened to traffic on June 26, 1993, 5 months ahead of schedule. The day of dedication activities began with a run/walk across the bridge, with more than 5,000 participants (shown in this view).

implementation the authority met a minimum of once a month in a public forum (more than 50 public meetings) to make decisions that would give the community the facility that it wanted.

Once the design was completed and the contract documents were ready for construction bids, contractors were notified and were prequalified by a process tailored for the needs of this project. Thirteen major contractors (including general contractors, precasters, and pile drivers) were prequalified and construction bids were received. The low-bid contractor's price resulted in a bridge cost of \$44/ft<sup>2</sup>.

To sell the bonds after bids were received, potential investors were brought to the project site to meet the authority and research the area to help in evaluating their own financial rating for these unrated bonds.

In April 1991 the underwriters sold these unrated revenue bonds for this start-up and stand-alone toll facility. Within 10 min 25 buyers had made offers for \$150 million. The authority was able to negotiate lower interest rates because only \$81 million was needed to finance this project. On April 24, 1991, the bond clos-

ing was held and bonds were purchased by 18 buyers with interest rates lower than those for rated transportation bonds sold on the market on that same day. The toll rates are \$1.00 each way for prepurchased trips and \$2.00 for nonprepurchased trips.

Construction of the bridge began with special incentives in the contract for the contractor to complete the 30-month construction ahead of schedule. There was a \$5,000/day incentive for each day that construction was completed ahead of schedule and \$15,000 in liquidated damages for each day of construction past the scheduled completion date. Three payments of \$500,000 each were tied to achieving certain milestones in the CPM schedule.

The bridge itself was a precast, post-tensioned segmental box girder bridge comprising 141 spans with typical span lengths of 41.5 m (136 ft) and a main span over the Intracoastal Waterway of 68.6 m (225 ft). The completed bridge is shown in Figure 2. The substructure consisted of precast, post-tensioned box piers for the high-level portion and cast-in-place piers for the low-level portion, all of which was supported on concrete pile



FIGURE 3 Typical 41.5-m (135-ft) spans were erected by span-by-span methods by using an assembly truss. The contractor was routinely able to erect four spans per week. During the week of September 20, 1992, the contractor was able to erect seven spans in 7 days [290 m (952 ft) of completed bridge in 1 week], a world record for span-by-span erection speed.

foundations. The bridge was built by the span-by-span method of construction, as shown in Figure 3. The contractor was typically able to place four spans per week. However, a world record for span-by-span erection was achieved when seven spans were completed in 7 days, for 290 m (952 ft) of completed bridge in 1 week.

In April 1993, when the construction was 4.5 months ahead of schedule and the interest rates on bonds were dropping significantly, the authority decided to refinance the bridge before the completion of construction. The construction costs were as expected and under budget, and the authority was able to obtain BBB and BBB- ratings on the senior and junior bonds, respectively. The new interest rates dropped by 2.02 and 2.85 percent, respectively. The interest rates for both the April 1991 and April 1993 bond sales were as follows:

	<i>Interest Rates (%)</i>	
	<i>April 1991</i>	<i>April 1993</i>
Senior lien bonds, \$56 million	8.09	6.07
Junior lien bonds, \$26 million	9.25	6.40

On June 26, 1993, the bridge opened 5 months ahead of schedule (it was built in 25 months). The bridge opened to traffic 6 years from the time that the consultants began the feasibility studies. The community achieved its dream and helped to create a new way for other community transportation projects to be financed.

#### **HOW MID-BAY BRIDGE'S SUCCESS HELPS FUTURE TRANSPORTATION**

The partnerships, special insurance, loans, no backings of governments, and construction incentives were all

part of this first-of-a-kind unrated revenue bond issue for an \$81 million stand-alone start-up toll facility. The revenues are only backed by the 5,000 vehicles per day that each pay by \$1.00 (prepurchased) and \$2.00 tolls. This demonstrates how a transportation project can meet a significant challenge by using innovation. ISTEA expands on the options for innovation, allowing more opportunities for the use of federal and state monies and using small investments and loans to achieve major transportation projects. More facilities can be built with less money.

The Mid-Bay Bridge is resulting in the achievement of more stand-alone, unrated transportation projects. Our \$90 million Santa Rosa Bay Bridge in Santa Rosa County, Florida, will begin construction in 1995. It will be supported on 6,000 vehicles per day as a start-up, stand-alone facility building on the lessons learned from the Mid-Bay Bridge.

#### **ACKNOWLEDGMENTS**

The Mid-Bay Bridge Authority is the owner of the Mid-Bay Bridge Project and hired Figg Engineering Group as their engineers for design and management of the project. Figg Engineering Group managed eight subconsultants, provided the bridge design, and provided construction management and inspection. The authority's underwriters were Smith Barney and Harris Upham & Co., Inc., and the authority's attorneys were Stowell, Anton & Kraemer. The traffic and revenue analysis was accomplished by URS Coverdale & Colpitts. The contractor was Traylor Bros., with C. W. Roberts handling roadway construction. Michaels Building Corporation built the toll plaza. The members of the team, along with the partnerships with Okaloosa County and the FDOT, made this project successful.

# BRIDGE AESTHETICS

---



# Innovation and Aesthetics

---

Frederick Gottemoeller and Alicia Buchwalter, *Frederick Gottemoeller and Associates, Inc.*

Throughout engineering history, innovation and aesthetics have been intertwined. The introduction of new materials inspires the creation of forms that exploit their structural capabilities. These forms generate new aesthetic responses and create new opportunities for aesthetic pleasure. Although the acceptance of new ideas and forms is often slow, new materials and thus innovations are constantly on the horizon. Eventually the public recognizes and appreciates the beauty of them. Thomas Telford proved this with his development and use of iron. Telford's breathtaking proposal for a cast iron bridge in London was denied, but by the mid-19th century his ideas were standard for major metropolitan areas. Today we look forward to a similar but, it is hoped, faster acceptance of the innovations made possible with high-performance steel, high-strength concrete, and composites of the two. Furthermore, with the new load and resistance factor design (LRFD) specifications, designers will have greater flexibility in creating more efficient and aesthetic structures. With today's methodology and experience, it is possible to provide engineering solutions to issues tailored to the specifics of the bridge at hand. The challenge for designers of these structures is to develop forms that exploit and display the inherent advantages of laciness and transparency while at the same time addressing modern criteria of simplicity and the expression of structural forces. The structures that result will evoke new aesthetic reactions. We will see then how long it will be this time before general public acceptance follows.

Throughout engineering history innovation and aesthetics have been intertwined. The introduction of new materials inspires an engineer to create forms that take full advantage of the structural capabilities of the new materials. These forms generate new aesthetic responses and create new opportunities for aesthetic pleasure. The most creative engineers recognize the aesthetic potential of new forms and exploit their characteristics for the same purposes that an artist would, to maximize their emotional and aesthetic impacts. Yet, because of the general public's reluctance to change, many new technologies do not immediately get the amount of use they merit, and often, innovations are left to emerge only slowly as practical solutions to modern problems. As they emerge, artists and art critics see them and adopt the aesthetic ideas into other areas of art. Then new forms become generally accepted.

The history of innovation in structural art is a series of these cycles. Each cycle begins with the acceptance and support of a standard method of bridge construction both by the public and, as the methodology is refined, by institutions such as the fine arts commissions and the academies of art and by critics of art and architecture. Then a new material or technique is introduced, and a particularly creative engineer with the vision to understand the opportunities presented creates a new type of structure. The new form is often unfamiliar and therefore seems to violate the accepted norm.

Consequently, the public and the art establishments resist the change, and its use is restricted to out-of-the-way places where the art establishment is not involved in the decision making and the economy of the structure is the overriding political concern.

Then the new technique begins to attract supporters. People experience a new type of aesthetic reaction and consequently recognize a new type of beauty in its form. As the more forward thinking critics see its virtues, the new technique is invited into the centers of major cities. In time its acceptance grows and the innovation becomes the new standard for design and, in many cases, an inspiration for other art forms.

New materials and thus innovations are constantly on the horizon. Today we look forward to high-performance steel, high-strength concrete, and composites of these materials. In addition, we can anticipate innovations in design encouraged by the change to load and resistance factor design (LRFD) specifications. Although we may not be able to predict the specifics of the bridges that these materials will produce or who will bring these new potentials to the fore, we can expect the cycle to continue. There will be a new type of structure, probably in an out-of-the-way place, greeted by anguished criticism from the art community. Then, over time, acceptance, widespread use, and perhaps even a spin-off into other realms of art will emerge. The speeding up of modern life and an increasing acceptance of modern materials and techniques have reduced the time for each cycle, but the basic cycle remains.

By taking a look at examples from the past and by thinking about the structural capabilities of the new materials in the light of this history, we can develop some ideas about how the introduction of these new materials will result again in new structural as well as aesthetic ideas.

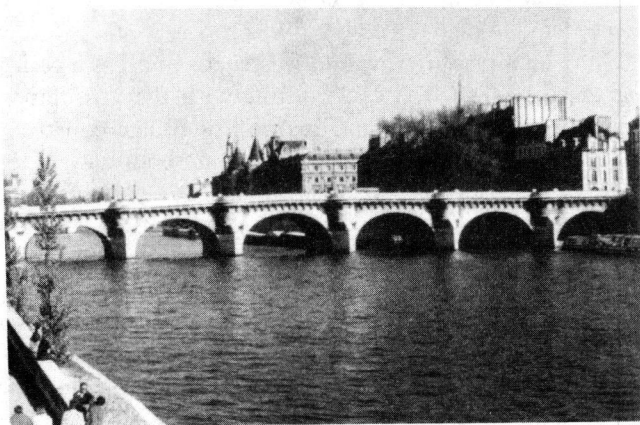


FIGURE 1 Pont Neuf, Paris, 1736.

## EXAMPLES FROM THE PAST

Bridge engineering for many centuries was dominated by the semicircular stone Roman arch, and bridges built as much as 15 centuries apart looked remarkably similar. The Pont Neuf in Paris, built in 1736, has nearly the same elevation as bridges built in Rome more than 1,400 years earlier (Figure 1). In all of Europe, for centuries the "proper" way to build an important bridge was to build a monumental stone arch.

## Iron and Steel

The modern history of engineering begins with the introduction of cast iron and wrought iron as structural materials in the late 7th century. The first structural artist to recognize the possibilities of these materials was Thomas Telford, the founder of the civil engineering profession. Telford realized that the material provided an opportunity for different forms and different methods of fabrication. His Craiglechie Bridge in Scotland puts most of the material into a flat, segmental arch and then connects the arch and the deck with a lightweight lattice of bars. This design, with its lightness, transparency, and relative horizontality, was immediately accepted for structural reasons and became the structural standard for metal bridges from that point forward (Figure 2).

Aesthetic acceptance took longer. People who were raised all their lives on the solid stone masonry of Roman arches were uncomfortable with the tracery of the Craiglechie Bridge. Consequently, Telford's breathtaking proposal for a cast iron bridge in London with a 600-ft span was denied (Figure 3). Telford and his metal bridges were relegated to the outer reaches of the British Isles. It was not until the mid-19th century that bridges of this form and material were built in major metropolitan areas.



FIGURE 2 Craiglechie Bridge over Spey River, Thomas Telford, Elgin, Scotland, 1814.

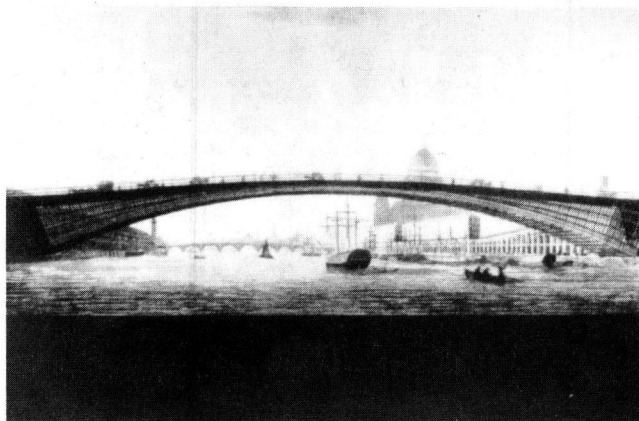


FIGURE 3 Telford's proposal for a cast iron London bridge, 1800.

The Pont Alexandre III in Paris (Figure 4), in contrast to the Pont Neuf (Figure 1) just a few meters downstream, shows how far the basic form eventually evolved. Here it is very decorated, but the flat arch and lightweight spandrel connections, as introduced by Telford, are easily discernible.

The next structural artist to come on the scene was Gustave Eiffel. His railroad bridges in southern France, which took advantage of the strength of the new material, steel, also introduced new shapes designed to more efficiently withstand or reduce the force of wind. The towers and arch rib of the Garabit Viaduct are widened at the bottom to provide a stronger base to resist horizontal wind forces. The bracing takes advantage of the strength of the material to reduce member thickness and thus reduce the area on which the wind is acting (Figure 5).

Eiffel's way of thinking found its ultimate expression in his famous Tower. The Tower, in spite of the initial grumbling of academic critics, found fast acceptance both with the public and with the art community [Figure 6 (left)]. It introduced a whole new way of seeing not only structure itself but space and time as well. The process of rising through the structure on the elevators and viewing the city from constantly changing angles through the lacework of structural members inspired a whole new approach to art. The Cubist movement, aimed at showing the same objects from multiple vantage points and at multiple points in time [Figure 6 (right)] grew out of this new way of seeing things.

At about the same time John Roebling applied his structural artistry to another new material, steel wire, developing new and improved structural forms. The Brooklyn Bridge represents the most complete and successful example of his vision [Figure 7 (left)]. Like the Eiffel Tower, this structure introduced new aesthetic themes and captured the imagination of the public and

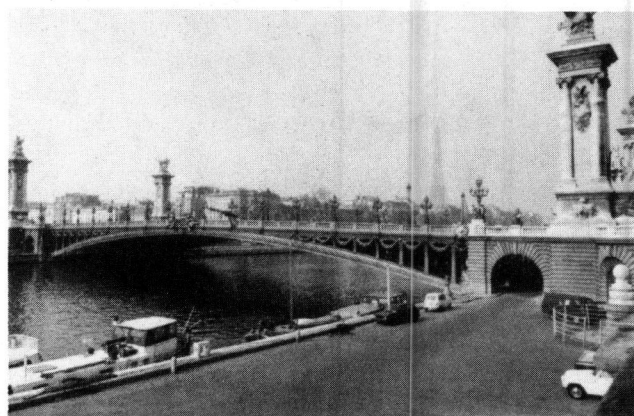


FIGURE 4 Pont Alexandre III, Paris, 1899.

the art community. As one moves across the bridge one sees the city from various vantage points, often through the veil of the stays and suspenders, and with a constant sweep of the main cables and deck curves interacting with each other. Artists have fastened onto these images, and the bridge has been a theme of many paintings, photographs, sculptures, and even poetry [Figure 7 (right)].

## Concrete

The introduction of reinforced concrete in the late 19th century presented additional opportunities. The master in this medium was the Swiss engineer Robert Maillart. He began with the forms of stone masonry very much in mind. However, as he began to understand the tensile capabilities of the material, he began to carve away the areas of structure that were not necessary to support

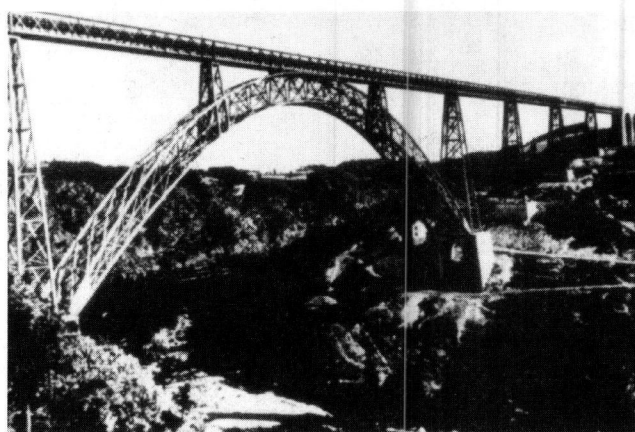


FIGURE 5 Garabit Viaduct over Truyère River, Gustave Eiffel, St. Flour, France, 1884.



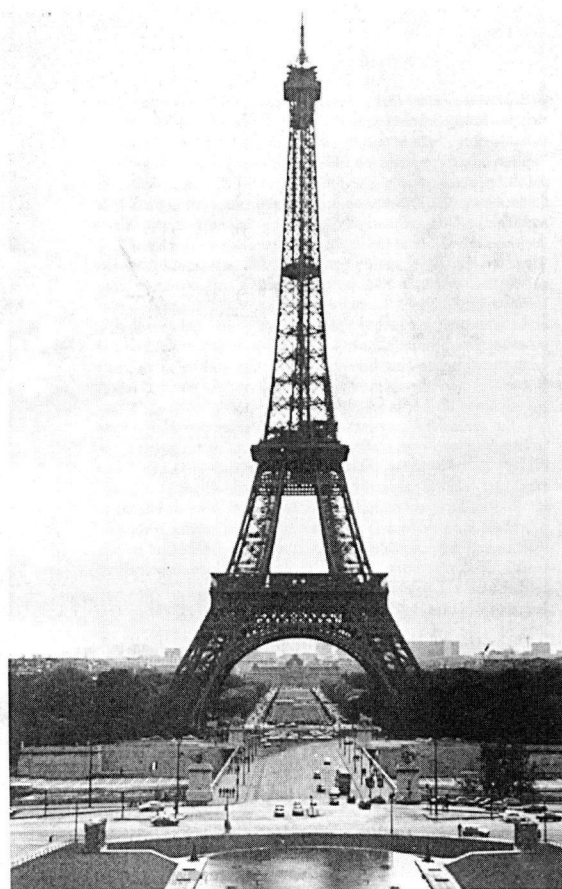


FIGURE 6 *Left*, Eiffel Tower, Gustave Eiffel, Paris, 1899. *Right*, Cubist painting of Eiffel Tower.

the load, until he had created very thin arch structures and three-hinged arches. Both represented new, dynamic forms of the arch bridge. His most famous structure, the Salginatobel Bridge in Switzerland, has become an icon of modern art (Figure 8).

The next great innovation in technique was prestressed concrete. The economic and structural capabilities of this material encouraged the move away from arch forms to girder forms. The girder form is most efficient when its depth changes to reflect the concentration of forces at the supports. The result is a haunched girder. These have been built as both cast-in-place and precast bridges. The masters of this form, such as John Muller and Christian Menn, have found ways to refine the materials into structures of outstanding grace (Figure 9).

The combination of higher-strength concrete and higher-strength steel strand has made possible the stayed girder concept. These new structures have been refined into very attractive bridges that, as in the past, have captured the public's imagination. The Tampa Skyway Bridge is now the accepted standard in the popular imagination for a "signature bridge," and com-

munities all over the country are asking for one like it, whether or not the situation lends itself to this type of structure.

Menn has further refined the use of concrete and high-strength steel strand into a structure that follows a horizontal curve. His Ganter Bridge in Sweden encases the stays in concrete to allow them to follow the curvature of the roadway (Figure 10). It has taken its place alongside the Salginatobel Bridge as an icon of 20th century technology and structural art.

All of the aforementioned designers and designs have a number of things in common. None of these engineers were pursuing art for art's sake when they developed their works. None depended on the addition of unneeded decorative materials for their effects. All were built under the pressure of economy and efficient use of resources and had to respond to the fabrication techniques and materials available. All continue to withstand their assigned loads many years after their completion. Finally, by expressing in the form of the structure the forces on it and the materials it was made of, the engineers found ways to produce bridges that are works of art.

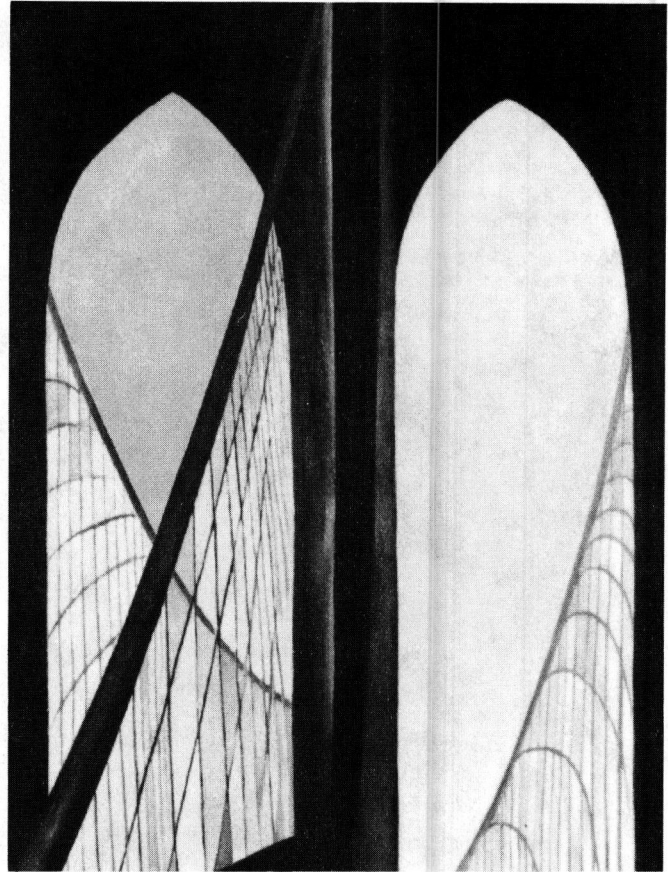


FIGURE 7 *Left*, Brooklyn Bridge, John Roebling, New York, 1886. *Right*, Brooklyn Bridge in art, Georgia O'Keeffe.



FIGURE 8 Salginatobel Bridge, Robert Maillart, Switzerland, 1930.

## EXPECTATIONS FOR THE FUTURE

What kind of innovations are on the horizon for bridges? With the potential of high-performance steel, high-strength concrete, and composites of the two, coupled with the flexibility of the LRFD specifications, many possibilities exist.

### High-Performance Steel

High-performance steels are steels with improved ductility and weldability. They will make field welding more practical and will reduce concerns about fatigue and fracture-critical fabrication. Consequently, designers may once again become interested in truss and tied-arch bridges. However, as these forms regain popularity, they will be subject to aesthetic review. Previously, with their intricate and apparently weighty systems, trusses



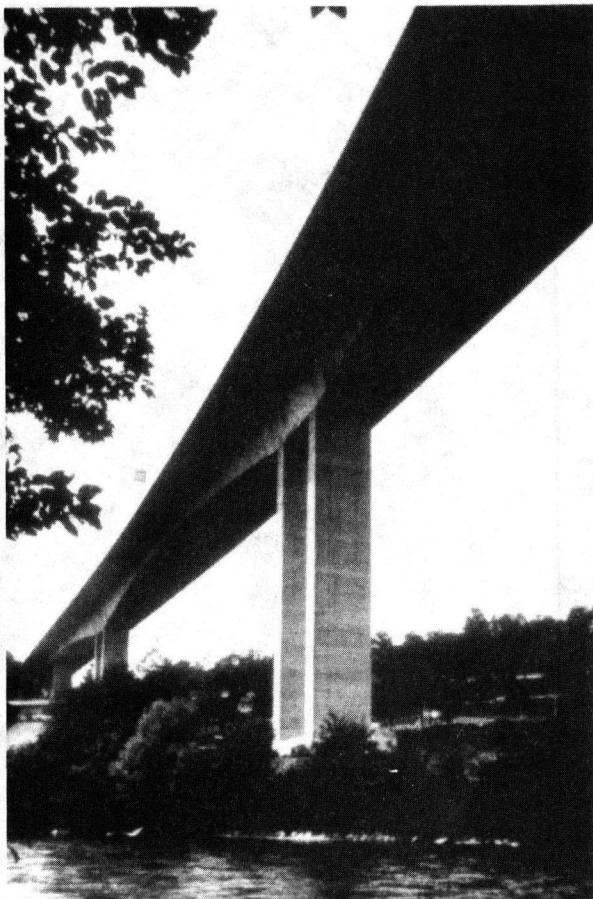


FIGURE 9 Felsenau Bridge, Christian Menn, Bern, Switzerland, 1974.

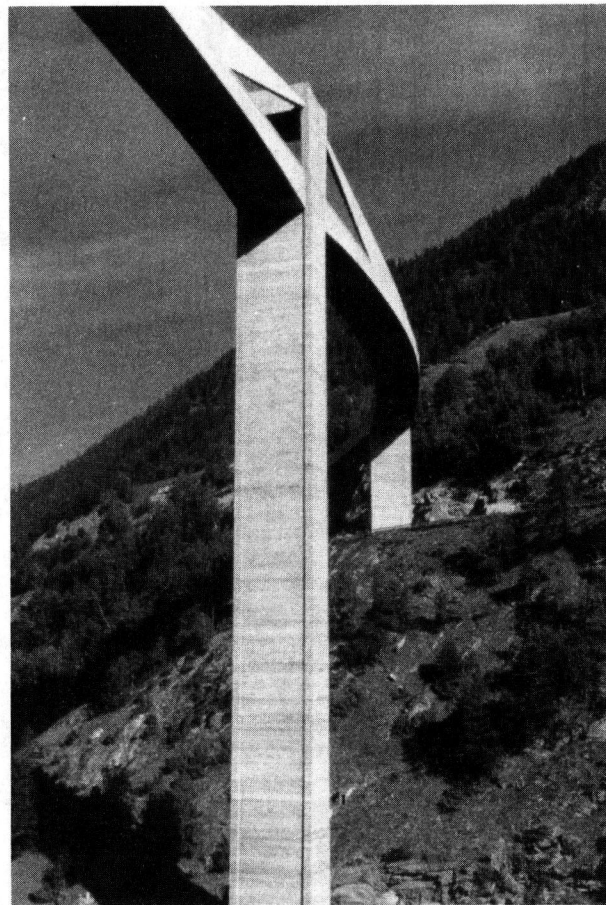


FIGURE 10 Ganter Bridge, Christian Menn, Switzerland, 1980.

had earned the reputation of being the ugly ducklings of the bridge world. Now, with the use of high-performance steels, there is a lacy quality with truss bridges that can be very attractive (Figure 11).

The key to success with truss bridges is to arrange the members in some easily recognizable pattern so that the eye can read the pattern and understand the logic involved. Although the equilateral triangles of the recently built Wando River Bridge provide one successful example of this approach (Figure 12), the fanned members of the famous Firth of Forth Bridge provide a unique pattern of their own (Figure 13). When they are seen in elevation, it appears that they are all arranged to intersect at two points in space, the compression members at a point below the bridge and the tension members at a point above the bridge. The tension members are laced steel structures and almost disappear at a distance. The compression members are tubular and have the appearance of solidity consistent with their function in the structure.

High-strength steel has allowed for innovations in the design of arched bridges as well as in the design of

truss bridges. By using higher-strength steel and new steel building techniques, the appearance of arches could be improved. The Swiss engineer Santiago Calatrava has produced a striking proposal for an arched bridge in which tubular steel members reflect the light, lacy appearance of trussed structures (Figure 14).

Tubular members have inherent advantages for compression members because of their stiffness. They can also be more attractive because their stiffness allows for the use of thinner members, thus reducing the visible surface area and making them easier to understand than wide flange members. Finally, they offer less wind resistance than rectangular members.

Although in the past it has been difficult to calculate the stresses at the intersections of tubular members and to fabricate these intersections, computerized design can now facilitate both of these issues. In addition, the experience gained in the fabrication of drilling platforms with tubular members for the oil industry should be transferrable to bridge construction as well. Therefore, the improved weldability of high-performance steel in combination with improved welding techniques and

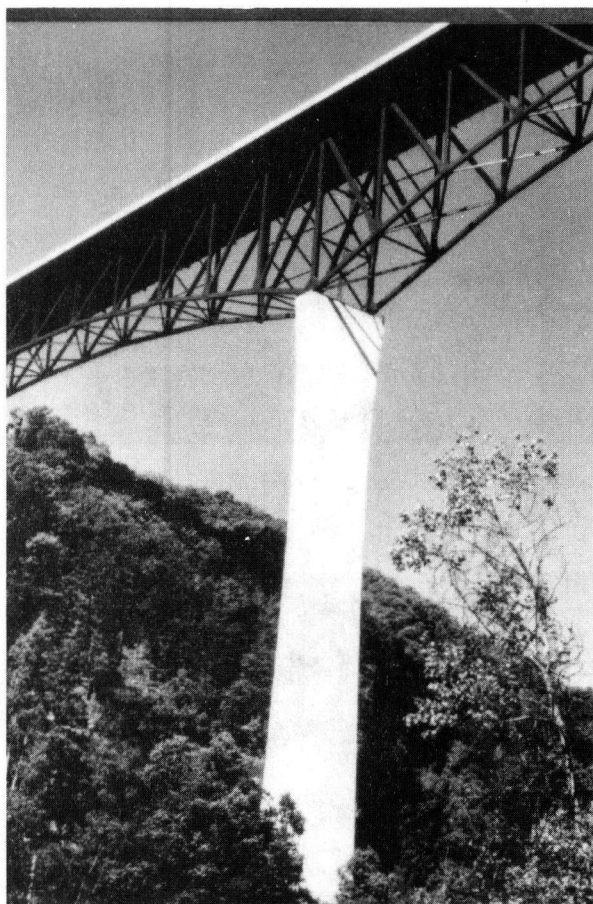


FIGURE 11 Glade Creek Bridge, West Virginia.

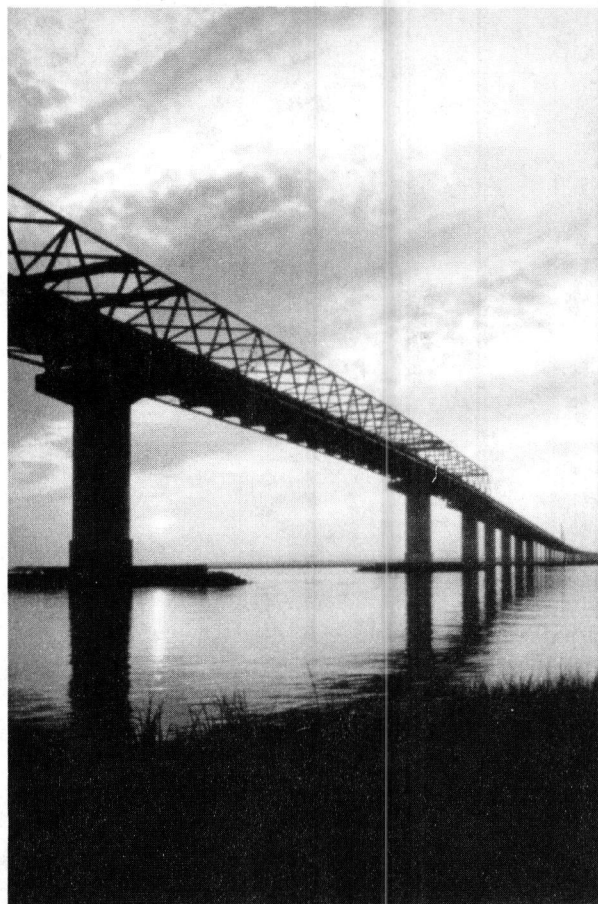


FIGURE 12 Wando River Bridge, South Carolina.

computer-driven machinery makes the use of tubular steel members more feasible.

Tied-arch bridges should also make a comeback with high-performance steels because it makes the fracture-critical tie less of a concern. The I-255 bridge over the Mississippi River illustrates the slenderness that can be achieved with this familiar but now rarely used structural type (Figure 15). If there is a return to these types of structures, it is hoped that they will be built with similar grace.

Finally, the new weldability of high-performance steel may make it more economical to design steel structures as thin and light and continuous as many contemporary concrete structures. The key is to be able to economically fabricate structures with integral cross girders.

The typical problem with steel girders is the need to support and brace every single girder, which requires a heavy concrete pier cap as well as a plethora of under-structure bracing. As one attendee at a public hearing put it, "Looking under a steel bridge is like sticking your head under an old car." Integral cross girders, as



FIGURE 13 Firth of Forth Rail Bridge showing varying angles of the diagonals.



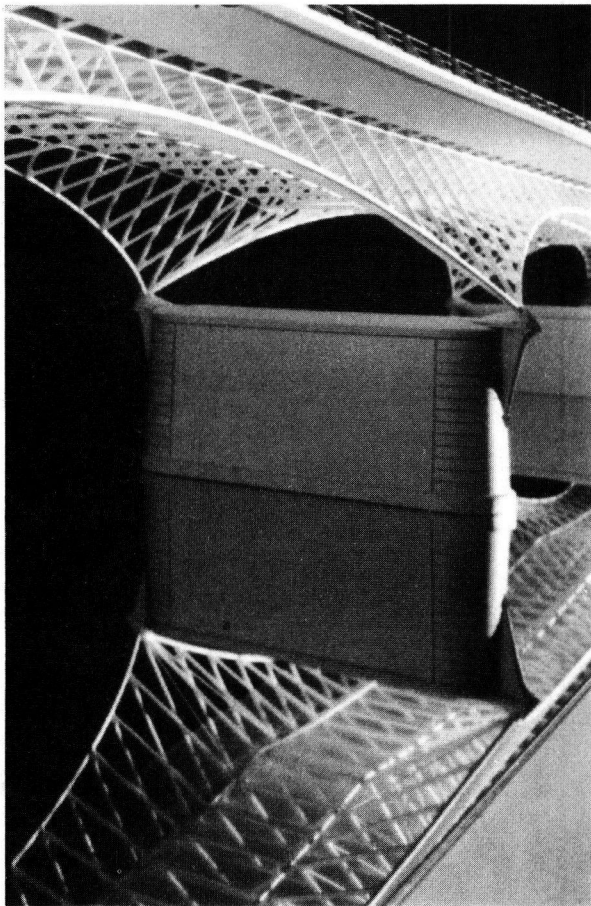


FIGURE 14 Proposed truss arch for Basel, Santiago Calatrava.

in the I-15 Tropical Boulevard flyover in Las Vegas (Figure 16), eliminate the heavy pier cap, simplify the main lines of the structure, and allow it to directly reflect the lines of movement of the ramps overhead. The goal is the same kind of clean lines and simple structure that have been available in concrete structures.

### High-Strength Concrete

Simultaneously with high-performance steel, innovations are appearing in the area of concrete strength and in techniques for joining precast concrete members.

The ability to achieve higher concrete stresses will result in thinner cast-in-place and precast members with higher levels of prestressing. Ontario has built hundreds of excellent post-tensioned concrete structures, but the designs have been limited by the strength of the available concrete. The development of reliable higher-strength concrete would allow continued development of such thin continuous concrete structures (Figure 17).



FIGURE 15 I-255 tied arch over Mississippi River.

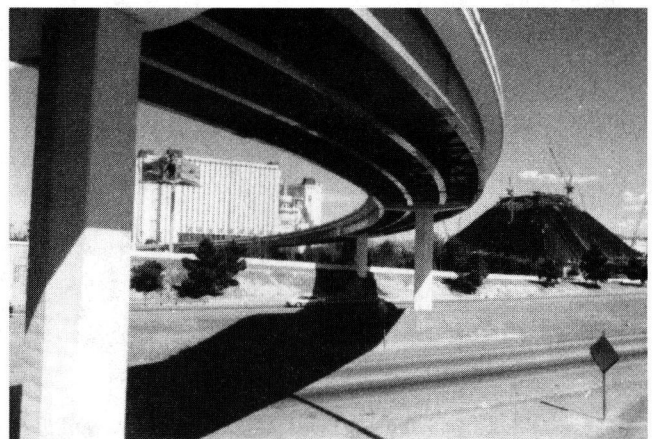


FIGURE 16 I-15 Tropical Boulevard overpass, Las Vegas.

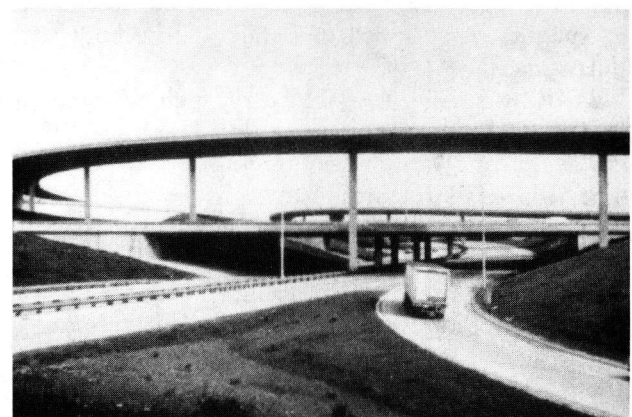


FIGURE 17 Highway 404 ramp, Toronto.



Furthermore, the development of higher-strength concretes should allow for longer spans and more economical construction of cable-stayed bridges. The integrity of these bridges depends on the balancing of compressive strength and weight within the deck, and therefore depends on the concrete composition of the deck. The advantages of higher-strength concrete in bridge decks are not limited to cable-stayed bridges alone. The same concerns that governed the development of cable-stayed bridges now govern the development of new types of suspension bridges, such as this self-anchored single-cable design from Japan (Figure 18).

One of the main goals in the development of precast concrete construction is to enable engineers to design longer spans. However, joining precast segments at the piers, the point of maximum moment, has proven difficult and expensive. In order to provide full live load continuity engineers and designers must continue to develop new techniques. Experience in Kentucky and Colorado shows that the joining of continuous precast beams at their inflection points simplifies the process somewhat and allows significantly longer spans for the same depth of member (Figure 19). Methods under development at the University of Nebraska with expansive concrete also show promise for gaining full live load participation in precast concrete members.

### LRFD Specification

Another area that may result in some change is due to the move to LRFD specifications. Recently, design has been dominated by guidelines about girder spacing, bracing spacing, and other parameters that came out of the current AASHTO specifications. In many cases these requirements aided designers with problems that are difficult to calculate without computers.

The new specifications permit more flexibility, provided that the designer is able to demonstrate the effects

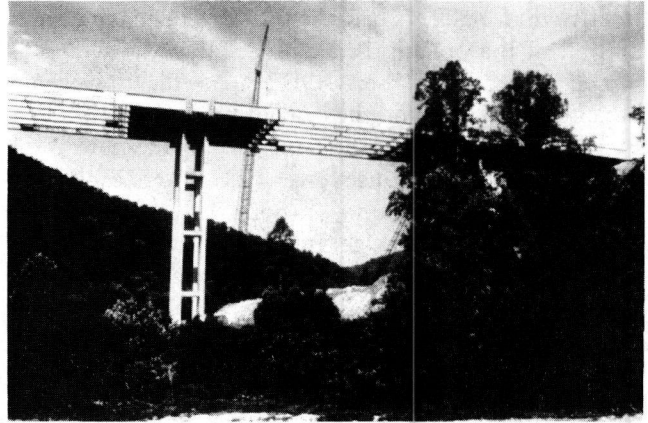


FIGURE 19 Shelby Creek Bridge, Kentucky.

of his or her design. With today's methodology and recent experience with bridges of various types, it is now possible to provide engineering solutions to issues that are tailored to the specifics of the bridge at hand. These solutions in turn have the potential to significantly improve bridge appearance.

For example, wider girder spacing requires more robust girder sections that, taking into account the stiffness provided by the slab itself, make bracing less necessary. This will result in a cleaner underside and make girder bridges more attractive for areas where there is pedestrian traffic underneath. Wider girder spacing also allows additional overhang, which in turn provides a major improvement in the appearance of girder structures. Larger overhangs create larger shadow lines, breaking the bridge up into three horizontal stripes: light, dark, and light. The stripes make the bridge appear thinner than it actually is.

Recent experience with steel box girders shows a similar result. Steel box girders are inherently more at-



FIGURE 18 Hokko Bridge, Japan.

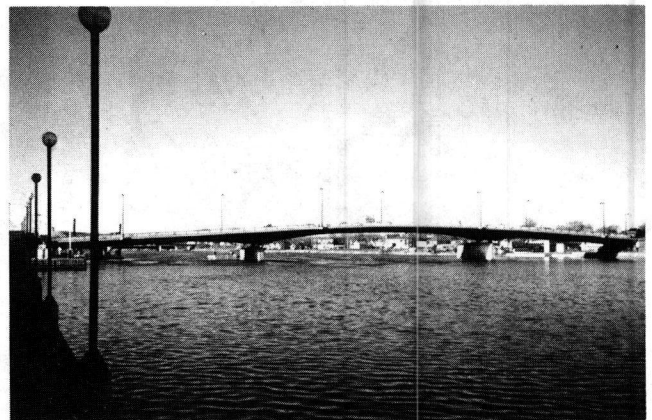


FIGURE 20 Dundas Street over Trent River, Trenton, Ontario.

tractive than I-girders because they can be made thinner and all of the bracing is enclosed. However, when designed according to the AASHTO specifications many boxes are required and the bridges become costlier than I-girder bridges. Given the flexibility of the new specifications, bridges that use fewer box girders can be developed. This saves money in both the fabrication and construction of the bridge. In addition, with fewer box girders the deck overhang is again increased, leading to an apparently thinner and more attractive structure (Figure 20).

## CONCLUSION

Some of the improvements described here represent a continuation of the development of contemporary innovations in, for example, girder bridges. We may expect that those changes will be greeted with approval

and appreciation. However, other changes, particularly those that have to do with truss bridges, represent a return to structural types that some believed had been left behind because of their supposedly poor appearance. With these structures we may expect to see a recurrence of the cycle: new method, disapproval, grudging acceptance, and eventually, accepted practice.

The challenge for the designers of these structures will be to develop structures that exploit and display the inherent advantages of laciness and transparency in their forms while at the same time addressing modern criteria of simplicity and the expression of structural forces.

Beyond these ideas, the new materials offer the potential for structural forms as yet unimagined. We may see again new and exciting structural forms in our midst. We should attempt to welcome these innovations, seek to understand their aesthetic implications, and avoid the historical cycle of adamant disapproval, grudging adoption, and final acceptance.

# Bridge Architecture: The Good, the Bad, and the Ugly

---

R. Ralph Mays, *Washington State Department of Transportation*

The aesthetic element of bridge design is more complex than many bridge design engineers realize. Some view aesthetics as something that gets in the way of a true engineering solution, adds excessive costs, and slows up the project. Others consider visual quality to be as important as structural integrity. A truly beautiful structure has the balance of visual elements that will give it a pleasing appearance throughout time. To achieve visual quality it is important to include an architect who is experienced in transportation architecture on the design team at the very beginning of a project. This early involvement on the design team will give the architect a chance to ask questions and make suggestions in the early stages that will affect the visual quality of the whole project. Individual components, such as bridges, retaining walls, noise barriers, location and style of light standards, sign bridges, transfer facilities, utility conduits, or other attachments to transportation structures, all need to be visually coordinated. Study models and sketches during the design process will give the architect and design engineers the ability to coordinate the visual and structural requirements. Our transportation environment deserves our best efforts.

**T**his paper will not give any magical rules or mathematical formulas that can be used to create beautiful bridges, just as no article of this length could convey the expertise required to design bridges. The important point is the need to consider

appearance during the early design of bridges and other transportation structures. An effective process that can be used to incorporate aesthetics into the design of bridges and other structures in the transportation corridor is sketched out here. Good aesthetics create both a pleasant journey and a safer one. The big picture includes the design of all transportation structures, but the focus of this paper will be mainly on bridge aesthetics.

At this point we should decide what beauty is as it relates to a bridge. Bridge design must be governed by valid visual properties that create order and good proportion. Generally, if we consider the development of bridge design from an aesthetic viewpoint, there is a preference for very slender structures supported by slender, well-proportioned piers. Simplicity and a minimum of elements are also preferable, along with continuous and steady longitudinal lines, either straight or in smooth curves that relate to moving traffic. These qualities make a bridge, sign, or transportation corridor safer and more comfortable for drivers. For example, by limiting distracting visual clutter, signs are easier to read.

We have all heard the saying "Beauty is in the eye of the beholder," which is true. The task is to help create more "beholders" who look at your bridge as beautiful. More beholders are created by considering and incorporating aesthetics into the bridge design process.

We have also heard that beauty is only skin deep but that ugly goes clear to the bone. This seems to be true

with bridge design, because the whole structure must be considered from the very start of design to incorporate aesthetics. If aesthetics are not considered until after the structural design is completed, it is virtually impossible to make an ugly structure attractive by adding surface textures or some kind of false panels (the skin).

Why, then, are some bridges beautiful (and therefore have more beholders) and others are visually unattractive or downright ugly? Maybe some designers do not know how to incorporate aesthetics into their designs. Perhaps some are not concerned with the visual quality of our built environment, wanting only to get from here to there. But, whatever the reason, the features of an ugly bridge result from using principles opposite those that are inherent in beautiful bridges.

What leads to the creation of a beautiful bridge? The most important element is early involvement of someone experienced in transportation architecture. The second important principle is coordination of the designs of all structures in the transportation corridor (bridges, retaining walls, noise walls, signage, sign bridges, lighting, landscaping, rest areas, information centers, etc.). Architectural design guidelines were developed and published in a booklet used by design engineers on the \$2.5 billion I-90 freeway in Seattle (1). A completely new corridor is designed differently from an existing corridor where some structures remain or where a bridge is being replaced. The third important principle is the formation of a multidisciplinary design team.

The multidisciplinary design team consists of all of the design professionals who will collaborate on the project (such as the bridge designer, foundation or geotechnical engineer, traffic engineer, illumination designer, utilities engineer, acoustics engineer, landscape architect, the project engineer, and the transportation architect). The disciplines and size of the team depend on the complexity of the project. One way to explain the effect of such a team is that it "greases the skids" on the design process by drawing on the expertise of a diverse group from the very beginning of the design. For example, if a noise wall ends or starts at a bridge, the acoustics engineer and the bridge designer will find they need to create a junction of some type before they start designing their portions of the project.

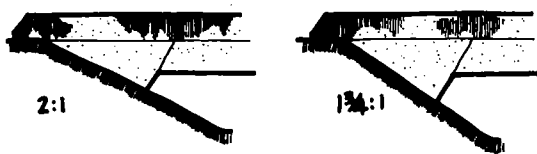


FIGURE 1 Abutments can appear too massive if the slope angle is increased.

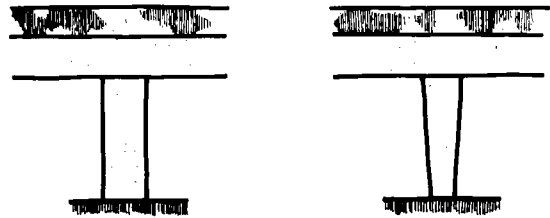


FIGURE 2 Avoid short, stubby piers. Note the visual improvement obtained by making a slight change of the shape of the pier.

As mentioned, this paper will not give rules or mathematical formulas, but the following are insights into the vital visual design elements that should be considered during the design process:

- Scale and proportion: the size as it relates to the surroundings and other parts of the bridge. This involves the abutments, piers, the depth of the superstructure, the span, and the sizes of openings between the piers.
- Line and mass: the appearance of lightness; the flow of the horizontal line.
- Harmony: the relationship to the environment and other structures.
- Order and balance: the orderly arrangement of visual elements.
- Clarity of function: how the form serves its structural purpose.
- Simplicity: a form's lack of complication. Seek simplicity and purity of structure and limit complicated elements. Avoid all useless additives or ornamentation.
- Color and texture: the placement of texture and color to highlight the design elements.
- Aesthetics: the creative combination of all of these elements to form a beautiful structure.
- Constructability: this is not a visual element but must be considered in the design process.
- Economics: just because a bridge has a pleasing appearance does not mean it has to cost more. A beautiful bridge may even cost less than an unattractive bridge. Early involvement by an experienced design team will provide the most economical results.

How do we apply the visual elements listed here to the different parts of a bridge? The following are some useful methods and some parts of a bridge that should be looked at when gathering aesthetic contributions from the design team:

- Sketches and drawings: the quantity and the amount of detail depend on the size, visual impact, and complexity of the bridge.

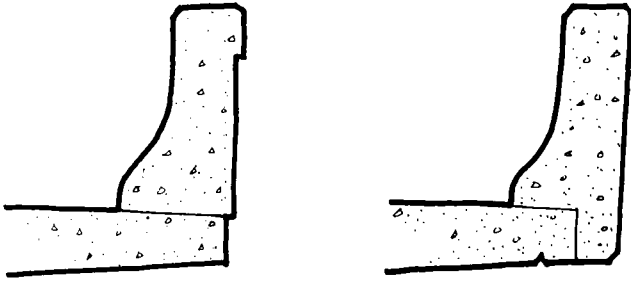


FIGURE 3 Textures and shapes on the bridge barrier face will affect the appearance of the bridge. Also, note the drip groove on the bottom of the deck slab.

- Models: use models to study conceptual ideas during the design process and to present options or proposals to the public or governing bodies.
- Abutments: the size of the abutment must be in proportion to the span and depth of the bridge. A steep slope may make an abutment appear too massive (Figure 1).
- Slope protection: the materials used for slope protection should relate to the bridge or to the surrounding landscape.
- Piers or columns: the type and size of piers depend on the style, width, length, and height of the bridge. Tapered piers are more pleasing than stubby ones (Figure 2).
- Traffic barriers: traffic barriers should have simple clean lines and extend to the bottom of the roadway slab. Put a texture on the outside face to control staining and slope the top to drain to the inside. Specify a sample panel of the texture to be constructed for ap-

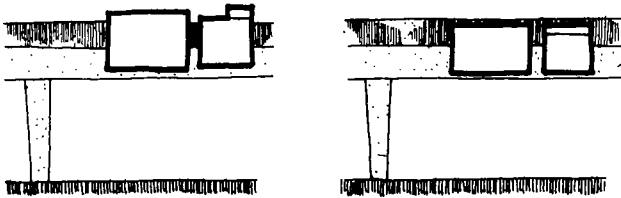


FIGURE 4 As a last resort, attach signs to a bridge, but keep them within the silhouette of the bridge.

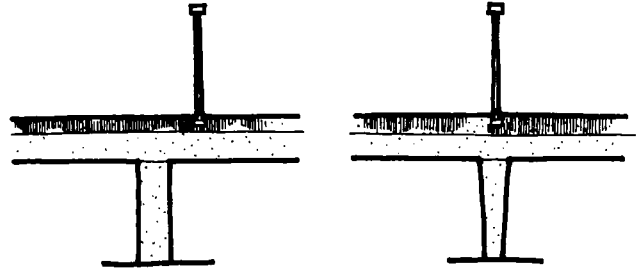


FIGURE 5 Poor placement of light standards can unbalance the visual appearance.

proval before the actual construction of the barrier (Figure 3).

- Signs: if signs must be attached to a bridge, they should fall within the silhouette of the bridge. If there is more than one sign, they should be the same height if possible. Exit number signs should be the same width as the sign below. These guidelines also work with sign bridges (Figure 4).
- Light standards: light standards and other attachments to the bridge that extend above the deck should line up with the pier lines (Figure 5).
- Drip grooves: drip grooves on the underside of the overhang will control staining of the outside face of the bridge girder caused by the construction of the concrete traffic barrier (Figure 3).
- Concrete stain: the use of concrete stains substantially improves the appearance of concrete structures. It not only hides blotchy surfaces but seals and protects the concrete. Graffiti is easier to remove if the concrete stain is also a sealer.

It is up to us to form our own design teams and apply these principles. We can develop a growing following of beholders. It is critical to make the extra effort to gather this team early in the design process. The built environment is worth our best efforts.

#### REFERENCE

1. *I-90 Architectural Design Standards*, revised edition. Washington State Department of Transportation, Olympia, Dec. 1986.

# Humane Urban Aesthetic: US-183 Elevated Project in Austin, Texas

---

Dean Van Landuyt, *Texas Department of Transportation*

Designers at the Texas Department of Transportation were faced with building an elevated bridge 1.3 million ft<sup>2</sup> through the city of Austin. Limited right-of-way and the inherent size of an overhead highway meant that there existed the possibility of building an oppressive architecture among the homes and businesses of the US-183 corridor. Instead of applying the accepted techniques of modern bridge aesthetics, engineers used new fundamentals for designing appropriate regional bridge architecture. The aesthetic design philosophy was to build this important public structure so that it expressed the spirit of Austin as defined by the city's innovative high-technology industry, traditional state architecture, and most importantly its humane, livable quality. Engineers tapped into the iconoclastic creativity common to so many Austin artists. Aesthetics was given equal importance with the other constraints of bridge design: functional requirements and economic demands. Integrity of structure can only be achieved when all three of these elements are fully examined and integrated into every level of decision making. The result is a sound, economical structure that reawakens the notion of creative detailing in large-scale bridge architecture.

**M**uch of the bridge aesthetic design today is a result of engineers simply following technique. Acceptable practices such as reducing the number of structural elements, thinning members, and creating clean lines are readily embraced. Unfor-

tunately these practices have dulled creativity and resulted in ubiquitous, sterile architecture. By immediately applying the near-universal technique, many designers bypass (or aren't allowed to ask) the fundamental question that begins the creative aesthetic process: "What are we trying to express?"

The designers at The Texas Department of Transportation (TxDOT) were faced with building 1.3 million ft<sup>2</sup> of elevated bridge through the city of Austin. Limited right-of-way and the inherent size of an overhead freeway meant that there existed the possibility of building an oppressive architecture among the homes and businesses of the US-183 corridor. Engineers developed the philosophy that they should create an architecture that reflected the values and culture of the community.

## THE CITY

Austin is a highly educated university city that is known for its progressive technological and arts communities and the high quality of life that its residents enjoy. Innovation abounds in this city that is only the 27th largest in the country but 7th in the number of patents its citizens are granted. A total of 480 software firms are headquartered here. The University of Texas is a major cultural force not only in the curriculum it provides but also in its progressive atmosphere for ideas that it fos-

ters. Students as well as artists are attracted to this oasis of creative expression. Many of the arts are embraced here, but Austin is perhaps best known for its thoroughly original music scene.

Visitors and new residents are often surprised by the unexpected beauty of a Texas city. Set on the edge of the hill country, Austin has an abundance of trees and lakes. Austinites are protective of their environment, including the neighborhoods and architectural treasures. With a population of 500,000, the city provides a delicate balance of economic and cultural opportunities without compromising its humane, small-town characteristics that make it so livable.

## DESIGN PHILOSOPHY

The design philosophy for the US-183 elevated project is to balance the functional requirements, economic constraints, and aesthetic qualities of the bridge. The functional requirements consist of project geometrics and structural demands. Economic considerations include first cost and long-term maintenance of the structure. The visual elements should contribute to the overall aesthetic theme. Integrity of structure could be achieved only if all three of these factors were fully examined and incorporated into the bridge.

Only a general aesthetic theme could be outlined before the structural design. Thereafter the myriad of aesthetic decisions were made within the context of structural design where they were balanced by the functional and economic constraints. Consequently, designers had to be sufficiently skilled to move quickly between and capably within all three requirements.

## Functional Requirements

### *Geometrics*

US-183 is an urban corridor with two functions: to carry express traffic across the northern part of the city and to operate as an arterial with extensive commercial and residential development. To meet both of these needs, the corridor will consist of an elevated freeway and at-grade frontage roads that provide access to city streets and adjacent driveways. The elevated freeway will be composed of two separate, parallel structures that each carry three lanes of mainline traffic for a distance of 2 mi. A gap 2.2 m (7 ft) wide between them will allow for a possible future high-occupancy-vehicle bridge. To limit the purchase of expensive right-of-way, the elevated structures will be supported on columns in the wide median and will cantilever over the frontage roads. The frontage roads have already been completed

in a previous construction contract and currently carry all US-183 traffic. The elevated project was let in November 1993, and expected completion is March 1997.

The project is complicated by the need for four elevated entrance and exit ramps that provide access to the elevated mainlanes. Three of these ramps also need to cross at-grade roads at a heavy skew. The other is a direct connector on the fourth level of the IH-35 interchange that also crosses lower roadways at a large skew. The US-183 mainlanes will rise to the third level to pass over the second level IH-35 mainlane bridges. US-183 frontage roads remain on the ground level.

## *Structural Requirements*

Generally speaking, the structural demands are not unusual for a project of this type. The fourth-level direct connector requires a girder deep enough to span 54.9 m (180 ft). Mainlanes are required to span 36.6 m (120 ft) over IH-35. Typical of most interchanges, the structural system has to be able to accommodate flaring roadway widths where ramps merge with mainlanes. Perhaps the most unique feature is that the mainlanes have to cantilever 6.7 m (22 ft) over the frontage roads (Figure 1).

## Economic Requirements

The project is so large that it consumes a significant portion of the budget of the local TxDOT district. Engineers were creative in their efforts to design a bridge that would be as inexpensive as possible. However, department officials were willing to spend more money than for a typical bridge if all three frontage road lanes could remain open during the daytime construction operations and aesthetics were improved. Because of the elegant shape of winged box girders, the ability to set segments at night while one lane of frontage road traffic was shut down, and the potential for a low square-foot cost, a decision was made to build a precast segmental concrete superstructure.

## Aesthetic Requirements

Bridge architecture in the United States has become standardized to the point that there is little regional identity. Fueled by the creative energy of Austin's artistic environment, engineers took on the ambitious task of designing a bridge that embodied the spirit of Austin. Three ideas were adopted to convey this feeling: expressing high technology, referencing architectural tradition, and creating a humane environment.

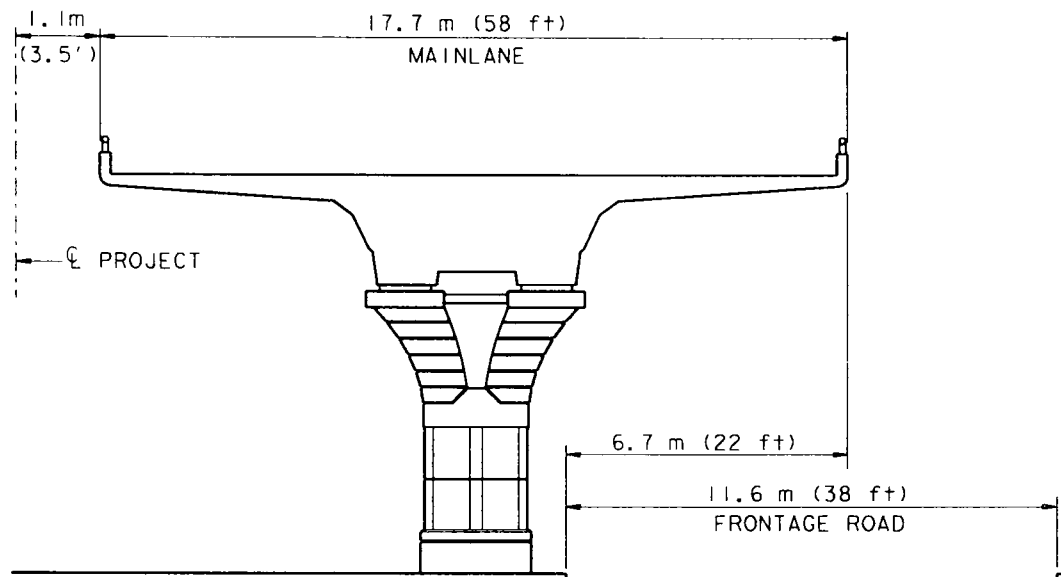


FIGURE 1 Mainline column and superstructure adjacent to frontage road.

### High Technology

US-183 is also known as Research Boulevard—so named because of the large number of high-technology firms located there. This area is home not only to innovative software and microelectronic firms but also to the Phil M. Ferguson Structural Engineering Laboratory. This University of Texas laboratory is known worldwide for its outstanding research in the design and behavior of segmental concrete bridges, much of which is funded by TxDOT. Engineers chose to expose the high-technology structure of the bridge as much as possible. Elements typically hidden in other bridges were to be revealed where appropriate.

### Architectural Tradition

It is proper that Austin's largest highway project reference other state architecture located in the city. Perhaps the greatest architectural treasure is the century-old neoclassical state capitol building. Nearby buildings on the original 40-acre campus at the University of Texas are richly detailed in a Spanish mediterranean style. While referencing these wonderful structures, it was imperative that new designs not be hackneyed or slavishly old fashioned.

### Humane Environment

The most important aesthetic principle is to build a humane architecture for commuters, workers, and residents of the area. There are many ways to create a humane environment, but three principles are followed.

Monotony can rarely, if ever, enrich the visual experience. Unfortunately there is an explosion of sameness in today's bridge designs. TxDOT designers sought first to create a variety of elements but maintain harmony—a delicate proposition. Second, because of the large size of the project and the number of commuters and residents on the frontage roads and city streets, it is important that a personal scale be used where possible. Large elements could be divided into smaller, human-size parts. Finally, the structure should manifest a human presence. Too many of today's bridges exude a coarse, simple, and austere appearance. US-183 designers were free to utilize creative talents to build a bridge with fine proportions and visual complexity and delight.

### DESIGN PROCESS

#### Superstructure

The structural design began by optimizing span lengths originally set by roadway designers. Lower roadway geometrics force a direct connector span arrangement of 38.1 m–54.9 m–43.3 m–54.9 m–38.1 m (125 ft–180 ft–142 ft–180 ft–125 ft) that is best built by the balanced cantilever method. A minimum girder depth of 2.1 m (7 ft) is required for these spans. The remainder of the project (195 spans) can be most economically constructed with the span-by-span construction method. Because the direct connector ties into the mainlanes, a 2.1-m (7-ft) girder depth was chosen for the entire project. Roadway designers had set columns for the span-by-span bridges such that the average span length was 29.5



m (97 ft). Structural designers fully utilized the girder depth and rearranged the column layout. By extending the maximum span to 40.9 m (134 ft), the average length increased to 38.4 m (126 ft). More than 60 foundations, columns, and span construction cycles were thus eliminated.

Geometric requirements dictate that the mainlane cross section be very large. An overall width of 17.7 m (58 ft) is necessary to support three lanes and shoulders. A 4.9-m (16-ft) nominal width box is required for stability. A smaller scale is achieved by chamfering the transverse joints between the segments. Thus the segmental persona of the bridge is suggested rather than hidden. Box girders typically are cast with a rigid corner at the intersection of the web and bottom slab of the box. A large chamfer creates a more organic feel that visually lightens the superstructure. Plinths, necessary to provide level bearing when the roadway surface is in a grade or cross slope, are accentuated to make the superstructure appear less earthbound. Moreover, they create a sense of order within the superstructure. These unique segments, which are designed to handle the heavy bearing and post-tensioning anchorage forces, are visually differentiated from typical segments. Harmony is achieved by incorporating these same elements into the smaller ramp girders [8.5 m (28 ft) wide] (Figure 2).

### Substructure

Engineers started substructure design by examining the structural and geometric demands of the 260 columns on the project. Necessary bearing areas for the superstructure, available footprints, and type and magnitude of loadings were all categorized. It was determined that all demands could be met with as few as three column

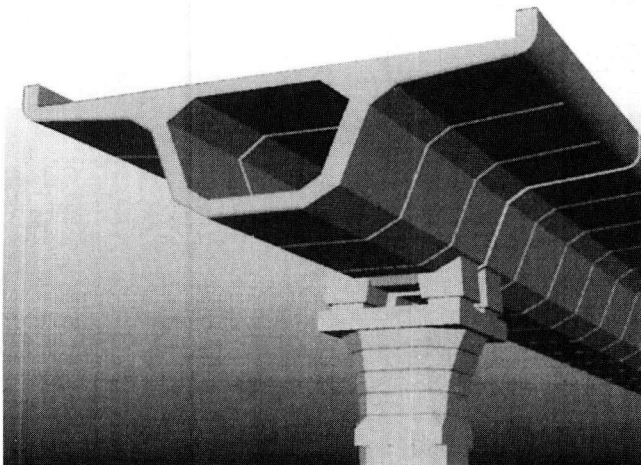


FIGURE 2 Ramp girder and small ramp capital.



FIGURE 3 Small ramp piers in tandem to support flaring box girder.

types. These include 115 mainlane piers, 132 small ramp piers, and 13 large ramp piers. The large ramp piers are needed to sustain severe balanced cantilever loadings from the direct connector. The small ramp piers are versatile enough to support ramp box girders, straddle bents, and the entire flaring superstructure region (Figure 3). The small number of pier types meant that costs could be reduced because of reuse of forms and repeatability of tasks. Visual harmony is also more easily achieved when assimilating fewer elements.

All of the columns on this project were originally designed as precast segmental piers post-tensioned with vertical tendons. Designers thought that this would be the most economical way to construct elements that were so repetitive. Close proximity to adjacent frontage roads, reduced field construction time, better quality control for casting complex column shapes, and the availability of the casting yard also made this an appealing economic option. The resulting segmented appearance of the columns would also fulfill the aesthetic vision. Similar to the superstructure segments, the con-



FIGURE 4 Mainline capital.

struction history of the piers would be revealed and a more human scale presented at the all-important frontage road level. After much deliberation, the winning bidder, Eby Contruction, asked the state to redesign the mainlane and small ramp piers as cast in place in return for a small savings. TxDOT obliged. In keeping with the already established aesthetic concept and creating harmony with the still-precast large ramp piers, the appearance of the cast-in-place piers remained almost identical to that detailed in the original plans. Transverse joints at 1.2-m (4-ft) intervals were maintained as were the oversized bases originally designed as cast-in-place connections between the first precast segment and the foundation.

The columns are the visual focal point of the project because of their close proximity to frontage roads and city streets. All three column types require superstructure bearing areas larger than the column cross sections

needed to resist axial loads and moments. The larger bearing area combined with the large bases required for constructability hinted at the possibility of classical three-part columns.

### *Mainlane Columns*

The bearings of the mainlane superstructure are so widely spaced that ill-proportioned, top-heavy piers commonly seen in bridges across the United States could have easily been designed. There was little to be done about the required top width of 5.2 m (17 ft), so engineers created the illusion of a smaller capital by eliminating the concrete between the bearings (Figure 4). Load is directed downward by diagonal concrete compression struts. Four steel pipes 0.20 m (8 in.) in diameter act as tension ties and reduce much of the flexural moment in the diagonals. The pipes are anchored on the exterior of the capital to create a well-confined structural node. The concrete was also removed with the intention of providing a bearing ledge for erection equipment (Figure 5). The contractor will dispense with tower scaffolding and instead fit a bracket into the opening to efficiently carry the tremendous weight of longitudinal erection trusses and unstressed segments [about 635 Mg (700 tons)].

The pier maintains an element of drama throughout its height balanced by reassuringly correct structural forms (Figure 6). Proportionally undersized tension pipes at the top of the capital tenuously tether two large diagonals. All of this is revealed by slicing away the concrete between the bearings and abruptly interrupting the horizontal rustications. The thrusts of opposing diagonals are balanced by a single, inverted keystone but the visual duality is only briefly unified. A deep rustication, defined by tracing the parabolic inside edges of

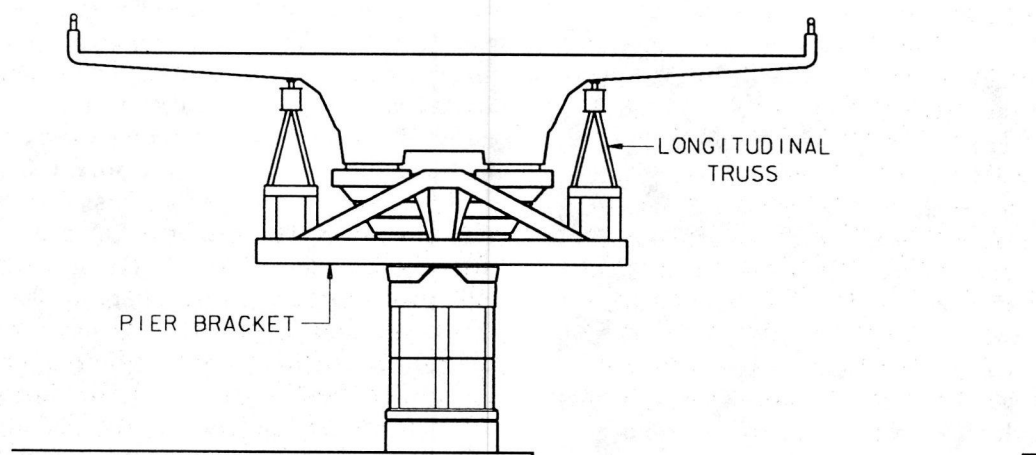


FIGURE 5 Mainline capital notch used to support erection equipment.



FIGURE 6 Mainline column.

the diagonals to their origin as vertical tangents, resumes the duality and slims the shaft. The division is finally and convincingly resolved by a large, banded base.

A large abacus (the flat slab at the top of the column) crowns the diagonals for a variety of reasons. It increases the available bearing area not quite given by the flaring diagonals, references classical architecture, and should improve the long-term appearance of the pier. In spite of sealed fingered joints in the superstructure, it is almost a certainty that water will trickle down the bearings and reach the top of the column. Smoothly detailed columns that flare to follow the shape of the girder historically have provided a large canvas to display stains. All US-183 piers are detailed to channel the water to confined, shadowed areas. A berm 32 mm (1¼ in.) tall on the top of the capital is broken only above vertical rustications on the side of the abacus (Figure 7). A drip bead formed with a 25-mm (1-in.) chamfer strip on the underside of the abacus should prevent water from reaching the compression diagonals.

### *Ramp Columns*

The small ramp and large ramp piers harmonize with the mainlane piers. Because the ramp superstructure bearings are close together, a single undivided capital is used. The abacus, closely spaced horizontal rustications, and oversized lower capital terminus piece are similar to those on the mainlane piers. The shaft cross section is a square with its corners removed by the same heavy 0.20-m (8 in.) chamfers that are used on the mainlane piers. The segmented shaft is supported on the base that visually balances the capital.

### **Balancing Functionality, Economics, and Aesthetics**

Good design requires the integration of functional requirements, economic restraint, and aesthetic quality. Functional demands of the structure provide the origin for all design. From this the engineer relies on creativity

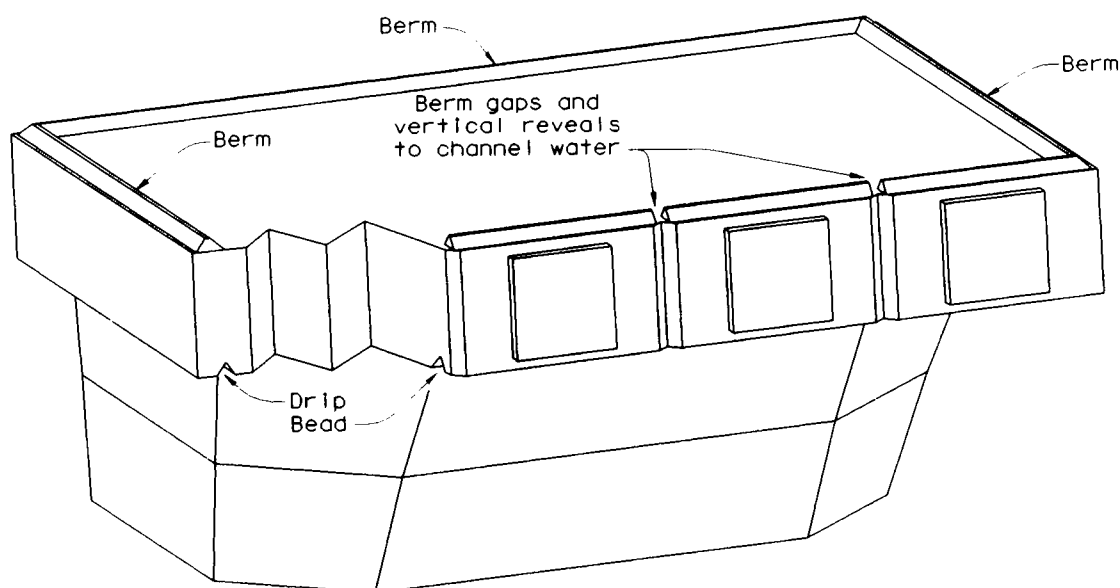


FIGURE 7 Mainline column berm, rustications, and drip bead to reduce water staining.

to instill beauty and meaning while respecting the economic burden of the taxpayers. Most of the unique architectural features probably added little to the overall cost of the bridge. The project bid at \$39.00/ft<sup>2</sup>, about the same as other more traditional span-by-span segmental bridges in Texas, but well below an average U.S. bridge cost of approximately \$70.00/ft<sup>2</sup>. The interplay of the three requirements can perhaps best be understood by examining the design of the mainline column.

Aesthetic design of bridge columns is frequently constrained by a need to build columns of varying height. Costs will increase slightly when a gracefully changing cross section is introduced for a large number of constant-height columns; building designers often use economy of scale to afford their constant-height columns with gentle tapers or classically styled entasis (the subtle convex shape of the column shaft). However, costs become prohibitive for a project such as US-183 where mainline columns range from 3 m (10 ft) to 13 m (43 ft). Therefore, unlike true classical columns the column shaft cross section was kept constant.

It became an economic maxim then that visual complexity could be given to repetitive elements of constant dimension. The capital could thus be flared on a number of planes if it was maintained at a constant height and only the length of the shaft varied. Reveals and chamfers were inexpensive additions because they were detailed with respect to necessary reinforcing steel cover requirements, cage construction, and form assembly and removal. The void in the capital supports erection equipment, visually lightens the capital and reveals the structural requirements of the capital but is probably

the single most expensive architectural enhancement. While the extra cost of a complex form is essentially a one-time cost amortized over many piers, the fabrication of the transverse pipes and the flaring reinforcing cage are incurred at every pier. Nonetheless details were assimilated to control costs and meet structural demands. The void was shaped by smooth planes perpendicular to the upstation and downstation faces of the capital to allow a collapsing interior form to be easily removed.

Realities of structural demands dashed hopes of a more graceful mainline pier. Early sketches were drawn to fine proportions using a smaller cross section for the entire column below the level on the capital void. Moments in the diagonal capital arms resulting from unbalanced gravity loads and wind mandated the use of a wider column.

## PUBLIC REACTION

All artists must first meet their own personal tests of truth and beauty. The individual painter or sculptor need go no further, but the government designer has a duty to provide aesthetic quality to a diverse public. The unusual visual styling of the US-183 elevated project was determined by the engineers and technicians of the TxDOT Design Division and supported at the administrative level both at the division and the Austin district. The public did not provide any input into the architectural theme. Public reaction, however, has been overwhelmingly favorable as evidenced by news re-



ports, letters to the editor of the local paper, letters to TxDOT, and enthusiastic citizen comments made to the designers. Of course, all innovative public art will have its detractors (and perhaps it should lest it not be very innovative), but they have been very few.

## CONCLUSION

Engineers at the TxDOT were challenged by the task of designing a large elevated highway in the city of Austin that enhanced the human aesthetic appeal of the city. Rather than applying the accepted techniques of modern bridge aesthetics, engineers used new fundamentals for designing appropriate regional bridge architecture. The aesthetic design philosophy is to build this important public structure so that it expresses the spirit of Austin as defined by the city's innovative, high-

technology industry, traditional state architecture, and most importantly its humane, livable quality.

To accomplish this, engineers tapped into the iconoclastic creativity common to so many Austin artists. Integrity of structure can be achieved only when aesthetics is fully integrated with functional and economic demands at every level of decision making. The result is a bridge that reawakens the notion of creative expression in large-scale bridge architecture.

## ACKNOWLEDGMENT

A project of this magnitude requires the combined talents of a great number of people. There are many responsible for the so-far successful completion of this bridge, but the author would like to specifically thank the many engineers and technicians who worked so diligently on the design.

# Discovery Bridge

---

Ronald K. Mattox, *Burgess & Niple, Ltd.*

The Discovery Bridge in downtown Columbus, Ohio, is a one-of-a-kind structure that provides unique solutions to historic, aesthetic, and technical issues. Because the bridge was a contributing element in the Civic Center Historic District and was federally funded, FHWA entered into a memorandum of agreement (MOA) with the State Historic Preservation Office. To comply with stipulations within the MOA, FHWA assembled a community interest task force, representing regional planning, Columbus development, historic preservation, and arts organizations. This task force identified architectural design parameters/criteria for the replacement bridge. To incorporate the input from the task force, public agencies, and private individuals, a unique and innovative bridge study process was developed. The new process included separate and intense engineering workshop sessions followed by presentations to the task force and general public. Within each session, the design team reviewed all input, developed ideas, evaluated alternatives, and prepared presentation sketches and renderings. The resulting structure is reminiscent of the previous bridge, respectful of the historic district, and a center for civic activities, and it was constructed using the latest in bridge design and construction technology.

**T**raditionally, federal, state, and local agencies have been responsible for maintaining the nation's transportation system at the highest level of service possible with limited resources. This has meant construction of new facilities and repair or replacement of existing facilities at a cost of billions of

dollars annually. These expenditures, however, have not been sufficient to gain ground on the ever-increasing deterioration of the system. To stretch the budget as far as possible and provide a sufficient level of service, responsible agencies have had to provide a no-frills system. This can be seen in the Interstate system designed and constructed primarily in the 1950s and 1960s. This system was designed to meet the basic purpose of transporting goods and people across this nation. Many standard bridge types and details were developed to reduce design and construction time and minimize costs. Some of the details do incorporate aesthetic considerations; however, the primary purpose was to develop utilitarian structures that could be applied as frequently as possible without changes. Some very notable structures have been exceptions. These bridges, because of their location, history, or significance, have received special attention during design and construction.

In recent years, the utilitarian attitude has shifted. It is no longer enough to provide facilities that just get people from Point A to Point B. It has become apparent that these facilities will be around for many decades. At every level of government more consideration is being given to the impacts these facilities have on our living environment. New bridges, rehabilitations, and replacement bridges are being evaluated for their visual impact and, depending on the location and significance of each bridge, the aesthetics are given a much more significant role in the design. Not all bridges warrant more than just minimum aesthetic consideration, but in some situations it may be given a role equal to or greater than

the technical design. One such bridge is the Discovery Bridge over the Scioto River in downtown Columbus, Ohio.

As the primary access across the Scioto River in downtown Columbus, the Discovery Bridge has always been a major structure. The current bridge, completed in June 1992, is the latest of six bridges to exist at this site. It replaces a bridge that stood for 60 years serving the public until time and deterioration took its toll. This fifth bridge was constructed between 1918 and 1921 at a cost of \$659,000, replacing a truss bridge destroyed in the 1913 floods that devastated much of the Ohio River Valley.

The bridge constructed at that time was a concrete seven-span, barrel-arch structure with an overall length of 679 ft (Figure 1). The bridge carried six 10-foot traffic lanes on an earth fill supported by the arches and spandrel walls. On each side, 12-ft sidewalks spanned between the interior earth walls and the exterior fascia to form a vault used by utilities to get across the river. The fascia incorporated columns at each pier and at the abutments to highlight these locations and break up the large areas of concrete. A limestone balustrade was located along the bridge and was later extended along the top of the floodwall.

For many years, the bridge served the people of Columbus; however, in 1962 the sidewalks had to be overlaid, and in the early 1980s inspections reported significant deterioration. In 1983, the Franklin County Engineer's Office initiated a study to determine the structural condition of the bridge. This study included an in-depth inspection and destructive tests of core samples. In 1985, representatives from FHWA, the Ohio Department of Transportation (ODOT), the Franklin County engineer's office, the City of Columbus, and the inspection consultant met and decided that replacement

of the bridge versus rehabilitation was the only feasible alternative.

That bridge was both graceful and elegant while conveying a feeling of strength and permanence. The bridge served for many years as the gateway to the city and as a focal point for city events. At the time of construction, the bridge was considered to be an outstanding structure. In spite of this and its importance to the area, the bridge was never considered to be historically significant in its own right. It was, however, a contributing structure in the Civic Center Historic District eligible for listing in the National Register of Historic Places. This district is composed of seven buildings and three bridges. To mitigate the impact of the bridge replacement on the historic district and the significance to the city, FHWA entered into a memorandum of agreement (MOA) with the State Historic Preservation Office (SHPO) and the Advisory Council on Historic Preservation (Council). Within the MOA were four stipulations:

1. Recordation,
2. Plaque,
3. Coordination, and
4. Dispute resolution.

The third stipulation required that "FHWA continue to coordinate with the SHPO and other local agencies in the selection of the architectural design parameters for the replacement structure." To comply with this, FHWA created a community interest task force (CITF). This group included representatives from the following organizations:

- Mid-Ohio Regional Planning Commission,
- Downtown Columbus Community Improvement Corporation,
- Development Committee for Greater Columbus,
- Franklin County Commissioners,
- Columbus Historic Resources Commission,
- Columbus Landmarks Foundation,
- City of Columbus,
- Greater Columbus Arts Council, and
- Ohio Preservation Alliance.

CITF was charged with developing design parameters for design of the new Broad Street Bridge. In addition, CITF would review the preliminary bridge design and provide comments to the SHPO, which had review and approval authority of the preliminary design. In June and July of 1988, CITF met and developed 15 parameters. The following parameters were submitted to the Franklin County engineer for utilization by the design consultant.

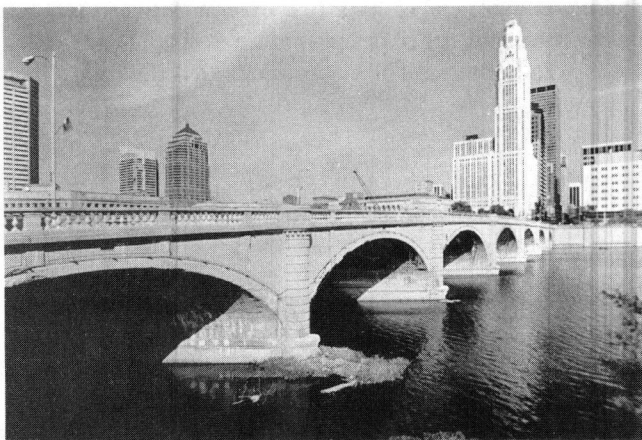


FIGURE 1 View of Broad Street Bridge in 1989.

1. Feeling of permanence/established/older,
2. Feeling of pedestrian friendliness/safety and security,
3. Articulated surfaces/sculptural form (molding, rustication) balustrades, railings,
4. Preference for curved arches (seven) (roundness)/full vaults (solid barrelvault),
5. Graceful/uncluttered line/open,
6. Continuity between bridges (Broad and Town) and railings and walkways,
7. Setting for Civil Center activities,
8. Well-defined entrance/exit,
9. View of bridge and district; view from bridge,
10. Connection between two sides of river,
11. Feeling of serenity/peaceful,
12. Use of concrete or masonry, color/texture/blend into district/warmth versus cold,
13. Use of bridge balustrades to blend into materials of district,
14. Unified classical design (irregular surface—shadow effect), and
15. Classical scale and proportion.

In August 1988 the "world class" team of Burgess & Niple, Limited; Leonhardt, Andrä und Partner; and H2L2 Architects/Planners was selected to design the replacement for the Broad Street Bridge. Burgess & Niple was the team leader assigned with overall coordination and management of the project, bridge design, and all plan preparation. Leonhardt, Andrä und Partner, from Stuttgart, Germany, was responsible for conceptual and final design of the bridge superstructure. H2L2 Architects, from Philadelphia, provided the bridge architectural expertise.

From the beginning of the project, the Franklin County engineer recognized that many people would be concerned about the design and aesthetics of the replacement structure. They were also aware of FHWA policies about alternate designs. To achieve the county's goal of obtaining approval for a single bridge design, a process that was sensitive to local concerns and that met FHWA and ODOT requirements, was critical. Burgess & Niple developed a process that included two separate design sessions followed by presentations to both CITF and general public. Each of the sessions was extremely intense and focused.

The first design session was held in early September 1988. Participants included representatives from the Franklin County engineer's office, the city of Columbus, and the design team. For 1 week, this design group met in an isolated conference room away from all outside distractions. This allowed full concentration on the session goal of developing approximately 12 preliminary alternatives.

The session was divided into five separate phases:

1. Information phase,
2. Creative phase,
3. Judgment phase,
4. Development phase, and
5. Analytical phase.

The objective of the information phase was to present the design group with all relevant data on the project firsthand. During this phase, all representatives of utilities affected by the project were invited into the session to discuss their on-site existing facilities, construction aspects, and future needs. Representatives from FHWA, the city of Columbus, and the Franklin County engineer's office were also invited to discuss the project from agencies' and communities' perspectives. All pertinent data and previous work were collected and reviewed by the design group.

Following the review of all data, concerns, and information concerning the project, the design group entered the creative phase. This phase was a brainstorming session to list all the possible alternatives that could serve as a solution to the Broad Street Bridge replacement. Judgment of the ideas was suspended to allow a free flow of ideas. The design group listed over 115 possible alternatives.

In the judgment phase, alternatives not worth further development were eliminated. The first step in this phase was to list all parameters that would affect the structure. Included were CITF's parameters, construction cost, safety, historic compatibility, ability to accommodate future riverfront development, and more. Advantages and disadvantages about the parameters were then listed for each alternative.

On the basis of the design team's judgment, each of the alternatives was rated on a scale of 1 to 10 (10 most desirable, 1 least desirable). All alternatives receiving a rating of less than 6 were dropped, reducing the number of alternatives to approximately 50. The parameters were then refined and consolidated into five encompassing categories. To avoid confusion between CITF's parameters and other design parameters, the categories were called criteria. The criteria included the following:

- Life cycle costs
  - Initial costs of construction,
  - Maintenance costs (including service life), and
  - Inspection costs;
- Compatibility
  - Ability to accommodate riverfront development,
  - Ability to accommodate festivals and special events;
- Constructibility
  - Construction time,
  - Simplicity, availability of local contractors,



- Accommodation of utilities, and
- Availability of materials and equipment;
- Fundability
  - FHWA and ODOT participation in construction costs and
  - Alternate sources of available funds;
- Historical/Aesthetics
  - Visual impact,
  - Historical compatibility,
  - Proportions, continuity,
  - Scale, and
  - Obstructiveness/openness.

Criteria were then inserted into a scoring matrix with the purpose of comparing categories and assigning a measure of importance to each. The result was as follows:

<i>Criterion</i>	<i>Weight</i>
Life cycle cost	6
Compatibility	7
Constructibility	3
Fundability	4
Historic/aesthetic elements	10

The remaining alternatives (over 50) were then rated using the weighted criteria. The score for each alternative was totaled and a second list of alternatives was created.

The highest scoring alternative from each bridge type above-deck support structures, arch structures, girder structures, etc.) made up the short list of 19.

These alternatives were then investigated in some depth in the development phase. The following material was prepared for each alternative to aid the design team in further evaluation:

- Sketches,
- Preliminary design calculations,
- Critique on aesthetic and historical impact, and
- Relative cost estimates.

On completion of the development phase, the design team began the analytical phase. Using the new material, the remaining alternatives (19) were again rated. Thirteen alternatives were short listed on the basis of the score. These 13 alternatives were the preliminary alternatives presented to FHWA, ODOT, CITE, and the general public.

On October 12, and 13, 1988, the 13 preliminary alternatives were presented to FHWA, ODOT, CITE, and the public, respectively. Preliminary alternatives were presented in soft-line, black-and-white sketch format illustrating basic shape and form (Figures 2 through 5). Aesthetic elements (i.e., texture, lighting, railing) had not been developed at this time and were not presented. The design group requested feedback on basic form of the preliminary alternatives. To facilitate

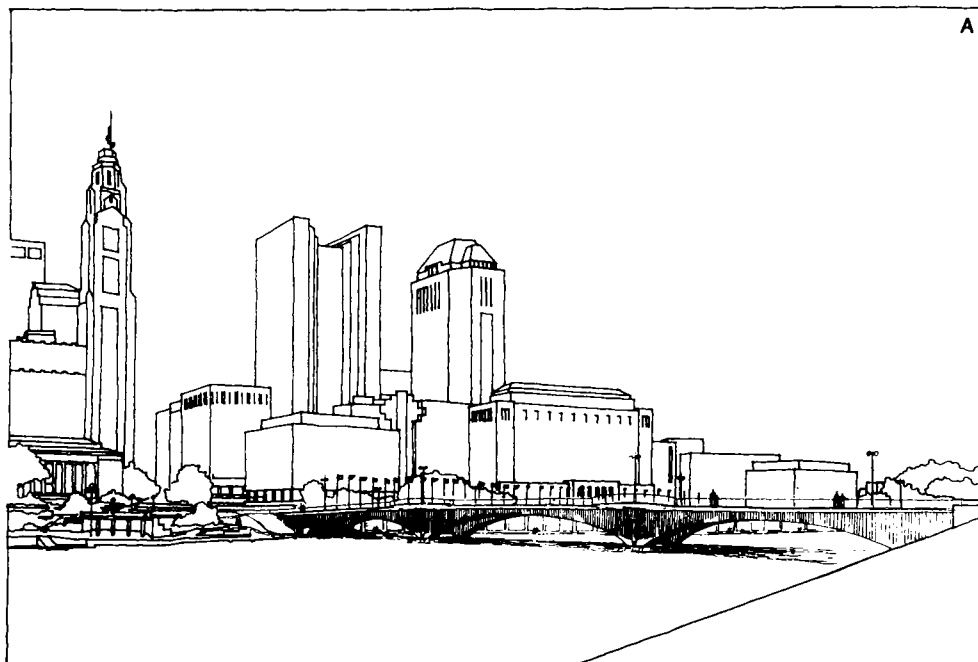


FIGURE 2 Preliminary Alternative A.

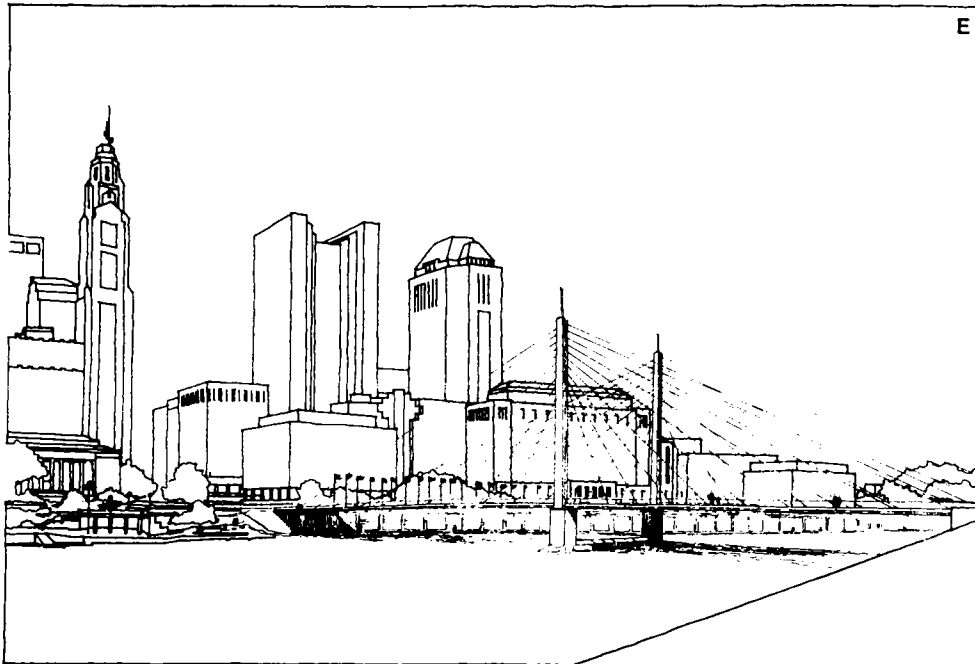


FIGURE 3 Preliminary Alternative E.

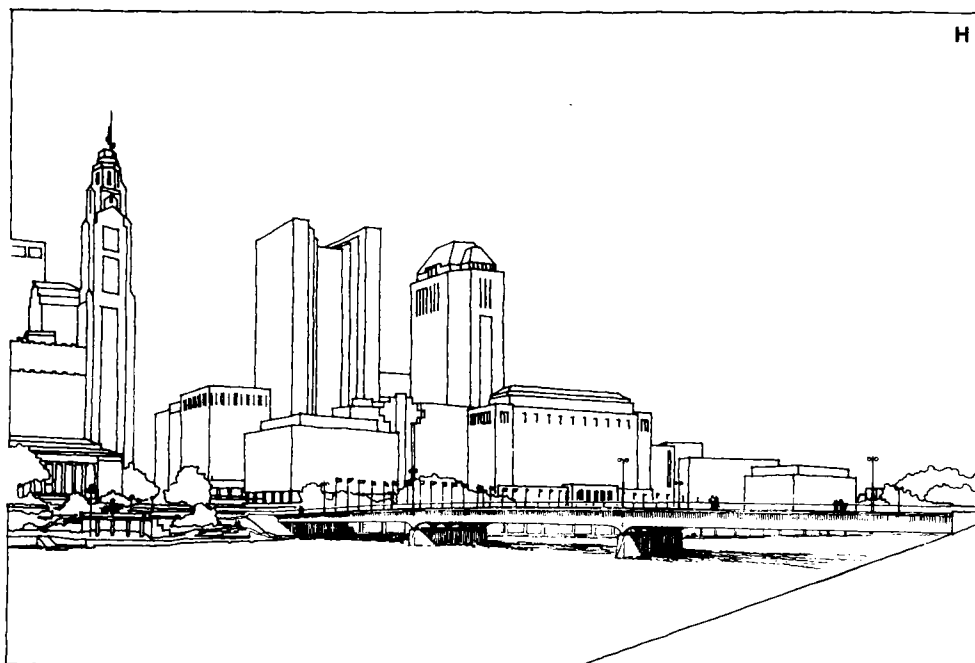


FIGURE 4 Preliminary Alternative H.

this process, a handout with survey was presented and distributed.

Each participant was urged to fill out all of the survey forms. The following was concluded from responses:

1. The majority of those responses ranked criteria the same way as the design team.
2. Constant depth structures were not well received.
3. The public either hated or loved the cable-stayed structure.
4. Steel structures were not well received.
5. Arch-shaped structures were well received, with the plate arch family receiving the most acceptance.
6. There was concern regarding the length of deck cantilevers and the resulting shadow effect.
7. A five-span arch-shaped structure should be developed for further consideration.
8. Significant visual elements should be included, such as railing lighting.

During the week of October 24, 1988, the second design session was held. The first order of business was to review responses from the task force public meetings. On the basis of responses and engineering judgment, the following preliminary alternatives were eliminated from further development:

- Constant-depth bridges,
- Cable-stayed bridge, and

- Steel bridges.

This reduced the preliminary alternative list from 13 to the following:

- Three-span concrete plate arch,
- Three- and four-span concrete twin frame,
- Three- and four-span concrete continuous haunched girder, and
- Three- and four-span concrete continuous deep haunched girder.

The list of alternatives was also expanded to include five 5-span structures. This created a new list of alternatives for further study during the design session.

Before the design session, a model of the site (scale: 1 in. = 30 ft) had been prepared. Study models of each of the alternatives on the new list were developed for review and evaluation while the design team proceeded to its next task of the design session.

On the basis of input received from the meetings, the criteria used to arrive at the preliminary alternatives were modified as follows:

- Life cycle costs,
- Compatibility,
- Constructibility,
- Fundability,
- Aesthetics, and
- Historic elements.

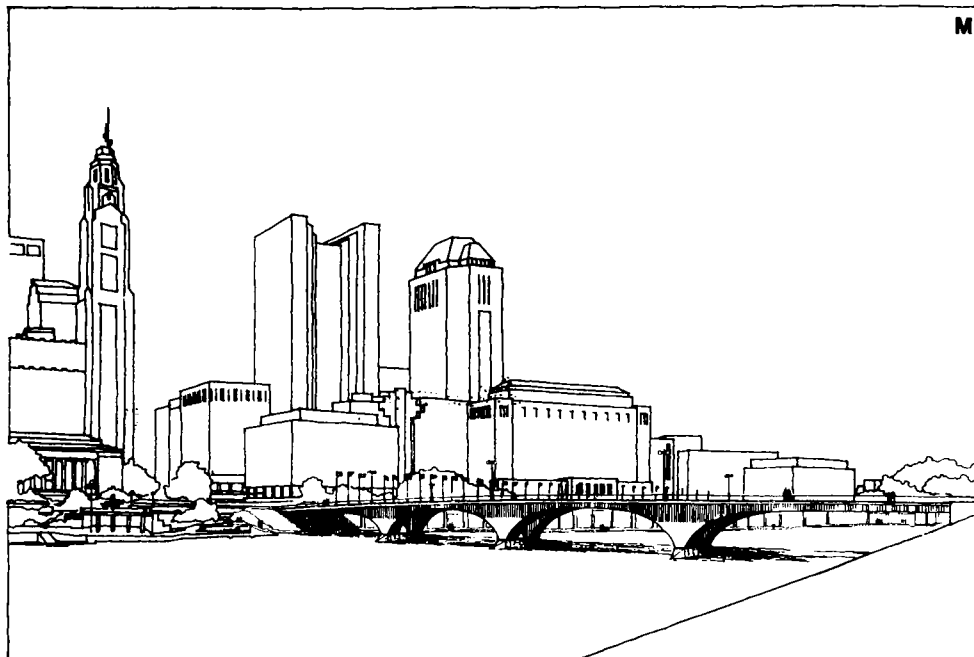


FIGURE 5 Preliminary Alternative M.

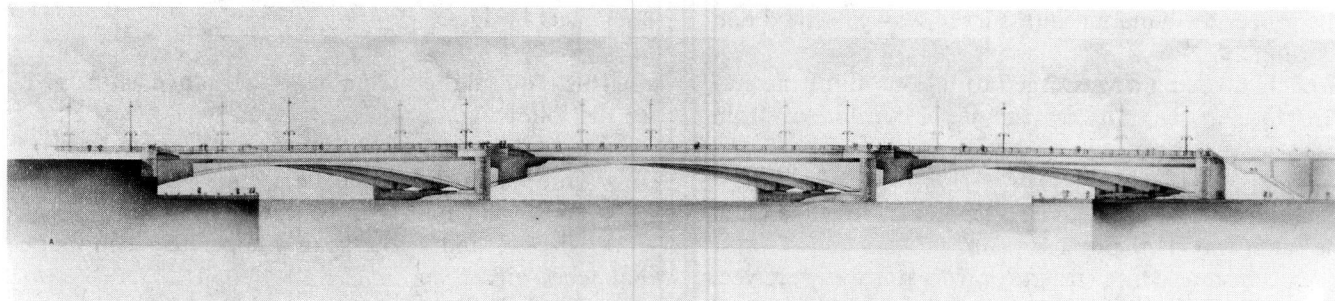


FIGURE 6 Rendering of Feasible Alternative A (7 ft long).

In a manner similar to Design Session 1, the criteria were inserted into a scoring matrix and the following measures of importance were determined:

<i>Criterion</i>	<i>Weight</i>
Life cycle cost	4
Compatibility	6
Constructibility	2
Fundability	3
Historic elements	6
Aesthetics	10

Using all available information and the model, each of the alternatives was rated. The three highest scoring alternatives became the proposed feasible alternatives.

Feasible alternatives included two 5-span and one 3-span plate-arched bridges. The difference between the five- and the 3-span alternatives was the termination location of the end arches, either high or low. All three were scaled and proportioned along lines appropriate for geometric limitations of the site. They also retained key visual elements of the existing bridge and surrounding architecture.

On December 8 and 15, the feasible alternatives were presented to FHWA, ODOT, SHPO, CITF, and the public, respectively. At those meetings the design team presented color renderings of each feasible alternative (Figures 6 through 8) and presented ideas on lighting,

texture, color, railing, and shadows, emphasizing that the elements shown were only ideas illustrating possibilities and not finalized items (Figures 9 and 10).

Participants were asked to focus primarily on shape. Survey forms given to CITF requested that they rank their parameters in order of importance and evaluate each alternative on the parameters. The public was requested to comment on preference. Both CITF and the general public were also requested to provide input on architectural elements presented.

After the presentations, the design team again evaluated the responses. These were in general a statement of which of the three alternatives was preferred. As could be expected, there was no single alternative that stood out clearly as the preferred, although the five-span alternatives were preferred over the three-span. Since no clear preferred alternative came out of the presentations, it was decided to carry all three for further development. Responses about the architectural elements were also reviewed and applied to each of the three feasible alternatives.

Responses received on the proposed alternatives did not indicate a need for further refinement of the evaluation criteria. Therefore, each alternative was further developed and evaluated on the basis of life cycle cost, compatibility, constructibility, fundability, and historic elements/aesthetics. In addition, the design team evaluated the feasible alternative on the basis of the CITF

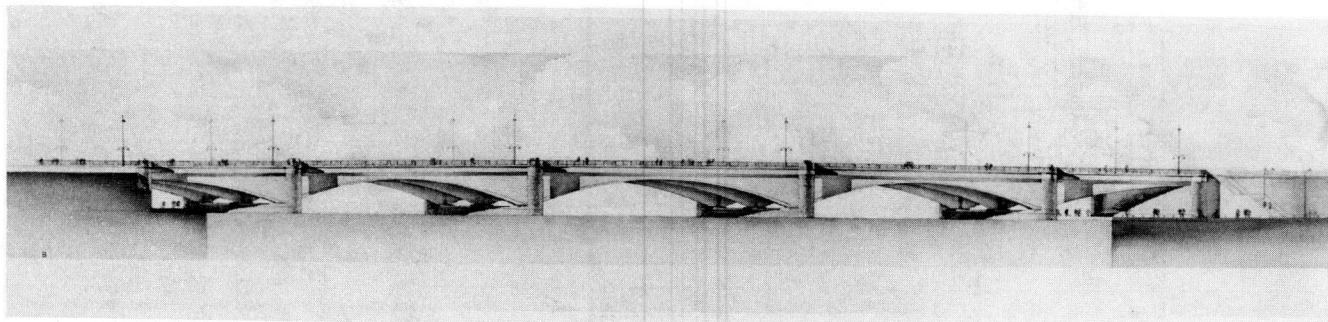


FIGURE 7 Rendering of Feasible Alternative B (7 ft long).

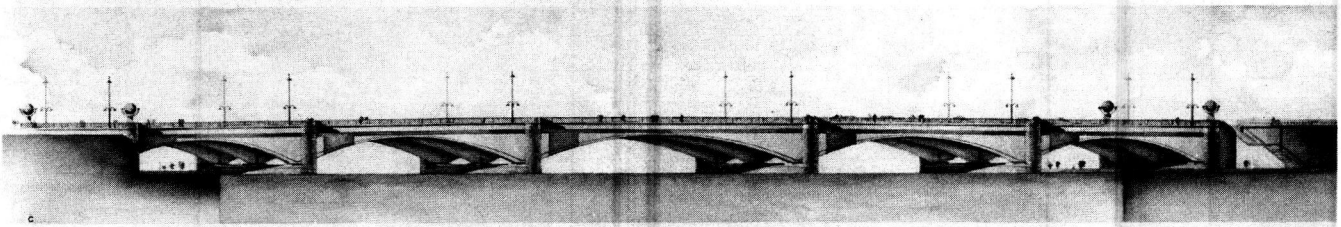


FIGURE 8 Rendering of Feasible Alternative C (7 ft long).

parameters. Each of the alternatives met the parameters to various extents.

In February 1989, all three feasible alternatives were submitted to ODOT for review and approval. The design group recommended the five-span alternative having end arches ending high. This recommendation was based on the input received from all organizations and

the public and on basic engineering judgment. In August 1989, the recommended alternative was approved by ODOT and FHWA, and the design team was authorized to begin final design.

Incorporation of historic and aesthetic elements into the final bridge design required a unique design concept. All elements were integrated into the structural design

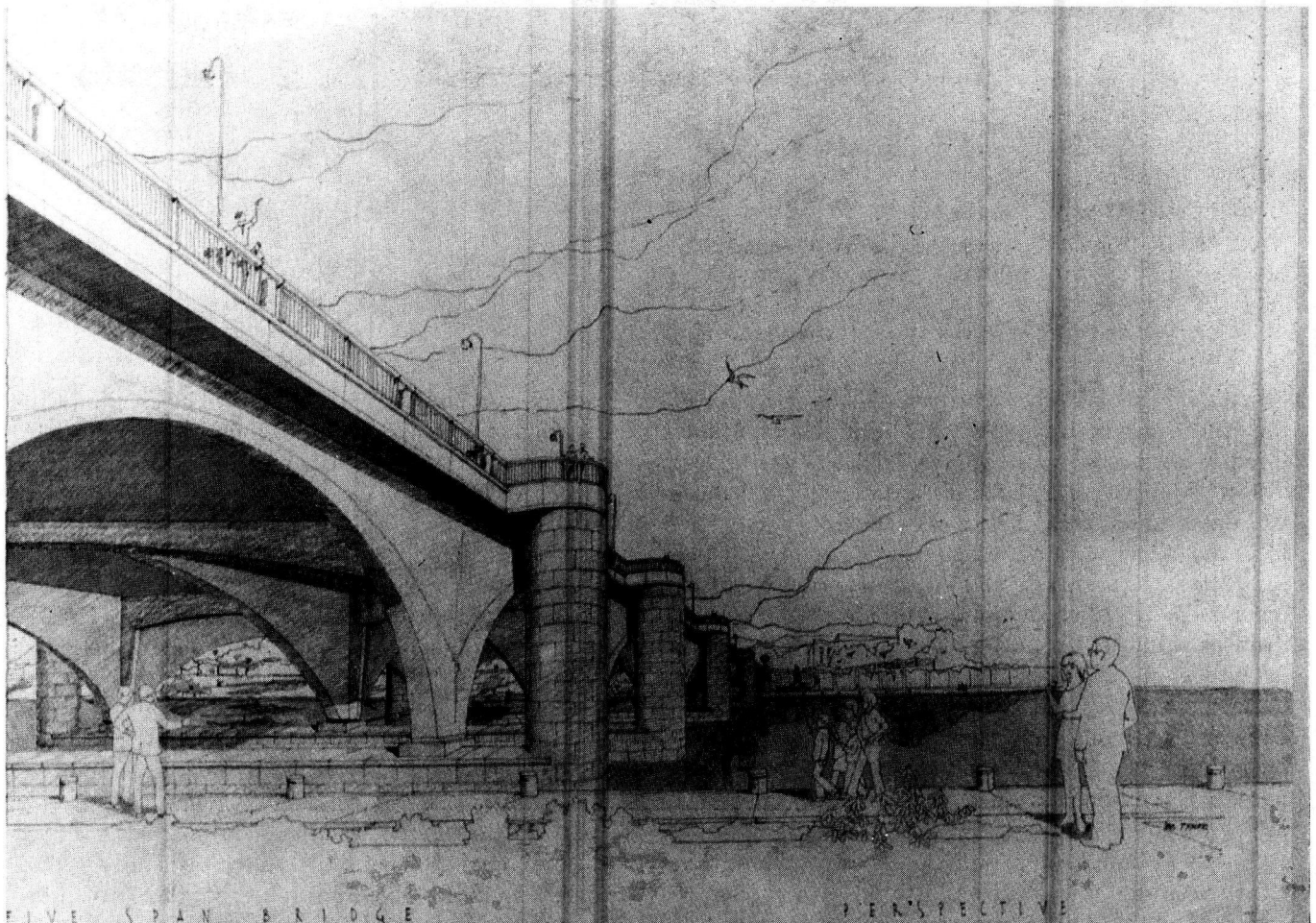


FIGURE 9 Feasible Alternative A: perspective view.



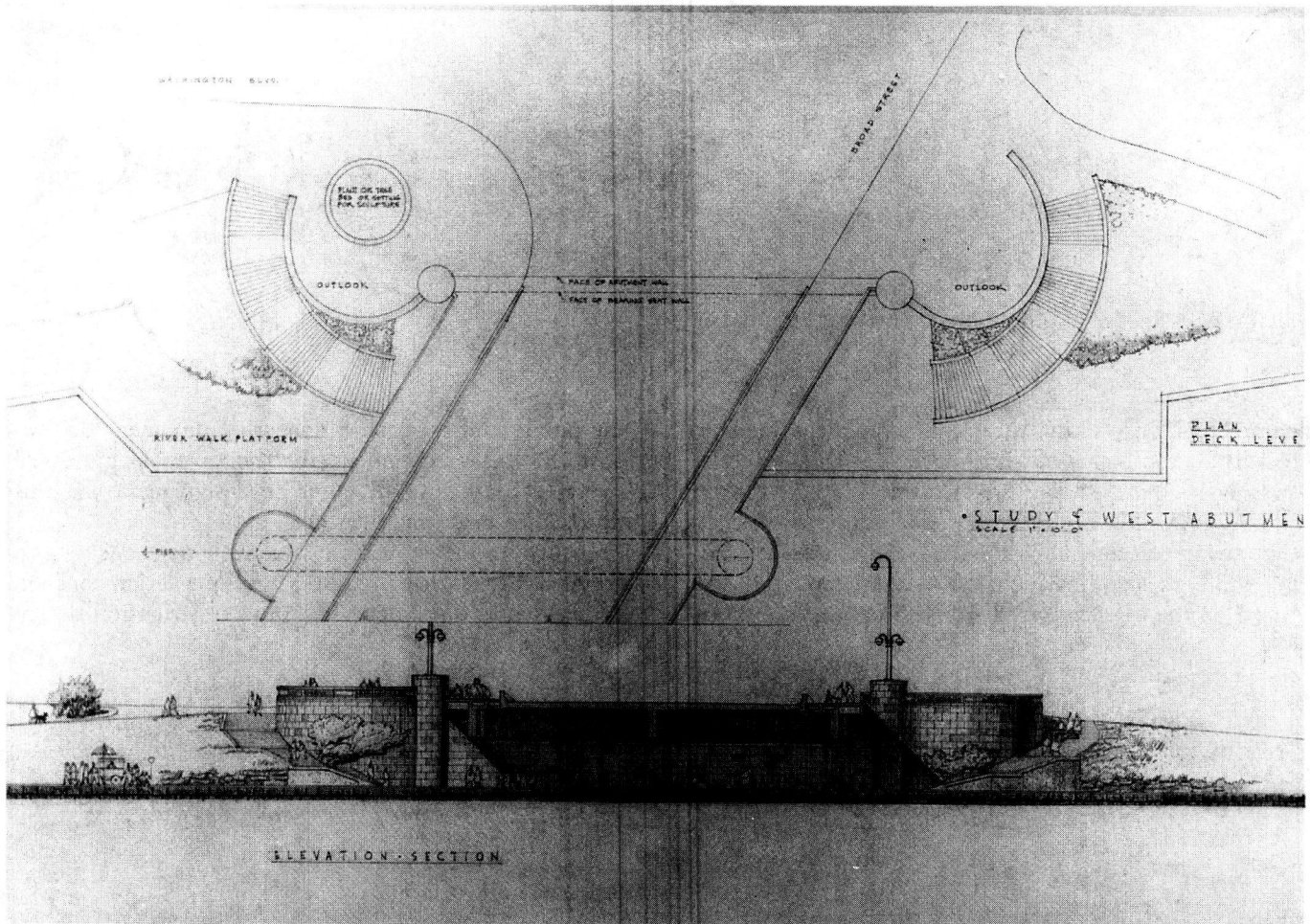


FIGURE 10 Plan and elevation views of west abutment.

instead of being add-ons or afterthoughts. For example, the balconies provide pedestrians with a comfortable location to view the river, the riverwalks, and the bridge. The preliminary concept for the balconies placed them on large columns separated from the bridge. These were to be reminiscent of the pilasters that existed at each pier of the previous bridge. From a structural perspective, the separated columns created several problems. But placing them back into the arched girders as on the old bridge allowed enough area at the bottom of the pilaster to carry the extreme bridge loads to the bearings. These extreme loads required design of the largest known bearings of this type in the United States. At the top of the pilaster, a transition to the 8-ft balcony projection was achieved with a trumpeted cap (Figure 11).

Another example of integrating historic and aesthetic elements within the structural design is seen in the bridge rail and plaza balustrade. The rail is designed to meet current federal standards for static loads and is

reminiscent of the previous bridge rail by creating a similar rhythm and openness. Rectangular concrete posts evenly spaced between balconies frame structural rail segments. Each segment incorporates slender vertical pickets between vertical and horizontal structural members, a brass handrail, and cast bronze medallions (Figure 12). Each medallion located at the center of each segment depicts either the Columbus coat of arms or three sailing ships on the ocean. The plaza balustrade is also designed to current standards and replicates the previous balustrade.

Plazas, like the balconies, provide areas for pedestrians to relax and enjoy the surroundings. At the west end, circular plazas include landscaping at the center, walkways to other attractions, and circular stairways down to the river (Figure 13). At the east end, the plazas provide a comfortable transition from the hectic downtown streets to the relaxed atmosphere found down the stairways, along the riverwalk.

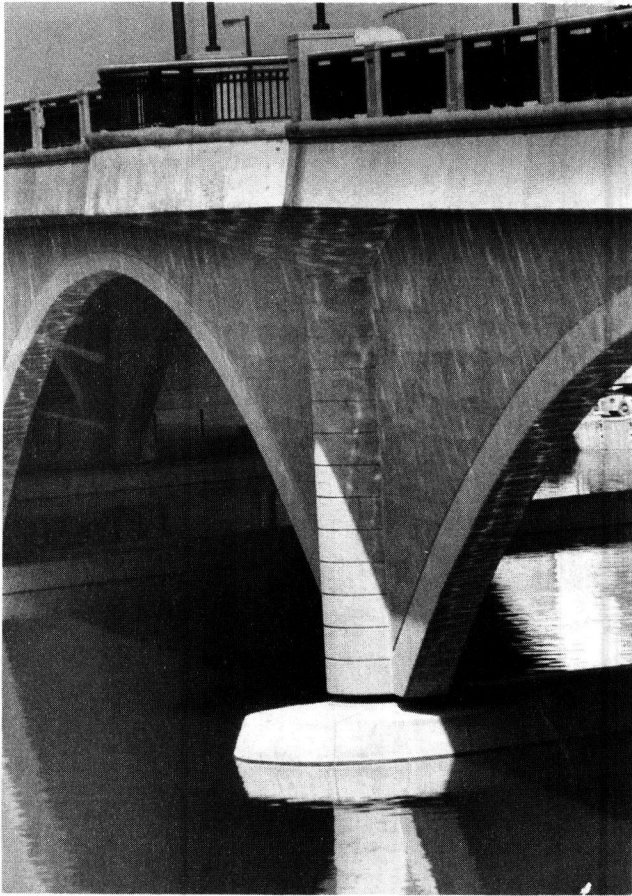


FIGURE 11 Pier pilaster, trumpet, and balcony.



FIGURE 12 Rail segment with bronze cast center medallion.

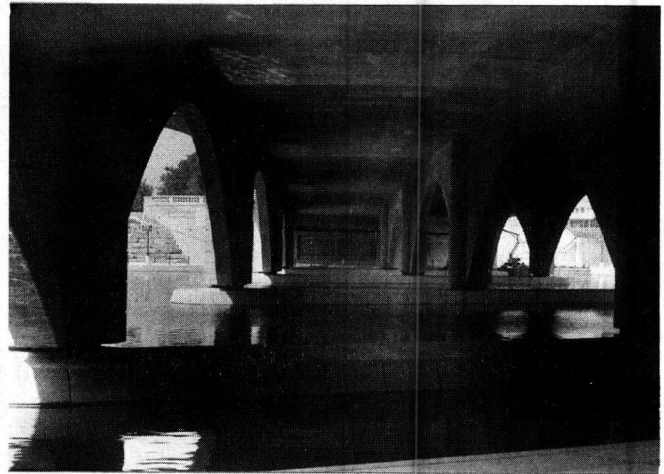


FIGURE 14 View of circular southwest plaza.

The riverwalks extend along the river and under the bridge and connect into adjacent parks. Walking along the river people experience a friendly, peaceful feeling. The bridge itself provides a feeling of safety and permanence. The view of the bridge and abutments from the riverwalks shows the graceful, uncluttered lines and the repetition of the arch form and articulated surfaces (Figure 14).

The design concept for the bridge itself is a unique solution to both the technical and nontechnical issues of this project. Six lanes of traffic and two sidewalks are carried by a deck 100 ft wide. A deck thickness of only 1 ft 6 in. is achieved through the use of the post-tensioning structural system. The deck is supported by three plated arched girders. Post-tensioning allows the heavy loads to be carried by these girders that are only 2 ft 6 in. wide. The interaction between the deck and

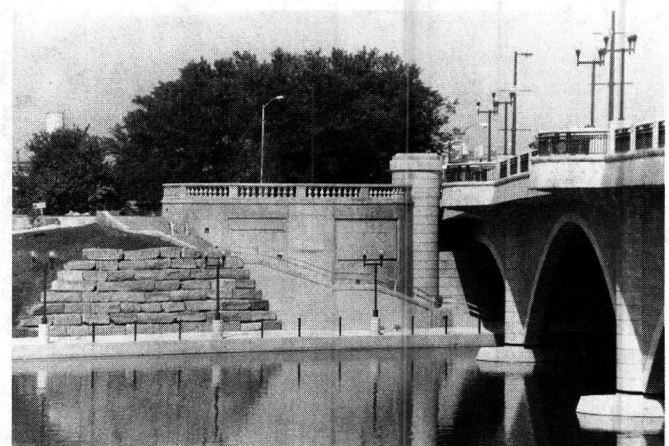


FIGURE 13 View beneath bridge from riverwalk.



girders maintains the stability of the entire bridge without the use of cross frames that would add clutter and block the view below the bridge (Figure 14). Each arch forms three full arches and two half arches at each end. These are reminiscent of the previous bridge and provide a continuity with the adjacent Town Street bridge and a feeling of openness (Figure 15).

The entire bridge is made of concrete. This is in harmony with the district that surrounds the bridge. The color of the concrete used was modified through the use of the same local natural sand used in the previous bridge and existing floodwalls. Concrete also provided an opportunity for surface textures, sculptural forms, and rustications. This greatly enhanced the visual appeal of the bridge, abutments, piers, and riverwalks.

The urban setting of the project made the nighttime appeal of the bridge as important as the daytime appeal. A portion of these architectural designs focused on the project lighting. Riverwalk, sidewalk, and roadway lighting were designed together to complement each other and the district. The light also creates a feeling of safety and comfort. In addition to the normal street and pedestrian lighting, aesthetic lighting has been designed. This system of fiber optic lights and floodlights highlight features of the bridge.

Early in the project the design team recognized the significance of the bridge with regard to the 1992 Columbus's Discovery of America celebrations. The new bridge, appropriately named "The Discovery Bridge," is dedicated to the spirit and accomplishments of Christopher Columbus and other great discoverers. An arts program was conceptualized to commemorate this theme. The program would create specific elements on the bridge that would focus on a specific subject. These elements and their subjects would include the following:



FIGURE 16 Overall view of bridge.

- Portal sculptures—discoverers of the cosmos;
- International discovery medallions—global discoverers;
- Ohio discovery plaques—Ohio discoverers; and
- Landscaped plazas—local discoverers.

Throughout the design, major efforts were made to integrate the historic, aesthetic, and structural elements. The overall view and feel of the completed bridge is proof of how well this was accomplished (Figures 16 and 17).

Looking back on the design process, there are several lessons to be learned. The primary lesson is that the process is as important as the final outcome. Without the support developed through the process, the project will not reach its ultimate potential. Involvement of all

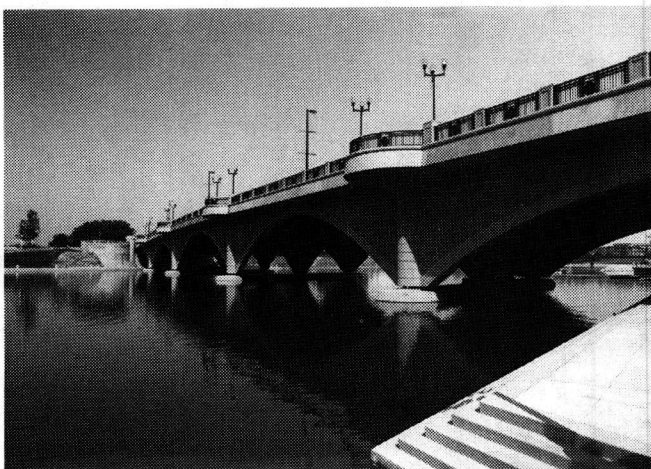


FIGURE 15 Overall view of bridge from east riverwalk.



FIGURE 17 View of Discovery Bridge from Civic Center Drive.



interested parties from the beginning of conceptual design to the final design is crucial. However, this involvement must be channeled and focused on the issues of the bridge. Part of this involvement will be honest debate and disagreement. This controversy is an important part of the project, and how it is dealt with and incorporated into the project may determine the overall level of success.

Another lesson learned is that the design team should be involved from the beginning with the task force in

the development of the design parameters. This would help in the development of parameters that could be more easily incorporated into the design and would provide a thorough understanding by the design team of the meaning behind each parameter.

#### ACKNOWLEDGMENTS

The author expresses his gratitude for the work done by Teresa Hammond in preparing this paper.

# Alsea Bay Bridge Replacement

---

Maurice D. Miller, *HNTB Corporation*

As the nation's infrastructure ages, replacement of bridges has become more commonplace. Many of the bridges to be replaced will have historic significance and may have established an identity for the local community. Replacement of these historic bridges may be the only feasible option when the structure can no longer safely serve its transportation function. This is especially true when the cost of rehabilitation becomes prohibitively high. When replacement has been determined to be the only option left, owners are often faced with the challenge of justifying replacement to the community. Opposition can be overcome or reduced by education of the community to the need for replacement. An effective means to mitigate the loss of the historic bridge is to provide a replacement structure that meets the needs and aesthetics of the community. The Alsea Bay Bridge at Waldport, Oregon, is one example of how an owner can successfully overcome local opposition and provide a replacement structure that enhances the community. This paper will document how the Oregon Department of Transportation was able to replace a high-profile, extremely popular structure that could no longer meet the transportation needs of the highway system with a new bridge that provides aesthetic features complementing the local community. The tradition established by the previous bridge was preserved by adapting parts of the old bridge into waysides and bridgeheads. The resulting structure, which incorporates the old with the new, has provided the community with a new focal point.

**T**he aging of the transportation infrastructure has resulted in more than 30 percent of the 588,150 bridges in the United States being substandard and in need of rehabilitation or replacement. Many of these bridges will be eligible for inclusion in the National Register of Historic Places. The characteristics that make them historic—integrity of location, design, and setting—are the very issues that cause the local community to want to save the bridge. However, replacement becomes necessary when the bridge can no longer safely meet its transportation function.

The Alsea Bay Bridge is one example of the successful replacement of a historic bridge. The existing bridge met all of the requirements for a historic bridge, enjoyed both local and statewide support, and provided an identity to the local community. Through a combination of community involvement and education, the Oregon Department of Transportation (DOT) was able to replace the bridge by providing a structure meeting the aesthetic requirements of the local community.

In the following comments, a brief review of the requirements for historic bridges is first presented; this is followed by a discussion of how the existing Alsea Bay Bridge met these requirements and why the bridge could no longer safely fulfill its transportation function. The measures developed to mitigate the loss of the existing bridge and how aesthetics were an important element of the mitigation are also presented.

## HISTORIC BRIDGE REQUIREMENTS

To be eligible for inclusion in the National Register of Historic Places a bridge must meet only two requirements:

- It must be at least 50 years old.
- It must have historic significance. Historic significance in architecture and engineering is present in structures of state and local importance possessing integrity of location, design, setting, material, workmanship, feeling, and association. In addition, bridges have historical significance if they
  - are associated with events that have made a significant contribution to the broad patterns of history;
  - are associated with the lives of persons significant in the past;
  - embody the distinctive characteristics of a type, period, or method of construction;
  - represent the work of a master; and
  - possess high artistic values.

The rehabilitation of a historic bridge must meet two criteria: the rehabilitated structure must be safe, and the restored structure must fulfill its function in the overall transportation system.

The hierarchy of actions to preserve a historic bridge is as follows:

- Identify, retain, and preserve the historic structure.
- Protect and maintain the historic structure.
- Rehabilitate the historic structure.
- Replace the historic structure.

When the last action is deemed necessary, mitigation of the loss of the structure is required. This mitigation can be as simple as photographic documentation and preservation of the plans of the existing bridge. Bridges providing historic and cultural significance and local identity to the community require more complicated mitigation measures. In these cases, the owner must develop strong local and state support for replacement of the bridge. In addition, the replacement structure should fulfill the cultural and aesthetic desires of the community.

Such was the situation facing the Oregon DOT when replacement of the bridge carrying Oregon Coastal Highway US-101 over Alsea Bay became necessary. The Alsea Bay Bridge project demonstrated that bridge replacements involving strong opposition and controversy can be successful. The Oregon DOT overcame both local and state opposition to replacement of the bridge through community education, development of community ownership of the project, and strong measures to mitigate the loss of the existing bridge (1,2).

## FIRST ALSEA BAY BRIDGE

The Alsea Bay Bridge is located in central Oregon on Coastal Highway US-101 at Waldport, in Lincoln County. A location map is shown in Figure 1.

The bridge spans Alsea Bay at the mouth of the Alsea River, where this waterway meets the Pacific Ocean. The bay is about 3,000 ft wide and is relatively shallow at the crossing. At high tide the water fills the bay, but at low tide about half of the bay is exposed and becomes a popular area for walking, wading, and beachcombing.

The first bridge, of reinforced concrete construction, was opened to traffic in 1936 and is shown in Figure 2. From the north end the bridge consisted of a 124-ft approach span; three 150-ft deck arch spans; three through tied-arch spans of 154, 210, and 154 ft; three 150-ft deck-arch spans; and 1,469 ft of deck girder approach spans. The total length of the bridge was 3,028 ft. It had a 24-ft roadway with a 3.5-ft sidewalk on each side (Figure 3). The three through arches provided 70 ft of vertical clearance above low water, allowing small watercraft, including sailboats, to enter Alsea Bay from the ocean.

Concrete pylons, shown in Figure 4, were placed at both ends of the bridge. These pylons were 17 ft high and had raised decorative designs. Concrete spires accentuated the portals of the tied-arch spans. The through-arch spans were braced with concrete cross frames, which accented the arch spans. These features are shown in Figure 3.

The overall appearance of the bridge was described as one of grace, rhythm, and harmony with the marine setting (Environmental Impact Statement, Draft 4(f), Evaluation). Acting as the focal point in the scenic backdrop of the Waldport community, the bridge provided height, dimension, and aesthetic qualities to the bay area.

The bridge also had regional significance, because it was one of five structures built on the central portion of the Oregon Coast to replace existing ferries. The five bridges, ranging in length from 1,570 to 5,305 ft, were all multispan arch structures. The Alsea Bay Bridge was the only bridge in the group that was built entirely of reinforced concrete. To add further historic significance, the bridge was reputed to have been the longest reinforced concrete tied-arch bridge in the Northwest.

In addition to being ranked as one of the finer examples of concrete bridges in America, the Alsea Bay Bridge was noteworthy because of its designer. The five coastal bridges, in addition to several hundred others, were designed under the supervision of Condon B. McCullough, a noted bridge engineer who served the Oregon State Highway Department from 1919 to 1946. McCullough, a nationally recognized pioneer in the de-

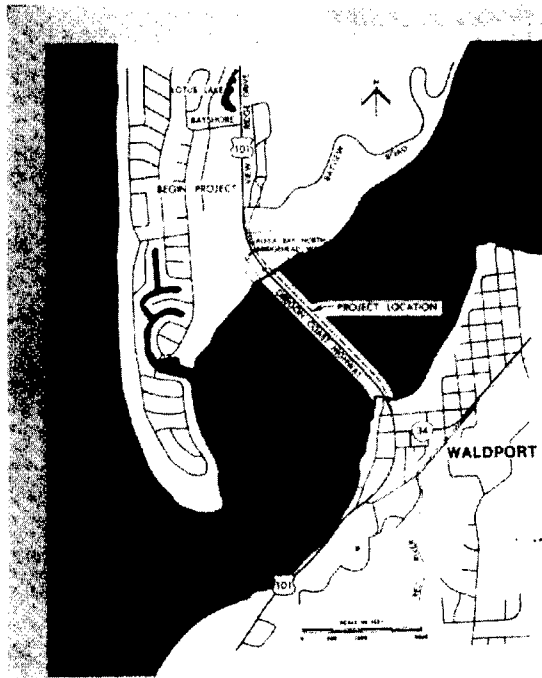
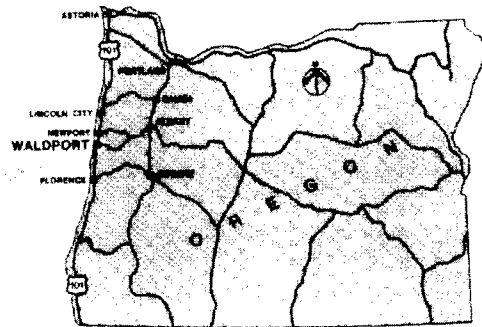


FIGURE 1 Location map.



sign of concrete bridges, promoted sound structural and architectural principles in his designs. The Alsea Bay Bridge was an excellent example of how his bridge designs enhanced and conformed to the environment.

As the bridge owner, the Oregon DOT had to make a difficult decision when this bridge became functionally obsolete and deteriorated to a point where repair was not economically justifiable. This decision was further complicated because the bridge's design and designer made it eligible for inclusion in the National Register of Historic Places.

Several factors contributed to the obsolescence of the existing bridge: narrow roadway widths (two 12-ft traffic lanes), a lack of shoulders, and a restricted load-carrying capacity. In addition, because of the harsh marine environment, the bridge had deteriorated significantly.

In 1967 a marine borer infestation of the timber piles caused the collapse of 17 of the supports for the south deck girder approach spans. Emergency repairs were made; however, these repairs were considered to be only temporary.

Chloride intrusion from the marine atmosphere caused severe corrosion of the reinforcing steel in the concrete members. The bottom of the concrete deck had a chloride ion content 3 times greater than the level recommended for repair of concrete structures. Corrosion of the reinforcing steel, due to the penetration of

the chloride ion, had cracked and broken the deck extensively along its entire length. The beams and girders supporting the deck also had absorbed chloride in amounts 2 to 4 times greater than the level at which repairs are recommended. The concrete arches had similar problems. The high chloride ion content coupled with the humid conditions of the bay area resulted in corrosion of the embedded reinforcing steel, which caused cracking of the concrete throughout the length of the structure.

Bridge rehabilitation was rejected when the Oregon DOT concluded that a restoration would not satisfy safety and transportation criteria. There could be no assurance that the rehabilitation would be effective or would increase the life span of the bridge. Continued deterioration of the timber piles could not be prevented. The integrity of some of the reinforcing steel in the concrete members had been lost, and the chloride ion content in the concrete made rehabilitation impractical. The need to replace the bridge was confirmed by an independent study prepared by Parsons Brinkerhoff Quade and Douglas.

Even though the Oregon DOT presented a very strong case that replacement of the existing bridge was justifiable for both safety and economic reasons, there was strong opposition to replacement. The bridge was described as "the crown jewel of the Oregon Coastal



**FIGURE 2** First Alsea Bay Bridge (looking southwest).

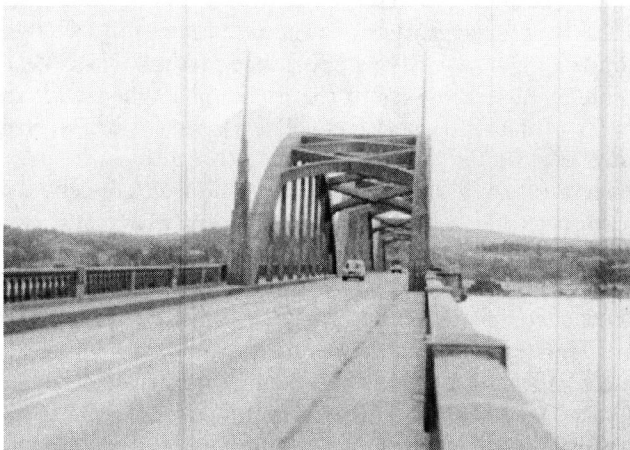


**FIGURE 3** First Alsea Bay Bridge showing roadway at through concrete arch spans. Concrete spires provided emphasis to arch span.



**FIGURE 4** South abutment of first Alsea Bay Bridge showing concrete pylons.

Highway," and a Save the Bridge group was started and enjoyed both local and statewide support.

Through a program of education and involvement, the Oregon DOT successfully overcame this opposition and developed an acceptable replacement bridge project. The Oregon DOT held information meetings with the local Waldport community to describe the need for the project and the serious condition of the existing bridge, to present alternative alignments, and to discuss the environmental impact study process. Measures were taken to make the community a part of the decision-making process and to develop a sense of community ownership of the new bridge.

A Citizens Advisory Committee was formed in 1980 to work with the Oregon DOT during the development of the project. This committee was composed of representatives of the historic community, local governments, businesses, and citizens. The committee's duties included helping the Oregon DOT identify community concerns and values and identify environmentally sensitive areas and alternative solutions for study. In addition, the committee was instrumental in selecting the preferred alternative for the bridge site.

## TYPE SELECTION

At the conclusion of the environmental impact study, HNTB Corporation was selected by the Oregon DOT to prepare preliminary bridge concept studies for a new crossing of Alsea Bay on the existing alignment. These concept studies were developed in enough detail so that the Oregon DOT, working with the Citizens Advisory Committee, could select three alternatives for preliminary design studies.

The bridge types studied included the following:

- Cable-stayed concrete girders,
- Cable-stayed concrete box girder,
- Concrete arch with Vierendeel bracing,
- Concrete arch with cross bracing,
- Twin-cell concrete box girder,
- Concrete finned box girder,
- Cable-stayed steel box girder,
- Cable-stayed steel girder with twin H-pylons,
- Cable-steel girder with single pylon,
- Steel through tied-arch with Vierendeel bracing,
- Steel through tied-arch with cross bracing,
- Steel deck arch,
- Steel tied-arch with Vierendeel bracing,
- Steel tied-arch with cross bracing, and
- Haunched steel girders.

Elevations and cross sections of the bridge types and cost estimates were prepared for each alternative. Esti-

mated costs ranged from \$31,112,000 for the twin-cell concrete box girder alternative to \$44,300,000 for the cable-stayed steel girder with a single pylon. In August 1985 the studies were presented to the Oregon DOT, FHWA, and the Citizens Advisory Committee for the purpose of selecting three alternatives for further study.

The three representatives of the Citizens Advisory Committee unanimously selected the tied-arch bridge with Vierendeel bracing for the main span with concrete delta-pier approach spans as the preferred alternative. This unanimous selection of the tied-arch bridge type allowed the project to proceed with preliminary development of the arch concept. For comparative purposes, a concrete box girder main span with box girder and bulb-tee approach spans was also developed in the preliminary planning stage.

After selecting the approved bridge type, the Citizens Advisory Committee was asked to assist in presenting the preferred alternative to their fellow citizens. The Oregon DOT also took part in these presentations to continue the dialog with the community and to answer questions about the construction of the new bridge. This procedure helped to obtain community support and acceptance of the recommended alternative.

The Citizens Advisory Committee's selection of the bridge type was influenced by their feelings toward their community and toward Condon McCullough. The bridge type was selected to reflect McCullough's arch concept used for the first bridge and the other four bridges on Oregon Coastal Highway US-101. The delta-pier approach spans were selected as a concept that McCullough might have used if he were designing a current bridge. In addition, the appearance of the bridge, both as it related to Waldport and as the individual parts related to the whole, was also a strong factor in the bridge type selection.

Care was taken in the preliminary design to balance the structural and aesthetic requirements of the bridge. This was especially true for the support of the arch span on the delta piers. For appearance reasons it was desirable to have the axes of the arch ribs aligned with the axes of the delta-pier struts. The placement of the bearings for the tied arch offset the arch rib from the delta-pier struts. To remedy this the tied-arch concept was dropped and a two-hinged arch was used. The two-hinged arch, with bearings placed at the intersection of the arch rib and delta pier and centered on the axes of both, satisfied the structural and aesthetic requirements.

The aesthetic requirements are satisfied because the arch ribs line up with the inclined struts of the delta pier. The solution is also very functional because the thrust vector from the two-hinged arch flows directly into the centroidal axes of the inclined struts. Since the reactions of the arch are centered on the axis of the delta-pier strut, axial forces, with very little bending



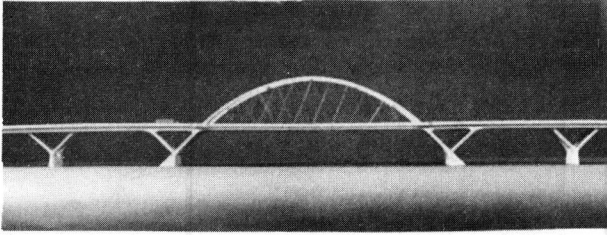


FIGURE 5 Arch rib and delta elevations.

moments, are produced in the strut. Figure 5 provides an elevation of the arch ribs and delta piers.

The spatial relationship of the delta-pier height and width to the span height and length was a crucial element of the visual design of the structure. As the profile grade descends, the spans are shortened and the heights of the deltas are decreased proportionately. These relationships are shown in the aerial photograph of the bridge shown in Figure 6.

Spans starting from the northwest are 235 and 235 ft; 450-ft arch span; and 235, 230, 225, 215, 205, 195, 155, 145, 140, 135, and 120 ft. The roadway provides two 12-ft traffic lanes in each direction, separated by a 4-ft median. On the outside of the 12-ft lanes are 6-ft shoulder/bikeways with 6-ft sidewalks. The total width, out-to-out of structure, is 79 ft.

In addition to the consideration given to the design and appearance of the new Alsea Bay Bridge, care was also given to preserve the character and history of the

first Alsea Bay Bridge. The Oregon DOT provided measures to preserve the historical aspects of the first bridge.

### MITIGATION MEASURES

Before demolition of the first bridge, photographs and documentation were made in accordance with the Historic American Engineering Record standards. To make this documentation readily available to the public, a visitors' center was constructed at the south end of the bridge (Figure 7). The theme of the visitors' center is Transportation Development on the Oregon Coast. To preserve the historical aspect of the design of the first bridge, a biography of Condon B. McCullough was included along with photographs of other Oregon coastal bridges designed by McCullough.

The wayside also includes features that can be used to teach children about bridge engineering. A computer is available at the center to demonstrate the basics of bridge engineering. Facilities for building model bridges are also available. Because of its educational appeal, the visitors' center has become a field trip destination for area schoolchildren.

The wayside has also become a popular tourist attraction, with several hundred people visiting weekly. This popularity is due in part to the details that were incorporated into the wayside to preserve the historical aspects of the first Alsea Bay Bridge. The incorporation of these details into the visitors' center allows the user to view the old and new features of the Alsea Bay Bridge and at the same time enjoy beach activities.

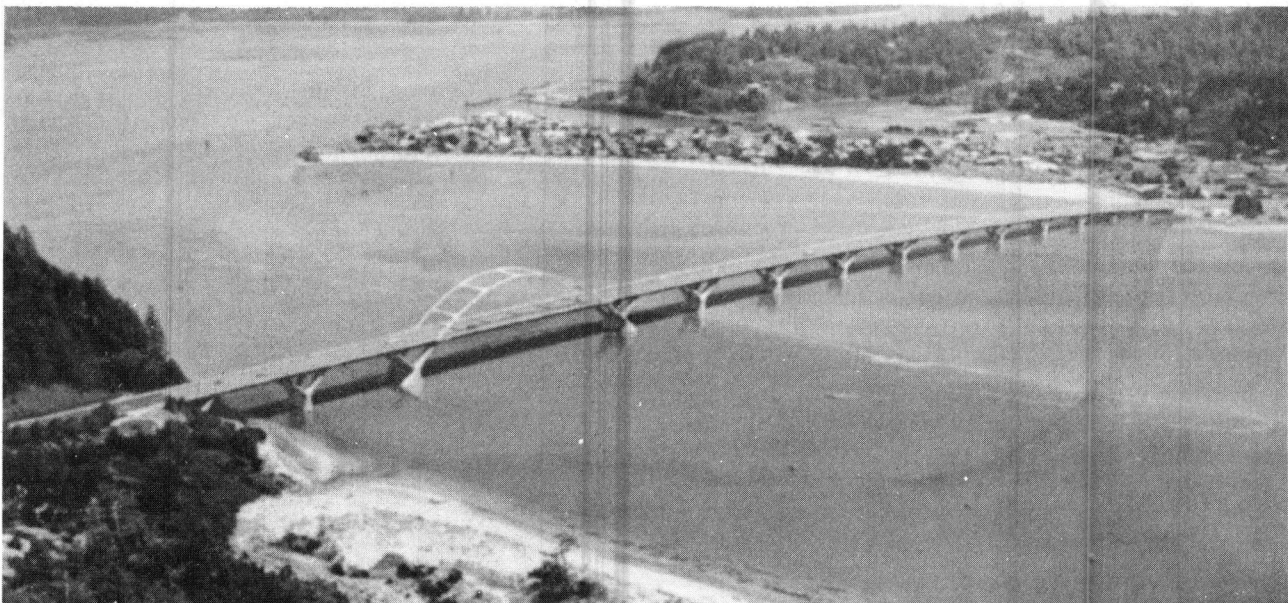


FIGURE 6 New Alsea Bay Bridge.

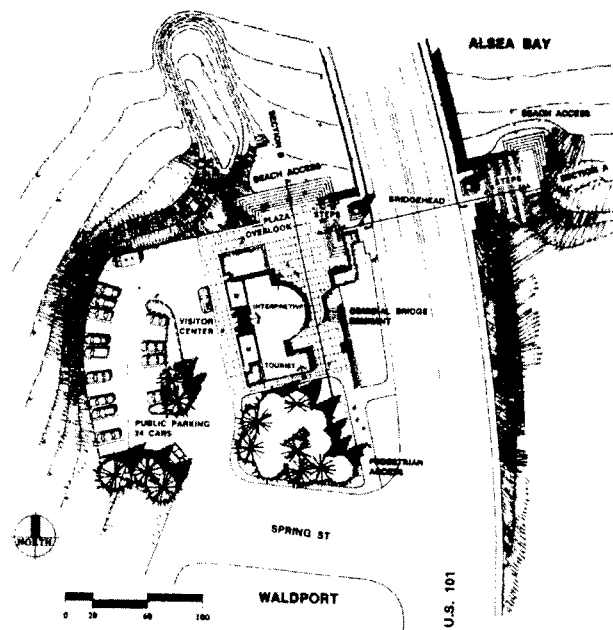


FIGURE 7 Plan view.

The pedestrian leaving the wayside to enter the beach is provided a viewing area of both the bay and the bridge. Handrails from the first bridge were preserved and reused. The original concrete pylons at the south abutment have been retained and serve as a bridgehead (Figure 8). These pylons are mounted on arch-shaped concrete supports and are placed over the sidewalks at the new south abutment location. The gothic arches of the pedestrian walk-throughs reflect the shape of the piers in the first Alsea Bay Bridge.

A wayside was also built at the north end of the bridge. This wayside, located well above the bay, offers a scenic vista of the city of Waldport, the bay, and the bridge. The concrete pylons at the north abutment of the first Alsea Bay Bridge have been left in place to enhance the view. These pylons are connected by a concrete handrail salvaged from the first bridge. The concrete spires that defined the entrance way to the through concrete arch spans of the first bridge, seen in Figure 3, now provide definition to the north wayside.

Lighting has also been provided to enhance the appearance of the bridge. Reflective architectural lighting of the arch spans, the delta piers, and the bridge head were provided in addition to the roadway illumination.

## CONCLUSION

Historic bridges that can no longer safely serve their transportation function can be replaced with the sup-

port of the local community. Education of the community as to the necessity for replacement and then involving the community in key design decisions can be an effective means of obtaining support for the bridge replacement. Preservation of elements of the existing bridge in the new structure can also mitigate the loss of the bridge.

The successful completion of the new Alsea Bay Bridge demonstrates that historic bridges can be re-



FIGURE 8 Bridgehead at south abutment.



placed and the replacement can satisfy the local community's needs. The new bridge is not only serving its transportation function but it is continuing the tradition of the first bridge. The bridge continues to provide a focal point for the city of Waldport. The concrete piers and superstructure carry on the material composition of the first bridge. The delta piers and the post-tensioned concrete of the superstructure use current technology, similar to the designs of Condon McCullough. The two-hinged steel arch reflects the structure type of the first bridge.

The bridge is owned by the Oregon DOT. The design of the bridge was completed by the HNTB Corporation in 1987. CH2M Hill provided geotechnical engineering and structural design, CENTRAC Associates provided

approach roadway design, and Zimmer-Gunsul-Frasca Partnership provided urban design. The bridge was constructed by General Construction Company for \$38,000,000 and was opened to traffic in 1991. Upon completion of the bridge, the existing bridge was torn down, but not forgotten.

#### REFERENCES

1. Keune, R. V. AIT ed. *The Historic Preservation Yearbook: A Documentary Record of Significant Policy Development Issues*. Adler & Adler, Bethesda, Md., 1985, p. 517.
2. Chamberlin, W. P. *NCHRP Synthesis of Highway Practice 101: Historic Bridges—Criteria for Decision Making*. TRB, National Research Council, Washington, D.C., Oct. 1983.

# BRIDGE PERFORMANCE

---

# British Practice in Arch Bridge Assessment

---

W. J. Harvey and F. W. Smith, *University of Dundee, United Kingdom*

The bridge at Aldochlay in the Strathclyde region is small and is constructed from random rubble masonry. It shows no sign of distress, but it became clear very early in the assessment process that different types of analysis yielded very different answers for this structure. The example describes the root causes of some of these conflicts. Bargower is a semicircular bridge constructed from dressed sandstone and has a 10-m span. Its behavior is influenced by various effects of soil pressure and soil-structure interaction that are not well represented in many analytical approaches.

**T**he bridges of Britain are not unique but are quite unusual in that a very large number of bridges with masonry arches are still in use on the highway system. India probably has a larger stock of arch bridges, but it is a much larger country. China certainly has an enormous stock, but knowledge of its assessment procedures is only just filtering out of the country. The ravages of land-based war in Europe means that the European mainland arch bridge stock is drastically reduced and nearly all bridges are modern.

In Britain we have a special interest in arch bridge assessment. Of the stock of approximately 70,000 arches on the highway system, by far the majority were built before the introduction of any loading standards. It is therefore clear that they were designed entirely empirically. There are considerable regional variations in the style of bridges and also more local variations in the quality of workmanship and the standard of design. Nonetheless, that proportion of the arches that did not

collapse early in their lives and that are still carrying traffic has proved well able to sustain the steadily increasing loads imposed on them, provided they are reasonably well maintained. The Department of Transport regulations in Britain require a major inspection and assessment at least every 6 years for all trunk road bridges, and the same rules are usually applied to bridges on locally owned roads.

Interest in arch assessment techniques tends to run in 30-year cycles, with a long period of consolidation using the techniques that have been developed followed by a burst of effort. There has been a substantial amount of activity on arch assessment in Britain since 1980, largely influenced by Heyman's (1) work on the application of plastic theorems to arches. His proposals were incorporated in the Department of Transport's Departmental Standard BD21/84 (2) as an alternative to the long-established empirical method originally developed by Pippard in the 1930s. Working engineers were, on the whole, happy with the application of the MEXE method after 40 years of use, with no known failures of bridges that had passed assessments.

The new approach offered in BD21/84 (2) was slightly modified from Heyman's and attempted to present a limit state method of assessment. Engineers were much less confident that the limit state proposed would yield both safe and satisfactory results. Their concerns are heightened by the fact that after 10 years and probably nearly £2 million (£1 = \$1.60) worth of research work, the clauses on the use of Heyman's method were deleted from the updated version of the standard that

appeared in 1993. Indeed, an appendix casts considerable doubt on those computerized approaches that were based on Heyman's methods. It is perhaps surprising that similar doubts were also cast on the range of finite-element methods that have been developed since 1990.

Although this paper is written by the authors of one of the programs based on Heyman's techniques, an attempt will be made to present a reasoned view of the tools available for arch assessment and the way that they might be applied and to offer suggestions as to how further progress might be made.

### PROCESS OF ASSESSMENT

The assessment of the capacity of a masonry bridge requires three elements:

1. A field inspection,
2. A desktop study, and
3. Reflection and the application of judgment by a competent and experienced engineer.

There is considerable desire to remove the need for the third element, but it will be demonstrated that it is extremely unlikely that it will ever be possible to do so.

### Field Inspection

Three things are required. The first and most obvious is a geometric survey. Arch bridges depend on their shape for their strength to a greater extent than any other form of bridge. Ideally, the assessing engineer wants to know the basic geometry of the intrados or soffit of the arch, that is, the span, the rise, the shape of the curve, and the plan shape (whether square or skewed). The assessing engineer would clearly like to know the height and thickness of the abutments and the nature of the foundations on which those abutments stand. Knowledge of the thickness of the arch ring and any variation in that thickness over the span is also important, as is knowledge of the thickness and height of the spandrel walls and the depth and quality of the fill, which brings a steeply curved arch up to a reasonably level surface for the road.

Many of these details are completely hidden. In particular, it is extremely difficult to obtain dimensions for the abutment and ring thicknesses and for the nature and quality of the foundations. BD21/84 (2) and BD21/93 (3) avoid the most difficult of these problems by saying that if there is no sign of distress in the abutments, then they should be assumed to be adequate.

This seems a very strange response in the light of the concern that is expressed about the performance of the arch itself.

Once the basic geometry is noted, the engineer will proceed to consider the condition of the bridge. The masonry units, brick or stone, may have deteriorated with time, particularly if moisture has been allowed to penetrate from the road surface through the fill and into the masonry. Some of the poorest stones and bricks used in arches deteriorate progressively with time, even when they are kept in relatively benign condition. The mortar in the joints between the masonry units presents rather more problems. Although on some bridges that the authors have inspected it is still possible after 300 years to see the impression of the formwork on the mortar between the stones, on others the mortar has been completely eroded. It cannot be emphasized too strongly that the mortar is at least as important as the masonry units to the performance of an arch, not least because the forces must flow through the structure, and if there is a gap between two adjacent stones, then no force can pass between them.

Another important question for the field inspector is whether the bridge is cracked in any way. Cracks in the arch barrel are regarded as particularly important. Transverse cracks, except for a single crack very close to the crown, are very uncommon and are in any case unlikely to be particularly important. Longitudinal cracks, however, indicate some sort of breakdown of the structural system. They occur most commonly at the inside face of the spandrel walls and, particularly in railway bridges, between opposing traffic lanes. Cracks of this nature can hardly be caused by direct tension in the masonry. It is sometimes suggested that the pressure of fill on the inside of the spandrel walls will push the walls outward, and they will sometimes take the arch with them and crack it. Bearing in mind that the spandrels are supported off the arch usually with a very soft mortar, this mechanism seems extremely unlikely. However, the flexural stiffness of the spandrel walls and the fill behind them is very different, and the result is that the arch attempts to deform between the spandrel walls and is held in shape by the walls themselves, generating large displacements and enormous strains and stresses that cause longitudinal cracks. Once the cracks have formed, the broken edge of the arch may well push the spandrel walls outward. The spandrel walls may bulge as a result of pressure from the fill. This problem is not a matter for the present paper.

Diagonal cracks are rare but are of rather more concern since they can only occur as a result of some form of twisting deformation of the arch barrel. Whether the twist takes place between abutments that remain firm or whether the abutments themselves move is a matter for inspection and measurement. It is, of course, ex-

tremely important that the inspecting engineer exercise judgment, deciding what features of the structure are important and what can be ignored.

Some data that the inspecting engineer would very much like to have can only be obtained at considerable expense and probably by doing damage to the structure. It is possible to take cores from a bridge to ascertain unit strength and so develop the strength and, indeed, calculate elastic properties for the masonry. If these cores are well preserved and the assessing engineer is certain that they will not change with time, then coring may be justified. However, the enthusiasm some assessing engineers have shown for knocking holes in bridges in this way must be questioned.

A full understanding of the internal geometry of the structure and of the properties of the fill material can only be obtained by digging trial pits. Drilling or coring through the arch barrel or spandrel walls is notoriously ineffective in providing adequate, accurate data.

## Analysis

The constraints on the data available from a field survey must be borne in mind in deciding what analysis might be carried out. If a method demands particular items of data and these data are not available, reasonable estimates must be made. The sensitivity of the analysis to them must then be investigated. An engineer's experience in this is extremely important since the sensitivity of different shapes and sizes of bridge to different items of data will vary and a complete parameter study cannot be carried out on every structure that is assessed. In the end, an assessment is a matter of developing the confidence of the engineer in the structure that the engineer is assessing.

Most assessments are now carried out by consulting engineers who, because of the nature of their work, must carry insurance. The cost of that insurance is critically dependent on the engineer's success. At the same time, the engineer must submit to fee competition in obtaining work and therefore must minimize the amount of effort that he or she puts into a particular assessment.

The authors therefore suggest that analysis for assessment should be a matter of exploration and confidence building and should progress from simple, relatively understood techniques to more complex ones only if the engineer requires more support to improve his or her confidence. This approach is common practice among many engineers, but it is discouraged by the working of the design standard used.

## Analytical Tools

### MEXE Analysis

The MEXE routine completes the assessment of an arch on one piece of paper. For most engineering groups this is on a standard form. The engineer begins by inserting leading dimensions. A nomogram or formula gives a capacity for a perfect arch (the Provisional Axle Loading, or PAL). A series of reduction factors is then applied to take account of

1. a less than "perfect" shape,
2. a ratio of ring thickness to fill depth that differs from the assumed value,
3. quality and geometry of the masonry units and the joints between them, and finally,
4. an entirely empirical condition factor.

The result of the final assessment may be 20 percent or less of the initial value extracted from the nomogram.

The nomogram itself is based on an elastic analysis. It was assumed that the arch is completely elastic and is supported on a pin at each end, that the fill only acts as dead load, that the critical position for a load is at the center of the span, and that the only important control is the compressive stress in the arch ring. With time it has become increasingly clear that this model does not in any way represent the true behavior of an arch. Nonetheless, the results obtained have proved satisfactory, although no one knows whether the actual factor of safety achieved is 1.1 or 11.

In BD21/93 (3) an updated version of this procedure (described as the computerized Pippard/MEXE method) is recommended. It uses a frame analysis program to analyze an elastic arch ring on two hinges. The authors believe that the benefits of this procedure are wholly imaginary and that the dangers are considerable. The MEXE procedure has stood the test of time, whereas no attempt has been made to check that the new method either leads to results that are similar to those of MEXE or that it produces conservative results for a range of bridges that are demonstrably in sound condition. The system has, however, been calibrated against a series of full-scale tests to destruction that are of questionable value for this particular application.

### Equilibrium Analysis

In 1676 Robert Hooke "solved" the problem of the functioning of a masonry arch (4). Essentially, he said that an arch works in the same way, but inverted, that a chain supports a system of loads. For 300 years now engineers have sought to find the pattern of the chain for a particular system of loads and thereby prove that,

the chain being contained within the depth of the arch material, the arch is sound. Through the 19th century and a large part of the 20th century many engineers have attempted to find a particular solution to this hanging chain problem. Barlow (5) in 1846 demonstrated that the attempt was doomed to failure but in any case was unnecessary. It is sufficient to show that a particular polygon or line of thrust can be contained within the arch without knowing precisely which line of thrust is used to carry the loads.

Pippard understood this well and knew that at the limit of arch behavior, a mechanism was formed involving alternate hinges on the intrados and extrados (Figure 1). Despite this and despite the historical context of his work exactly at the period at which Baker was advancing the plastic theorems, Pippard clung to inadequate elastic analysis for his assessment method. It was left to Heyman (1) to pick up French work from the 18th and 19th centuries on the collapse of arches and develop a limit state procedure based on the collapse mechanism. Heyman worked with Hooke's line of thrust and continued to treat the fill as unrealistic.

The present authors found that this had two disadvantages, one of which was picked up by the writers of the Departmental Standard. Using the line of thrust as a test for stability of a structure ignores the fact that stability can be destroyed by material failure. BD21/84 (2) required that the line of thrust never approach closer to the boundaries of the arch than half the width of a rectangular stress block capable of carrying the thrust at that point, whereas the authors took this one step further and drew a zone of thrust (6,7) which was at all points through the arch capable of sustaining the applied thrust (Figure 2). Applying this analysis to real bridges produced unacceptably low results, and it quickly became clear that the soil fill could exert an enormous stabilizing influence on the arch. Approaches that take account of this influence, however, lead to more complication in the analytical procedures and to a demand for more data. The approach taken in the ARCHIE program was therefore to allow an engineer to explore the limits of influence of various parameters in a very fast analytical cycle.

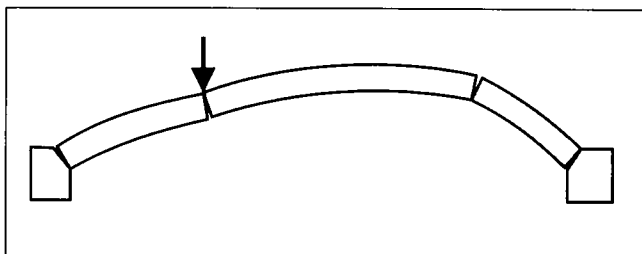


FIGURE 1 Mechanism forming in a loaded arch.

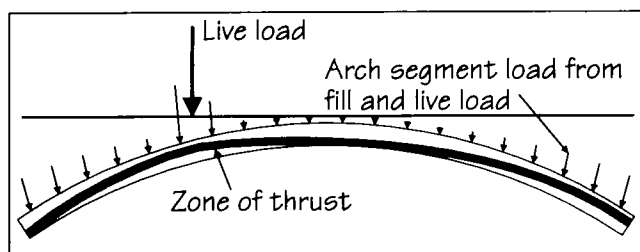


FIGURE 2 Zone of thrust is the minimum arch capable of supporting these loads.

### Finite-Element Analyses

During the late 1980s and early 1990s a number of workers developed specialized finite-element packages for analyzing masonry arch bridges. Crisfield (8) at the Transport & Road Research Laboratory adapted an existing program to treat the soil fill as a Mohr-Coulomb material to allow elasto-plastic cracking behavior in the arch ring and to take account of the ensuing changes in geometry. The program produces interesting and valuable results, but it takes several hours to produce a solution for a single load case and is therefore entirely impractical for assessment use.

Bridle and Hughes (9) at Cardiff developed a computerized version of Castigliano's analysis. They computed elastic and, indeed, inelastic deformation of the arch and progressively removed from the computation those zones of the material that were cracked, shifting the centerline of their elastic arch rib appropriately.

Choo at Nottingham used plane strain elements to represent the arch ring but tapered them progressively to remove from the calculations that part of the material that would be in tension. Unlike the Cardiff approach, his analysis did not take nonlinear geometry into account.

Both of these finite-element programs treat the soil fill as a set of horizontal-yielding elastic springs. The results obtained are obviously critically dependent on the spring constant used. The model used by Choo is not known, but it is known that Bridle and Hughes calibrated their soil springs to produce analytical results that match test failures as closely as possible.

### Examples

Two examples are presented. They show to some extent the problems of bridge assessment and also the limitations of the tools that are in use. In particular they will emphasize the role of judgment in bridge assessment.

### Aldochlay Bridge, Strathclyde Region

This small-span bridge had been repaired by guniting at some time. It is a trunk road bridge owned by the Scottish Development Department for whom the Strathclyde Regional Council acted as agent. The owners required an assessment to be carried out by the traditional MEXE approach but also for a rating to be produced for heavy vehicles, which necessarily involved more advanced analysis. The advanced analysis that was used involved a very simple version of the mechanism, or equilibrium analysis, and produced a result substantially lower than that yielded by MEXE. The authors were asked to carry out a review of the analysis and explain why these anomalies occurred.

The MEXE analysis (Figure 3) considers a load at midspan, whereas a properly constituted mechanism analysis (Figure 4) searches for the most critical position for a load. It was clear that the view of the geometry of the arch barrel that had been taken was simplistic. The masonry was hidden behind gunite, but it seemed likely that the stone was selected random rubble, and experience showed that the old masons tended to select bigger stones for the springings and smaller ones for the crown and then to hide this on the exposed spandrel face by carefully choosing stones of similar depth to express a parallel ring. Experience has shown that it is usually safe to assume that, provided the zone of thrust does not leave the arch until a point on the extrados vertically above the face of the abutment (Figure 5), the structure will be secure since there will be material to carry the thrust.

An excavation was carried out on site at a cost of some £2,500, and it was found that the arch was in fact much thicker than this near the springings, as shown by the broken line in Figure 5. This example clearly shows (a) the need for experience in bridge assessment,

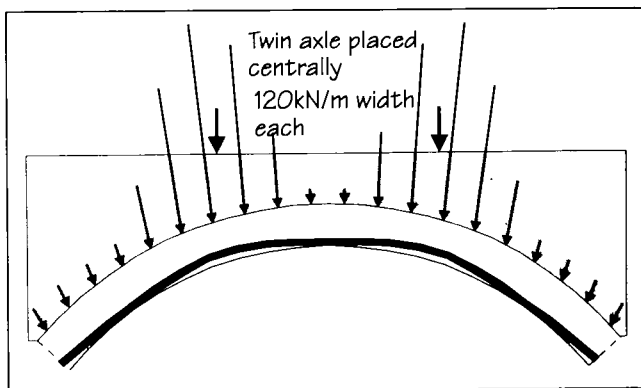


FIGURE 3 Zone of thrust view of MEXE analysis.

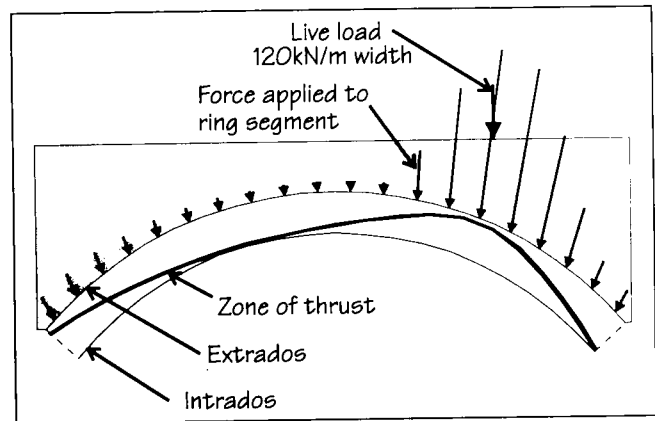


FIGURE 4 Zone of thrust with a single asymmetric load.

preferably backed up by regular observation of such bridge excavations and demolitions that take place, and (b) the need not to take analyses at face value.

Whatever form of rational analyses was applied to the structure, taking into account the additional material in the arch would produce a substantially higher result than ignoring it. The option of taking such material into account is not available in the MEXE method and is actually likely to have a detrimental effect in the computerized Pippard/MEXE method because taking a hinge at the centerline of the arch depth at the springings would in this case result in a much shallower arch curve without a corresponding increase in effective depth at the critical points.

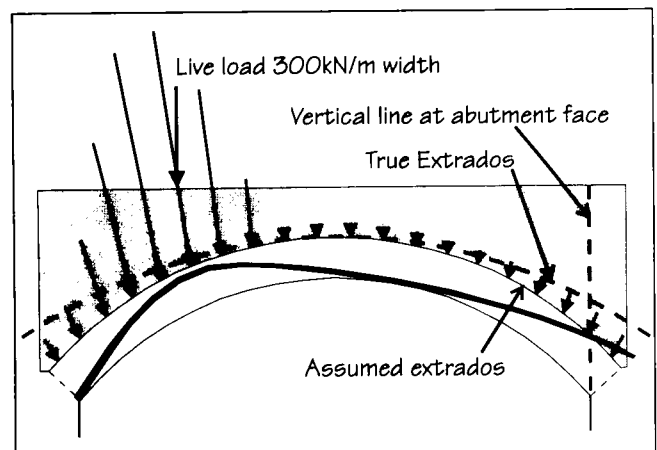


FIGURE 5 Increased capacity from a small amount of additional material.

### Bargower Bridge

The bridge at Bargower was one of a series tested to destruction in a program sponsored by the Department of Transport and carried out under the direction of the Transport & Road Research Laboratory. The bridge has a span of 10.54 m and is semicircular and apparently still in its true shape. It stands on abutments 5 m high and is slightly skewed, although not sufficiently to have any significant effect on the assessment. At the time of the test cracks were evident at the inside face of the spandrel walls over the middle half of the span. For this example it is worth running through the actual MEXE analysis.

#### Assessment

The first step in the assessment is to determine the PAL (in metric tons). This can be found from either a nomogram or an equation (which would appear to be dimensionally incorrect). The following actual dimensions are used for the bridge at Bargower:

Span, 10.54 m ( $L$ )

Rise, 5.18 m ( $r_c$ )

Q pt rise, 4.49 m ( $r_q$ )

Ring thickness, 0.588 m ( $d$ )

Cover to crown, 1.71 m ( $h$ )

$$\text{PAL} = \frac{740(d+h)^2}{L^{1.3}} = \frac{740 \cdot (0.588 + 1.71)^2}{10.54^{1.3}} = 183T$$

The various factors that must be applied are then considered.

The span/rise factor ( $F_{sr}$ ) makes allowances for the fact that steeper arches are stronger than flat arches. For arches for which the span/rise ratio is greater than 4 the value is read from a graph. For values of less than 4, as with the bridge at Bargower, for which the span/rise ratio is approximately 2,  $F_{sr}$  is 1.

The profile factor ( $F_p$ ) makes allowance for arches that do not conform to the ideal profile, which is assumed by this method to be parabolic. The value may be obtained from a graph or an equation.

$$F_p = 2.3 \cdot \left( \frac{r_c - r_q}{r_c} \right)^{0.6} = 2.3 \cdot \left( \frac{5.18 - 4.49}{5.18} \right)^{0.6} = 0.686$$

The material factor ( $F_m$ ) is based on two other factors, barrel factor  $F_b$  and fill factor  $F_f$ , which are obtained by reference to tables. The barrel factor ranges from 1.5 for built-in-course masonry to 0.7 for masonry in poor condition. The fill factor varies from 1.0 for concrete fill to 0.5 for weak materials. This would be the case if wheel tracking were evident. For the bridge

at Bargower the values chosen were an  $F_b$  of 1.5 and an  $F_f$  of 0.7.  $F_m$  is then obtained from the formula

$$\begin{aligned} F_m &= \frac{(F_b \cdot d) + (F_f \cdot h)}{d + h} \\ &= \frac{(1.5 \cdot 0.588) + (0.7 \cdot 1.71)}{0.588 + 1.71} \\ &= 0.90 \end{aligned}$$

The joint factor ( $F_j$ ) takes account of the joint width, mortar condition, and depth of mortar loss and is the product of three other factors, one for each of the elements given earlier. Wide joints, joints with missing mortar, and loose friable mortar all reduce the value of this factor.

$$F_j = F_w \cdot F_d \cdot F_{mo} = 0.9 \cdot 1.0 \cdot 1.0 = 0.9$$

The condition factor ( $F_c$ ) is intended to take account of any cracking or deformation, which could affect the load capacity of the bridge and is perhaps the most subjective of all the factors. The bridge at Bargower exhibited longitudinal cracks under the inner edge of the spandrel walls. The suggested condition factor for this type of defect gives an  $F_c$  of 0.8. However, it is unlikely that those cracks would have had any significant effect on the capacity of the arch, although they may have reduced the stability of the spandrel walls.

#### Modified Axle Load

All of the various factors listed above are used to determine the modified axle load. This value is then multiplied by axle factors to get the safe load for a particular axle arrangement. For a bridge with a 10.5-m span such as the bridge at Bargower the single axle factor is 1.6. The safe axle load is given by

$$\begin{aligned} F_{sr} \cdot F_p \cdot F_m \cdot F_j \cdot F_c \cdot \text{PAL} \cdot A_f \\ = 1.0 \cdot 0.686 \cdot 0.9 \cdot 0.9 \cdot 0.8 \cdot 183 \cdot 1.6 = 130T \end{aligned}$$

Exploring the performance of the structure by the equilibrium analysis presents some interesting difficulties. Figure 6 shows the effect of applying a load at the critical point on the span, roughly the third point for a semicircular arch of this scale, with the soil acting simply as vertical dead load. It is clear that under these circumstances the bridge is quite incapable of supporting a load. Figure 7 shows the same load but with the soil exerting a horizontal component of pressure with the at-rest coefficient,  $(1 - \sin\phi)$ , for a value of  $\phi$  of 35 degrees. Clearly, the performance is dramatically improved. Applying a proportion of passive pressure to that part of the arch that would rise as it failed (shown



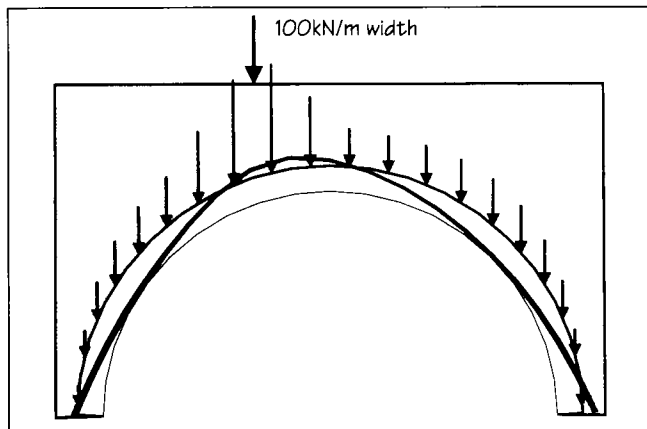


FIGURE 6 Fill acting as dead load only, negligible capacity, for bridge at Bargower.

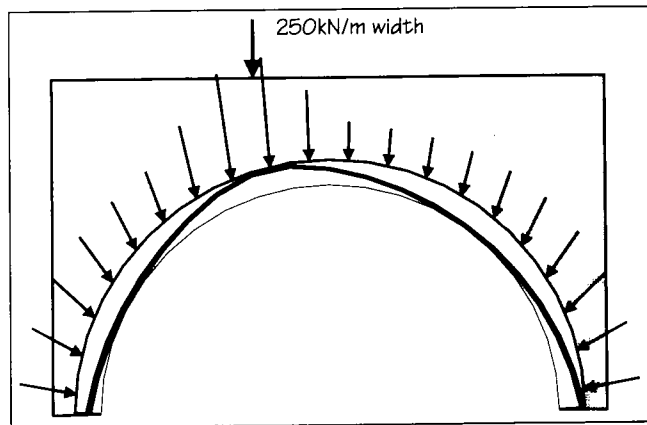


FIGURE 7 Fill exerting at-rest horizontal pressure for bridge at Bargower.

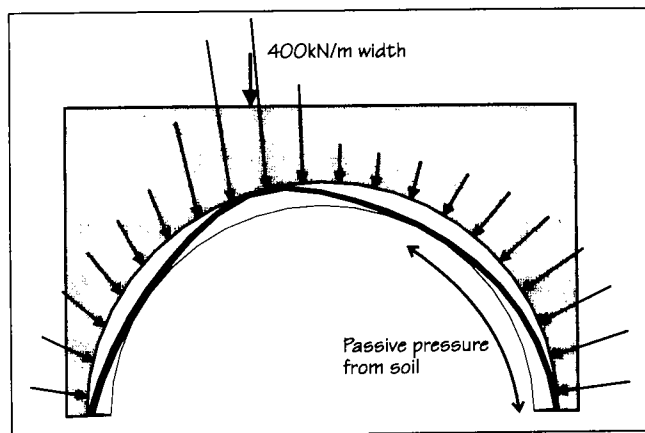


FIGURE 8 Fill exerting passive pressure for bridge at Bargower.

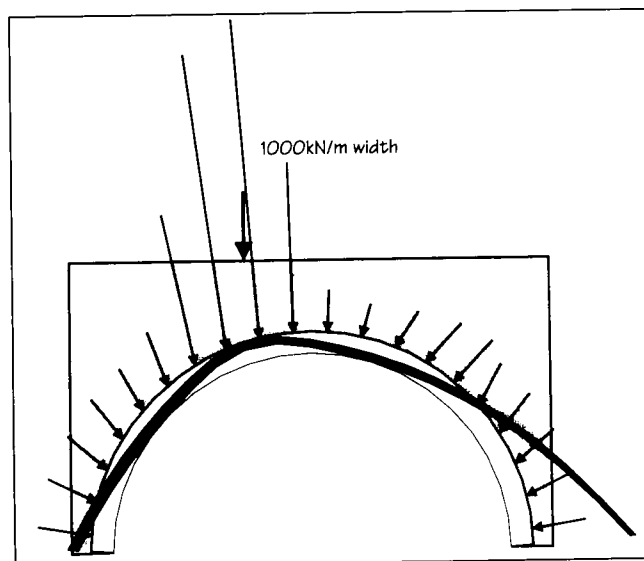


FIGURE 9 Assuming masonry backing to quarter point for bridge at Bargower.

by the arrow in Figure 7) increases the load capacity by a factor of 2 (Figure 8).

Allowing the thrust to escape from the arch at roughly the quarter point (Figure 9) increases the capacity by an additional factor of 2.5. This is a realistic scenario because on demolition it was found that the bridge had masonry support to the arch ring up to this depth. Even assuming a depth of backing as suggested above increases the load capacity to 400 kN/m of width (Figure 10).

It is clear from this example that a detailed survey of the bridge is necessary and that if a realistic assessment

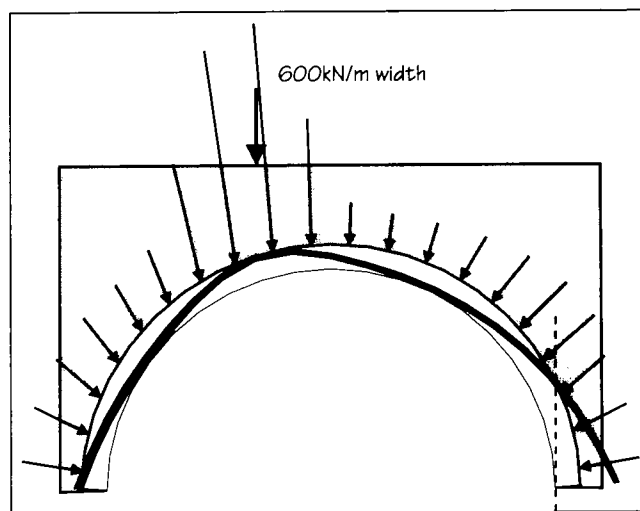


FIGURE 10 Assuming minimum masonry backing for bridge at Bargower.

is to be made, estimates are required for the complex geometry of the bridge interior. It is hoped that this also indicates the value of taking an exploratory approach to analysis for bridge assessment, progressively exploring more complex geometries.

### ANALYSIS IN APPLICATION

It is clear that the MEXE analysis, if analysis it can be called, is very simple to use and has the confidence of engineers. Any approach that is more difficult to use is unlikely to be welcome. Thus, until such time as someone writes a program to speed its application, the computerized Pippard/MEXE method recommended by the Department of Transport is unlikely to come into regular use. There are other pieces of software known to the authors, but ARCHIE, the Cardiff program CTAP, and the Nottingham program MAFEA are all characterized by specially written data input modules that speed operation.

Nonetheless, all three have major drawbacks. Perhaps the most important, shared by all of them, is the fact that they are essentially two-dimensional analyses of three-dimensional structures. They all ignore the potential stiffening effect of spandrel walls and can only take account of load distribution by the use of empirical effective widths.

It is clear from the nature of the Cardiff and Nottingham programs that although they are capable of providing rather more information at loads less than the ultimate limit, once the limit is reached, the results should be very similar to those produced by the much simpler ARCHIE program. Only in the case of very large flat arches in which substantial elastic deformation takes place before failure will the CTAP program produce noticeably different results for the ultimate limit, and then they might be substantially lower.

### CONCLUSIONS

1. Arch bridge assessment is a complex and difficult operation made more difficult by the lack of firm data on which to base an analysis.
2. Exploratory analysis investigating the effects of various parameters is extremely valuable, increasing an engineer's confidence in his or her results.
3. Such exploratory analysis would be too expensive to carry out without efficient, specially designed software.
4. Analysis based on unreasonable structural theory is unlikely to lead to confidence in the output.

### REFERENCES

1. Heyman, J. *The Masonry Arch*. Ellis Horwood Ltd., Chichester, United Kingdom, 1981.

2. Department of Transport. *The Assessment of Highway Bridges and Structures*. Departmental Standard BD21/84. 1984.
3. Department of Transport. *The Assessment of Highway Bridges and Structures*. Departmental Standard BD21/93. 1993.
4. Hooke, R. *A Description of Helioscopes, and Some Other Instruments*. London, 1676.
5. Barlow, W. H. On the Existence (Practically) of the Line of Equal Horizontal Thrust in Arches and Modes of Determining It by Geometric Construction. *Minutes of the Proceedings of the Institution of Civil Engineers*, Vol. 5, 1846, p. 162.
6. Harvey, W. J. The Application of the Mechanism Analysis to Arch Bridges. *Journal of the Institution of Structural Engineers*, Vol. 66, No. 5, March 1988, pp. 77–84.
7. Harvey, W. J. Stability, Strength, Elasticity and Thrust Lines in Masonry Structures. *Journal of the Institution of Structural Engineers*, Vol. 69, No. 9, May 1991, pp. 181–184.
8. Crisfield, M. A. *A Finite Element Computer Program for the Analysis of Masonry Arches*. Report LR1115. Transport & Road Research Laboratory, Crowthorne, Berkshire, England, 1984.
9. Bridle, R. J. and T. C. Hughes. An Energy Method for Bridge Analysis. Discussion. *Proceedings of the Institution of Civil Engineers*, Part 2, Vol. 89, Sept. 1990, pp. 617–630.

### APPENDIX

#### MEXE Method

The MEXE approach began with a series of assumptions. The arch is assumed to be parabolic to ease the calculations, it is assumed to be elastic but supported on pins, the span/rise ratio is assumed to be 4, and the ratio of ring thickness to fill depth is assumed to be 1. All loads are assumed to act vertically on the arch. The live load is a twin axle placed centrally. With this layout a formula can be written for the value of live load axle that will produce a compressive stress of 200 lb/in.<sup>2</sup> or 1.4 MPa at the crown. This calculated stress was found empirically to correspond to the first crack in a series of real arches tested in Britain in the 1930s and 1950s. The approach therefore takes empirical account of such factors as load distribution and stiffening of the arch by the spandrels. For ease of use a nomogram (Figure 11) was produced, relieving military engineers working under stress from the need to carry out calculations.

Clearly, arches are not all parabolic, nor do they all have a span/rise ratio of 4 or equal depths of ring and fill. Modification factors were computed to take account of each of these changes. It is worth noting that however the factors were computed, they are demonstrably wrong since the shape factor indicates the para-

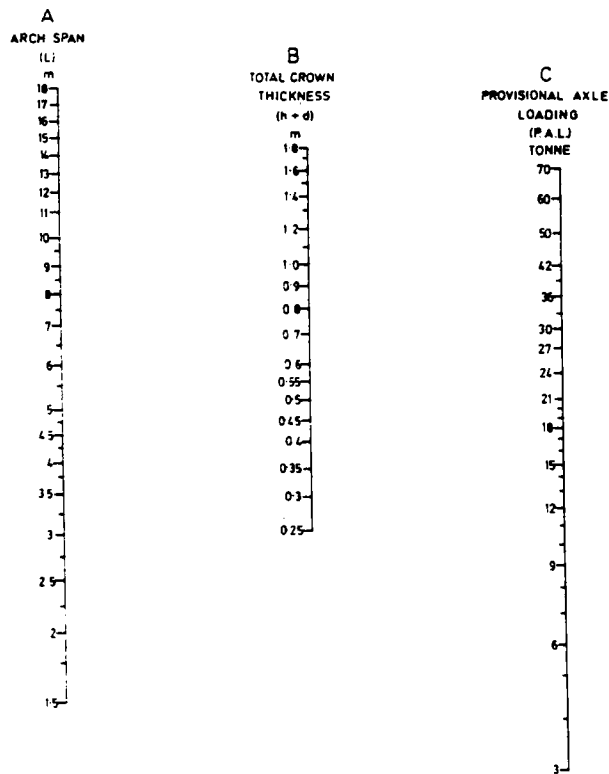


FIGURE 11 Nomogram for determining provisional axle loading of masonry arch bridges before factoring.

bolic shape to be the best, whereas for a typical real arch with realistic soil pressures, the best shape will vary considerably with the span and rise. There are additional factors to take account of the strength and stiffness effects of different materials, a lost section as a result of loss of mortar in the joints, and finally, a general condition factor for the bridge. The condition factor is entirely a matter of judgment, although guidance is provided in the Department of Transport standard by the use of photographs. There is no indication of how the factors were actually derived, nor is there any evidence that the loss of capacity indicated has been checked against test results. The nomogram for the various factors is presented below.

### Computerized Pippard-MEXE Method

The computerized Pippard-MEXE method is essentially a modernized basic MEXE method. The arch is divided into a number of segments and is analyzed as a rigid jointed frame with pinned supports. All loads are assumed to be vertical and concentrated at the nodes, but the true shape of the arch and the correct loading can be used. Despite these improvements the method remains empirical since it is recognized that the analytical model does not represent the real behavior of the arch.

# Case Study of Concrete Deck Behavior Without Top Reinforcing Bars

---

Li Cao and P. Benson Shing *University of Colorado, Boulder*  
John Allen, *Allen Research & Development Corporation*  
Dave Woodham, *Colorado Department of Transportation*

A major cause of the deterioration of bridge decks is the spalling and delamination caused by the corrosion of the top mat of reinforcing bars. Empirical evidence has indicated that the tensile bending stresses developed at the top of a bridge deck subjected to traffic loads are relatively low. As a result the need for top reinforcing bars for sustaining the negative bending moment induced by traffic loads is questionable. To explore the possibility of eliminating top reinforcing bars, and thereby reducing the vulnerability to corrosion, the performance of a four-span bridge deck is investigated. In the bridge studied one span has an experimental deck with no top reinforcement, whereas the remaining spans have both top and bottom reinforcements that conform to AASHTO specifications. The response of the bridge deck under a test truck was monitored with embedded strain gauges. It was found that the peak transverse tensile strains developed at the top of the deck were less than 30 percent of the cracking strain of the deck concrete. The behavior of the bridge deck under the test truck and other combinations of truck loads has also been investigated by means of elastic finite-element analysis. The results show that the tensile stresses developed at the top of the deck tend to be much less than the modulus of rupture of the deck concrete. The study confirms that a properly designed bridge deck does not require the top reinforcement for sustaining the negative bending moment induced by traffic loads.

The deterioration of bridges in the United States is a serious problem. As bridges age, repair and replacement needs accrue. It has been estimated that 41 percent of the nation's 578,000 bridges are either structurally deficient or functionally obsolete (1). An estimated investment of \$51 billion is needed to bring all of the nation's bridges to an acceptable and safe standard by either rehabilitation or replacement. On the basis of national bridge inventory data obtained from the U.S. Department of Transportation, about one third of the nation's bridges have deficient decks, whereas 24 percent of the nation's bridge decks are structurally deficient. An effective means of preventing such deterioration is to eliminate top reinforcing bars from a deck. This can lead to substantial savings in construction, maintenance, and repair.

To explore this new design concept an experimental deck was designed and constructed without top reinforcement for an end span of a four-span bridge by the Colorado Department of Transportation. The main objective of the study was to determine the maximum tensile stresses that can be developed in such a deck in order to assess its durability in the absence of top reinforcement. The investigation consisted of the development of a linearly elastic finite-element model for evaluating the response of the deck under truck loads and the monitoring of the actual response of the bridge

deck under a test truck as well as normal traffic loads. Results of the study have been documented in detail by Li et al. (2,3). This paper summarizes the design of the experimental deck, the field tests, and the experimental and numerical results.

## BRIDGE DECK DESIGN

### Background

In North America most short- and medium-span bridges are constructed with slab-on-girder decks, in which a reinforced concrete slab is supported by several steel or precast, prestressed concrete girders. Generally, the design of reinforced concrete decks has been based upon the Westergaard theory (4), which assumes that a slab is continuous over fixed linear supports. The current AASHTO slab design provisions (5) are based on empirical rules derived from earlier adaptations of the Westergaard theory (6,7).

According to the conventional design method, bridge slabs over three or more girders are designed as continuous slabs, which are assumed to have the same positive and negative bending moments that are 80 percent of the simple span moment specified in the AASHTO code (5). As a result nearly the same quantities of steel have been used to resist the positive and negative bending moments in a slab. Until the late 1960s bridge decks had a top concrete cover of only 1.5 in. (38 mm) and a bottom cover of 1.0 in. (25 mm). In the early 1970s the top cover was increased to at least 2.0 in. (51 mm) or 2.5 in. (64 mm) for situations in which deicing chemicals were used. It was thought that the additional cover would significantly delay the penetration of chlorides to the reinforcing bars.

The increased top cover did not extend the lives of bridge decks dramatically. In many states where salt usage was prevalent, decks have been made more impervious to moisture and salt penetration. Concrete mixes with a high percentage of cement are known to be more impervious, so that their use has become standard practice. To protect the top reinforcing bars several barrier techniques, such as the use of membranes, dense concrete, or latex-modified concrete, have been developed. These techniques have moderate success, but the use of epoxy-coated bars has proven to be the most effective and widely accepted strategy.

In spite of attempts to prevent the deterioration of bridge decks due to the corrosion of reinforcing bars, deck cracking has worsened dramatically. In recent years the incidence of transverse cracking has increased. It has been observed that transverse cracks, which appear shortly after deck placement, often occur over the

upper reinforcing bars, permitting increased exposure to chlorides from deicing chemicals.

The need for top transverse reinforcing steel has recently been questioned by Allen (8). Investigations of the behaviors of bridge decks by Beal (9) and Fang et al. (10) have shown that the negative bending moments in bridge decks and the resulting transverse tensile stresses at the top of a deck are usually very low, much less than the positive bending moments and the bottom tensile stresses. Analysis of their work and other empirical evidence by Allen (8) indicates that the deflection of girders tends to significantly reduce the transverse bending stresses at the top of a deck. Hence, the best way to prevent the corrosion of reinforcing bars is to eliminate the top mat of reinforcing steel. Without top reinforcing bars the predominant cause of bridge deck deterioration can be eradicated. To explore the new design concept of removing the top reinforcement, an experimental deck was designed and constructed by the Colorado Department of Transportation (CDOT), as discussed in the following section.

### Design and Configuration of Prototype Bridge

The bridge selected for the project described here is located on Colorado State Route 224 over the South Platte River near Commerce City. It is 420 ft (128 m) long and 52 ft (15.85 m) wide. The superstructure consists of four equal continuous spans. The supporting girders are standard precast Colorado Type G-54 girders spaced at approximately 8.0 ft (2.44 m) on center. The thickness of the bridge deck is 8.0 in. (203 mm), which complies with the new design requirement adopted by CDOT. The configurations of the four-span bridge and typical girder sections are shown in Figure 1.

In the four-span deck, the west end has an experimental deck, from which most of the top reinforcement has been omitted. It consists of the entire 104-ft (31.7-m) end span and 36 ft (10.97 m) of the adjacent interior span. The remaining deck has both top and bottom reinforcement that conforms to AASHTO specifications (5). The span at the east end serves as the control deck. The reinforcing steel details of the control and the experimental decks are shown in Figure 2. Both decks are instrumented with strain gauges.

In the midspan of the control deck, the top and bottom transverse reinforcement consists of No. 5 bars with a 5.5-in. (140-mm) center-to-center spacing. The top longitudinal reinforcement consists of No. 5 bars with an 18-in. (457-mm) center-to-center spacing, and the bottom longitudinal reinforcement consists of No. 5 bars with a 9.5-in. (241-mm) center-to-center spacing.

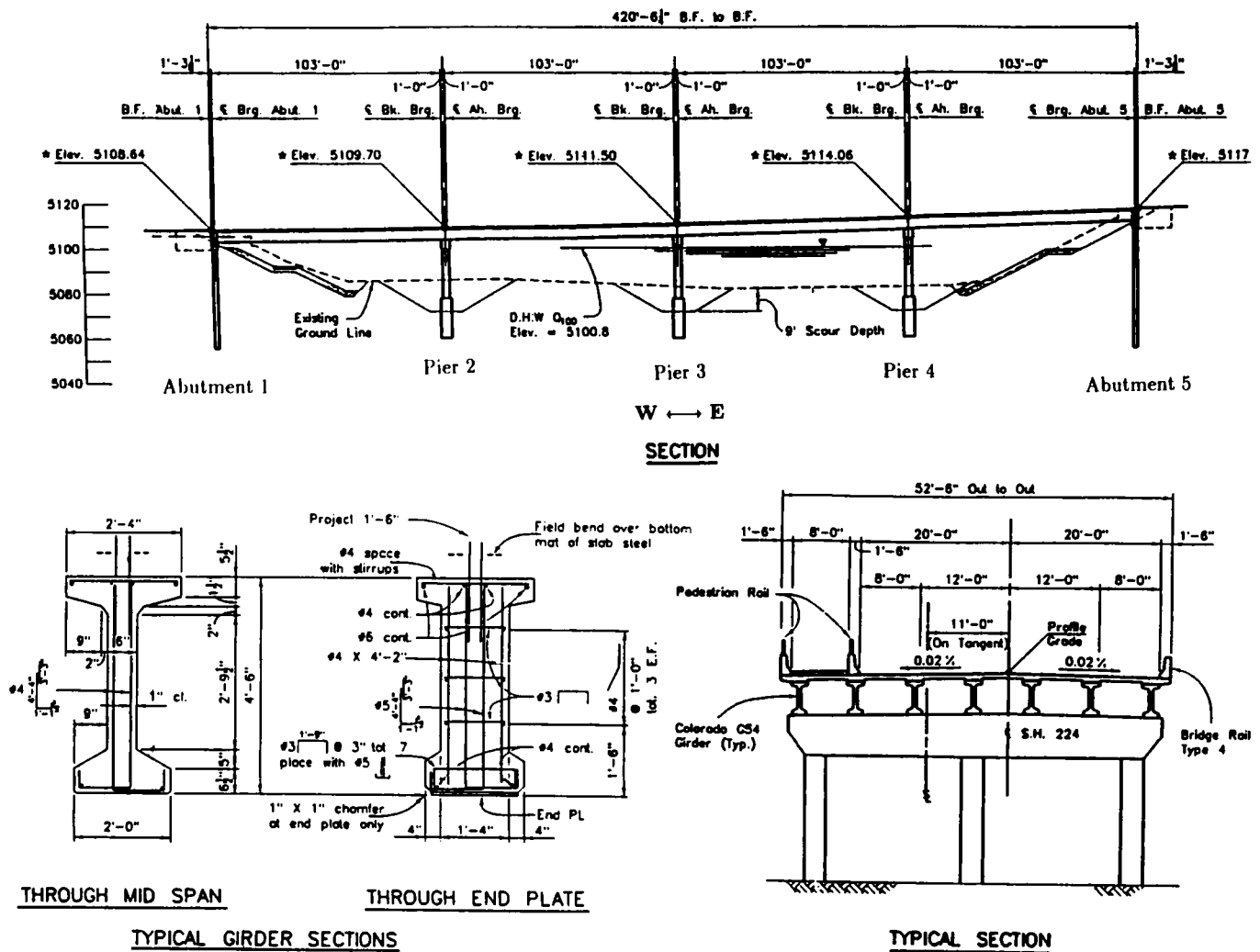


FIGURE 1 Configuration of the bridge deck (1 in. = 25.4 mm).

In the midspan of the experimental deck, the top reinforcement is removed. On the basis of an allowable stress of 24,000 lb/in.<sup>2</sup> (165.36 MPa) for steel, this deck slab can sustain a positive transverse bending moment of 6,990 ft-lb/ft (31.1 kN-m/m). From the finite-element analysis of the bridge deck conducted by Li et al. (2), it has been found that the maximum transverse tensile stress that can be expected at the bottom of the deck is 550 lb/in.<sup>3</sup> (3.80 MPa), with the deck thickness taken to be 7.5 in. (190 mm) on the basis of the preliminary design. This tensile stress corresponds to a positive bending moment of 5,160 ft-lb/ft (23.0 kN-m/m). According to AASHTO specifications (5), the design bending moment of the slab under an HS20 truck is 4,910 ft-lb/ft (22.0 kN-m/m), not including the continuity factor of 0.8. Hence, it has been concluded that the quantity of bottom transverse reinforcement adopted here is sufficient to carry the design load, even if the slab is not continuous over the girders.

Furthermore, from the finite-element analysis (2), the maximum transverse tensile stress at the top of the deck above the center of a girder is expected to be 286 lb/in.<sup>2</sup> (2.0 MPa). The maximum top transverse tensile stress at a point 12 in. (305 mm) away from the center of a girder, which is approximately above the edge of the flange of a girder, is expected to be 140 lb/in.<sup>2</sup> (1.0 MPa) for a slab 7.5 in. (190 mm) thick. This tensile stress is reduced to 123 lb/in.<sup>2</sup> (0.85 MPa) for a slab 8.0 in. (200 mm) thick, which is way below the expected tensile strength of the deck concrete. Hence, it has been concluded that no top transverse reinforcement is required to sustain the negative bending moment.

In both the control and experimental decks, the same amount of top longitudinal continuity reinforcement was placed. This consisted of 56-ft (17.1-m)-long No. 9 bars spaced at 9 in. (229 mm) on center across the piers. The top cover on these bars was 3 in. (76 mm)

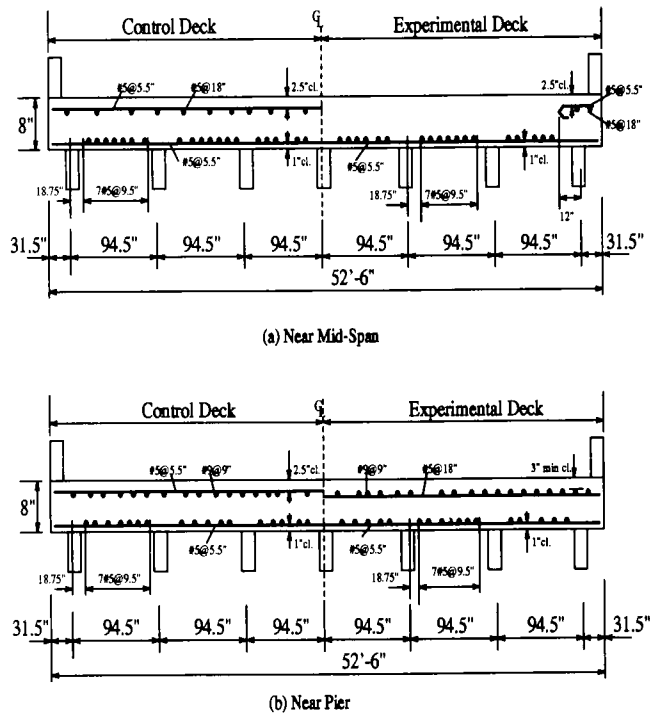


FIGURE 2 Reinforcing steel details for the bridge deck (not to scale; 1 in. = 25.4 mm).

in the experimental deck, so that these bars are at the same elevation as those in the control deck.

A small amount of polypropylene fiber (1.5 lb/yd<sup>3</sup> of concrete) was added to the deck concrete to help control cracking. The deck concrete was membrane cured. Based on 28-day laboratory-cured specimens, the average compressive strength and the modulus of rupture of the deck concrete are measured to be 5,740 and 590 lb/in.<sup>2</sup> (39.6 and 4.1 MPa), respectively. The average compressive strength of the girder concrete is 8,500 lb/in.<sup>3</sup> (58.6 MPa).

The bridge was constructed in two phases to facilitate the flow of traffic. The Phase 1 portion of the deck consists of a slab 34 ft (10.36 m) wide supported over five girders. It was cast in January 1993. The Phase 2 portion of the deck was cast in July 1993. After the bridge had been opened to traffic for 6 months, a series of load tests was conducted on a single day in September 1993, with the complete bridge temporarily closed to traffic.

## FIELD TESTS

### Test Truck and Truck Load Positions

As shown in Figure 3, the test truck included a front axle transmitting a force of 16.5 kips (73 kN). The total force transmitted by the rear tandem axles of the test

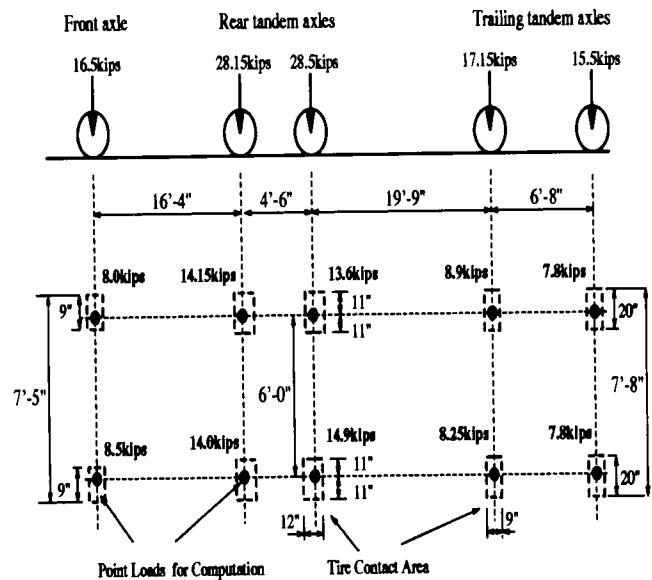


FIGURE 3 Test truck (1 kip = 4.45 kN, 1 in. = 25.4 mm).

truck was 56.7 kips (252 kN), and the total force exerted by the trailing axles was 32.8 kips (146 kN). The total weight of the test truck was 106 kips (472 kN), which is 47 percent more than that of a conventional HS20 truck. The axle and wheel spacings of the test truck were similar to those of a standard HS20 truck.

To investigate the maximum tensile stresses that could be developed in the transverse direction at the top and bottom of the deck, it was decided that the test truck should be positioned at three different locations along the longitudinal direction of the bridge, as shown in Figure 4. The first truck position was close to the abutment in the experimental deck at the west end, resulting in rear tandem axle loads being approximately 8 ft (2.44 m) away from the abutment. The deflection of the girders was small when the truck was at this position. The trailing axles and the front axle were not used in this load case, since it is expected that these axle loads would increase the girder deflections and thereby decrease the transverse tensile stresses at the top. The second truck position in the longitudinal direction was near the mid-span of the experimental deck, with the resulting rear tandem axle loads being approximately 44 ft (13.41 m) away from the abutment. This induced differential deflections among the girders. The third truck load position in the longitudinal direction was in the vicinity of the pier in the experimental deck, with the resulting rear tandem axle loads being approximately 6 ft (1.83 m) away from the pier. The above positions are identified as Load Groups 1, 2, and 3, respectively. As illustrated in Figure 5, the wheels of the test truck were positioned at six to seven different locations along the transverse direction of the deck for each of these load groups.

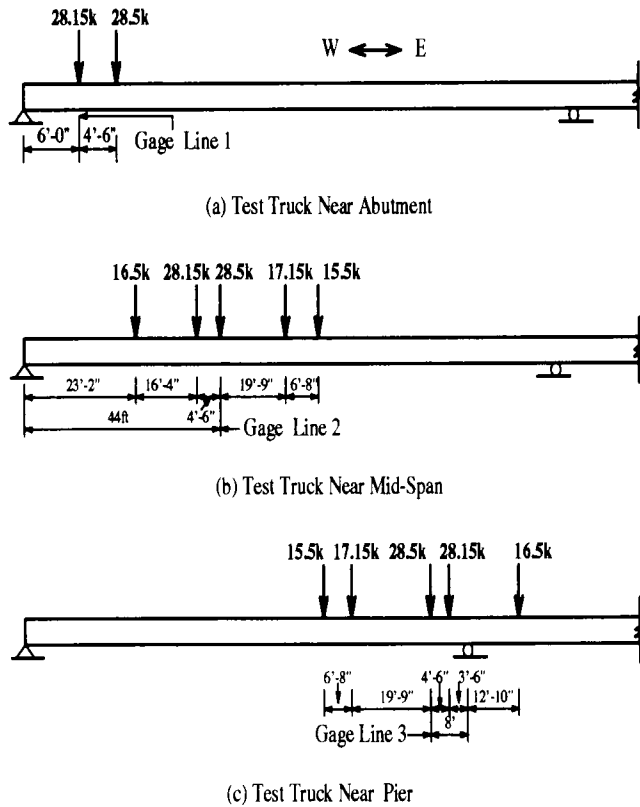


FIGURE 4 Longitudinal positions of test truck on the bridge (1 kip = 4.45 kN, 1 in. = 25.4 mm).

The truck load positions were determined from the finite-element analysis (2). Each position results in a most severe stress condition when compared with the stress conditions at other positions in the vicinity. In addition to the three longitudinal positions, the test truck was also placed on the control deck. Load Groups 4 and 5 correspond to the midspan and abutment positions, respectively, on the control deck in the east span, which are similar to Load Groups 2 and 1, respectively.

### Instrumentation

The response of the bridge deck under the test truck was monitored by strain gauges embedded at different locations in the deck. These locations are associated with the designated positions of the test truck discussed earlier. Five gauge lines are selected, as shown in Figure 6. The first three gauge lines are located in the experimental deck, and the other two are located in the control deck. In the experimental deck, the first and second gauge lines are 6 ft (1.83 m) and 44 ft (13.41 m) away from the abutment, respectively. The third gauge line is

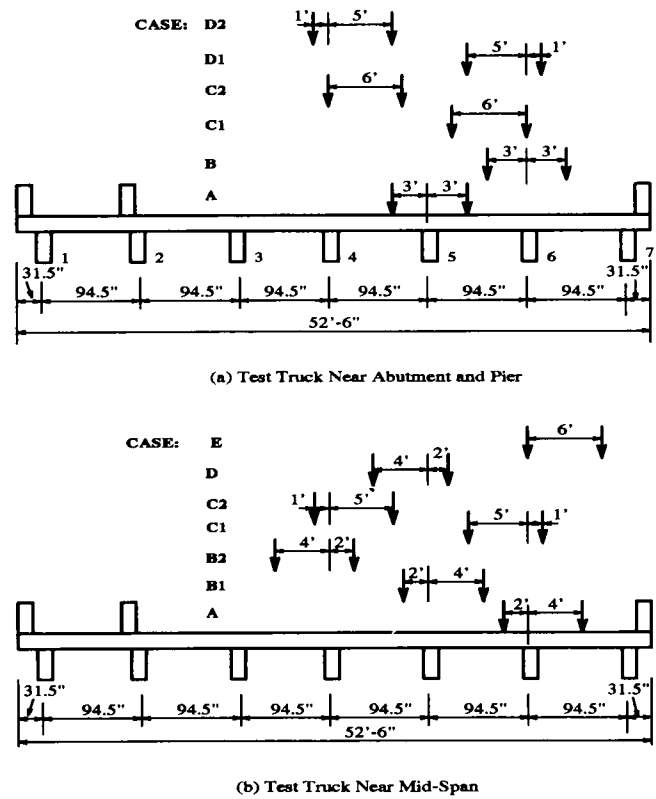


FIGURE 5 Test truck positions along transverse direction of the deck (1 in. = 25.4 mm).

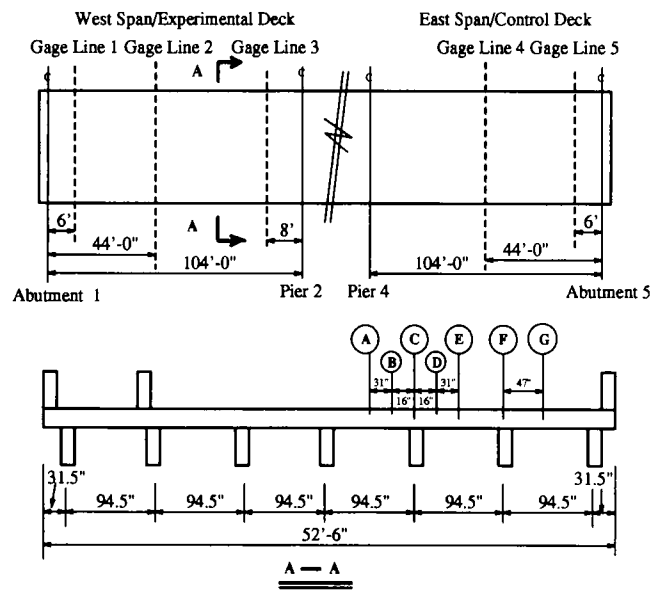


FIGURE 6 Locations of strain gauges in the bridge deck (1 in. = 25.4 mm).



**TABLE 1 Maximum Strain Readings in the Transverse Direction at Top and Bottom of Slab**

Gage Point	Gage Line				
	1	2	3	4	5
A	+3.1/+66.5	-52.3/+117.9	-53.3/+54.9	-/-	-/-
B	-/-31.5	-24.5/-	-/-	-/-	-/-
C	+20/-	+6.8/-	+19.2/-	+5.6/-	+13.8/-
D	+18.3/-	-/+50.7	-/-	-/-	-/-
E	-32.6/+76.7	-53.9/+173.8	-51.1/+73.4	-46.5/+133.2	-39.6/+30.2
F	+15.4/-	+13.0 /-	+18.7/-	-/-	+15.7/-
G	-14.8/+30.8	-/+176.2	-/-	-/-	-/-

Note: The plus and minus signs refer to the tensile and compressive strains, respectively. The locations of gage lines and gage points are illustrated in Fig. 6. The strain readings in each column are obtained under a load group which has the same number as the gage line.

8 ft (2.44 m) away from the pier. Gauge Lines 4 and 5 are located in the control deck.

There are seven gauge points (A through G) along each of the gauge lines, as shown in Figure 6. Each gauge point usually has top and bottom gauges, which are oriented in the transverse and longitudinal directions of the deck. The top and bottom gauges are about 1 in. (25 mm) away from the top and bottom surfaces of the deck, respectively. The strain gauges were welded on 21-in. (0.53-m)-long No. 4 bars that have anchoring hooks. These bars are embedded in concrete. The gauge mounting technique was verified with a reinforced concrete beam subjected to third-point loading (3).

## Results of Field Tests

The response of the bridge deck to the test truck positioned at the different locations mentioned previously was measured by embedded strain gauges. The maximum strain readings at the top and bottom of the deck are summarized in Tables 1 and 2.

The modulus of rupture of the deck concrete was measured to be 590 lb/in.<sup>2</sup> (4.1 MPa) with standard third-point loading tests, and the modulus of elasticity of the deck concrete was calculated to be 4,230 lb/in.<sup>2</sup> (29 1500 MPa) on the basis of the formula of the American Concrete Institute (ACI) formula (11). Hence, the corresponding cracking strain of the deck concrete is estimated to be  $140 \times 10^{-6}$ . Based on the plane section assumption, the strains at the top and bottom surfaces of the deck can be determined with the strain measured at a gauge point. Since the distance from an embedded gauge to the top or bottom of the deck is about 1 to 2 in. (25 to 51 mm) and the thickness of the deck is 8 in. (203 mm), it is expected that the strains at the top and bottom surfaces of the deck will reach the cracking strain when the strain at an embedded gauge near the surface is about  $70 \times 10^{-6}$  to  $105 \times 10^{-6}$ .

It can be seen from Table 1 that when the test truck was close to the abutment the maximum transverse ten-

sile strains at the top gauge positions of the deck along Gauge Line 1 were less than  $20 \times 10^{-6}$  and those at the bottom gauge positions of the deck were about  $60 \times 10^{-6}$  to  $80 \times 10^{-6}$ . When the test truck was near the midspan the transverse tensile strains at the bottom gauge positions of the deck along Gauge Line 2 became very large and were about  $110 \times 10^{-6}$  to  $180 \times 10^{-6}$ . At the same time the transverse tensile strains at the top gauge positions of the deck were less than  $15 \times 10^{-6}$ . Comparison of these readings with the readings obtained at Gauge Line 1 indicates that the deflection of the girders increases the transverse tensile stresses at the bottom of the deck and reduces those at the top. When the test truck was close to the pier, the transverse tensile strains at the top gauge positions of the deck along Gauge Line 3 were less than  $20 \times 10^{-6}$ , and those at the bottom gauge positions of the deck were about  $50 \times 10^{-6}$  to  $80 \times 10^{-6}$ .

It can be seen from Table 2 that the longitudinal tensile strains developed in the deck under the test truck were less than  $28 \times 10^{-6}$  for all three load groups. It is also noted from the test results that the behaviors of the experimental and control decks are similar.

## NUMERICAL RESULTS

### Finite-Element Models

To investigate the stress state of a bridge deck, the most refined approach is to use the finite-element method. A

**TABLE 2 Maximum Strain Readings in the Longitudinal Direction at Top and Bottom of Slab**

Gage Point	Gage Line				
	1	2	3	4	5
A	-/+0.4	-61.8/+1.0	-10.9/+10.7	-/-30.2	-/-
C	+6.2/-	-41.9/-	-/-	-/-	+10.0/-
E	-24.3/+27.5	-35.7/-23.4	-/-	-/-21.9	-/-
F	-17.3 /-	-51.7/-	-/-	-/-	-/-

number of different finite-element models have been used for the analysis of bridge decks (10,12). In the present study two layers of eight-node solid elements are used to model the concrete slab, and rigid beams are used to connect the nodes at the bottom of the slab to the centroids of the girders, which are represented by three-dimensional beam elements. The cross-sectional area and moment of inertia of each girder of the bridge are 630 in.<sup>2</sup> (0.41 m<sup>2</sup>) and 242,590 in.<sup>4</sup> (10 097 360 cm<sup>4</sup>), respectively. Finite-element program SAP90 (13) is used for the stress analysis. Nonconforming solid elements are used to eliminate possible shear locking.

Furthermore, since only a single end span of the four-span bridge is considered, the remaining three spans are modeled by equivalent beam elements only. Each equivalent beam has a rectangular section of 54 in. (1.37 m) height and 43.45 in. (1.1 m) in width whose moment of inertia is equal to that of a fully coupled composite T-beam section consisting of a girder and a slab. The effective width of the flange is equal to the center-to-center distance between the girders, in accordance with the recommendations of ACI (11).

In the finite-element model 50 solid elements are used in the transverse direction of the bridge deck, with 8 solid elements used between two girders. The mesh along the transverse direction remains the same for all three load groups. The mesh along the longitudinal direction is adjusted in accordance with the locations of the axle loads of the test truck. Twenty-four solid elements are used along the longitudinal direction in a single span. For all three load groups, a fine mesh is used in the vicinity of the rear tandem axle loads, where the maximum stresses are expected to occur. The meshes used for the stress analysis are shown in Figure 7.

In the finite-element analysis of the bridge deck, the elastic moduli for the deck and girder concrete are taken to be 4,230 ksi (29 150 MPa) and 5,260 ksi (36 240 MPa), respectively. The Poisson's ratio is assumed to be 0.2 for both the deck and girder concrete. There is a steel diaphragm consisting of a C15 × 33.9 channel at the middle of each span, which is modeled by bar elements connected to the girders. The elastic modulus of the bars is assumed to be 29,000 ksi (199 810 MPa). The bridge deck has an 8-degree angle of skew. However, because the angle of skew is small, it is ignored in the stress analysis. The wheel loads of the test truck are treated as concentrated point loads.

### Comparison of Test and Numerical Results

The behavior of the bridge deck under the 19 load cases was analyzed with the finite-element models presented earlier. The corresponding normal stresses along the

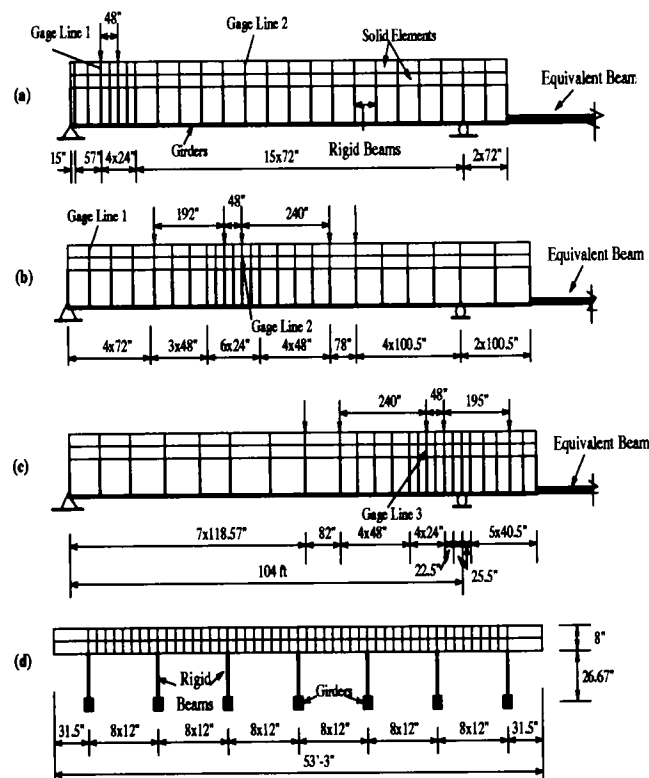


FIGURE 7 Finite-element meshes: (a) Longitudinal section for Load Group 1; (b) longitudinal section for Load Group 2; (c) longitudinal section for Load Group 3; (d) transverse section for all three load groups (1 in. = 25.4 mm).

transverse and longitudinal directions of the bridge deck have been determined.

Since two layers of eight-node solid elements have been used to model the bridge deck, the stresses have been computed at three nodal points along the depth of the slab. The stresses at the gauge locations have been evaluated from the nodal stresses with a linear interpolation, which happens to fit the nodal stresses very well. In spite of the small variations in gauge positions, it has been assumed that all strain gauges are 1.0 in. (25 mm) away from the top or bottom of the deck. Since the normal strains in both the longitudinal and transverse directions were measured at most of the gauge positions, the normal stresses in the deck have been calculated with a biaxial stress-strain relation, in which the modulus of elasticity and the Poisson's ratio of the deck concrete are the same as those used in the finite-element model.

The test and numerical results from selected load cases are compared in Figures 8 and 9. These correspond to Case A of Load Group 1 (Case 1A) and Case B1 of Load Group 2 (Case 2B1). The wheel load positions along the transverse direction of the deck are similar for these two cases, as shown in Figure 5. These

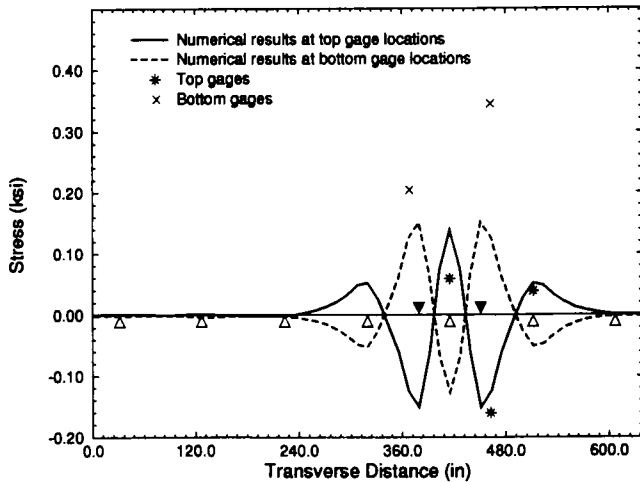


FIGURE 8 Normal stresses in transverse direction along Gauge Line 1 for test truck near abutment (Case 1A) (1 in. = 25.4 mm, 1 ksi = 6.89 MPa).

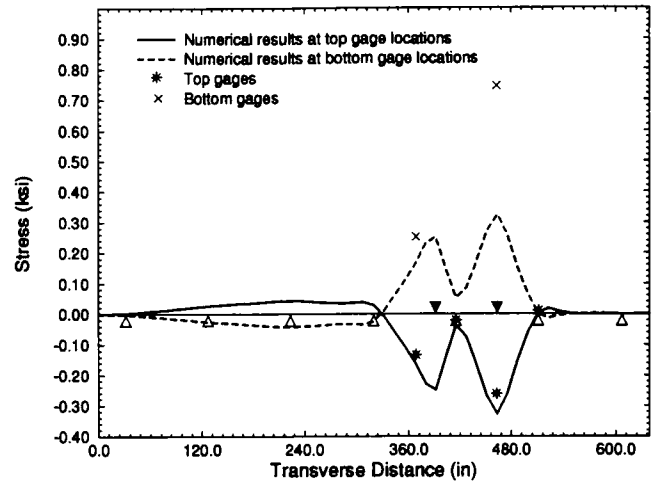


FIGURE 9 Normal stresses in transverse direction along Gauge Line 2 for test truck near midspan (Case 2B1) (1 in. = 25.4 mm, 1 ksi = 6.89 MPa).

two load cases demonstrate the effect of girder deflection on the normal stresses in the transverse direction of the deck. It can be seen from the figures that the numerical results are quite close to the test results for these two load cases. Nevertheless, the tensile stresses developed at the bottom of the deck in the field tests are about twice as large as the numerical results. This can be attributed to the cracking at the bottom of the deck, which is not accounted for in the analysis.

It can be seen from Figure 8 that when each of the wheel loads was near the midspan between two girders, the transverse normal stresses obtained from the tests at the top of the girders are only about 50 percent of the numerical results. This discrepancy is also found in other load cases in which the truck was close to a pier. This is probably caused by the flanges of the girders, which are not considered in the finite-element model. This effect is not significant when the truck loads are near the midspan, since in this case the transverse normal stresses at the top of the girders are significantly influenced by the deflection of the girders. In addition, it is found that the test and numerical results for truck loads near the pier are similar to those for truck loads close to the abutment.

It can be seen from Figure 9 that when the test truck was near the middle of the experimental deck, the transverse tensile stresses at the bottom of the deck were relatively high. This phenomenon can be observed from both the numerical and test results.

### Analysis with Two Trucks

The prototype bridge has one lane of traffic in each direction. To simulate the most severe loading condi-

tions that can be expected for the bridge, the response of the bridge deck under two test trucks was investigated. This response can be obtained with the superposition of the numerical results obtained with one test truck.

Figure 10 shows the combined effects of different load cases with the truck loads close to the abutment. The resulting maximum transverse tensile stress at the top of the deck is 230 lb/in.<sup>2</sup> (1.59 MPa). Figure 11 shows the combined effects when the truck loads were near the midspan. In this case the maximum transverse tensile stress at the top is 100 lb/in.<sup>2</sup> (0.69 MPa). The deck section at which the maximum tensile stress occurs is referred to as the critical section in the figures.

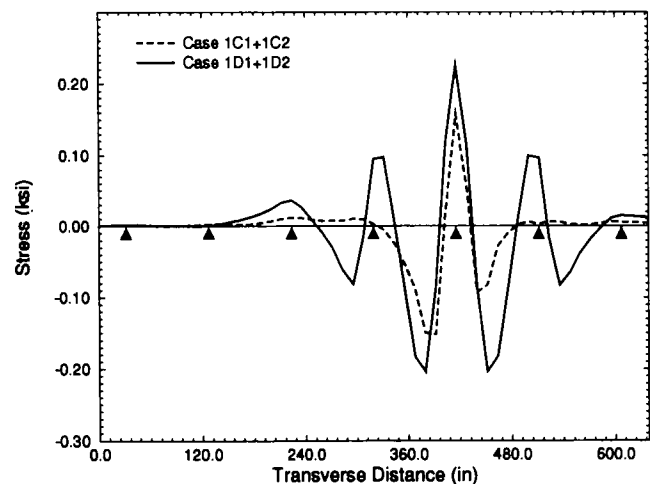


FIGURE 10 Top normal stresses in transverse direction along the critical section for two trucks near abutment (1 in. = 25.4 mm, 1 ksi = 6.89 MPa).

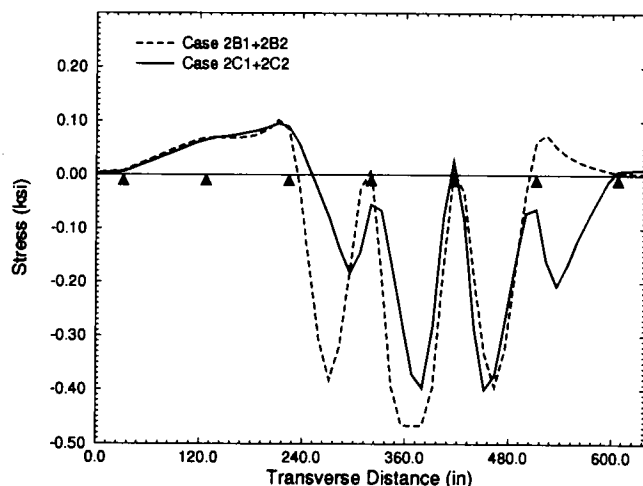


FIGURE 11 Top normal stresses in transverse direction along the critical section for two trucks near midspan (1 in. = 25.4 mm, 1 ksi = 6.89 MPa).

In summary, it has been found from the finite-element analysis that the maximum transverse tensile stress that can be developed at the top of the bridge deck is 230 lb/in.<sup>2</sup> (1.59 MPa). If an impact factor of 0.3 is considered, this maximum transverse tensile stress is 300 lb/in. (2.06 MPa), which is much less than the modulus of rupture of the deck concrete.

A highway bridge is normally subjected to about 100,000 to 10 million cycles of repeated loadings during its lifetime (14). It has been observed from test results that the fatigue strength of plain concrete is about 60 percent of its rupture strength when concrete specimens were subjected to 10 million load cycles (15–17). If the bridge deck studied is going to be subjected to about 10 million load cycles, the tensile strength of the deck concrete is expected to be reduced from 590 lb/in.<sup>2</sup> (4.1 MPa) to 355 lb/in. (2.45 MPa), which is still higher than the maximum tensile stresses expected at the top of the deck. Since the truck load used in the stress analysis of the deck was 47 percent heavier than a standard HS20 truck, the analysis is considered conservative.

## CONCLUSIONS

The test results show that for all the load cases considered here, the transverse tensile strains at the top of the deck were always substantially lower than the cracking strain of the deck concrete. The behavior of the bridge deck under a test truck was analyzed by the finite-element method. The numerical results showed a good correlation with the test results. It was found from the analysis that even under more severe load cases with

two test trucks, the normal tensile stresses at the top of the deck are less than the expected fatigue strength of concrete. Hence, the results of the present study strongly support the fact that top transverse reinforcement is not necessary for sustaining the negative bending moment induced by traffic loads. Nevertheless, further research on the control of temperature and shrinkage cracks in the absence of top reinforcement is warranted.

Nonlinear stress analysis of the bridge deck, considering the cracking of concrete, is under way. These analyses will provide a better understanding of the behavior of concrete bridge decks subjected to extreme traffic loads, as well as of the influence of shrinkage and temperature cracks on deck stresses. Furthermore, the bridge considered in the present case study has relatively stiff girders. Hence, further parametric studies should be conducted with the finite-element model to develop rational design guidelines that cover a range of girder flexibilities.

## ACKNOWLEDGMENTS

The authors gratefully acknowledge the financial support provided by the CDOT for the present study.

## REFERENCES

1. *The Status of the Nation's Highways and Bridges: Conditions and Performance—Highway Bridge Replacement and Rehabilitation Program*. FHWA, U.S. Department of Transportation, 1989.
2. Li Cao, J. H. Allen, and P. B. Shing. A Case Study of Elastic Concrete Deck Behavior in a Four-Span Prestressed Girder Bridge: Finite Element Analysis. *Report CDOT-DTD-CU-93-7*, Colorado Department of Transportation, Denver, Jan. 1993.
3. Li Cao, J. H. Allen, P. B. Shing, and D. Woodham. A Case Study of Concrete Deck Behavior in a Four-Span Prestressed Girder Bridge: Correlation of Field Tests and Numerical Results. *Report CDOT-CU-R-94-8*, Colorado Department of Transportation, Denver, April 1994.
4. Westergaard, H. M. Computations of Stresses in Bridge Slabs Due to Wheel Loads. *Public Roads*, March, 1930, pp. 1–23.
5. *Standard Specifications for Highway Bridges*, 15th ed. AASHTO, Washington, D.C., 1992.
6. *Standard Specifications for Highway Bridges*, 2nd ed. AASHTO, Washington, D.C., 1935.
7. *Minutes of AASHTO Bridge Subcommittee*. FHWA, AASHTO, Washington, D.C., 1957–1961.
8. Allen, J. H. Cracking, Serviceability and Strength of Concrete Bridge Decks. In *Transportation Research Record 1290*, TRB, National Research Council, Washington, D.C., 1991, pp. 152–171.

9. Beal, D. B. Load Capacity of Concrete Bridge Decks. *Journal of the Structural Division*, ASCE, Vol. 108, No. ST4, 1982, pp. 814–882.
10. Fang, I. K., J. A. Worley, N. H. Burns, and R. E. Klinger. Behavior of Isotropic R/C Bridge Decks on Steel Girders. *Journal of Structural Engineering*, ASCE, Vol. 116, No. 5, 1990, pp. 659–678.
11. *Building Code Requirements for Reinforced Concrete* (ACI 318-89). American Concrete Institute, 1989.
12. Mufti, A. A., et al. Fiber Reinforced Concrete Deck Slabs Without Steel Reinforcements. *Report 1-1991*, Department of Civil Engineering, Technical University of Nova Scotia, July 1991.
13. Wilson, E. L., et al. *SAP90 Program User's Manual*. Computers & Structures, Inc., 1989.
14. Hsu, T. T. C. Fatigue of Plain Concrete. *ACI Journal*, July-Aug., 1981, pp. 292–305.
15. Ballinger, C. A. Cumulative Fatigue Damage Characteristics of Plain Concrete. In *Highway Research Record* 370, HRB, National Research Council, Washington, D.C., 1971, pp. 48–60.
16. Tepers, R., and T. Kutti. Fatigue Strength of Plain, Ordinary, and Lightweight Concrete. *ACI Journal*, May, 1979, pp. 635–652.
17. Oh, B. H. Fatigue Analysis of Plain Concrete in Flexure. *Journal of Structural Engineering*, ASCE, Vol. 112, No. 2, 1986, pp. 273–288.

---

*The opinions expressed in this report are those of the authors and do not necessarily represent those of the sponsor.*

# Probabilistic Assessment of Prestressed Concrete Bridge

---

J. A. Sobrino, *PEDELTA, S.L. Civil Engineering Consultants, Spain*

J. R. Casas, *Technical University of Catalonia, Spain*

The structure of an existing bridge cannot be assessed using the same nominal parameters and safety factors calibrated for the design of new bridges. The direct use of probabilistic methods allows a determination of the safety and serviceability of an existing structure. The uncertainties involved with load and resistance values in the assessment of concrete bridges are usually lower than in the design stage because the strength and load effects can be estimated accurately by using information from inspections, experimental tests, traffic measurements and other supplementary data. After that, a full probabilistic analysis is performed, as with design code calibration, but for each particular case of study. A practical example is presented, including the assessment of a prestressed concrete bridge, to illustrate the abilities of probabilistic methods to assess existing structures.

**T**he assessment of existing concrete bridges is becoming an important task for structural engineers. Approximately 72 percent of U.S. bridges are older than 25 years (55 percent in Western Europe), and most of these bridges were made of concrete [in 1989, 70 percent in Western Europe and 52 percent in the United States (1)]. In addition, many of these bridges have been classified as deficient (1). In this way, the development of new structural evaluation methods will have important safety and economical implications.

Using semiprobabilistic methods, with safety factors and nominal resistance or loads that have been calibrated for the design of new structures, to assess existing structures is not always best. The safety factors and nominal parameters used in design have been obtained for a set of specifications included in the design codes, but for existing bridges these criteria can be different:

1. Safety factors include global uncertainties that are possible to find in structures designed with the same codes when substantially different construction methods and technologies are used. For example, the average error of concrete slab depths built in situ usually varies between 1 and 3 cm. These values affect significantly the evaluation of self-weight of slabs between 20 and 40 cm thick, as used in building construction. In prestressed concrete slab bridges these errors usually are not relevant because depth varies between 80 and 150 cm. Nevertheless, design codes usually specify the same dead load factor for both types of construction. For an existing structure it is possible to estimate accurately the geometry and deficiencies of the structural elements.

2. In the assessment of existing bridges, the resistance parameters can be updated with data from experimental tests (static or dynamic load, cores of concrete or steel bars, etc.). Variations of resistance in the structure are estimated accurately using Bayesian tech-

niques. In general, the uncertainties are less than those assumed in current standards.

3. Traffic loads can be measured in specific places (weigh-in-motion techniques, traffic flow control, etc), and expected maximum values of loads can be obtained for the study. For each case, it is possible to consider allowances in truck weights, increasing and heavier traffic, or other circumstances.

4. Some existing bridges have been designed with codes including structural verification criteria and rules different than current methods. In other old structures, lower nominal live loads were used in design. In most cases, these bridges would be classified as unsafe if the current design code requirements were imposed.

The safety factors and nominal parameters included in the codes are based on and calibrated with a probabilistic approach. The reliability theory provides tools to determine the parameters necessary for safe structures, if design rules are verified.

The use of probabilistic methods has been accepted as the more rational analysis for assessing existing concrete bridges. On such structural evaluations, the reliability level shall be at least the level accepted for new bridges in national or international standards. The recent European codes have been calibrated for a maximum failure probability of collapse between  $P_f = 10^{-4}$  to  $10^{-6}$  during a lifetime (1–3). In the United States a probability of failure  $P_f = 10^{-3}$  has been accepted for a reference period of 50 years. Instead of using probability of failure, the reliability index,  $\beta$ , has been used more as a convenient measure of the structural safety level. For the aforementioned probabilities, the reliability index is between 3.5 (United States) and 3.8 to 5.0 (Europe).

The reliability index generally is defined as a function of the probability of failure:

$$\beta = \Phi^{-1}(P_f) \quad (1)$$

where  $\Phi^{-1}$  is the inverse standard normal probability density function. Values of reliability index versus probability of failure are as follows:

$\beta$	$P_f$
0.0	0.500
1.0	0.159
2.0	$0.23 \cdot 10^{-1}$
3.0	$0.14 \cdot 10^{-2}$
4.0	$0.32 \cdot 10^{-4}$
5.0	$0.29 \cdot 10^{-6}$
6.0	$0.13 \cdot 10^{-9}$

More advanced definitions and concepts related to the reliability theory can be found elsewhere (4,5).

## STRUCTURAL ASSESSMENT PROCEDURE

The exposed method for evaluating the safety of existing concrete bridges is based on a probabilistic approach. The traditional formulation of the ultimate limit states (ULS) can be written as

$$M = R - S \quad (2)$$

where

$M$  = safety margin

$R$  = structural response (resistance), and

$S$  = load effects.

$M$ ,  $R$ , and  $S$  should be modeled as random variables to evaluate the reliability index,  $\beta$ , as the more rational structural safety measure for the assessment of existing bridges considering its real structural capacity and actual or future load conditions. The more relevant parameters are updated for a specific case using information derived from inspections, tests, traffic measurements, and so on.

The formulation of the limit states concerning flexural behavior is presented in the following sections for the case of a simply supported beam. For continuous bridges, Sobrino and Casas proposed a method that takes into account the nonlinear behavior of concrete decks in evaluating ultimate load-carrying capacity (6,7).

## Evaluation of ULS of Collapse Due to Moment Carrying Capacity

The failure function of the ULS of collapse due to bending moment, in a simply supported beam, can be formulated for the critical section as

$$M_u - (M_{g1} + M_{g2} + M_{q,T}) = 0 \quad (3)$$

where

$M_u$  = ultimate bending moment capacity,

$M_{g1}$  = bending moment due to self weight,

$M_{g2}$  = bending moment due to dead load (pavement, fascia beams, etc.), and

$M_{q,T}$  = maximum bending moment due to traffic load for time  $T$ .

All of these should be modeled as random variables. The safety of the bridge will be ensured if the reliability index of this ULS ( $\beta_u$ ) is greater than the minimum accepted value  $\beta_{u,min}$ .

The same ULS is verified with the rules provided by the current Spanish design code. In this case, the load





In this example, the following situation is assumed:

1. It is supposed that during the construction of bridge one of the ducts is broken and it is not possible to place one of the prestressing tendons.

2. A higher quality of concrete has been obtained. A C35 concrete was specified, and the result of quality controls provided the following parameters:

$$f_{c,mean} = 42 \text{ MPa}$$

The coefficient of variation  $V_{fc} = 8$  percent.

3. A higher quality of prestressing and reinforcement steel has been obtained. The result of quality controls provided the following parameters:

–Yield tensile stress of prestressing steel:

$$f_{yp,mean} = 1820 \text{ MPa} \quad (f_{yp,nom} = 1620 \text{ MPa})$$

The coefficient of variation is assumed to be 3 percent.

–Yield tensile stress of reinforcement steel:

$$f_{y,mean} = 560 \text{ MPa} \quad (f_{y,nom} = 500 \text{ MPa})$$

The coefficient of variation is assumed to be 5 percent.

In both cases, the coefficient of variation is assumed from recent studies and a large data bank collected in Spain (6). These data have been updated with the results of quality control using Bayesian techniques.

4. The mean elongation of the cables during execution was practically coincident with the theoretical calculated values, with a coefficient of variation of 6 percent.

5. During the revision of the load effects in the design project, the effect of eccentric live load was not considered because of human error.

The objective of this paper is to evaluate the serviceability and load-carrying capacity of the deck with nine tendons under the real traffic loads.

## Load Effects

The dead loads have been modeled as random variables using Monte Carlo techniques. The data used for the uncertainty modeling of geometry are derived from available data collected in concrete bridges in Spain (6). These models allow the consideration of common errors and uncertainties in concrete depths, real position of steel, real depth of pavements and so forth. The ob-

**TABLE 1 Bending Moment at Midspan (MN·m)—Nominal Values and Probabilistic Models (Including Model Uncertainties) for Evaluation of ULS**

	Nominal Value (1)	Mean	Coefficient of Variation	Type of distribution
Self-weight	15.60	15.93	0.025	Normal
Imposed dead load	3.75	4.12	0.080	Normal
Traffic T=50 years	7.92	8.25	0.060	Gumbel

(1) Nominal values for traffic according to current Spanish code (including eccentricity effect of loads) and mean values of geometry for dead loads.

tained values of bending moment at midspan due to self-weight and dead load in the case of study, for a good construction are given in Table 1. The mean thickness of the pavement is 80 mm.

The traffic load effects have been obtained using numerical simulations with a model developed by Sobrino (6) and improved to simulate traffic using a grillage structural model. The traffic has been simulated passing over the bridge under real conditions. The traffic is 20 percent trucks with a typical highway composition of vehicles, classified by the number of axles (Figure 2). The average intensity is 12,000 vehicles per day in the period of study. The loads are derived from real measurements in Spain (6). Figures 3 and 4 show the mean and maximum truck weights obtained in measuring more than 16,000 trucks in 1 week during 1990 and 1992 near Barcelona. In some weigh stations more than 60 percent of vehicles exceed the legal limit (380 kN for more than four axles).

The maximum traffic load effects have been obtained for two situations: (a) free traffic with a maximum intensity of 1,000 vehicles per hour (2 h/day), and (b) full-stop traffic, with an average value of 4hr/week. The results of the simulations are presented in Tables 1 and

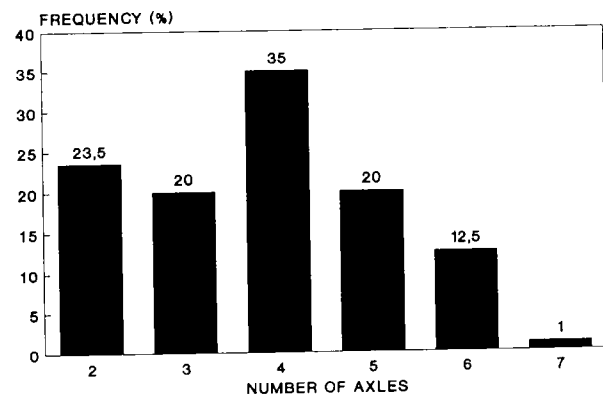


**FIGURE 2 Heavy traffic composition classified by number of axles.**

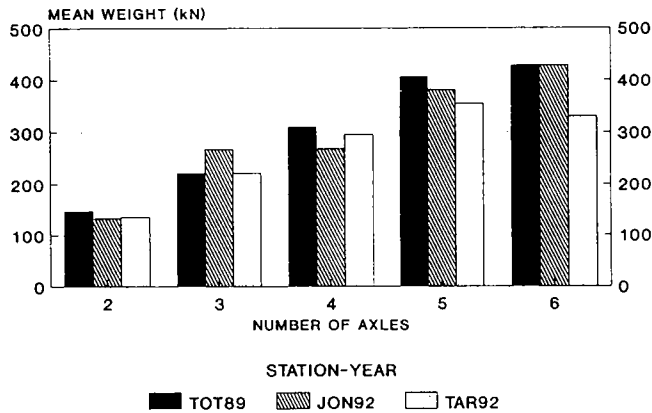


FIGURE 3 Mean truck weight observed in three weigh stations, 1990 and 1992, Spain.

2, in terms of bending moment at midspan, including the impact factor and the effect of load eccentricities on the deck.

### Structural Response

The structural capacity of the bridge has been evaluated in terms of flexural response of the critical cross section. The probabilistic models for material strengths are based on a data bank collected in Spain; the values are similar to those measured in other countries for a high quality of control (6). The Monte Carlo techniques have been used to obtain the cross-sectional response, including the nonlinear behavior of steel and concrete in the calculation of the bending moment–curvature relationships and for the ultimate flexural capacity. Results are given in Table 3.

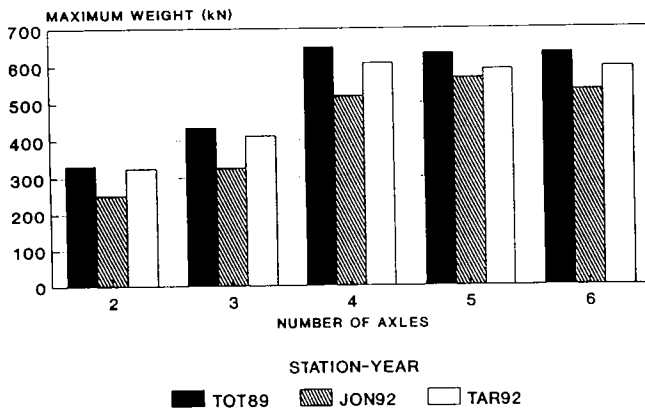


FIGURE 4 Maximum truck weight observed in three weigh stations, 1990 and 1992, Spain.

TABLE 2 Traffic Bending Moments for Evaluation of the SLS

	Bending Moment (MN·m)
Frequent loads	6.08
Infrequent loads	7.15

Note: These values were obtained by means of numerical simulations with real traffic loads and configurations.

### Evaluation of Ultimate Limit Flexural Capacity

A reliability analysis has been performed to evaluate the safety of the bridge under the actual conditions with nine cables. The minimum value of  $\beta_{u,min} = 5$  has been accepted. The results are shown in Figure 5. In Figure 6 the load safety factor is shown, defined as Expression 4.

The load safety factor for the girder with nine cables is  $\gamma = 1.42$  (less than the minimum required  $\gamma_{min} = 1.50$ ), but the reliability index is  $\beta_u = 6.6$  (probability of failure  $P_f = 10^{-11}$ ).

If the design condition is checked (deck with 10 prestressing cables), the measures of the safety level are

$$\gamma = 1.55$$

$$\beta_u = 7.8 \text{ (probability of failure } P_f = 10^{-14})$$

As a consequence of this study, it is noticed that the semiprobabilistic analysis gives very conservative criteria for the structural safety of the bridge compared with the more rational probabilistic study. The bridge should be considered safe enough under real traffic conditions for 50 years.

The safety of the bridge has also been verified with the same traffic configuration, assuming 40 percent of trucks in the traffic flow. In this case, the reliability index was very similar ( $\beta_u = 7.6$ ) because the mean value of live load moment at midspan increases an 8 percent but the coefficient of variation is about 3.5 percent (not including the statistical or model uncertainties).

TABLE 3 Cross-Sectional Response at Midspan with 10 and 9 Prestressing Cables (MNm)

	No. of Cables	Nominal Value	Mean	Coefficient of Variation	Type of distribution
Mu	10	43.63 (1)	53.33	0.059	Lognormal
	9	40.17	48.09	0.059	Lognormal
Mcr	10	25.46 (2)	26.83	0.074	Normal
	9	22.82	24.21	0.075	Normal

(1) Nominal values are calculated with characteristic values of material strengths and partial safety factors.

(2) Nominal values calculated with characteristic values of strengths and prestressing force. The values of the mean and the Coefficient of Variation include model uncertainties.

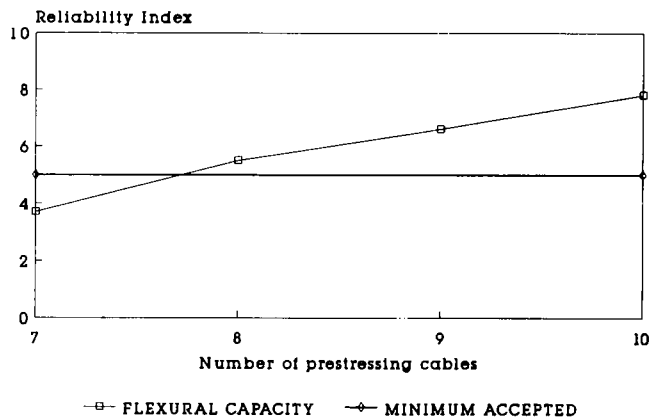


FIGURE 5 Reliability index for ULS flexural carrying capacity;  $T = 50$  years. Index has been calculated for different numbers of prestressing cables in deck. Bridge would be considered safe with eight cables.

### Evaluation of SLS of Cracking

The SLS of cracking has also been checked with 10 and 9 cables. In this case, the results are

$$(M_{g1,k} + M_{g2,k} + M_{q,freq}) = 27.1 \text{ MN}\cdot\text{m}$$

$$(M_{g1,nom} + M_{g2,nom} + M_{q,nom}) = 27.6 \text{ MN}\cdot\text{m}$$

Design condition with 10 cables:  $M_{cr,k} = 25.5 \text{ MN}\cdot\text{m}$

Design condition with 9 cables:  $M_{cr,k} = 22.8 \text{ MN}\cdot\text{m}$

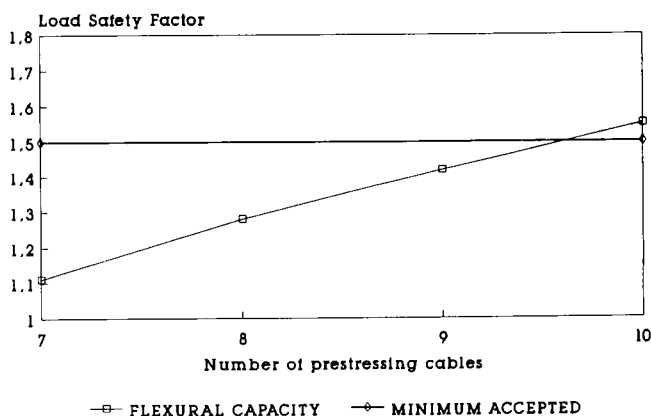


FIGURE 6 Load safety factor for ULS of flexural carrying capacity. Safety factor is calculated by means of Expression 4 for different numbers of prestressing cables. Minimum accepted value by Spanish design code is 1.50. Bridge would be considered safe with 10 prestressing cables.

In both cases, the SLS of cracking is not verified, and crack width should be checked under permanent and frequent traffic load effects. The crack width has been calculated using the rules of Eurocode 2 (9). The obtained values are

Design condition with 10 cables:  $W_k = 0.08 \text{ mm}$

Design condition with 9 cables:  $W_k = 0.17 \text{ mm}$

The maximum characteristic value of the crack width is, in both cases, less than the maximum design value accepted under frequent combination of loads and non-aggressive environment  $W_{max} = 0.2 \text{ mm}$ . So the actual situation of the deck, with nine cables, should be considered satisfactory under real traffic conditions.

### CONCLUSIONS

The use of probabilistic methods allows a rational evaluation of existing structures. The more relevant features of the probabilistic assessment method are presented using a simple example.

For evaluating existing prestressed concrete bridges, the use of the same safety factors and nominal design properties and loads does not allow the real condition of the structure—or further information about materials, test, and loads—to be taken into account. Because the probabilistic assessment leads to a more rational evaluation, it is an efficient tool for managing existing bridges.

### ACKNOWLEDGMENT

This work is part of the Ph.D. dissertation of J. A. Sobrino, which was financially supported by the Education Department of the Government of Catalonia.

### REFERENCES

1. *Bridge Management*. Road Transport Research, Organization for Economic Cooperation and Development, Paris, France, 1992.
2. European Committee for Standardization. *Eurocode 1: Basis of Design and Actions on Structures. Part 1: Basis of Design*, 6th draft. March 1993.
3. Nowak, A. S. Calibration of LRDF Bridge Design Code. *Proc., ICOSSAR '93 Conference, Structural Safety and Reliability*, Vol. 2, Austria, 1993, pp. 927–932.
4. *Conceptional Preparation of Future Codes*. Bulletin 147. Comité Euro-International du Béton, Feb., 1982.

5. Thoft-Christensen, P., and M. J. Baker. *Structural Reliability Theory and Its Applications*. Springer-Verlag, 1982.
6. Sobrino, J. A. *Evaluation of Structural Safety and Serviceability of Existing Reinforced and Prestressed Concrete Bridges* (in Spanish). Doctoral thesis. Technical University of Catalonia, Barcelona, Spain, Dec. 1993.
7. Sobrino, J. A., and J. R. Casas. Random System Response of Reinforced and Prestressed Concrete Bridges. *Proc., ICOSSAR '93 Conference, Structural Safety and Reliability*, Vol. 2, Austria, 1993, pp. 985–988.
8. European Committee for Standardization. *Eurocode 1: Basis of Design and Actions on Structures, Vol 3: Traffic Loads on Bridges*. 10th draft, 1993.
9. European Committee for Standardization. *Eurocode 2: Design of Concrete Structures*. Revised final draft, 1989.

# Effect of Cross Frames on Behavior of Steel Girder Bridges

---

Atorod Azizinamini, *University of Nebraska–Lincoln*

Steve Kathol, *Schemmer Associates, Inc.*

Mike Beacham, *Nebraska Department of Roads*

Although cross frames are required before construction, their usefulness after construction has been questioned. A combination of experimental and analytical studies was conducted to investigate the performance of steel girder bridges that use different types and spacing of cross frames. The experimental investigation included construction and testing of a full-scale steel girder bridge in the laboratory. Unique characteristics of the bridge include a concrete slab designed on the basis of AASHTO's 1994 empirical design approach, which requires a minimal amount of reinforcement. Elastic and ultimate load tests were carried out, and punching shear tests were conducted after the ultimate load tests. Results of the research indicate that for bridges with zero skew, the influence of cross frames is minimal. Ultimate tests indicate that steel girder bridges have large reserve capacities. Very large punching shear capacity of the slab was also observed.

The 15th edition of the AASHTO manual requires intermediate cross frames in steel girder bridges with maximum spacing of 7.63 m. Although these cross frames may be needed for temporary loads, their effectiveness after construction has been a point of debate for short- and medium-span bridges.

Cross frames with different configurations have been used in bridge construction. Besides increasing construction costs, cross frames may contribute to many prob-

lems in steel girder bridges. For instance, many states have observed cracking in the girder web of bridges in the vicinity of the cross frame's connection to the girder, especially in details for which stiffeners are not connected rigidly to top and bottom flanges.

To address this issue, a combination of analytical and experimental investigations was conducted. A summary of the experimental investigation related to the use of cross frames is presented in this paper.

## EXPERIMENTAL INVESTIGATION

### Bridge Description

A series of tests was carried out on a full-scale bridge constructed in the structural laboratory. The bridge was a simple span 21.35 m long and 7.93 m wide. Figure 1 shows a photograph of the completed bridge in the laboratory. The superstructure consisted of three welded plate girders built compositely with a 190.5-mm-thick reinforced concrete deck. The girders, each 1.37 m deep, were spaced 3.05 m on center, and the reinforced concrete deck had a 0.915-m overhang. The concrete barrier structure was an open concrete bridge rail, with 280- × 280-mm posts spaced 2.44 m on center. The construction sequence was identical to that of field practice.

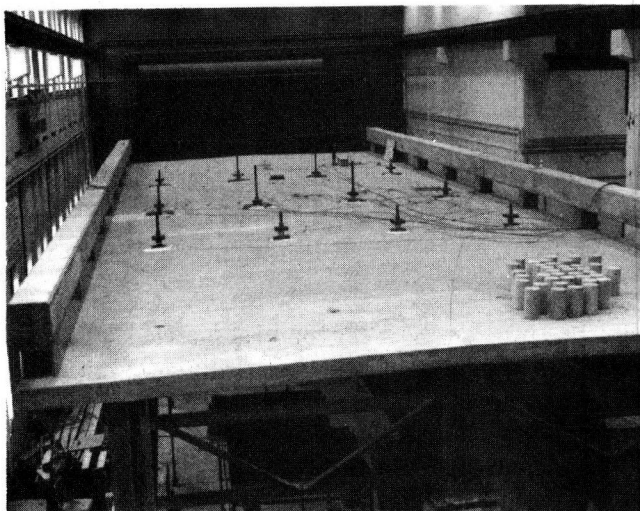


FIGURE 1 Completed bridge.

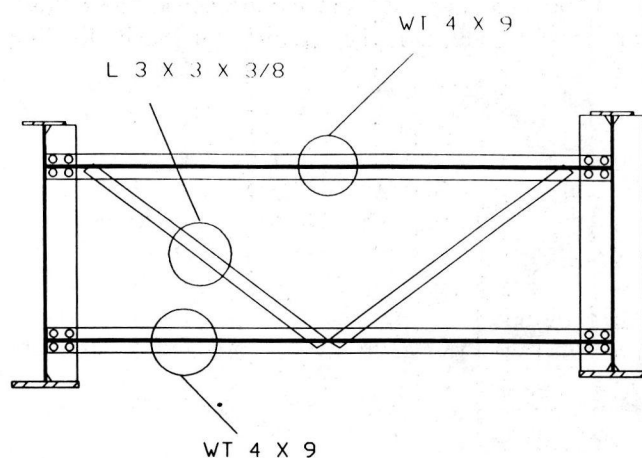


FIGURE 2 Member sizes used for K-type cross frames.

During construction, K-type cross frames at 3.42-m spacing, as shown in Figure 2, were used. This resulted in a total of seven cross frames in each lane.

A series of strain gauges and potentiometers was attached to the bridge to measure strains and bridge deflections at different locations.

The behavior of the bridge was monitored continuously for approximately 102 days following casting of the concrete deck before live load tests were conducted to evaluate the effect of cross frames. During this period, strains in the cross frames resulting from creep and shrinkage of the concrete deck were measured using vibrating wire strain gauges. In general, the maximum strain resulting from dead load and creep and shrinkage was very small; the resulting stress did not exceed 11.72 MPa in members of the cross frames monitored.

### Live Load Test Setup

Live loads were applied by using 12 hydraulic rams, shown in Figure 1. Each ram simulated one wheel load. Six rams were placed on each lane of the bridge to simulate the wheel configuration of one AASHTO HS20 truck load. Figure 3 shows the locations of all 12 rams, which simulated two trucks side by side on the bridge. The spacing of axles, as shown in Figure 3, is 3.66 and 4.58 m instead of 4.27 and 4.27 m as specified by AASHTO. This spacing was a result of laboratory constraints. Using this hydraulic ram configuration, it was possible to simulate having (a) only one truck in the north or south lane (by activating only six rams in the desired lane), (b) on truck straddling the centerline (by activating the middle six rams), or (c) one truck on each lane (by activating all rams). Steel plates were used to simulate the footprint of trucks at each load point. The

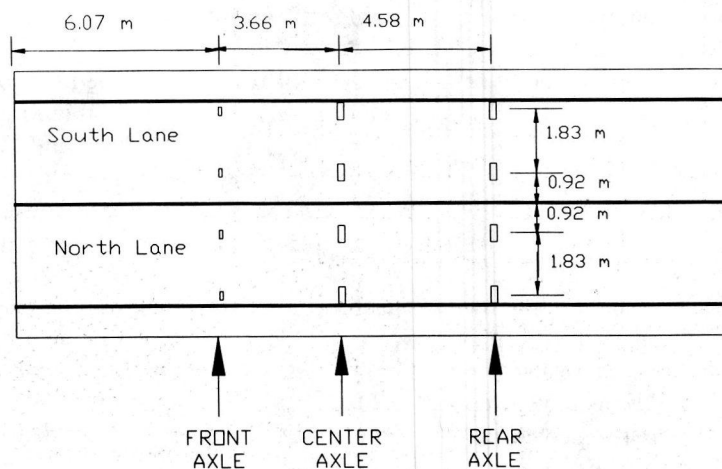


FIGURE 3 Location of 12 hydraulic rams used for applying live load.



size of the footprint was determined from the AASHTO manual. The plates used in the rear and front axles were  $508 \times 203 \times 50.8$  mm and  $254 \times 101.6 \times 50.8$  mm, respectively.

## Test Descriptions and Results

Table 1 gives a list of 12 tests. Each test consisted of applying three cycles at the indicated load level. Also shown in Table 1 are the type and spacing of cross frames used in each test. For instance, during Test 1, K-type cross frames at 3.42-m spacing were used. In this test all 12 rams were activated to stimulate two trucks side by side. Further, during Test 1, the bridge was loaded and completely unloaded three times at a load level corresponding to having trucks weighing 2.5 times the AASHTO HS20 truck load (800 kN) on each lane. This load level was achieved by increasing load points on rear and front axles to 178 and 44.48 kN, respectively.

During Tests 2 through 5, K-type cross frames at 6.83-m spacing were used. All but the end cross frames were removed during Tests 6 through 9. Tests 10

through 12 used X-type cross frames of the configuration shown in Figure 4 at 6.83-m spacing.

The effect of cross frame types and spacing on response of the bridge to applied live loads will be discussed in terms of maximum strain in steel girders, maximum girder deflections, and load distribution factors.

## Strain in Steel Girders

The effect on the behavior of steel girders of altering cross frame spacing and type will be discussed in terms of maximum tensile strain in the bottom flange of interior and exterior girders at the mid- and quarter spans of the bridge. In all cases the applied live load corresponds to one or two trucks being on the bridge, each truck weighing 800 kN. A summary of strains measured at midspan and quarter span of the bridge for different cross frame configurations and loading conditions is given in Table 2. The reported strains are all measured in the bottom flange at indicated locations. The following sections discuss the results for each loading condition.

TABLE 1 Descriptions of Live Load Tests

Test Number <sup>+</sup>	Cross frame Type	Cross frame Spacing, meters	Loading Condition <sup>#</sup>	Maximum Load <sup>*</sup>
1	K	3.42	Both Lanes	2.5 x HS-20
2	K	6.83	Both Lanes	2.5 x HS-20
3	K	6.83	South Lane	2.5 x HS-20
4	K	6.83	North Lane	2.5 x HS-20
5	K	6.83	Straddling	2.5 x HS-20
6	None	-----	Both Lanes	2.5 x HS-20
7	None	-----	South Lane	2.5 x HS-20
8	None	-----	North Lane	2.5 x HS-20
9	None	-----	Straddling	2.5 x HS-20
10	X	6.83	Both Lanes	2.5 x HS-20
11	X	6.83	North Lane	2.5 x HS-20
12	X	6.83	Straddling	2.5 x HS-20

<sup>+</sup> Each test consisted of applying three complete cycles of loading. Each cycle is defined as increasing the loads in rear rams to 178 kN and front rams to 44.48 kN load levels.

<sup>#</sup> Both Lanes = All 12 hydraulic rams were activated, simulating having two truck side by side

South Lane = The six rams in south lane were activated, simulating having one truck in south lane. See Fig. 3 for definition of south and north lanes

North Lane = The six rams in north lane were activated, simulating having one truck in north lane

Straddling = The middle six rams were activated, simulating one truck straddling the centerline

<sup>\*</sup> During each test applied loads in front and rear wheels simulated having one or two trucks weighing 800 kN each.

This weight corresponds to 2.5 times the weight of AASHTO's HS-20 truck

<sup>%</sup> The maximum concrete strains reported are transverse strains (perpendicular to traffic direction) measured in top surface of the slab at midspan in middle of the two girder lines. Compressive and tensile strains are represented by negative and positive signs respectively

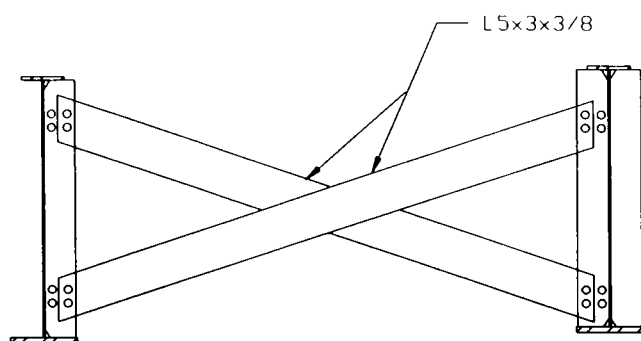


FIGURE 4 Configuration of X-type cross frames.

### Both Lanes Loaded

Table 2 gives maximum bottom flange strains at midspan and quarter point for the cases in which both lanes are loaded. Comparison of test results for K cross frames at 3.42- and 6.83-m spacing indicates that the maximum tensile strain in the bottom flange of the center girder increased slightly as the spacing of cross frames increased. The difference in exterior girder strain is not significant enough to make definite conclusions. As indicated in Table 2, the maximum strains in both interior and exterior girders are not significantly affected by using X-type cross frames instead of K type. The case in which all cross frames are removed resulted in higher tensile strain in the center girder and smaller strains in exterior girders when compared with cases in which X- or K-type cross frames at 6.83-m spacing are used. The increase in maximum tensile strain in the bottom flange of the center girder at midspan resulting from removal of all cross frames is only 6.4 percent over

the case in which K-type cross frames are used at 6.83-m spacing. This behavior indicates that load distribution factors are affected only slightly by the presence of intermediate cross frames.

### Straddling the Center Lane

Table 2 also gives the maximum bottom flange strains observed for each cross frame configuration at midspan and quarter point with applied load simulating one 800-kN truck straddling the bridge centerline. Results indicate that X- and K-type cross frames result in the same behavior. From this table it can be observed that in the case of no cross frames, the resulting strain in the center girder is 14.5 percent higher than it is with K cross frames at 6.83-m spacing. In evaluating this result two points are important. First, the difference is relatively small. Second, although the case of one truck straddling the centerline results in higher percentage differences, the magnitude of the resulting strain in the bottom flange is much smaller than it is when both lanes are loaded. This is important when considering that the design situation will be governed when both lanes are loaded.

### Loading One Lane Only

Table 2 presents maximum bottom flange strains observed at midspan and quarter point with only the south lane loaded with a truck weighing 800 kN. As expected, the influence of removing all cross frames is more pronounced for the exterior girder farthest from the loaded lane (north lane). As noted in Table 2, although the percentage difference in exterior girder (north lane)

TABLE 2 Maximum Bottom Flange Strains

Loading Condition	Cross frame Type and Spacing meter	Maximum Strain at Midspan ( $\mu\epsilon$ )			Maximum Strain at Quarter span ( $\mu\epsilon$ )		
		North Exterior Girder	Center Girder	South Exterior Girder	North Exterior Girder	Center Girder	South Exterior Girder
Both Lanes Loaded	K at 3.42	359	425	358	335	371	329
	K at 6.83	372	473	367	340	393	331
	X at 6.83	367	481	368	339	402	330
	None	349	505	351	320	424	317
Straddling Center Lane	K at 6.83	160	302	161	152	245	150
	X at 6.83	156	309	155	155	253	147
	None	139	353	138	133	294	130
South Lane Loaded	K at 6.83	35	237	334	32	199	297
	X at 6.83	29	237	331	28	204	299
	None	23	253	324	25	216	290

strain is larger than that with K-type cross frames at 6.83-m spacing (23 micro strain compared with 35 micro strain), the magnitude of resulting strains in exterior girders is much smaller than when both lanes are loaded (23 microstrain compared with 349 microstrain).

### Girder Deflections

A summary of the effects on deflection of interior and exterior girders of altering cross frame spacing and type is given in Table 3. The deflections are reported at mid-span and quarter point of the interior and one of the exterior girders. All deflections are the maximum values observed and correspond to loading that simulates one or two 800-kN trucks on the bridge in a position producing the maximum moment in the girders. For the loading condition designated as "one lane loaded," deflections are reported for the exterior girder located in the side of the loaded lane. All deflections are corrected for the end displacements produced by the flexibility of the bearing pads.

From the results given in this table, the following conclusions can be drawn:

- In the case of K cross frames, increasing the spacing from 3.42 to 6.83 m has a negligible effect on girder deflection, for both exterior and interior girders.
- The deflection of the girders for tests with X- and K-type cross frames differs very slightly.
- In the case of no intermediate cross frames, the deflections of the exterior girders are decreased while the deflection of the interior girder is increased. How-

ever, again, this change in deflection is small. The main reason for this behavior is that the contribution of the slab in distributing load between girders is more pronounced than that of the cross frames. When there are no intermediate cross frames, the percentage difference in deflection of girders compared with having X- or K-type cross frames at 6.83-m spacing is higher when only one lane is loaded or when the load straddles the centerline. However, the resulting deflections for both interior and exterior girders in these cases are approximately 50 percent of what they are when both lanes are loaded.

### Load Distribution Factors

By using the experimental results, load distribution factors for different cross frame configurations were obtained. First, however, load distribution factor, as used in this paper, will be defined briefly.

A load distribution factor is needed because current design approaches use two-dimensional models to approximate the real behavior of a bridge. Therefore, the load distribution factor can be viewed as a correction or correlation factor relating specific responses (such as a maximum stress in the bottom flange of the girder) of a bridge component in a real structure to the same response of a simple model of that component. So, if one is interested in approximating the maximum tensile stress in the bottom flange of girders in a bridge, one should use an appropriate correlation factor (or load distribution factor) that was based on stress considerations.

In the current design approach, an important limit state criterion is the level of stresses in the steel girder

TABLE 3 Maximum Girder Deflections

Loading Condition	Cross frame Type	Cross frame Spacing meter	Maximum Deflection			
			Quarter Point		Mid Span	
			Interior Girder (mm.)	Exterior Girder (mm.)	Interior Girder (mm.)	Exterior Girder (mm.)
Both Lanes Loaded	K	3.42	11.38	10.08	16.54	14.25
	K	6.83	12.12	10.19	17.45	14.4
	X	6.83	12.7	10.16	18.21	14.5
	None	-----	13.1	9.78	19	13.95
Straddling Center Line	K	6.83	7.32	4.9	10.69	6.73
	X	6.83	7.67	4.62	11.3	6.48
	None	-----	8.84	4.09	12.93	5.79
One Lane Loaded	K	6.83	5.94	9.22	8.71	13.03
	X	6.83	6.4	9.07	9.04	12.98
	None	-----	6.5	8.86	9.42	12.65

portion of the bridge. Therefore, in this study the distribution factor from experimental results was obtained using stress considerations. The procedure used to calculate the distribution factors can be summarized as follows.

First, a simply supported beam was loaded with three concentrated loads with spacing corresponding to axle spacing used in the experimental investigation (approximately the same axle spacing as that of an AASHTO HS20 truck). The three concentrated loads had relative magnitudes corresponding to HS20 truck wheel loads as indicated in Figure 5. The  $\alpha$ -factor in front of each concentrated load in Figure 5 is the distribution factor. From Figure 5, the maximum moment,  $M_a$ , as a function of the  $\alpha$ -factor is then calculated. Next, from the experimental results, the maximum observed strain in the bottom flange of the interior and exterior girders was obtained. The values were taken from tests simulating two trucks side by side at a load level corresponding to AASHTO HS20 truck loads (i.e., 17.8 and 71.2 kN under the front and rear wheels, respectively). Using the average modulus of elasticity obtained from material tests, these strains were converted to stress. Using these stresses, experimentally obtained moments were calculated using the following formula:

$$M_{exp} = f_t S_b$$

where

- $M_{exp}$  = maximum moment obtained from experimental results,
- $S_b$  = section modulus of composite section with respect to bottom flange, and
- $f_t$  = experimentally obtained tensile bottom flange stresses.

To ensure compatibility with assumptions used in AASHTO procedures for the design of composite sections, in calculating the  $S_b$ , the section modulus, it was assumed that the effective width of the slab is the same as that specified by the AASHTO manual. Finally, by equating the maximum moment obtained from experi-

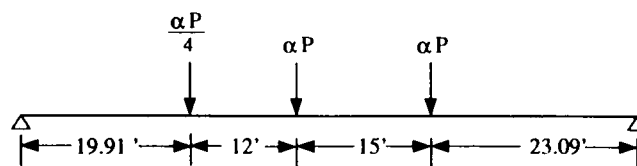


FIGURE 5 Girder model and loading condition.

mental results,  $M_{exp}$ , to that obtained from Figure 5  $M_a$ , the load distribution factor,  $\alpha$ , was obtained. Table 4 provides a summary of distribution factors obtained for different cross frame configurations. Also given in this table are the distribution factors predicted by current AASHTO procedures and those given by AASHTO's new provisions, *Guide Specifications for Distribution of Loads for Highway Bridges* (Ibsem formulas) (1).

The following observations can be inferred from the data reported in this table:

- Distribution factors obtained experimentally are smaller for exterior girders than for interior girders. This result can be attributed mainly to the strengthening effects of the railing system. The analytical model used in developing Ibsem formulas does not include the effect of railing systems.
- The X- and K-type cross frames spaced at 6.83 m resulted in almost the same distribution factors.
- In the case of no cross frames, the increase in distribution factor for interior girder and decrease in distribution factor for exterior girder were very small when compared with the case of X- or K-type cross frames spaced at 6.83 m. However, the distribution factors obtained experimentally are still smaller than what the AASHTO or Ibsem formulas predict.

## ULTIMATE LOAD TEST

After the elastic load test just described, the bridge was loaded to collapse. During the ultimate load all 12 hydraulic rams were activated, to simulate having two HS20 trucks side by side. During the ultimate load test

TABLE 4 Load Distribution Factors

Cross frame Type	Cross frame Spacing, meter	Experimental		Current AASHTO		1994 AASHTO Provisions (1)	
		Interior	Exterior	Interior	Exterior	Interior	Exterior
K	3.42	1.21	1.03	1.82	1.82	1.62	1.62
K	6.83	1.34	1.05	1.82	1.82	1.62	1.62
X	6.83	1.38	1.06	1.82	1.82	1.62	1.62
None	-----	1.42	1.01	1.82	1.82	1.62	1.62

all cross frames were removed except those at the end. Figure 6 gives the resulting deflection at midspan of the middle girder versus the total applied load. The applied loads are given in terms of the number of HS20 truck loads weighing 320 kN each. A safety concern arose during the ultimate load test when the applied total load was approximately equal to 14 times the HS20 truck load. Consequently, the bridge was unloaded to correct the problem. Upon reloading, the load deflection curve followed the unloading path as indicated in Figure 6. This indicates that even loading and unloading the bridge at such a high load level did not alter the composite action between the girders and the concrete slab. The bridge failed when the total applied load approached the equivalent of 16 AASHTO HS20 truck loads. Failure was by punching shear at one of the loading points. At the time of failure, the maximum strain in the bottom flange of the interior girder at midspan was 10,900 microstrain. The permanent deflections of interior and exterior girders after complete unloading after failure were approximately 36 and 102 mm, respectively.

It is interesting that the bridge was designed for an AASHTO HS20 truck load (320 kN) and that the ultimate live load capacity of the bridge according to load factor design approach stated in the 15th edition of the AASHTO manual is approximately 2.7 times the HS20 truck load (in each lane). On the other hand, the bridge failed at a load corresponding to eight times the HS20 truck load in each lane, indicating a large reserve load-carrying capacity. This large reserve capacity could be attributed to (a) actual material properties that are higher than assumed smaller values in design, (b) a conservative approach to calculating distribution factors, (c) simplified two-dimensional analysis approaches to

calculate induced moments in bridge girders, and (d) conservative effective width values used in the design process.

## PUNCHING SHEAR TESTS

After the ultimate load tests, a series of punching shear tests was conducted on the bridge. These tests consisted of applying a single concentrated load at various locations over the concrete slab. Because of the 'ultimate load tests, the concrete slab bridge had experienced extensive cracking. Four punching shear tests were conducted, and despite the extensive cracking over the slab, the punching shear capacities obtained were between 543 and 694 kN: the capacity of 543 kN was obtained in the area where extensive cracking from the ultimate load test took place, and that of 694 kN was obtained in the area where relatively no cracking was present before the punching shear tests. These results indicate that the empirical design rule procedure as stated in the AASHTO 1994 load resistance factor design (LRFD) manual results in large punching shear capacity, even in the absence of cross frames and relatively large girder spacing.

## CONCLUSIONS

From the results of this investigation, the following conclusions can be made.

For a steel bridge with small skew, cross frames may be needed during construction, but their presence has little influence on the behavior of the bridge after construction. After construction, the stiffness of the slab is sufficient to distribute the live load to adjacent girders. It can be argued that cross frames are needed to provide redundancy in the bridge—that is, cross frames could be used to provide alternative load paths if such elements as the concrete deck were to fail. In this scenario—failure of one of the main load-carrying members—it is unlikely that cross frames could provide such a function and the bridge would fail anyway. This is especially important given the fact that many problems in steel bridges are caused by the presence of cross frames to begin with. Results of this research indicate that if it is desired to leave cross frames in place, the use of simpler forms of cross frames such as the X type provides behavior as good as that of the more expensive K or other types. Another application of this conclusion could be in retrofitting old steel girder bridges. Where cracking in elements connecting cross frames to the girder or girder webs is observed, the cross frames could be removed altogether to avoid costly repair expenses.

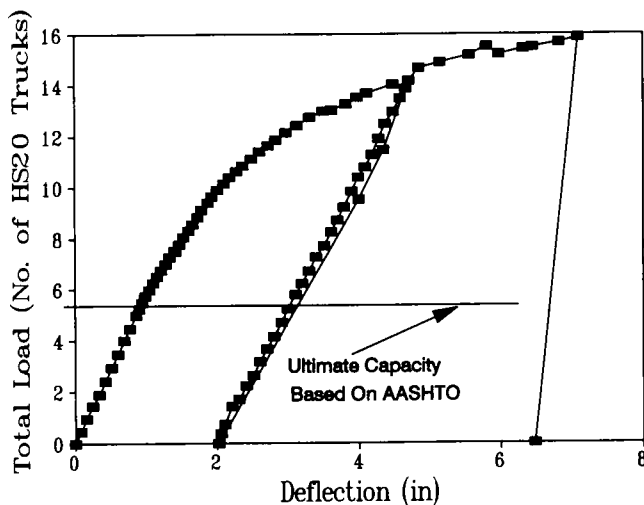


FIGURE 6 Load deflection response of interior girder at midspan during ultimate load test.

Results of ultimate load tests conducted on the bridge without any intermediate cross frames indicate that simplified and conservative assumptions made during design have given steel girder bridges a very large reserve capacity. If a bridge is in good condition, this reserve capacity could be used in rating older bridges designed for smaller truck loads than they are required to carry.

Results of punching shear tests indicate that the empirical design rule stated in the AASHTO 1994 LRFD manual results in a very adequate slab design procedure.

#### ACKNOWLEDGMENT

This research project is sponsored by the Nebraska Department of Roads (NDOR), to which the authors are

very appreciative. Valuable input by Gale Barnhill, Structural Engineer; Lyman Freemon, Bridge Engineer; and Mo Jamshidi, Assistant Bridge Engineer, Bridge Division of NDOR, is gratefully acknowledged. During the course of the investigation Robert Nickerson provided technical input, for which the authors are thankful. The assistance of Jim Luedke, Yerapalli Shekar, and Bruce Keeler in conducting the experimental and analytical studies is acknowledged. Additional support was provided by the Center for Infrastructure Research at the University of Nebraska–Lincoln.

#### REFERENCE

1. *Guide Specification for Distribution of Loads for Highway Bridges*. AASHTO, Washington, D.C., March 1994.

# On the Use of Measured Vibration for Detecting Bridge Damage

---

Sreenivas Alampalli, Gongkang Fu, and Everett W. Dillon, *New York State Department of Transportation*

Bridge condition monitoring using modal properties, which has been suggested and studied recently, is perceived to supplement or even replace current inspection practice. However, its applicability is still unclear. A study conducted on a fracture-critical bridge, supplementing earlier studies on a scaled model bridge, is presented. The detectability of damage using measured vibration is addressed. Results indicate that modal frequencies can be used to detect the existence of damage or deterioration simulated here. However, the damage location cannot be identified with high confidence using mode shapes and their derivatives because damage affects mode shapes comparably at both damaged and undamaged locations.

Many highway bridges in the United States are structurally deficient or functionally obsolete. Periodic inspection has become a major part of maintaining the safety of these bridges, so that potentially hazardous conditions can be identified early enough to prevent serious consequences. Currently, FHWA requires every bridge be inspected at least every 2 years (1), but some deficiencies may develop and cause serious failure between inspections. The near failure of a viaduct in Rhode Island (2) and other recent bridge failures in several states (3) prompted researchers to look for new inspection tools. It is believed that remote bridge monitoring systems based on measured

structural vibration will be helpful in bridge inspection in the future. It is well-known that modal frequencies and mode shapes will change with altered structural condition. Theoretically, the monitoring of these modal properties may be used for bridge diagnosis. The technique is commonly referred to as experimental modal analysis, modal testing, or dynamic monitoring.

Modal testing (4) recently received intensive attention because of the availability of Fourier analyzers, which instantaneously perform fast Fourier transforms. Several researchers have investigated changes in modal parameters due to simulated damages using laboratory bridge models and field bridges (5–8). Great efforts have been made to correlate measured modal parameters with simulated damages. Yet little attention has been paid to the sensitivity of modal parameters to common damage or deterioration of interest, which is critical in real-world application to bridge inspection. The major issue is that modal testing, like other experimental techniques, produces variable results when repeated, because of inevitable noise attributable to such causes as environment, electrical disturbance, and operators. This variation may be higher than the changes in modal parameters due to damage or deterioration, resulting in incorrect diagnosis.

This paper presents partial results of a study to examine the sensitivity of modal parameters in detecting fatigue cracks using frequencies, damping ratios, mode



shapes, and their derivatives. Modal tests were conducted on a 1/6 scale model of a multiple-steel-girder simple-span bridge including both intact and damaged states. Sensitivity of the modal parameters to changes of structural condition were studied using statistical methods. Results indicated that modal frequencies can be used in conjunction with mode shapes to identify the existence of commonly observed fatigue-related damages in steel highway bridges (9). However, it is difficult to identify damage locations using these modal parameters. The work described here was aimed at supplementing and verifying the previous laboratory work by conducting tests on a fracture-critical bridge and using commercially available modal-testing instrumentation and the latest analytical techniques for diagnosis of simulated damage.

### STRUCTURE AND INSTRUMENTATION

A fracture-critical bridge with two steel girders of 6.76-m span was the test structure. Located over Mud Creek on Van Duesen Road in Claverack, New York, the bridge was built in 1930 and was closed to service in 1988. It had two W18×64 steel beams supporting floor beams and a reinforced concrete deck, as shown in Figure 1. Its floor beams were fastened to the main beams

by bolts. The main beams appeared to be embedded in the concrete abutments at both ends. A total of 54 data points were chosen, as shown in Figure 2, for modal testing measurements. (For practical applications, measurement points or sensor locations may have to be determined by considering expected damage or instrumentation costs.)

The general test setup is shown in Figure 3. It consisted of an impact hammer, a dynamic signal analyzer, signal conditioners, a stationary accelerometer, and a microcomputer. An impulse force hammer, PCB Model 086B50, with a plastic tip was used to excite the test structure, and the excitation induced was measured using a PCB load cell (with sensitivity of 10 mV/lbf) attached to the hammer tip. Acceleration responses of the structure were measured using PCB accelerometers (Flexcel Model 336A04 with 100 mV/g sensitivity). The accelerometers were fixed to the structure using magnets supplied by PCB Piezotronics. A dynamic signal analyzer (Tektronix Model 2630) obtained time domain data, transfer functions, power spectra, and coherence functions (4).

The locations of the data points (Figure 2) for obtaining transfer functions were chosen to represent the behavior of the structure for the modes of interest (0–200 Hz). Only the vertical vibration response perpen-

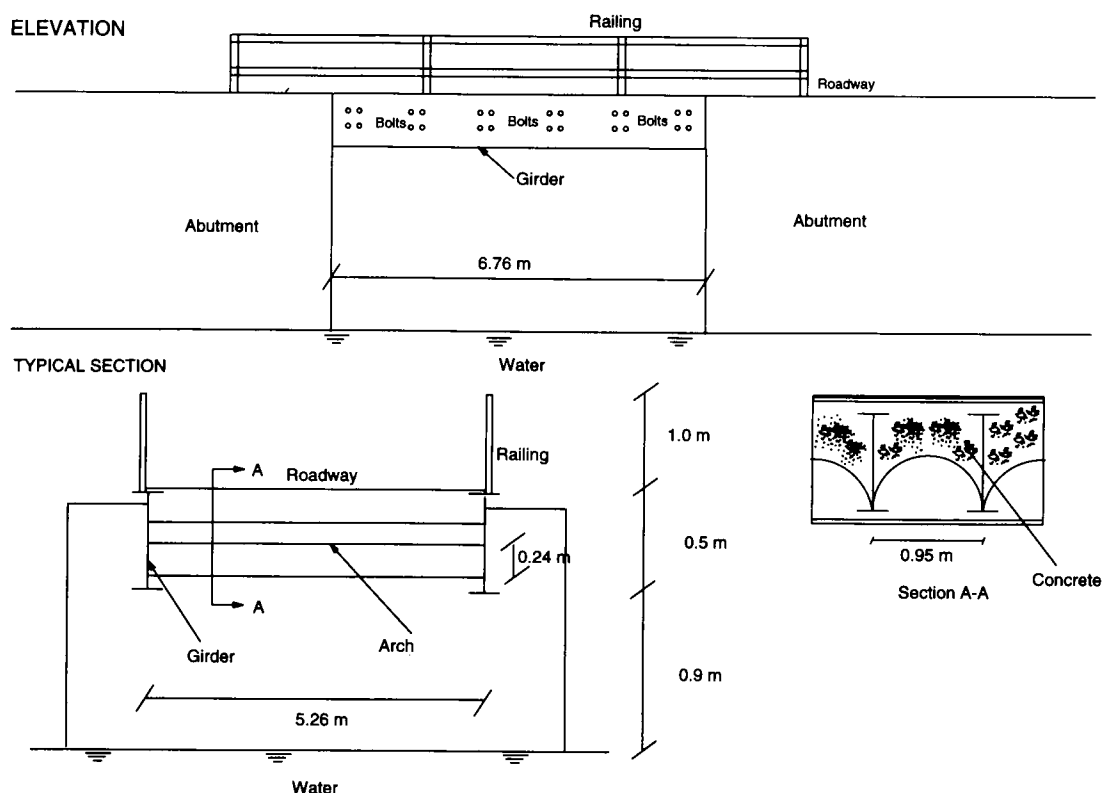


FIGURE 1 Test bridge (not to scale).

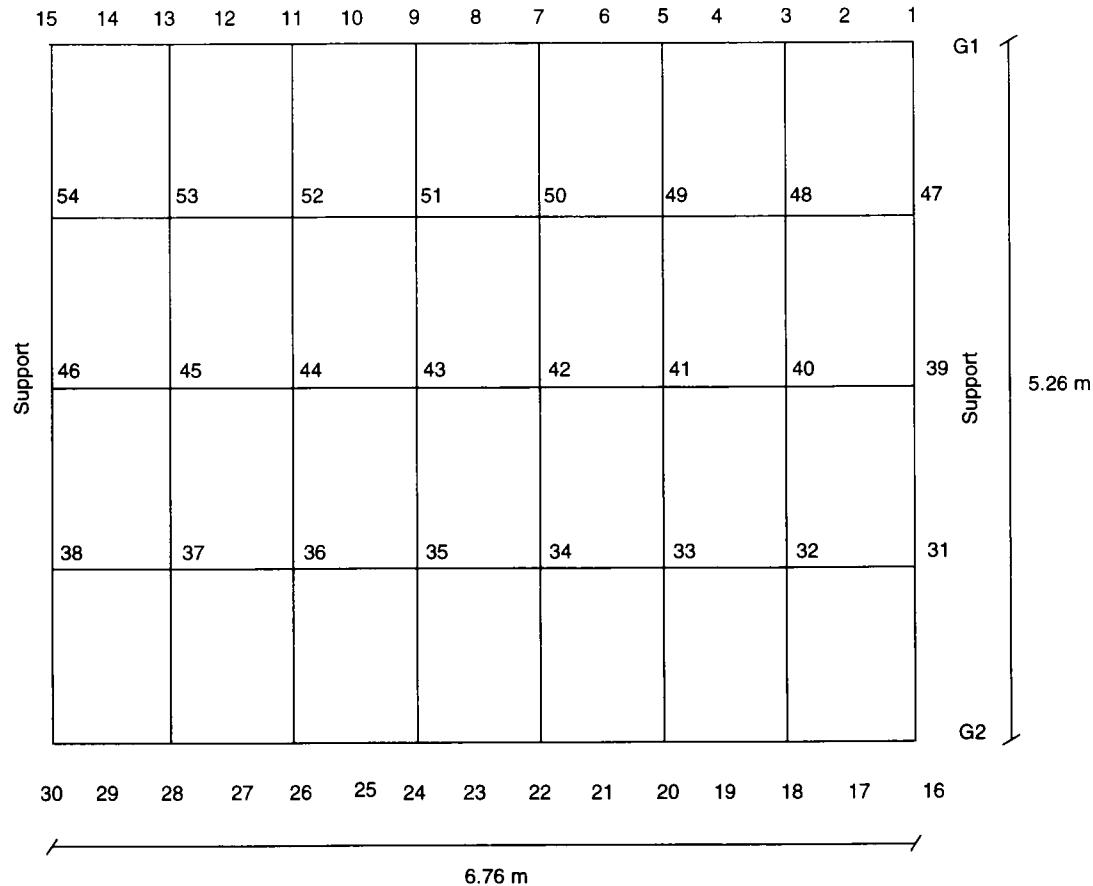


FIGURE 2 Data measurement points on test bridge.

dicular to the plane of the concrete deck was measured. The excitation input was given by the hammer at every data point shown in Figure 2, and the frequency response function (FRF) was obtained by measuring force input (of the impact hammer) and the response output of a stationary accelerometer at Point 27 (Figure 2). This location was chosen such that it was perceived and later verified not to be a modal node (i.e., a point theoretically having no motion for the mode) within the frequency range of interest. For each test, this procedure was repeated several times for the same point, and an average of FRFs was then stored with observation of good coherence. The coherence function indicated the consistency of the obtained data: 1.0 for perfect consistency and 0 for no consistency. For all the data collected, almost perfect coherence values (greater than 0.95) were recorded in the frequency range of interest. Reciprocity was also confirmed at the beginning of the test program by comparing FRFs with interchanged input and output locations. The required analyses were performed using software developed by Structural Measurement Systems, Inc., of San Jose, California, to obtain modal frequencies, modal damping values, and mode shapes.

## STRUCTURAL SIGNATURES AND TEST PROGRAM

### Candidates of Structural Signature

The following structural signatures were used for damage detection on the basis of their measured values: modal frequencies, modal damping ratios, mode shapes, modal assurance criterion factors (MAC), and coordinate modal assurance criterion factors (COMAC). The first three are inherent modal parameters of the structure, and the other two are derived from mode shapes

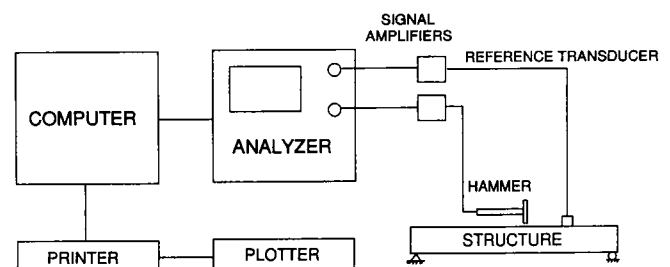


FIGURE 3 General test setup for impact hammer test.

as inherent structural indexes (10,11). Their intended functions in damage detection are discussed next.

MAC indicates correlation between two measured mode shapes from two different tests. Let  $[\phi_A]$  and  $[\phi_B]$  be the first and second sets of measured mode shapes in matrices form of sizes  $n \times m_A$  and  $n \times m_B$ , respectively, where  $m_A$  and  $m_B$  are the number of modes in the respective sets and  $n$  is the number of coordinates (or number of data points) included. MAC is then defined for Modes  $j$  and  $k$  as follows:

$$\text{MAC}(j,k) = \frac{\left| \sum_{i=1,2,\dots,n} i\{\phi_A\}_j i\{\phi_B\}_k \right|^2}{\left[ \left( \sum_{i=1,2,\dots,n} i\{\phi_A\}_j i\{\phi_A\}_j \right) \left( \sum_{i=1,2,\dots,n} i\{\phi_B\}_k i\{\phi_B\}_k \right) \right]}$$

$$j = 1, 2, \dots, m_A \text{ and}$$

$$k = 1, 2, \dots, m_B \quad (1)$$

where  $i\{\phi_A\}_j$  is the  $i$ th coordinate of the  $j$ th column (mode) of  $[\phi_A]$ , and  $i\{\phi_B\}_k$  is the  $i$ th coordinate of the  $k$ th column (mode) of  $[\phi_B]$ .

MAC indicates the degree of correlation between the  $j$ th mode of the first set and the  $k$ th mode of the second set. MAC values vary from 0 to 1, with 0 for no correlation and 1 for full correlation. If Eigen vectors  $\{\phi_A\}_j$  and  $\{\phi_B\}_k$  are identical (e.g., for the same mode), Equation 1 will be unity indicating full correlation. Theoretically, mode shapes are invariable if the structure is not altered. Thus, MAC was used in this study to detect the existence of damage by identifying MAC values altered from their original values near 1 for individual modes.

COMAC is intended to identify locations where mode shapes from two sets of test data do not agree, indicating damage locations. For Location  $i$  and including  $L$  modes, COMAC is defined as

$$\text{COMAC}(i) = \frac{\left[ \sum_{j=1,2,\dots,L} i\{\phi_A\}_j i\{\phi_B\}_j \right]^2}{\left[ \sum_{j=1,2,\dots,L} i\{\phi_A\}_j^2 \sum_{k=1,2,\dots,L} i\{\phi_B\}_k^2 \right]} \quad (2)$$

where the summation is carried out over  $L$  modes and  $i\{\phi_A\}_j$  and  $i\{\phi_B\}_j$  are the  $j$ th mode shapes at Point  $i$  from Tests A and B, respectively. Note that if  $[\phi_A]$  and  $[\phi_B]$  are identical, COMAC for all the measurement points will theoretically be unity, indicating no difference (damage) between the results of Tests A and B.

### Random Variation of Measured Structural Signatures

Practically, instrumentation systems possess only certain degrees of accuracy, test environments may add noise to measured physical quantities, and required manual

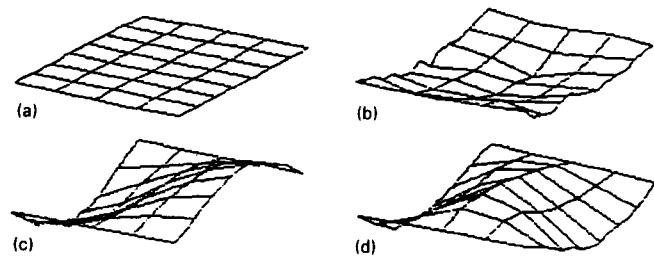


FIGURE 4 Mode shapes of test bridge: (a) undeformed, (b) Mode 1, (c) Mode 2, and (d) Mode 3.

operations may also introduce fluctuation to test results. Identifying and quantifying such variation are necessary for practical applications. Ten impact tests were conducted between October 28, 1992, and November 6, 1993, to understand and evaluate variation in measured modal parameters in the field. The data were obtained using a 0–200 Hz base band, with a 0.125 Hz frequency resolution. The exponential window was used on the vibration response, and the force window was used on the hammer excitation. The mode shapes are shown in Figure 4. Tables 1 and 2 contain means, standard deviations (STD in Table 1), and coefficients of variation (COV) of the obtained modal parameters. MAC and COMAC values were calculated with the first set of test data as reference.

TABLE 1 Random Variation of Measured Modal Parameters and MAC

	Modal Frequencies (Hz)		
	Mode 1	Mode 2	Mode 3
Mean	10.895	20.212	36.792
STD	.03740	.05313	.08588
COV (%)	.34326	.26288	.23343
	Modal Damping Ratios (%)		
	Mode 1	Mode 2	Mode 3
Mean	3.034	2.762	2.386
STD	0.301	0.140	0.176
COV (%)	9.921	5.069	7.376
	MAC Factors (with first data set as reference)		
	Mode 1	Mode 2	Mode 3
Mean	0.848	0.976	0.963
STD	0.025	0.017	0.007
COV (%)	2.948	1.742	0.727

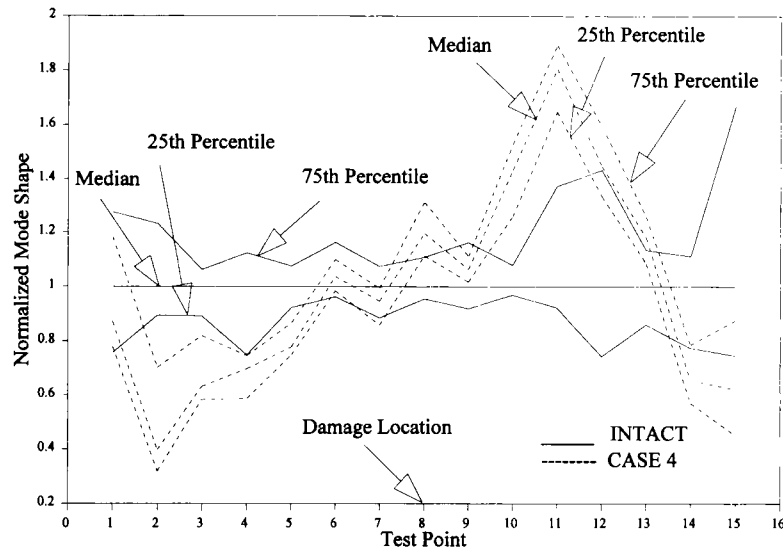
TABLE 2 Random Variation of Measured COMAC (First Data Set as Reference)

Pt #	MEAN	STD	COV (%)	Pt #	MEAN	STD	COV (%)
1	0.837	0.077	9.156	28	0.955	0.048	4.986
2	0.955	0.030	3.177	29	0.921	0.056	6.045
3	0.992	0.006	0.571	30	0.870	0.158	18.178
4	0.994	0.007	0.720	31	0.917	0.115	12.535
5	0.996	0.003	0.300	32	0.984	0.013	1.295
6	0.992	0.009	0.889	33	0.995	0.006	0.629
7	0.997	0.002	0.240	34	0.997	0.003	0.337
8	0.997	0.003	0.332	35	0.995	0.007	0.713
9	0.988	0.012	1.168	36	0.996	0.004	0.367
10	0.996	0.004	0.424	37	0.992	0.010	0.971
11	0.991	0.010	1.040	38	0.986	0.012	1.175
12	0.981	0.020	2.069	39	0.861	0.045	5.188
13	0.988	0.009	0.959	40	0.982	0.010	1.003
14	0.877	0.055	6.289	41	0.996	0.004	0.430
15	0.670	0.213	31.840	42	0.997	0.001	0.137
16	0.902	0.095	10.571	43	0.993	0.005	0.517
17	0.966	0.042	4.368	44	0.987	0.007	0.666
18	0.984	0.011	1.153	45	0.994	0.004	0.395
19	0.994	0.005	0.497	46	0.869	0.066	7.545
20	0.987	0.020	1.999	47	0.944	0.049	5.163
21	0.996	0.008	0.789	48	0.995	0.004	0.360
22	0.969	0.004	0.385	49	0.996	0.003	0.320
23	0.973	0.013	1.357	50	0.998	0.003	0.254
24	0.996	0.003	0.343	51	0.996	0.006	0.584
25	0.973	0.025	2.551	52	0.997	0.006	0.579
26	0.981	0.020	1.997	53	0.998	0.002	0.215
27	0.970	0.024	2.460	54	0.926	0.084	9.073

As seen from the results in Table 1, the maximum standard deviation and COV were 0.086 Hz and 0.0034, respectively. These random changes appeared to be insignificant for identifying the corresponding frequencies. The obtained damping ratios showed much more significant variation, highlighted by the maximum COV of 0.0992. This can be attributed mainly to the very low damping typically observed in steel structures. In general, measuring low damping reliably is difficult.

No significant changes in the mode shapes were observed during these consecutive tests. Figure 5 shows the variation of a typical mode for Girder 1 by solid lines. Their derivatives, MAC and COMAC, are given in Ta-

bles 1 and 2. The maximum standard deviation in MAC was 0.025 for Mode 1. The maximum COV of MAC was 0.0295, and the maximum COV in COMAC was 0.0629, excluding data points at supports (Points 1, 15, 16, 30, 31, 38, 39, 46, 47, and 54). These points showed little movement, resulting in high noise-to-signal ratios. COMAC values at these points thus were not reliable, showing high COV values. COV values in Tables 1 and 2 generally show less significant variations in MAC and COMAC than in the damping ratios. On the other hand, they were more significant than those in the modal frequencies. This is because the MAC and COMAC values were defined and calculated from the



Note: All mode shapes are normalized by the median mode shape at intact.

**FIGURE 5** Variation in Mode 1 due to damage Case 4 (all mode shapes are normalized by the median mode shape when intact).

mode shapes, which were in turn determined using the modal frequencies.

These results indicate that frequencies, mode shapes, and MAC and COMAC values can be estimated with relatively higher consistency than damping ratios. This is also in agreement with the test results obtained from earlier laboratory tests (9). Hence, it was decided that they were to be used as candidates for fundamental structural signatures. Their sensitivity to damage was a focus of this study. The results indicate that structural damage will not be detectable if it results in less deviation in modal parameters than the corresponding random variation.

### Test Program

Modal testing was conducted on the test bridge to confirm the results obtained in the laboratory (9) and to gain field experience. Three simulated damage scenarios were introduced by a sawcut 1.6 mm wide:

- Scenario 1: Flange cracking at midspan.
- Scenario 2: Flange cracking at one-third span.
- Scenario 3: Web cracking at midspan.

Table 3 gives more details of the damage cases. These simulated damages were introduced progressively in steps as indicated there. At least three modal tests were conducted for each case, except for Case 2, which included only one test. These data were obtained at temperatures above freezing. Note that these simulated

damage cases are more severe than fatigue cracks visible during actual inspection, which were simulated in the earlier laboratory study (9). The intention was to examine whether the earlier conclusions would be valid for cases of more critical damage.

### RESULTS AND DISCUSSION

The first three modes of the field bridge were used in analyzing data for damage diagnosis. Measured modal frequencies, mode shapes, MAC, and COMAC are discussed here. Mean modal frequencies for each damage case are given in Table 4. Corresponding mean MAC and COMAC values (calculated with the first set of test data as reference) were also estimated accordingly for each damage case, as shown in Tables 5 and 6, respectively. These mean values are not adequate for damage diagnosis because of the random variation observed. For example, Table 4 shows the mean of the second modal frequency increasing and decreasing for Cases 3 and 4, although damage severity increased monotonically. These results also indicate that mean frequencies generally decrease with damage (as stiffness of the structure decreases), with several exceptions. Statistical techniques were then used to analyze the data obtained, and results are discussed in the following paragraphs.

Analysis of variance (ANOVA) was performed using the Tukey range method to estimate 95 percent confidence intervals for the means of modal frequencies for all damage cases (12). In other words, the mean values of another sample for modal frequencies will be within

TABLE 3 Damage Scenarios and Test Program

Scenario	Case	CRACK DETAILS			No. of repeated tests
		Location*	Length, l (mm)	Depth, d (mm)	
1	1	G1, MS, Point 23	207.65 (FFW)	8.71 (HFT)	4
1	2	G1, MS, Point 23	207.65 (FFW)	17.42 (FFT)	1
1	3	G2, MS, Point 8	207.65 (FFW)	8.71 (HFT)	3
1	4	G2, MS, Point 8	207.65 (FFW)	17.42 (FFT)	10
2	5	G1 & G2, 1/3S, Points 5 & 20	207.65 (FFW)	8.71 (HFT)	3
2	6	G1 & G2, 1/3S, Point 5 & 20	207.65 (FFW)	17.42 (FFT)	3
3	7	G1 & G2, MS, Points 8 & 23	10.24 (FWT)	152.40 (HWD)	3

\* MS = Midspan, 1/3S = One-Third Span, FFW = Full Flange Width, FWT = Full Web Thickness, HFT = Half Flange Thickness, FFT = Full Flange Thickness, and HWD = Half Web Depth.

these intervals with a probability of 95 percent. All modal tests were performed in a temperature range of 3.9 to 27.2°C. The confidence intervals were first estimated by assuming both temperature and simulated damage as influencing factors and adjusting the means with temperature effects filtered. Typical results for Mode 1 are given in Table 7. The confidence intervals were estimated again with the simulated damage as the only influencing variable (i.e., assuming no influence of temperature). These results for Mode 1 are given in Table

8. Comparison of Tables 7 and 8 indicates that these results are virtually the same. Results for other modes showed similar behavior. It was thus concluded that, for practical purposes, temperature had no significant effect.

Results given in Table 4 also indicate a tendency of frequency shift with progressive damage cases. The two-sample *t*-test was used to quantify this tendency (12). This statistical analysis tests the hypothesis if the mean values of two populations are identical, using the two mode shapes (before and after damage) of respective

TABLE 4 Mean Modal Frequencies for Intact and Damage Cases

Case	Mode		
	1	2	3
int	10.90	20.21	36.79
1	10.57	20.23	36.67
2	10.78	20.15	36.70
3	10.63	20.31	37.16
4	10.00	19.69	35.24
5	10.07	19.64	35.30
6	9.94	19.63	34.89
7	9.49	18.56	34.01

TABLE 5 Mean MAC for Intact and Damage Cases (First Data Set as Reference)

Case	Mode		
	1	2	3
intact	0.848	0.976	0.963
1	0.838	0.987	0.964
2	0.866	0.967	0.957
3	0.829	0.965	0.940
4	0.829	0.967	0.936
5	0.852	0.980	0.942
6	0.862	0.975	0.941
7	0.818	0.975	0.901

TABLE 6 Mean COMAC for Intact and Damage Cases (First Data Set of Impact Case as Reference)

Pt #	CASE							
	intact	1	2	3	4	5	6	7
1	0.837	0.969	0.759	0.809	0.800	0.891	0.908	0.942
2	0.955	0.914	0.927	0.975	0.891	0.853	0.920	0.706
3	0.992	0.976	0.993	0.988	0.991	0.992	0.976	0.980
4	0.994	0.995	0.986	0.986	0.989	0.990	0.989	0.988
5	0.996	0.983	0.997	0.992	0.995	0.995	0.997	0.992
6	0.992	0.996	0.989	0.989	0.993	0.987	0.989	0.995
7	0.997	0.986	0.998	0.996	0.996	0.995	0.997	0.993
8	0.997	0.995	0.994	0.993	0.992	0.987	0.994	0.993
9	0.988	0.995	0.991	0.974	0.983	0.971	0.972	0.977
10	0.996	0.991	0.979	0.978	0.983	0.964	0.974	0.974
11	0.991	0.977	0.969	0.957	0.958	0.949	0.967	0.946
12	0.981	0.982	0.945	0.966	0.960	0.956	0.961	0.968
13	0.988	0.982	0.992	0.983	0.977	0.984	0.986	0.972
14	0.877	0.792	0.938	0.919	0.907	0.889	0.941	0.917
15	0.670	0.787	0.983	0.440	0.906	0.821	0.949	0.796
16	0.902	0.831	0.851	0.922	0.864	0.832	0.903	0.845
17	0.966	0.978	0.995	0.977	0.945	0.928	0.915	0.937
18	0.984	0.975	0.997	0.991	0.977	0.982	0.963	0.981
19	0.994	0.984	0.983	0.987	0.979	0.971	0.970	0.972
20	0.987	0.986	0.993	0.998	0.993	0.993	0.985	0.996
21	0.996	0.997	0.999	0.997	0.996	0.998	0.998	0.995
22	0.969	0.951	0.971	0.969	0.941	0.947	0.936	0.937
23	0.973	0.988	0.999	0.997	0.995	0.995	0.995	0.991
24	0.996	0.990	0.999	0.999	0.996	0.997	0.994	0.997
25	0.973	0.985	1.000	0.996	0.967	0.976	0.979	0.995
26	0.981	0.977	0.975	0.947	0.984	0.970	0.980	0.949
27	0.970	0.960	0.985	0.997	0.902	0.962	0.991	0.937
28	0.955	0.963	0.978	0.919	0.869	0.968	0.965	0.931
29	0.921	0.808	0.714	0.746	0.780	0.927	0.859	0.710
30	0.870	0.968	0.989	0.973	0.921	0.973	0.956	0.963
31	0.917	0.895	0.620	0.715	0.717	0.676	0.768	0.906
32	0.984	0.972	0.978	0.989	0.986	0.994	0.949	0.977
33	0.995	0.995	0.992	0.998	0.996	0.999	0.991	0.994

(continued on next page)

TABLE 6 (continued)

34	0.997	0.995	0.999	0.993	0.996	0.999	0.995	0.996
35	0.995	0.993	0.999	0.999	0.997	0.998	0.991	0.983
36	0.996	0.993	0.997	0.994	0.977	0.978	0.983	0.973
37	0.992	0.980	1.000	0.981	0.951	0.975	0.985	0.990
38	0.986	0.947	0.840	0.991	0.978	0.988	0.961	0.672
39	0.861	0.869	0.915	0.827	0.883	0.884	0.798	0.850
40	0.982	0.988	0.987	0.996	0.955	0.971	0.948	0.984
41	0.996	0.998	0.999	0.998	0.981	0.993	0.982	0.995
42	0.997	0.998	1.000	0.996	0.993	0.998	0.998	0.999
43	0.993	0.994	1.000	0.997	0.993	0.993	0.994	0.998
44	0.987	0.991	0.994	0.993	0.977	0.984	0.977	0.999
45	0.994	0.993	0.991	0.993	0.969	0.972	0.964	0.983
46	0.869	0.817	0.963	0.921	0.807	0.936	0.894	0.900
47	0.944	0.937	0.841	0.882	0.896	0.801	0.853	0.734
48	0.995	0.990	0.975	0.992	0.992	0.993	0.996	0.994
49	0.996	0.992	0.989	0.994	0.994	0.994	0.996	0.999
50	0.998	0.997	0.996	0.996	0.992	0.998	0.995	0.998
51	0.996	0.998	0.999	0.997	0.994	0.995	0.997	0.996
52	0.997	0.998	0.996	0.998	0.993	0.990	0.995	0.985
53	0.998	0.989	0.931	0.974	0.979	0.977	0.962	0.978
54	0.926	0.945	0.935	0.978	0.954	0.942	0.993	0.826

TABLE 7 ANOVA Assuming Temperature and Simulated Cracks To Be Effective (with Temperature Effect Filtered)

Damage Case	95 % Confidence interval for Mean	
	Lower (Hz)	Upper (Hz)
intact	10.845894	10.944106
1	10.487356	10.642644
2	10.620712	10.931288
3	10.516195	10.735805
4	9.950594	10.048806
5	9.979011	10.158322
6	9.854344	10.033656
7	9.399344	9.578656

TABLE 8 ANOVA Assuming Only Simulated Cracks To Be Effective

Damage Case	95 % Confidence interval for Mean	
	Lower (Hz)	Upper (Hz)
INTACT	10.845200	10.944800
1	10.486259	10.643741
2	10.618518	10.933482
3	10.514643	10.737357
4	9.949900	10.049500
5	9.977744	10.159589
6	9.853078	10.034922
7	9.398078	9.579922



populations. Because of the uncertainty inherent in the problem, the test gives the result associated with a probability, which is interpreted here as probability of damage or detectability for damage. Table 9 gives results of the detectability for all the damage cases with reference to the intact condition, except for Case 2, which had only one measured data point and thus was not eligible for the statistical analysis. Except for Modes 2 and 3 under Case 1 and Mode 1 under Case 3, damage detectabilities are higher than 95 percent for all damage cases and all modes, indicating that most of the simulated damage can be detected with high confidence. Table 10 shows damage detectability using MAC values for all damage cases. Most of these detectabilities are lower than those for frequencies in Table 9, indicating lower sensitivity of MAC to damage for this bridge. However, they still can be used to supplement diagnostic decisions. For example, Case 1 damage would not be diagnosed using only the modal frequencies in Table 9, because only one mode showed high damage probability. Supplemented by Table 10 using MAC, this diagnosis can be made with higher confidence because an additional mode (Mode 2) shows a higher damage probability of 92.5 percent. This example has also shown that a limited number of modes may be inadequate for damage diagnosis with higher confidence, either because certain modes are not significantly affected by the damage or because random variation in obtained data is too high; both cases result in difficulty of diagnosis based on a limited number of modes.

Because modal frequencies and MAC refer to individual modes of vibration, diagnosis using these structural signatures can only indicate whether damage or deterioration exists. In practice, when this question is answered positively, the often-needed next step is to identify where the damage is, or at least in which area it has occurred. Without this information, the diagnosis may be considered incomplete. Mode shapes and their derivatives (e.g., COMAC) as structural signatures are

**TABLE 9 Percentage of Damage Detectability Using Modal Frequencies**

Mode	Damage Case w.r.t. Intact					
	1	3	4	5	6	7
1	100	85.2	100	99.3	100	100
2	37.3	98.1	100	100	100	100
3	53.0	99.0	100	96.7	100	100

Note: Detectability was not estimated for Case 2, as only one test was conducted.

**TABLE 10 Percentage of Damage Detectability Using MAC**

Mode	Damage Case w.r.t. Intact					
	1	3	4	5	6	7
1	37.6	96.2	67.2	10.8	80.7	90.8
2	92.5	73.5	59.9	52.6	5.2	5.4
3	0.5	68.8	99.5	100	97.8	100

Note: Detectability was not estimated for Case 2, as only one test was conducted.

natural choices for this purpose because they provide information on vibration patterns for individual points in structures.

Table 11 presents damage detectability using COMAC by the two-sample *t*-test. Note that the detectabilities in Table 11 refer to the intact condition for all damage cases. The shaded cells indicate the damage locations for each case. For example, Column 1 of Row 5 shows the probability of Point 5 being a damage location due to damage in Case 1. If a 95 percent confidence in diagnosis is required, Points 1, 7, 14, 23, 48, and 49 will be identified as damage locations, simply because they all have damage probabilities of more than 95 percent. Even if Point 1 is excluded because of its location at a support, the rest still do not definitely lead to the correct damage location (i.e., Point 23). Using the same criterion, damage detectabilities for Case 3 show Points 4, 15, 23, 25, 27, 40, and 44 as the damage locations, failing to simultaneously identify Points 8 and 23. Further, Case 7 includes damage locations as Points 5, 8, 20, and 23. The same damage location identification criterion will lead to 11 points being identified as damage locations, with three actual damage locations missing.

Table 12 shows damage detectability by the two-sample *t*-test for four arbitrarily selected locations and four actual damage locations, directly using mode shapes. The shaded cells indicate actual damage locations for the respective damage cases. Unfortunately, they do not always show highest detectabilities. In other words, other points will be falsely identified as damage locations if the real damage locations are identified. Note that this was also observed when all data points were included in the analysis. These results indicate that mode shapes were affected comparably at points beyond and within the damage vicinity.

This situation can be illustrated more intuitively using the results shown in Figure 5. For a damage Case 4 at Points 8 and 23 (midspan of girders), it shows the variation of Mode 1 of Girder 1 at intact and after dam-

TABLE 11 Percentage of Damage Detectability Using COMAC

Mode	Damage Case w.r.t. Intact						Mode	Damage Case w.r.t. Intact					
	1	3	4	5	6	7		1	3	4	5	6	7
1	99.9	32.6	63.4	84.7	94.8	96.9	30	88.0	89.7	56.1	89.6	83.4	83.4
2	72.6	56.0	90.9	62.6	58.8	100	31	27.6	57.1	98.4	68.7	74.4	17.9
3	88.5	36.8	7.1	2.2	46.8	88.0	32	54.1	69.9	21.0	92.5	79.4	83.0
4	26.1	98.1	70.6	58.2	31.0	61.0	33	10.5	60.0	30.7	86.1	68.4	27.6
5	90.9	40.3	70.6				34	52.4	56.7	44.7	71.7	49.7	44.4
6	78.3	15.2	25.8	56.6	39.3	52.5	35	31.4	90.1	65.1	80.1	35.5	63.3
7	99.4	16.3	25.9	39.9	1.8	95.1	36	56.7	42.4	100	95.1	97.9	99.5
8	34.8						37	81.6	57.2	81.2	73.0	57.7	37.1
9	79.6	85.1	66.1	99.1	84.0	72.3	38	53.8	74.7	78.8	28.2	65.1	61.4
10	40.9	85.7	99.1	96.6	96.7	87.2	39	15.7	26.4	57.1	59.3	40.9	21.5
11	83.0	90.9	100	88.5	90.1	93.7	40	70.7	99.6	98.5	55.7	100	35.5
12	1.6	53.6	96.9	91.0	96.1	80.9	41	55.6	80.8	100	52.9	99.9	16.1
13	51.0	65.6	97.1	50.1	28.7	82.5	42	61.3	23.7	59.0	43.0	83.8	91.1
14	95.7	80.8	79.5	24.0	96.3	86.3	43	31.3	58.0	14.1	5.9	4.6	97.3
15	69.4	96.8	98.6	69.1	99.3	66.3	44	78.8	97.1	97.3	25.4	85.3	99.9
16	57.6	28.6	65.0	52.7	0.7	33.4	45	35.3	14.5	100	77.8	99.6	98.6
17	46.0	43.0	78.8	64.5	97.0	59.9	46	58.1	88.9	74.3	90.0	36.0	55.2
18	26.1	49.4	73.8	16.2	82.8	38.4	47	24.1	54.0	96.2	87.8	100	90.6
19	72.6	47.9	99.6	79.8	83.1	90.6	48	99.5	58.1	76.8	45.4	59.8	8.9
20	10.2	83.0	52.8				49	95.2	86.9	61.4	50.3	9.2	96.5
21	34.6	16.0	10.1	58.7	53.5	9.8	50	30.3	58.8	75.4	43.6	50.5	16.2
22	87.7	3.2	100	97.9	92.7	98.3	51	76.5	55.5	29.5	33.0	56.5	7.3
23							52	4.8	24.1	90.4	90.5	55.5	97.4
24	83.9	83.0	4.9	14.4	38.9	33.7	53	76.6	77.0	99.9	100	91.9	96.7
25	61.3	97.4	36.4	13.0	37.3	96.4	54	40.5	88.0	54.9	39.5	94.8	83.7
26	23.0	36.9	24.4	51.6	6.1	94.3							
27	40.5	98.8	89.7	25.4	96.5	40.7							
28	27.6	35.8	94.1	40.9	33.8	56.1							
29	86.6	54.0	94.9	7.3	40.8	67.3							

Note: Detectability was not estimated for Case 2, as only one test was conducted. Shaded cells indicate damage locations.

**TABLE 12 Percentage of Damage Detectability Using Mode Shapes**

Mode 1	Damage Case w.r.t. Intact					
Pt #	1	3	4	5	6	7
5	99.8	93.9	98.9			
8	48.2					
11	76.8	94.5	100.0	91.1	95.0	96.6
20	20.1	75.1	16.7			
23						
26	39.2	26.7	49.5	80.5	38.7	99.7
33	64.5	75.5	100.0	98.8	97.9	80.4
52	90.4	27.0	56.9	75.9	48.1	21.9

Mode 2	Damage Case w.r.t. Intact					
Pt #	1	3	4	5	6	7
5	1.1	59.1	81.8			
8	48.1					
11	89.9	82.5	89.5	84.6	92.0	95.2
20	6.5	86.4	68.0			
23						
26	12.0	86.0	47.0	27.6	49.4	86.2
33	96.6	80.5	100.0	100.0	100.0	98.4
52	94.3	26.3	88.7	97.4	98.2	78.9

Mode 3	Damage Case w.r.t. Intact					
Pt #	1	3	4	5	6	7
5	65.2	81.2	96.3			
8	42.2					
11	27.4	29.3	97.3	88.4	91.1	100.0
20	30.5	18.0	98.7			
23						
26	92.9	90.8	42.3	5.9	36.0	99.6
33	99.9	1.9	100.0	99.5	100.0	54.4
52	38.0	69.6	88.5	84.5	7.3	98.9

Note: Shaded cells indicate damage locations.

age, described by the median, 25th-percentile, and 75th-percentile values. For clarity, these values are normalized by the median mode shape of the intact structure. Note that Point 23 is transversely at the same location as Point 8 but on the other girder (Figure 2). It can be seen that the mode shape changed at all locations along the girder (including damage location); Points 2 and 11

changed the most, being 2.9 and 1.45 m away from the damage location points.

Using mode shapes or their derivatives for identifying the location of damage is essentially based on an assumption that local damage will change mode shapes at or near the damage location more significantly than in other areas. Figure 5 shows that this assumption is

not verified and instead demonstrates proportional changes of the mode shapes at various locations. This happens because upon local damage, adjacent structural elements autogenously distribute load effects through an altered load path system, and local damage effects are thus distributed to other elements of the structure. This self-adjustment capability is believed to have been provided by intentional and unintentional redundancy.

The preceding results also confirm the findings from the earlier laboratory tests (9). It should be noted that these consistent findings are associated with the specific test instrumentation used. They may indicate the need to improve instrumentation by reducing measurement noise and attaining more extensive simultaneous coverage over the structure.

## CONCLUSIONS

Modal frequencies may be used to detect the existence of damage or deterioration simulated here for highway bridges. Cross-diagnosis using multiple signatures such as mode shapes, MAC, and COMAC is warranted for such detection, because a single signature may not be conclusive due to inevitable variation of measured data. Criteria for warning triggering that use these signatures need to be determined by taking into account their random variation affecting sensitivity of detection. However, damage locations cannot be identified using mode shapes and their derivatives, because damage affects mode shapes comparably at all damaged and undamaged locations. For complete damage diagnosis, including existence and location, improved instrumentation may be needed for lower noise and more extensive simultaneous coverage.

## ACKNOWLEDGMENTS

This project was partially supported by the U.S. Department of Transportation. Many New York State Department of Transportation personnel contributed to

make this study possible, and their efforts are deeply appreciated.

## REFERENCES

1. FHWA, U.S. Department of Transportation. National Bridge Inspection Standards: Frequency of Inspection and Inventory. *Federal Register*, Vol. 52, No. 66, April 7, 1987.
2. R. I. Shores Cracked Viaduct. *Engineering News-Record*, Feb. 4, 1988, pp. 20–28.
3. Collapse of New York Thruway (I-90) Bridge over the Schoharie Creek near Amsterdam, New York, April 5, 1987. Report PB 88-916202, NTSB/HAR-88/02. *Highways Accident Report*, National Transportation Safety Board, 1988.
4. Ewins, D. J. *Modal Testing: Theory and Practice*. John Wiley, New York, 1984.
5. Mazurek, D. F., and J. T. DeWolf. Experimental Study of Bridge Monitoring Technique. *Journal of Structural Engineering*, ASCE, Vol. 116, No. 9, Sept. 1990, pp. 2532–2549.
6. Pandey, A. K., M. Biswas, and M. M. Samman. Damage Detection from Changes in Curvature Mode Shapes. *Journal of Sound and Vibration*, Vol. 145, No. 2, March 1991.
7. Wolf, T., and M. Richardson. Fault Detection in Structures from Changes in the Modal Parameters. *Proc., 7th International Modal Analysis Conference*, Las Vegas, Nev., Jan. 1989, pp. 87–94.
8. Hearn, G., and R. B. Testa. Modal Analysis for Damage Detection in Structures. *Journal of Structural Engineering*, ASCE, Vol. 117, No. 10, Oct. 1991, pp. 3042–3063.
9. Alampalli, S., G. Fu, and E. W. Dillon. Measured Bridge Vibration for Damage Detection. Final report. New York State Department of Transportation, Albany (in preparation).
10. Allemang, R. J., and D. L. Brown. A Correlation Coefficient for Modal Vector Analysis. *Proc., 1st International Modal Analysis Conference*, Bethel, Conn., 1982, pp. 110–116.
11. Lieven, N. A. J., and D. J. Ewins. Spatial Correlation of Mode Shapes, The Coordinate Modal Assurance Criterion (COMAC). *Proc., 6th International Modal Analysis Conference*, Kissimmee, Fla., Feb. 1988, pp. 690–695.
12. Box, G. E. P., W. G. Hunter, and J. S. Hunter. *Statistics for Experiments*. John Wiley & Sons, New York, 1978.

# BRIDGE CONSTRUCTION

---

# FHWA's Bridge Temporary Works Research Program

---

John F. Duntemann, *Wiss, Janney, Elstner Associates, Inc.*  
Sheila Rimal Duwadi, *Federal Highway Administration*

Approximately 35,000 state or federal-aid highway bridges were built in the United States during the past decade. Most of these bridges were built without incident, which is a credit to the construction industry. During this period, however, several major bridge failures occurred during construction and were attributed to construction practices and procedures. Statistically, bridge falsework represents more than a third of the total recorded falsework collapses, most of which occurred during construction of conventionally reinforced concrete beam or box-girder bridges. Falsework design in the United States, because of its temporary nature, has traditionally been delegated to the contractor or contractor's engineer under the premise that the contractor is responsible for the means and methods of construction. Although there are potential economies in this type of assignment, the design engineer of record for the bridge relinquishes some control of the project, which, in turn, increases the probability of construction complications or failures. The possibility of construction problems is compounded by the fact that until recently very few detailed standards existed for the construction of these temporary systems and, in many cases, the design assumptions were left to individual engineering judgment. Following the collapse of the Route 198 bridge over the Baltimore Washington Parkway in 1989, FHWA determined that there was a need to reassess, on a national level, the specifications currently used to design, construct, and inspect

falsework for highway bridge structures. Toward that end, FHWA sponsored a study to identify the existing information on this subject and develop a guide specification for use by state agencies to update their existing standard specifications for falsework, formwork, and related temporary construction. The results of this study, which included a survey of U.S. and Canadian highway departments and a comprehensive literature search, will be presented. The paper will focus on the current state of the practice in the United States and abroad. FHWA's *Guide Design Specification for Bridge Temporary Works* will be discussed in detail.

In 1991, FHWA initiated a study to identify the current state of the practice in the United States and abroad for designing, constructing, and inspecting the falsework and formwork used to construct highway bridge structures. The findings of this study were published in *Synthesis of Falsework, Formwork, and Scaffolding for Highway Bridge Structures* (1). The results of this study, which included a survey of U.S. and Canadian highway departments and a comprehensive literature search, are summarized in this paper. An overview of *Guide Design Specification for Bridge Temporary Works* (2) is also presented.

## EXISTING NATIONAL STANDARDS

### United States

In the United States, few existing national standards apply solely to falsework construction. Perhaps the most widely recognized standard is American National Standards Institute (ANSI) A10.9-1983, *American National Standard for Construction and Demolition Operations—Concrete and Masonry Work—Safety Requirements*. This standard was formulated by the ANSI Committee on Safety in Construction and Demolition Operations. The current version was based on the American Concrete Institute's (ACI's) 347-88, *Guide to Formwork of Concrete*, and therefore contains similar provisions (3).

The AASHTO Division II 1991 interim specifications contain a newly created section entitled "Temporary Works," which includes subsections on falsework and forms, cofferdams and shoring, temporary water control systems, and temporary bridges (4). This section was developed, in part, to update Division II and consolidate information found in other parts of the AASHTO *Standard Specifications for Highway Bridges* (5). The section on falsework and forms includes general design criteria as well as guidelines for removal of these temporary structures.

### Canada

In 1975 the Canadian Standards Association (CSA) published a national standard entitled *Falsework for Construction Purposes*, designated CSA S269.1-1975 (6). As stated in its scope, this standard provides rules and requirements for design, fabrication, erection, inspection, testing, and maintenance of falsework. The falsework standard was prepared by the Technical Committee on Scaffolding for Construction Purposes and is one of the first national standards developed on this subject.

CSA S269.1 adopts the National Building Code of Canada and existing CSA standards by reference, including CSA S16, *Steel Structures for Buildings*; CSA 086, *Code of Recommended Practice for Engineering Design in Timber*; and CSA W59.1, *General Specification for Welding of Steel Structures*. Materials that cannot be identified as complying with specified standards are not allowed for falsework construction.

In addition to material and design standards, CSA S269.1 specifies design loads and forces, analysis and design methods, erection procedures, and test procedures for steel shoring systems and components. Vertical loads are prescribed generally in terms of a uni-

formly distributed load. Loads due to special conditions such as impact, unsymmetrical placement of concrete, and overpressures due to pneumatic pumping are discussed but not quantified. Horizontal loads are specified as either the lateral wind force found in the National Building Code of Canada or 2 percent of the total vertical load, whichever is greater. Design capacity is determined by existing CSA design codes or, where proprietary components are used, based on test results with prescribed factors of safety. Additional requirements for tubular scaffold frames and wood falsework are also specified.

A questionnaire distributed to Canadian provincial bridge engineers indicated that most provinces adopt the CSA standard for falsework. Four of the provinces' highway standards supersede sections of the CSA standards. Ontario is currently developing its own falsework manual.

### Great Britain

In 1973 the British Standards Institution began to draft a code of practice for falsework; the draft British *Code of Practice for Falsework* was published in late 1975. The document was subsequently revised and published as the *Code of Practice for Falsework* (BS5975) in 1982 (7).

The British code is similar in format to the Canadian falsework standard in that the content is organized under the general headings of procedures, materials, and components, loads, foundations and ground conditions, design, and construction. However, it also contains a considerable amount of in-depth commentary and several detailed appendixes, which include properties of components in tube and coupler falsework, design of steel beams at points of reaction or concentrated load, effective lengths of steel members in compression, and so forth.

Like the Canadian standard, the British *Code of Practice for Falsework* references existing British design and material standards. One of the unique features of the British code is its distinction between maximum wind force during the life of the falsework, which represents an extreme condition, and maximum allowable wind force during construction operations. Forces from both of these conditions are used to check the stability of the falsework at appropriate stages of construction.

With the exception of piles, the British code is relatively complete with respect to foundations and ground conditions for temporary works. Pile foundations are addressed in a separate British standard on foundations. BS5975 includes allowable bearing pressures for a wide range of rock and soil types and modification factors that, depending on the reliability of site information, magnitude of anticipated settlement, and fluctuations in

groundwater level, are applied to the prescribed bearing pressure. The code also contains some specific guidelines for the protection of foundation areas.

### Australia and New Zealand

Temporary structures for Australian bridge projects are governed by provisions in the *Bridge Design Specifications* as set forth by the National Association of Australian State Road Authorities (NAASRA) (8). Section 12, entitled "Design for Construction and Temporary Structures," reviews formwork and falsework design and is supplemented with appendixes on lateral concrete pressure and testing requirements for components. As in the United States, each Australian state transportation department has provisions that supplement or supersede the national specifications.

Falsework for government bridge projects in New Zealand is regulated by the *Code of Practice for Falsework—Volumes 1 and 2*, which are internal documents. Volume 1 contains the code and appendixes, and Volume 2 serves as commentary. Like the Canadian and British standards, the content of the New Zealand code of practice is organized under the general headings of procedures, materials, foundation and soil conditions, loadings, design, and construction. The New Zealand code also contains several detailed appendixes, which include scaffold tube falsework, proprietary components, foundation investigation, and lateral concrete pressure on forms.

The New Zealand code of practice includes specific provisions for lateral loads generated by nonvertical support members and a horizontal seismic force. The latter force is obtained from a basic seismic coefficient multiplied by factors representing the risk associated with the falsework exposure period and the consequences of failure. The New Zealand code also includes detailed provisions for both working stress and ultimate strength design and prescribes load combinations and related load factors. The section on foundations and soil conditions is similar in detail to the British code of practice and includes a fairly comprehensive review of soil properties and foundation design.

### STATE SPECIFICATIONS

As part of the FHWA study, a questionnaire was sent to the 50 U.S. highway departments. Information relating to design and administrative policies for falsework and formwork construction and the bridge construction activity for each state was requested. A summary of the findings is tabulated in Figures 1 and 2.

Virtually every state was found to have general requirements and guidelines for the construction and re-

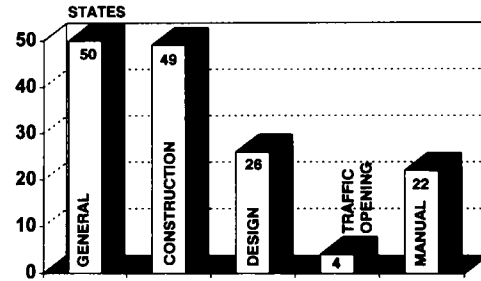


FIGURE 1 Summary of state specification requirements.

moval of falsework and formwork. However, only about half the states specified design criteria. Similarly, only 22 states had accompanying design or construction manuals that included specific design information. States that are more active in constructing cast-in-place concrete highway bridges generally were found to have more comprehensive specifications and guidelines. As evident in Figure 3, the complexity of these systems tends to dictate the need for more comprehensive standards.

Besides identifying the content of state specifications, the survey also provided some insight into each state's administrative policies concerning falsework and formwork. About two-thirds of the states require the submittal of plans and calculations, sealed by a registered professional engineer, for any significant falsework construction. By definition, significant falsework was generally considered as anything that spans more than 4.9 m (16 ft) or rises more than 4.3 m (14 ft) in height. The survey showed that most states also conduct their own reviews and inspections, subject to availability of staff, complexity of design, and so forth.

### Loads

Many state specifications are consistent with respect to minimum uniform load requirements and contain pro-

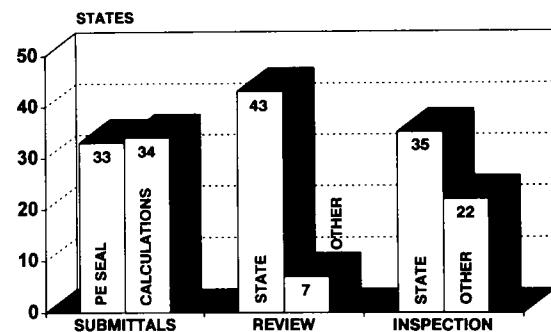


FIGURE 2 State administrative policies.



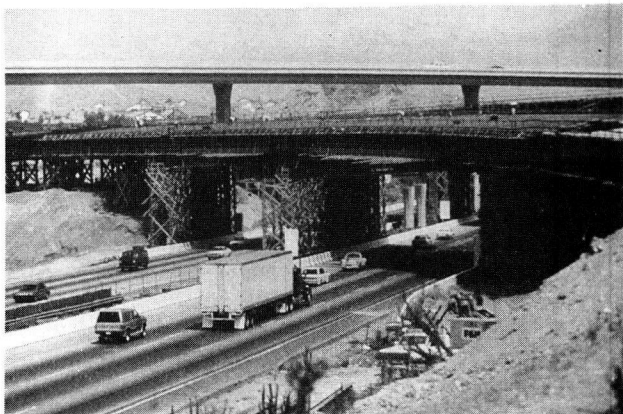


FIGURE 3 Falsework construction over existing roadway.

visions similar to both ANSI 10.9 and AASHTO's 1991 interim specifications. Dead loads include the weight of concrete, reinforcing steel, formwork, and falsework. The weight of concrete, reinforcing steel, and formwork is generally specified to be  $2550 \text{ kg/m}^3$  ( $160 \text{ lb/ft}^3$ ) for normal-weight concrete or  $2100 \text{ kg/m}^3$  ( $130 \text{ lb/ft}^3$ ) for lightweight concrete. Some states also specify a minimum vertical load requirement of  $4.8 \text{ kN/m}^2$  ( $100 \text{ lb/ft}^2$ ).

Live loads typically consist of equipment weights applied as concentrated loads and a uniform load not less than  $0.96 \text{ kN/m}^2$  ( $20 \text{ lb/ft}^2$ ), plus  $1.1 \text{ kN/m}$  ( $75 \text{ lb/ft}$ ) applied at the outside edge of the deck overhangs. In California, the latter requirement applies only to overhang falsework and not to falsework components below the deck overhang system. In order to avoid being overly conservative, the  $1.1\text{-kN/m}$  ( $75\text{-lb/ft}$ ) loading generally is distributed over a length of  $6.1 \text{ m}$  ( $20 \text{ ft}$ ) when falsework components are designed below the level of the bridge soffit.

The horizontal load used to design the falsework bracing system includes the sum of lateral loads due to wind; construction sequence, including unbalanced hydrostatic forces from fluid concrete; and stream flow, where applicable. Superelevation, inclined supports, out-of-plumbness, thermal effects, post-tensioning, and less predictable occurrences (such as impact of concrete during placement, stopping and starting of equipment, and accidental impact of construction equipment) can also introduce horizontal loads into the falsework system.

In general, AASHTO and many state specifications require that the horizontal design load correspond to the actual sum of potential lateral loads but not less than 2 percent of total dead load. Exceptions include Georgia, where "the assumed horizontal load shall be the sum of the actual horizontal loads due to equipment, construction sequence or other causes, and a

wind load of  $2.4 \text{ kN/m}^2$  ( $50 \text{ lb/ft}^2$ ), plus 1 percent of the vertical load to allow for unexpected forces, but in no case shall the assumed horizontal load to be resisted in any direction be less than 3 percent of the total dead load," and Kansas, which requires that "falsework supporting bridge roadways over  $0.04 \text{ ft/ft}$  superelevation shall use a minimum lateral load equal to 4 percent of the total dead load."

Most states do not prescribe wind loads in their falsework and formwork specifications, and there are inconsistencies between states that have established values. Several states adopt a slightly modified version of the *Uniform Building Code* provisions for open-frame towers (9).

For posttensioned construction, it is generally recognized that redistribution of gravity load occurs after the superstructure is stressed. The distribution of load in the falsework after posttensioning depends on factors such as spacing and stiffness of falsework supports, foundation stiffness, superstructure stiffness, and tendon profile. The amount of load redistribution can be significant and may be a governing factor in the falsework design. The AASHTO 1991 interim specifications and some state specifications recognize this potential but do not offer specific design guidelines.

Similar problems have been identified with respect to the redistribution of vertical load due to deck shrinkage. This problem has been researched by the California Department of Transportation (Caltrans) and is addressed indirectly in its specification. Caltrans found that depending on the falsework configuration, type of construction, and construction sequence, the maximum load imposed on the falsework developed within 4 to 7 days after the concrete was placed and varied between 110 and 200 percent of the measured load at 24 hr (10).

## Stresses

Twenty-two of the 50 states specify design criteria for falsework that includes allowable stresses for steel and timber construction. Most states with established design criteria adopt the AASHTO provisions for structural steel, and the rest use the American Institute of Steel Construction (AISC) allowable stress provisions (11). Because AASHTO adopts the *National Design Specification for Wood Construction* (NDS), only the distinctions between this and other specifications will be discussed (12,13).

Table 1 gives a summary of the allowable stresses for structural steel prescribed by AISC, AASHTO, and several states with variations of these provisions. For the states, provisions for axial tension, tension in flexure, and shear provisions are generally consistent with either

TABLE 1 Allowable Stress for Structural Steel (lb/in.<sup>2</sup>)

Specification	Axial Tension "F <sub>t</sub> "	Flexure, "F <sub>b</sub> " Tension	Compression	Axial Compression "F <sub>c</sub> "	Shear "F <sub>v</sub> "
AISC <sup>a</sup>	0.60 F <sub>y</sub>	0.60 F <sub>y</sub>	0.60 F <sub>y</sub> <sup>b</sup>	AISC Eqn E2-1 <sup>c</sup>	0.40 F <sub>y</sub>
AASHTO <sup>d</sup>	0.55 F <sub>y</sub>	0.55 F <sub>y</sub>	20,000 - <sup>e</sup> 7.5 (L/b) <sup>2</sup>	16,980 - <sup>e</sup> 0.53 (KL/r) <sup>2</sup>	0.33 F <sub>y</sub>
Iowa <sup>f</sup> (F <sub>y</sub> = 30 kip/in <sup>2</sup> )	0.55 F <sub>y</sub>	0.55 F <sub>y</sub>	16,500 - 5.2 (L/b) <sup>2</sup>	14,150 - 0.37 (KL/r) <sup>2</sup>	0.33 F <sub>y</sub>
Kansas <sup>g</sup>	-	18,000	$\frac{12,000,000}{Ld/bt} \leq 18,000$	16,000 - 0.38 (L/r) <sup>2</sup>	11,000
Kentucky <sup>h</sup>	-	0.55 F <sub>y</sub>	-	AISC Eqn E2-1	0.40 F <sub>y</sub>
Maryland <sup>i</sup>	24,000	0.55 F <sub>y</sub>	20,000 - 7.5 (L/b) <sup>2</sup>	16,980 - 0.53 (KL/r) <sup>2</sup>	0.33 F <sub>y</sub>
Minnesota <sup>j</sup>	1.33(0.55F <sub>y</sub> )	25,000	1.33(AASHTO Eqn)	16,980 - 0.53 (KL/r) <sup>2</sup>	1.33(0.33F <sub>y</sub> )

1 lb/in<sup>2</sup> = 6895 Pa, 1 kip/in<sup>2</sup> = 6.895 MPa, 1 ft = 0.305 m, 1 in = 25.4 mm

<sup>a</sup> California, Colorado, Georgia, Idaho, and Nevada adopt AISC allowable stresses for identifiable grades of steel. Louisiana, Maryland and South Dakota permit AISC, subject to approval.

<sup>b</sup> Refer to AISC Manual of Steel Construction - Allowable Stress Design for compact sections or compact and non-compact sections with unbraced length greater than L<sub>c</sub>.

<sup>c</sup> AISC Eqn E2-1:

$$F_a = \frac{F_y}{F.S.} \left[ 1 - \frac{(KL/r)^2 F_y}{4\pi^2 E} \right] \quad \text{when } KL/r < C_c$$

$$F_a = \frac{\pi^2 E}{F.S. (KL/r)^2} \quad \text{when } KL/r > C_c$$

<sup>d</sup> States not identified in table or footnote a. adopt AASHTO provisions.

<sup>e</sup> Corresponds to A36 steel.

<sup>f</sup> Iowa adopts AASHTO provisions, but specifies F<sub>y</sub> = 30 kip/in<sup>2</sup>.

<sup>g</sup> Allowable stresses discussed in Bridge Manual, but not specified in Standard Specifications.

<sup>h</sup> Allowable stresses discussed in Construction Manual, but not specified in Standard Specifications.

<sup>i</sup> Maryland specifies allowable axial tension and adopts AASHTO for remaining stresses.

<sup>j</sup> Standard specifications adopt AASHTO with an allowable one-third increase. Exceptions noted in Bridge Construction Manual.

AISC or AASHTO, whereas allowable axial compression and compression in flexure tend to vary. Despite the difference in the constants used in these expressions, most of the equations have the same form and predate the 1963 specifications, when the Structural Stability Research Council formula (AISC Equation E2-1) was adopted (14).

Some states also specify allowable stresses for unidentified, or salvaged, steel grades, as indicated in Table 2. For salvaged steel, states tend to subscribe to older and more conservative allowable stress criteria as opposed to using more current criteria with a reduced

yield stress. The exception is Iowa, which appears to acknowledge the likelihood of salvaged steel being used in falsework construction by limiting the maximum design yield strength to 207 MPa (30 ksi), roughly corresponding to the A7 steel common in older bridge construction.

With respect to timber falsework, 16 states reference AASHTO or NDS in their standard specifications. In addition, several states specify allowable unit stress values and, in some cases, note exceptions to the national standards. These states and their prescribed stresses are presented in Table 3. In general, the tabulated values

TABLE 2 Allowable Stress for Salvaged Steel (lb/in.<sup>2</sup>)

Specification	Axial Tension "F <sub>t</sub> "	Tension	Flexure, "F <sub>b</sub> " Compression	Axial Compression "F <sub>c</sub> "	Shear "F <sub>v</sub> "
California, Georgia, Idaho, Nevada	0.60 F <sub>y</sub>	0.60 F <sub>y</sub>	$\frac{12,000,000}{Ld/bt} \leq 22,000$	16,000 - 0.38 (L/r) <sup>2</sup>	0.40 F <sub>y</sub>
Colorado	18,000	18,000	$\frac{20,000}{1 + \frac{L^2}{2,000 b_f^2}}^a$	$\frac{18,000}{1 + \frac{L^2}{18,000 r^2}} \leq 15,000^b$	12,000

1 lb/in<sup>2</sup> = 6895 Pa, 1 kip/in<sup>2</sup> = 6.895 MPa, 1 ft = 0.305 m, 1 in = 25.4 mm

<sup>a</sup> 18,000 for L < 15b<sub>f</sub>

<sup>b</sup> 18,000 for L/r < 25

are unit stresses and subject to modification due to slenderness, moisture content, and other factors. However, contrary to NDS, some states do not require an allowable stress reduction for wood with a moisture content greater than 19 percent. California also allows a 50 percent increase in design values for bolts in single-shear connections, a specification based on in-house research (15). The allowable stresses specified by Wisconsin and Minnesota include a 25 percent increase to account for short-term load duration.

## Deflection

Many specifications, including the AASHTO 1991 interim specifications, prescribe a maximum allowable deflection for falsework flexural members corresponding to  $1/240$  of their span. Idaho limits deflection to  $1/500$  of the span. The limitation is intended to ensure a reasonable degree of rigidity in the falsework, in order to minimize distortion in the forms. The *California Falsework Manual* states that deflection generally is based on the assumption that all the concrete in the bridge superstructure is placed in a single pour (16). However, most specifications are not specific as to how this deflection should be determined. The actual deflection will depend on the sequence of construction when two or more concrete placements are required for a given span.

Caltrans has conducted research on curing effects and concrete support periods on dead load deflections of reinforced concrete slab bridges. Its findings indicate that variation in curing time from 7 to 21 days did not significantly affect deflections; however, the difference between 7- and 10-day support periods and 10- and 21-day support periods was significant. The end result was

a revision to the "effective modulus" used to calculate ultimate deflections (17).

## Stability

Stability is not addressed in detail by any of the state specifications. However, some of the accompanying bridge design or construction manuals contain related commentary. The *California Falsework Manual* contains perhaps the best available commentary (16).

In falsework construction, overall stability is a function of both internal and external conditions. Internally, falsework can be subject to a wide variety of local horizontal forces produced by out-of-plumb members, superelevation, differential settlement, and so forth. Therefore, the falsework assembly must be connected adequately to resist these forces. In practice, however, the inherent temporary nature of falsework construction does not always translate to a well-connected assembly. Although friction often provides means of load transfer, so-called positive connections eliminate or at least reduce the probability of underestimating the necessary restraint. The need for positive load transfer is particularly apparent when superelevation exists or the soffit is inclined.

External stability and overturning due to lateral or longitudinal loads are generally considered synonymous. If a falsework frame or tower is theoretically stable, external bracing is not necessarily required. However, if the resisting moment is less than the overturning moment, the difference must be resisted by bracing, cable guys, or another means of external support. Depending on the applicable standard, the minimum factor of safety against overturning can vary anywhere

TABLE 3 Allowable Unit Stress for Structural Lumber (lb/in.<sup>2</sup>)

Specification	Extreme fiber in bending "F <sub>b</sub> "	Tension parallel to grain "F <sub>t</sub> "	Horizontal shear "F <sub>v</sub> "	Compression perpendicular to grain "F <sub>c⊥</sub> "	Compression parallel to grain "F <sub>c</sub> "	Modulus of elasticity "E"
AASHTO <sup>a</sup>	1450 <sup>b</sup>	850	95	625	1000	1,700,000
California <sup>c</sup>	1500-1800	1200	140	450	$\frac{480,000}{(L/L_d)^2} \leq 1600$	1,600,000
Indiana <sup>d</sup>	1800	-	185	-	$1800 \left(1 - \frac{L}{60d}\right)^e$	1,600,000
Iowa <sup>f</sup>	1200	1000	120	390	1000	1,600,000
Kansas <sup>g</sup>	1200	-	120	250	850 <sup>h</sup>	1,500,000
Kentucky <sup>i</sup>	1600	-	125	405	1000	1,600,000
Maryland <sup>j</sup>	1.3(AASHTO) ≤ 1800	-	150-200	1.25(AASHTO)	1.25(AASHTO)	Ref. AASHTO
Minnesota <sup>k</sup>	1875	-	120	480	1560	1,800,000
Wisconsin <sup>l</sup>	1875	-	150	500	1500	-

1 lb/in<sup>2</sup> = 6895 Pa, 1 kip/in<sup>2</sup> = 6.895 MPa, 1 ft = 0.305 m, 1 in = 25.4 mm

<sup>a</sup> The current AASHTO Specifications (14th Edition) are based on the National Design Specification for Wood Construction (NDS), 1982 Edition. The allowable unit stresses in this table correspond to No. 2 Douglas Fir - Larch used at 19-percent maximum moisture content.

<sup>b</sup> Allowable stress corresponds to single member use.

<sup>c</sup> Georgia, Idaho and Nevada have similar specifications.

<sup>d</sup> The tabulated values correspond to Douglas-Fir.

<sup>e</sup> L = length of column, d = least dimension.

<sup>f</sup> Allowable stresses correspond to lumber 5 in thick or greater.

<sup>g</sup> Allowable stresses discussed in Bridge Manual, but not specified in Standard Specifications.

<sup>h</sup> Refers to NDS Section 3.7 for intermediate and long columns.

<sup>i</sup> Allowable stresses discussed in Construction Manual, but not specified in Standard Specifications.

<sup>j</sup> Maryland references AASHTO and prescribes allowable increases.

<sup>k</sup> MnDOT adapts AASHTO. Tabular values correspond to No. 1 Douglas Fir - Larch and include 25-percent increase for short-term load duration.

<sup>l</sup> Allowable stresses correspond to No. 1 Douglas Fir and includes 25-percent increase for short term load duration.

between 1 and 2. Many states also require the falsework system to be stable enough to resist overturning before the concrete is placed.

## Foundations

In general, the contractor is responsible for designing temporary foundations. Beyond this type of assignment, however, many state specifications are vague with respect to foundation requirements. As with permanent structures, the type of foundations required for temporary works is a function of soil conditions and design loads. Depending on the falsework system, foundation

loads can be distributed over the entire length of a supported span or concentrated at temporary bents. In either case, simple foundation pads may be adequate to support the falsework and construction loads.

With an increase in leg load, the method of foundation support on intermediate and heavy-duty shoring towers becomes more significant. Some states require that foundations be designed for uniform settlement under all legs of the tower and under all loading conditions. For heavy-duty shoring, this necessitates the use of concrete mats or pile foundations, as opposed to timber cribbing or simple pads. Pile foundations are required when site conditions preclude timber cribbing or concrete pads and generally are specified to support

falsework for bridge structures over water or where conventional pad foundations are not feasible because of poor soil conditions. In some cases, temporary construction loads are supported by brackets off the permanent piers and abutments, but several states do not permit this practice.

The AASHTO *Standard Specifications for Highway Bridges* contains several sections that relate to foundations (5). Many of these provisions, however, apply to permanent pier construction and sections applicable to falsework construction, for example, pile and framed bents, and timber cribbing, generally are more qualitative. For the most part, basic design information for both permanent and temporary construction is limited to pile design criteria and forces due to stream current and ice loads. The AASHTO Division II interim specifications for temporary works do not contain specific guidelines for foundation design (4).

## Traffic Openings

Traffic openings in falsework are relatively common, particularly for bridge construction over public roads. As such, the specifications of California and three other states contain special provisions for traffic openings, including clearance requirements and special load conditions. Clearance requirements are also identified in a related ACI-ASCE committee report (18). California devotes a chapter of its falsework manual to this subject (16) and has some of the most comprehensive specifications. Falsework over or adjacent to roadways or railroads, which are open to traffic, must be designed and constructed so that the falsework remains stable if subjected to accidental impact.

## FHWA'S GUIDE DESIGN SPECIFICATION

FHWA's *Guide Design Specification for Bridge Temporary Works* was developed for use by state agencies to update their existing standard specifications for falsework, formwork, and related temporary structures. The guide specification provides unified design criteria that reflect the current state of practice. The specification was prepared in a format similar to AASHTO's *Standard Specifications for Highway Bridges*.

For the purposes of this document, "falsework" is defined as temporary construction used to support the permanent structure until it becomes self-supporting. "Shoring" is generally considered a component of falsework, such as horizontal or vertical support members, and the term is often used interchangeably with falsework. "Formwork" is a temporary structure or mold used to retain plastic or fluid concrete in its designated

shape until it hardens. "Temporary retaining structures" are both earth-retaining structures and cofferdams. These definitions are not intended to be exclusive, but generally consistent with the common use of these terms.

## Falsework

The FHWA falsework provisions include four general topics: materials, loads, design considerations, and construction. Allowable stress provisions for steel and timber, as well as modification factors for salvaged (used) materials, are identified. Safety factors and limitations of manufactured (proprietary) components are also specified. Four general load categories, including environmental loads, are defined. The basic reference for computation of wind load is the *Uniform Building Code* (9). General design topics such as load combinations, stability against overturning, traffic openings, and foundations are addressed. Presumptive soil-bearing values are also provided. Construction topics include foundation protection, erection tolerances, clearances of traffic openings, adjustment methods, and removal.

The guide design specification is supplemented with commentary and several detailed appendixes, which include design values for ungraded structural lumber, provisions for steel beam webs and flanges under concentrated forces, design wind pressures from selected model codes, and foundation investigation and design.

## Formwork

ACI 347-88 (3) along with ACI SP-4, *Formwork for Concrete* (19), served as the principal reference documents for this section. The objective is to address many of the common bridge forming methods, such as those shown in Figures 4 and 5. Formwork includes materials, loads, and construction. Requirements for sheathing, form accessories, prefabricated formwork, and stay-in-place formwork are specified, as are minimum vertical and horizontal loads. The ACI equations for lateral pressure of fluid concrete are adopted, and the limitations of these equations are discussed in the commentary. Construction topics such as form removal, placement of construction joints, and tolerances are also discussed.

## Temporary Retaining Structures

Although developed primarily to address earth-retaining systems more common to bridge construction, such as the soldier pile/lagging shown in Figure 6, this section



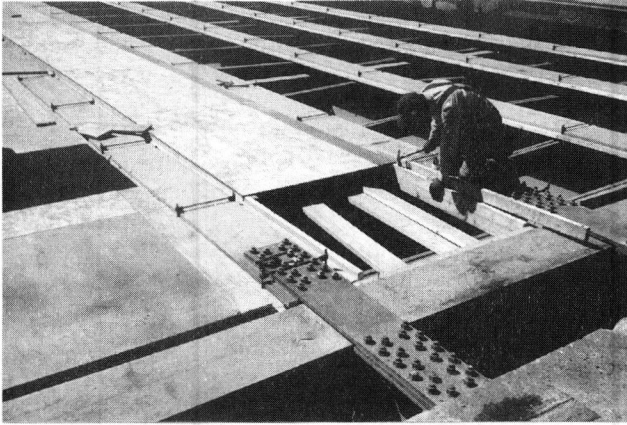


FIGURE 4 Bridge deck formwork.

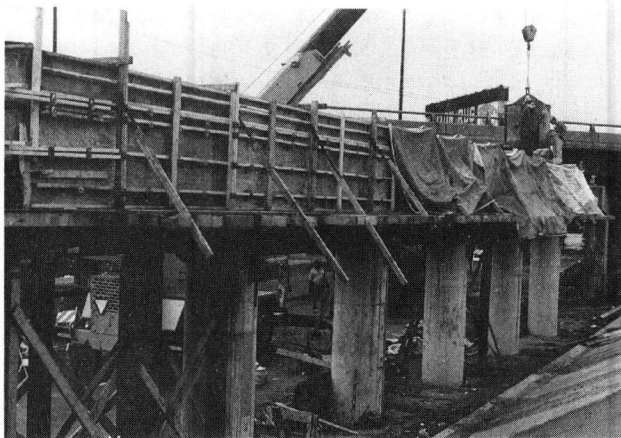


FIGURE 5 Job-built formwork.



FIGURE 6 Soldier piles retained with soil anchors.

also applies to temporary cofferdams. General requirements and types of excavation support are identified. Federal standards of the Occupational Safety and Health Administration and other regulations are referenced. Empirical methods for determining design lateral pressures in various soils and their limitations are identified. The simplified earth pressure distributions presented in the AASHTO's 1991 interim specifications are adopted. Related topics such as stability, sealing and buoyancy control, seepage control, and protection are discussed in a companion document (20).

## SUMMARY

The objective of this paper has been to familiarize the reader with existing standards and specifications for temporary works used to construct highway bridge structures. In the United States, these standards include AASHTO's 1991 interim specifications (4) and ANSI A10.9-1983. Since the first edition in 1977, the *California Falsework Manual* (16) has also served as an authoritative document on this subject and has influenced the specifications of other states as well as the development of standards abroad.

In 1975 and 1982, respectively, Canada and Great Britain produced model standards for falsework that apply to bridge and building construction. As noted in its foreword, the British standard represents "a standard of good practice which has drawn together all those aspects that need to be considered when preparing a falsework design, and in so doing has included recommendations for materials, design and work on site." Since then, the Works and Development Services Corporation in New Zealand has produced a similar code of practice.

In 1991 FHWA initiated a study to identify the current practice in the United States and abroad for designing, constructing, and inspecting the falsework and formwork used to construct highway bridge structures. The findings of this study were published in the *Synthesis of Falsework, Formwork, and Scaffolding for Highway Bridge Structures* (1). More recently, FHWA has published the *Guide Design Specification for Bridge Temporary Works* (2), which is summarized briefly in this paper. Three other publications—*Guide Standard Specification for Bridge Temporary Works* (21), *Certification Program for Bridge Temporary Works* (22), and *Construction Handbook for Bridge Temporary Works* (23)—were also developed as part of the Bridge Temporary Works Research Program.

The reports produced under this program are available through the National Technical Information Service, 5285 Port Royal Road, Springfield, Virginia 22161.

## NOTATION

- $b$  = actual width of stiffened or unstiffened compression element,  
 $b_f$  = flange width of rolled beam,  
 $d$  = overall depth of steel member or least dimension of timber member,  
 $E$  = modulus of elasticity,  
 $F_a$  = allowable axial compressive stress,  
 $F_b$  = allowable bending stress,  
 $F_c$  = allowable axial compressive stress parallel to grain,  
 $F_{c\perp}$  = allowable axial compressive stress perpendicular to grain,  
 $F_y$  = specified minimum yield stress of steel,  
 $F_t$  = allowable axial tension stress,  
 $F_T$  = allowable axial tension stress parallel to grain,  
 $F_v$  = allowable shear stress,  
 F.S. = factor of safety,  
 $I$  = moment of inertia,  
 $K$  = effective length factor,  
 $L$  = unbraced length of column or compression flange,  
 $r$  = governing radius of gyration,  
 $t$  = thickness of compressed element.

## ACKNOWLEDGMENTS

The work described herein was sponsored by FHWA and directed by the Scaffolding, Shoring, and Forming Task Group of FHWA. The U.S. and Canadian transportation departments are thanked for their participation in this study. The assistance of the authors' professional colleagues abroad in locating foreign literature is also gratefully acknowledged.

## REFERENCES

1. Duntemann, J. F., N. S., Anderson, and A. Longinow. *Synthesis of Falsework, Formwork, and Scaffolding for Highway Bridge Structures*. Report FHWA-RD-91-062. FHWA, U.S. Department of Transportation, Nov. 1991.
2. Duntemann, J. F., L. E. Dunn, S. Gill, R. G. Lukas, and M. K. Kaler. *Guide Design Specification for Bridge Temporary Works*. Report FHWA-RD-93-032. FHWA, U.S. Department of Transportation, March 1993.
3. Guide to Formwork for Concrete (ACI 347R-88). *ACI Manual of Concrete Practice, Part 2*, American Concrete Institute, Detroit, Mich., 1990.
4. *Interim Specifications for Bridges*, AASHTO, Washington, D.C., 1991.
5. *Standard Specifications for Highway Bridges*, 14th ed., AASHTO, Washington, D.C., 1989.
6. *Falsework for Construction Purposes* (CSA S269.1-1975). Canadian Standards Association, Rexdale, Ontario, 1975.
7. *Code of Practice for Falsework* (BS5975: 1982). British Standards Institution, London, 1982.
8. *NAASRA Bridge Design Specification*. National Association of Australian State Road Authorities, Sydney, 1976.
9. *Uniform Building Code*. International Conference of Building Officials, Whittier, Calif., 1988.
10. Nelsen, B. H., and P. J. Jurach. *Long Span Bridge Deflection*. Report FHWA/CA/SD-82/01. Office of Structure Design, California Department of Transportation, Sacramento, Dec. 1983.
11. *Manual of Steel Construction—Allowable Stress Design*, 9th ed. American Institute of Steel Construction, Chicago, Ill., 1989.
12. *National Design Specification for Wood Construction*. National Forest Products Association, Washington, D.C., 1986.
13. *NDS Supplement—Design Values for Wood Construction*. National Forest Products Association, Washington, D.C., 1988.
14. *Manual of Steel Construction*, 6th ed. American Institute of Steel Construction, New York, 1963.
15. Hallis, K. *Capacities of Bolted Joints for Bridge Timber Falsework Bracing*. Report FHWA/CA/SD-85-02. Office of Structure Construction, California Department of Transportation, Sacramento, May 1985.
16. *California Falsework Manual*. California Department of Transportation, Sacramento, 1988.
17. Roberts, J. E. *Effects of Curing and Falsework Support Period on Dead Load Deflections of Reinforced Concrete Slab Bridges*. Report CA-HY-BD-4106-1-72-8. Bridge Department, California Division of Highways, Sacramento, Dec. 1972.
18. Analysis and Design of Reinforced Concrete Bridge Structures (ACI 343R-88). *ACI Manual of Concrete Practice, Part 4*, American Concrete Institute, Detroit, Mich., 1990.
19. Hurd, M. K., and ACI Committee 347. *Formwork for Concrete (SP-4)*, 5th ed. American Concrete Institute, Detroit, Mich., 1989.
20. Duntemann, J. F., F. Calabrese, and S. Gill. *Construction Handbook for Bridge Temporary Works*. Report FHWA-RD-93-034. FHWA, U.S. Department of Transportation, Nov. 1993.
21. *Guide Standard Specification for Bridge Temporary Works*. Report FHWA-RD-93-031. FHWA, U.S. Department of Transportation, 1993.
22. *Certification Program for Bridge Temporary Works*. Report FHWA-RD-93-033. FHWA, U.S. Department of Transportation, 1993.
23. *Construction Handbook for Bridge Temporary Works*. Report FHWA-RD-93-034. FHWA, U.S. Department of Transportation, 1993.

*The contents of this paper reflect the views of the authors and do not necessarily reflect the official view of the sponsor.*

# Constructability Reviews: An Opportunity for Partnering

---

William J. Schmitz, *Berger, Lehman Associates, P.C.*

The partnering concept of working together toward common goals has proven to be highly successful during construction. Constructability reviews offer the opportunity to expand this idea to include the design process. The definition, objectives, and benefits of constructability reviews are examined. The composition of the review team and procedures for conducting a constructability review are also discussed. Case histories of the author's involvement in a number of constructability reviews are related. It is concluded that constructability reviews are the direction of the future, but there is a need for an effective methodology to permit contractor participation in the process.

**C**onstructability is a new word that has been coined to express an idea that is as old as the pyramids and integral to the meaning of engineering: the concept that what has been designed must be capable of being built. The term "constructability" is so new that to date there is no consensus on how to spell the word. Many people use the spelling "constructibility," derived from the spelling of the adjective form "constructible."

Regardless of its spelling, engineers have a clear understanding of what the term means. Constructability review is a form of peer review to determine if the proposed construction can be built as presented in the contract documents. This review includes ascertaining whether the design is feasible, practical, and conducive

to accomplishing the necessary construction operations in a reasonable and efficient manner. Its objective is to determine if the contract work can be completed, as specified, within the contract's time frame and without significant changes. For the owner of a project, the benefits of a constructability review include an independent review of the contract documents, a reduction in the possibility of claims and change orders, additional expertise to suggest economies of construction, and a better product. For the designer, the review serves as a risk management tool. For the construction contractor, an improvement in the quality of the construction documents decreases the possibility of lose-lose delays and therefore increases the profit potential. Because everyone benefits, the process is an ideal candidate for partnering.

## NEW YORK STATE DEPARTMENT OF TRANSPORTATION CRITERIA

Berger, Lehman Associates' experience in performing formal constructability reviews has been primarily for the New York State Department of Transportation (NYSDOT), which has been a leader in using this process. NYSDOT's scope of services for constructability reviews of highway and bridge design requires that biddability and buildability be addressed.



## Biddability

Issues of biddability include the following:

- Is sufficient information contained in the contract documents to allow uninterrupted construction of the project and to avoid major field changes?
- Are the bidders unnecessarily restricted in their bids or has the appropriate degree of flexibility been included in the bidding documents?
- Have the appropriate parties been coordinated during design and have agreements reached with those parties been provided for in the bidding documents (or are such actions in progress)?
- Have all necessary permits been identified and is there enough time to secure those permits before construction?
- Are the maintenance and protection of traffic plans adequate and complete? Are they too restrictive?

## Buildability

Issues of buildability include the following:

- Has sufficient field investigation been made during design so that the project can physically be built?
- Is sufficient right of way available to the contractor for all construction operations and storage required during construction of the project?
- Are the type and sequence of construction activities realistic?
- Can the project be built in the time frame allowed for each individual stage and the amount of time allowed for each construction season?
- Are the materials specified in the contract documents readily available?
- Can the details as shown be constructed using the standard practices of the industry? If unusual contract expertise, special equipment, or nonstandard operations are required, are the performance characteristics and quality of the end product clearly established?

## PROCEDURE

Performing a constructability review requires the formation of a special team that may comprise design experts, contract administrators and resident engineers, specification writers, and claims experts. Ideally, the team should also include a construction contractor. Few design professionals or resident construction engineers can provide better insight than someone whose success or failure depends on his or her ability to understand and implement the contract documents. Unfortunately,

because such participation would preclude the contractor from bidding on the project because of a perceived information advantage, it is difficult to obtain such assistance.

Constructability reviews are a form of peer review. Reviews often require questioning the fundamental premises of a project or owner's standard procedure; therefore, they are most successfully conducted by an outside consultant. They can, however, be conducted by the owner's engineering staff or the designer.

For a constructability review, or any other review, to be effective, it must be performed in a timely manner so that changes, if necessary, can still be incorporated in the contract documents. This generally means that the review must be conducted at the advance detail plan submission stage (approximately 80 percent completion), when the documents are expected to be essentially complete but may not yet be checked.

This can be an inopportune time for the designer because internal quality control procedures and checking may still be occurring and certain details may still be in development. The designer naturally will feel vulnerable to unjust criticism, particularly by an outside reviewer in front of the designer's client. Therefore, it is incumbent on the review team to conduct the review in a professional, nonconfrontational manner and to make constructive criticisms. In a real sense, the constructability reviewers must engage in "partnering" with the owner and the designer.

The constructability review ideally begins with the designers briefing the constructability review team on the project. Then the reviewers must become thoroughly familiar with the project scope, project site, and review documents. Next, each member of the review team formulates comments based on his or her area of expertise. Group discussion and brainstorming of initial comments serve to synthesize the individual comments into an overall picture. Finally, the review team project manager edits these comments to create a comprehensive report that is presented to the client and the designer at a joint meeting.

Frequently, constructability review comments relate to items that result from policies or directions given by the owner or client. This should not stop the reviewers from questioning them. The owner is entitled to this insight, even if other considerations may preclude implementation of the suggestions. The owner, in turn, must be willing to take a second look at prior decisions and policies to determine if they meet present needs.

The decision of whether to implement particular constructability review comments must ultimately be made by the owner, subject only to the limitation of the designer's professional responsibility. The constructability reviewers must recognize this hierarchy, as well as the fact that the design must be guided by the comments

and requirements of other agencies. Although contradictory opinions may develop, honest resolution of these issues through an open, professional discussion will result in a better design. Again, this is most successfully accomplished in a partnering atmosphere, wherein each party acknowledges the common goal.

## CASE HISTORIES

### Oak Point Link Rail Connection

The Oak Point project required the completion of a 1.8-m-long railroad trestle along the shoreline of the Harlem River in the South Bronx, New York, between the south end of the Highbridge Yard and the west end of the Harlem River Yard. A previous construction contract had been terminated because of problems with the caisson foundations.

Berger, Lehman Associates, the designer for the completion contract, was also charged with conducting an unbiased constructability review. The impartiality of the review team was maintained by making a senior officer of the firm, who was not involved in the design, responsible for the review. The unique feature of the panel was the inclusion of the president of a preeminent marine construction contractor. His firm had to waive its right to bid on the project in order to participate. The team also included an independent marine construction consultant and a geologist.

By working with the design team and the client, NYSDOT, the panel was instrumental in developing more progressive and equitable payment items to compensate the construction contractor for unknown foundation conditions. Contractor representatives on the panel and the NYSDOT's specification writers had many lively discussions on this subject. Through these discussions, each party learned from the other, and together they reduced a new, equitable payment system. Previously, a single payment item was provided for length of caisson installed, which would have forced the contractor to assume all risk for unknown subsurface conditions. The new specifications provided separate payment for ordered length of pipe shell, driven length, and removal obstructions. Another major recommendation of the review was to conduct a pile driving and load testing program, in advance of construction, to verify the driving criteria for the redesigned caissons without rock sockets. The full-time, on-site presence of a geotechnical design engineer during construction to facilitate real-time decisions about foundation conditions was also recommended. These recommendations were implemented, and construction operations to date have proven their value.

### Mineola Grade Crossing Elimination

The Mineola project provides for the elimination of the grade crossing of the Long Island Rail Road main line at Herricks Road in Mineola, Long Island. It involves raising the Long Island Rail Road's two-track line for a length of  $5,000 \pm$  ft. Herricks Road, a four-lane roadway, is an important north-south connector in Nassau County. It will be depressed approximately 7 ft at the railroad intersection to provide a roadway clearance of 14 ft 6 in.

The project involves the construction of new east-bound and westbound mainline tracks and a third track within the northern portion of the existing right of way. This requires the temporary relocation of the two main line tracks southward within the railroad right of way and the use of temporary easements.

Berger, Lehman Associates undertook an independent constructability review of this project for NYSDOT that was based on the advance detail plan submission prepared by others. The primary recommendation was to retain a construction manager or coordinator to ensure that the design and construction of railroad work, utility work, roadway work, easements, acquisitions, and long-term procurement of materials would be accomplished in a timely and coordinated manner. A construction agreement between all parties would be required to facilitate coordination and empower the construction manager. Further, to accomplish the necessary coordination, all parties would address and accept a critical path method schedule embracing all critical elements.

### Bruckner Expressway

Two contracts for the Bruckner Expressway project provide for deck, parapet, superstructure, and substructure rehabilitation of a 2-mi viaduct carrying the Bruckner Expressway (I-278) in the Bronx.

The Bruckner Expressway, which carries six lanes of traffic, links the Triborough Bridge/Major Deegan Expressway (I-87) and points west and south to the Sheridan Expressway (I-895), the New England Thruway/Cross Bronx Expressway (I-95), and points north and east. In the project area, the Bruckner Expressway is on a viaduct. Bruckner Boulevard, a nine-lane urban arterial, runs underneath and parallel to the viaduct.

Traffic requirements dictate the performance of construction in stages. The intent of this staging is to provide a minimum of two traffic lanes in each direction at all times. Up to half of the traffic that normally uses the viaduct will be detoured onto Bruckner Boulevard during construction.

Berger, Lehman performed an independent constructability review for NYSDOT. The contract documents were found to present a clear picture of the work to be performed and were considered to be biddable and constructible. The following is a sampling of the recommendations made:

1. The proposed starting date for construction should be coordinated with an adjacent construction contract that is behind schedule and will not be completed in time.
2. Shielding is required for pedestrian undercrossings, including a pedestrian bridge used by schoolchildren.
3. Incident management procedures need to be included in the contract to clear stalled vehicles in areas of single lane operation.
4. Incentive and disincentive provisions should be incorporated for work on critical ramps, particularly where it is otherwise advantageous to the contractor to not reopen the ramp because doing so would increase traffic problems.
5. Coordination with the city of New York is required to retime signals on the detour routes.
6. The construction schedule does not provide for winter shutdowns.
7. Maintenance and protection of traffic schemes are needed for bearings replacements, which require falsework in the streets below the viaduct.
8. A full-time traffic coordinator should be provided.
9. The plans should be updated to indicate protective shielding placed by others since the designer's field investigation.
10. The tops of lampposts beneath the viaduct will interfere with specified shielding between the bottom of girder flanges.
11. Traffic signal heads and conduits mounted on some of the concrete piers must be relocated to permit required concrete repairs.
12. A number of specifications need to be coordinated with the drawings so information "as shown on the plans" is provided.

## Other Projects

On a highly complex truss rehabilitation project, the constructability review recommended that the owner enter a formal partnering agreement with the contractor, the designer be engaged to provide construction support services, and the precision steelwork involved in strengthening the truss members be declared a specialty item. All these recommendations were departures from previous policies of the owner. It was also recommended that the contractors be allowed extra time to prepare their bids because of complexity of the project. The anticipated construction schedule was found to require reevaluation because of unrealistic required contractor staffing levels and potential conflicts with sporting events.

## SUMMARY

The concept of working together toward common goals has proven to be successful during construction. Constructability reviews enable this idea to be expanded to include the design process. Doing so requires a professional, constructive attitude from the review team; a positive, cooperative approach by the designer; and flexibility on the part of the owner. Hopefully, when an equitable methodology is found, contractor participation will be a routine part of constructability reviews.

Just as partnering has gained widespread acceptance, constructability reviews may be the direction of the future for complex projects. Designers, owners, contractors, and the public will all benefit.

## ACKNOWLEDGMENTS

The author wishes to acknowledge the role of NYSDOT in conducting the described constructability reviews and the suggestions and support of James M. O'Connell, Assistant Deputy Chief Engineer (Structures), NYSDOT; Edward J. Petrou, Regional Construction Engineer, Region 11 NYSDOT; and Richard Schmalz, Regional Planning Engineer, Region 11 NYSDOT in the preparation of this paper.

# High-Performance Concrete for a Floating Bridge

---

M. Myint Lwin, Alan W. Bruesch, and Charles F. Evans, *Washington State Department of Transportation*

A high-performance concrete mix was developed for the construction of the new I-90 Lacey V. Murrow Floating Bridge (LVM Bridge) on Lake Washington in Seattle, Washington. The LVM Bridge is 2013 m (6,600 ft) long, consisting of 20 prestressed concrete pontoons rigidly connected to form a continuous structure. A typical pontoon measures 110 m (360 ft) long, 18.3 m (60 ft) wide, and 5.4 m (17.85 ft) deep. About 38,000 m<sup>3</sup> (49,600 yd<sup>3</sup>) of high-performance concrete went into the construction of the pontoons. The high-performance concrete contains silica fume and fly ash, and its average 28-day compressive strength is more than 69 MPa (10,000 psi). The high-performance concrete has low permeability and low shrinkage. The contractor learns to work with the high-performance concrete by constructing test sections. The lessons from the test sections are put into practice, resulting in improved placement, finishing, and curing procedures. The construction of the LVM Bridge has shown that it is feasible and cost-effective to use high-performance concrete in highway structures for which high strength, impermeability, and durability are of prime importance.

**W**ashington State has been building concrete floating bridges since 1938 (1,2). Floating bridges form major transportation links in the state and Interstate highway systems. The first concrete floating bridge was opened to traffic in July 1940

(1). The concrete strength for this bridge ranged from 21 to 24 MPa (3,000 to 3,500 psi). In the early 1960s (3), the strength of concrete for floating bridges ranged from 24 to 31 MPa (3,500 to 4,500 psi). Concrete pontoons built in the 1980s (4) had concrete strength ranging from 28 to 45 MPa (4,000 to 6,500 psi).

In the early 1990s, there was a need to build another concrete floating bridge across Lake Washington, Seattle (5). The new bridge is known as the Lacey V. Murrow Floating Bridge (LVM Bridge). The LVM Bridge is 2013 m (6,600 ft) long, consisting of 20 prestressed concrete pontoons connected to form a continuous structure. Figure 1 shows the layout of the new LVM Bridge. A typical pontoon measures 110 m (360 ft) long, 18.3 m (60 ft) wide, and 5.4 m (17.85 ft) deep. Figure 2 shows a typical cross section of the pontoons. In planning the new bridge, it was again recognized that watertightness and durability were of prime importance for long-term performance of a floating structure, because of the exposure to water and severe environmental conditions. The concrete must be extremely dense and impermeable to water, highly resistant to abrasion due to wave action, and relatively crack free. As the design was progressing, an effort was launched to research and develop a concrete mix that would give the above properties. Additionally, the concrete must be readily available locally, have good workability, have low demand on labor skills, and require no special equipment.

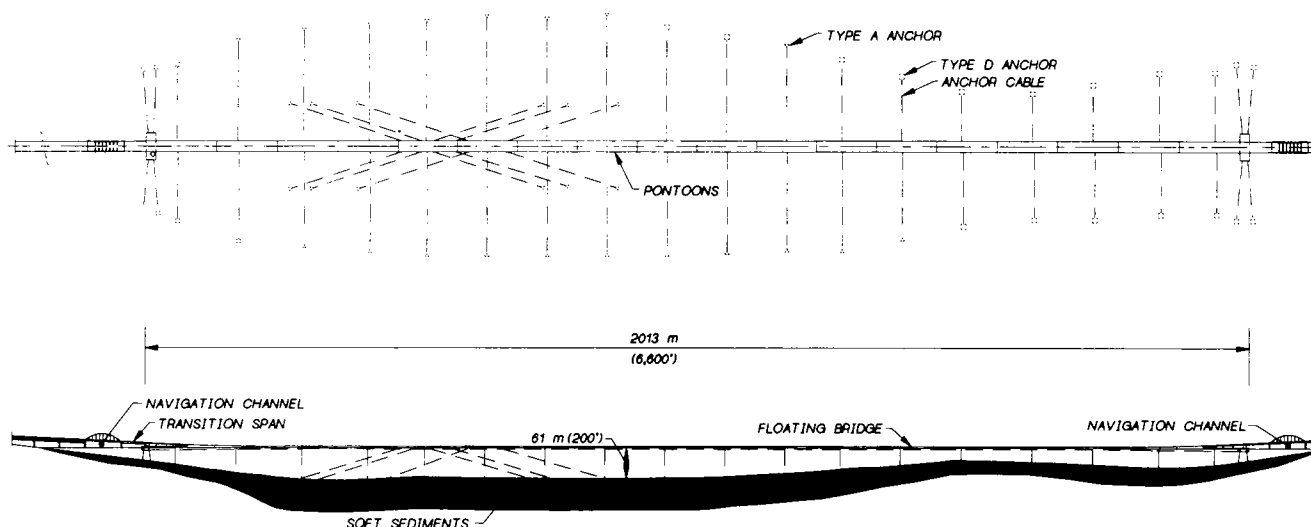


FIGURE 1 Lacey V. Murrow Floating Bridge: *top*, plan; *bottom*, elevation.

The objectives of this paper are to describe the procedures used to develop a high-performance concrete mix and the methods for placement, consolidation, and curing of the high-performance concrete.

#### CONCRETE MIX DESIGN DEVELOPMENT

The concrete mix development program was conducted in three phases. The first phase was to conduct preliminary trial mixes to evaluate cement types, effects of silica fume, fly ash, and admixtures. The trial mixes confirmed the performance characteristics of the material as follows:

1. Silica fume
  - Reduces permeability,

- Increases early compressive strengths,
- Reduces bleeding, and
- Increases heat of hydration.

2. Fly ash
  - Increases workability,
  - Reduces heat of hydration, and
  - Increases ultimate compressive strength.
3. Retarders
  - Increase workability,
  - Extend slump life, and
  - Improve concrete set control.
4. Superplasticizers
  - Increase workability, and
  - Decrease water demand.

The second phase was to provide a design mix that would meet watertightness, durability, constructability,

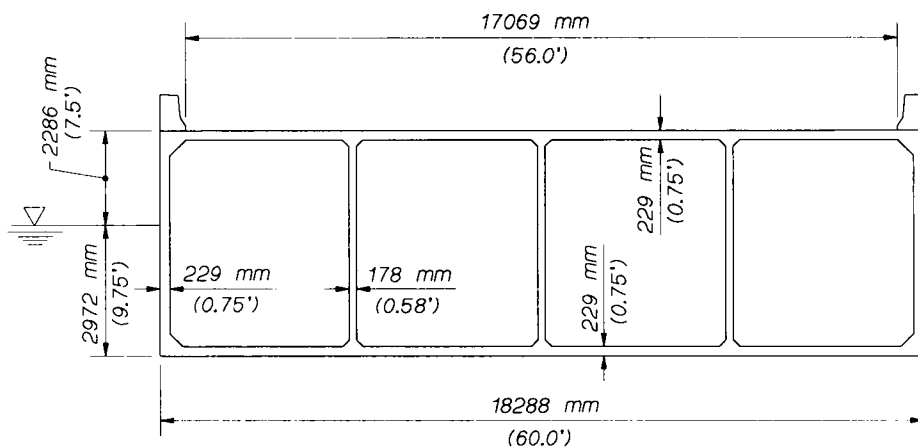


FIGURE 2 Cross section of typical pontoon.

and compressive strength. From the results of the first-phase trial mixes, the final mix was developed with the following proportions per cubic meter (per cubic yard) of concrete:

- Cement Type II: 380 kg (640 lb)
- Silica fume: 38 kg (64 lb)
- Fly ash: 59 kg (100 lb)
- Water: 142 kg (240 lb)
- Coarse aggregate: 1078 kg (1,815 lb)
- Sand: 706 kg (1,189 lb)
- Retarder: 230 mL/59 kg (6 oz/100 lb cementitious materials)
- Superplasticizer
  - Initial dose: 310 mL/59 kg (8 oz/100 lb cementitious materials)
  - Final dose: 464 mL/59 kg (12 oz/100 lb cementitious materials)
- Air entrainment: none
- Slump: 210 mm (8.25 in.)

The average compressive strengths of the hardened concrete were as follows:

- 7 days: 54 MPa (7,800 psi)
- 14 days: 72 MPa (10,420 psi)
- 90 days: 86 MPa (12,480 psi)

The third phase was to construct full-size test sections to test the constructability of the mix. The test sections consisted of wall and slab combinations including reinforcing bars and posttensioning conduits. The test sections also provided information on finishability, consolidation, curing requirements, and construction joints. The following observations were made from the tests carried out on the test sections:

- The concrete was easily placed and finished.
- The concrete appeared “sticky;” however, a float finish was achieved easily.
- A light mist helped achieve a smooth and dense surface finish.
- Effort to prepare construction joint was minimal.
- Construction joint had low permeability.
- Retarder applied to the construction joint resulted in an inferior joint.
- Curing compound must be applied immediately after finishing to avoid cracking.
- Wet burlap covered with polyethylene sheeting provided adequate moisture for proper curing.
- External vibration was the most desirable method for consolidation of concrete in the walls.
- Free-fall of concrete did not show sign of segregation.

- Two-hr cold joint could be reconsolidated into concrete of the new lift.

- Walls must be continuously supplied with moisture while forms were in place; otherwise surface crazing would occur.

The information gathered in the three phases of concrete mix development was used in preparing the construction specifications for the project.

## CONSTRUCTION SPECIFICATIONS

The Washington State Standard Specifications for Road, Bridge, and Municipal Construction have provisions for contracting agency-provided mix designs for concrete with 28-day strength of up to 34.5 MPa (5,000 psi). For higher-strength concrete, the contractors are required to submit a mix design for the state's approval under the terms of the standard specifications.

The concrete mix for this project was designated as Class LVM with emphasis on watertightness, low permeability, and low shrinkage. The structural designers needed 45 MPa (6,500 psi) at 28 days to satisfy the structural requirements.

Consequently, the contractor was to provide a mix design with a minimum compressive strength of 45 MPa (6,500 psi) at 28 days. Besides meeting the requirements of the standard specifications, the mix per cubic meter (cubic yard) was to meet the following specifications:

1. Minimum portland cement Type II content shall be 370 kg (625 lb).
2. Microsilica shall be used at a rate of not less than 30 kg (50 lb) or more than 40 kg (70 lb).
3. Fly ash shall be used at a minimum content of 59 kg (100 lb).
4. The combined microsilica and fly ash should not exceed 25 percent of total cementitious materials by weight. Total cementitious materials should be defined as the combined weight of cement, microsilica, and fly ash.
5. Aggregate gradation proportions shall be determined by the contractor to be suitable for the placement conditions and methods of placement. Aggregate gradations shall be submitted to the engineer for approval.
6. Water content shall not exceed 166 kg (280 lb). Maximum ratio of water to cementitious materials shall not exceed 0.33 by weight.
7. Both normal and high-range water reducing admixtures shall be used.
8. The contractor shall submit a plan for admixture dosage. The initial application rate shall not exceed that shown in the mix design. A subsequent dosage, prior to

acceptance of the concrete by the engineer, will be permitted but shall not exceed half of the initial dosage.

9. The concrete shall not be air entrained.

The contractor was also required to submit the following test data on permeability and shrinkage with the proposed mix design for approval:

1. Rapid chloride permeability (AASHTO T277): two samples shall be tested from laboratory-cured cylinders at 28 days. The maximum allowable electrical charge passed shall not exceed 1000 coulombs.
2. Length change of hardened concrete (AASHTO T160): the maximum allowable shrinkage shall not exceed 400 millionths at 28 days.

### CONTRACTOR'S FINAL MIX DESIGN

The approved contractor-provided mix design conformed closely to the project specifications. A 9.5-mm ( $\frac{3}{8}$ -in.) maximum aggregate was used, as was a silica fume in slurry form. The slurry contained about 45 percent silica fume solids, water, and a small amount of high-range water reducer. The proportion of the contractor's final mix design per cubic meter (cubic yard) was as follows:

- Portland cement Type II: 370 kg (624 lb)
- Silica fume (AASHTO M307): 30 kg (50 lb)
- Fly ash (AASHTO M295): 59 kg (100 lb)
- Paving sand: 770 kg (1,295 lb)
- Coarse aggregate: 1050 kg (1,770 lb)
- Water: 150 kg (255 lb)
- Water reducer (ASTM C494): 965 mL (25 oz)
- Superplasticizer (ASTM C494): 5065 mL (131 oz)
- Air entrainment: none
- Water/cementitious materials ratio: 0.33
- Slump: 180 mm (7 in.)

The average 28-day compressive strength of this mix was above 69 MPa (10,000 psi). The average permeability as tested in accordance with AASHTO T-277 was as follows:

- 28 days: 1,198 coulombs (C)
- 56 days: 790 C
- 90 days: 584 C

At 28 days the permeability did not meet specifications. However, at 56 days the permeability was well below 1,000 C, which was considered very low. Future specifications should require that the permeability at 56 days be less than 1,000 coulombs.

### TEST SECTION

The contract specifications required that the contractor build a test section of a cell of a typical pontoon before pontoon construction began. The test section was to include the reinforcement, posttensioning ducts, and anchorages. Tests were conducted to evaluate the concrete mix, forms, concrete placement method, consolidation technique, and curing method proposed for the pontoon construction. The test demonstrated the necessity for adequate external vibration and strict quality control in mixing, placing, vibrating, and curing of the concrete.

Additionally, the contractor conducted several tests of the concrete mix and placement procedure for two walls 6 m (20 ft) high. The tests were performed to measure form pressures, evaluate vibration methods, and measure form deformation. The form pressures at the bottom of the wall were between 48 and 58 kPa (1,000 and 1,200 lbf/ft<sup>2</sup>) and about 31 kPa (650 lbf/ft<sup>2</sup>) near the top. The information gathered from these tests was valuable to the contractor in designing forms, estimating rate of slump loss, and planning quality-control procedures.

### CONCRETE PLACEMENT

The workability of the concrete was good. A slump of 180 to 230 mm (7 to 9 in.) allowed the concrete to be pumped without difficulty. A set time of 6 to 8 hr was achieved during construction. However, once the mix started to set, it set very rapidly. The longer set time was important for casting and finishing the flatwork such as the bottom and top slabs of the pontoons. Figure 3 shows the initial strength gain of the LVM concrete mix as compared with the normal concrete mix. The normal concrete mix has a compressive strength of 28 MPa (4,000 psi) and no silica fume. Concrete was placed in the walls in multiple lifts. The long set time allowed internal vibration full height of the walls. The concrete mix was very cohesive and resistant to segregation.

A modified structural tube attached to the concrete pump hose was used as a tremie to place concrete in the tall walls. The tremie was lowered to the bottom of the wall and slowly raised as the level of concrete rose. The tremie was inserted at 3.7 to 4.3 m (12 to 14 ft) centers for depositing concrete. The concrete flowed 1.8 to 2.4 m (6 to 8 ft) laterally from the point of deposit through the heavily reinforced wall. The upper lifts of concrete were placed from the top of the wall without the tremie.

Figure 4 shows that the bottom slab of a pontoon had been completed and that wall forms were being erected. Figure 5 shows that a pair of pontoons was

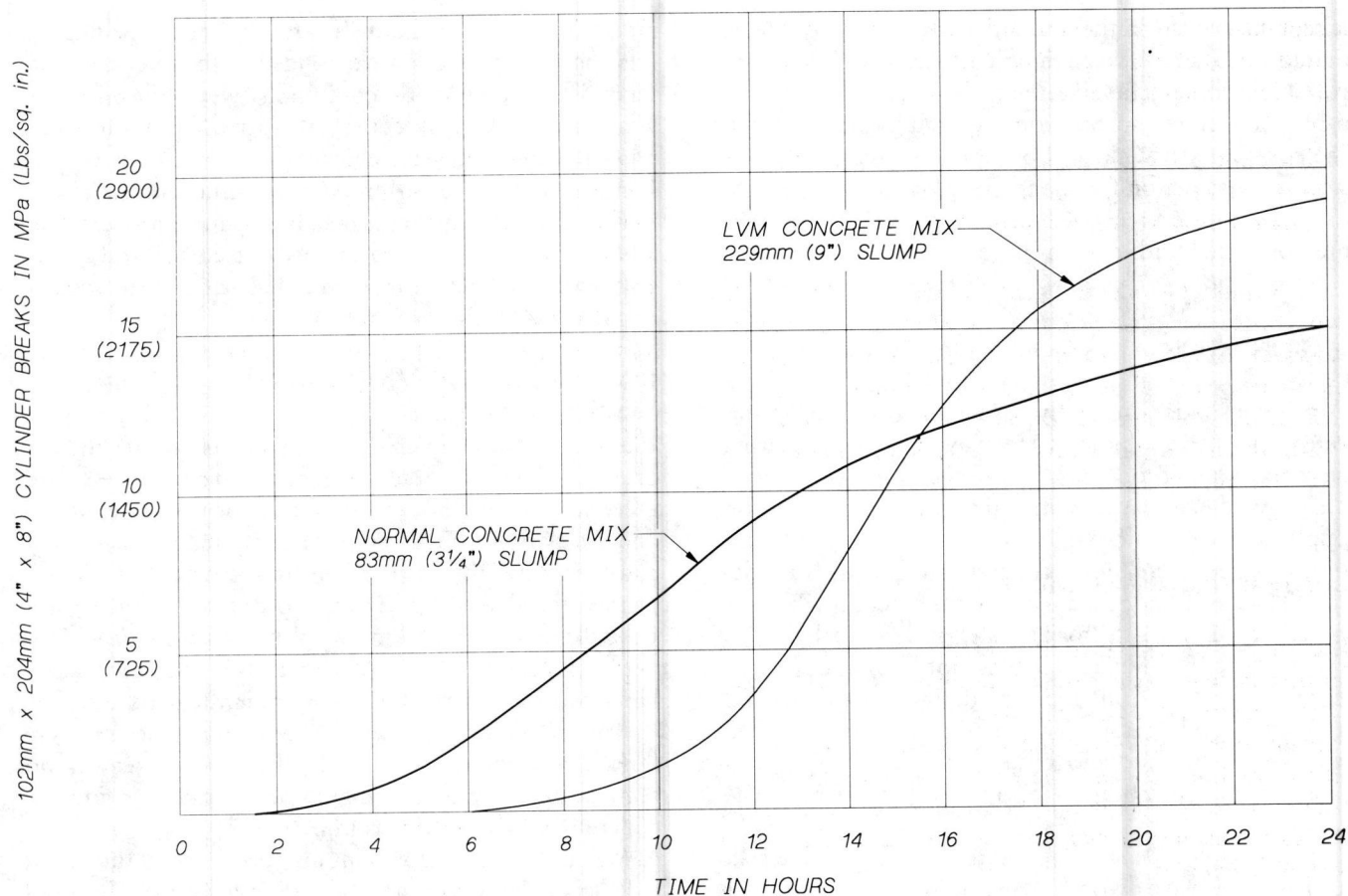


**FIGURE 3** LVM concrete mix initial strength gain.



**FIGURE 4** Completion of bottom slab and erection of wall forms.

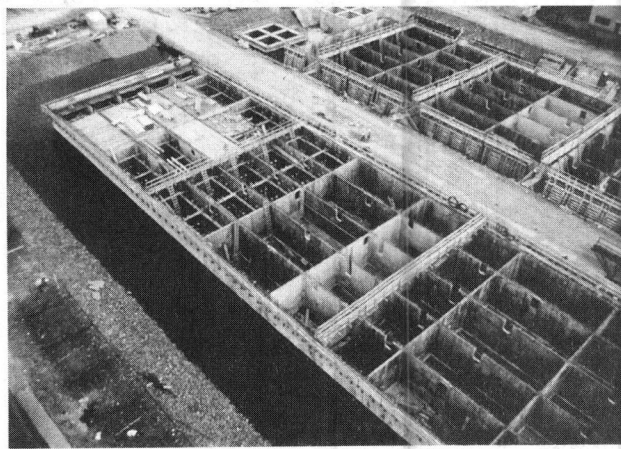


**FIGURE 5** View of pontoon interior with watertight compartments.



being constructed in the graving dock. Each pontoon is divided into small watertight compartments for controlling flooding. The exterior walls were made of cast-in-place concrete construction required by the contract. The contractor had the option of using cast-in-place or precast construction for the interior walls. The contractor chose to use precast elements for the interior walls interconnected with cast-in-place concrete.

### CONSOLIDATION OF CONCRETE

Proper consolidation is key to achieving durable concrete. It was the subject of extensive discussion during the development of project specifications. For silica fume concrete, it was determined that external vibration supplemented by internal vibration was essential to ensure dense concrete and a concrete surface without defects. The contractor used rotary-type external vibrators spaced at 1.2 m (4 ft) horizontally and vertically.

Quantitative information was not available on the design of forms. Forms must be designed to withstand the lateral fluid pressure of concrete and the repeated reversing stresses induced by external vibration and to transmit the vibration in a uniform manner to the concrete.

Steel was the generally preferred forming material, but it is expensive. Wood forms perform adequately if properly designed. The final construction specifications allowed wood, steel, or a combination of the two materials. The contractor was required to design and fabricate the forms to ensure proper consolidation. The test sections provided some needed information on the design of the forms and placement of vibrators.

Wood forms with plywood lining were used for the project. The system performed satisfactorily. However, after three or four cycles of reuse, the wood forms and liners began to show signs of damage and were in need of repair or replacement. Steel forms would have lasted much longer and might be more cost-effective in the long run.

### CURING OF CONCRETE

Silica fume concrete mixes yielded little or no bleed water to the surface, creating a high potential for difficulty in finishing surfaces of flatwork and for plastic shrinkage cracking and short cracks just before final set of the concrete. Fog spraying immediately after the concrete was placed and screeded helped avoid such problems.

Moisture curing of the exposed concrete surface was essential to ensure crack-free and impermeable concrete. The unformed concrete surfaces were fog sprayed im-

mediately and continuously after initial screeding or floating. The surfaces were ponded with water soon after finishing to provide continuous wet curing for not less than 14 days. A concrete relatively free of cracks and other trouble was achieved.

Wall forms were permitted to be removed 72 hr after final set, which was defined as penetration resistance of 3445 kPa (500 psi). Continuous wet curing had to begin within 4 hr after form removal and continue for not less than 14 days.

### PERFORMANCE OF LVM CONCRETE

The contractor had very limited experience with the use of silica fume concrete when the project started, and there was some concern about the concrete's stickiness and workability. The contractor started learning by constructing a mockup section that was representative of the typical work. The mockup gave the contractor a valuable lesson in working with the relatively new high-performance concrete. Subsequently, the contractor built two more test sections to refine the procedure.

The contractor soon discovered that the concrete flowed readily with adequate vibration, there was no segregation despite the high slump, and the finished concrete was relatively trouble-free.

When the contractor went into production, the initial casting cycle of a pontoon took 19 weeks. The contractor had start-up problems and had to learn to work with the new mix. Through constant effort in improving construction techniques and skills, the casting cycles were reduced to 12, 9, and finally 8 weeks. The contractor was pleased with the results. The contractor also benefited from several cost-saving features of the high-performance concrete mix. The finished concrete required very little patching or repair. The high early strength of the concrete enabled posttensioning to be done sooner than with conventional concrete. Part way into the construction the contractor asked to use the high-performance concrete in other parts of the pontoons where normal concrete was specified. The substitution was made with no additional cost to the state. This demonstrated the contractor's satisfaction with the mix and the successful application of high-performance concrete.

Figure 6 shows a completed pair of pontoons arriving at the job site and being maneuvered into position. The concrete was uniformly dense and impermeable. There were very few signs of repair, rework, or patching.

### COST INFORMATION

Concrete suppliers indicated that adding 8 percent silica fume to normal concrete mix would add about \$60/m<sup>3</sup>



FIGURE 6 Pair of pontoons being maneuvered into position.

(\$50/yd<sup>3</sup>). For example, if 440 MPa concrete, including fly ash, cost \$130/m<sup>3</sup> (6,000 psi concrete at \$100/yd<sup>3</sup>), silica fume concrete would cost \$190/m<sup>3</sup> (\$150/yd<sup>3</sup>) delivered to the job site. The contractor would have to add other costs associated with the use of silica fume concrete to arrive at the in-place cost of concrete. On the basis of the average bid prices of the three low bidders, the in-place cost of concrete was \$986/m<sup>3</sup> (\$754/yd<sup>3</sup>). The higher in-place cost reflected the additional care and requirements of working with the high-performance concrete. The test sections added cost to the concrete work but were worth every dollar in improving efficiency and avoiding construction problems. The formwork had to be designed for external vibration and higher form pressures because of the slow initial set of the concrete. The complexity of pontoon construction also added to the cost of concrete. The high average bid prices of the concrete reflected the concerns of the contractors and suppliers in dealing with a relatively new high-performance concrete with silica fume. About 38 000 m<sup>3</sup> (49,600 yd<sup>3</sup>) of concrete were specified for the project.

This information is based on 1991 costs and is included here for general information only. The actual cost will depend on many factors, such as location, complexity of the structure, volume of work, and experience of the suppliers and contractors. The price is expected to drop as more silica fume concrete is used in highway construction.

## CONCLUDING REMARKS

High-performance concrete containing silica fume and fly ash is very cohesive, will not segregate, and has good

workability when properly proportioned. Enhanced with high-range water reducers, the concrete can be placed with a very high slump with no loss in strength or density.

Silica fume content of about 8 percent of total cementitious materials was used in the concrete mix for the project. However, the mix can be adjusted with different proportions of silica fume and fly ash to meet the strength, permeability, and durability requirements of a project. Some cost savings can be realized with mix modifications to meet objectives of the mix and performance demands of the fresh and hardened concrete. Research and development of concrete mixes should be carried out before or during project development to meet the project objectives. The data and findings should be incorporated into the project specifications and made available to the contractor.

The quality of plant mixing equipment, competence of plant personnel, experience with the specialized concrete mixes, commitment to quality, and team effort are necessary for successful development and application of high-performance concrete.

Valuable qualitative and quantitative information can be obtained by constructing test sections of typical



FIGURE 7 New LVM Bridge, on left.

portions of the work. The test sections should be constructed before production to gain experience in rate of pour, form pressures, effectiveness of vibration, and other construction techniques.

High-performance concrete has many applications in bridge construction. Some examples are

- Reinforced and prestressed concrete structures requiring high strength, corrosion resistance, and long-term durability;
- Bridge decks to reduce chloride intrusion;
- Precast, prestressed concrete girders to reduce weight, reduce depth, decrease number of lines of girders, or increase span lengths;
- Overpass structures subject to salt spray from traffic;
- Structures with thin or heavily reinforced walls; and
- Floating and other marine structures.

Figure 7 shows the new LVM Bridge alongside the Third Lake Washington Floating Bridge. The new bridge was completed and opened to traffic on September

12, 1993. The construction of the LVM Bridge has demonstrated that it is feasible and cost-effective to use high-performance concrete in highway structures for which high strength, impermeability, and durability are of prime importance.

#### REFERENCES

1. Murrow, L. V. A Concrete Pontoon Bridge To Solve Washington Highway Location Problem. *Western Construction News*, July 1938.
2. Lwin, M. M. Floating Bridges—Solution to a Difficult Terrain. *Proc., International Conference on Transportation Facilities Through Difficult Terrain*, Aspen, Colo., Aug. 1993.
3. Nichols, C. C. Construction and Performance of Hood Canal Floating Bridge. *ACI Publication SP-8*, American Concrete Institute, 1962.
4. Gloyd, C. S., and M. M. Lwin. Rebuilding the Hood Canal Floating Bridge. *Concrete International*, June 1984.
5. Lwin, M. M. The Lacey V. Murrow Floating Bridge, USA. *Structural Engineering International*, International Association for Bridge and Structural Engineering, Aug. 1993.

# Premature Cracking of Concrete Bridge Decks: Causes and Methods of Prevention

---

Ron Purvis and Khossrow Babaei, *Wilbur Smith Associates*

Nalin Udani and Abid Qanbari, *Pennsylvania Department of Transportation*

William Williams, *Federal Highway Administration*

Newly constructed bridge decks were examined in order to identify the factors that cause cracking and ways in which the cracking might be reduced. The research included field surveys that showed transverse cracking to be the prevalent type associated with new bridges. Factors potentially influencing transverse cracking were studied and compared with the design and construction practice of the Pennsylvania Department of Transportation. Preliminary findings indicated that the main cause of transverse cracking is the shrinkage of hardened concrete. Further study and tests provided conclusive evidence of thermal shrinkage and drying shrinkage. Correlation of the cracking performance of several newly constructed decks with the shrinkage actually measured in the deck concrete showed that transverse cracking occurred where the shrinkage measurements were high. The findings further indicated that the type of aggregate used in the mix was a major factor associated with shrinkage cracking. Thermal shrinkage is affected by the amount of temperature change during the curing period as well as the coefficient of thermal expansion of concrete, which is mainly aggregate-related. It was noted that thermal shrinkage and cracking were especially severe in concretes that were subjected to large temperature changes associated with cold-weather curing. The research recommends the maximum acceptable

shrinkage, implementation of a shrinkage verification test for use in approving mix designs, and temperature control during cold-weather curing.

Increased cracking has been observed in recent years in newly constructed concrete highway bridge decks in Pennsylvania. Premature cracking is a concern, because the Pennsylvania Department of Transportation's (PADOT's) experience has shown that cracks can cause steel to corrode and concrete to deteriorate, resulting in decreased deck service life. Prevention of premature cracks can provide longer deck lives and lower maintenance costs. A PADOT research project was initiated with the following objectives:

1. Identify factors that may cause premature concrete cracking,
2. Relate factors to PADOT bridge deck cracking, and
3. Recommend changes to reduce the cracking.

Initially, a literature search was performed and a questionnaire distributed to determine the extent of the problem and if others had identified causes or solutions.

This paper will focus on the final stage of the work, which was conducted in three phases:

1. Examination of existing bridge decks, so that the types, significance, and causes of cracking, as well as methods to minimize it, could be determined (1).
2. Observation of bridge deck construction to identify specific construction procedures contributing to cracking, if any (2).
3. Performance of laboratory experiments to verify or modify the research findings (3).

## PHASE 1: EXAMINATION OF EXISTING BRIDGE DECKS

### Walk-By Surveys

The research team conducted visual walk-by surveys of 111 bridge decks that were selected by superstructure type from a group of 623 bridges to represent bridges built in Pennsylvania no more than 5 years before the surveys. The following number were selected from each type to represent this bridge group: 51 prestressed concrete I-beam bridges, 41 prestressed concrete spread box-beam bridges, and 19 steel-beam bridges. To the extent possible, various types of cracks were identified and their extent was quantified. Transverse cracking was identified as the prevalent type.

Transverse cracking occurred both in the positive and negative moment regions, which indicated that the cracking was not necessarily a load-related problem. The nature of the transverse cracks observed indicated that their cause was most likely shrinkage in hardened concrete and restraint provided by longitudinal beams. Concrete shrinkage is caused by the loss of heat of hydration and cooling during the curing period (short-term thermal shrinkage) and by the loss of mix water after curing and during the service (long-term drying shrinkage).

### In-Depth Surveys

Of the 111 bridge decks, 12 were selected for in-depth surveys. The bridges were selected so as to include transverse crack intensities ranging from none to 87 m of cracks per 100 m<sup>2</sup> (265 ft/1,000 ft<sup>2</sup>) of deck. The types selected also represent the majority of bridges being built in Pennsylvania. The in-depth surveys included crack mapping, crack width measurement, rebar location and depth survey (pachometer survey), and concrete coring. Background design and construction records of the 12 bridge decks were also obtained and reviewed as part of the in-depth surveys.

### Field Observations

The following crack characteristics were observed during the in-depth field surveys:

- Almost all transverse cracks followed the line of the top transverse bars, regardless of the type of superstructure. This observation was revealed by pachometer surveys and verified by coring.
- Coring concrete showed that transverse cracks' depth extended to the level of the top transverse bars and beyond.
- The width of transverse cracks was generally narrow or medium, with the majority being medium.

0.1 mm < narrow < 0.25 mm (0.004 in.

< narrow < 0.01 in.)

0.25 mm < medium < 0.76 mm (0.01 in.

< medium < 0.03 in.)

[According to ACI Report 224 (4) Table 4.1, cracks wider than 0.18 mm (0.007 in.) contribute to deterioration of concrete and corrosion of reinforcing steel in the presence of deicing chemicals.]

- The average depth of cover for the top transverse bars ranged from 70 to 76 mm (2.75 to 3.00 in.). The nominal depth was 63.5 mm (2.5 in.). Thicker cover depths cause wider cracks, since the longitudinal crack control reinforcement is embedded too deeply in the concrete.

- Concrete cores examination showed that transverse cracks often intersected coarse aggregate particles. This indicated that the cracks occurred in the hardened concrete as opposed to the plastic concrete and that the cause of cracking was most likely drying shrinkage and thermal shrinkage, and not factors such as plastic shrinkage (caused by surface evaporation prior to curing) or settlement of plastic concrete between the top transverse bars.

- Concrete settlement cracking is not likely to have occurred in the bridge decks examined because their bar cover was relatively deep and their slump was relatively low [see *NCHRP Report 297: Evaluation of Bridge Deck Protective Strategies* (5)]. The cover depth was from 70 to 76 mm (2.75 to 3.0 in.) and slump was 51 to 102 mm (2 to 4 in.). However, vertical planes of weakness directly above the transverse bars are present because of the initial settlement-induced strains in the plastic concrete in that region. Later, transverse shrinkage cracking would form in the weakened concrete directly above the bar, as noted in the field surveys.

### *Estimate of Bridge Deck Shrinkage*

Total concrete shrinkage strain (drying shrinkage plus thermal shrinkage) was estimated roughly for each bridge deck included in the in-depth surveys. To do this, the number of transverse cracks in each span was multiplied by the crack width and the product was divided by the length of the span. The number of transverse cracks for each span was obtained from the crack maps. An average crack width of 0.25 mm (0.01 in.) was assumed on the basis of the crack surveys. The shrinkages estimated for the spans were then averaged to represent the bridge. In continuous bridges, estimating shrinkage was limited to positive moment areas to eliminate the effects of negative moments on cracking.

It was found, analytically, that a residual long-term shrinkage of about 400 microstrain would be needed to initiate cracking. To find the residual shrinkage strain (tensile strain), the tensile strength was divided by the modulus of elasticity. Since shrinkage-induced tension is not an instantaneous phenomenon, an "effective" modulus of elasticity was used. The effective modulus of elasticity was the instantaneous modulus of elasticity divided by the sum of one plus the creep factor. The creep factor was found from the information available in ACI Report 209 (6). A creep factor of 2.5 was used to determine the residual long-term shrinkage. Detailed information is provided elsewhere (2, Appendix D). The residual shrinkage was added to the shrinkage estimated from the crack maps. On the basis of field data gathered in the second phase of the study (see Phase 2), a thermal shrinkage of 150 microstrain was assumed for all 12 decks. The thermal shrinkage was subtracted from the shrinkage estimated to approximate the deck drying shrinkage.

The deck drying shrinkage was multiplied by 2.5 to represent shrinkage of standard laboratory specimens. Laboratory specimens [ $76 \times 76 \times 254$  mm ( $3 \times 3 \times 10$  in.)] have a much lower volume-to-surface ratio than a typical bridge deck slab, and drying shrinkage increases with a decrease in the volume-to-surface ratio [ACI Report 209 (6)]. The specimen drying shrinkage varied from 625 to 1,228 microstrain, a shrinkage difference of approximately 600 microstrain.

Next, background design and construction information for the 12 bridges was reviewed to identify the potential factors contributing to the range of shrinkage estimated.

### *Factors Affecting Drying Shrinkage*

#### *Mix Water*

The content of concrete mix water affects drying shrinkage. The more water in the mix, the more evaporation

after curing and consequently more drying shrinkage to be expected. Information from ACI Report 224 (4) shows that for a typical concrete specimen,  $1309 \text{ N/m}^3$  ( $225 \text{ lb/yd}^3$ ) water content results in about 300 microstrain drying shrinkage, and the drying shrinkage increases at a rate of about 0.5 microstrain per  $1 \text{ N/m}^3$  ( $3 \text{ microstrain per } 1 \text{ lb/yd}^3$ ) increase in water content.

For the 12 bridges studied, the mix water content reported varied from  $1552$  to  $1698 \text{ N/m}^3$  ( $267$  to  $292 \text{ lb/yd}^3$ ), a difference of  $146 \text{ N/m}^3$  ( $25 \text{ lb/yd}^3$ ). That variation in water content increases the drying shrinkage by about 75 microstrain. This figure is only 13 percent of the difference between the minimum and maximum shrinkage determined for the 12 bridge decks in the study (i.e., 600 microstrain). Thus, it appeared that concrete mix water content was not the prime cause of the significant difference in the performance of the bridge decks with respect to transverse cracking.

#### *Aggregate*

Aggregate contributes to drying shrinkage of concrete in two quite different ways: first, certain aggregates need more water in the mix to produce the desired slump and workability, and the extra water increases shrinkage; and second, certain aggregates yield to the pressure from the shrinking paste and do not provide sufficient restraint against the shrinkage of the paste.

1. *Aggregates demanding water:* aggregates that need more water in the mix to produce the same workability have smaller coarse aggregate, rough texture, or flat and elongated particles. However, since the water content of the concrete is measured and controlled through its maximum allowable water-cement ratio, this characteristic of aggregate cannot unexpectedly increase shrinkage of concrete.

2. *Aggregates yielding to pressure from shrinkage:* aggregates that yield to the pressure from the shrinking paste are soft and have low stiffness and high compressibility. Absorption of an aggregate (coarse and fine) is a measure of its porosity, and the porosity influences the stiffness and compressibility. Generally, concretes made with high absorption aggregates tend to be more compressible and thus yield higher shrinkages. Also, aggregates with high absorption may themselves shrink an appreciable amount upon drying.

The information provided in ACI Report 224 (4) shows that the drying shrinkage can increase from 320 to 1,160 microstrain (about a 250 percent increase) when the aggregate absorption is increased from 0.3 to 5.0 percent. Quartz, limestone, dolomite, granite, feldspar, and some basalt are generally classified as aggre-



gates that produce low shrinkage. Sandstone, slate, trap rock, and some types of basalt aggregates often produce high shrinkage concretes.

For the 12 bridge decks studied in the project, the coarse aggregate absorption varied from 0.34 percent (dolomite) to 1.17 percent (gravel), and the fine aggregate absorption varied from 0.43 percent (dolomite) to 1.97 percent (gravel). That variation in the absorption corresponds to an increase of at least about 300 microstrain in drying shrinkage on the basis of the limited information provided by ACI Report 224 (4). That figure is 50 percent of the difference between the maximum and minimum shrinkage noted in the 12 bridge decks studied (i.e., 600 microstrain). Thus, it appeared that aggregate softness or hardness had an important role in the performance of the bridge decks with respect to transverse cracking.

### Concept of Thermal Shrinkage

Concrete temperature rises during the initial hydration and curing process because of the release of heat of hydration. This initial temperature rise and expansion induces no residual compressive stresses in the concrete in changing from a plastic state to a solid state. This is because of the extremely low modulus of elasticity of the concrete at this plastic-to-solid state. When the concrete reaches its peak temperature, it has also solidified. Subsequently, the hardened concrete begins to cool to the ambient temperature.

During the cooling process, longitudinal beams restrain the deck shrinkage. This phenomenon in turn will cause tensile stresses and transverse cracking in the deck. The magnitude of thermal shrinkage in the deck depends on the difference between the peak concrete temperature and the temperature of supporting beams at the time of peak temperature. The temperature of supporting beams is usually equal to the ambient temperature, unless the deck is heated underneath as part of cold-weather curing.

The difference in deck and beam temperatures contributes to thermal shrinkage at a rate of 6.8 to 11.9 microstrain per degree Celsius (3.8 to 6.6 microstrain per degree Fahrenheit) depending on the type of aggregate used [average of 9.9 microstrain per degree Celsius (5.5 microstrain per degree Fahrenheit) (7)]. Typically, quartz and sandstone have very high coefficients of thermal expansion, and limestone has a very low coefficient of thermal expansion.

Unlike deck drying shrinkage, which may take over a year, thermal shrinkage affects the concrete in a short period (a few days); thus concrete creep properties cannot be fully used to relax the concrete and mitigate cracking. As a result, the shrinkage required to trigger

cracking will be less than that required to trigger cracking under drying shrinkage. Analytical work found that 228 microstrain thermal shrinkage would be needed to initiate cracking. The analytical work was similar to that for residual long-term shrinkage, except that a creep factor of 1 was assumed. Detailed information is given elsewhere (2, Appendix D).

### Factors Affecting Thermal Shrinkage

Thermal shrinkage increases as the rise in concrete temperature during curing increases. The heat generated during the hydration and the subsequent rise in temperature increase with increase in cement content, cement fineness (ASTM C115 or C204), or 28-day cement heat of hydration (ASTM C186).

ACI Report 207.2 (8) provides a procedure to estimate the rise in concrete temperature on the basis of the factors discussed. An attempt was made to quantify the impact of the factors discussed on the thermal shrinkage of the decks selected. The cement content of the 12 concrete mixes studied (Type I cement) varied from 377 to 418 kg/m<sup>3</sup> (635 to 705 lb/yd<sup>3</sup>). However, no information was available on the fineness and 28-day heat of hydration of these cements.

Two additional factors were unaccounted for in the ACI 207.2 procedure. First, retarder admixtures were used in the concrete. The authors' field observation in the second phase of the research was that depending on the dosage of the retarder, the rise in concrete temperature during curing may be almost nil. Second, the field practice in hot weather is to lower the placing temperature of the concrete by using ice in the mix. Doing so will also reduce the rise in concrete temperature.

Because of these reasons, estimating thermal shrinkage was not possible. However, on the basis of the field data obtained in the second phase of the study, it is reasonable to assume that the difference between the peak concrete temperature and ambient temperature varied from 0 to 17°C (0 to 31°F) for the 12 bridge decks studied. Those figures correspond to a difference of 170 microstrain deck thermal shrinkage, considering an average thermal coefficient of expansion of 9.9 microstrain per degree Celsius (5.5 microstrain per degree Fahrenheit) for concrete.

That amount of thermal shrinkage is relatively high and is 27 percent of the difference between the maximum and minimum shrinkage noted in the 12 bridge decks studied (i.e., 600 microstrain). Although 170-microstrain thermal shrinkage is not sufficient to initiate cracking in the concrete when the concrete is cooled gradually (less than the threshold of 228 microstrain), it is later superimposed on the drying shrinkage.

### *Thermal Shrinkage Caused by Cold-Weather Curing*

Further investigations of the background information of the selected existing decks revealed that two of the sample decks were subjected to special cold-weather curing conditions that involved heating or insulating the concrete or both. Cold-weather curing can contribute greatly to thermal shrinkage and cracking of concrete.

#### Springfield Road Bridge

Springfield Road Bridge is a two-span continuous bridge supported by prestressed concrete I-beams. Its deck had the highest level of transverse cracking among the 12 decks studied. Its cracking was measured as 87 m of transverse cracks per 100 m<sup>2</sup> (265 ft/1,000 ft<sup>2</sup>) of deck area, equivalent to full-width cracks spaced about 1.2 m (4 ft) apart.

Because of the cold weather during the placing and curing of the concrete, the deck was heated underneath. When the concrete placement began, the ambient temperature was 1°C (35°F). At that time the temperature of the metal deck forms was 10°C (50°F) as a result the deck's being heated underneath overnight. Upon placement, the concrete was covered and insulated with blankets and straw.

One day after placing the concrete, the surface temperature of the concrete was recorded as 48°C (118°F). Since the concrete was insulated, it can be assumed that the surface temperature recorded is the same as the peak concrete temperature. However, the temperature of the supporting concrete beams in the enclosed heated area was the same as the temperature of the metal deck forms [i.e., 10°C (50°F)]. This condition translates to a difference of 38°C (68°F) [48°C – 10°C (118°F – 50°F)] between the peak deck temperature and the temperature of the supporting beams. Interestingly, a quartz aggregate, which has a high coefficient of thermal expansion, was used in this concrete. Assuming a thermal coefficient of expansion of 10.8 microstrain per degree Celsius (6.0 microstrain per degree Fahrenheit) for this concrete, its thermal shrinkage is estimated as at least 408 microstrain.

As discussed previously, a thermal shrinkage strain of about 228 microstrain may trigger cracking in the concrete in its early ages (gradual cooling). If crack widths are assumed to be 0.25 mm (0.01 in.), the thermal shrinkage in excess of the cracking threshold shrinkage (i.e., 408 – 228 = 180 microstrain) is capable of developing transverse cracks 1.5 m (5 ft) apart, which is in agreement with the overall crack pattern noted in the deck.

#### SR 0079 Bridge

SR 0079 Bridge is an eight-span continuous bridge supported by steel girders. The span with the highest level of cracking had 27 m of cracks per 100 m<sup>2</sup> (82 ft/1,000 ft<sup>2</sup>), equivalent to full-width cracks spaced about 3.7 m (12 ft) apart.

Upon placement, the deck was insulated with blankets because of the cold weather. The deck, however, was not heated underneath. The maximum surface temperature of the deck was 28°C (82°F) a day after placement. Since the concrete was insulated, it can be assumed that the surface temperature recorded is the same as the peak concrete temperature.

During concrete placement, the minimum day time temperature was 4°C (40°F). The peak concrete temperature most likely occurred at night (8 to 12 hr after placement). The night temperature may be assumed to be at least 3°C (5°F) less than the minimum day temperature, or 1°C (35°F). This temperature is almost the same as the temperature of the steel beams at the time of the peak concrete temperature. This condition translates to a maximum difference of 26°C (47°F) [28°C – 2°C (82°F – 35°F)] between the peak deck temperature and the temperature of the supporting beams. Assuming the average thermal coefficient of expansion of 9.9 microstrain per degree Celsius (5.5 microstrain per degree Fahrenheit) for this concrete, the thermal shrinkage is estimated at 259 microstrain.

A thermal shrinkage strain of only 228 microstrain may trigger cracking in the concrete in its early ages. If crack widths are assumed to be 0.25 mm (0.01 in.), the thermal shrinkage in excess of the crack threshold shrinkage (i.e., 259 – 228 = 31 microstrain) is capable of developing transverse cracks 8 m (26 ft) apart. Although the actual cracking is more intense than the cracking estimated, in time drying shrinkage can increase the intensity of cracking.

### **PHASE 2: OBSERVATION OF BRIDGE DECK CONSTRUCTION**

#### **Field Observations**

The second phase of the research involved observing bridge deck construction to identify procedures contributing to shrinkage and cracking. Eight concrete bridge deck constructions were observed. All constructions were performed in late spring and summer. Construction procedures were monitored during the observations for any evidence that the procedures may contribute to cracking in concrete. The general observation was that the construction procedures would not affect the per-



formance of the eight sites observed with respect to cracking.

### Shrinkage of Field Concrete

Observations of bridge deck construction provided an opportunity to determine shrinkage. During the observations, concrete temperature was recorded during curing to determine the thermal shrinkage. The concrete used in the observed deck constructions was also sampled and tested in a laboratory to determine the drying shrinkage.

#### Thermal Shrinkage

The internal temperature of concrete was recorded during curing at each bridge deck construction site up to 8.5 hr after casting. Concrete thermometers were inserted in the concrete for this purpose. The concrete curing temperature (peak temperature) for each construction is presented in Table 1. The difference between the concrete curing temperature and ambient temperature (recorded at the time that the concrete temperature was recorded) ranged from 0 to 17°C (31°F). The lower end of the range corresponded to concretes that were highly dosed with a retarder: the retarder slows the cement hydration process, thus reducing the rate of heat of hydration generated and temperature rise.

The temperature of the beams supporting the decks was assumed to be the same as the ambient temperature, since the air surrounding the beams was not artificially heated. Therefore, the difference between concrete curing temperature and beam temperature would also range from 0 to 17°C (31°F). That differential temperature contributes to thermal shrinkage of concrete at an average rate of 9.9 microstrain per degree Celsius (5.5 microstrain per degree Fahrenheit) (7). Accordingly, the thermal shrinkage for each bridge deck was determined and is presented in Table 1; it ranged from 0 to 170 microstrain.

#### Drying Shrinkage

Concrete was sampled at each construction site for shrinkage tests. Each sample consisted of three unrestrained concrete specimens 76 × 76 × 254 mm (3 × 3 × 10 in.). The shrinkage specimens were taken to the laboratory and cured for 7 days, the same as the bridge decks. Twenty-four hours after casting the specimens were demolded and specimen lengths were measured; specimen lengths were measured up to 112 days after casting. The length measurement was performed in accordance with ASTM C157/C878, and shrinkage was determined accordingly. The values of specimen drying shrinkage (corresponding to 112 days) are given in Table 1; they ranged from 480 to 1,450 microstrain.

TABLE 1 Thermal and Drying Shrinkage Information for Eight Construction Sites

WSA Br. No.	1	2	3	4	5	6	7	8
SR No.	0092	4021	0087	0108	1050	0079	0234	2007
District & County	4 Wyoming	8 York	4 Wyoming	10 Butler	12 Westmor.	12 Greene	8 Adams	10 Jefferson
Weather	Overcast Clear	Clear	P. Cloud	P. Cloud	Cloud Clear	Clear P. Cloud	Overcast	P. Cloud
Air Temp., °C (°F)	16 - 33 (60 - 92)	23 - 36 (74-96)	13 - 26 (55 - 78)	21 - 27 (70-80)	23 - 34 (74-94)	17 - 27 (63-81)	24 - 35 (76-95)	20 - 33 (68 - 92)
Concrete Curing Temp. °C (°F)	38 (100)	31 (88)	39 (102)	27 (80)	40 (104)	44 (111)	37 (99)	44 (112)
Ambient Temp. <sup>1</sup> , °C (°F)	26 (78)	33 (92)	24 (75)	27 (80)	34 (94)	27 (80)	35 (95)	33 (92)
Assumed Beam Temp. <sup>1</sup> , °C (°F)	26 (78)	33 (92)	24 (75)	27 (80)	34 (94)	27 (80)	35 (95)	33 (92)
Differential Conc./Beam Temp. °C (°F)	38-26=12 (100-78= 22)	31-33= -2 (88-92= -4)	39-24=15 (102-75= 27)	27- 27=0 (80- 80=0)	40-34=6 (104-94= 10)	44-27=17 (111-80= 31)	37- 35=2 (99- 95=4)	44-33=11 (112-92= 20)
Deck <sup>2</sup> Thermal Shrinkage, Micro-Strain	22x5.5= 121	-4x5.5= -22	27x 5.5= 148	0x5.5= 0	10x 5.5= 55	31x 5.5= 170	4x 5.5= 22	20x 5.5= 110
Specimen Drying Shrinkage, Micro-Strain	905	533	1450	508	480	805	710	867
Deck Drying Shrinkage, Micro-Strain	905: 2.5= 362	533:2.5 =213	1450: 2.5= 580	508:2.5 =203	480: 2.5= 192	805:2.5= 322	710:2.5 =284	867: 2.5= 347

1: At the time when concrete cure temperature was recorded.

2: Since temperatures were recorded in °F the average coefficient of thermal expansion of 5.5 micro-strain per °F is used (7).

Deck drying shrinkage, however, is much less than specimen drying shrinkage because of the lower volume-to-surface ratio of the specimen. Drying shrinkage of the deck may approximately be assumed  $\frac{1}{2}$  times the drying shrinkage of the specimen considering the difference in the volume-to-surface ratio (6). The values of deck drying shrinkage are presented in Table 1 for the eight construction sites.

### Relationship Between Deck Shrinkage and Deck Cracking

The eight newly constructed bridge decks were surveyed for crack occurrence after construction; the results are presented in Table 2. The survey revealed cracks in four bridge decks.

As discussed previously, it was found on the basis of analytical work that a thermal shrinkage strain of 228 microstrain may initiate cracking in the concrete in its early ages (gradual cooling). It was also found that for long-term shrinkage (i.e., thermal shrinkage plus drying shrinkage), the cracking threshold shrinkage strain would be 400 microstrain, since concrete creep properties would be further used. Detailed information is provided elsewhere (2).

By definition, the thermal shrinkage in excess of the cracking threshold strain of 228 microstrain is called effective thermal shrinkage. Effective thermal shrinkage is capable of developing transverse cracks in the deck in its early ages (when the concrete cools during curing). The authors have estimated the amount of effective thermal shrinkage for the eight newly constructed decks in Table 3. As noted in the table, the effective thermal shrinkage of the eight decks is 0, since the thermal shrinkage is always less than the cracking threshold of 228 microstrain. All of the thermal shrinkage, thus, will be in the form of residual shrinkage and will be added to the long-term drying shrinkage later.

By definition, the long-term shrinkage in excess of the cracking threshold strain of 400 microstrain is called effective long-term shrinkage. Effective long-term shrinkage is capable of developing transverse cracks in the deck within about 1 year after the construction. The authors have estimated the amount of effective long-term shrinkage for the eight newly constructed bridge decks in Table 3. On the basis of the effective long-term shrinkage estimated, the average transverse crack spacing for each bridge deck has been predicted in Table 3. A crack width of 0.25 mm (0.01 in.) has been assumed for this purpose.

As noted in Table 3, the authors have predicted the development of transverse cracks in four decks and the absence of transverse cracks in four decks on the basis of the shrinkage determined for each bridge deck. A

visit to the eight decks validated the prediction of transverse cracking as shown in Table 3. These results further support shrinkage as the prime cause of transverse cracking in bridge decks.

On the basis of the crack prediction procedure, the crack spacing will exceed 9 m (30 ft) if the 4-month specimen drying shrinkage is kept below 700 microstrain [equivalent to 400 microstrain 28-day shrinkage (6) provided the thermal shrinkage is limited to 150 microstrain] [corresponding to a maximum concrete temperature rise of 12°C (22°F)]. Note that the specimens are unrestrained and  $76 \times 76 \times 254$  mm ( $3 \times 3 \times 10$  in.). The information in Tables 2 and 3 supports this statement.

## PHASE 3: LABORATORY EXPERIMENTS

### Experiment Design

The laboratory experiments focus on examining the effects of the aggregate source, cement source, and fly ash on shrinkage. The experiments were designed using the types of aggregate, cement, and fly ash typically used in Pennsylvania. Accordingly, concrete mixes were produced and tested for temperature rise during curing (indication of thermal shrinkage), and they were tested for drying shrinkage.

Three  $76 \times 76 \times 254$ -mm ( $3 \times 3 \times 10$ -in.) unrestrained shrinkage specimens were produced from each concrete mix designed. Drying shrinkage was measured up to 4 months using applicable ASTM C157/C878 provisions. For each mix, concrete temperature was recorded during curing while the concrete was in an insulated  $152 \times 305$ -mm ( $6 \times 12$ -in.) steel cylinder.

It is important to note that the results reported here are all based on limited experiments. They indicate only the potential for a shrinkage increase, or decrease, when aggregate, cement, or fly ash sources and types are varied. The results are not sufficient to be used to approve, or reject, certain products.

### Effect of Aggregate Type on Shrinkage

Table 4 gives the concrete drying shrinkage for four types of aggregate that were selected on the basis of their mineralogy. As the table shows, when sandstone coarse aggregate (Mix 1.4) was substituted for dolomite coarse aggregate (Mix 1.2) in the concrete mix, drying shrinkage increased from 420 to 1,012 microstrain (i.e., 141 percent increase).

Unlike dolomite, sandstone, by nature, is a soft aggregate with low stiffness and high compressibility. Therefore, it yields to the pressure from the shrinking

TABLE 2 Crack Information for Eight Construction Sites

WSA Br. No.	1	2	3	4	5	6	7	8
SR No.	0092	4021	0087	0108	1050	0079	0234	2007
District & County	4 Wyoming	8 York	4 Wyoming	10 Butler	12 Westmor.	12 Greene	8 Adams	10 Jefferson
Br. Type	Steel I Smp. & Cont.	SPD Box Cont.	Steel I Cont.	ADJ Box Simple	SPD Box Cont.	Steel I Smp. & Cont.	SPD Box Smp. & Cont.	Steel I Simple
No. of Spans	1 Smp. & 4 Cont.	2	2	1	2	1 Smp. & 7 Cont.	1 Smp. & 2 Cont.	1
Pour Length & Width, m (ft)	42.7x14.6 (140x48)	11.3x9.8 (37x32)	19.8x11.0 (65x36)	31.1x4.9 (102x16)	2@ 18.3x9.8 (60x32)	22.6/23.8/26.8 x11.3 (74/78/88x37)	19.8x11.6 (65x38)	42.7x9.8 (140x32)
Moment at Pour Location	Positive Moment	Positive Moment	Positive Moment	Positive Moment	Positive Moment	Positive Moment	Positive Moment	Positive Moment
Ave. Trans. <sup>1</sup> Crack Spacing of Pour Observed	2.1 m (7 ft)	None	2.1 m (7 ft)	None	None	5.8m/4.9m/None (19ft/16ft/None)	None	21 m (70 ft)
Age of Pour when observed	12 to 14 months	12 to 14 months	12 to 14 months	12 to 14 months	12 to 14 months	12 to 14 months	12 to 14 months	12 to 14 months

1: Determined by dividing the pour length by the number of cracks observed plus one.

TABLE 3 Comparison of Predicted and Observed Cracks for Eight Newly Constructed Bridge Decks

WSA Br. No.	1	2	3	4	5	6	7	8
SR No.	0092	4021	0087	0108	1050	0079	0234	2007
District & County	4 Wyoming	8 York	4, Wyoming	10 Butler	12, Westmor	12 Greene	8 Adams	10, Jefferson
Deck <sup>1</sup> Thermal Shrinkage, Micro-Strain	121	-22	148	0	55	170	22	110
"Effective" Thermal Shrinkage, Micro-Strain	121-228=0	-22-228=0	148-228=0	0-228=0	55-228=0	170-228=0	22-228=0	110-228=0
Residual Thermal Shrinkage, Micro-Strain	121	-22	148	0	55	170	22	110
Deck Drying <sup>1</sup> Shrinkage, Micro-Strain	362	213	580	203	192	322	284	347
"Effective" Long Term Shrinkage, Micro-Strain	121+362-400=83	-22+213-400=0	148+580-400=328	0+203-400=0	55+192-400=0	170+322-400=92	22+284-400=0	110+347-400=57
Predicted <sup>2</sup> Crack Spacing .25mm width (0.01"width)	3 m (10 ft)	None	0.9 m (3 ft)	None	None	2.7 m (9 ft)	None	4.6 m (15 ft)
Observed <sup>3</sup> Average Crack Spacing	2.1 m (7 ft)	None	2.1 m (7 ft)	None	None	5.8m/4.9m/None (19ft/16ft/None)	None	21 m (70 ft)

1: From Table 3.

2: Crack spacing in ft =  $833.33 \times 10^{-6} / \text{"Effective Long-Term Shrinkage Strain, micro-strain"}$

3: From Table 4.

TABLE 4 Effects of Aggregate Type on Shrinkage

Mix No.	1.1	1.2 <sup>1</sup>	1.3 <sup>1</sup>	1.4 <sup>1</sup>
Cement Content, kg/m <sup>3</sup> (lb/y <sup>3</sup> )	418 (705)	418 (705)	418(705)	418(705)
Cement Source	Hercules Cement (Type I), Stockertown, PA			
Water Content, kg/m <sup>3</sup> (lb/y <sup>3</sup> )	172 (290)	172 (290)	172 (290)	172 (290)
Fine Aggr. Content, kg/m <sup>3</sup> (lb/y <sup>3</sup> ) SSD	601 (1013)	635 (1070)	592 (997)	578 (975)
Fine Aggregate Source	Honeyhole Sand & Gravel, Hazleton, PA (Gravel)	New Enterprise Stone & Lime, New Enterprise, PA (Dolomite)	Dravo Basic Materials, Pittsburgh, PA (Gravel)	Glacial S&G, Tarrtown Hill (Type A) (Gravel)
Fine Aggregate Absorption	1.42%	0.51%	1.34%	2.10%
Fine Aggregate S.G.	2.65	2.80	2.61	2.55
Coarse Aggr. Content, kg/m <sup>3</sup> (lb/y <sup>3</sup> ) SSD	1082 (1824)	1152 (1941)	1054 (1776)	1087 (1831)
Coarse Aggregate Source	Honeyhole Sand & Gravel, Hazleton, PA (Gravel)	New Enterprise Stone & Lime, New Enterprise, PA (Dolomite)	Dravo Basic Materials, Pittsburgh, PA (Gravel)	State Aggregates Inc., Clifford, PA (Sandstone)
Coarse Aggregate Absorption	1.17%	0.25%	2.17%	1.61%
Coarse Aggregate S.G.	2.65	2.82	2.58	2.66
Air Admixture	Yes	Yes	Yes	Yes
Water Reducer	No	No	No	No
Retarder	Yes	Yes	Yes	Yes
Four-Month Shrinkage, <sup>2</sup> micro-strain	792	420	922	1012

1: Same as Mix 1.1, Except Different Aggregate Source

2: Unrestrained Specimens; Applicable ASTM C157/C878 Provisions.

cement paste and results in higher concrete shrinkage. Absorption of an aggregate is a measure of its porosity, and porosity influences stiffness and compressibility. Concretes made with high absorption aggregates tend to be more compressible and thus yield higher shrinkages. The absorption of the sandstone used in the experiment was 1.6 percent, whereas the absorption of the dolomite was 0.25 percent (Table 4, coarse aggregates).

Also note that the absorption of the fine aggregate used with the sandstone coarse aggregate (Mix 1.4, 2.10 percent) is much higher than the absorptoin of the fine aggregate used with the dolomite coarse aggregate (Mix 1.2, 0.51 percent). Soft fine aggregates also contribute to drying shrinkage, but not as much as soft coarse aggregates. The fine aggregate with a lower absorption is dolomite. The fine aggregate with a higher absorption is designated gravel (as distinguished from crushed stone). Gravels need petrographic examinations to identify their predominant mineral.

Table 4 also compares the drying shrinkage of two mixes with that of different types of gravel (Mixes 1.1 and 1.3). It is seen that the mix with the higher absorption gravel (Mix 1.3, coarse aggregate, 2.17 percent) has gained more shrinkage than the mix with the lower absorption gravel (Mix 1.1, coarse aggregate, 1.17 percent). Note that the absorption of coarse aggregate is the governing factor in this case, since the absorption

of fine aggregate does not change significantly. Drying shrinkage increased from 792 to 922 microstrain (i.e., 16 percent), when the higher-absorption gravel was used.

For mixes with different gravel (i.e., Mixes 1.1 and 1.3), the effect of aggregate absorption on drying shrinkage is not as pronounced as in the case of the mixes with sandstone and dolomite (i.e., Mixes 1.2 and 1.4). This indicates that aggregate absorption reflects the softness or hardness of the aggregate, but a clear relation may not exist. Thus, there may be exceptions in which an aggregate with a relatively higher absorption may achieve relatively lower drying shrinkage.

## Effect of Cement Source and Type on Shrinkage

### Drying Shrinkage

Table 5 presents the concrete drying shrinkage for four cements from various sources. The table shows the significant effect of cement source on drying shrinkage. Drying shrinkage increased from 378 to 785 micro-strain (i.e., 108 percent increase) when Type I independent cement (Mix 2.2) replaced Type I Lehigh cement (Mix 2.3). As stated in ACI Report 224 (4), chemical composition of cement has a definite effect on the dry-

TABLE 5 Effects of Cement Source and Type on Shrinkage

Mix No.	2.1	2.2 <sup>1</sup>	2.3 <sup>1</sup>	2.4 <sup>1</sup>
Cement Content, kg/m <sup>3</sup> (lb/y <sup>3</sup> )	405 (682)	405 (682)	405 (682)	405 (682)
Cement Source	Lone Star Cement, (Typ I) Nazareth, PA	Independent Cement, (Typ I) Hagerstown, MD	Lehigh Cement (Typ I), Union-bridge, MD	Lone Star Cement, (Typ II) Nazareth, PA
Water Content, kg/m <sup>3</sup> (lb/y <sup>3</sup> )	174 (293)	174 (293)	174 (293)	174 (293)
Fine Aggr. Content, kg/m <sup>3</sup> (lb/y <sup>3</sup> ) SSD	654 (1102)	654 (1102)	654 (1102)	654 (1102)
Fine Aggregate Source	Mays Landing Sand & Gravel, Dorchester, NJ (Quartz Sand)			
Fine Aggr. Absorption	0.44 %	0.44 %	0.44 %	0.44 %
Fine Aggregate S.G.	2.62	2.62	2.62	2.62
Coarse Aggr. Content, kg/m <sup>3</sup> (lb/y <sup>3</sup> ) SSD	1092 (1841)	1092 (1841)	1092 (1841)	1092 (1841)
Coarse Aggr. Source	Glasgow Inc., King of Prussia, PA (Dolomite)			
Coarse Aggr. Absorption	0.36 %	0.36 %	0.36 %	0.36 %
Coarse Aggregate S.G.	2.85	2.85	2.85	2.85
Air Admixture	Yes	Yes	Yes	Yes
Water Reducer	No	No	No	No
Retarder	Yes	Yes	Yes	Yes
Four-Month Shrinkage, <sup>2</sup> micro-strain	488	785	378	367

1: Same as Mix 2.1, Except Different Cement Source

2: Unrestrained Specimens; Applicable ASTM C157/C878 Provisions.

ing shrinkage of the paste and concrete. Currently, information in the literature in this area is limited, and there are no relations established between those factors and drying shrinkage.

The experiments also explored the effect of the type of cement. As shown in Table 5, when Lone Star Type II cement (Mix 2.4) substituted Lone Star Type I cement (Mix 2.1), drying shrinkage decreased from 488 to 367 microstrain (i.e., 25 percent).

### Thermal Shrinkage

As discussed previously, cement type can be a major factor affecting the heat of hydration generated and thermal shrinkage of concrete. The heat generated increases with increases in cement fineness (ASTM C115 or C204) and in 28-day cement heat of hydration (ASTM C186). In the course of the laboratory investigations, concrete curing temperatures were measured in 152- × 305-mm (6- × 12-in.) insulated cylinders. Those curing temperatures gave an indication of the extent of thermal shrinkage of the four cements used in the study.

As shown in Figure 1, the mix with Lone Star Type I cement had the highest temperature rise in the cylinder: about 9°C (16°F), compared with about 6°C (11°F) for the other mixes (i.e., 45 percent increase in temper-

ature rise). Note that the temperature rise in a bridge deck will be much higher than temperature rise in a small cylinder because of the greater mass of concrete. Although sufficient information is not available from this experiment to quantify the effects of the cements used on thermal shrinkage, it is evident that the source of cement can affect thermal shrinkage significantly.

The experiments also explored the effect of Type II cement on thermal shrinkage. As shown in Figure 1, when Lone Star Type II cement (Mix 2.4) was substituted for Lone Star Type I cement, the temperature rise decreased from 9 to 6°C (16 to 11°F), the same as the temperature rise of the other two mixes with Type I cement.

### Effect of Fly Ash on Shrinkage

The effect of fly ash on drying shrinkage was based on limited tests (Table 6). As shown in Table 6, drying shrinkage increased from 510 to 895 microstrain (i.e., 75 percent increase) when fly ash partially substituted for cement in one mix. That increase was higher than expected. It is possible that this finding is applicable only to certain types of cement and fly ash, and the finding may not be generalized.

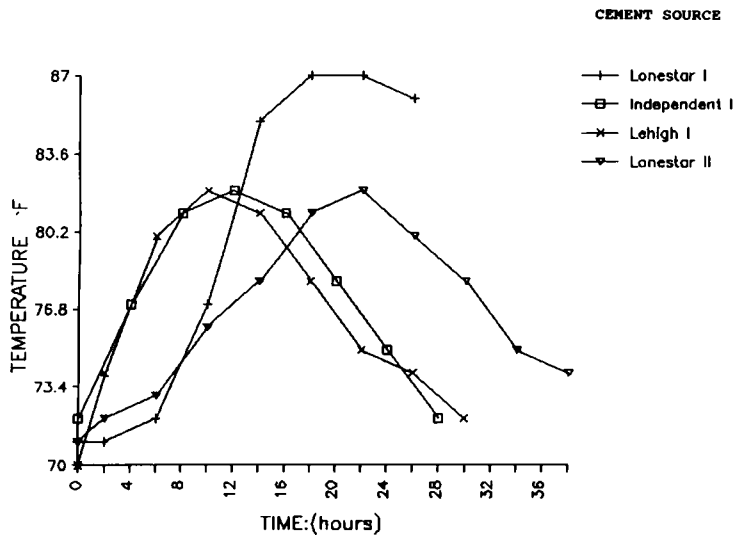


FIGURE 1 Effects of source and type of concrete on curing temperature.

TABLE 6 Effects of Fly Ash on Shrinkage

Mix No.	3.1 Mix with Fly Ash	3.2 Same as 3.1, Except no Fly Ash
Cement Content, kg/m <sup>3</sup> (lb/y <sup>3</sup> )	377 (635)	443 <sup>1</sup> (746)
Cement Source	Armstrong Cement (Type I), Cabot, PA	
Fly Ash Content, kg/m <sup>3</sup> (lb/y <sup>3</sup> )	67 (113)	0
Fly Ash Source	National Mineral (Type F)	-
Fly Ash S.G.	2.25	-
Water Content, kg/m <sup>3</sup> (lb/y <sup>3</sup> )	173 (291)	173 (291)
Fine Aggr. Content, kg/m <sup>3</sup> (lb/y <sup>3</sup> ) SSD	572 (963)	594 <sup>2</sup> (1001)
Fine Aggregate Source	Glacial S&G, Tarrtown Hill (Type A) (GLG-03C), (Gravel)	
Fine Aggregate Absorption	2.10%	2.10%
Fine Aggregate S.G.	2.55	2.55
Coarse Aggr. Content, kg/m <sup>3</sup> (lb/y <sup>3</sup> ) SSD	1042 (1756)	1042 (1756)
Coarse Aggregate Source	Latrobe Construction, Longbridge (#57) (LAT-64A), (Calcareous Sandstone)	
Coarse Aggregate Absorption	0.43%	0.43%
Coarse Aggregate S.G.	2.68	2.68
Air Admixture	Yes	Yes
Water Reducer	No	No
Retarder	Yes	Yes
Four-Month Shrinkage, <sup>3</sup> micro-strain	895	510

1: Cement content is based on water-cementitious ratio of 0.39.

2: Aggregate is adjusted to partially substitute fly ash.

3: Unrestrained Specimens; Applicable ASTM C157/C878 Provisions.

## RECOMMENDATIONS

### Recommended Pennsylvania Deck Concrete Shrinkage Specification

#### *Maximum Differential Deck/Beam Temperature*

The first recommendation of this research to reduce thermal shrinkage is to require in the Pennsylvania specification for deck concrete construction that the differential deck/beam temperature be maintained under 12°C (22°F) for at least 24 hr after the concrete is placed.

#### *Maximum Drying Shrinkage*

The second recommendation is to include a requirement in the Pennsylvania specification for deck concrete mix design limiting the 4-month specimen drying shrinkage to 700 microstrain (equivalent to 28-day shrinkage of 400 microstrain). Drying shrinkage is to be verified by performing a shrinkage test on a trial batch, using the materials that will be used in the bridge deck concrete, before the mix is approved. Specimens are 76- × 76- × 254-mm (3- × 3- × 10-in.) unrestrained prisms.

### Suggestions for Complying with PADOT Shrinkage Specification

The Pennsylvania deck concrete shrinkage specification is a first step toward eliminating premature cracking of bridge decks. More testing will be necessary to refine the mix design process so that the shrinkage can be predicted accurately before the trial batch. The following suggestions are based on the limited testing and observations made during this project to assist in achieving the Pennsylvania deck concrete shrinkage specification and reducing premature cracking of bridge decks.

#### *Aggregates*

The research suggests that the use of soft aggregates (usually high in absorption and low in specific gravity) such as sandstone tends to result in increased drying shrinkage and that the use of hard aggregates (usually low in absorption and high in specific gravity) such as quartz, dolomite, and limestone tends to result in decreased shrinkage. The research further suggests that coarse aggregate absorption should not exceed 0.5 percent and that fine aggregate absorption should not exceed 1.5 percent.

#### *Mix Water*

Specifications now allow maximum mix water content to be 192 kg/m<sup>3</sup> (323 lb/yd<sup>3</sup>). However, a lower mix

water content will reduce drying shrinkage. A mix designed for the lower end of the slump range should shrink less than one in which the slump is toward the high end. The mix water should be controlled rigidly from the batch plant until it is discharged at the site. The addition of a water-reducing admixture should also improve shrinkage.

#### *Cement*

Specifications allow the maximum cement content to be 446 kg/m<sup>3</sup> (752 lb/yd<sup>3</sup>). The less cement that is used, the less heat is generated and the less water is required for hydration. Type II cement has lower heat of hydration than Type I. The research also suggests that some brands of cement may contribute more to shrinkage of concrete than others. However, the research is much too limited to use to select specific brands. There is certainly justification for additional research in this area, which may result in shrinkage limitations for cement used in bridge decks.

#### *Thermal Controls*

Retarders reduce the rise in temperature of the concrete and should be used, particularly when ambient temperature is expected to reach 24°C (75°F) or more. In hot weather, attempts should be made to cover concrete with wet burlap no more than 30 min after finishing and texturing the surface, and the burlap should be kept wet continuously. Doing so will minimize heat buildup from exposure to direct sunlight. In hot weather it is preferable to place concrete at night to minimize heat that builds up from cement hydration and ambient heat.

#### *Cold-Weather Concreting*

During cold-weather curing, the concrete surface should not be insulated without heating and increasing the temperature of the air underneath the deck. The insulation will promote the rise in temperature of the deck, while the temperature of supporting beams will be the same as the cold ambient air. Heating the air underneath the deck will raise the temperature of the beams, consequently reducing the differential temperature.

The surface insulation should be controlled such that the concrete surface temperature is maintained between 12 and 24°C (55 and 75°F) during curing with emphasis on the lower end of the range. The area underneath the deck should be enclosed and heated such that the temperature of the surrounding air is kept as close as possible to the temperature of concrete [i.e., 12 to 24°C (55 to 75°F)].

After the cold cure is complete, the concrete temperature should be lowered gradually to the ambient tem-

perature. The maximum allowable temperature drop during first 24 hr after end of curing period should be 14°C (25°F). The recommended temperature drop of concrete can be accomplished by reducing sources of heat slowly and by allowing insulation to remain until the concrete has essentially reached equilibrium with the ambient temperature.

#### ACKNOWLEDGMENTS

The research reported herein was performed by Wilbur Smith Associates (WSA) as part of a project for the PADOT, Office of Research and Special Studies. The research is sponsored by PADOT and FHWA, U.S. Department of Transportation. Since it is in progress, not all the findings have been accepted as official views of either PADOT or FHWA.

Managing the research for PADOT and providing liaison between the PADOT research panel and WSA was Steve Davis from the Office of Research and Studies. The panel, headed by Nalin Udani from the Bureau of Design Bridge Division, includes Abid Qanbari, Gordon Bell, Dave Reidenouer, Ron Arner, Gary Hoffman, and John Ekiert of PADOT and William Williams of FHWA.

The WSA team of Ron Purvis (principal investigator) and Khossrow Babaei are performing the research. Sub-consultants assisting WSA are Mike Boyle, Valley Forge Testing; Ken Clear, Kenneth C. Clear Inc.; Gajannan

Sabnis, Howard University; and Heintz Koretzky, private consultant.

#### REFERENCES

1. Babaei, K., and R. L. Purvis. *Prevention of Cracks in Concrete Bridge Decks: Report on Surveys of Existing Bridge Decks*. Report for Research Project 89-01. Pennsylvania Department of Transportation, Oct. 1994.
2. Babaei, K., and R. L. Purvis. *Prevention of Cracks in Concrete Bridge Decks: Report on Observations of Bridge Deck Construction*. Report for Research Project 89-01. Pennsylvania Department of Transportation, Jan. 1995.
3. Babaei, K., and R. L. Purvis. *Prevention of Cracks in Concrete Bridge Decks: Report on Laboratory Investigations of Concrete Shrinkage*. Report for Research Project 89-01. Pennsylvania Department of Transportation, Jan. 1995.
4. *Control of Cracking in Concrete Structures*. Report 224R-80. American Concrete Institute, Detroit, Mich., rev. 1984.
5. *NCHRP Report 297: Evaluation of Bridge Deck Protective Strategies*. TRB, National Research Council, Washington, D.C., 1987.
6. *Prediction of Creep, Shrinkage, and Temperature Effects in Concrete Structures*. Report 209R-92. American Concrete Institute, Detroit, Mich., 1992.
7. *Design and Control of Concrete Mixtures*. PCA Engineering Bulletin, Portland Cement Association, 1968.
8. *Effects of Restraint, Volume Change, and Reinforcement on Cracking of Massive Concrete*. Report 207.2R-73. American Concrete Institute, Detroit, Mich., rev. 1986.



# Design and Construction of North Halawa Valley Viaduct

---

Tim J. Ingham, Rafael Manzanarez, and Karen Cormier,  
*T. Y Lin International*

The North Halawa Valley Viaduct is a 2-km-long prestressed concrete box girder bridge on the island of Oahu, Hawaii. It is the first cast-in-place cantilever segmental bridge in the United States to be built from an overhead erection gantry. The design features of the project are described, and the reasons for choosing that construction method are given. The main features of the operation of an erection gantry are described, and some of the problems arising during the construction of the bridge are discussed. Finally, the instrumentation of the structure to monitor its long-term performance is detailed.

**T**he North Halawa Valley Viaduct is a part of the so-called Interstate route H-3 project on the island of Oahu, Hawaii. As shown in Figure 1, the project runs from the Halawa interchange on H-1, north of Honolulu, across the Koolau Mountains (which form the backbone of Oahu), to Kaneohe, on the windward side of the island. The project is intended to relieve congestion on the existing Pali and Likelike highways, connect the Pearl Harbor naval station with the Marine Corps station at Kaneohe, and provide for future trans-Koolau travel demand.

## PROJECT DESCRIPTION

The H-3 project, besides including several miles of at-grade highway, includes three major structures: the

trans-Koolau tunnel, which runs approximately a mile beneath the crest of the island; the recently completed Windward Viaduct immediately to the east of the tunnel; and the North Halawa Valley Viaduct immediately to the west of the tunnel. The North Halawa Valley Viaduct was designed by Nakamura & Tyau, of Honolulu, Hawaii, and T. Y. Lin International, of San Francisco, California.

## Site Conditions

The bridge runs through the upper North Halawa Valley, which is typical of the deep erosional valleys that have formed on the flanks of the ancient Koolau volcano. The valley is generally V-shaped, with irregular side valleys and ridges extending to the valley bottom; slopes along the project alignment are frequently as steep as 2h:1v to 1h:1v.

The viaduct design reflects the fact that the North Halawa Valley is an environmentally sensitive site. Several native Hawaiian burial sites have been found in the valley; these are now the subject of archaeological investigation. The valley is also a watershed area and will be closed to the general public after the H-3 project is completed. The viaduct has been designed and constructed so as to minimize disturbance to the site.

The North Halawa Stream meanders along the viaduct alignment as shown in Figure 2. The stream is sub-

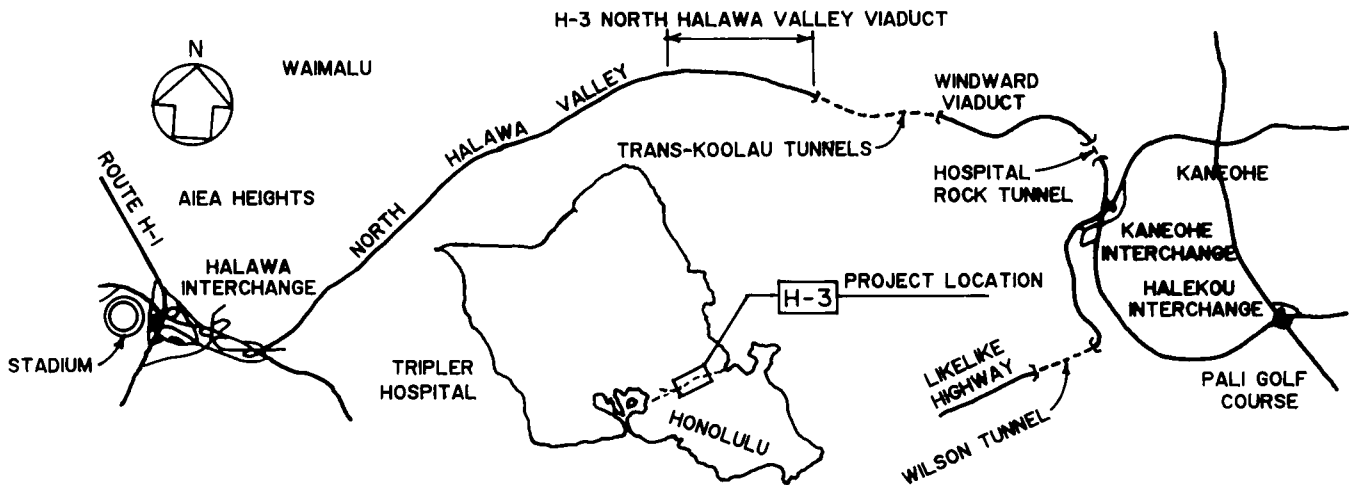


FIGURE 1 Project location.

ject to frequent floods because of an average of 150 in. of rain annually at the top of the valley. An important part of the project involves improving the stream to protect the viaduct foundations from scour.

### Description of Structure

A general plan and elevation of the bridge are shown in Figure 2. The project actually consists of two parallel viaducts, one carrying two lanes of traffic inbound to Honolulu and one carrying two lanes of outbound traffic. The inbound viaduct is 1897 m (6,225 ft) long and the outbound viaduct is 1667 m (5,470 ft) long. Both viaducts are aligned horizontally on curves with radii of approximately 1800 m (5,906 ft) at the lower end of the valley and 2900 m (9,514 ft) at the upper end of the valley. The viaducts are on a nearly constant 6 percent grade sloping up toward the mountains (the vertical scale is exaggerated by a factor of two in Figure 2). The typical (and maximum) span length is 109.728 m (360 ft), with some span lengths as small as 91.44 m (300 ft) to accommodate the vagaries of the terrain and the stream in the valley bottom.

Figure 2 shows the viaducts to be divided into three structural units each, averaging 565 m (1,854 ft) in length between expansion joints. Each unit has two fixed piers toward its center and two or three flanking expansion piers on either side. Each unit was constructed by the segmental cantilever method using an overhead erection gantry.

The expansion joints between the units are located at the top of so-called end piers. This was done to avoid the excessive deflections that sometimes accompany midspan hinges and the construction problems that often accompany cantilever construction past a quarter-

point hinge. The fact that the end piers, located at what would otherwise appear to be the middle of a span, are perhaps unattractive was discounted because the valley will eventually be closed to the public. The rather large movement ratings of the expansion joints, up to 21 in., combined with the steep 6 percent grade of the bridge led to an unusual design detail. At each end pier the bearings were aligned along the grade of the structure in order to constrain the movement of the bridge to be parallel to the expansion joint. If the bearings had been set horizontally, as is done normally, the movement of the bridge would have had a component perpendicular to the expansion joint, causing a jog in the roadway surface of  $1\frac{1}{4}$  in. Of course, inclining the bearings induces a slope load into the pier and footing, equal to the grade of the bridge times its dead load. But the dead load reactions on the end piers are relatively small, and, fortuitously, most of the end piers are fairly short.

The viaduct cross section is shown in Figure 3. The out-to-out width of the bridge is 12.497 m (41 ft), which accommodates two lanes of traffic plus shoulders. The cross section varies in depth from 2.438 m (8 ft) at midspan to 5.468 m (18 ft) near the piers. These dimensions are typical of cast-in-place structures of about 100-m (328-ft) span length.

### Piers

The bridge piers are designed conventionally. They are of hollow construction with a wall thickness of 457 mm (1 ft 6 in.) and exterior dimensions of  $3.048 \times 7.010$  m ( $10 \times 23$  ft). They vary in height from 8.336 to 31.766 m (27 ft 4 in. to 104 ft 3 in.). The piers were built in tall lifts of concrete, up to 12.192 m (40 ft), using flying forms. The construction took place without incident.

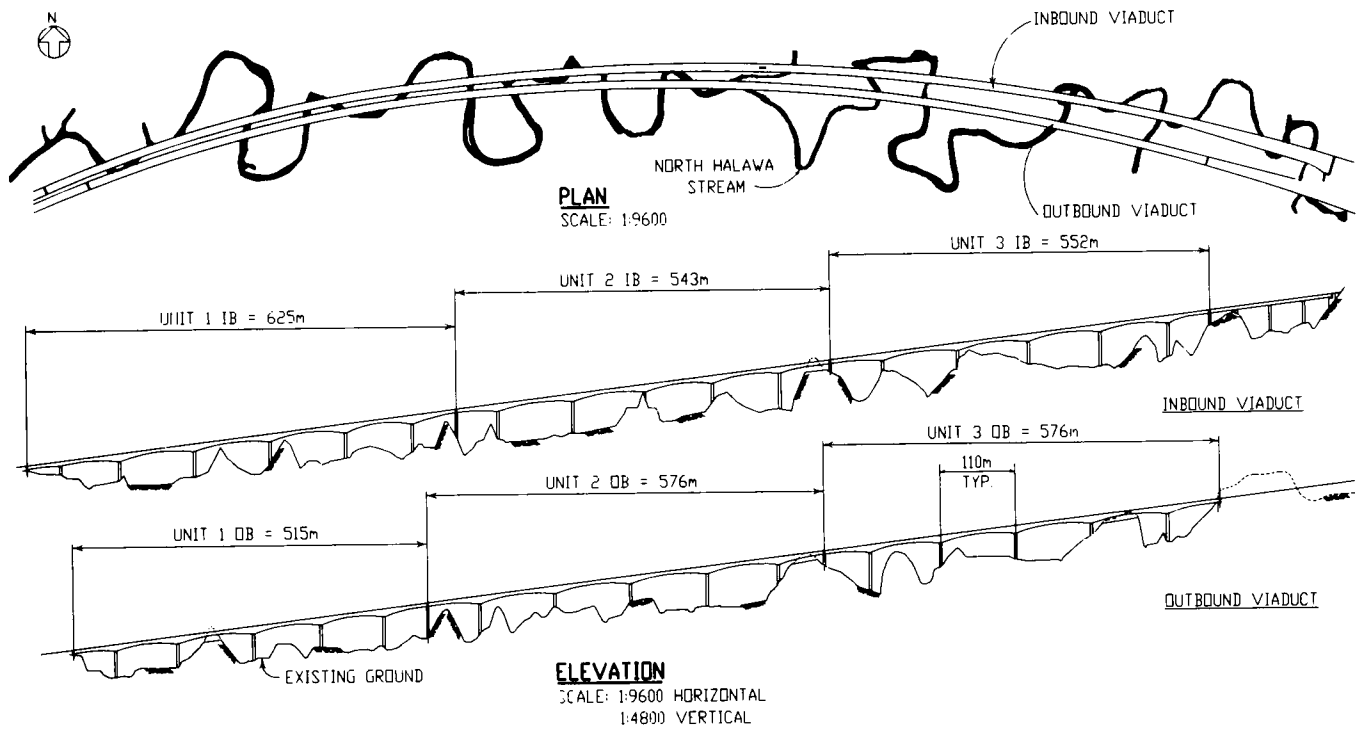


FIGURE 2 General plan and elevation of viaduct.

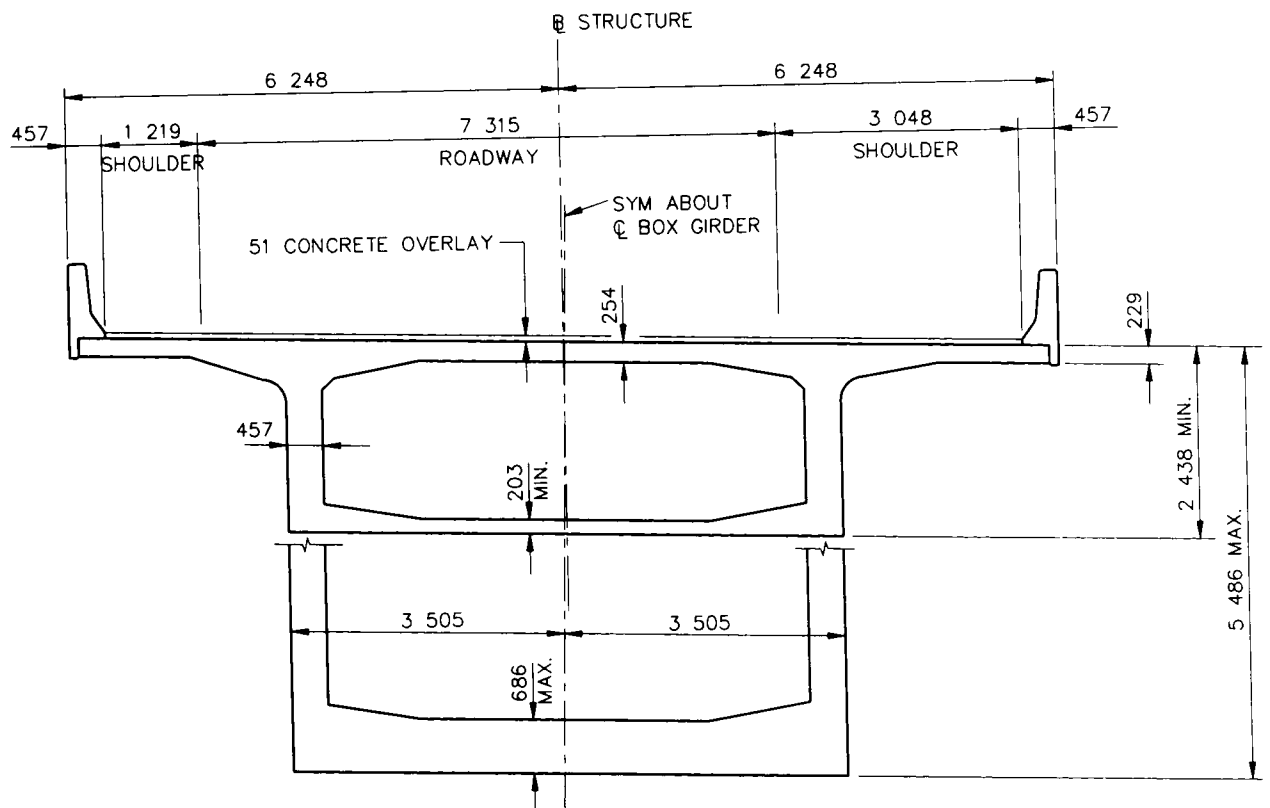


FIGURE 3 Bridge cross section.

## Foundations

The soils along the bridge alignment consist of surficial layers of alluvium and colluvium underlain by thick layers of residual soils and saprolite decomposed from basalt. At depths approaching 30.480 m (100 ft), the saprolite gradually gives way to slightly weathered and unweathered basalt rock.

Both prestressed concrete pile and drilled shaft foundations were designed and fully detailed and bid as alternatives. A typical pile foundation consisted of octagonal piles 70 508 mm (20 in.) in diameter. Because at depth the ground is fairly hard, it was anticipated that these piles would be driven through predrilled holes 457 mm (18 in.) in diameter to depths ranging from 15.240 to 30.480 m (50 to 100 ft). Not surprisingly, no contractor bid the pile alternative—it probably does not make sense to predrill piles if one can just make a drilled shaft.

The successful drilled shaft alternative was only the second application of this construction method in Hawaii. A  $3 \times 3$  pattern of drilled shafts 1.524 m (5 ft 0 in.) in diameter is typically used, with one or two shafts occasionally omitted from the pattern. The shafts vary in length from 24.384 to 36.576 m (80 to 120 ft). Further details are given later in the paper.

Three site factors complicated the foundation work. The construction of drilled shafts near the stream had to contend with large fields of boulders. These boulders were deposited over the years as the stream meandered back and forth over the valley bottom. (The boulders were another reason that drilled shafts were favored over piles.) Footings near the stream had to be constructed in cofferdams to protect them from scour, because flooding was a possibility at any time of the year. And several of the viaduct foundations fall on the ridges that intersect the valley bottom; each of these required a large excavation.

## Transition Area Box Girder

In addition to the three segmentally constructed units, the inbound viaduct also has a portion 178.308 m (585 ft) long that is built on falsework. This is a conventional multicell box girder at which the viaduct widens so rapidly (to accommodate some transition lanes before the trans-Koolau tunnels) that segmental construction was considered impractical.

## Bridge Types and Construction Methods Considered

Only segmental construction methods were considered when the bridge type was selected. Both precast and

cast-in-place superstructures were considered, with span lengths ranging from 48.768 to 109.728 m (160 to 360 ft). Balanced cantilever construction, with either form travelers or erection gantries, was considered for both the precast and cast-in-place alternatives. Span-by-span construction was also considered for the cast-in-place alternative.

The precast alternatives were thought to be relatively expensive because there was no suitable location for a segment precasting yard near the bridge site. The only suitable locations were several miles away, outside of the North Halawa Valley. Unfortunately, the access road to the site was long and narrow and had to be shared with several other construction projects in the valley. The Hawaii Department of Transportation and the bridge designers favored cast-in-place construction over precast for subjective reasons: the greater durability of cast-in-place bridges and their possibly better behavior during earthquakes.

In considering only cast-in-place construction, erection from conventional form travelers was thought to be expensive because of the time-consuming assembly and disassembly of the form travelers on each pier (31 in number). Erection from an overhead gantry (as shown in Figure 4) was thought to offer several advantages with respect to erection from form travelers.

The fundamental advantage of this construction method is that, except for the pier segment, the superstructure construction is independent of the ground; all of the necessary materials, equipment, and personnel can be delivered to the point of work from overhead, along the completed structure and over the gantry. And the difficult topography of the valley and the project's environmental restrictions made it desirable to work from overhead as much as possible.

To be sure, 3564 m (11,695 ft) of viaduct is a lot of bridge. Once mobilization costs are overcome, construction with an erection gantry is inherently fast, because large segments are possible and because the launch of the gantry from one pier to another can be quick. Savings are also possible in piers and foundations because the gantry can absorb some of the unbalanced moment of the cantilever. And although the erection gantries themselves are expensive, there are offsetting savings in auxiliary equipment, which is not required to service cantilever construction at each pier, and in spur roads and lay-down areas at each pier, which are not required to service the same volume of material as for conventional construction with form travelers.

The typical span length of 109.728 m (360 ft) is thought to be about the maximum practical span length for this method of construction. The maximum span length was chosen in order to minimize the number of piers and foundations to be built in the difficult terrain. The North Halawa Valley Viaduct is the first cantilever

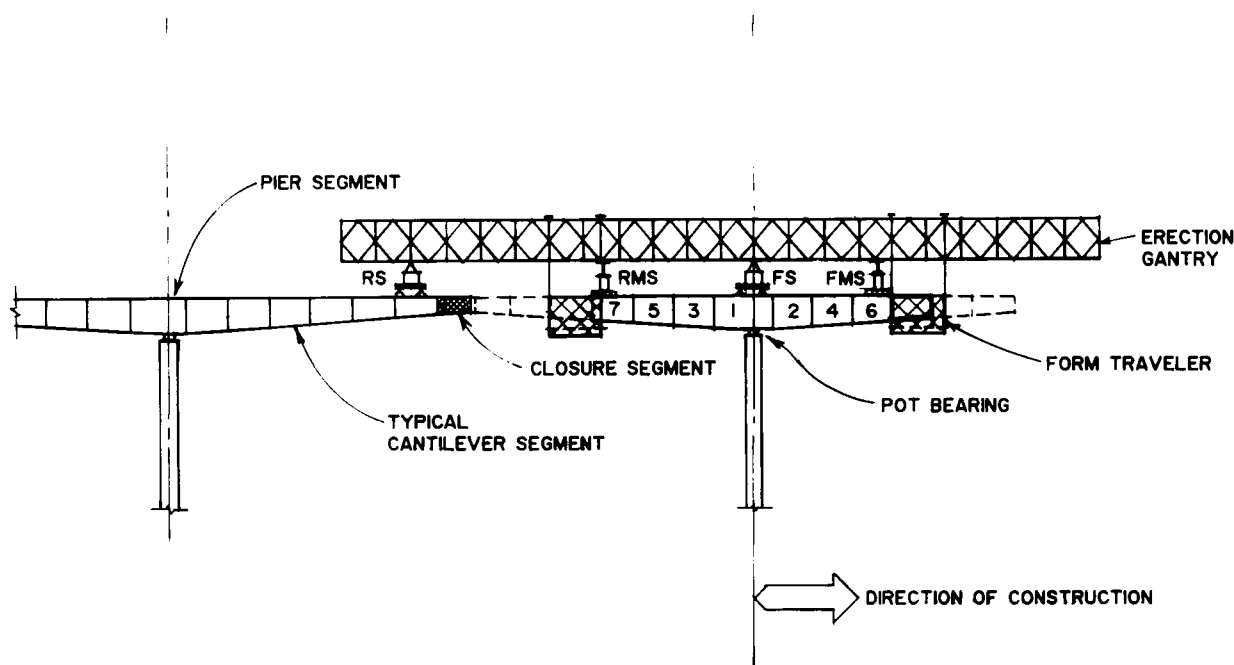


FIGURE 4 Operation of erection gantry.

segmental bridge in the United States to be cast in place from an overhead gantry. The method has been used several times in Europe, however.

## CONSTRUCTION

After a very competitive bidding process, a contract for construction of the viaduct was awarded to the Kiewit Pacific Company on December 19, 1991, with a notice to proceed on February 21, 1992. The bid price was approximately \$141 million, for the viaducts and the ancillary site work; the viaduct itself cost about \$105 million. Nine hundred ninety calendar days were allowed for the construction of the viaducts and for the site work. Major subcontractors to Kiewit Pacific included the VSL Corporation, for erection gantry design and superstructure construction engineering, and the Malcolm Drilling Company, for drilled shaft construction.

## Foundations

Drilling the shafts was the first construction activity on the site. They were constructed both in the dry and by tremie inside a casing near the stream. The boulder fields were found to be a significant obstacle to the drilling. In fact, the drilling subcontractor filed a successful claim against the state, charging that the boulders were larger and more densely packed than indicated by the

test borings. Boulders smaller than one shaft diameter were usually removed with a choker; the subcontractor was generally able to drill through larger boulders, but some shafts were cut off when very large boulders were encountered. Aside from this problem, however, the construction of the drilled shafts was straightforward. The drilling subcontractor was able to drill about one shaft a day, on average. A total of 6781 m (22,429 ft) of shaft 1.524 m (5 ft) in diameter and 2856 m (9,370 ft) of shaft 914 mm (3 ft) in diameter were drilled and cast in just over a year.

## Superstructure

### *Cantilever Construction*

The superstructure was built by cantilever construction about each pier. Each cantilever (or pair of cantilevers) was cast in place in segments using an erection gantry, as shown in Figure 4. At each pier, the construction was started by casting a pier segment directly on top of the pier; this was actually cast in place in formwork supported on the pier shaft. In each case, the pier segment was eccentric with respect to the centerline of the pier, thus applying an unbalanced moment to the pier shaft. The eccentric length of the pier segment was equal to half of the typical segment length.

After casting the pier segment, the typical cantilever segments were cast in place in formwork supported

from the erection gantry. The segments were cast alternately to either side of the pier, starting from the side opposite the pier segment cantilever. When released from the formwork, each segment potentially applied a net unbalanced moment to the pier shaft corresponding to half of the segment length times the remainder of the cantilever length minus a quarter of the segment length.

The cantilever construction at each pier was concluded by casting a closure segment between the rear cantilever segment (relative to the direction of construction) and the tip of the previously completed cantilever. The closure segments were cast using the same formwork as for the cantilever segments (with some revisions to the support of the interior formwork).

Because the end spans in each structural unit are longer than a typical cantilever length, often 76.200 m (250 ft) versus about half the span length, or 54.864 m (180 ft), a portion of each end span was cast in place in formwork supported on the ground. These supported segments were typically 12.192 to 18.288 m (40 to 60 ft) long.

### *Contractor Modifications*

Although segmental construction using an erection gantry was anticipated in the design of the viaducts and shown on the contract plans, the actual construction involved two important modifications to the original design. Each of these modifications was made to increase the rate of construction, relative to the conservative assumptions made by the designers of the bridge. One modification made by the contractor was to increase the segment length from the 6.401-m (21-ft) length assumed in the original design to 7.315 m (24 ft). (The original design would have allowed construction with conventional form travelers.) Another modification was to increase the rate of casting of segments from an assumed 5-day cycle (in effect a weekly cycle without working on the weekends) to a 4-day cycle.

Taken together these modifications allowed the contractor to build the bridge with three erection gantries rather than the four shown on the contract plans. One gantry was used on each of the inbound and outbound viaducts, moving uphill from the abutments to construct Units 1 and 2. The third gantry (actually the first to be launched since it was on the critical path) was used to construct Unit 3 of both viaducts; it started on the outbound viaduct, moving downhill from the abutment toward one of the other gantries. When Unit 3 of the outbound viaduct had been completed, this gantry was pushed back up the completed structure and then sideways onto the transition area box girder. It was then launched downhill again, to build Unit 3 of the inbound viaduct.

The posttensioning layout was also revised by the contractor to accommodate the revised segment length; the overall posttensioning scheme was maintained, however. The changes to the segment and posttensioning layouts, and particularly the increased rate of construction of the bridge, made it necessary for the contractor and the designer to reanalyze the bridge, because the creep and shrinkage of concrete renders the behavior of the bridge time-dependent.

### *Casting Cycle*

As mentioned previously, a 4-day cycle was used for casting cantilever segments (indeed, occasionally the contractor was able to build a segment in 3 days). The daily operations in the typical cycle were as follows:

- Day 1: Install the reinforcing and posttensioning in the bottom slab of the cross section.
- Day 2: Install the reinforcing and posttensioning in the webs and the top slab, adjust the forms, and perform a button-up survey.
- Day 3: Perform a prepour survey and cast the segment.
- Day 4: Stress the posttensioning tendons anchored in the segment, break down and move the forms forward, and perform an as-built survey.

The superstructure concrete mix designed by the contractor was an important factor in the success of the 4-day cycle. A strength of 24 MPa (3,500 psi) (70 percent of the design concrete strength) was required for posttensioning of the structure. The mix used had a high cement content, low ratio of water to cement, and superplasticizers. In the insulated forms used, the required strength routinely was reached at about 18 hr after casting. [The 28-day strength of the mix is about 48 MPa (7,000 psi).] Frequently, when the required strength for full posttensioning was not achieved on schedule, partial posttensioning at 17 MPa (2,500 psi) strength was used to allow the forms to be moved forward.

### *Creep and Shrinkage Testing*

As required by the specifications, the contractor performed creep and shrinkage testing of his proposed superstructure concrete mix, both to prove the suitability of the mix for construction and to confirm the characteristics used in the design. Although the creep and shrinkage properties of Hawaiian concrete were researched by the designers of the bridge, such tests are always necessary because of the high variability of concrete as a material.

The original research suggested that the shrinkage of Hawaiian concrete (in general) was much larger than

predicted by the CEB-FIP model of the creep and shrinkage of concrete (commonly used for bridge design). The designers assumed the shrinkage of concrete to be  $2\frac{1}{2}$  times that predicted by the model, and this factor was confirmed by the shrinkage testing. (Hawaiian aggregates are of volcanic origin, which is not common elsewhere.) The original research did not reveal any systematic difference between the creep of Hawaiian concrete (considering materials from several sources) and that predicted by the CEB-FIP model, but this particular assumption was not confirmed by the testing, which showed the mix proposed by the contractor to have about 25 percent higher creep than predicted. Consequently, the reanalysis of the bridge, made necessary by the contractor's increased rate of construction, used this higher creep coefficient. From the testing, the ultimate shrinkage strain of the superstructure concrete mix was taken to be 0.000449 and the ultimate creep coefficient was taken to be 2.47, for 28-day loading.

### *Increased Continuity Posttensioning*

The increased rate of construction of the bridge and the higher creep coefficient both led to a small increase in the amount of continuity posttensioning needed in the bridge. The so-called continuity tendons are draped tendons in the webs in each span. They are an important factor in eliminating tension in the bottom fibers of the bridge at midspan; the design criteria did not allow any tensile stress in the structure under combinations of live load and temperature gradient. The aforementioned factors both cause tensile stress at midspan. The additional continuity posttensioning needed to compensate for this stress took the form of additional strands placed in the existing ducts; no additional tendons were required. The contractor was compensated for the additional posttensioning required to offset the higher creep coefficient but not for that required to offset the increased rate of construction, since that was his choice relative to the contract plans.

### *Gantry Design and Operations*

The erection gantries, illustrated in Figure 4, were designed and built by the contractor. Each gantry had a crane rail and two cranes of 5.9-ton (13-kip) capacity running along its soffit. The cranes were used to deliver reinforcing bars and other materials to the point of work. Each gantry also had a 480V power line running along its soffit to power equipment at the point of work. Each gantry was 140 m (450 ft) long, weighed about 613 tons (1,350 kips), and cost about \$2.5 million, including the form travelers and auxiliary equipment.

As can be seen in Figure 4, the form travelers were suspended from the gantry rather than from "horses" supported on the cantilever, as in conventional cantilever construction. The form travelers themselves were fairly conventional (except in one respect to be discussed later). During cantilever construction, each gantry was balanced on a front main support (FS) on the forward pier (in the direction of construction) and a rear main support (RS) on the tip of the previously completed cantilever. The sequence of casting concrete, stressing tendons, and moving the form travelers was the same as for conventional cantilever construction.

An important feature of the gantry operation was the use of struts between each gantry and the viaduct—the front mobile support (FMS) and rear mobile support (RMS) shown in Figure 4. These were jacks placed immediately behind the form travelers to support the gantry on the bridge deck. They took advantage of the inherent strength and stiffness of the structure to help the gantry carry the load of freshly cast segments. They were moved with the form travelers so as to be always just behind the segment being cast.

Also, at expansion piers, where the superstructure is supported on pot bearings, the struts were used to balance the cantilever on top of the pier. One strut, at least, was always maintained in compression between the gantry and the structure to react the weight of the unbalanced segment on the opposite side of the cantilever. Form travelers and struts being moved to the next segment were always on the heavy side of the cantilever (where a segment had just been cast), so that the strut on the opposite side was compressed naturally by the unbalanced moment. When the form travelers were stationary, both struts were maintained in compression. This scheme enabled the contractor to avoid a complicated moment restraint to stabilize the cantilever against the pier shaft.

### *Geometrical Control*

Because struts were used to share loads between the gantry and the structure, they formed a system that had to be analyzed to determine its behavior under load. This use made the geometrical control of the structure more complicated than it is for conventional cantilever construction. But using the gantries to stabilize the cantilevers at expansion piers (by using the struts just described) allowed those cantilevers to be "rocked" in order to compensate for geometrical errors, in effect providing an additional variable for solving geometrical control problems.

In accordance with the specifications, the contractor wrote a geometry control plan that subsequently was reviewed by the designer. The goal of the plan was to compensate for the deflection and movement of the

bridge during construction (due to the method of construction and construction operations) and for the creep and shrinkage of the bridge after construction (up to 20 years). In accordance with the geometry control plan, the bridge was cast to a cambered "control line" so that it would eventually deflect into the required vertical alignment. The plan also contained provisions to compensate for errors in construction (differences from the control line) of more than 25.4 mm (1 in.).

The successful geometrical control of the structure was due to a cooperative effort between the contractor and the designer. Both the contractor and the state of Hawaii maintained a team of bridge surveyors in the field, who independently monitored the position of the bridge at each stage of construction as well as the loads in the gantry front and rear mobile supports (struts). Both the contractor's engineer and the designers ran detailed computer simulations of the construction of the bridge, using the measured mobile support loads at each step. These simulations were compared with each other and with the measured geometry of the bridge before and after the casting of each segment. For each segment, the contractor and the designer agreed to a preset elevation of the segment to meet the control line.

A difficult part of the geometrical control of the bridge was compensating for the deflection of the tip of the previous cantilever, because of creep of the bridge under the gantry rear main support reaction. This deflection was as much as 50 mm (1.97 in.) because of the large lever arm of the reaction. Any deviations from the planned construction schedule led to relatively large deviations from the control line as well.

### *Closure Segments*

Another interesting challenge was the geometrical control of the closure segments between the cantilever under construction and the previous cantilever. The closure segments were usually 7.315 m (24 ft) long, and occasionally 8.534 m (28 ft) long. It was found necessary to place struts on both sides of the closure segments in order to minimize the relative displacements between the tips of the cantilevers during casting. Even with struts on both sides of the closure segments, small relative displacements required compensation by an opposing camber.

### *Gantry Launching*

Subsequent to the closure of each cantilever to the tip of the previous cantilever, the gantry was launched to the next pier, carrying the form travelers with it. The form traveler bottom platforms could split open so that they could pass around the piers.

Each gantry was launched by hydraulic rams mounted on the rear main support. The rams would either push the gantry uphill or lower it downhill, according to its overall direction of motion. Each gantry was held in position by toothed grippers acting between its bottom flange and the rear main support while the rams were recycled. These grippers were used to hold the gantry firmly in position during cantilever construction also.

The launching of a gantry was a complicated operation requiring many steps. Three basic operations were involved. The most basic of these was moving the gantry forward over the front and rear main supports by pushing against the rear main support. The gantries moved over Hilman rollers on the main supports. Another basic operation was the temporary support of each gantry on either the front or the rear mobile support (strut), which relieved the load of the gantry on the corresponding main support and allowed that support to be moved. The third basic operation was moving the form travelers to reposition the center of gravity of the gantry/form traveler system to change the reactions on the gantry supports.

At each pier, a sequence of these operations was planned to simultaneously maintain the equilibrium of the gantry and avoid any overstress of the structure. The launch sequence was summarized by the contractor in a launch manual that was carefully reviewed by the designer.

Perhaps the most critical step in the launch procedure was the relocation of the front main support to the next pier for cantilever construction. This relocation was accomplished by launching the gantry tip as far the next pier, in steps as described earlier. The front main support was then moved to the next pier while the gantry tip was supported temporarily on that pier by the front mobile support. Similarly, the rear main support was relocated to the tip of the just-completed cantilever; it was then posttensioned to the bridge to carry uplift forces.

The typical launch of a gantry involved about 100 steps. Despite this evident complexity, the typical launch took only 2½ days once the contractor gained experience. This speed was possible because each of the steps was simple and the operations of the gantry were highly automated.

### INSTRUMENTATION

An unusual aspect of the project is the instrumentation of one of the structural units, specifically, Unit 2 of the inbound viaduct (the last unit to be completed). The instrumentation program will gather data on the behavior of the structure for comparison with the design



assumptions and the predicted behavior. The instrumentation program was a joint effort between T.Y. Lin International; the Construction Technologies Laboratory, Chicago, Illinois; and the University of Hawaii, Manoa. It will continue for 5 years after the completion of the bridge. The measurements include:

1. The forces in six posttensioning tendons will be measured by load cells placed behind the anchor heads.
2. At instrumented sections of the bridge, the strains in the concrete will be measured by cast-in-situ vibrating wire strain gauges and mechanical extensometers. There are four instrumented sections: two at midspan locations and two near piers.
3. At instrumented sections, the strains in some of the reinforcing bars will be measured by resistance strain gauges, adjacent to the concrete strain gauges.
4. At instrumented sections, the average temperature of the concrete and the temperature gradients over the depths of the section and the top slab will be measured by thermocouples placed around the perimeter of the box.
5. The vertical deflections of the bridge will be measured by reference to a high-strength piano wire stretched over the length of the unit and supported inside the cross section at the piers.
6. The rotations of the bridge over the piers will be measured by tiltmeters.
7. The horizontal displacements of the bridge will be measured at the joints by linear variable differential transformers spanning between the soffit of the box and the tops of the piers.
8. Any lateral displacements of the bridge will be surveyed from the ground.
9. The creep and shrinkage properties of the concrete used in the instrumented sections will be determined by testing under laboratory and site conditions.



FIGURE 5 Partly completed structure.

Hopefully, comparison of the collected data with the design assumptions and the predicted behavior of the bridge will lead to an improved understanding of long-span posttensioned bridges in general, as well as to improved design methodologies.

## CONCLUSIONS

Figure 5 shows a photograph of the two viaducts, one of them completed and one of them with an erection gantry in place. When this paper was written, the construction of the superstructure had been completed. Only the deck overlay and expansion joints and some site work remained to be completed. A total of 445 superstructure segments were cast in place in just over 2 years. The successful use of the overhead gantries shows the viability of this construction method where conditions make other methods unsuitable.

# **BRIDGE MANAGEMENT SYSTEMS, PART 2**

---

# Development and Implementation of New York State's Comprehensive Bridge Safety Assurance Program

---

A. M. Shirolé, *New York State Department of Transportation*

Since 1990 the New York State Department of Transportation has been proactively involved in the planning, development, and implementation of its long-range comprehensive bridge safety assurance program. This program will be integrated into the department's bridge management system to provide important safety-based bridge information for capital and maintenance program planning. The development and implementation of procedures used to assess the vulnerability of existing bridges to six potential causes or modes of failure—hydraulic, structural steel detail deficiencies, collision, overload, structural concrete detail deficiencies, and earthquake—are discussed. Furthermore, the development and implementation of an overall bridge safety assurance policy aimed at the design and construction of new bridges, retrofitting bridges during their planned rehabilitation, and programming the remaining bridges for necessary actions to eliminate or reduce their vulnerability to catastrophic failure are also discussed.

**D**uring the past decade the New York State Department of Transportation (NYSDOT) has introduced several programs to ensure the structural integrity and safety of the bridge network in the state. In April 1987 the New York State Thruway Authority's bridge over Schoharie Creek collapsed during

heavy floods, further underscoring the need for such programs. As a result the state's Highway Law was amended in 1989 to include the requirements for comprehensive bridge management and safety assurance programs and a uniform code of bridge inspection. Subsequently, the department began developing a systematic method to reduce the vulnerability of New York State's bridges to all potentially significant modes of failure. The planning aspects of this effort were previously reported by Shirolé and Holt (1).

In 1991 NYSDOT conducted an extensive survey of all states to determine the most common causes of bridge failure. A review of the 1,322 bridge failures reported revealed six failure modes as being the most significant in terms of the potential damage that they can cause to highway bridges in New York State. Three of these failure modes—hydraulic, overload, and collision—were found to be significant from the standpoint of frequency of incidence. Steel and concrete detail deficiency failure modes were considered significant in that they address potential vulnerability due to built-in design obsolescence in the existing bridge population. The earthquake failure mode was included in the program because of the severe consequences if even a single significant seismic event occurred in the Northeast. Based on significance and consequence, these failure modes are listed in prioritized order as follows:

1. Hydraulic,
2. Overload,
3. Structural steel detail deficiencies,
4. Collision,
5. Structural concrete detail deficiencies, and
6. Earthquake.

These failure modes are based on a nationwide survey of bridge failures since 1950 and were compiled by NYSDOT.

This paper discusses the development and implementation of procedures that can be used to assess and evaluate the extent of vulnerability of individual bridges to one or more of the identified failure modes. It presents an overview of the vulnerability assessment and evaluation procedures developed thus far for four of the six failure modes, and it discusses the development and implementation of an overall bridge safety assurance (BSA) policy aimed at the design and construction of new bridges, vulnerability retrofitting of bridges during their planned rehabilitation, and programming of the remaining bridges for necessary actions to eliminate or reduce their vulnerability to catastrophic failure.

## VULNERABILITY ASSESSMENT AND EVALUATION PROCEDURES

### Conceptual Framework

The vulnerability of a structure to failure is a measure of its susceptibility to failure or collapse because of loads or environmental conditions not anticipated in the design. Failure, for the purpose of the BSA program, is defined as any physical change of a bridge that creates a threat to public safety or the complete loss of service. Failure could result from excessive displacement or distortion, structural instability, component collapse, and so forth.

To simplify the vulnerability assessment of New York State's large bridge population (Table 1) NYSDOT decided to use a multilevel process. Each level of this process successively refines the list of bridges so that those

structures with greater vulnerabilities can be given a more detailed evaluation. This process comprises screening, classification, and rating steps that are intended to be performed sequentially and on a priority basis. Each step provides an increasing understanding of the specific vulnerability of a bridge. Bridges with greater vulnerabilities are first progressed through the various steps to focus the corrective actions on the most critical bridges in the shortest time. This results in a staggered progression of bridges through the assessment process.

Completion of the vulnerability assessment process requires a review of construction plans, inspection reports, bridge files, and other related documentation. Site visits may also be necessary to confirm information and gather additional data.

The process begins by screening the entire bridge population to identify bridges that exhibit the characteristics relevant to individual failure modes and progresses through the classification of individual bridges into a high, medium, or low vulnerability class on the basis of their vulnerability relative to those of other bridges in that particular failure mode. The vulnerability rating is determined by using the results of the classification process and, when available, results of further analyses, for example, a hydraulic analysis combined with an evaluation of the consequences of a failure. The actual vulnerability rating is determined in a manner similar to that in the classification process, in that rating scores are assigned to evaluate the likelihood and the consequence of a failure and are then added together to determine the vulnerability ratings.

The rating step is common to all six identified BSA failure modes, and it is intended to provide a uniform measure of a structure's vulnerability to failure on the basis of the likelihood of a failure and the consequences should one occur. The likelihood of a failure event is a measure of the probability of an external load condition exceeding the structural capacity, whereas the consequence of a failure refers to the impact of a bridge failure in terms of loss of life, injury, traffic disruption, or economic loss. There are six possible ratings, from 1 to 6. These ratings indicate what type of corrective action is needed to reduce or eliminate vulnerability to failure and the urgency with which this action should be implemented. On the basis of the vulnerability rating, an interim action such as load posting or bridge closing may be necessary until a detailed evaluation can be completed and more permanent vulnerability reduction measures taken. The following are the six possible ratings:

1. Safety priority action. This rating designates a vulnerability to failure resulting from loads or events

TABLE 1 Composition of New York State Bridges

Characteristic	Number of Bridges		(a) + (b)	% of Total
	State (a)	Non-State (b)		
Steel	5386	8669	14055	72%
Concrete	1699	1493	3192	16%
Prestressed Concrete	586	926	1512	8%
Timber	10	355	365	2%
All Other Types	38	345	383	2%
Total	7719	11788	19507	100%

that are likely to occur. Remedial work to reduce the vulnerability must be given immediate priority.

2. Safety program action. This rating designates a vulnerability to failure resulting from loads or events that may occur. Remedial work to reduce the vulnerability does not need immediate priority, but waiting for capital program action would be too long.

3. Capital program action. This rating designates a vulnerability to failure resulting from extreme loads or events that are possible but not likely. This risk can be tolerated until a normal capital construction project can be implemented.

4. Inspection program action. This rating designates a vulnerability to failure presenting minimal risk, provided that anticipated conditions or loads on the structure do not change. Unexpected failure can be avoided during the remaining life of the structure by performing special inspections.

5. No action. This rating designates a vulnerability to failure that is less than or equal to the current design standards. The likelihood of failure is remote.

6. Not applicable. This rating designates that there is no exposure to a specific type of vulnerability.

Figure 1 shows a typical six-digit vulnerability rating code for a bridge developed to assist in prioritizing BSA actions. Each digit in the six-digit code reflects the vulnerability rating for a specific failure mode. By this coding system, all bridges that have a rating of 1 in any failure mode will take precedence in maintenance, repair, or replacement decisions. The presence of an individual bridge on the vulnerability list is thus determined by having at least one rating of 1 within its rating number and is further prioritized by the position of any 1 (starting from the left) in the vulnerability rating code.

Results from the rating steps for each vulnerability mode provide input to the overall structural integrity evaluation (SIE), which is a detailed engineering evaluation covering all aspects of a bridge's structural condition and integrity as well as present and future needs for preserving or upgrading the safety and serviceability

of the bridge. This evaluation covers all identified vulnerability factors and failure modes and is expected to be done for bridges with a vulnerability rating of 1, 2, or 3.

Vulnerability assessment and evaluation procedures have been under development and follow this conceptual framework. Procedures for determining hydraulic, structural steel detail deficiency, overload, and collision vulnerabilities to failure have been developed and are in various stages of implementation. An overview of these procedures is presented herein specifically for each failure mode. Since the rating step is common to all modes, discussion of the rating step is presented in its entirety only in the section on hydraulic vulnerability procedures and is not repeated in the sections on the other procedural discussions.

## Hydraulic Vulnerability

The goal of the hydraulic vulnerability assessment is to identify bridges prone to failure due to scour or related hydraulic forces and, if necessary, to initiate measures such as NYSDOT's Floodwatch and Post-Flood Inspection Programs, interim retrofits, and capital improvements to reduce hydraulic failure vulnerability. This is accomplished through a series of assessment steps that result in a hydraulic vulnerability rating for each structure.

Figure 2 provides an overview flow chart of hydraulic vulnerability assessment procedures. A detailed discussion of this procedure has been presented previously by Shirolé and Loftus (2) and is summarized here.

## Screening

The hydraulic vulnerability assessment process begins with the inventory screen. This screen uses information contained in the department's Bridge Inventory and Inspection System (BIIS) data file to identify structures that do not span water (summarized in Table 2). These structures are assigned a vulnerability rating of 6 (not applicable) and are eliminated from the assessment process. The remaining bridges are subjected to a two-part susceptibility screening that consists of a review of bridge plans, construction documents, inspection reports, and other available information to place bridges in four susceptibility groups, numbered groups 1 through 4. The susceptibility groups are used to indicate a bridge's relative susceptibility to damage from hydraulic forces and to determine the order in which they progress to the classification step. Figure 2 contains a tabulated list of factors that are used in the first part of the susceptibility screen to identify structures with low susceptibilities to scour damage. Those structures are

H			C		E
Y	O		O	C	A
D	V		L	O	R
R	E		L	N	H
A	R	S	I	C	Q
U	L	T	S	R	U
L	O	E	I	E	A
I	A	E	O	T	K
C	D	L	N	E	E
2	3	2	3	6	5 (Example)

DECREASING ORDER OF SIGNIFICANCE - Left to Right  
(Based on Frequency of Occurrence)

FIGURE 1 Bridge vulnerability rating code.

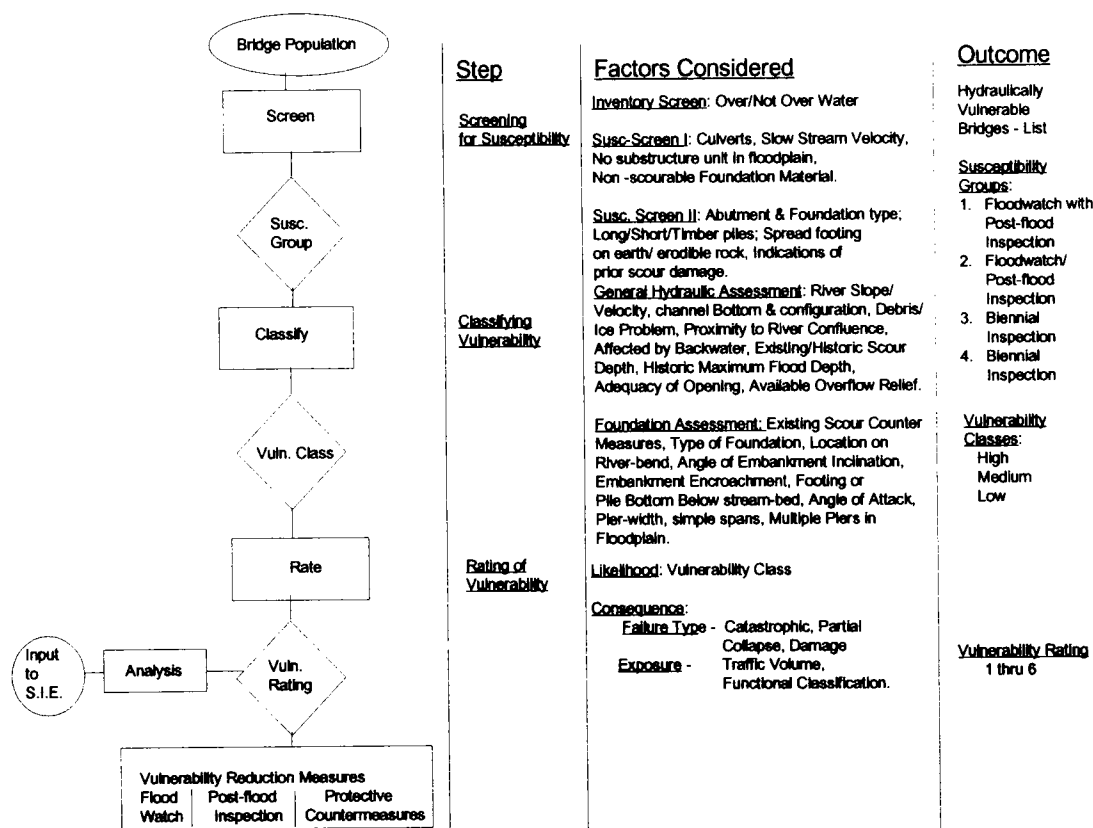


FIGURE 2 Hydraulic vulnerability assessment.

placed in susceptibility group 3 or 4. The second part of the susceptibility screening places bridges in the first, second, or third susceptibility group on the basis of their substructure configurations and assessment of scour conditions by considering factors listed in tabulated form in Figure 2.

### Classification

The second step in the hydraulic vulnerability assessment process is to evaluate a structure's vulnerability to scour damage on the basis of its site hydrology and hydraulic characteristics. This classification step consists of general hydraulic and foundation assessment procedures. The considerations on which these procedures are based are listed in tabulated form in Figure 2. This step quantifies the potential vulnerability of a structure to hydraulic damage relative to the vulnerabilities of other bridges in the classification process and places the structure in a high, medium, or low hydraulic vulnerability class. These classes indicate the likelihood of failure and are used to determine the vulnerability rating for a structure and also whether a structure should be placed on a floodwatch list or a postflood inspection list (3). NYSDOT's Floodwatch Program is intended to

ensure that bridges with a high susceptibility to damage or failure from hydraulic forces are monitored during periods of flooding, as long as the bridge remains vulnerable. The Post-Flood Inspection Program monitors the performance of hydraulically vulnerable bridges following a major flood event.

### Rating

The hydraulic vulnerability rating is determined by using the results of the classification process, combined with an evaluation of the consequences of a failure. The actual vulnerability rating is determined in a manner similar to that in the classification process, in that rating

TABLE 2 New York State Bridges over Water

Characteristic	Number of Bridges		(a)+(b)	% of Total
	State (a)	Non-State (b)		
Non-Navigable	3407	8054	11461	59%
Navigable	58	127	185	1%
NYS Canal	224	107	331	2%
Unknown	300	177	477	2%
Total	3989	8465	12454	64%

scores are assigned to evaluate the likelihood and the consequence of a failure and are added together to determine the hydraulic vulnerability rating.

### Evaluation

A detailed hydraulic analysis of vulnerable bridges is conducted on a prioritized basis to provide a quantitative assessment of the performance of an existing bridge in comparison with current hydraulic design requirements. The results of this analysis are then used in an SIE to determine the stability of a bridge against hydraulic forces. The analysis is also necessary to design hydraulic improvements and scour protection countermeasures at a bridge, and the results can supplement and refine the data used in the classification and rating procedures. The most commonly used hydraulic vulnerability reduction measures are riprap, stone fill, and gabions installed at a pier or abutment. Some of the other available methods include constructing guide banks and dikes to protect abutments, improving the channel to lessen the potential for the occurrence of scour, installing sills or drop structures to stabilize the channel, and strengthening the existing foundations or

increasing the bridge opening to lessen the vulnerability of the structure.

### Steel Detail Deficiency Vulnerability

The goal of the steel detail deficiency vulnerability assessment is to identify bridges prone to failure due to steel detail deficiencies or deterioration and, if necessary, to initiate measures to reduce failure vulnerability. This is accomplished through a series of assessment steps that result in a steel detail deficiency vulnerability rating for a structure. Figure 3 provides an overview flow chart of the steel detail deficiency vulnerability assessment procedures.

### Screening

The screening step consists of an inventory screen and a more refined bridge-type screen. The inventory screen is a preliminary screening procedure that identifies non-metal, closed, and abandoned bridges and structures that do not carry truck traffic, such as parkway and pedestrian bridges, through a review of information

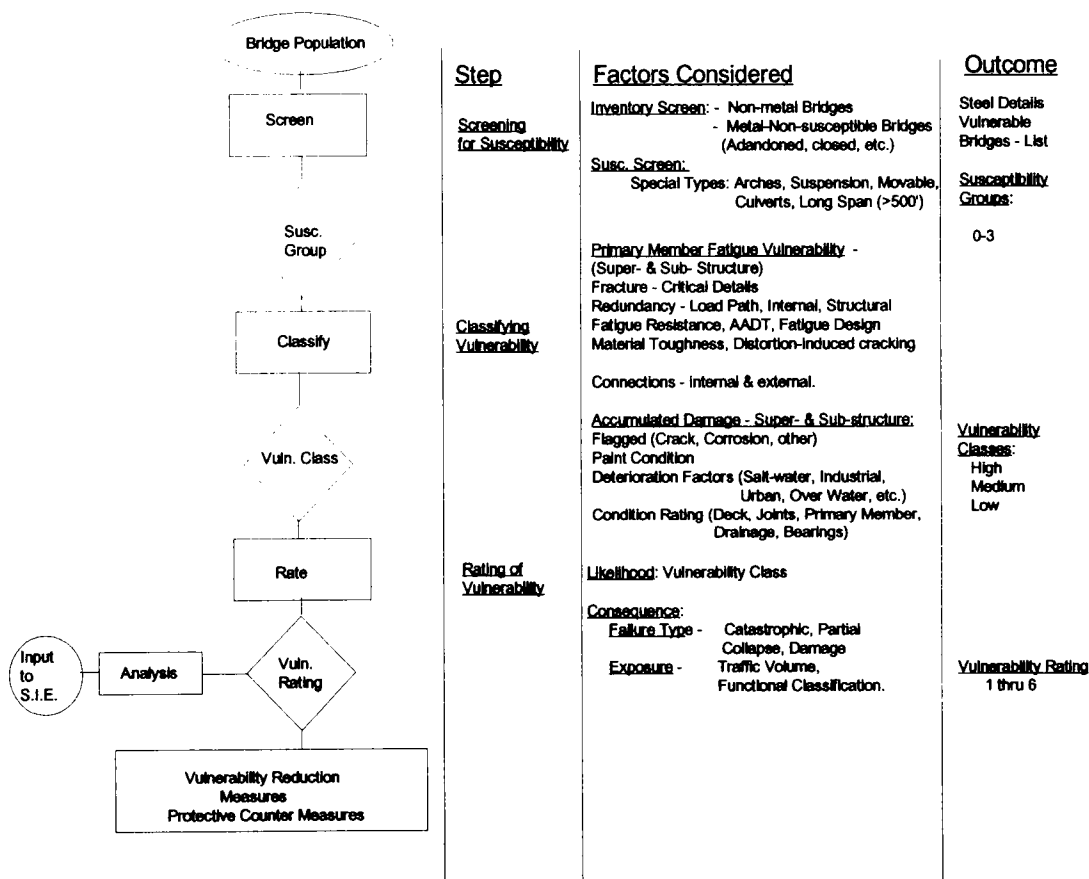


FIGURE 3 Steel detail vulnerability assessment.

contained in the BIIS data files and the Superstructure Code Database. These structures are assigned a vulnerability rating of 6 (not applicable). No further actions are required for these structures.

The first stage of the bridge-type screen is to segregate special types of bridges that are not easily analyzed through the standardized vulnerability assessment procedure. These bridges, which are evaluated directly through an SIE, include all culverts, arches, tied arches, suspension bridges, moveable bridges, steel plate pipes, pipe arches, railroad bridges, and long-span (>500-ft) bridges. The second stage sorts each of the remaining bridges into one of three susceptibility groups on the basis of their respective superstructure types. These groups imply a relative susceptibility to failure due to fatigue, deterioration, or other steel detail-related causes and are used to determine the order in which bridges progress to the classification step. At the completion of the bridge-type screen, bridges in susceptibility group 1 are progressed to the classification step first; this is followed by groups 2 and 3, respectively.

### *Classification*

The classification step evaluates the vulnerability of a structure to failure on the basis of its structural steel details, as well as its traffic, design, deterioration, and environmental conditions. This step quantifies the potential vulnerability of a structure to steel detail deficiency failure relative to that of other bridges in the classification process and places the structure in a high, medium, or low vulnerability class. The vulnerability classes describe the relative potential that a structure has for failure because of steel detail-related problems. These classes are used to determine the vulnerability rating of a structure.

A field evaluation by a trained engineer may be necessary to complete the vulnerability classification step for some bridges. During the field inspections the evaluating engineer is required to look for catastrophic failure-prone conditions that could lead to a sudden collapse of the structure. If any potentially catastrophic conditions are observed, then appropriate interim vulnerability reduction measures are to be recommended to safeguard the bridge against a failure until a more detailed evaluation and remediation plan can be developed.

Figure 3 indicates in a tabulated form the criteria used in the classification step. They include consideration of primary member fatigue vulnerability for both super- and substructures, the vulnerabilities of connections, and accumulated super- and substructure damage. The score from the classification step is used to place a bridge in its appropriate vulnerability class.

### *Rating*

The steel detail deficiency vulnerability rating is determined by the procedures described in the hydraulic vulnerability discussion.

### *Evaluation*

Structures with a vulnerability rating of 1 or 2 are immediately considered for retrofit work as a vulnerability reduction measure. If the decision to retrofit the structure is made, the work is programmed, and when the retrofit work is completed, the structure is given a new rating taking into consideration the work that was done. Structures with a vulnerability rating of 3 that are included in the capital improvement program are evaluated during their design phase. If the decision is not to retrofit, the vulnerability ratings for the other five failure modes are also considered. On the basis of all of these ratings, a priority list is established and SIEs are performed in this priority order.

### *Overload Vulnerability*

The goal of the overload vulnerability program is to identify the relative vulnerability of the state's bridges to failure due to overload so that necessary vulnerability reduction measures can be implemented in an efficient and effective manner. Figure 4 presents an overview flow chart of the overload vulnerability assessment process.

### *Screening*

The screening process begins with an inventory screen of the BIIS data file to identify highway bridges. These bridges progress to the classification step. Non-highway bridges and culverts are assigned a vulnerability rating of 6 (not applicable) and are eliminated from the assessment process.

### *Classification*

The classification step begins with a preliminary classification stage that consists of load expectancy and structural capacity assessments. The factors considered at this stage are listed in tabulated form in Figure 4. The assessments use bridge inventory information on bridge load types as well as structural strength and condition to assess the vulnerability to overload failure and result in a preliminary classification score. Local conditions such as load restrictions on bridge approaches, heavy truck traffic, level of truck weight limit enforcement, and physical site restrictions for trucks entering



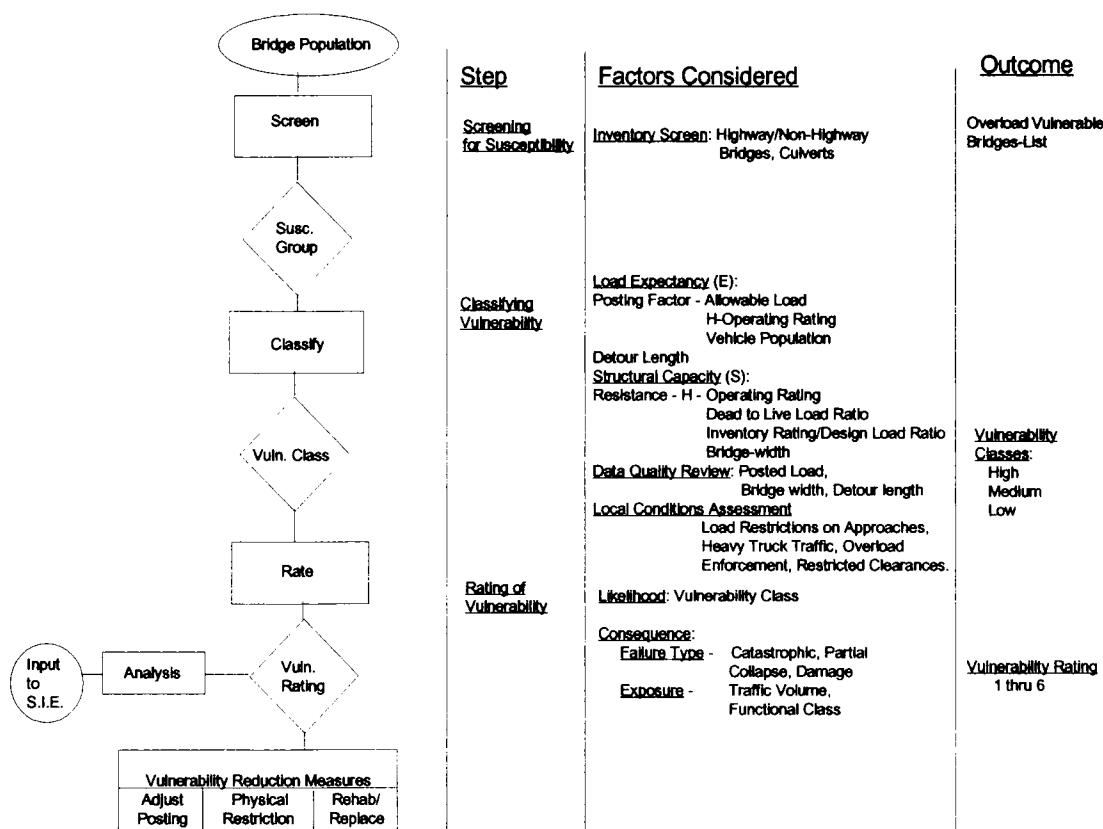


FIGURE 4 Overload vulnerability assessment.

a bridge are also considered. On the basis of this information the preliminary classification scores are then adjusted as necessary to arrive at a final vulnerability classification score. This classification score quantifies the structure's overload vulnerability relative to those of other bridges in the classification process and places the structure in a high, medium, or low vulnerability class. The vulnerability class describes the relative potential that a structure has for failure due to overloads and is used in determining the vulnerability rating.

### Rating

The overload vulnerability rating is determined by the procedures described in the hydraulic vulnerability discussion.

### Evaluation

The evaluation step provides a quantitative engineering analysis of a bridge's vulnerability to overload failure in comparison with current design standards. It is conducted immediately for structures with a vulnerability rating of 1 or 2. Structures with a vulnerability rating of 3 that are included in the capital improvement pro-

gram are evaluated during their design phase. The results of this evaluation are used in conjunction with evaluations for other failure modes to compile an SIE report for a bridge and to develop any required vulnerability reduction measures.

An evaluation of overload vulnerability will typically consist of a load rating analysis to determine the load-carrying capacity of a structure and also to provide information for use in the development of retrofit plans. In some cases a physical load test may also be necessary or useful. Typical overload vulnerability reduction measures consist of load posting, closing, rehabilitation or replacement.

### Collision Vulnerability

The goal of the collision vulnerability assessment procedure is to identify the relative vulnerability of the state's bridges to failure due to vehicle, vessel, or train collision impact damage so that any necessary vulnerability reduction measures can be implemented in an efficient and effective manner. Figure 5 presents an overview flow chart of the collision vulnerability assessment process.

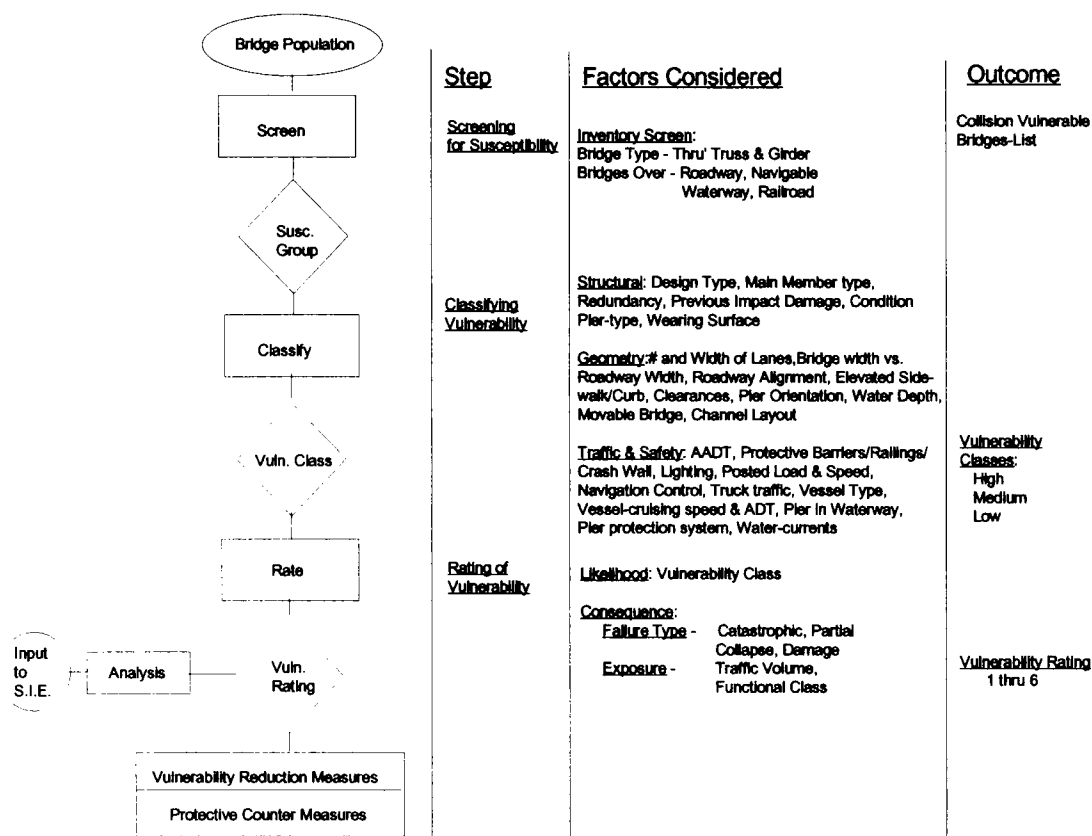


FIGURE 5 Collision vulnerability assessment.

### Screening

The collision vulnerability assessment process begins with an inventory screen of the BIIS data file to identify bridges vulnerable to collisions on the basis of their structure type (e.g., thru truss/girder) and whether they span a roadway, navigable waterway, or railroad. Structures that do not meet the screening parameters are assigned a vulnerability rating of 6 (not applicable) and are eliminated from the assessment process.

### Classification

The classification step uses information (tabulated in Figure 5) such as impact factors, exposure factors, characteristics of traffic, and the geometrics of the structure and its approaches to evaluate the vulnerability to collision impact damage or collapse. The product of this step is a vulnerability classification score and an assignment to a high, medium, or low vulnerability class. The vulnerability classes describe the relative potential that a structure has for failure due to collision impact dam-

age, and it is used in the rating step to determine the vulnerability rating for a structure.

### Rating

The collision vulnerability rating is determined by the procedures described in the hydraulic vulnerability discussion.

### Evaluation

The evaluation step provides a quantitative engineering assessment of a bridge's vulnerability to collision impact damage or collapse. The results of this evaluation are used, in conjunction with evaluations for other failure modes, to compile an SIE report for a bridge and to develop any required vulnerability reduction measures. Typical vulnerability reduction measures consist of installing or constructing protective features or developing rehabilitation or replacement plans for the structure. A typical collision vulnerability protection measure for a "thru" type of structure would be installation, or up-

grade, of a bridge railing or barrier system that is sufficient to mitigate an impact. Other possible vulnerability reduction measures may include rehabilitation or removal of previous impact damage.

### Status of Implementation

The development of the assessment and evaluation procedures has been performed in a sequential manner, and extensive training and implementation activities have followed the completion of development activities for each failure mode. The training activities have entailed the development of new training materials and organization of available training materials with hands-on training exercises in the use of assessment and evaluation procedures for each type of vulnerability. Table 3 summarizes the implementation status of the assessment and evaluation procedures for each of the six failure modes.

### NYSDOT'S COMPREHENSIVE BSA POLICY

Since 1990 the NYSDOT BSA activities have progressed systematically through the development of vulnerability assessment and evaluation procedures, specialized training in their application, and implementation of vulner-

ability reduction measures deemed necessary as the process was being implemented. The knowledge and experience gained through these activities enabled the department to develop its comprehensive BSA policy (4). Adopted in 1992, this policy clearly outlines the department's commitment to ensuring public safety and minimizing adverse economic impacts due to the loss of service of the state's bridge network. It states NYSDOT's objective to implement a proactive system to assess and evaluate all state-owned bridges for their failure vulnerabilities and outlines a specific policy and plan of action for each failure mode organized in a prioritized manner.

The specific plan of action for each failure mode consists of the following:

- Development of vulnerability assessment procedures. Each type of failure is to be analyzed and an assessment procedure is to be developed to rate each bridge on the basis of the contributing vulnerability factors. The vulnerability rating system will ensure that bridges are rated on a uniform scale for the respective factors and will be compatible with the comprehensive bridge management system being developed by the department.

Each failure mode will require an individual assessment procedure that will be very technical in nature and that will require specialized training in some instances. Owing to the variety of field conditions, this process will require enough flexibility to allow for engineering judgment at all stages of the assessment. This procedure is merely a tool for the engineer to use in making comparative assessments of a large population of bridges.

- Vulnerability assessment of existing bridges. All state bridges shall be assessed for each of the six failure vulnerabilities described in this paper and shall be rated from 1 to 6 for each failure mode, consistent with the likelihood and consequence of failure of each bridge. Structures rated 1, 2, or 3 shall be programmed for appropriate action, whereas those rated 4 shall be scheduled for special monitoring inspections to preclude unexpected failures. The vulnerability ratings will be used to prioritize bridges for an SIE that will provide documentation for any vulnerability reduction action considered.

- Programmed vulnerability reduction actions. Structures scheduled for replacement are to be designed according to the current AASHTO standard specifications for highway bridges, as modified/supplemented by appropriate NYSDOT bridge design and construction standards and specifications. Special attention shall be given to site-specific considerations to ensure that the replacement structure is not vulnerable to failure modes. Structures scheduled for rehabilitation shall be designed and detailed to significantly reduce or elimi-

TABLE 3 Status of Implementation

FAILURE MODE	STATUS
HYDRAULIC	Assessment Procedures Manual developed and promulgated <u>State-owned Bridges:</u> Assessments 96% (3761) completed Over 300 evaluated through hydraulic analysis & scour calculation, Over 500 have vulnerability reduction projects either in progress or completed. 551 are on Floodwatch to ensure public safety during flood events, and 877 are on Post-flood Inspection Program. <u>Locally owned Bridges:</u> Assessments for 7973 bridges started in 1995. Results to be forwarded to owners. During past two years, computer inventory screen lists were provided to local bridge owners, with recommendations for a floodwatch program for certain bridges.
STEEL DETAILS	Assessment Procedures Manual developed and promulgated <u>State-owned Bridges:</u> Assessments 56% (3107) completed Prior Programs: Pin and Hanger - 21 bridges evaluated and retrofits completed 2 and 3 Welded Girder - 108 bridges evaluated and retrofits completed Vulnerability reduction projects for 75 bridges.
OVERLOAD	Assessment Procedures Manual developed and promulgated <u>State-owned Bridges:</u> Assessments 25% (1882) completed Currently 96 bridges load-posted <u>Locally owned Bridges:</u> Computer Inventory Screen list to be sent to local bridge owners in 1995
COLLISION	Assessment Procedures Manual developed and promulgated
CONCRETE DETAILS	Assessment Procedures development scheduled to be completed in 1995
EARTHQUAKE	Interim Assessment procedures and policies promulgated Final Assessment procedures scheduled for completion in 1995

nate their vulnerabilities to failure modes by incorporating vulnerability reduction measures in the rehabilitation plans.

The BSA program shall be an ongoing and proactive approach aimed toward the assessment, evaluation, and mitigation of the failure vulnerability of New York State bridges.

This policy shall apply only to NYSDOT-owned bridges. However, the department will provide information on its BSA policies and practices to other bridge-owning governmental agencies in the state and encourage their implementation.

## CONCLUSION

NYSDOT's comprehensive BSA program has successfully progressed from its planning phase to development and implementation phases. Six modes of failure—hydraulic, overload, structural steel detail deficiencies, collision, structural concrete detail deficiencies, and earthquake—were identified as significant after a nationwide survey of bridge failures. The vulnerability assessment procedures for the first four modes of failure have been developed; this has been followed by inten-

sive training in the use of those procedures, guidance and monitoring of their actual application, and the use of vulnerability reduction measures that have been implemented or that are under way. NYSDOT's comprehensive BSA policy, developed through the knowledge and experience it gained through the development process and subsequently adopted in 1992, clearly outlines New York State's approach and commitment to ensuring the safety of its extensive bridge network.

## REFERENCES

1. Shirolé, A. M., and R. C. Holt. Planning for a Comprehensive Bridge Safety Assurance Program. In *Transportation Research Record 1290*, Third Bridge Engineering Conference, Vol. 1, Bridges and Structures. TRB, National Research Council, Washington, D.C., 1991, pp. 39–50.
2. Shirolé, A. M., and M. J. Loftus. Assessment of Bridge Vulnerability to Hydraulic Failures. Presented at 71st Annual Meeting of the Transportation Research Board, Washington, D.C., 1992.
3. *NYSDOT Bridge Flood Warning Action Plan for State Bridges*. Structures Design and Construction Division, New York State Department of Transportation, May 1989.
4. *Policy on Bridge Safety Assurance*. New York State Department of Transportation, 1992.

# Pontis Version 3: Reaching Out to the Bridge Management Community

---

Paul D. Thompson, *Cambridge Systematics, Inc.*

AASHTO, through its AASHTOWare software joint development and support program, has recently adopted the Pontis bridge management system and has completed development of Release 3, to be known as AASHTOWare Pontis. With the participation of 46 state-level departments of transportation (DOTs) and FHWA, the project represents a significant effort to advance the implementation of the system and broaden its audience to include large and small transportation agencies, including local governments working in cooperation with their state DOTs. The Release 3 software will be a major advance in the product: it will be highly graphical in its user interface, work with a wide variety of commercial data base managers, employ an innovative system for coordinating the work of multiple decision makers, and include a state-of-the-art project-level analysis to complement its already-advanced network-level capabilities. Cambridge Systematics, Inc., as a contractor to AASHTO, developed the product.

Pontis was conceived in 1989 by a unique team consisting of FHWA, six state departments of transportation (DOTs) (led by California, which administered the contract, and including Minnesota, North Carolina, Tennessee, Vermont, and Washington) TRB, and three consulting firms (Cambridge Systematics, Inc., and Optima, Inc. in a joint venture, and the Urban Institute). At the time, development of bridge

management systems was just beginning to bloom, with many states beginning creative efforts. The Pontis project was initiated by FHWA through its Demonstration Project 71 as a way for states to cooperate on the development of a core system that would address difficult central issues in bridge management while leaving unlimited room for innovation by the states.

Initially the focus of the effort was a methodology for combining engineering and economic concerns in network-level policies, priority setting, and project scheduling. Pontis 1.0 was completed in February 1992 and beta-tested over the remainder of that year by 13 states and 1 local government. From the beta-testing results, it was clear that the project had defined and addressed an important need recognized by almost all the states. The beta-testers had accumulated a long list of enhancements to make the software easier to use and recommended the standardization of an improved procedure for assessing bridge condition and the eventual development of a more comprehensive bridge management system that would include full-scale data base management and project-level features.

With participation by 21 states, a standardized condition assessment system, called the commonly recognized (CoRe) elements, was developed in 1993. Combined with a slate of small and medium-size software enhancements, this work resulted in the completion of Pontis Release 2 in November 1993. FHWA distributed the software and manuals to the states in summer 1994,

when AASHTO assumed ownership and support responsibilities for the project participants.

Release 2 represented an incremental enhancement of Pontis, in that the fundamental modeling methods and network-level orientation of the system were unchanged from Release 1. Some of the beta-testing recommendations, however, were much more ambitious: many of the states foresaw that Pontis could be extended to cover a broader range of bridge management needs, including providing a software framework that ultimately could house new developments in the science of project-level bridge management models. Many Pontis users could also see the potential for the open-system philosophy of Pontis to be extended to work seamlessly with diverse external systems such as data base managers; doing so would greatly enhance the agency's ability to access Pontis and use its results.

Finally, the experience gained by the many states using Pontis 1.0 has led to a new vision of ways in which the perspectives of budgeting, levels of service, project programming, and project-level bridge management could be closely integrated. By taking advantage of newly available computing power and computer graphics, it is now possible to maintain multiple consistent models of an agency's bridge management health and its future plans, with an intuitive way of looking at bridge management problems from all sides. This could allow local bridge managers to maintain a comfortable project-level perspective without losing the link to network-level budgets and performance standards. Combining the need for support of Release 2 and the development of this new concept in Release 3, AASHTO secured the financial support of 46 states and FHWA to begin the effort, which was completed in summer 1995 under a contract with Cambridge Systematics, Inc.

## NEW VISION FOR PONTIS

By providing an objective way of reconciling budget limitations with service expectations, Pontis filled an important need, proving the value of network-level bridge management systems. Even so, Pontis Releases 1 and 2 were in many ways embryonic. Although the software is fast and not difficult to learn, system users must devote considerable attention to maintaining the software itself, such as paying constant attention to the use of the correct models in the correct order and keeping track of exceptions and overrides to the many network-level generalizations about costs, deterioration, and service levels. When beta-testers encountered difficulties in using the system, it was often because of missteps in the modeling process or difficulty in determining what features should be used to accommodate project-level factors. As in the first generation of any completely new

system, it has been necessary to observe people using the system the way that they envision that it should work, in order to discover how the system should best be presented.

What emerged from the first 2 years of active Pontis implementation is a much-improved understanding of how different people in a transportation agency can use Pontis to help them improve their understanding of bridge conditions and the implications of their decisions. Although Pontis already includes an extensive toolbox with all the tools necessary to build and operate valid network-level models, it became clear that a higher level of operation of the system is needed, one in which users do not have to be so strongly aware of the mechanics of the engineering and economic models in order to answer their questions related to bridge management. The network-level models can be made more intuitive by the use of graphics and a more flexible optimization method, and the relevance to the agency can be greatly enhanced by the full implementation of a true project-level perspective. Moreover, these features can be best implemented not by adding menu items to the existing software but by completely redesigning the way in which the system will be perceived and used. Thus even though the same network-level modeling methods and data are used, their organization and appearance have been changed greatly.

In the conceptual development of Release 3, a major challenge for the team was to conceive an organizing framework for the new system that is simple, familiar to all users, and exhaustive of the major features of the system. This framework should describe the system in a way that makes it obvious which parts any particular user will need at any particular time, and it must completely include all of the features that exist in the earlier versions.

This latter point has great short-term importance: since Release 3 was developed at the same time that Release 2 was being implemented, it was vital that users clearly perceive Release 2 as a partial implementation of Release 3, that adopting Release 2 is the best path toward the ultimate adoption of Release 3, and that no work done previously using Release 2 must be discarded once Release 3 is available.

Figure 1 is a conceptual framework that meets these requirements. The diagram shows a project-level dimension of bridge management intersecting with the network level. In the network-level box is the set of major modeling features that currently exist in Pontis; in the project-level box is a new set of features for analyzing a selected bridge. Where these two boxes intersect is the domain of project prioritization and scheduling, which must satisfy both the network and project-level perspectives. Every transportation agency has responsibilities in all of the domains of this diagram, but each

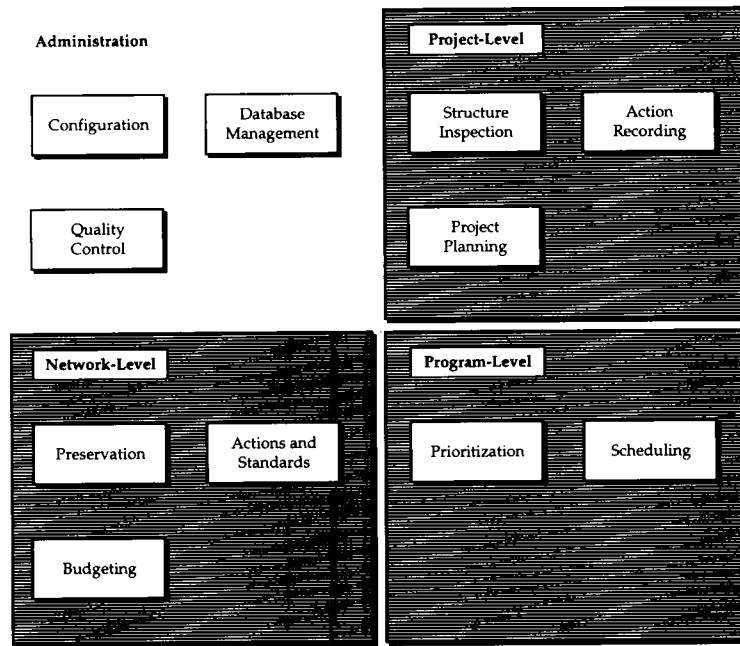


FIGURE 1 Conceptual framework for Pontis 3.0.

individual tends to concentrate on just one part. Through a common data base and an integrated set of models, Pontis can allow each individual to work in the domain for which he or she is responsible, while maintaining access to up-to-date information on how the other domains affect his or her own concerns.

Through this conceptual framework, budgets and service policies can constrain programming decisions and guide project-level decisions; at the same time, project-level decisions can provide detail to program plans, influence priorities, and supply refined alternatives to network-level decision making. Through this framework, the differing perspectives can work together to achieve an agency direction that meets both sets of needs. Given the availability of a graphic user interface, it has become possible to have a software package whose overall appearance follows the general outlines of this diagram.

## NETWORK-LEVEL DOMAIN

The network-level perspective of Pontis uses an engineering economic model of the agency's bridge inventory, its cost structure, and its aggregate life-cycle behavior to analyze questions of budget allocation and policy that affect large subsets of the inventory. Among the major management concerns at this level are

- Ensuring that funding is adequate to deliver expected levels of service,

- Determining the economic and opportunity costs of new policy commitments that the agency may need to make,
- Making satisfactory progress in reducing the accumulated backlog of deferred maintenance,
- Ensuring that new preservation needs are identified and met in a strategically timed manner,
- Forecasting and coping with new functional needs that may arise, and
- Communicating the agency's capabilities and needs in a consistent manner to elected officials and the public.

Although this domain, by definition, does not include bridge-level analysis, it is important that network-level planning values be consistent with the aggregated body of project-level concerns and that project-level activities be constrained by network-level policies. When such consistency exists, then the agency is most likely to be able to meet its commitments to the public with the limited budget available.

Figure 2 summarizes the key trade-offs in the network-level domain. In this diagram, maintenance, repair, and rehabilitation (MR&R) needs and functional/structural needs are brought side by side. The shaded bars for each need category indicate decreasing benefit/cost ratios, increasing annual funding requirements, and increasing accomplishments over several years. Each bar begins at the zero funding level and ends at the level at which all possible actions considered by the models are taken in the first year. Any horizontal line drawn across the

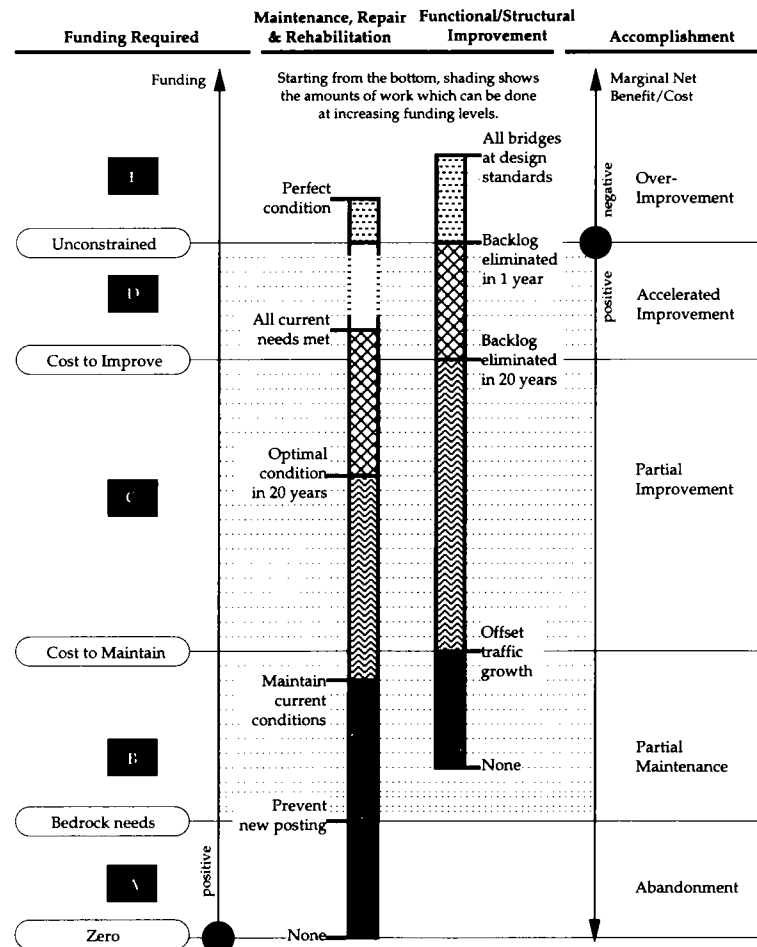


FIGURE 2 Network-level perspective: investment and accomplishment trade-offs.

two bars must cross both bars at the same benefit/cost ratio, and thus it represents a particular funding level and allocation of funding between MR&R needs and functional/structural needs. This is equivalent to saying that the two lists of needs are combined and priority ranked together.

In Funding Interval A in Figure 2, the highest-priority needs may be the MR&R actions that would prevent bridges from becoming posted if they are not already. If funding is maintained continuously within this interval, then new postings and closings must occur, since there is not enough money to prevent it. This funding interval is therefore referred to as abandonment. As funding increases to the top of Interval A, called "bedrock needs," only enough money is spent to prevent any additions to the structural needs list. Funding Interval B represents additional funding between the level of preventing new postings and the level at which current conditions can be maintained in the MR&R model. At the end of this interval, there is at least enough funding to

offset deterioration and enough to address the highest-priority functional and structural needs, up to the point at which the total backlog of needs does not increase.

Funding Interval C represents sufficient funding to improve the condition of the bridge inventory. MR&R policy in this interval is geared toward reducing the backlog of deferred maintenance, eventually achieving a condition level at which a long-term cost-minimizing maintenance policy can be put in place. Funding Interval D represents accelerated improvement, where the backlog of functional and structural needs is exhausted in fewer than 20 years. This interval extends to funding levels for which the backlog might be funded as quickly as the first year. Since the MR&R needs are based on a life-cycle cost optimization, they represent not the maximum possible expenditure, but only the maximum expenditure on projects having positive net benefits. Similarly, functional and structural needs represent only the possible expenditures on bridges that are below desired service standards. As Interval E indicates, it is possible



to spend beyond the total unconstrained needs, implementing projects that have a negative net benefit according to the assumptions of the models. As with the abandonment interval, this overimprovement interval is considered unrealistic and therefore is not included in the capabilities of the models.

As Figure 2 suggests, the Pontis models generate a continuous range of funding and policy alternatives and use benefit/cost models to recommend relative priorities. For policies that are not "optimal" according to the economic models (but that may be attractive for non-economic reasons), Pontis can offer feedback in terms of the economic performance of such policies and the amount of deviation from economic optimality.

To make the network-level analysis quick and convenient, Pontis Release 3 will feature graphic controls in the user interface that control bridge allocations, MR&R policies, and service objectives. The trade-offs among these factors will be managed by a set of optimization models nearly identical to the Release 2 models (based on Markovian deterioration probabilities and linear programming optimization), with considerable input from the project-level and programming domains of the system. Users can set funding and policy decisions of interest and receive responses by means of presentation graphics, showing the resulting adjustments to other planning factors. For example, a user can lower the functional standard for clear deck width for a particular functional class and see either the amount of money that it saves or the best alternative use of the saved money.

## PROJECT-LEVEL DOMAIN

For many (perhaps most) users of bridge management systems, it is most intuitive to view bridge management problems from the perspective of one or more specific bridges for which immediate analysis is needed. Such analysis can take into account the particular site-specific factors that often dominate decisions on cost estimation and project development. It is essential that project-level planning be conducted within the context of a consistent network-level model, because only then is it possible to be sure that a project is affordable, will not be displaced later by a project of higher priority, and meets the requirements of an affordable set of agency policies. When the marriage of network- and project-level concerns is inadequate, the symptoms can be obvious: scope creep (cost escalation due to work added relatively late in project development), deferred work (usually maintenance and repairs), expensive stop-gap actions, unenforceable policies, and loss of credibility with elected officials. One of the most important planned features of Pontis Release 3.0 will be the addition of a

project-level domain and a set of models which link them to the network-level domain. Major project-level concerns to be addressed are:

- Describing correctly the elemental configuration of the bridge and maintaining an up-to-date picture of the elements' conditions;
- Developing a programmatic strategy for the bridge that ensures its continued health;
- Recognizing past trends that may indicate changing conditions and possible unexpected needs;
- Identifying and resolving functional deficiencies;
- Recognizing project interrelationships that may affect the bridge's programmatic strategy;
- Estimating cost accurately, accounting for unique characteristics of the bridge;
- Selecting actions that consider unique characteristics of the bridge; and
- Performing efficient routine inspections.

Cost estimation will receive special emphasis, because it is widely considered to be the weakest component of bridge management analysis. In particular, the software has the ability to incorporate traffic control, mobilization, and work zone user costs, can supply these estimates at the project level, and uses the same information to ensure that these costs are included in network-level analysis. The Pontis database stores all historical actions which have been recorded in it, and this information is used in a cost updating procedure similar to the deterioration model updating procedure which was already available.

## PROGRAMMING DOMAIN

The programming domain includes information and models which integrate the network-level and project-level perspectives. This includes an analysis of project priorities, including the possibility of multiple project alternatives on the same bridge, and a scheduling capability which can recognize the constraints of multiple funding sources. Changes to network-level budgets and service levels can be reflected in the priority lists and schedules. Changes in project-level information, including new inspections, can have an immediate impact on the project's standing in the program. Unlike the step-by-step "batch-oriented" analysis of earlier versions of Pontis, Release 3 automatically finds the models it needs to update the program.

To enhance the convenience and relevance of programming information, users can organize it into goal-oriented program categories, such as bridge replacement, deck overlay, painting, etc. This will make it easy to see the costs and priorities within these programs,

and to see how the programs overlap on specific bridges. Programs based on vulnerability factors such as seismic, fatigue, and scour can also be developed.

Although the primary emphasis of Pontis is on economic analysis of bridge programs, the system has features to provide alternative ways of prioritizing projects, in order to take into account important issues such as vulnerability, equity, mobility, and air quality.

## SOFTWARE FEATURES

Pontis Release 3 was developed for Microsoft Windows and is compatible with Windows NT. Taking advantage of the Windows user interface, the software is highly graphical, including statistical graphics as well as specialized graphic controls and icons. Special emphasis is given to making it easy to navigate around the system. Software features are organized into user-focused perspectives: thus, for example, bridge inspectors will be provided with a full-featured inspection module that appears separate from other system features which the inspector would not normally need. It is possible to have multiple windows, possibly from multiple perspectives, open at the same time. All windows have the same set of features for printing and exporting, and a very flexible reporting facility is provided.

Recent developments in the standardization of software interfaces has made it possible to adopt an open-systems approach to Pontis. Instead of limiting the system to just one data base manager, Pontis uses the open data base connectivity (ODBC) standard to provide

access to multiple data base managers such as Access and Oracle. Pontis is delivered with just one data base manager, but agencies have the option of replacing it with one meeting their own standards. Pontis is a true multi-user system with appropriate security and access controls.

An important feature of the new software is the total elimination of the "black box" feel of the models. It is often possible to work backward from results to inputs, which should be tremendously helpful in grasping the underlying analytical process. Users can attach textual notes to any data record, which can help to call out unresolved issues or to document model assumptions. Complete context-sensitive help features at several levels of detail are provided, including an on-screen tutorial and automatic look-ups of glossary items and element/state/action definitions.

## CONCLUSIONS

Release 3 of Pontis is intended as a total bridge management system package, which can replace and upgrade the older systems now in existence in many state DOTs. Release 3 represents a comprehensive effort to reach out to the entire bridge management community, providing a balanced approach to meeting the needs of a diverse user group which includes local agencies and decentralized state DOTs. The new version is intended to be easier to use than Release 2, and more flexible in its ability to adapt to multiple data bases and customized models.

# Environmental Classification Scheme for Pontis

---

Dixie T. Wells, *Virginia Transportation Research Council*

In efforts to comply with the federal mandate for bridge management systems, many states are implementing Pontis. Pontis is the network-level bridge management system developed through FHWA's Demonstration Project 71. One component of the Pontis implementation process involves assigning the bridge elements to one of four environments. The environments used in Pontis—benign, low, moderate, and severe—represent relative distinctions among rates of deterioration resulting from operating practices and climatic exposure. Because of this, each agency should develop its own criteria for assigning elements to environments. A systematic strategy for developing a definition of these environments suitable to the needs of individual states is presented, and a step-by-step procedure for collecting data is explained. Regression analysis can then be used to analyze the data, thereby providing a way of defining the environments. To illustrate the method, an application is described for concrete bridge decks that uses operating practices and climatic exposures specific to Virginia.

**T**he 1991 Intermodal Surface Transportation Efficiency Act mandated the use of bridge management systems. These systems predict the future condition of bridges within a network both with and without intervening actions (1). To make this prediction, it is necessary to model the deterioration of the bridges. The Markov process is one method that captures the stochastic nature of this deterioration. Through use of only the current state of the bridge sys-

tem, the future conditions are predicted through a probabilistic mechanism. One-step transition probabilities depict the probability of the system deteriorating from its current state, or condition, to its next (future) state in a given interval. When all of the one-step transition probabilities for a specific time are grouped, the result is a transition probability matrix.

Because some parts of a bridge deteriorate more rapidly than other parts, transition matrices are needed to predict the rate of deterioration of each part. Modeling at this level of detail provides the information needed to specify corrective actions that should be taken. This method of modeling deterioration is used by Pontis, the network-level optimization and planning program developed through FHWA Demonstration Project 71 (2).

During the development of Pontis, it was recognized that the component condition ratings required as part of the National Bridge Inspection Standards program were inadequate. This inadequacy is because these components are a collection of various elements, each of which has a distinct deterioration pattern. To enable better predictive modeling and more representative feasible actions, Pontis uses individual elements of the bridge with clearly defined condition states and costs of actions.

To refine this predictive model further, it is helpful to examine a single bridge element. Consider, for example, two identically constructed concrete bridge decks, one of which is on a seldom traveled secondary road and the other on a heavily traveled interstate highway. To allow for the difference in deterioration rates because

of climatic exposure and operating practices (e.g., average daily traffic or annual chloride applications), Pontis requires the elements to be classified in one of four environments. Essentially, these are deterioration classes. These four environments—benign, low, moderate, and severe—must be defined by individual agencies.

### PURPOSE AND SCOPE

The purpose of this research was to develop a method to be used to determine how to assign bridge elements to one of the four environments—benign, low, moderate, or severe—within Pontis. [A more detailed explanation of the development and results appears in Wells (3).] Such a method would allow an agency to develop quantitative definitions of the environments on the basis of the appropriate operating practices and climatic exposure for every element in the agency's bridge population. To illustrate the method, an application is described for concrete bridge decks using operating practices and climatic exposures specific to Virginia.

### APPROACH

The problem posed by Pontis is that every element of a bridge must be assigned to an environment. Because most previous studies addressed the deterioration of individual bridges, the results cannot be used to generate environmental categories at this level. Because the definition of the environments should be tied to realistic situations anticipated within an agency's bridge population, the definition of the environments needs to be tailored to each state agency. For these reasons, a survey was created to collect the data for the initial environmental classification. The result of using the surveys is an easily implemented methodology that allows quick assignment of the elements to the appropriate environments. A review of the classification after several cycles of use will determine the method's effectiveness. If the method performs unsatisfactorily, the historical data collected in the intervening time can be used to reformulate the model.

Using the results from the surveys, a process was devised for creating the definitions of the four environments from the collected data. Steps include the organization of the data, the selection of the appropriate sample of the data, and the classification method to be used to develop the definitions. The method that emerged from a process of trial and error is discussed in the following section.

### FINDINGS AND INTERPRETATION

The methodology developed to quantify the definitions for the environments is a 10-step procedure:

1. Determine the element or group of elements of a structure for which the survey is to be developed.
2. Gather information about climatic conditions and operating practices that may affect the deterioration of the specified element or elements.
3. Determine the applicable, state-specific, quantitative ranges over which the selected factors may vary.
4. Create a survey for the element selected.
5. Distribute the survey.
6. Collect the survey and review the responses.
7. Create a data base of the responses and classify the elements into environmental categories.
8. Analyze the results of the environmental assignments on the basis of the definitions developed.
9. Distribute the results to survey respondents for verification.
10. Use the results to assign defined elements to the appropriate environment.

An application to concrete bridge decks in Virginia illustrates the method.

### Selection of Elements

Elements affected by the same operating practices and climatic conditions may be grouped. For example, all decks and slabs can be covered in one survey for the purpose of environmental classification, but the deck and the substructure elements should not be grouped together. Expert elicitation and historical records can be used to distinguish between the deterioration behaviors resulting from the use of different materials or structural properties.

### Information About Deterioration

One source of information is previous research studies. A second source is what experts in the field believe affects deterioration rates. For example, in the application of this method to concrete bridge decks, the type of span (e.g., simple versus continuous), age of the deck, average daily traffic, number of chloride applications per year, average daily truck traffic, and construction and maintenance procedures were found to be significant factors that influence the deterioration rates of concrete decks (4–7). In addition to the factors identified through the literature search, various experts at the Virginia Transportation Research Council mentioned freeze/thaw cycles. For this application, average daily truck traffic, freeze/thaw cycles, and chloride applications were selected.

It is important to ensure that the factors determined to affect the rate of deterioration are not used to dif-

ferentiate between Pontis elements. For example, the presence of epoxy-coated reinforcing steel is generally considered to affect the rate of deterioration of concrete decks. However, a concrete deck with epoxy-coated reinforcing steel is a separate Pontis element; thus, it should not be incorporated into the definition of the environment.

Another caution is that the surveys should focus on information that is easily available for the bridge elements. For example, in the case described, average daily truck traffic is measured easily, and the information generally can be found on record. However, the state of Virginia does not track the number of chloride applications. Because it is uncertain where and how frequently chloride is applied, the inspector must estimate the number of chloride applications, which adds inaccuracy and complexity. Freeze/thaw data can be derived from historical climatological information since most states are divided into climatological regions. However, this information is not recorded on bridge records.

### Determination of Applicable Ranges

For general survey construction, the ranges of the variables should include all of the possible responses for bridges in the agency's Pontis data base. In the example, a range of 0 to 800 was selected for average daily truck traffic, 0 to 75 for chloride applications, and 0 to 60 for freeze/thaw cycles. These ranges suggest that no bridge included in the state's Pontis data base is expected to have less than the minimum or more than the maximum value.

### Creation of Survey

The purpose of the survey is to relate the factors found to affect the deterioration of an element and their impact on the rate of deterioration. A graph like the one shown in Figure 1 is easily adapted to various elements and is an easy format for the respondent to understand. In this figure, an example was taken from the application to bridge decks in Virginia. The climatic and operating practices were average daily truck traffic (ADTT), annual freeze/thaw cycles (F/T), and annual chloride applications (C1).

The heavy line represents the particular characteristics of the deck the respondent is being asked to consider. In the graph in the top left corner, the respondent is asked to evaluate the rate of deterioration of the concrete bridge deck with high values of the three factors, as compared with all the other concrete bridge decks in the agency. Enough graphs should be depicted to allow subsequent analysis. One suggestion is that the user be

given  $3^f$  graphs, where  $f$  is the number of factors that will be used. This allows a high, medium, and low range for each variable. In the example shown in Figure 1, there are three factors; therefore, there should be a total of  $3^3 = 27$  graphs. Using the various combinations in the survey, many different combinations of variables can be surveyed. Other methods that can survey this wide range of possible responses were found to take much longer to answer.

### Distribution of Surveys

The information used to develop the definition of the environments will be based on the survey results. Because the responses from the survey will be used to determine to which environment the elements are assigned, it is important that careful consideration be given to the selection of the people to be surveyed. In Virginia, the survey was distributed to district bridge engineers.

### Review of Returned Surveys

If enough responses state that a particular relevant factor was initially disregarded, the survey should be reformulated so that the factors determined originally to influence the rate of deterioration and the other factors can be included. For example, respondents in Virginia noted that the type of span and the class of road or the speed of the traffic on the road should be considered in subsequent deck surveys.

### Classification into Environments

The classification will use the data collected from the surveys to create a definition of the four environments for a particular element for the bridges in the agency. If the data set is split, then part of the data can be used to "train" the model and the other part can be reserved to "test" the model. One way of estimating the error of the various approaches is to divide the sample data ( $\mathcal{L}$ ) into two sets ( $\mathcal{L}_1, \mathcal{L}_2$ ). The data in  $\mathcal{L}_1$  are used to train or build the model. The data in  $\mathcal{L}_2$  are then used to test, or validate, the model for its ability to assign the described cases to the appropriate environment (8). In this case, the appropriate environment is the one to which the experts in the survey assigned the described element.

Because the Pontis environments are categorical variables, the environments were mathematically manipulated into real, ordered variables. In this manipulation, the set of environments {benign, low, moderate, severe} was translated into {1, 2, 3, 4}, where 1 represents the

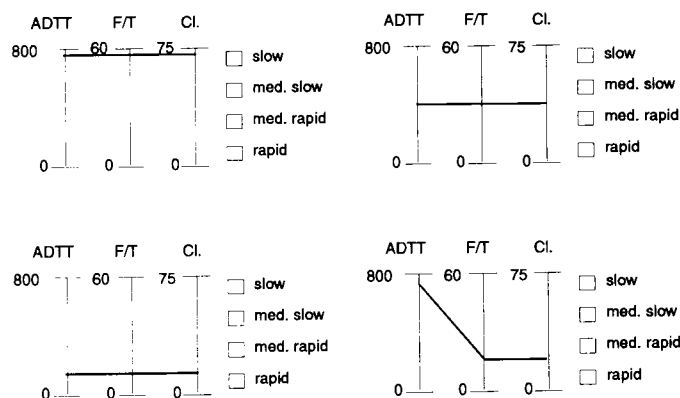


FIGURE 1 Suggested format for the survey.

class with the slowest deterioration rate for the area of use. This manipulation was possible because the environmental classes represent increasingly greater rates of deterioration, and it allowed a broad selection of modeling approaches.

One method used to quantify the environments was regression analysis. In this case, an equation is generated that can be used to estimate the output for future variable sets. The value produced using the equation is rounded to the nearest integer to find the appropriate environmental assignment (where 1 is benign and 4 is severe). In this application, the following equation is given:

$$En = 0.001347 (ADTT) + 0.005533 (F/T) + 0.024999 (Cl) + 0.677581$$

where

$En$  = the environment,  
 $ADTT$  = average daily truck traffic  
 $F/T$  = freeze/thaw cycles, and  
 $Cl$  = the number of chloride applications per year.

## Analysis of Results

In general, the model should provide accurate and realistic classification, be easy to use, and be familiar to agency staff. When several classification methods were compared, multiple regression was found to provide a good model of the data (3). In addition, it is a common statistical method, and most agencies have software available for regression analysis. Regression analysis did not predict any class that was more than 1 off the actual class predicted by the respondents.

A weakness of the type of regression analysis used is that all of the input variables will appear in the output

equation with some weight. If a variable is found to have no impact on the environmental classification, some other methods do not use it in the model. The inclusion of all of the variables in the resulting model is tolerable if all of the factors influence the deterioration to some degree. If sufficient previous research exists, as was the case with bridge decks, then the factors can be verified.

As the survey method is developed and later used, there are two major sources of error. The first is the classification method itself. The second is that the information used to train and then evaluate the model was gathered from a survey of people who may have different frames of reference, experience, and exposure. Because the responses from the survey will be used to determine the assignments of the environments, it is important that careful consideration be given to the selection of the people to be surveyed. It is important that these people have experience in the field. It is also important that they be willing to spend the time to complete the survey as accurately as possible.

If an element is assigned to an environment that is not a true representation, the predictions of the future condition of the element will be off because the element will deteriorate either slower or faster than was anticipated. Any critical deterioration should be noticed on the 2-year inspection cycles, and the problem should be flagged. If the element is deteriorating at a slower rate than is expected, the condition assigned during the bridge inspection will reflect this, and no action will be taken.

In addition, as the bridge management system is used, the deterioration of the elements of particular bridges can be tracked using the historical data base. If the rate of deterioration is not consistent with the class assignment, the element can be reassigned. If this occurs often, then the deterioration rates tracked historically can be used to redefine the environments.

**TABLE 1 Matrix of Actual Responses Versus Predicted Responses**

Predicted Class	True Class			
	Benign	Low	Moderate	Severe
Benign	36	12	0	0
Low	0	29	14	1
Moderate	0	6	37	5
Severe	0	1	6	29

## Verification of Results

The construction of a matrix is one way to evaluate how well the method classifies the data (see Table 1). The values in the matrix display the results predicted from the model versus the respondents' answers from the survey. A strong diagonal with 0's in the upper and lower diagonals is desirable. Ideally, 100 percent of the values would be along the diagonal, but in most cases, since the opinions of experts vary, the "true" classes are not uniform. In general, the values along the diagonal should be maximized, whereas those values outside the diagonal should be minimized. Preferably, the more extreme triangular regions are equal to 0. However, the results must be examined outside of these restrictions. For example, if nine experts predict severe and one expert predicts benign, it is preferable for the model to predict severe and have one prediction three classes off than for it to predict moderate and have nine predictions one class off and one prediction two classes off.

Various classification methods can be compared by developing matrices for each method and comparing the diagonals. Review of the assignments by experienced field staff is also beneficial.

## Implementation of Classification

The results are used to assign defined elements to the appropriate environment.

## CONCLUSIONS AND RECOMMENDATIONS

The classification of the elements of the bridge population into the four environments helps improve the accuracy of the model used by Pontis. The result is a more realistic representation of the actual behavior of the bridge network. As the model of the behavior becomes more refined, the projections of where resources are best expended become more accurate. Whether this method for developing environment definitions or another is used, the development of objective criteria for assignments of the elements to the environments should not be sacrificed for a slight initial savings in time. The method presented in this report is easily adaptable to

any Pontis element or group of elements, and it was found in the application to yield reasonable results.

Once Pontis has been in use for four cycles (8 years), it is recommended that the environments be evaluated. At that time, it may be found that the transition matrices for the different environments are not distinct. Only after a review like this is made should the number of environments used by an agency be reduced.

Another topic that should be considered for future research is the development of a self-correcting environmental assignment procedure that could be incorporated into the Pontis computer code. The motivation for using a survey in this research was that historical data did not exist at the element level. Once the Pontis system has been in place for several inspection cycles, sufficient data will exist so that such a system could automatically partition the elements into the appropriate four environments on the basis of actual inspection data. Such a mechanism would increase the accuracy of the prediction of deterioration and subsequently improve the cost projections of the model. However, additional study is needed before such a procedure is implemented. Because of the updating procedures for deterioration and cost, research must be developed in such a way that the validity of these models is not sacrificed.

Another area in which research is needed is the development of costs that are appropriate at the network level and significant at the project level. (Preliminary phases of this research are currently under way at Clemson University.) Although not addressed in this research, this area should be considered in conjunction with the development of the criteria for the environments. Because costs are required for each element in each environment, work is needed to increase the understanding of how the two are best linked. Although the factors that affect deterioration often affect the cost of the repair—for example, average daily traffic—this is not always the case. Division of the cost of maintenance, repair, and rehabilitative actions into environments is meaningful only in the cases in which the factors affect both deterioration and cost. On the other hand, experience may show that the rates of deterioration are not distinct enough to warrant the environments and that the division is better allocated to the difference in costs. Regardless, it is necessary that the environmental definition be tied with the cost model in such a way that the environments serve a twofold purpose. First, the environments function as a type of deterioration class representing operation practices and climatic exposure, as has been emphasized throughout this study. Second, the definition of the environments might be expanded to include factors that lead to significant cost differences. Such a possibility was beyond the scope of this research but should be explored in future research.

The implementation of Pontis requires devotion of extensive resources. This survey method of defining environments will give a good environmental class without sacrificing the staff hours that are needed in other aspects of implementation. Use of such a method will result in clear definitions for environments so that costs can be adjusted accordingly. With the use of this type of method, objective criteria exist for the assignment of bridge elements to environments. Without such a rational basis for assignment, many of the problems with subjectivity that have been mentioned with the National Bridge Inventory ratings are introduced back into the element-level inspection process.

#### ACKNOWLEDGMENTS

This study was supported by the Virginia Transportation Research Council and is based on the author's thesis for the master of science in systems engineering degree. William T. Scherer was the advisor for this research.

#### REFERENCES

1. U.S. Department of Transportation. Management and Monitoring Systems; Proposed Rule. *Federal Register*, Vol. 58, No. 39, 1993, pp. 12096–12125.
2. *Pontis Executive Summary, Technical Manual, and User's Manual: A Network Optimization System for Bridge Improvements and Maintenance*. Cambridge Systematics, Inc.; Optima, Inc., Cambridge, Mass., 1991.
3. Wells, D. T. *Environmental Classification Scheme for Pontis*. VTRC Report 94-R20. Virginia Transportation Research Council, Charlottesville, 1994.
4. McGhee, K. K., G. R. Allen, and W. T. McKeel. *Development of Performance and Deterioration Curves as a Rational Basis for a Structure Maintenance Management System*. VTRC Report 94-R1. Virginia Transportation Research Council, Charlottesville, 1993.
5. O'Connor, D. S., and W. A. Hyman. *Bridge Management Systems*. Report FHWA-DP-71-01R. FHWA, U.S. Department of Transportation, 1989.
6. Allen, G. R., and W. T. McKeel. Development of Performance and Deterioration Curves as a Rational Basis for a Structure Maintenance Management System. *Official Proc.*, 6th Annual International Bridge Conference, Pittsburgh, 1989, pp. 60–64.
7. Fitzpatrick, M. W., D. A. Law, and W. C. Dixon. Deterioration of New York State Highway Structures. In *Transportation Research Record 800*, TRB, National Research Council, Washington, D.C., 1981, pp. 1–8.
8. Breiman, L., J. Friedman, R. Olshen, and C. Stone. *Classification and Regression Trees*. Wadsworth and Brooks, Pacific Grove, Calif., 1984.



# Development of Life-Cycle Activity Profiles in BRIDGIT Bridge Management System

---

Hugh Hawk, *National Engineering Technology Corporation*

The objectives of NCHRP Project 12-28(2)A were to develop a microcomputer-based bridge management system (BMS) that could be implemented by departments of transportation and local bridge authorities as well as satisfy the requirements for bridge management systems mandated in the interim final regulations for Intermodal Surface Transportation Efficiency Act management systems. Phase 2 of the project was completed in 1994 and resulted in the development of the BRIDGIT BMS. The various models used in BRIDGIT to produce life-cycle activity profiles (LCAPs) for each bridge in a network are discussed. In developing repair and functional improvement strategies for any selected group of bridges, it is necessary to identify and compare feasible alternatives. As part of its optimization analysis, BRIDGIT develops different LCAPs for individual bridges and determines the present value of life-cycle costs and benefits for each one. The costs considered include agency costs for the various repair or improvement actions as well as user costs associated with accidents or detours due to load capacity deficiencies, vertical clearance deficiencies, or bridge width deficiencies.

As part of the inventory data requirements in BRIDGIT, it is necessary to define the physical and geometric characteristics of each bridge in a network. Bridges can be divided into segments that can represent different bridge units such as approach

spans, main spans, or spans of similar construction. Agencies are required to define the various elements and protection systems that make up each segment.

BRIDGIT uses a condition rating system similar to that used in the Pontis bridge management system (BMS) software, whereby inspectors must report the quantity of a bridge element that is in each of the condition states defined for that element. Up to five condition states can be identified for any element model, with the first state representing the best condition. The condition state definitions correspond to different types and severities of defects for the element. Protection systems such as deck overlays are reported separately from the underlying element by using the same condition rating format.

In order to produce accurate life-cycle costs, predict future deterioration of elements and protection systems, and define feasible repair or improvement alternatives for each bridge, agencies must provide cost and deterioration information for each of the element and protection system models. The following data are required for each model. Unless otherwise noted, any references to elements are also applicable to protection systems.

- Repair actions and associated costs. For each condition state a repair action and associated unit cost may be defined. BRIDGIT uses this information to calculate the costs associated with repair of the element on the

basis of the quantities of an element identified in each condition state.

- **A/M/U factors and threshold value.** The A/M/U factor is used to define the acceptability of each condition state. This factor indicates whether a condition state is considered to be acceptable (A), marginally acceptable (M), or unacceptable (U). For example, Condition State 1 usually represents a condition that would not require any repair actions and that would always be considered acceptable. Condition State 2 usually corresponds to only a small amount of deterioration and would necessitate, at most, carrying out minor preventive maintenance actions to those element quantities. Thus, it would also be considered an acceptable condition state. Condition State 3 is generally defined as having significant deterioration but with little loss of structural capacity or performance. An agency would usually consider this state to be marginally acceptable. In other words, repair actions would be performed only if sufficient funds were available. Condition State 4 is usually associated with significant deterioration and with the loss of structural capacity or performance. This would no doubt be considered unacceptable and would require repair if the quantity of element in this state exceeds some defined threshold value percentage.

As part of the element model information, BRIDGIT requires agencies to define this threshold value, which represents the maximum permissible quantity (in percent) of an element that may be present in any unacceptable condition state before a repair action should be triggered. As part of the development of individual bridge life-cycle activity profiles (LCAPs), the threshold value is therefore used to determine the timing of future repair actions.

- **Element deterioration models.** BRIDGIT has been initially loaded with deterioration information for four environments: benign, low, moderate, and severe. It is expected that agencies will customize these data to reflect their own experience and judgment. Because little information that can be used to assist agencies in initially defining deterioration model parameters is available, any BMS should assist agencies in improving the accuracy of this information in the future. To accomplish this BRIDGIT provides a routine for automatically updating the deterioration models from an analysis of historical inspection data.

BRIDGIT also provides a means for agencies to specify additional factors that can be used to modulate the rate of deterioration of the average element deterioration models on the basis of average daily traffic (ADT). These factors are defined for each functional route classification and are applied to any element or protection system model that has been identified as being affected by ADT. In general, deck elements, joints, and overlays are affected by ADT.

## DEVELOPMENT OF AGENCY AND USER COSTS

Two types of costs are considered in any year of a bridge's life cycle: agency costs and user costs. Agency costs are incurred with initial construction as well as routine maintenance, repair, or improvement actions over the life of the structure. These costs are borne directly by the agency. User costs are incurred by bridge users as a result of functional deficiencies. The occurrence of accidents is higher on bridges with narrow deck widths or low vertical clearances than on bridges without these deficiencies. Bridges with low vertical clearances or insufficient load capacities will force a certain volume of truck traffic to be detoured to alternate routes, resulting in increased vehicle operating costs.

### Development of Agency Costs for Repair and Improvement Actions

A number of repair or improvement cost alternatives are developed by BRIDGIT for any given year in a bridge's life cycle. These include

1. Scheduled actions,
2. Level 1 (U) repairs,
3. Level 2 (U-M) repairs,
4. Protection system replacement in a bridge segment,
5. Element replacement in a bridge segment,
6. Superstructure replacement in a bridge segment,
7. Segment replacement,
8. Load capacity improvements,
9. Bridge raising improvements,
10. Bridge widening improvements, and
11. Bridge replacement.

### *Scheduled Actions*

Scheduled actions are defined as repairs that form part of a scheduled maintenance program for bridges and that include such actions as repairing railings or joints as well as painting steel elements or overlaying decks. BRIDGIT considers scheduled actions for all protection systems as well as any minor unprotected elements. The term "scheduled actions" denotes that this level of maintenance is programmed and should be performed as required. It does not compete with other actions during optimization. Scheduled actions are initiated when the element or protection system deteriorates to the point at which the quantity of an element in an unacceptable state exceeds the threshold value defined for the model. At that time, all unacceptable marginally acceptable states are repaired and returned to Condition State 1. A scheduled action within 5 years of a selected

repair, rehabilitation, or replacement action will be deferred. For example, repainting of a steel girder element should not occur if the girders are to be repaired within 5 years. Painting would be deferred until the year of repair.

### ***Level 1 (U) Bridge Repairs***

Level 1 bridge repairs are defined as actions that remove only the quantities of elements in an unacceptable condition state. This is referred to as a “U” repair in BRIDGIT. Level 1 repairs do not remove functional deficiencies, with the possible exception of load-carrying capacity. This repair scenario would normally be applicable to situations in which it is desirable to extend the service life of the bridge until a more comprehensive action can be afforded (such as replacement of the entire bridge). Level 1 repairs can often be the most cost-effective bridge repair action, even though they do not completely restore the bridge to an acceptable condition level.

### ***Level 2 (U-M) Bridge Repairs***

Level 2 bridge repairs are defined as those repairs that are intended to remove all quantities of elements in unacceptable and marginally acceptable condition states. This is referred to as a “U-M” repair in BRIDGIT. Level 2 repairs do not remove functional deficiencies, with the possible exception of load-carrying capacity.

### ***Protection System Replacement in a Bridge Segment***

When a protection system receives a repair, BRIDGIT checks to see whether complete replacement of the protection system for that bridge segment may be a more economical choice. This verification is made by comparing the cost of repairing the protection system with the cost of replacing the protection system.

### ***Element Replacement in a Bridge Segment***

When an element receives a scheduled Level 1 or Level 2 repair, BRIDGIT checks to see whether complete replacement of that element and any associated protection system may be warranted. This check is made by comparing the cost of repairing the element and protection system for a particular bridge segment with the cost of replacing the entire element and protection system. BRIDGIT also recognizes the fact that a new element and associated protection system generally have longer lives and thus reduced life-cycle costs. Therefore, BRIDGIT selects an element and protection system replacement if the cost of repairs exceeds 70 percent of

the cost of replacement. This value is based on evaluations of life-cycle costs associated with various types of bridge repairs and represents a conservative level. Element replacement is usually considered to be economical when the repair costs exceed 65 to 85 percent of the replacement costs.

### ***Superstructure Replacement in a Bridge Segment***

In the same way that the cost-effectiveness of element replacement is evaluated against element repairs, BRIDGIT also examines replacement of the entire superstructure including the deck, bearings, joints, and railing elements. This situation is difficult to evaluate because replacement of a superstructure for only one segment of the bridge usually involves a number of considerations:

1. Should the superstructure be replaced to the same dimensions that already exist when only a portion of the total bridge is being considered for replacement?
2. Should the bridge be locally widened in anticipation of a possible future widening of the remaining segments?
3. Does replacement of, say, one span remove a load capacity deficiency or does it still exist at another location?
4. Does a localized bridge raising, if possible, through a more slender superstructure design or adjustment of the vertical profile remove a vertical clearance deficiency, or does it still exist in another location? If there is at least a partial removal of a vertical deficiency, how much traffic under the bridge is affected?

BRIDGIT sidesteps these issues by not evaluating superstructure replacement as a bridge improvement alternative to be considered during the optimization analysis. Instead, BRIDGIT evaluates superstructure replacement after optimization is complete by notifying the user in the analysis work plan reports that superstructure replacement may be warranted for a particular bridge if the combined cost of repairs for a particular segment for the superstructure, deck, joints, bearings, and railing elements exceeds 70 percent of the cost of replacing the entire superstructure.

### ***Segment Replacement***

The issue of segment replacement is treated in the same way as superstructure replacement is (i.e., not during optimization). In the case in which both superstructure replacement and segment replacement may be warranted, only replacement of the segment is reported. The cost of segment replacement is calculated by using

the bridge replacement unit costs defined for the replacement bridge model identified for that segment.

### **Load Capacity Improvements**

If a bridge has been identified as being posted, BRIDGIT assumes that Level 1 repair, Level 2 repair, and replacement actions to superstructure elements will result in increased load capacity for the bridge. The amount of increase is determined by the following rules:

1. A Level 1 repair restores the load capacity 85 percent of the way back to its load capacity in the new condition, provided that the percentage of the total quantity remaining in any marginally acceptable states after repairs for any critical superstructure element does not exceed 25 percent.
2. A Level 1 repair restores the bridge load capacity only 50 percent of the way back to its load capacity in the new condition if the percentage of the total quantity in any marginally acceptable states after repairs for any critical superstructure element exceeds 25 percent.
3. A Level 2 repair restores the bridge load capacity 85 percent of the way back to its load capacity in the new condition.
4. Bridge replacement results in a bridge load capacity 25 percent higher than the maximum legal load or nonposted single-vehicle capacity.

### **Bridge Raising Improvements**

A bridge raising improvement is intended to remove functional deficiencies due to vertical clearance. As part of the inventory information required for each bridge, users are required to define whether each bridge segment can be raised (on the basis of physical as well as economic constraints). BRIDGIT will verify if all segments in the bridge can be raised. If this is possible, BRIDGIT will estimate the cost to remove the vertical deficiency.

BRIDGIT assumes that once bridge raising improvements have been performed, no future user costs due to vertical clearance deficiencies will be incurred over the remaining life of the bridge.

### **Bridge Widening Improvements**

A bridge widening is intended to remove functional deficiencies due to clear deck width. As part of the inventory information required for each bridge, users are required to specify if each bridge segment can be widened. BRIDGIT will verify whether it is possible to widen all segments in a bridge. If so, BRIDGIT will consider widening the bridge to the desirable level-of-service goals for clear deck width defined by the agency for a pro-

jected level of traffic 20 years beyond the date of the widening. Widening can be of two types:

1. Minor width adjustments to remove lane width and shoulder deficiencies and
2. Major width adjustments to add new lanes. This may be a twinning of an existing structure.

It is recognized that the unit costs of minor widenings are higher because of the difficulties of integrating new structural elements with existing ones. For this reason BRIDGIT permits agencies to define a multiplying factor that is used to increase the unit cost for widenings less than a prescribed width. For widenings greater than this prescribed value, the unit costs defined for the replacement bridge models identified for each segment of the bridge are used without modification.

### **Bridge Replacement**

A bridge replacement removes all functional deficiencies and is designed to accommodate levels of traffic 20 years beyond the year of replacement being considered. The new bridge width will be based on the desirable level-of-service goals defined by the agency for vertical clearance, number of lanes, lane widths, and load capacity. The new length of the bridge is assumed to be longer than that of the structure being replaced and is calculated from an equation that is modifiable by the agency.

### **Development of Agency Costs for Routine Maintenance**

BRIDGIT estimates the present value of annual costs associated with routine maintenance of a bridge over its service life. In BRIDGIT routine maintenance represents strictly preventive actions such as deck washing, drain cleaning, and bearing cleaning. Spot repairs to bridge elements and protection systems are considered scheduled actions. In order to calculate routine maintenance costs for all bridge elements of any bridge  $i$ , BRIDGIT multiplies the quantities of the element reported in each element condition state by the unit maintenance costs defined by the bridge agency for each corresponding element model. It is assumed that these costs increase as the conditions of the bridge elements deteriorate. Elements that have an associated protection system receive maintenance to the protection system only. This can be represented by the equation

$$\text{ARMC}(i, t) = \sum_{c=1}^{\text{NB}(i)} \text{MCB}(i, c, t) + \sum_{c=1}^{\text{NP}(i)} \text{MCP}(i, c, t) \quad (1)$$

where

$t$  = time; time is generally considered to be a continuum but is sometimes discretized to integer years; the first year is denoted as year 0 and year 1 is defined as being from  $t = 1.0$  to  $1.999$ ;

$ARMC(i, t)$  = annual routine maintenance cost for bridge  $i$  at the beginning of year  $t$ ;

$MCB(i, c, t)$  = maintenance cost for bare bridge element  $c$  of bridge  $i$  at the beginning of year  $t$ ;

$MCP(i, c, t)$  = maintenance cost for bridge protection system  $c$  of bridge  $i$  at the beginning of year  $t$ ;

$NB(i)$  = total number of bare bridge elements for bridge  $i$ ; and

$NP(i)$  = total number of protection systems for bridge  $i$ .

The present value (PV) of routine maintenance (RM) costs from time  $T1$  to  $T2$  for bridge  $i$  can then be calculated as follows:

$$PV\_RM(i, T1, T2) = \sum_{t=T1}^{T2} \frac{ARMC(i, t)}{(1 + RRRR)^t} \quad (2)$$

where RRRR is real required rate of return or discount rate.

### Development of User Costs

User costs are generated because of deficiencies associated with narrow deck width, insufficient load capacity, and low vertical clearance. The various concepts used in BRIDGIT for estimating these costs have been developed by Chen and Johnston (1), Aabed-Al-Rahim and Johnston (2), and Al-Subhi et al. (3) for use in the optimization portion of the OPBRIDGE program, developed for the North Carolina Department of Transportation.

The occurrence of accidents is higher on bridges with narrow deck widths, poor approach alignments, or low vertical clearances than on bridges without these deficiencies. Bridges with low vertical clearances or insufficient load capacities force a certain volume of truck traffic to be detoured to alternate routes, resulting in increased vehicle operating costs. As the volume of traffic increases the number of accidents or detoured vehicles also increases.

For each bridge in the network BRIDGIT determines if a geometric or load capacity deficiency exists by comparing the bridge's vertical clearance, deck width, and load capacity with the level-of-service goals defined by

the agency. The calculation of annual user costs considers the following three terms:

- User costs associated with deficient deck width. User costs associated with deficient deck width are a function of traffic volume, structure length, acceptable deck width, and the actual deck width.

The present value of user costs for bridge  $i$  due to deck width deficiency within the time interval of  $T1$  to  $T2$  years can be expressed as

$$PV\_WIDTH(i, T1, T2) = \sum_{t=T1}^{T2} \left[ \frac{COST\_WIDTH(i, t)}{(1 + RRRR)^t} \right] \quad (3)$$

where  $COST\_WIDTH(i, t)$  is user costs associated with width deficiency in year  $t$  for bridge  $i$ .

- User costs associated with vertical clearance deficiencies. Vertical clearance deficiencies can generate user costs due to accidents that occur on the bridge (overhead deficiencies) or under the bridge (underpass deficiencies) as well as detour costs due to deficient clearance under or over the bridge. The following equation expresses these costs in any year  $t$  for bridge  $i$ :

$$\begin{aligned} COST\_VERT(i, t) = & COSTVERT\_AO(i, t) \\ & + COSTVERT\_AU(i, t) \\ & + COSTVERT\_DO(i, t) \\ & + COSTVERT\_DU(i, t) \end{aligned} \quad (4)$$

where

$COST\_VERT(i, t)$  = annual user cost due to vertical clearance deficiencies for bridge  $i$  in year  $t$ ;

$COSTVERT\_AO(i, t)$  = annual user cost due to accidents on the bridge attributed to vertical clearance over the bridge;

$COSTVERT\_AU(i, t)$  = annual user cost due to accidents under the bridge attributed to vertical clearance under the bridge;

$COSTVERT\_DO(i, t)$  = annual user cost due to detouring of traffic from on the bridge because of vertical clearance deficiency over the bridge; and

$COSTVERT\_DU(i, t)$  = annual user cost due to detouring of traffic from under the bridge because of a vertical clearance deficiency under the bridge.

The present value of accident and detour costs for bridge  $i$  due to vertical clearance deficiencies within the time interval of  $T1$  to  $T2$  years can be expressed as

$$PV\_VERT(i, T1, T2) = \sum_{t=T1}^{T2} \frac{COST\_VERT(i, t)}{(1 + RRRR)^t} \quad (5)$$

- Annual user costs associated with load capacity deficiency. Reduced load capacity results in a percentage of the traffic being detoured, thus generating user costs. These user costs can be expressed as a function of traffic volume, detour length, and the percentage of trucks detoured at the reduced load capacity.

The present value of user costs for bridge  $i$  due to posting within the time interval of  $T1$  to  $T2$  can be expressed as

$$PV\_POST(i, T1, T2) = \sum_{t=T1}^{T2} \frac{COST\_POST(i, t)}{(1 + RRRR)^t} \quad (6)$$

where  $COST\_POST(i, t)$  is user cost due to reduced load capacity in year  $t$  for bridge  $i$ .

- Calculation of total user costs. The total annual user cost associated with geometry and load capacity deficiencies of bridge  $i$  in year  $t$  is calculated as follows:

$$COST\_USER(i, t) = COST\_WIDTH(i, t) + COST\_VERT(i, t) + COST\_POST(i, t) \quad (7)$$

and the present value of user costs for bridge  $i$  within the interval  $T1$  to  $T2$  years and discounted to year 0 is

$$PV\_USER(i, T1, T2) = PV\_WIDTH(i, T1, T2) + PV\_VERT(i, T1, T2) + PV\_POST(i, T1, T2) \quad (8)$$

## DEVELOPMENT OF LIFE-CYCLE ACTIVITY PROFILES

A life-cycle activity profile (LCAP) represents a series of repair and improvement actions expected to occur over the life of a structure. The cost to an agency for a bridge is seldom a one-time cost. It is a long-term, multiyear investment. Throughout its useful life, a bridge requires periodic maintenance and possibly repair or rehabilitation actions. At the end of its useful life, the bridge must be replaced.

As part of its optimization analysis, BRIDGIT compares the cost-effectiveness of different repair and improvement options for each bridge in the network by determining the present value of costs and benefits of each option by using a life-cycle approach. The various

alternatives to be considered for economic analysis are selected from knowledge-based decision rules that examine overall strategies over the life cycle of each bridge. BRIDGIT calculates the present value of life-cycle costs for the following maintenance, rehabilitation, and replacement alternatives at each analysis period:

1. Replacement,
2. Rehabilitation (Level 2 repairs to all bridge elements and removal of all functional deficiencies),
3. Level 2 (U-M) repairs to all bridge elements, and
4. Level 1 (U) repairs to all bridge elements.

In addition, the present value cost of doing nothing except routine maintenance and scheduled actions until the end of the analysis horizon (year 20) is calculated; this is followed by an LCAP based on the bridge's condition and functionality at the end of the analysis horizon.

The development of the LCAPs includes the costs associated with immediate as well as future actions. BRIDGIT ages the bridge network to project the future conditions of elements and protection systems in order to calculate future repair or improvement costs. In addition, future ADT levels are predicted in order to determine future user costs. The LCAP models select feasible repair and functional improvement actions and determine the appropriate timing of such actions over the life cycle of each bridge.

## Replacement LCAP

The replacement LCAP assumes that all bridges require complete replacement at some year  $t_R$  in the future. BRIDGIT permits bridge agencies to define replacement bridge models and associated unit construction costs for different road classifications and span length ranges. This information is used to develop the LCAP.

Agencies are required to supply all of the information necessary to calculate the replacement LCAP in the models section of BRIDGIT. It is therefore a "hard-wired" LCAP in that the calculated present values of present and future costs are fundamentally characteristic of the model and not site dependent. They depend only on the size of the new bridge.

## Initial Bridge Replacement Costs

The estimated initial cost of a bridge replacement alternative for any existing bridge  $i$  at the beginning of year  $t$  can be expressed as a function of the existing bridge length, the width required to accommodate future traf-

fic volumes, the type of replacement bridge, and the cost per unit deck area for that replacement bridge type.

### User Costs

When the bridge is replaced in year  $t_R$  it is assumed that the design will meet all functional requirements over its service life. Therefore, no user costs associated with geometric deficiencies will be incurred over the life of the new structure. Load capacity is assumed to be related to the condition of the key bridge superstructure elements. Initially, the bridge does not have any load capacity deficiencies and therefore does not have any associated user costs. It is also assumed that the new bridge receives timely repairs that would ensure that the bridge would not require posting at any time. User costs are thus zero.

### Routine Maintenance and Minor Repair Costs

The bridge replacement models defined by the agency in BRIDGIT include an average unit annual cost of maintenance over the life of the bridge model. This value represents both routine preventive maintenance as well as minor repair actions to the bridge. A new bridge is assumed to not require any maintenance repairs until a significant quantity of one of its bridge elements has deteriorated to Condition State 2 or 3. Costs then increase annually as the condition of the new bridge deteriorates and until the bridge is rehabilitated.

When elements have been improved by rehabilitation, the maintenance costs are reduced or eliminated, depending on the condition of other bridge elements at the time of rehabilitation. As the structure deteriorates, these costs again increase until the next rehabilitation and then again to the next replacement. The present value of the maintenance costs accumulated from the time of replacement until the next bridge replacement thus assumes that maintenance varies through time.

### Major Repairs and Rehabilitation

The replacement LCAP includes up to two major repairs during the life of the bridge. The timing of these actions as well as their associated unit costs are taken from the replacement bridge model defined by the agency.

### Calculation of Replacement Life-Cycle Costs

The present value of the replacement life-cycle costs for the replacement LCAP for bridge  $i$  applied at the beginning of year  $t_R$  and discounted to year 0 and assuming

perpetual replacements every  $t_{NB}$  years can be expressed as

$$PV\_REPL(i, t_R) = \left[ \frac{ICNB(i, t_R)}{(1 + RRRR)^{t_R}} + \frac{COSTRH1(i)}{(1 + RRRR)^{t_R + t_{RH1}}} + \frac{COSTRH2(i)}{(1 + RRRR)^{t_R + t_{RH2}}} + \sum_{t=t_R}^{t_R + t_{NB}} ARMC(i, t) \right] \cdot \frac{1}{[1 - (1 + RRRR)^{-t_{NB}}]} \quad (9)$$

where

$ICNB(i, t_R)$  = initial cost of a bridge replacement for bridge  $i$  in year  $t_R$ ;

$COSTRH1(i)$  = initial cost of the first rehabilitation of bridge  $i$  at the beginning of year  $t_R + t_{RH1}$ ;

$COSTRH2(i)$  = initial cost of the second rehabilitation of bridge  $i$  at the beginning of year  $t_R + t_{RH2}$ ;

### Rehabilitation LCAP

The purpose of a major rehabilitation is to extend the service life of a bridge before replacement. Usually, a bridge receives one major rehabilitation in its lifetime involving the replacement or rehabilitation of all deficient bridge elements and the removal of all functional deficiencies. At the end of the extended service life  $E$ , BRIDGIT assumes that the rehabilitated bridge may receive one more repair cycle and then be replaced.

The rehabilitation LCAP assumes that the rehabilitated bridge is improved to meet all functional requirements established by the bridge agency for the remainder of its extended service life (i.e., the bridge is widened or vertical clearance is increased to the level-of-service standards defined by the agency). Therefore, no user costs due to geometric deficiencies are incurred during the extended life of the bridge. If a bridge's geometric deficiencies cannot be removed because of some constraint, then the rehabilitation alternative is rejected as infeasible.

Routine maintenance costs are generally reduced because of the rehabilitation but increase over the extended service life of the bridge as it deteriorates.

The present value of the life-cycle costs of the rehabilitation LCAP,  $PV\_UMF(i, t)$ , is the sum of the dis-

counted initial cost of rehabilitation at year  $t$ , the present value of annual routine maintenance and user costs during the extended service life period  $E$ , and the minimum of the present value of the replacement LCAP applied at the end of the extended service life or the present value of another rehabilitation cycle. This can be expressed as

$$\begin{aligned}
 PV\_UMF(i, t) = & COST\_UM(i, t)/(1 + RRRR)^t \\
 & + COST\_WIDEN(i, t)/(1 + RRRR)^t \\
 & + COST\_RAISE(i, t)/(1 + RRRR)^t \\
 & + PV\_SCHED(i, t, t + E) \\
 & + PV\_RM(i, t, t + E) \\
 & + PV\_USER(i, t, t + E) \\
 & + \text{MIN}[PV\_REPL(i, t + E), \\
 & PV\_UM(i, t + E)]
 \end{aligned} \quad (10)$$

where

$$\begin{aligned}
 COST\_UM(i, t) &= \text{cost of a repair to remove all unacceptable and marginal states in year } t; \\
 COST\_WIDEN(i, t) &= \text{cost of widening bridge;} \\
 COST\_RAISE(i, t) &= \text{cost of raising bridge;} \\
 PV\_SCHED(i, t, t + E) &= \text{present value of scheduled maintenance from year } t \text{ to } t + E; \\
 PV\_RM(i, t, t + E) &= \text{present value of routine maintenance from year } t \text{ to } t + E; \\
 PV\_USER(i, t, t + E) &= \text{present value of user costs from year } t \text{ to } t + E; \\
 \text{MIN}[\dots] &= \text{minimum value of the terms inside the brackets;} \\
 PV\_REPL(i, t + E) &= \text{present value of a replacement LCAP in year } t + E; \text{ and} \\
 PV\_UM(i, t + E) &= \text{present value of a Level 2 repair LCAP in year } t + E.
 \end{aligned}$$

### Level 1 (U) or Level 2 (U-M) Repair LCAPs

The third type of repair or improvement alternative to be considered during optimization is the Level 1 or Level 2 repair LCAP. The purpose of this level of action is to repair elements that are in unacceptable or marginally acceptable condition states without initiating any functional improvement such as widening or raising. At the end of the extended service life  $E$ , it is as-

sumed that either a rehabilitation or a replacement action takes place at year  $t + E$ .

Two LCAP scenarios are possible:

1. Removal of all unacceptable condition states, a Level 1 (U) repair; and
2. Removal of all unacceptable and marginally acceptable condition states, a Level 2 (U-M) repair.

The Level 1/Level 2 repair LCAP does not involve removal of any geometric deficiencies that may be present. Therefore, user costs due to geometric deficiencies may be incurred until the year that a rehabilitation or replacement is carried out. Routine maintenance costs are calculated in the same way as for the rehabilitation LCAP.

The present values of the two life-cycle costs for the repair alternatives  $PV\_U$  and  $PV\_UM$  are calculated as the sum of the discounted initial cost of the repair alternative in year  $t$ , the present value of annual routine maintenance and user costs during the extended service life period, and the present value of the rehabilitation or replacement LCAP applied at the end of the extended service life. This can be expressed as

$$\begin{aligned}
 PV\_U(i, t) = & COST\_U(i, t)/(1 + RRRR)^t \\
 & + PV\_SCHED(i, t, t + E_U) \\
 & + PV\_RM(i, t, t + E_U) \\
 & + PV\_USER(i, t, t + E_U) \\
 & + \text{MIN}[PV\_REPL(i, t + E_U), \\
 & PV\_UMF(i, t + E_U)]
 \end{aligned} \quad (11)$$

where  $COST\_U(i, t)$  is the cost of a repair to remove all unacceptable states in year  $t$  for bridge  $i$  and  $E_U$  is extended service life due to a Level 1 repair; all other terms were defined earlier.

Similarly, the present value of the Level 2 repair LCAP can be expressed as

$$\begin{aligned}
 PV\_UM(i, t) = & COST\_UM(i, t)/(1 + RRRR)^t \\
 & + PV\_SCHED(i, t, t + E_{UM}) \\
 & + PV\_RM(i, t, t + E_{UM}) \\
 & + PV\_USER(i, t, t + E_{UM}) \\
 & + \text{MIN}[PV\_REPL(i, t + E_{UM}), \\
 & PV\_UMF(i, t + E_{UM})]
 \end{aligned} \quad (12)$$

where  $E_{UM}$  is the extended service life due to a Level 2 repair, and all other terms have been defined earlier.



### Base Case—The “Do-Nothing” LCAP

As part of the optimization analysis, BRIDGIT compares the present value of costs associated with each of the feasible alternatives defined for replacement, rehabilitation, or Level 1/Level 2 repair of a bridge with the present value of the do-nothing LCAP. In developing this base case it is assumed that no bridge repair or improvement actions are performed on the bridge during the optimization analysis horizon of 20 years. Two different scenarios can result from this assumption:

- Case 1: Bridge becomes functionally deficient during the analysis horizon. At the end of the 20-year analysis horizon a functionally deficient bridge is assumed to require either rehabilitation or replacement. Level 1 and Level 2 LCAPs are not considered acceptable.
- Case 2: Bridge does not become functionally deficient during the analysis horizon. If by the end of the analysis horizon no “critical” bridge elements have deteriorated to the point that quantities in unacceptable condition states have exceeded the defined threshold values, the time beyond 20 years at which a critical threshold is reached is determined and the LCAP with the least present value of costs at that point is applied. If a critical bridge element has already exceeded the defined threshold, then the LCAPs are applied immediately after the 20-year analysis horizon.

The do-nothing LCAP forms the base case against which all other alternatives are evaluated. Since BRIDGIT assumes that scheduled actions can form part of the do-nothing alternative, it is not a zero-cost alternative. For each period all elements are deteriorated from their condition at the beginning of the period to their condition at the end of the period, suitably adjusted for ADT effects. This process may initiate scheduled actions to minor elements and to protection systems.

At this point all of the costs and associated present values for scheduled actions and for user costs up to year 20 have been calculated. It is now necessary to calculate the number of years from year 20 that it will take until a critical element arrives at its threshold value. This is the point at which a repair or improvement action is initiated. It may happen that at the end of 20 years a critical element will have already deteriorated beyond its threshold value. In this case the number of years from the end of year 20 until an action is initiated will be zero (i.e., the action is initiated at the beginning of year 21).

The number of years until a critical element reaches its threshold value is determined by deteriorating the elements of the bridge through time until the threshold value for any critical element is exceeded. It is then nec-

essary to calculate the user costs and routine maintenance costs associated with the time period from year 20 to the just-calculated year. At this point an action is taken, namely, the most cost-effective life-cycle activity profile, based on the calculated present value of the Level 1 or Level 2 repair, rehabilitation, or replacement LCAPs.

We now have the total present value in year zero of doing no repair, rehabilitation, or replacement in the first 20 years followed by some action after 20 years, with proper account taken of user costs, routine maintenance, and scheduled actions within the first 20 years and beyond.

The present value of the life-cycle costs,  $PV\_DN(i)$ , for the do-nothing alternative is thus the sum of the present value of routine maintenance, scheduled maintenance, and user costs during the analysis horizon of 20 years and the minimum of the present values for the replacement, rehabilitation, and Level 1 or Level 2 repair LCAPs applied after the 20-year analysis horizon. This can be expressed as

$$\begin{aligned}
 PV\_DN(i) = & PV\_RM(i, 0, YR(i)) \\
 & + PV\_USER(i, 0, YR(i)) \\
 & + PV\_SCHED(i, 0, yr(i)) \\
 & + MIN[PV\_U(i, YR(i)), \\
 & PV\_UM(i, YR(i)), \\
 & PV\_UMF(i, YR(i)), \\
 & PV\_REPL(i, YR(i))] \quad (13)
 \end{aligned}$$

where  $YR(i)$  is the year beyond the analysis horizon at which a repair is required for bridge  $i$ , and all other terms have been defined earlier.

### Example: Calculation of a Level 2 Repair LCAP in Period 4

A Level 2 repair LCAP in Period 4 constitutes 1 of the 21 alternatives that BRIDGIT considers and has been selected to illustrate the basic methodology by which costs and present values are calculated for each alternative. Period 4 is defined as being from years 11 to 15 of the 20-year analysis horizon. BRIDGIT assumes that a Period 4 action will occur in year 13, approximately the median year for the period.

Up to year 13, the do-nothing LCAP is followed, except that scheduled actions in years 9 to 13 are dropped since they are within 5 years of the primary action.

Thus, up to year 13

$$\begin{aligned}
 PV(i, 0, 13) = & PV\_USER(i, 0, 13) \\
 & + PV\_RM(i, 0, 13) + PV\_SCHED(i, 0, 8) \quad (14)
 \end{aligned}$$

where

PV\_USER( $i, 0, 13$ ) = the present value of user costs from year 0 to 13 for bridge  $i$ ;

PV\_RM( $i, 0, 13$ ) = the present value of routine maintenance costs from year 0 to 13 for bridge  $i$ ;

PV\_SCHED( $i, 0, 8$ ) = the present value of scheduled maintenance from year 0 to 8 for bridge  $i$ ; and

PV( $i, 0, 13$ ) = the present value of all user costs, scheduled maintenance, and routine maintenance up to year 13 for bridge  $i$ .

In year 13 the Level 2 (UM) repair is undertaken. It should be noted that for the primary action the timing of the action is independent of the condition of the elements. Whether a critical element is under or over its threshold value has no influence on the timing of the principal action. It is simply a Period 4 repair option. Following the repair, the bridge elements are in an improved condition. It is now necessary to calculate the number of years that it takes for a critical element to deteriorate to the point at which its unacceptable condition quantity exceeds its defined threshold value.

This is done by deteriorating all of the elements of the bridge until one of the critical elements reaches its threshold (but not less than 10 years). As an example assume that superstructure steel box girders are deemed critical elements and that in year 29, 15 percent of the total element quantity is in Condition State 4 (and also that Condition State 4 is an unacceptable state with a defined threshold value of 15 percent). Year 29 thus becomes the year at which an action must be taken.

From year 13 to year 29 it is necessary to calculate the additional user costs, routine maintenance costs, and scheduled action costs to be included in the present value calculation. At year 29, according to the Level 2 repair LCAP, we have two choices: rehabilitate the structure or replace the structure. The least present value option will be selected. Thus,

$$\begin{aligned}
 PV(i, 0, \infty) = & PV(i, 0, 13) \\
 & + \text{COST\_UM}(i, 13)/(1 + \text{RRRR})^{13} \\
 & + \text{PV\_SCHED}(i, 13, 29) \\
 & + \text{PV\_RM}(i, 13, 29) \\
 & + \text{PV\_USER}(i, 13, 29) \\
 & + \text{MIN}[\text{PV\_REPL}(i, 29), \\
 & \text{PV\_UMF}(i, 29)] \quad (15)
 \end{aligned}$$

To simplify the discussion, assume that the rehabilitation option turns out to be the most economical.

Thus, in year 29 the structure receives a rehabilitation action. If the bridge is now (i.e., year 29) width deficient relative to the acceptable level-of-service goals, BRIDGIT will assume that the bridge must be widened to satisfy the desirable width goals for ADT levels 20 years hence (i.e., year 49). If the bridge is vertical clearance deficient relative to the acceptable level-of-service goals, BRIDGIT will assume that the bridge must be raised to the desirable level-of-service goal.

If after the rehabilitation action (Level 2 repair and removal of all geometric deficiencies) the bridge is still load capacity deficient relative to the defined acceptable level-of-service goals, then BRIDGIT will not consider rehabilitation as a feasible alternative. Similarly, if widening is required and not possible or raising is required and not possible, then rehabilitation is not considered feasible. It should also be noted that if there are no functional deficiencies relative to acceptable standards, then the rehabilitation option is really no different than the Level 2 repair option. Again, assuming that the rehabilitation option in year 29 was the best choice and that the bridge requires widening and raising, BRIDGIT now continues with the development of the LCAP by again determining the future year when a critical element reaches its defined threshold value. At that time BRIDGIT considers only one feasible option: replacement. If it is assumed that this occurs in year 57, then it is necessary to calculate the additional user costs, routine maintenance costs, and scheduled action costs from years 29 to 57 for inclusion in the present value calculations. At year 57 BRIDGIT determines the present value cost of the replacement LCAP, which is completely defined by the replacement bridge model specified for that bridge. These models include all of the future costs that are associated with replacement (in perpetuity). Thus,

$$\begin{aligned}
 PV(i, 0, \infty) = & PV(i, 0, 29) \\
 & + \text{COST\_UM}(i, 29)/(1 + \text{RRRR})^{29} \\
 & + \text{COST\_WIDEN}(i, 29)/(1 + \text{RRRR})^{29} \\
 & + \text{COST\_RAISE}(i, 29)/(1 + \text{RRRR})^{29} \\
 & + \text{PV\_SCHED}(i, 29, 57) \\
 & + \text{PV\_RM}(i, 29, 57) \\
 & + \text{PV\_USER}(i, 29, 57) \\
 & + \text{PV\_REPL}(i, 57) \quad (16)
 \end{aligned}$$

It should be noted that at each step of the way it is necessary to determine element condition state quantities and bridge load capacity before and after the repair or improvement actions have been implemented. In addition, ADT volumes and their effects on bridge width requirements and user costs must also be determined.

## COST-EFFECTIVENESS INDEX

Once the present values for each of the 20 repair LCAPs (four alternatives per period by five periods) as well as the do-nothing LCAP have been determined for a given bridge, the benefits and costs of each of the alternatives can be compared. The benefits associated with a particular alternative are represented by the reduction in the present value of costs for that alternative compared with that for the do-nothing case. Thus, benefits are considered to be reductions in future maintenance, repair, or user costs. Costs are considered to be the discounted initial cost of the alternative. It would also be valid to consider all costs within the 20-year time horizon or all life-cycle costs. The decision as to which costs to include is dependent on whether future costs are considered to be true costs or disbenefits. Use of only the initial cost in a benefit-cost ratio tends to favor low-cost repairs, provided that user costs are low, over more extensive repairs or functional improvements. The benefit-cost ratio (expressed as a cost-effectiveness index) can be defined in a modified form as

$$CEI(i, p, a) = \frac{PV\_DN(i) - PV\_ALT(i, p, a)}{COST\_ALT(i, p, a) / (1 + RRRR)^{t(p)}} + 1 \quad (17)$$

where

$CEI(i, p, a)$  = cost-effectiveness index for alternative  $a$  in period  $p$  for bridge  $i$ ;

$PV\_ALT(i, p, a)$  = present value of alternative  $a$  in period  $p$  for bridge  $i$ ;

$COST\_ALT(i, p, a)$  = cost of alternative  $a$  in period  $p$  for bridge  $i$ ; and

$t(p)$  = median year for period  $p$ .

Once the benefits and costs are determined, various optimization strategies can be used. BRIDGIT uses a multi-period modified incremental benefit-cost approach (4).

## CONCLUSION

This paper discussed the models used in BRIDGIT to produce LCAPs for each bridge in the network as well as the methodology used to determine the cost-effectiveness

of each option. For each bridge BRIDGIT considers four LCAP alternatives (Level 1 repairs, Level 2 repairs, rehabilitation, and replacement) in each period of the 20-year planning horizon, as well as a do-nothing LCAP. The costs calculated for different repair or improvement actions in any year of an LCAP include agency costs as well as user costs associated with vertical clearance, deck width, and load capacity deficiencies. As part of its optimization analysis, BRIDGIT compares the benefits and costs for each LCAP alternative with those for the do-nothing LCAP.

## ACKNOWLEDGMENTS

This work formed part of an NCHRP project and was sponsored by AASHTO in cooperation with FHWA and was conducted in NCHRP, which is administered by TRB of the National Research Council.

## REFERENCES

1. Chen, C.-J., and D. W. Johnston. *Bridge Management Under a Level of Service Concept Providing Optimum Improvement Action, Time, and Budget Prediction*. Center for Transportation Engineering Studies, North Carolina State University, Raleigh, Sept. 1987.
2. Abed-Al-Rahim, I. J., and D. W. Johnston. *Analysis of Relationships Affecting Bridge Deterioration and Improvement*. Draft report. Center for Transportation Engineering Studies, Department of Civil Engineering, North Carolina State University, Dec. 1991, 239 pp.
3. Al-Subhi, K. M. I., D. W. Johnston, and F. Farid. *Optimizing System-Level Bridge Maintenance, Rehabilitation, and Replacement Decisions*. Report FHWA/NC/89-001. Center for Transportation Engineering Studies, Department of Civil Engineering, North Carolina State University, Jan. 1989, 274 pp.
4. NET Corporation. *BRIDGIT Bridge Management System—Technical Manual*. NCHRP Project 12-28(2)A, Washington, D.C., Aug. 1994.

*The opinions and conclusions expressed or implied in this paper are those of the research agency. They are not necessarily those of TRB, the National Research Council, FHWA, AASHTO, or the individual states participating in NCHRP.*

# Calibration and Application of Deterioration Models for Highway Bridges

---

George Hearn, Dan M. Frangopol, and Milan Chakravorty, *University of Colorado at Boulder*

A correspondence between deterioration processes and the observed performance of bridges is established by creating new quantitative condition ratings. Condition ratings defined in terms of damage indexes are used to form Markov chain models that embody the performance of bridges in service. Markov chains in turn are used to generate mean transition times that can be used to compute parameters of deterioration process models. Variations in exposure of bridge beams and in regions of bridge beams are handled by a multiplicity of Markov chains. To calibrate multiple models, condition ratings must be tied to known locations in a bridge. For this purpose the practice of segment-based reporting is introduced. Quantitative condition ratings are linked to normalized remaining flexural and shear strengths of bridge beams. Normalized remaining strength, along with segment-based reporting, supports the estimation of live load rating of bridges. Four cases of an example steel beam bridge are considered under differing rates of corrosion and patterns of corrosion in cross sections. It is seen that the controlling segment for live load rating of a bridge may evolve under some corrosion environments and that estimated live load capacities based on quantitative condition ratings are reasonable approximations of the actual load ratings.

The performance of highway bridges may be measured as the ability of the bridges to remain strong and to provide adequate service over time. Bridges must withstand the actions of (a) a service environment defined by traffic loads, maintenance activities (or their lack), and operating practices such as application of deicing salts; and (b) a natural environment defined by temperature variations, freeze-thaw cycles, and air- and spray-borne chemical agents and salts. Collectively, these actions drive processes of deterioration that impair the strength of bridges. These deterioration processes can be modeled. With models, it is possible to examine the rates of deterioration processes and the importance of deterioration processes in the life cycle of bridges.

Deterioration rates for bridges in service, if known quantitatively, can provide direct evidence of the performance (success) of particular design details and structural materials. Most often, models of deterioration processes are taken as models obtained in exposure tests of material coupons and not from structures in service. Models of deterioration processes have been used to evaluate the strength and safety of bridges. Separately, there are models of time-domain changes in condition ratings. Condition ratings are, in present practice, qualitative indicators of the state of deterioration of a bridge, and models of condition ratings are used in bridge management systems (BMSs) to assist in the selection of repair strategies. The newest BMSs use

Markov chains to model condition ratings since these chains are easily calibrated to the observed changes in condition ratings for a network of bridges. Separately, then, there are models of deterioration process, methods for evaluating bridge strength that use deterioration models, models for condition ratings, and methods for calibrating models of condition ratings against the observed performance of bridges. What is lacking is a unified approach to modeling the observed performance of bridges, interpreting these models in terms of quantitative measures deterioration processes, and using the information obtained on processes to yield quantitative assessment of bridges.

This paper outlines a unified approach to modeling and calibration of models of deterioration processes for highway bridges and illustrates the use of modeling in the assessment of load ratings. Methods for modeling, calibration, and assessment are needed for the further development of BMS. Management systems are assuming a larger role in the planning of maintenance activities, but it is important both that BMS-derived planning be responsive to the strength and safety of bridges and that safety-related repairs, which now constrain BMS planning as an external factor, be included directly in BMS to achieve the best use of resources. The modeling and evaluation capabilities provided here require a modified practice of field inspection of bridges both to obtain the necessary condition ratings for elements and to link element ratings to specific locations within a bridge. The new inspection practice, which is the subject of an ongoing demonstration project being conducted with the Colorado Department of Transportation, is outlined.

## DETERIORATION MODELING

Mathematical representations of the performance of bridges, called "deterioration models," exist today in two distinct categories. First, there are models of deterioration processes such as fatigue, corrosion of steel, and spalling of concrete. Models of processes of deterioration often describe deterioration as a function of one or a few parameters related to environment, exposure, or use. Deterioration process models yield a measure of loss of material, of strength, or of endurance, and these measures are useful in the evaluation of strength and safety of structures. Models of processes of deterioration have been used to investigate the effect of deterioration on strength of bridges (1) and can be used in the optimization of inspection intervals and maintenance programs (2,3). The studies are similar in that the models allow a deterioration process to be recognized as a change (loss) in section properties of structural members and thereby permit a reevaluation of bridge strength by familiar design-level computations.

Models of deterioration processes require calibration. Rates of deterioration can respond strongly to environment and to exposure. This is evident in the models that have been developed for atmospheric corrosion of steel. Many studies of corrosion of steel coupons have used a power law relation to describe the progress of corrosion (4–6).

$$C = At^B \quad (1)$$

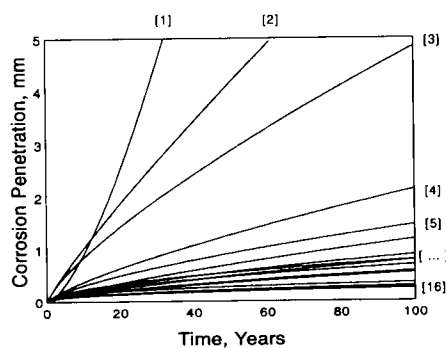
where

$C$  = average penetration of corrosion, often in microns,

$t$  = exposure time (years), and

$A, B$  = constants obtained from linear regression in log space.

Many studies of steel corrosion have employed a power law model, and it is observed that the rates of corrosion can differ significantly among studies. Figure 1 shows 16 power law models that have been reported for the corrosion of steel. It is seen that corrosion losses diverge sharply. Differences in corrosion rates are due to environment, exposure, and the method of modeling. Three severities of environment may be identified: benign, moderate, and severe (7). Exposure may be open or sheltered and is influenced by thermal lag if steel is part of a larger structure (8). Methods of modeling include linear regression log space, power law fitting in linear space (9), and composite modeling using a power law



### Corrosion Penetration - Models & Sources

[ 1] Marine, Albrecht 1984	[ 9] Marine, Albrecht 1984
[ 2] Industrial, Albrecht 1984	[10] Marine, Albrecht 1984
[ 3] Industrial, Albrecht 1984	[11] Rural, Albrecht 1984
[ 4] Industrial, Albrecht 1984	[12] Rural, Komp 1987
[ 5] Industrial, Albrecht 1984	[13] Industrial, Komp 1987
[ 6] Marine, Komp 1987	[14] Industrial, Komp 1987
[ 7] Marine, Albrecht 1984	[15] Industrial, Townsend 1982
[ 8] Rural, Albrecht 1984	[16] Industrial, Townsend 1982

FIGURE 1 Reported models of corrosion penetration for carbon steel.

for early-life corrosion and a linear rate for continuing corrosion (10). The models, different as they are, all represent the results of controlled tests of coupons.

For application to bridges, there may be a larger uncertainty in corrosion rates. Bridges are subject to all of the variables of environment and exposure and can be subject to service-related events, such as water runoff, that may encourage rapid local corrosion. Available models for corrosion of steel are almost all models of coupon studies, and nearly all are models developed using standard test methods for exposure of coupons. Some studies have placed coupons on (and underneath) bridges to simulate the exposure and environment of bridges (11, p. 717), and some work is available for corrosion rates measured on bridges in service (12, p. 16). But the overall indication of studies is that corrosion rates vary strongly, and the use of any model must be supported by frequent checking and calibration.

The second category of deterioration models is models of condition ratings. In U.S. practice, condition ratings have been assigned to bridges according to the condition rating scale of the National Bridge Inventory (NBI) (13) since the early 1970s. The condition ratings are broad, qualitative indicators of the health of a bridge. Condition ratings can be correlated with repair needs for bridges, and therefore both the ratings and models for changes in ratings over time are useful to BMSs that seek to assess repair needs and to formulate repair programs. Models for NBI condition ratings have been developed (14–16); these typically are obtained by regression analysis and can involve several factors such as bridge age, average daily traffic, and type of construction to express the changes in NBI ratings. More recently, Markov chains have been employed as models of condition ratings, and new BMSs have proposed new condition rating scales in combination with Markov chains to obtain superior models for the assessment of present and future repair needs for networks of bridges. Cesare et al. applied Markov chains to condition ratings obtained in the inspection of highway bridges in New York State (17).

Markov chains used for condition ratings are discrete-state/discrete-time chains. The condition rating for a population of bridges or of bridge elements is represented by a vector  $\{C\}$ , and the change in the population of condition ratings in a single inspection cycle is computed by operating on  $\{C\}$  with a matrix of transition probabilities  $[P]$  as

$$\begin{Bmatrix} C_1 \\ C_2 \\ C_3 \\ C_4 \\ C_5 \end{Bmatrix}_{n+1} = \begin{bmatrix} P_{1,1} & & & & \\ P_{2,1} & P_{2,2} & & & \\ & P_{3,2} & P_{3,3} & & \\ & & P_{4,3} & P_{4,4} & \\ & & & P_{5,4} & P_{5,5} \end{bmatrix} \begin{Bmatrix} C_1 \\ C_2 \\ C_3 \\ C_4 \\ C_5 \end{Bmatrix}_n \quad (2)$$

where

- $\{C\}_n$  = vector of current condition ratings
- $\{C\}_{n+1}$  = predicted vector of condition ratings after next inspection cycle and
- $P_{j,i}$  = probability that a bridge with condition rating  $i$  in current state will have condition rating  $j$  at next inspection.

Equation 2 shows a Markov chain that is typical of those for element-level BMSs. Condition State 1 is perfect, and higher rating numbers indicate increasing deterioration.

Discrete-state/discrete-time Markov chains are a natural choice for modeling discrete valued ratings that are collected at regular intervals. Discrete-state/discrete-time Markov chains require few parameters. Typically, Markov chains for condition ratings require a number of independent transition probabilities equal to the number of condition rating values. This is because it is observed that condition ratings change by not more than a single rating value in one inspection cycle (17). The transition probabilities are computed directly from inspection data as the number of bridges or elements that change from their present condition rating to the next higher rating in one inspection cycle. The transition probabilities and the model are tied directly to the observed performance of the network of bridges.

In comparison with functional forms of models for condition ratings, Markov chains do not explicitly indicate the dependence of condition ratings on factors such as bridge age or level of traffic. Instead, differences in traffic or type of structure or exposure or any other parameter that may influence the rate of change in condition ratings are handled by a multiplicity of Markov chains. For each unique element or environment, a separate Markov chain is formed. The overall model for condition ratings then is a collection of Markov chains, each independent and each dedicated to a particular combination of parameters. Using Markov chains BMSs directly address the problem of variable deterioration rates by employing separate models (chains) where required and by calibrating all models against the observed performance of the network of bridges. Variability in rates and condition is simply accepted and absorbed.

## QUANTITATIVE REPORTING AND MODELING OF DETERIORATION

Discrete Markov chains of the form used for condition ratings can be used in quantitative modeling of deterioration processes. Discrete-time chains naturally fit the regular intervals of data gathering that are standard practice for bridge inspections. The use of discrete-state

chains requires that observed deterioration be recorded as ratings that define ranges of deterioration severity—that is, a discrete-state Markov chain can indicate the probability that a bridge or bridge element is within a particular range of a quantitative measure of deterioration. For steel beams subject to corrosion, a rating scale defined in terms of a damage index based on the remaining thickness of a web plate has been proposed (18). Quantitative condition ratings for steel bridge beams are defined in terms of a damage index that is computed as a normalized thickness loss in the web plate as

$$DI = \frac{t_w - t_{wo}}{t_{wo}} \quad (3)$$

where

DI = damage index

$t_w$  = current thickness of web plate of beam (as observed/estimated in most recent inspection of the bridge), and

$t_{wo}$  = original thickness of web plate

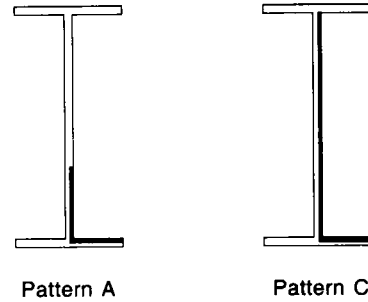
The condition rating scale is given in Table 1 and illustrated in Figure 2.

Quantitative condition ratings are used to form Markov chains in the same manner as present-day qualitative condition ratings. These Markov chains, in turn, allow the computation of parameters of models of deterioration process. This is illustrated for the *A* and *B* parameters of the power law model for corrosion of steel. A Markov chain for quantitative condition ratings defined for corrosion penetration is used to compute mean time to transitions to each of the four condition states 2 to 5. The mean time for transition from Condition Rating 1 to a deteriorated condition in rating *k* is

$$t_k = \sum_{i=1}^{\infty} P_{k,i-1} \{C_{i-1}\}_n \times n \quad (4)$$

**TABLE 1** Normalized Remaining Strengths in Condition States

Condition State	Pattern A		Pattern C	
	M/M <sub>0</sub>	V/V <sub>0</sub>	M/M <sub>0</sub>	V/V <sub>0</sub>
1	1.0	1.0	1.0	1.0
2	0.98	0.97	0.98	0.92
3	0.95	0.92	0.95	0.77
4	0.92	0.87	0.91	0.62
5	0.89	0.82	0.87	0.34



$$DI_w = \frac{t_{wo} - t_w}{t_{wo}}$$

Condition State	$DI_w$
1	0 - .05
2	.05 - .15
3	.15 - .30
4	.30 - .45
5	.45 - .60

**FIGURE 2** Corrosion patterns and quantitative condition ratings for steel beams.

$$\begin{Bmatrix} C_1 \\ C_2 \\ C_3 \\ C_4 \\ C_5 \end{Bmatrix}_n = \begin{bmatrix} P_{1,1} & & & & \\ P_{2,1} & P_{2,2} & & & \\ & P_{3,2} & P_{3,3} & & \\ & & P_{4,3} & P_{4,4} & \\ & & & P_{5,4} & P_{5,5} \end{bmatrix}^n \begin{Bmatrix} 1 \\ 0 \\ 0 \\ 0 \\ 0 \end{Bmatrix}_n$$

where  $t_k$  is the mean time for transition to condition rating *k*,  $[P]^n$  indicates the repeated application of the transition probabilities, and the initial vector of condition ratings has all of the bridges, or elements, in Condition Rating 1. The mean times to transition for the condition states each correspond to the values of damage index that are the limits of the condition ratings. The computation of mean transition times yields pairs of (time, damage index) data points that are used in a normal log-space regression to form a power law model for the corrosion process that underlies the Markov chain (19).

## SEGMENT-BASED CONDITION REPORTING

Rates of deterioration respond to the exposure of the beam, and there is a need to form several Markov chains to handle various severities of environment and exposure and several rates of corrosion. To recognize differences in exposure for beams on the same bridge and to achieve independent calibration of models for different exposures, it is necessary to link condition rat-

ings to specific portions of bridge beams. To achieve this, a process of segment-based condition reporting has been developed. In this process each bridge element is represented as a set of segments.

Segments are bounded by physical features of a bridge. Bridge beams are represented as segments between diaphragms. In Figure 3, a schematic plan of a single-span beam bridge is shown. The seven beams and four lines of intermediate diaphragms yield 35 segments for beam elements. The segments collectively form a model of the bridge that is useful both for focused modeling of deterioration processes and for estimation of load capacity. The bridge shown in Figure 3 is used in an example of load capacity estimation later in this paper.

In field inspections, two condition ratings are assigned to each beam segment (each end of the segments rated). The field report is accomplished on a graphic reporting form that indicates the segment boundaries and the locations of ratings along with a terse form of

the condition rating scale for reference. The assignment of ratings for individual segments entails many ratings for a bridge, but each rating is individually simple to assign. Inspectors can focus on a limited length of a single bridge beam and can report the ratings that correspond to their observations. This procedure is in contrast to NBI rating, in which the inspector must execute a form of mental averaging to assign a single rating for the superstructure (the item that the bridge beams would affect).

Segment-based reporting is also different from element quantity reporting required by new BMSs. The element quantities needed by BMS might require the measurement of quantities in the field, but in segment-based reporting the known quantities of individual segments may be summed in the various condition states as a part of the data processing that occurs in the office, after an inspection. Segment-based reporting for field inspections is the subject of a demonstration project being conducted by the University of Colorado and the Colorado Department of Transportation. Eight bridges, including steel, reinforced concrete, prestressed concrete, and timber bridges, are being inspected using a segment-based approach. This work will be reported separately.

### ESTIMATING LOAD CAPACITY

Quantitative condition ratings permit an estimation of the remaining strength of beams and of the load capacity of the bridge. To estimate remaining strength, both the severity of corrosion and the pattern of corrosion in the cross section must be known. The quantitative condition rating scale does not indicate the pattern of corrosion. The pattern must be reported separately as one of several characteristic patterns, or it may be assumed to be a characteristic pattern according to its position on the beam (1). Two common corrosion patterns for steel beams are shown in Figure 2. In Figure 4, normalized remaining flexural and shear strengths as a function of damage index are shown for four cross sections of bridge beams. The flexural strength plots are created for corrosion in Pattern A. Remaining shear strength has been created for corrosion in Pattern B. The close agreement of normalized remaining strength among different cross sections is a common finding for steel bridge beams.

Segment-based condition reporting links remaining strength with load demand, since load demand is a function of position within a bridge. The information provided by quantitative condition states and by segment-based reporting is enough to allow the estimation of load capacity of bridges by familiar means. Clearly, several choices are available here. The standard form of inventory rating for beams, with load demand com-

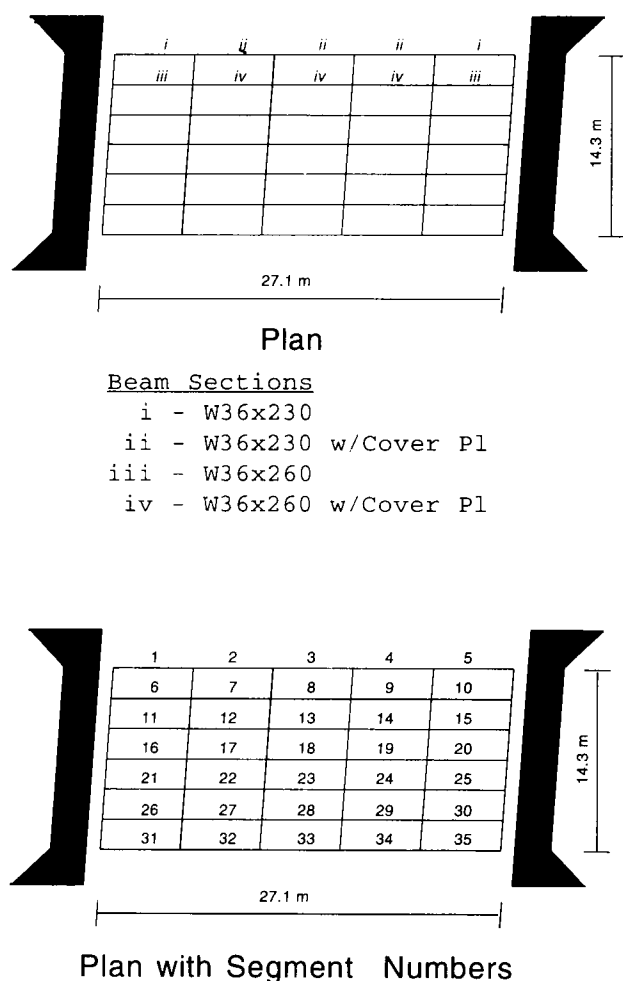


FIGURE 3 Bridge plan and segment model.



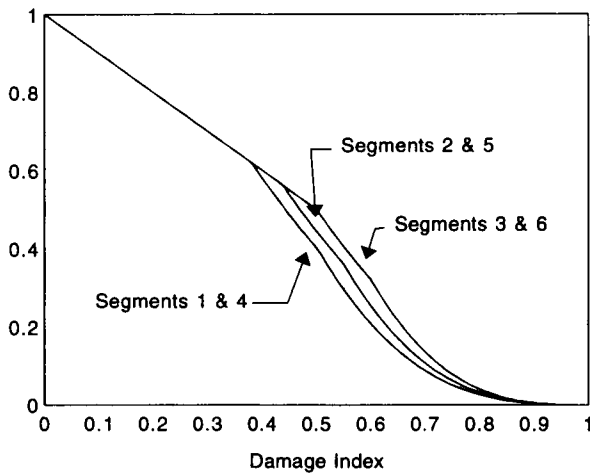
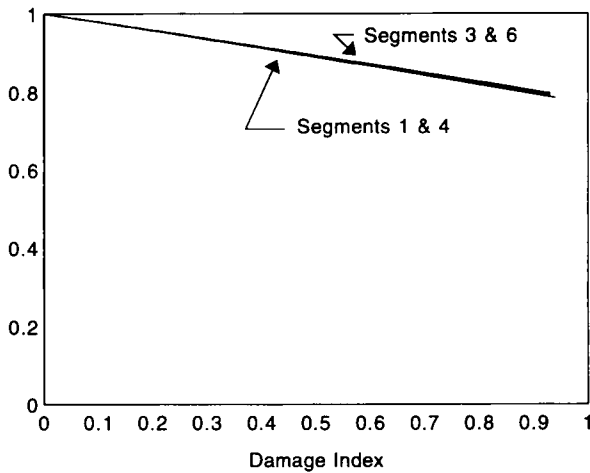


FIGURE 4 Beam strength versus damage index: *top*, flexure strength,  $M/M_o$ , Pattern A; *bottom*, shear strength,  $V/V_o$ , Pattern C.

puted on the basis of distribution factors, may be executed, and this is the method used in the example that follows. But other forms of load rating may be employed. Distribution factors may be eliminated in favor of a full three-dimensional analysis of load effects in the structure. Deterministic load effects may be replaced by an estimate of mean maximum load effects during a specified time interval (20, p. 1538), or load effects may be obtained from models that are either identified from field test data or calibrated against field test (21). In any of these approaches, the live load capacity of a bridge may be computed as

$$\begin{aligned} M_{LL+I} &\leq M_n - M_{DL} \\ V_{LL+I} &\leq V_n - V_{DL} \end{aligned} \quad (5)$$

where

$M_{LL+I}$ ,  $V_{LL+I}$  = available flexure and shear strength, respectively, for live load and impact  
 $M_n$ ,  $V_n$  = current (present-day) strength of bridge beams, and  
 $M_{DL}$ ,  $V_{DL}$  = flexure and shear dead load demand, respectively.

Using data on strength and load demand for individual beam segments, the quantities for live load capacity, segment strength, and dead load demand exist as a finite set of values  $M_{LL+I,i}$ ,  $M_{n,i}$ , and so on, where  $i$  indicates the segment number. Live load capacity is then computed for each segment individually as

$$\begin{aligned} M_{LL+I,i} &\leq M_{n,i} - M_{DL,i} \\ V_{LL+I,i} &\leq V_{n,i} - V_{DL,i} \end{aligned} \quad (6)$$

where all quantities refer to individual segments. The lowest live load capacity among all segments is taken as the live load rating of the bridge.

The estimates of live load capacity shown here are estimates for known conditions of segments. They are point-in-time estimates. Estimates at other times, future times specifically, are computed with new estimates of remaining strength in segments. These new estimates are obtained from either the Markov chains of condition ratings or the models of processes of deterioration derived from Markov chains. The use of Markov chains and discrete-valued condition ratings of course leads to discrete values of segment strength and a stepwise alteration (decrease) in load rating with continuing deterioration in members.

## EXAMPLE

The use of quantitative condition ratings, segment-based reporting, and deterioration models calibrated from condition ratings is illustrated in an example. A simple single-span steel beam bridge is shown in Figure 3. The span of the bridge is 26.8 m (88 ft), and the bridge has seven beams spaced at 2.4 m (7 ft 10 in.) on center. The bridge carries two lanes of traffic and a breakdown lane. Exterior beams are W36×230 with partial-length cover plates. Interior beams are W36×260, also with partial-length cover plates. The beams are composite with the 229-mm (9-in.) reinforced concrete deck. For this bridge without deterioration the inventory rating is controlled by the flexural strength of the exterior beams. In the segment model of this bridge (Figure 3), Segment 3 initially controls the live load rating.

Deterioration of the steel beams by corrosion will lessen the live load rating and could change the con-

trolling segment. For investigating this, three corrosion severities are assumed and their effects on the load rating of the bridge are examined. The three severities are termed benign, moderate, and severe. The power law models for these severities are given in Table 2, as are the transition probabilities that would be obtained from populations of bridge beams that experience corrosion damage according to these power laws. The transition probabilities have been determined through a simulation of aging in a population of bridges.

Benign, moderate, and severe corrosion severities are used with Corrosion Pattern A to examine the effect of overall environment on the load capacity of this bridge. In addition the severe corrosion model is used with Pattern C to simulate a special adverse local condition such as the failure of a deck joint and the resulting rapid corrosion of the ends of beams. Four cases are considered. They differ by rate of corrosion, corrosion pattern in the cross section of beams, and relative rates of corrosion for different regions of the bridge. The cases are

1. Moderate corrosion in Pattern A at all segments,
2. Severe corrosion in Pattern A at all segments,
3. Benign corrosion in Pattern A at the middle portions of beams combined with moderate corrosion at the ends of beams, and
4. Severe corrosion in Pattern C at beam ends combined with moderate corrosion in Pattern A on the middle portions of beams.

The cases are defined in Figure 5. In the figure, four cases are listed, the severity and pattern of corrosion are noted, and the application of corrosion models to three zones of the superstructure is identified. The zones recognize end, middle, and intermediate regions of beams. Additional zones might be identified. For example, interior beams and exterior beams could be considered as separate zones.

The influence of corrosion is examined by using the power law models to assess an exact corrosion penetration, by evaluating the remaining strength of segments for this corrosion, and by computing a live load rating for the controlling segment. In addition, the Markov models are used to compute condition ratings, and the

normalized remaining strengths of segments in condition states are used to estimate segment strength and to estimate live load rating. The results of live load rating using an exact value of corrosion penetration are compared with the results obtained as estimates from condition ratings.

### Case 1

Corrosion at one rate in all beams leads to nearly equal losses in normalized strength in all beams—losses of 8 percent of the beams' original flexural strength and 13 percent of the beams' original shear strength over the life of the bridge. Overall, the loss in inventory rating for the bridge is about 4 HS rating numbers, or approximately one-sixth of the initial rating of the bridge. The inventory rating is controlled by the flexural capacity of the exterior beam throughout this simulated service life. The controlling segment is Segment 3. Since this uniform corrosion process yields the same normalized losses of strength in all members, there is no evolution of the critical segment.

The inventory ratings for Case 1 are shown in Figure 6. The upper plot shows the inventory ratings for each segment as a function of time. The upper bound on the plot is the original inventory rating of the bridge. As the corrosion advances it is seen that there are decreases in the inventory rating associated with Segments 2 and 3. Both of these are segments in the exterior beam, and both are suffering losses in flexural strength that limit the inventory rating of the bridge. Segments 1, 4, 5, and 6 suffer losses of flexural and shear strength, and indeed are subject to the same corrosion process, but their losses relative to their load demand do not cause any reduction in inventory rating over a 100-year service life.

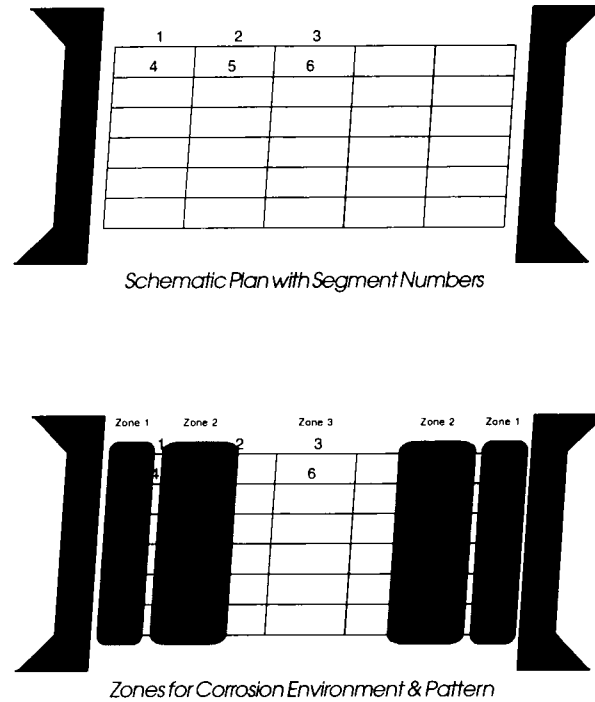
The application of segment condition ratings is shown in the lower plot. Each condition state corresponds to a range of corrosion losses, and therefore each condition state spans a range of values of flexural and shear strength. However, each condition provides a single value of normalized remaining strength. Here it is seen that the inventory ratings from condition state data decrease in a stepwise pattern as the controlling Segment 3 passes through States 1, 2, 3, and 4. The inventory ratings can be either over- or underestimates since the normalized remaining strength values are taken as the average strength in condition states. For this case, load ratings from condition states are within 1 HS number of the correct ratings.

### Case 2

Case 2 considers a faster rate of corrosion for all bridge beams. The results are similar to those of Case 1, but

**TABLE 2 Assumed Power Law Models and Derived Markov Chains for Corrosion of Steel Bridge Beams**

Corrosion Severity	Power Laws		Transition Probabilities				
	A (mm)	B	$P_{11}$	$P_{12}$	$P_{13}$	$P_{14}$	$P_{15}$
Benign	0.075	0.75	0.884	0.962	0.970	0.974	0.976
Moderate	0.171	0.75	0.718	0.895	0.915	0.925	0.931
Severe	0.390	0.75	0.502	0.727	0.782	0.804	0.819



<u>Case</u>	<u>Zone 1</u>	<u>Zone 2</u>	<u>Zone 3</u>
1	Moderate - A	Moderate - A	Moderate - A
2	Severe - A	Severe - A	Severe - A
3	Severe - A	Moderate - A	Benign - A
4	Severe - C	Severe - A	Severe - A

FIGURE 5 Cases for corrosion example.

losses of strength are more severe. The decrease in inventory rating is about 10 HS numbers, or 40 percent of the original strength of the bridge. The controlling segment is again Segment 3, and it is the flexural strength of this segment that limits the inventory rating of the bridge. The change in inventory rating over time for Case 2 is shown in Figure 7. Again, the upper plot shows the inventory ratings associated with various segments as a function of time. And again, only Segments 2 and 3 suffer losses of strength sufficient to alter the inventory rating. The loss of strength over time is approximately linear. The errors in stepwise inventory ratings obtained with condition ratings for elements differ from the correct results by 1 HS number. Notice that the inventory ratings derived from condition states stop at about 50 years. Here, corrosion losses are already severe, and the condition of the bridge is such that a more thorough review of the structure is warranted. Automated ratings, presented here, are no longer adequate

as the sole measure of strength once damage has become this severe.

### Case 3

Case 3 considers two rates of corrosion: slow corrosion in the middle of beams, and moderate corrosion at other locations. For these rates, there is an evolution in the controlling segment for inventory rating. For the first 70 years of service, the live load rating of the bridge is controlled by Segment 3. Beyond this time, corrosion losses in Segment 2 are so great that this segment comes to control the live load rating despite the lower load demand in this segment. The plots for live load ratings are shown in Figure 8. Live load ratings derived from condition states again yield reasonable estimates, and it is observed that the condition rating model (the Markov

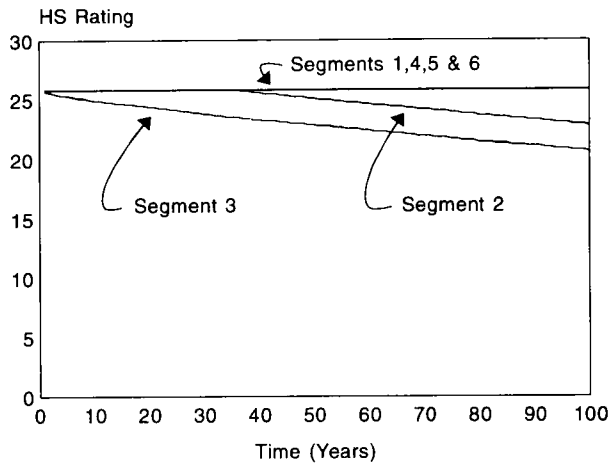


FIGURE 6 Case 1: moderate corrosion, inventory ratings.

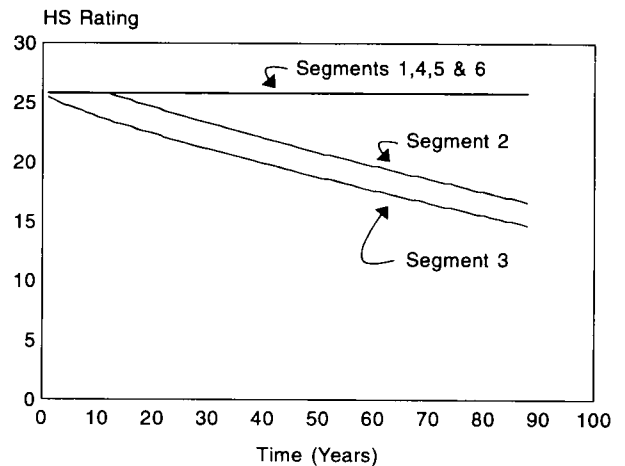


FIGURE 7 Case 2: severe corrosion, inventory ratings.

chain) recognizes the evolution of the controlling segment due to unequal corrosion rates.

#### Case 4

Case 4 considers a different, and more damaging, pattern of corrosion at the ends of beams. This case simulates a special, adverse condition such as the failure of a deck joint that produces a locally severe environment. The early part of the service life of the bridge is again controlled by the flexural strength of Segment 3. But accumulating damage in Segments 1 and 4 leads to severe and rapid losses in live load rating. This is a loss of shear strength in the ends of the beams due to corrosion attack on the entire height of the web. Figure 9 shows the plots of live load rating versus time; the rapid

loss of shear strength is seen as the dashed lines for Segments 1 and 4. The lower plot shows the live load ratings obtained from condition ratings. Again, these estimates follow the correct results. Errors in estimate ratings can be high since the bridge is undergoing large and comparatively rapid change in load capacity. Estimates from condition ratings are generally conservative, however. The only large overestimate of live load capacity is encountered after the bridge is severely impaired. This is in a range of conditions where automated estimates should not be relied on as the sole measure of bridge strength.

#### CONCLUSIONS

Deterioration rates vary, and calibration is a necessary task in the application and use of deterioration models.

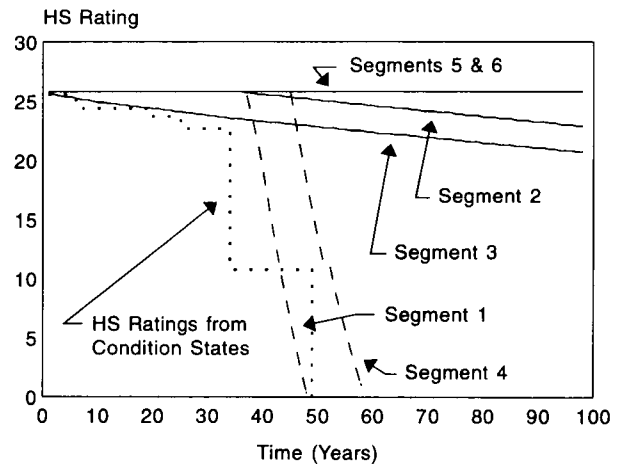
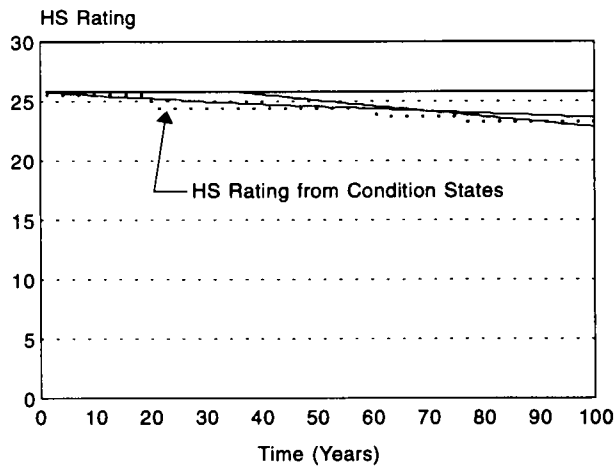
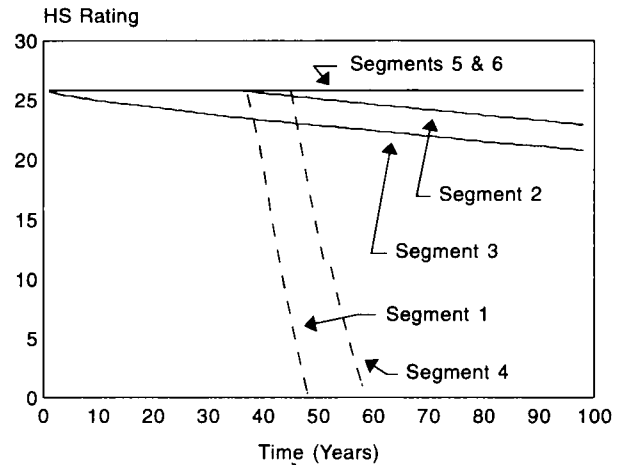
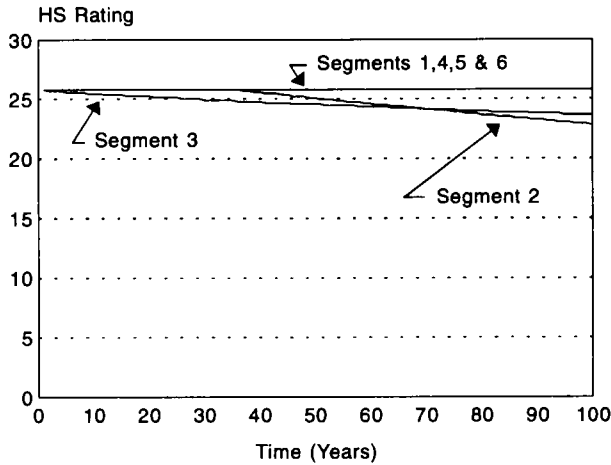


FIGURE 8 Case 3: moderate and benign corrosion, inventory ratings.

FIGURE 9 Case 4: severe and moderate corrosion, inventory ratings.

Calibrating deterioration models against the performance of bridges in service is desired but not easily achieved for standard forms of deterioration process models. The basic data on bridges and their conditions in service are provided by inspections, but such data often are not adequate to support calibration of deterioration models. In the United States, three condition ratings are the only formal data on the condition of a bridge that are routinely collected. Condition ratings are not quantitative data; condition ratings do not indicate the type or severity of deterioration observed on a bridge.

Condition ratings themselves can be modeled, and many BMSs employ models of ratings in planning and optimization procedures for maintenance programs. Management systems rely on correlations of condition ratings with repair actions to assess total costs of repairs

in a network of bridges. Management systems exploit forms of models that are calibrated easily against the historical record of condition ratings and updated easily with new data in each inspection cycle. Modeling and updating procedures available in BMSs offer much of the capability that is desired in the formation and maintenance of models of deterioration processes for highway bridges. The limitation is in the condition ratings themselves.

New quantitative condition ratings may be defined in terms of damage indexes for bridge members. New condition ratings employ the familiar integer-scale form of condition ratings currently in use. The quantitative definitions of new condition ratings make them useful in calibrating deterioration models and in evaluating bridge strength and safety. In addition, quantitative condition ratings allow BMSs to consider quantitative

safety-related impacts of decisions in maintenance programs. This is a new and important extension of existing functions of management systems.

In this paper, examples of quantitative condition rating are presented along with a protocol for condition recording that links ratings to specific elements in a bridge. Procedures for the calibration of deterioration models are presented, and the use of quantitative condition rating in load capacity evaluations is illustrated. It is found that live load rating estimates from quantitative condition ratings are accurate and that the evolution of the controlling segment, when it occurs, is recognized by models for condition ratings.

## REFERENCES

1. Kayser, J. R., and A. S. Nowak. Capacity Loss Due to Corrosion in Steel-Girder Bridges. *Journal of Structural Engineering*, ASCE, Vol. 115, No. 6, 1989, pp. 1525–1537.
2. Sorensen, J. D., and P. Thoft-Christensen. Inspection Strategies for Concrete Bridges. In *Reliability and Optimization of Structural Systems* (P. Thoft-Christensen, ed.), Springer-Verlag, London, 1988, pp. 325–335.
3. Sommer, A. M., A. S. Nowak, and P. Thoft-Christensen. Probability-Based Bridge Inspection Strategy. *Journal of Structural Engineering*, ASCE, Vol. 119, No. 12, 1993, pp. 3520–3536.
4. Copson, H. R. Long-Term Atmospheric Corrosion Testing on Low-Alloy Steels. *Proc. ASTM*, Vol. 60, 1960, pp. 650–660.
5. Komp, M. E. Atmospheric Corrosion Ratings of Weathering Steels—Calculation and Significance. *Materials Performance*, Vol. 26.
6. Albrecht, P., and A. H. Naeemi. *NCHRP Report 272: Performance of Weathering Steel in Bridges*. TRB, National Research Council, Washington, D.C., 1984.
7. Larrabee, C. P., and O. B. Ellis. Report of Subcommittee VII on Corrosiveness of Various Atmospheric Test Sites as Measured by Specimens of Steel and Zinc. *Proc.*, ASTM, Vol. 59, 19, pp. 183–201.
8. Upham, J. Atmospheric Corrosion Studies in Two Metropolitan Areas. *Journal of the Air Pollution Control Associates*, Vol. 17, No. 398, 1967.
9. McCuen, R. H., P. Albrecht, and J. Cheung. A New Approach to Power-Model Regression of Corrosion Penetration Data. In *ASTM STP 1137: Corrosion Forms and Control for Infrastructure* (V. Chaker, ed.), 1992, pp. 46–76.
10. McCuen, R. H., and P. Albrecht. Composite Modeling of Atmospheric Corrosion Penetration Data. In *ASTM STP 1194: Application of Accelerated Corrosion Tests to Severance Life Prediction of Materials* (Cragnolin and Sridhar, eds.), 1994, pp. 65–100.
11. McKenzie, M. The Corrosion Performance of Weathering Steel in Highway Bridges. *Atmospheric Corrosion*, 1982.
12. Raman, A. Atmospheric Corrosion with Weathering Steel in Louisiana Bridges. In *ASTM STP 965: Degradation of Metals in the Atmosphere*, 1987.
13. *Recording and Coding for the Structure Inventory and Appraisal of the Nation's Bridges*. FHWA, U.S. Department of Transportation, 1988.
14. O'Connor, D. S., and W. A. Hyman. *Bridge Management Systems*. Report FHWA-DT-71-01R. FHWA, U.S. Department of Transportation, 1989.
15. Fitzpatrick, M., D. Law, and W. Dixan. Deterioration of New York State Highway Structures. In *Transportation Research Record 800*, TRB, National Research Council, Washington, D.C., 1980, pp. 1–8.
16. Veshovsky, D., C. R. Beidleman, G. W. Buetow, and M. Demir. Comparative Analysis of Bridge Superstructure Deterioration. *Journal of Structural Engineering*, ASCE, Vol. 120, No. 7, 1994, pp. 2123–2155.
17. Cesare, M. A., J. C. Santamarina, C. Turksta, and E. H. Vanmarcker. Modeling Bridge Deterioration with Markov Chains. *Journal of Transportation Engineering*, ASCE, Vol. 118, No. 6, 1992, pp. 820–833.
18. Hearn, G., D. M. Frangopol, and M. Chakravorty. Towards Structural Strength and Safety Evaluation Within Bridge Management Systems. *Proc., ACSE Structures Congress XII* (N. C. Baker and B. J. Goodno, eds.), 1994, pp. 290–295.
19. Hearn, G., D. M. Frangopol, and M. Chakravorty. Quantitative Deterioration Modeling for Highway Bridges. *Proc., 4th Short and Medium Span Bridge Congress*, Halifax, Nova Scotia, Canada, 1994, pp. 397–408.
20. Verma, D. and F. Moses. Calibration of Bridge Strength Evaluation Code. *Journal of Structural Engineering*, ASCE, Vol. 115, No. 6, 1988.
21. Stallings, J. M., and C. H. Yoo. Tests and Ratings of Short Span Steel Bridges. *Journal of Structural Engineering*, ASCE, Vol. 119, No. 6, 1993, pp. 2150–2168.

# LONG-SPAN BRIDGES

---

# A Second High-Level Blue Water Bridge

---

Sudhakar R. Kulkarni, *Michigan Department of Transportation*

Planning, design, construction, and maintenance issues are presented for the proposed second high-level Blue Water Bridge, which crosses the St. Clair River between Port Huron, Michigan, and Point Edward, Ontario, Canada. The bridge design meets the requirements of AASHTO load resistance factor design specifications as well as the *Ontario Highway Bridge Design Code*. The construction plans are prepared in metric (SI) units. Main spans are a continuous tied arch bridge. The fracture-critical tie girder is fully bolted (no welding is allowed) to improve redundancy. The empirical design method is used to design the reinforced concrete deck. Approach spans are predominantly prestressed concrete I- or box beams with a reinforced concrete bridge deck.

**T**his paper presents issues related to the planning, design, construction, and maintenance of the proposed second high-level Blue Water Bridge, which will span the St. Clair River between Port Huron, Michigan, and Point Edward, Ontario, Canada. The new bridge will be constructed adjacent to the existing Blue Water Bridge and will provide an additional link between Interstate highways 94 and 69 in the United States and Highway 402 in Ontario. The proposed high-level bridge (a continuous steel tied arch) will provide a navigational clearance of 155 ft. (47.2 m) and have a center span of about 870 ft. (265.2 m). The total length of the bridge, including approach spans, is about 6,600 ft. (2001.7 m). The approach spans will be steel and prestressed concrete beam spans with reinforced

concrete decks. When the new bridge is completed, it will carry eastbound traffic to Canada; the existing bridge will carry westbound traffic to the United States. The estimated cost of the new bridge is about \$70 million, and it is expected to be opened to traffic in spring 1997. Figure 1 shows the proposed bridge, with the existing bridge in the background.

This international bridge is designed using AASHTO's new load resistance factor design (LRFD) specifications for highway bridges (1); it also meets the requirements of the *Ontario Highway Bridge Design Code* (2). The plans of the proposed bridge are prepared in the metric (SI) units.

The new and existing toll bridges are owned and operated by the Michigan Department of Transportation (MDOT) and the Blue Water Bridge Authority (BWBA), Canada. Both agencies will share the cost of the new project and provide equal design effort, labor, and materials for construction.

## PLANNING

### Traffic

Planning for the proposed structure took several years. The traffic studies indicated substantial growth in 1980 through 1991, from 3.5 million to 6.1 million vehicles a year. By 2031 the traffic is estimated to be 15.5 million vehicles a year. Currently the bidirectional annual truck traffic is estimated to be 1 million trucks. Recent





FIGURE 1 Proposed second high-level Blue Water Bridge; existing bridge in background.

passage of the North American Free Trade Agreement, or NAFTA, will generate more commercial traffic at this crossing. Truck traffic is forecasted to increase by 100 percent in the next 10 years. The existing bridge, which provides one lane of traffic each way, is not able to handle traffic growth. The proposed bridge will have three traffic lanes, shoulders, and a pedestrian sidewalk. It will carry eastbound traffic to Canada, and the existing bridge will carry westbound traffic to the United States. The toll plazas on the both sides will be upgraded for handling increased traffic.

### Funding

The second Blue Water Bridge will be a toll crossing, so the costs of construction of \$70 million will be repaid using the toll revenues.

### Environmental Report

An environmental impact study was conducted in order that final approvals could be received from the regulating agencies. The impact categories analyzed as a part of this study are as follows:

1. Natural environment: air quality, climate, geology, soils, vegetation, wildlife, aquatic environment, and special habits;
2. Social environment;
3. Cultural environment;
4. Local economics;
5. Archaeological resources;
6. Noise environment;
7. Built heritage resources; and
8. Traffic and transportation.

The study recommends mitigation for these impact categories. In particular, barges will not be allowed on the St. Clair River for construction and erection of the main span. This prohibition will require a construction method for the steel tied arch that uses a cantilevered erection of steel from the main piers on the river banks.

### SELECTION OF STRUCTURE TYPE

For spanning the St. Clair River the following bridge alternatives were considered:

- Cable-stayed (steel and concrete),
- Duplicate truss,
- Parallel-chord truss,
- Continuous tied arch, and
- Single-Span tied arch.

These alternatives were evaluated using the criteria of initial cost, life-cycle cost, construction disruption, maintenance/inspection, durability, redundancy or robustness, aesthetics, and engineering evaluation. The numerical results of these alternatives are presented in Table 1.

The evaluation indicated that cable-stayed (concrete and steel), duplicate truss, and continuous tied arch bridges were top choices. The public was given an opportunity to express its opinions on the three choices. The following is a summary of selected public input:

- Of those expressing an opinion, 63 percent preferred the duplicate existing alternative.
- By comparison, 19 percent preferred the continuous tied arch, and 16 percent the cable-stayed alternative.
- Bridge aesthetics was rated the most important evaluation factor in Port Huron, Michigan, and public health and safety was rated the highest in Point Edward, Canada.

Even though the public favored the duplicate truss bridge, the historical commission ruled in favor of the continuous tied arch bridge in order to preserve the historical uniqueness of the existing bridge. The commission also pointed out that the continuous steel tied arch bridge is aesthetically pleasing and blends with the existing bridge and the surrounding area.

Thus, the final selection was a continuous tied arch bridge for the river crossing. The adjacent three spans on each side of the arch bridge were selected to be of steel box girder spans for aesthetic reasons. The remaining approach spans, averaging lengths of about 25 to 35 m, are prestressed concrete I- or box beams. The structural and architectural features of the graceful con-

TABLE 1 Evaluation Matrix

Criteria	Weight	Cable-Stayed Steel Bridge	Cable-Stayed Concrete Bridge	Duplicate Truss Bridge	Parallel Chord Truss Bridge	Continuous Tied Arch Bridge	Simple Tied Arch Bridge
Initial Cost	3	85	85	85	100	85	85
Life Cycle Cost	1	85	90	60	90	75	100
Construction Disruption	1	100	100	90	90	85	80
Maintenance/Inspection	1	90	100	70	85	85	90
Durability	1	85	85	100	100	85	100
Robustness	3	100	100	90	85	80	75
Engineering Aesthetics	3	100	100	100	50	100	50
Engineer's Evaluation (Points)		1,215	1,230	1,145	1,070	1,125	1,000
Normalized Value		99	100	93	87	91	81

tinuous steel tied arch provide a pleasing view of the new bridge while preserving the uniqueness of the existing bridge, which has been an area landmark for a half century.

The bridge deck is reinforced concrete for the approach spans as well as for the tied arch span. The major steel tied arch bridges in North America have steel orthotopic decks with thin asphalt overlays. After considering winter conditions and the possibility of total deck replacement in the future, it was decided to not use steel orthotopic deck. The main span design will account for deck replacement in the future, using part-width construction to maintain one traffic lane.

### DESIGN/BUILD OR DESIGN/TENDER BID

Design/build was considered as an option for completing the project on time and within budget. From the owner's perspective, design/build offered the following important advantages:

- *Establishes single source of responsibility.* When both the design and construction functions are with a designer/contractor, this single entity has greater responsibility to the owner's concerns; this option also lowers the number of formal change orders.
- *Shifts risk.* The design/build team is responsible for errors and omissions in the design plans as well as defects in the construction.

- *Reduces project delivery time.* This option can reduce total project delivery time as construction of some phases can begin while later phases are still in the design stages.

- *Lowers cost.* Reducing project delivery time can provide an opportunity to reduce construction overhead and financing costs.

Disadvantages from the owner's perspective for design/build are as follows:

- *Lengthens review process.* The owner needs to define the scope of the project in great detail. Prequalification of design/build teams, request for proposal, review, selection, and award of the contract take considerable time, especially in the public agencies.
- *Decreases flexibility.* Any change in the predefined work is expensive.
- *Shifts control.* As more responsibility and control are placed with the design/build team, the owner loses a similar degree of control. Loss of control can result in a reduction of quality of materials and workmanship. Extensive specification and quality contract documentation is necessary to maintain some checks and balances.

After considering the preceding information, MDOT and BWBA decided to adopt the conventional design/tender bid method to complete this project. The selected design consulting team will be maintained for construc-

tion engineering of the project, and a second consulting team will be hired to perform an independent review of plans and quality assurance functions for the owner (MDOT).

### SELECTION OF CONSULTANT

The joint partnership between MDOT and BWBA required that the design consulting team be made up of consultants from the United States and Canada. In addition, the consultant team must have experience in designing long-span structures, in the LRFD highway bridge design specifications adopted by AASHTO, in the *Ontario Highway Bridge Design Code*, and in metrication of contract plans. The consulting team needs to include local subconsultants for surveys and geotechnical investigations. The consultants must show qualifications of the staff who will be assigned to complete the project.

### DESIGN CRITERIA

The bridge must be designed to meet the requirements of the LRFD specifications for highway bridges adopted by AASHTO (1) as well as those of the *Ontario Highway Bridge Design Code* (2). Measures must be taken to improve redundancy of the tie box girder of the continuous tied arch. The design live loading conditions must reflect operational situations on the bridge: namely, traffic tie-ups resulting in slow-moving but closely spaced commercial trucks, at least in one lane. It is possible that the concrete bridge deck will be replaced using part-width construction while maintaining one lane of traffic on the bridge. The contract plans must be prepared in metric units.

### ENGINEERING ISSUES

The following engineering issues were considered in the design phase:

- Geotechnical investigations. To provide complete data, at least one soil boring was taken at each substructure location; the borings were taken to rock depth. For main piers of the continuous tied arch, the borings were taken at least 10 ft (3.048 m) into the rock. The soil profile indicates layers of sand, gravel, and soft clay to an average depth of 100 ft (30.48 m). The hard shale rock layer is approximately 100 ft (30.48 m) below the natural ground.

Foundations for main piers and approach span piers will be supported on steel H-piles driven to bedrock. Because of the proximity of the existing bridge, care will

be taken to minimize vibrations due to the pile driving operation. Two pile load tests, one on each side of the river bank, were conducted to determine design pile capacity. Test piles were subjected to a 400-kip ultimate load; the design capacity of the piles is limited to 200 kips for the main piers.

- Hydraulics/scour protection. Since the St. Clair River flows from Lake Huron to Lake St. Clair in a well-defined channel, only minor river bank erosion control is required. The water level in the river does not vary much as it is controlled by the water levels in the Huron and St. Clair lakes. The main span piers are on the banks and out of the main river channel.

- Life-cycle/cost analysis. The analysis indicated that for the approach spans, using prestressed concrete beams is better because they eliminate the need for coating, as required for steel beams. Epoxy-coated steel will be used in the reinforced concrete deck and areas of splash zone of highway runoff containing deicing salts used during winter.

- Constructability. The plans will show a feasible scheme for erecting the continuous tied arch using a cantilevered construction from main river piers, thus avoiding use of barges in the St. Clair River.

- Maintainability. Ongoing maintenance will be a key to the durability of the bridge. To facilitate traffic and maintenance operations, the following provisions are made: (a) inspection walkways, (b) deck drainage system to drain into a pond, (c) lights, (d) waterline to fight emergency fires, (e) hazardous waste recovery system in case of truck spills, (f) crossover bridge between the new and existing bridges to divert traffic in case of repair or emergency on one of the bridges, and (g) use of slag material instead of salt for maintaining the riding deck surface during winter.

- Reinforced concrete deck design. The empirical method will be used to design the bridge deck with isotropic steel reinforcement. This method uses less steel reinforcement than does the traditional design. Epoxy-coated steel reinforcement will be provided in addition to a thin asphalt overlay with waterproofing membrane as corrosion protection.

- Bridge railings. Crash-tested railings with some modifications will be used for this bridge.

### CONSTRUCTION

Construction of the bridge will begin in March 1995, and it is expected that the bridge will be opened to traffic in spring 1997. The project will be divided into three major contracts. One contract will be for the continuous tied arch and adjacent three spans on each side, and the other two contracts will cover approach span construction of both the U.S. and Canadian sides. Approx-

imately 24 months of construction time will provide many challenges and opportunities for coordination and innovative construction methods. At this time, there is no plan to instrument this bridge for monitoring its long-term performance. However, during the construction phase the alignment and elevations and construction loads will be monitored.

## SUMMARY

In summary, this will be the first major international bridge between the United States and Canada designed

using the AASHTO and Ontario specifications, plans prepared in metric (SI) units, and featuring a deck design using isotropic steel reinforcement.

## REFERENCES

1. *LRFD Bridge Design Specifications*. AASHTO, Washington, D.C., 1994.
2. *Ontario Highway Bridge Design Code*. Ministry of Transportation and Communications, Ontario, Canada, 1991.

# Northumberland Strait Crossing, Canada

---

Gerard Sauvageot, *J. Muller International*

The Northumberland Strait Crossing is a bridge in Atlantic Canada; it is a prestressed, precast concrete structure that will provide a fixed link across the strait between Cape Tormentine, New Brunswick, and Borden, Prince Edward Island. It has been financed, designed, constructed, operated, and maintained for 35 years by the developer, a joint venture. The design service life of the structure is 100 years. The 13-km crossing comprises approaches with 93-m spans in shallow water near shores and a main bridge with 250-m spans in the strait. The scheduled completion date is the end of 1996. Because of the short construction time and the often adverse conditions for work at sea, precasting is used systematically on a large scale for the entire bridge. Precast pier bases are installed and grouted to bedrock at depths to 38 m below sea level. Precast shafts are erected on the bases. Typical cantilevers for marine spans weighing 78 MN are precast on shore and set in place with a floating heavy-lift crane, which is also used to place 52-m-long precast drop-in spans between cantilevers using a procedure that eliminates excessive erection moments in the piers. Innovative design features and the most advanced construction techniques and skills have been called on to match the challenge presented by such a major undertaking.

A fixed link between the provinces of New Brunswick and Prince Edward Island had been considered by Public Works Canada for a long time. It was not until 1988, however, that the idea materialized into a 13-km bridge, the Northumberland

Strait Crossing. This bridge would be financed, built, and operated by a private developer for 35 years, then turned over to Public Works Canada (Figure 1). In 1992 three international joint ventures were on the final list for consideration. Strait Crossing Joint Venture (SCJV) the successful low bidder, is composed of SCI of Canada, Morrison Knudsen of the United States, GTM of France, and Ballast Nedam of the Netherlands. The prime consultant is J. Muller International•Stanley Joint Venture. Construction started in spring 1994 and will last until the end of 1996; the facility is scheduled to open in 1997. Considering the size of the project, the short construction time, and the adverse conditions generally encountered at sea in this region, the realization of this bridge is a monumental work (Figure 2).

## DESCRIPTION OF PROJECT

### General

Deep water in the strait calls for long spans, whereas shallow water near shores is more suited for shorter spans. The extremely short completion time calls for extensive use of precasting, large precast elements carried by heavy marine equipment for the long spans, and more conventional elements for the shorter spans. These requirements naturally divide the bridge into two different structures: the long marine spans in deep water, and the shorter approach spans in waters not accessible by deep draft vessels.

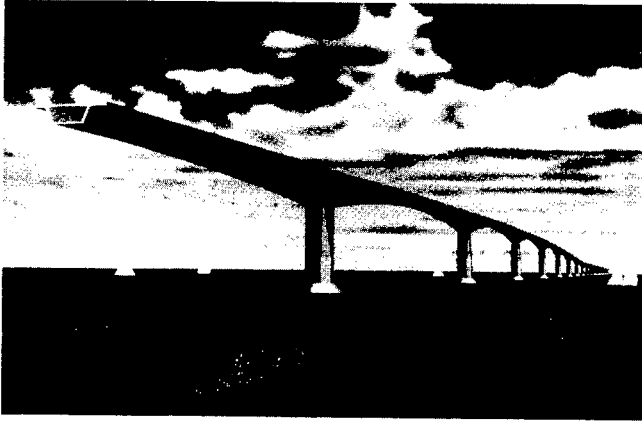


FIGURE 1 Northumberland Strait Crossing.

From Jourimain Island on the New Brunswick side to the village of Borden on the Prince Edward Island side, the bridge (Figure 3) comprises

- West approach, 1320 m long with 93-m spans;
- Main bridge across the strait, 10 990 m long with 250-m spans; and
- East approach, 600 m long with 93-m spans.

## Main Bridge

### Substructure

#### Foundations

The rock sequence across the strait consists of a series of interbedded sandstones, siltstones, and mudstones. These rocks are believed to have been deposited as sediments in a fluvial or estuarine environment, and a broad correlation can be made across the strait. However, at a small scale, the rock layers are not very consistent from pier to pier, and each pier location must be investigated fully and evaluated on its own. Thick layers of sandstone are interbedded with layers of relatively soft mudstone varying in thickness from 5 to 500 mm, most being 50 mm thick. Sandstone is competent rock, but mudstone layers underlying sandstone constitute weak planes for transmitting horizontal forces, such as those from ice and wind. Because of the uncertainty in assessment of the real geometry of these layers, it is assumed that they are present over 100 percent of the foundation areas.

The contractor chose to use spread footings for all the prefabricated piers. For the reasons explained earlier, the founding level must be on sandstone with the next layer of soft mudstone, if any, following at a depth not less than that determined by the geotechnical anal-

ysis on a pier-by-pier basis, but in no case less than 1.50 m. The dredging operations consist of first removing the overburden, which is up to 10 m thick, and excavating a trench to the competent sandstone level; a template is used to guide the dredging bucket in the circular pattern.

The prefabricated pier base ring footing is installed in the trench on three hard points about 0.5 m above the bottom. The three points determine a horizontal level on which to set the pier base and leave a space between the ring footing and the trench, which is then filled with a specially formulated tremie concrete, ensuring uniform bearing of the whole pier base on the rock (Figure 4).

Safety against sliding of the foundation is checked at the interface with the rock assuming a shear friction corresponding to 16 degrees/18 degrees for the undrained mudstone. The compressive stresses at ultimate limit state are in the range of 1.2 to 1.6 MPa; actual strength of the rock is twice that value or larger, depending on the pier location.

The modulus of subgrade reaction is in the magnitude of 110 MN/m<sup>3</sup>; long-term settlements are minimal. At the ultimate limit state, the eccentricity of the resulting force applied to the footing is limited to 0.30 of its diameter.

#### Pier Bases and Pier Shafts

All pier bases and pier shafts are prefabricated in the casting yard at Borden. They are prefabricated separately because of height and capacity limitations of the catamaran-type floating heavy-lift equipment, called Svanen, which has been upgraded after previous use in Denmark on the Great Belt Project and will be used to transport and erect all the components of the main bridge.

There are two types of pier bases: Type B1 for depths down to -27.0 m, and Type B3 for depths of -27.0 to -38.2 m. B1 has a ring footing, 22.0 m in diameter and 4 m wide, that fits exactly between the two hulls of Svanen. B3 has a ring footing 28.0 m in diameter but with two flat surfaces spaced 22.0 m so that it also fits into Svanen. Above the ring footing, a conical shell transfers the loads from the barrel, which varies in height according to the depth of the foundation. The barrel ends at elevation -4.00 m by a male cone used to connect the pier shaft to the pier base (Figure 5). The maximum weights of the B1 and B3 bases are 35 and 52 MN, respectively. The maximum height of B3 is 42.0 m.

Each pier shaft comprises the shaft itself and the ice shield. It is one of the most critical components of the whole structure because it will be in direct contact with the most aggressive and corrosive environment, seawater in the tidal range, salt-laden spray and air, and abra-

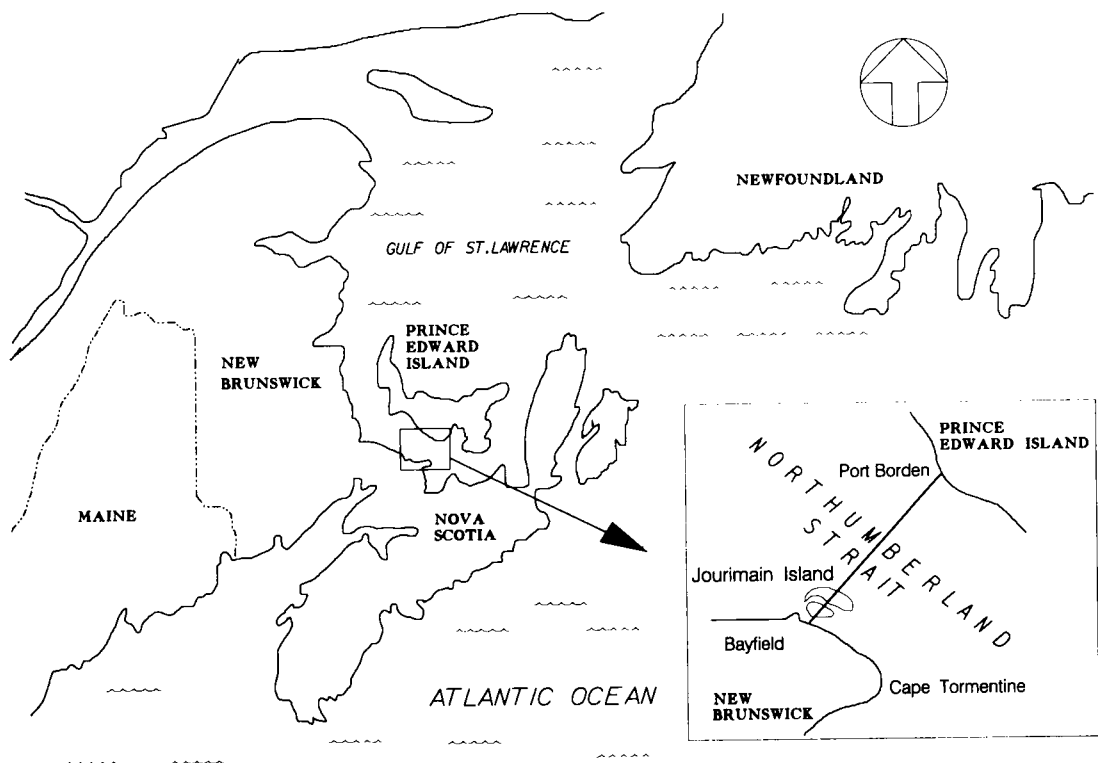


FIGURE 2 Project location.

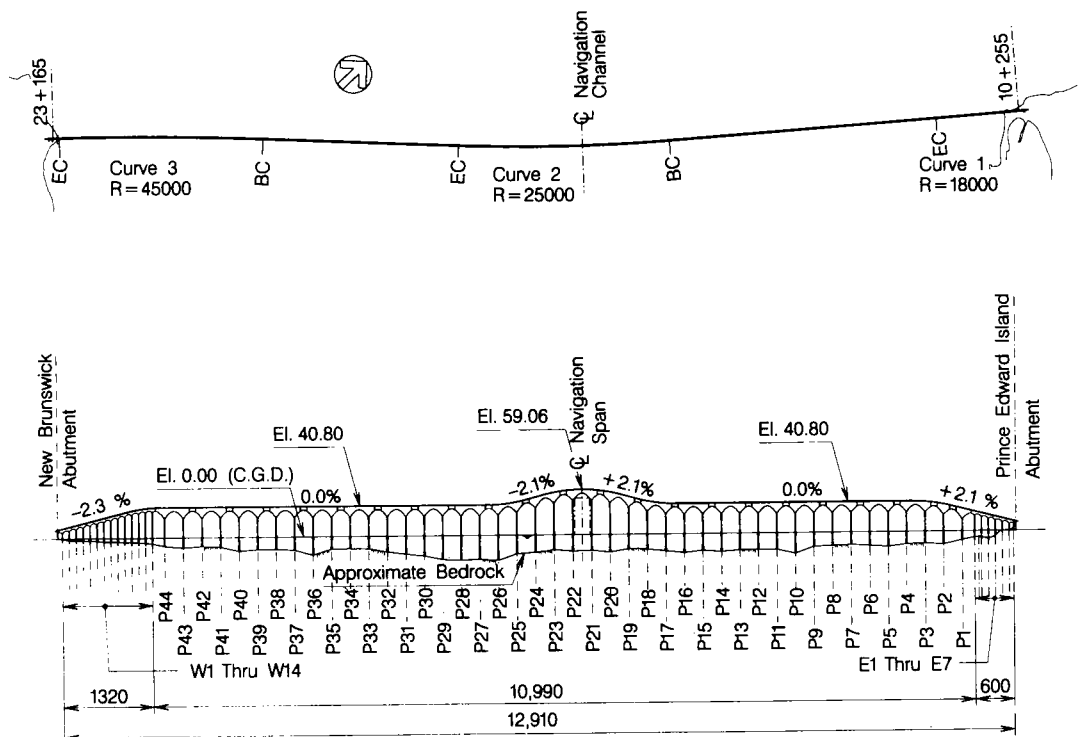


FIGURE 3 Bridge profile: top, plan; bottom, elevation.

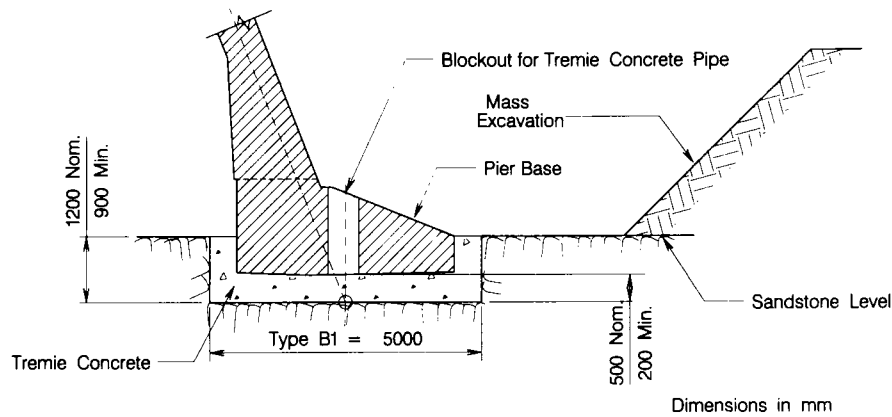


FIGURE 4 Trench and footing, main bridge.

sion from the ice; therefore, all exposed cast-in-place joints have been eliminated from this element, which is monolithic from the bottom of the ice shield to the top of the pier, with a maximum weight of 40 MN.

The ice shield is conical with a base diameter of 20.0 m, a height of 8.0 m, and a 52-degree angle on the horizontal. It is solid except for a central conical void that matches the top of the pier base. The ice shield itself extends between elevations  $-4.0$  and  $+4.0$  m; it is clad with a 10-mm mild steel sheet for abrasion protection.

The pier shaft has a box section, varying from an octagon at the top of the ice shield to a rectangle at the top of the shaft. The walls are 600 mm thick.

The pier shaft is assembled onto the pier base by being lowered until it rests on hydraulic jacks on top of the base; the position of the top of the pier shaft is adjusted by activating those jacks. The space left between the two cones is grouted, creating a continuous structure through the keyed joint, and vertical post-tensioning tendons crossing the joint are then stressed.

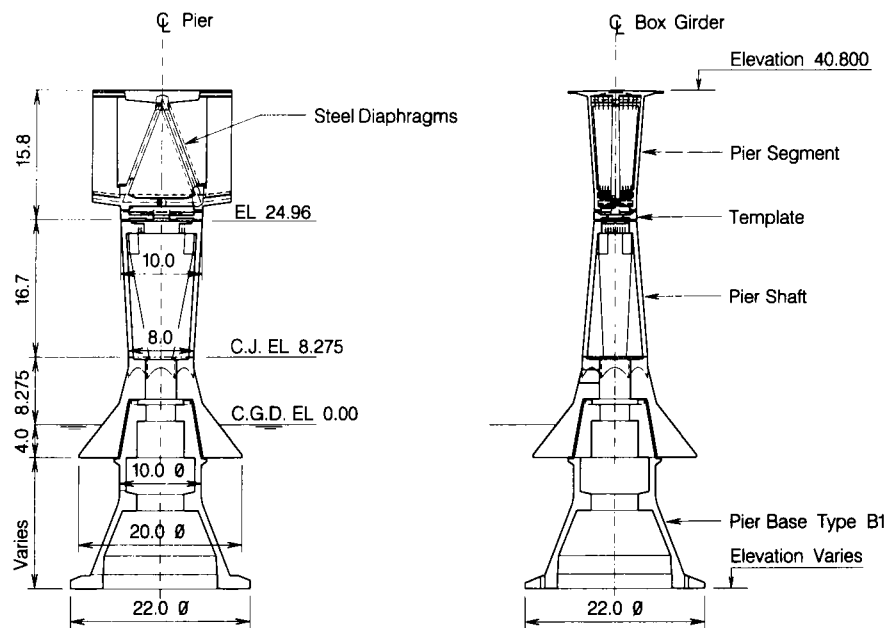


FIGURE 5 Typical pier, main bridge: *left*, longitudinal section; *right*, transverse section.



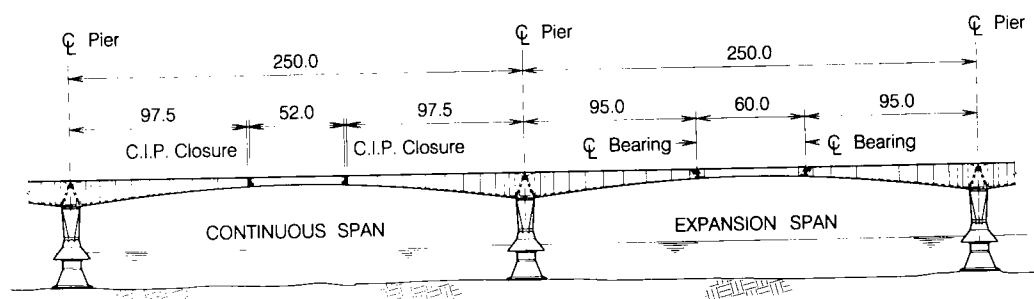


FIGURE 6 Typical superstructure, main bridge.

The top of the pier shaft is equipped with a template that is matchcast to the soffit of the pier segment. Once the pier shaft is in place, the template (1.0 MN) is grouted in position so that the future cantilever girder (78 MN) can be placed directly in its final position, thereby avoiding delicate and time-consuming adjustments of a heavy and unstable cantilever.

### Superstructure

The superstructure forms a series of frames connected by 60.0-m-long drop-in expansion spans. A frame consists of two cantilevers, integral with the piers and made continuous by inserting a 52.0-m drop-in span between the cantilever tips, pouring closure joints, and stressing

post-tensioning tendons to achieve a fully monolithic frame (Figure 6).

### Cantilever Deck

The 44 cantilevers, 192.0 m long, are prefabricated in the casting yard. Each is made up of 17 segments, one 17.0-m-long pier segment with eight segments on either side, their lengths varying from 7.5 to 14.5 m. Segment depths vary from 14.0 m at the pier to 4.5 m at mid-span. One end of the cantilever is equipped with a hinge to receive the simply supported drop-in span (Figure 7).

The pier segment has a composite post-tensioned inverted V diaphragm; its steel structure is used as form for casting of the segment and is supplied by the fab-

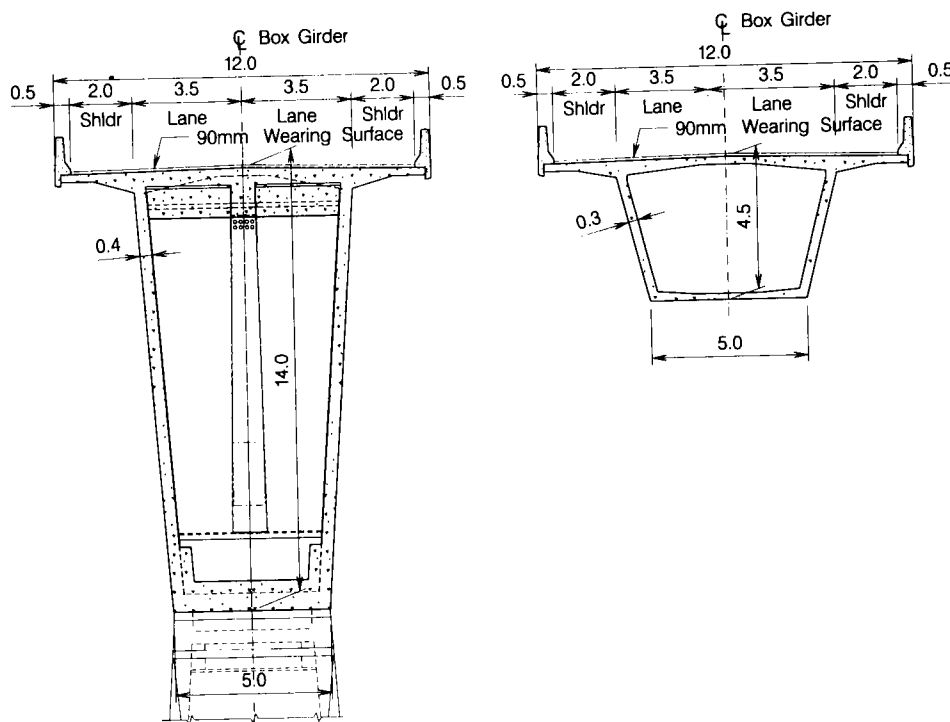


FIGURE 7 Typical cross section, main bridge: *left*, pier; *right*, midspan.

ricator with all the post-tensioning ducts installed to speed up fabrication. Steel diaphragms also help solve the congestion problem due to the large number of cantilever tendons needed for the long span that must be installed in a narrow cross section.

A moment-resisting connection between cantilever and pier is achieved through the matchcast template with vertical post-tensioning tendons, some of which are looped in the walls of the pier shaft and others that are external and replaceable, placed inside the pier shaft and anchored at the ice shield level.

In the precasting yard, the 16 cantilever segments are cast on 16 fixed beds, a pair at a time. The process starts with the pier segment, which is always cast at the same location; from there it is moved transversely until it aligns with the two first beds, where the first two cantilever segments are cast, one on each side, and post-tensioned. Then the assembly made of the pier segment and the two first segments is again moved transversely until it aligns with the next set of fixed beds, where another pair of segments is cast, and so on.

A system conceived to dampen the oscillations of the cantilever during load transfer from Svanen to the pier shaft is installed in the template (Figure 8).

### Drop-In Span

A drop-in span is used to close the remaining gap between cantilever tips. A typical 52.0-m drop-in span is used either to connect two cantilevers rigidly to create a frame or to connect two frames. When used within a frame, the drop-in span is made continuous with the cantilever using the following sequence. The 52.0-m span is picked up in the center by Svanen at the casting yard, brought out to the pier, and guided into position between the tips of the facing cantilevers. The gap between either end of the span and the adjacent cantilever

tip is closed by a shim-type device, whereafter the dead weight of the span is released by Svanen. If the cantilever tips were free to move longitudinally, toward each other, they would do so under the effect of the applied vertical loads, due to bending of the piers; such longitudinal movement is prevented, however, by the drop-in span acting as a strut; a compressive force is developed in the drop-in span counteracting the effect of its dead load, which otherwise would have induced adverse bending moments in the piers.

This horizontal force is such that no counterweights are needed. After the transfer of force, its magnitude is adjusted by means of hydraulic jacks to a design value, typically 18 MN, chosen to best compensate the long-term effects of creep and shrinkage. Then joints are cast and post-tensioning tendons stressed, whereby the continuity of the frame is achieved. When used to connect two frames, the basic 52.0-m span is fitted with hinge segments at either end to turn it into a 60.0-m simply supported span, which is always installed after the adjacent frames are completed.

### Approaches

West and east approaches consist of thirteen and five 93.0-m spans, respectively, and shorter abutment spans. The rectangular prismatic box piers rest on footings, shaped as ice breakers similar to those of the main bridge, and cast in place within cofferdams directly on sandstone. Each footing is equipped with six to eight keys, cast in vertical shafts, 2 m in diameter, 5 m long, drilled into the sandstone to increase resistance against ice loads.

For the footings, casting in place was selected because the water depths of 0 to 8 m did not allow heavy floating equipment to access all locations. For shafts and superstructure, precasting was chosen to reduce construction time and improve quality.

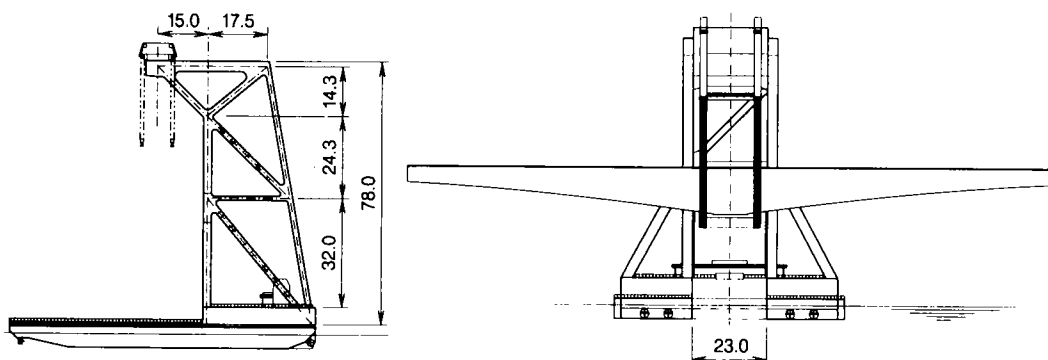


FIGURE 8 Floating heavy lift equipment, Svanen.



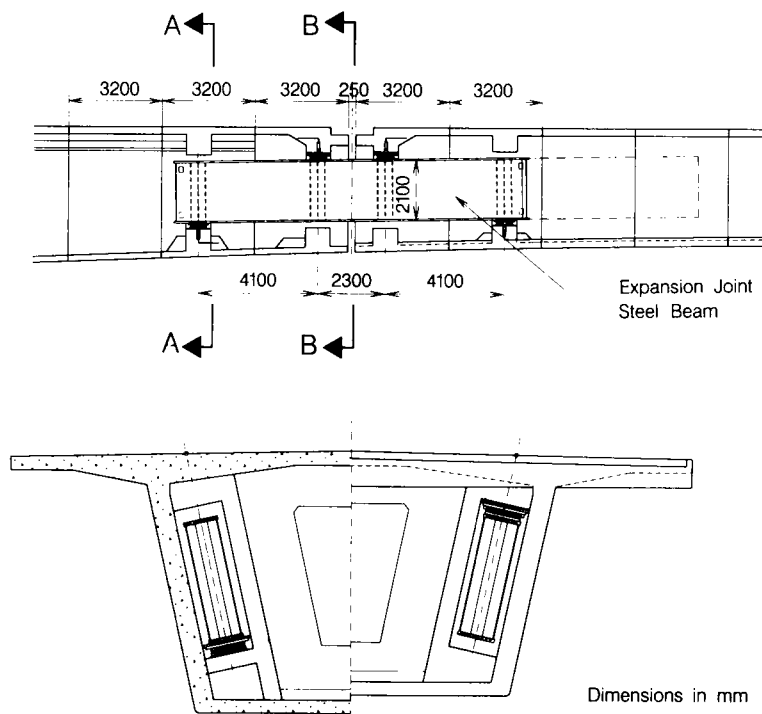


FIGURE 11 Expansion joint, approaches: *top*, longitudinal section; *bottom*, Sections A-A (*left*) and B-B (*right*).

Production time for a pier base is anticipated to be about 2 months, the same as for a pier shaft-ice shield. Twenty pier bases and 14 pier shafts can be stored.

## DESIGN REQUIREMENTS

The design requirements issued by Public Works Canada, as part of the 1988 call for proposals, have had a direct impact on the chosen structural concept. The most important of these requirements are listed here:

- The design service life of the facility shall be 100 years, with high-quality performance, and must be achieved through excellence of concept, design, construction, maintenance, and operation procedures.
- Consideration shall be given to the fundamentals of aesthetics.
- The progressive collapse criterion, saying that the failure or collapse of any one span shall not lead to progressive failure or collapse of other spans, has had a large influence on the choice of the static scheme of the bridge.
- Environmental loads, such as ice force and wind, in connection with the permanent loads are dictating the design of the substructures.

- Risk of ship impact in the vicinity of the navigation channel has led to either strengthened piers or protective islands.

- Roadway width is 11.0 m, providing a three-lane facility.

- The navigation channel has a 172-m horizontal clearance and 49.0-m vertical clearance, with a minimum depth of 13 m.

## Load Combinations and Load Factors

Public Works Canada requires that load combinations and load and resistance factors for ultimate and ser-

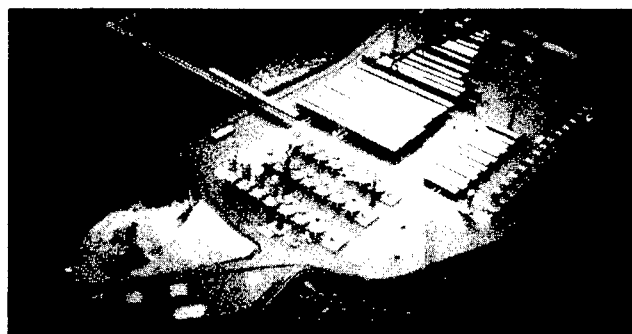


FIGURE 12 Model of precasting yard.

viceability limit states be derived specifically for the project through a full calibration process using probabilistic reliability techniques.

A target safety index  $\beta = 4.0$ , applies to each multi-load-path component of the bridge at ultimate limit states, for a 100-year design life. For single-load-path components,  $\beta = 4.25$  is imposed. The target safety index is a measure of the accepted risk of failure of a structural member.

As a result of the analysis, load factors different from those usually recommended in codes were obtained. For serviceability limit states, crack widths are related to the change of stress level in the reinforcement or tendon for a given spacing.

### Ice Loading

Generally, the ice season in the Northumberland Strait begins in December or early January, and conditions worsen until late March. The maximum thickness of ice floes (i.e., floating ice formed in large sheets at the surface of the sea) is about 0.30 m. Floe sizes occasionally reach 500 m, with a mean of 118 m.

Currents, waves, and wind induce ice movements, cause floes to break, and result in rafting and ridging; ice ridges consist of a consolidated core of refrozen ice at the waterline with loosely bonded blocks of ice forming a small sail on top of the ridge core and a much larger keel below it (Figure 13). Ridge dimensions are 50 to 75 m. The ridge keel depths can be evaluated from the number and location of scours seen on the bottom of the strait; the deepest is at 18 m, and the average is 8.5 m. The ridge core thickness may reach 2.5 m.

The critical case for the substructure of the bridge is the consolidated ridge core hitting the pier shaft. To minimize the horizontal force on the pier shaft, a con-

ical ice shield has been designed with an angle of 52 degrees to break the ridge core in bending, the ice riding up the cone and collapsing under its own weight, rather than crushing directly on a vertical surface, producing a much higher force. The ice shield is clad with steel plate to minimize ice abrasion and reduce friction.

Numerical models are used to calculate ice loads, which are given as a function of their expected occurrence, such as once in 100 years, once in 1,000 years, and so on.

The direction of ice forces has been studied; it is related to the direction of the prevailing currents and, to a lesser degree, the wind. Rose diagrams for currents, winds, and ice forces were developed at several locations along the bridge. It was found that the maximum force was perpendicular to the bridge and a force of about 65 percent thereof may act in the longitudinal direction of the bridge.

It should be noted that all assessment of ice loads carries a degree of uncertainty as relevant on-site measurements of ice forces are scarce; besides those made at Lighthouse KEMI-1 in the Gulf of Bothnia in 1985–1986, practically none have been reported, and laboratory test results can be only a guide.

Another aspect of ice loading is its dynamics. The dynamic response of the bridge allows the assessment of the dynamic loading characteristics of the ice. An analysis was carried out, taking into account ice force versus time histories derived from the consideration of all contributing features:

- Ice failure frequencies;
- Ice speed;
- Ridge core characteristics, ridge keel dynamics; and
- Rubble surcharge.

Failure of the ridge core is estimated to be the most likely source of dynamic ice loads for frequencies of less

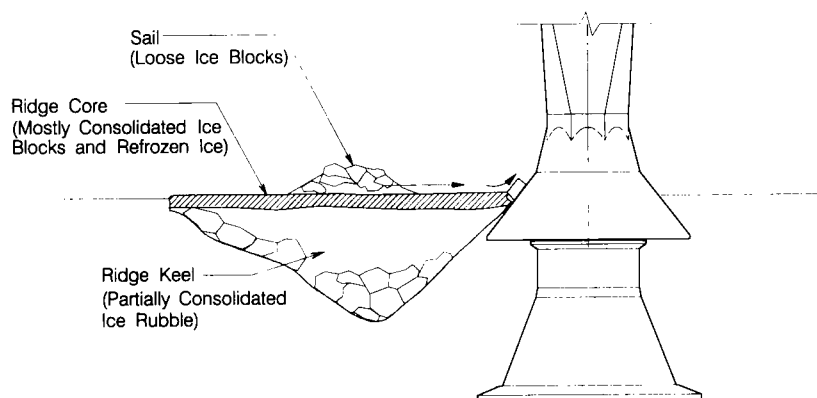


FIGURE 13 Ice ridge.

than 1.5 Hz; ridge keel dynamics activate frequencies below 1.0 Hz; the combination of ridge core and ridge keel effects is relevant only for frequencies less than 1.0 Hz. The lowest natural frequency to be considered for the completed bridge is 2.6 Hz, higher than the ice-induced frequencies.

Now, the design of the substructure is based on a transverse static ice force (perpendicular to the bridge) of 25 MN and a longitudinal static ice force (in the direction of the bridge) of 17.5 MN. For ultimate conditions a factor of 1.5 is applied to the loads, which are controlling the dimensions of the foundations.

### Wind Loading

Because of the location of the structure in the windy Northumberland Strait, a complete study was done to investigate the safety of the bridge for aerodynamic stability and maximum wind speed loadings, in construction stages and in service. Wind effects on vehicular traffic and snow accumulation were also investigated.

Experimental wind tunnel testing, involving a 1:60-scale section model for aerodynamic parameters and a 1:250-scale full aeroelastic model, was undertaken; the latter was tested in three construction stages, namely, free-standing double cantilever, frame completed, and bridge completed.

Reference wind speed for a 100-year return period is 29.5 m/sec, with the maximum component transverse

to the bridge being 26.4 m/sec, at 10 m above water. During construction, a wind speed of 22.5 m/sec corresponding to a 10-year return period is considered. In the casting yard, a wind speed of 15 m/sec is used. The wind load per unit length of bridge is given by

$$W(y) = q C_e [C(y) \pm C_{dyn} F(y)] B$$

where

$q$  = reference wind pressure ( $q = 0.44$  kPa for 26.4 m/sec),

$C_e$  = exposure coefficient (varies with height),

$C(y)$  = static coefficients in  $x, y, z$  varying with longitudinal position ( $y$ ),

$C_{dyn}$  = dynamic coefficient,

$F(y)$  = modal load distribution factor, and

$B$  = width of bridge deck.

The static part of the transverse wind load for a 250-m span is in the magnitude of 3.7 MN.

### Wave and Current Loading

The location of the bridge is somewhat protected from the ocean and from the swells of the Gulf of St. Lawrence by the island itself. The wave environment in the strait is governed by waves generated within the strait. The peak period for the extreme waves ranges from 6 to 9 sec. The maximum wave height in the mid-

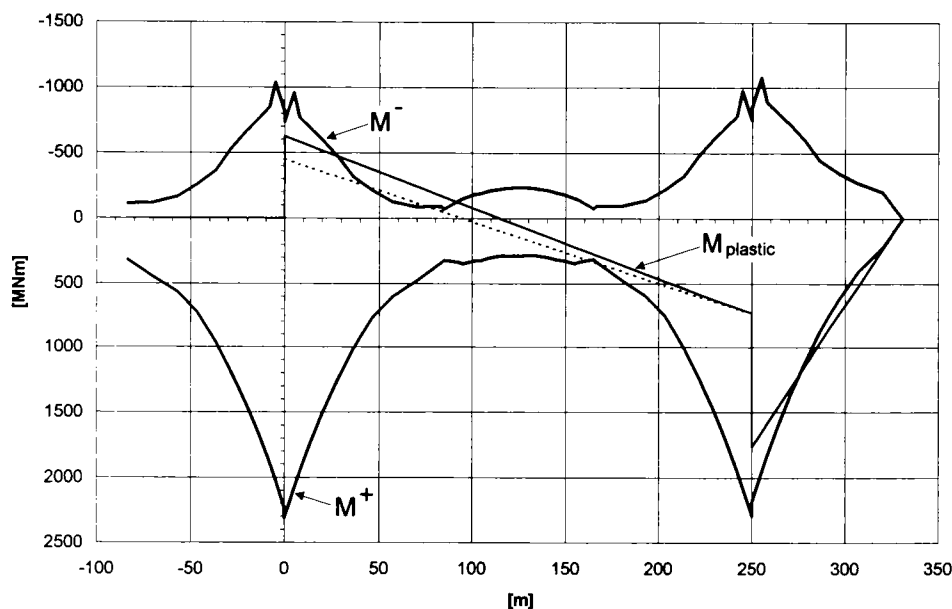


FIGURE 14 Progressive collapse, quasistatic analysis: bending moment after failure of hinge versus ultimate moment capacity, moment differences relative to dead load moment.

dle of the strait for a 100-year return period is 4.70 m. Tidal range is from +2.25 to -2.03 m. Maximum current velocity is 2 m/sec.

It was found that maximum forces develop at high tide and that a large part of the force is generated on the ice shield itself. Maximum horizontal and vertical forces are 8 and 4.3 MN, respectively.

### Progressive Collapse

Collapse of one pier or one span or destruction of a hinge-expansion joint must not trigger the collapse of the following spans, as is actually the case in most continuous structures. A simple and still efficient scheme was chosen, consisting of two piers with the cantilevers

rigidly connected by the drop-in span, the whole system forming a rigid frame. Frames are then linked with a drop-in span simply supported at the outer tips of the frames' cantilevers. Several analyses were carried out, including time-history analysis, and it was found that the quasistatic approach in which the weight of the missing drop-in span was replaced by an upward force equal to the reaction of the span yielded acceptable results. The graph in Figure 14 shows the result of such analysis where the "plastic moment" caused by the effect of the collapse must remain within the capacity of the span. The strengths of the pier-to-superstructure connection and of the superstructure were adjusted until this condition was satisfied. Progressive collapse criteria actually dictated the structural scheme of the bridge.

# Design and Construction of Tsurumi Tsubasa Bridge Superstructure

---

Mamoru Enomoto, Hisashi Morikawa, Haruo Takano, Masafumi Ogasawara, and  
Hiroyuku Hayashi, *Metropolitan Expressway Public Corporation, Japan*  
Wataru Takahashi, *Miyaji Iron Works Co., Ltd., Japan*  
Nobuo Watanabe and Masahito Inoue, *NKK Corporation, Japan*

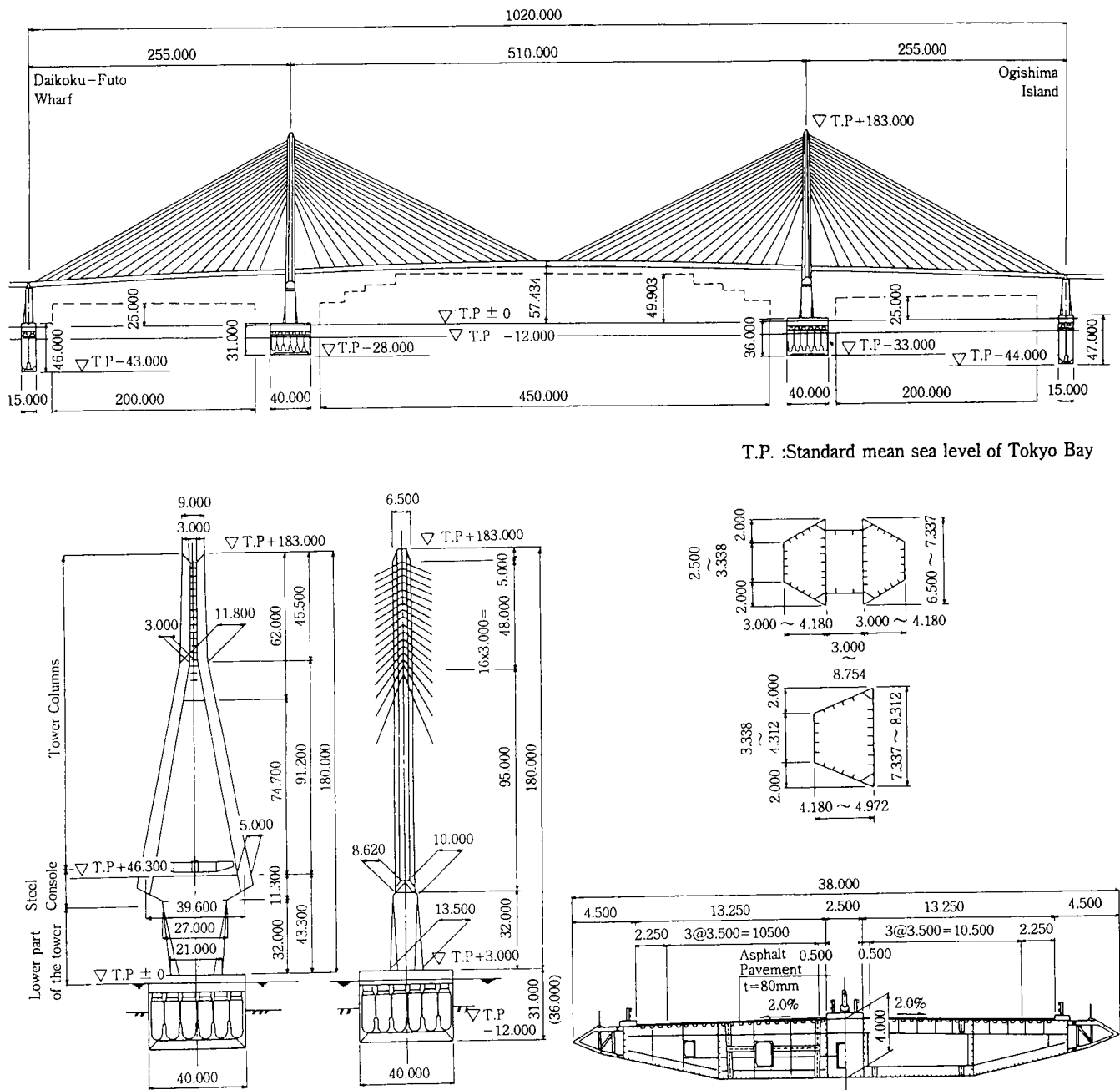
The Tsurumi Tsubasa Bridge is a single-plane, three-span continuous cable-stayed bridge 1020 m long, with a 510-m center span. It was constructed over the Tsurumi Fairway, which lies between the Daikoku-Futo Wharf and Ogishima Island in Yokohama. The total weight of the steel superstructure is about 38,000 tons with the foundation built on pneumatic caissons. This bridge was built for the Metropolitan Expressway. In the future, National Highway 357 will cross the Tsurumi Fairway on a separate bridge built parallel to and in the same style as the Tsurumi Tsubasa Bridge. Therefore, the appearance and the earthquake and wind resistance of the Tsurumi Tsubasa Bridge were studied not only with consideration being given to the first but also the second bridge standing parallel to the first. As for the construction of this new bridge, at each step of construction actual values were checked against design values to ensure safety and precision. Construction was accomplished with a high degree of precision, owing to the introduction of a precision control system.

**T**he Tsurumi Tsubasa Bridge, a 1020-m-long, single-plane, three-span continuous cable-stayed bridge with a 510-m center span, was constructed over the Tsurumi Fairway, which lies between the Daikoku-Futo Wharf and Ogishima Island in Yo-

kohama. The total weight of the steel superstructure is about 38,000 tons. Pneumatic caisson foundations were used. The general view is shown in Figure 1. This bridge was built for the Metropolitan Expressway. In the future, National Highway 357 will cross the Tsurumi Fairway on a separate bridge built parallel to and in the same style as the Tsurumi Tsubasa Bridge. Therefore, the appearance and the earthquake and wind resistance of the Tsurumi Tsubasa Bridge were studied with consideration being given not only to the first but also the second bridge parallel to the first.

Photomontage and computer graphics techniques were used to study the projected appearance of the two bridges standing parallel. The study revealed that with a double-plane, cable-stayed bridge design, the cables of the two bridges would appear to be entangled and that with a two-leg-type lower tower, the two pair of legs would appear to be intermingled. Therefore, a single-plane semi-fan-type cable arrangement was adopted. The lower part of the tower was designed as a concrete wall construction with an octagonal cross section, and the upper tower was configured as an inverted Y-shape with a trapezoidal cross section. To the extent possible, the block joints were welded at the construction site to provide a smooth, slender appearance.





T.P. :Standard mean sea level of Tokyo Bay

FIGURE 1 General view.

Because it stands in the sea, the concrete lower part of the tower was coated with a fluorine-containing resin to provide excellent durability and appearance. The color is white (N.9.5) to enhance its appearance in the blue of the sky and sea. An artist's conception of the twin bridges is shown in Figure 2.

The girder has a total width of 38 m, including fairings. It has a five-cell box section with a height of 4 m to increase torsional rigidity because the bridge has a single-plane, cable-stayed deck with very long spans.

Because the section is wide, a bending moment occurs in the transverse direction of the girder, and compressive stresses act on the lower flange in the spans and on the deck plate at the support points. Therefore, local and total buckling were studied for the members on which compressive stresses act in two directions (transverse and longitudinal). Verification was performed by three-dimensional finite-element method (FEM) analysis because stresses concentrate in the supports and at the cable anchoring sections. The maximum deflection of

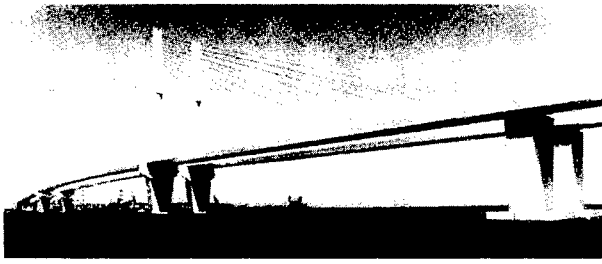


FIGURE 2 Artist's conception of the twin bridges.

the girder caused by live load (including the torsion-induced vertical displacement of the road shoulder) is  $\delta = 853$  mm. Vertical displacement of the road shoulder caused by a one-sided live load is  $\delta = 467$  mm and produces the largest torsion angle ( $\phi = 0.0123$  rad). Under normal conditions, however, the torsion angle is not so large.

The lower tower starts at the upper caisson slab and includes the steel console, which supports the girder and tower column. To smoothly transmit the load from the tower column and girder to the caisson foundation, a design was adopted that used a steel-frame reinforced concrete structure to about 20 m above the upper slab of the caisson foundation and a concrete steel multicell and steel console above it. The basic design concept was for the compressive force of the steel multicell section to be completely transferred to the concrete by a bearing plate and for the tensile force occurring during an earthquake to be borne by the steel frame. However, it was suspected that the total load could not be transferred by the bearing plate and, clearly, tensile force will flow to the reinforced concrete from the steel cell-plate structure. Dowels (D22 steel bars passing through holes cut in the steel cell plate) are used to provide a tensile load path between the steel cell-plate structure and the concrete and to permit smooth transfer of load. An experiment was performed using a large model to confirm the feasibility of these dowels. From the experiment, it was assumed in the design that 50 percent of the compressive force would be transferred from the bearing plate to the concrete and the remainder would be transferred through the dowels. The structure of the lower part of the tower is shown in Figure 3.

The tower column was made somewhat higher to reduce the deflections caused by the live load and the variations in cable tension. The tower height from the top of the foundation was set at 180 m. The tower column is subjected to high axial force and bending moment, and stresses concentrate at the cable anchoring locations and at the branch. Therefore, verification was performed by three-dimensional FEM analysis. Seismic resistance and elastic buckling analyses were carried out

to confirm the stability of the structural system of the whole tower column.

The cables were arranged as a semifan with 17 stay cables. The cables are nongrout-type parallel wire strands (PWS) that are made by bundling galvanized wires 7 mm in diameter and coating with polyethylene. The cable arrangement was studied using cables with 499 wires (coated outside diameter, 192 mm; unit weight, 156.8 kg/m), which is the maximum size that could be used in terms of production, transportation, and installation. Of the 34 cables attached to each tower 15 are maximum section cables. The cable tension was adjusted so that a dead load bending moment was not induced on the tower. A saddle-type cable anchorage was used on the tower side, whereas anchorage girders were used on the girder side. After the cable was anchored to the saddle on the tower, the girder end was pushed inside the girder into the anchorage girder from the upper side.

Attaching horizontal cables, set in the girder, were installed to restrain the relative horizontal displacement between the girder and tower. This is because the link structure increases the width of the tower and affects the clearance between the twin bridges and because oscillation of the girder must be restrained because of its low bending rigidity. The attaching horizontal cables were also made from PWS. Four 117-m cables are attached to each tower: two cables on the center span and the others on the side spans. Each cable has 367 wires and a coated diameter of 167 mm. The initial cable tension of 690 tons-force per cable was chosen to permit it to be maintained by the combination of live load and temperature change and to ensure that it did not exceed the allowable value during an earthquake.

Two vane-type dampers were installed on the tower steel console to help dampen longitudinal oscillation of the girder. The vane-type damper converts horizontal motion to rotational motion and is constructed so that flow is resisted when oil inside its left and right pressure chambers passes through orifices in the partition. This resistance induces a horizontal reaction in proportion to the square of the relative velocity of the girder and tower. To maintain the horizontal reaction at a fixed value above a certain relative velocity, a pressure control valve is installed in the partition. The vane-type damper scarcely resists low-speed motion such as the expansion and contraction of the girder caused by temperature changes. Results of the seismic response computations for the performance of these dampers in concert with the attaching horizontal cables indicate that, during an earthquake, they reduce horizontal displacement of the girder by about 30 percent and cable tension by 20 to 30 percent from the levels reported when only attaching horizontal cables are used. As a result, the attaching horizontal cables are kept in tension, re-

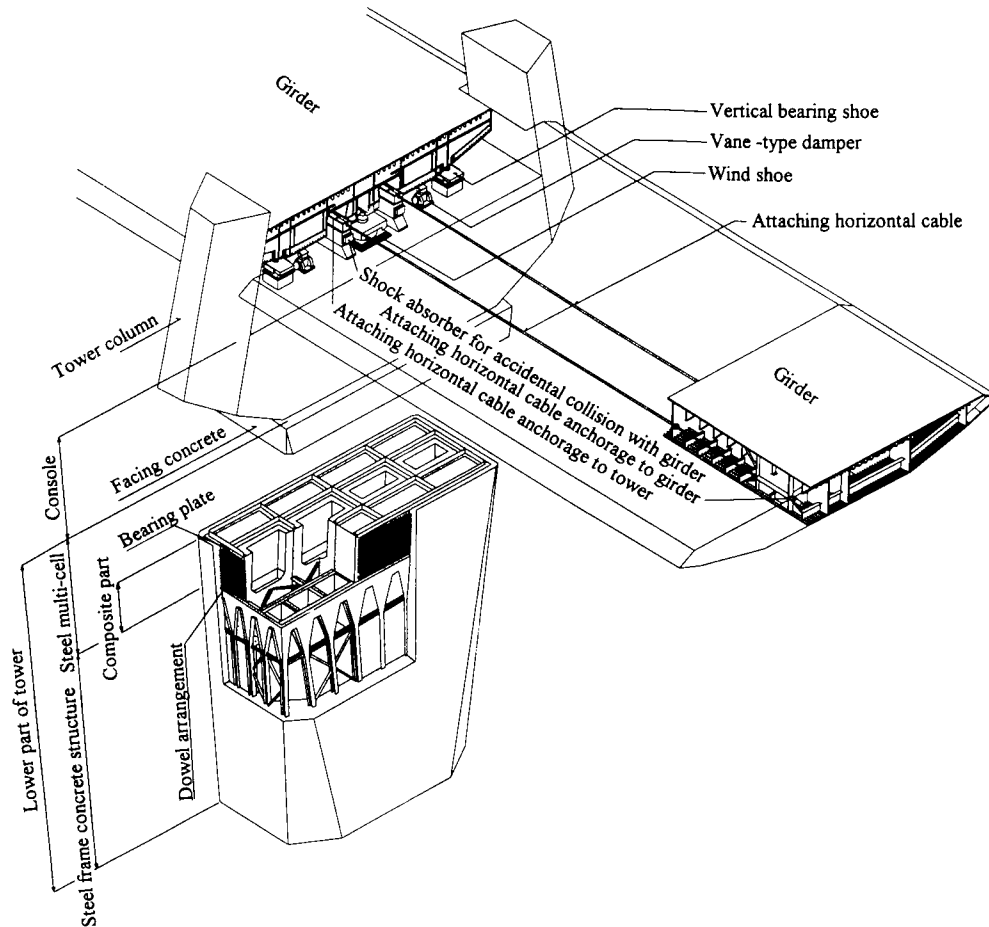


FIGURE 3 Structure of the lower part of the tower.

sulting in increased safety. The mechanism and the reaction properties of the vane-type damper are shown in Figures 4 and 5.

The span ratio between the side spans and the center span is approximately 1:2. Therefore, there is almost no vertical dead load reaction at the end supports, and both positive and negative reactions caused by the live load continually and repeatedly act on the pendulum supports of the end pier. Under normal conditions ( $1/2$  of the standard live load), the pendulum supports should be in compression at all times. To ensure this compression, 920 tons-force (about  $250 \text{ m}^3$ ) of concrete was poured inside the girder ends.

Two vertical bearing supports, one horizontal bearing support, two attaching horizontal cable anchorage systems, and two vane-type dampers were mounted on the tower. Two pendulum supports and one horizontal bearing support were mounted at the girder end.

Vortex shedding and wind/rain-induced vibration of the cables were often observed during the erection of the Tsurumi Tsubasa Bridge. To suppress these vibrations, both oil and (high damping) rubber dampers were

applied to the stays at the deck level. The rubber is especially effective not only in suppressing the vibration but also in reducing the additional stress caused by the live load. From the aesthetic point of view, these apparatuses were set at the same height as the handrail. The structure is shown in Figure 6.

## STUDY OF EARTHQUAKE RESISTANCE

### Magnitude of Earthquake and Incident Seismic Wave

On the basis of a survey of past major earthquakes, the expected value of the magnitude  $M$  of an earthquake with a return period of 75 years at the location of the Tsurumi Tsubasa Bridge was calculated as  $M = 7.8$  to  $8.2$  with an epicenter between 50 and 200 km away. To establish the acceleration response spectrum of the seismic waves on the bedrock (the target spectrum of the seismic waves on the bedrock), earthquake observation records for the Daikoku-Futo Wharf during the past 10

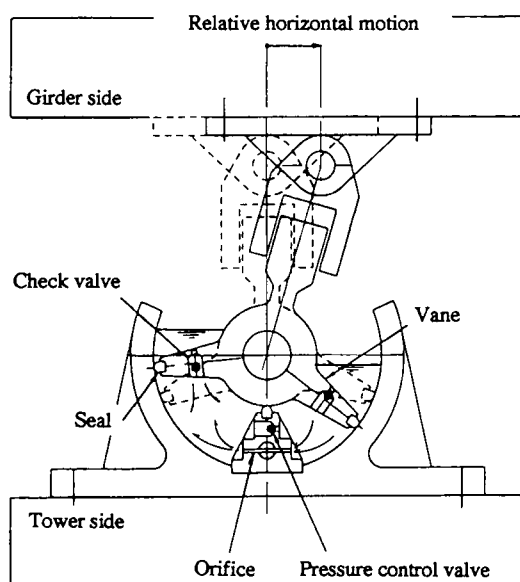


FIGURE 4 Vane-type damper mechanism.

years and other observed earthquakes were used as references. Artificial seismic waves were created that correspond to this target spectrum. The design acceleration spectrum is shown in Figure 7; the artificial seismic wave is shown in Figure 8.

### Analysis Model

Artificial seismic waves were applied to the bedrock. The dynamic characteristics (shear rigidity and damping ratio) were obtained by using the theory of wave superimposition (SHAKE), and a time-history response analysis was performed using a simplified three-dimensional FEM model. The reflection of waves (box effect) in the zone being analyzed, which is caused by treating the subsoil as a continuous, semi-infinite body in a finite zone, was considered using a simplified three-dimensional FEM model. Also, dissipation of the wave energy outside of the zone was considered by establishing the transfer and viscosity boundaries. The simplified three-dimensional model is shown in Figure 9.

### Earthquake-Resistant Design for Foundation Structure

The results of the dynamic analyses using the simplified three-dimensional FEM model indicated that there was a dynamic interaction between the foundation and the subsoil and that subsoil displacement mainly acts on the caisson foundation. This subsoil displacement was evaluated as a horizontal load in the static design.

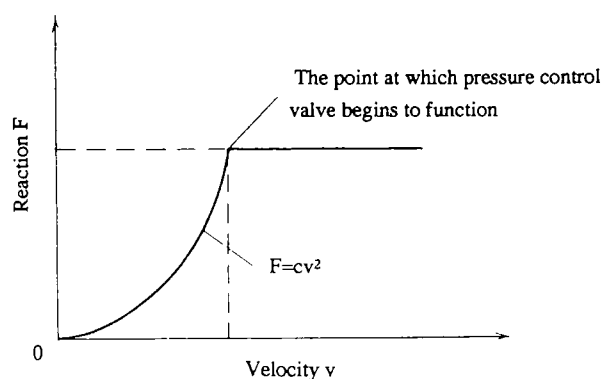


FIGURE 5 Reaction properties of vane-type damper.

### Earthquake-Resistant Design for Superstructure

The time history response analysis for the superstructure was performed by using a lumped mass model. A problem of this model is defining the strength and damping characteristics of the subsoil spring that models the connection of the foundation to the subsoil. These values were made equivalent to the results of the simplified three-dimensional FEM analysis. The time history response analysis using the lumped mass model was used to check the design, and the response spectrum method was used to do design computations. The distributions of bending moment of the towers do not match if a superstructure model is used that fixes the bottom ends of the towers, and a horizontal acceleration response spectrum is used for the top of the foundation. This is because the effect of rotation of the foundation is not included in the calculation. Therefore, the response spectrum method was used by extending the model down to the bottom of the foundation.

### WIND RESISTANT DESIGN

#### Design Wind Velocity

The design wind velocity was determined from the 100-year return expected value calculated from 10-min average wind velocity observations over the 55-year period since 1928 by the Yokohama Meteorological Observatory and over the past 4 years from the tower of the Daikoku Bridge, which is near the location of the proposed Tsurumi Tsubasa Bridge (girder,  $V_z = 53.0$  m/sec; tower and cable,  $V_z = 58.0$  m/sec).

#### Wind Tunnel Tests

Wind tunnel tests were performed on the completed bridge, the cantilevered erection of the girder, and the

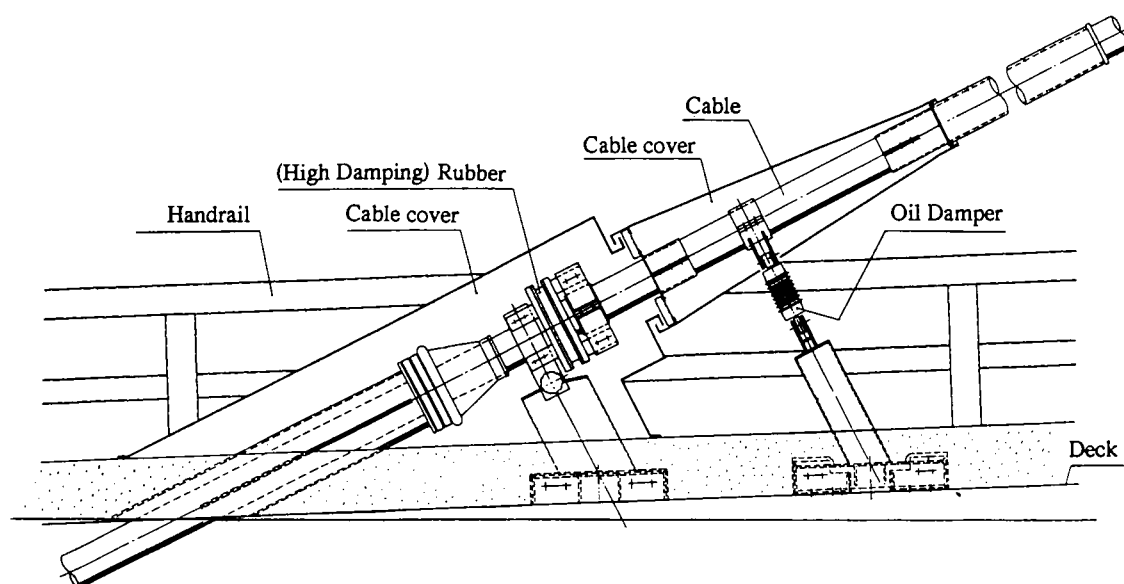


FIGURE 6 Cable damper.

erection of the tower. Tests were performed on the two-dimensional, spring-supported girder sectional model for attack angles of 0 degree and +3 degrees. The flutter wind velocity in the test of the single bridge model was far higher than the design wind velocity, and harmful vibrations did not occur at wind velocities up to 100 m/sec. The effectiveness of 2-m fairings attached to both edges of the girder was demonstrated. However, in the test of the twin bridge model, self-excited vibrations occurred at wind velocities of 69 to 72 m/sec. To increase

the flutter wind velocity, blocking of the medial strip guard fence (i.e., constructing a center barrier) was tried. This measure increased the flutter wind velocity above the design wind velocity of  $V_F = 74.4$  m/sec.

In the completed bridge model test, a test that is similar to that used on the girder sectional model was performed to check the effect of the center barrier. Flutter or other harmful vibrations did not occur regardless of the presence of the center barrier in the test of the single bridge model. The response characteristic of the test of

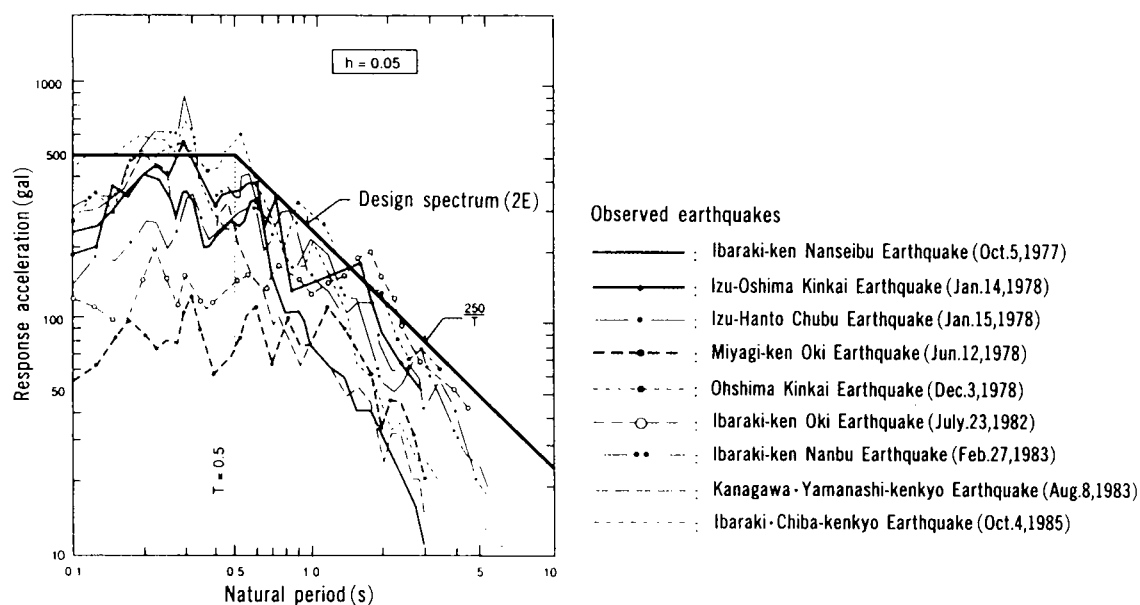


FIGURE 7 Design acceleration spectrum.

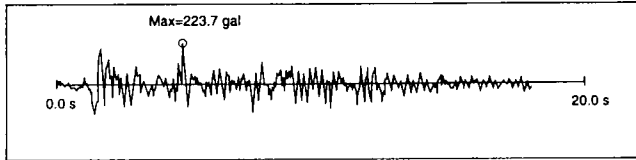


FIGURE 8 Artificial seismic wave.

the twin bridge model was almost the same as that of the single bridge model. In the uniform flow test flexural vibration did occur. However, this was prevented by the installation of the center barrier. It is therefore thought that a center barrier need not be installed as long as the bridge stands alone, but that it should be installed when the second bridge is built.

At an early stage of the design project, the tower column section was to be rectangular, and the occurrence of galloping was expected on the basis of preliminary test results. However, galloping was prevented by changing the cross section to a trapezoidal section.

## ERECTION OF THE SUPERSTRUCTURE

### Erection of the Foundation of the Tower

After the steel frames for the lower parts of the towers were assembled into single units on land, they were divided into top and bottom halves, carried to the site by

a 700-ton floating crane, and installed in the top slab of the caissons. Next the steel multicell located below the console bottom was erected, reinforced concrete was poured inside and outside of the steel multicell, and the whole composite was integrated into a single unit by the dowels, which were already set in place on the steel multicell. Finally, the steel consoles were erected as a single unit with a 3,500-ton floating crane.

### Erection of the Tower and the Girder

The construction stages are outlined in Figure 10. The girders of the side spans were divided into three large blocks. After two vents were set for the side spans, the girders were erected in large blocks by a 3,500 ton floating crane. The middle parts of the tower were constructed as large blocks by a 3,500 ton floating crane, and the upper parts of the tower were constructed by raising a single block by means of a 650-ton crawler crane set on the girder deck. They were then welded. Because vortex excitation occurred during erection of the tower column, measures were taken by installing a tuned mass damper device.

The tower side 115-m portions of the center span girder were supported by vents set approximately 80-m from the towers in the center span. These girder portions were erected in large blocks by a 3,500-ton floating crane. To permit the bridge to extend over the Tsurumi Fairway, approximately 240 m of the girder in the central portion of the center span was erected using the cantilever-type erection method in which the girder

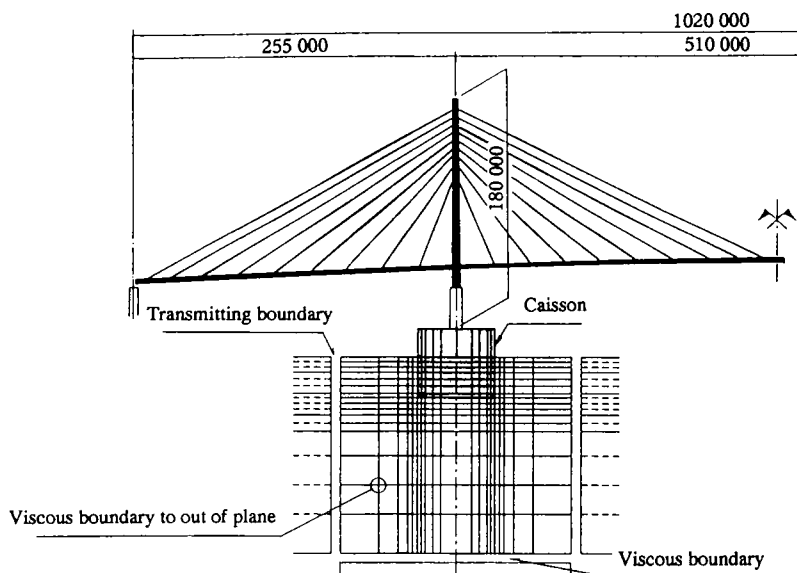


FIGURE 9 Simplified three-dimensional model.

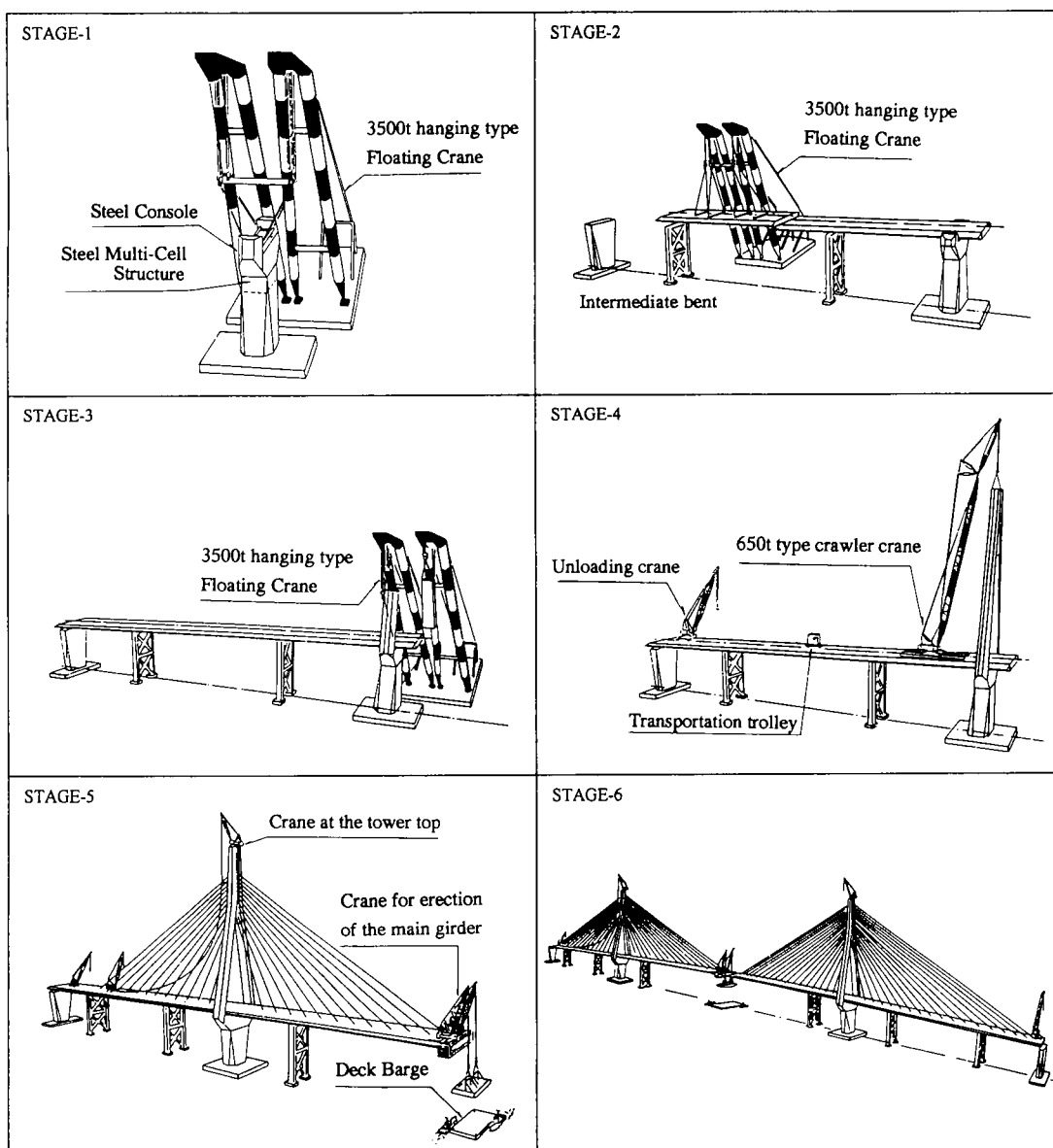


FIGURE 10 Construction stages.

was gradually extended from both sides as the cables were installed and tensioned—a method that took advantage of the mechanical characteristics of cable-stayed bridges. This method made it easy to control the process precisely, and procedures could be hastened at the site. Toward this aim, deck barges transported blocks of girder to a location directly below the place where they were to be installed, and they were raised to bridge level by 450 ton crawler cranes mounted on each side of the girder tips. Center-span girder closure was performed by using the cranes to raise the girder closure blocks to the correct position in the same manner as that for other blocks and then splicing both ends.

### Installation of Cables

The cable was unreeled on the deck, and the tower side end was lifted by a crane set on top of the tower. After it was anchored to the saddle on the tower, the girder side end was pushed inside the girder into the anchorage girder from the upper side.

### Precision Control During Construction

In the case of a cable-stayed bridge, deviation of stress and dimensions from the design values can be adjusted as the distance between fixed points can be changed by

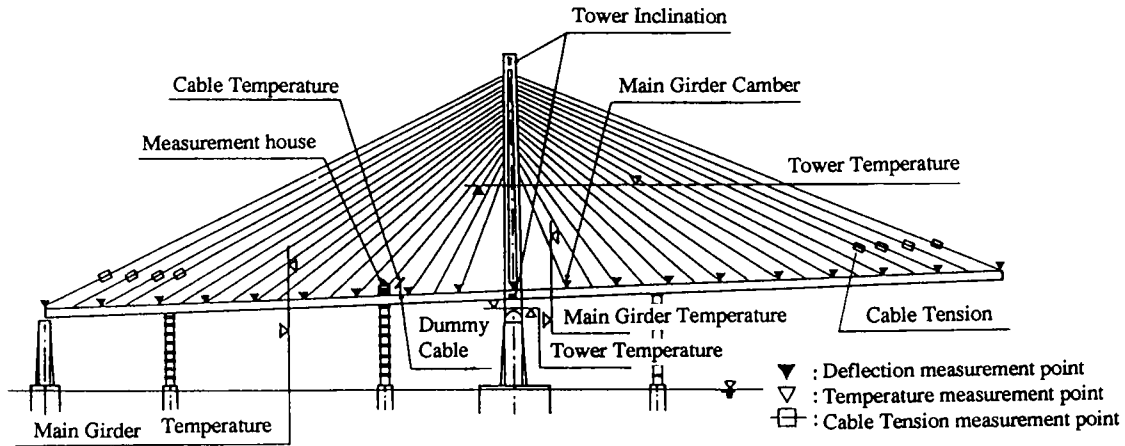


FIGURE 11 Arrangement of the measurement instruments.

means of shim plates installed at fixed points on the cables. To ensure safety during construction and high precision at completion, a computerized precision control system was applied.

As a preparation before the shim adjustment work, a calculation model was formed on the basis of the various errors and construction methods, and control limit values and influence values of shim plate thickness and temperature on cable tension and deformation were evaluated by analytic calculation, which was processed by a computer.

On the day of shim adjustment work, construction loads (mainly those on the bridge surface) were to be surveyed, and the resultant load data were input into the computers for precision control at the construction site linked with a central computer, and detailed control calculations were conducted. After confirmation that nighttime temperatures at each part of the bridge had been stabilized, measurements were taken. Vibration frequency of the cable was measured by an acceleration meter, the main girder camber was measured by level meter (communicating tube), and tower inclination was measured by laser level. These measurements were controlled by the centralized control system through com-

puters at the construction site. The arrangement of the measurement instruments is shown in Figure 11.

Conversion of the cable vibration frequency into tension and the temperature correction were processed by the computer. Measured data were transmitted to precision-control personal computers, which calculated optional solutions for shim adjustment by the least-squares method and expected values for any shim adjustment of choice. According to input data and control values, the final shim value for actual use was decided in reference to these computer calculations.

After shim adjustment work, if the comparison of measured values and control values mentioned earlier gave good results, the work for the day was finished, and work on the next step started the following day. Because of the introduction of the precision control system, construction was accomplished with the precision of half the control limit values. Control items and results of the precision control are shown in Table 1.

## SUMMARY

An outline of the design and construction of the superstructure for the Tsurumi Tsubasa Bridge has been pre-

TABLE 1 Control Items and Result of Precision Control

	Control Limit Value	Control Target Value	Results
Main Girder	$\pm [25 + (L - 40)] \times 0.5$ (L: Span Length)	1/2 of the Control	Center Span
Camber	Center Span $\delta = \pm 240\text{mm}$ (L=510m)	Limit Value	$\delta = +114\text{mm}$
	Side Span $\delta = \pm 120\text{mm}$ (L=255m)		Side Span
			$\delta = -58\text{mm}$
Tower	1/2000 of the Tower height	1/2 of the Control	$\delta = -10\text{mm}$
Inclination	$\delta = \pm 180000/2000 = \pm 90\text{mm}$	Limit Value	
Cable	$\pm 1$ allowable Tension - Design Tension	1/2 of the Control	$\Delta T = -55 \sim -78\text{t}$
Tension		Limit Value	



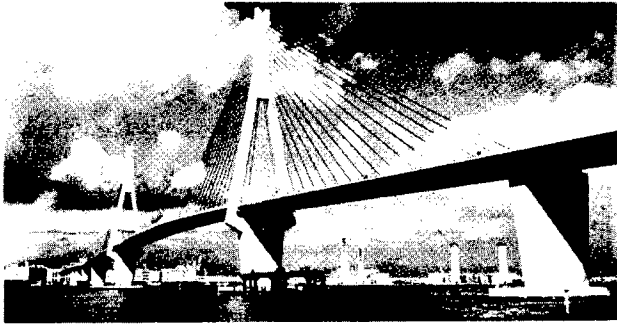


FIGURE 12 Tsurumi Tsubasa Bridge.

sented. The Tsurumi Tsubasa Bridge, which was completed at the end of 1994 as a result of the introduction of much new technology, is shown in Figure 12.

#### ACKNOWLEDGMENT

The Investigation and Research Committee Regarding the Design and Construction of the Tsurumi Tsubasa Bridge (Chairman, Manabu Ito of the University of Tokyo) was established to study technical questions in carrying out this project. The authors wish to thank those concerned with the design and construction of the Tsurumi Tsubasa Bridge, including the members of the committee.

# Kap Shui Mun Cable-Stayed Bridge

---

Steven L. Stroh and Thomas G. Lovett, *Greiner, Inc., Florida*

The Kap Shui Mun Bridge is one of the world's largest double-deck cable-stayed bridges and features the first fully enclosed lower deck. The bridge spans Kap Shui Mun Channel linking Lantau Island and Ma Wan Island, providing access to the proposed new airport in Hong Kong. The bridge carries six lanes of roadway traffic on the upper deck and two lanes of emergency roadway traffic and two tracks of light rail on the lower deck. The winning design/build tender is described; it is an innovative hybrid design with a steel composite superstructure for the central 387 m of the 430-m center span and an all concrete superstructure for the remainder of the main span and for the 160-m side spans.

A new system of access roads and railways is required as a part of the relocation of the Hong Kong airport from Kai Tak to Chek Lap Kok at the northern end of Lantau Island. A major part of this system is the Lantau Fixed Crossing, composed of a system of bridges linking Tsing Yi Island to Lantau Island. The Kap Shui Mun Bridge forms a major part of the Lantau fixed crossing, spanning the Kap Shui Mun Channel between Ma Wan Island and Lantau Island. Figure 1 presents a photomontage of the Kap Shui Mun Bridge, with Lantau Island in the foreground and Ma Wan Island in the central part of the photo. The Kap Shui Mun Bridge is a double-deck, five-span, cable-stayed bridge carrying both vehicular and rail traffic.

## DESIGN/BUILD TENDER

### Structure of the Design/Build Team

The winning design/build tender was prepared by a consortium of international contractors and engineers. The contracting team was composed of Kumagai Gumi, Maeda, Yokogawa, and Hitachi Zosen. The bridge was designed by the Greiner International Ltd. Tampa and Timonium offices in the United States and Leonhardt Andrä and Partner Ltd., Stuttgart, Germany, in conjunction with Fugro Hong Kong Ltd. for geotechnical engineering and site work, J. Roger Preston & Partners for electrical and mechanical work, Hong Kong, and Kennedy & Donkin Ltd., Hong Kong, for track work.

### Geometric Requirements

The crossing of the Ma Wan Channel requires a navigation channel width of 275 m and a vertical clearance of 47 m above reference datum. The horizontal alignment of the cable-stayed portion of the bridge is straight with the exception of approximately 45 m of one side span, which is located in a transition spiral. The vertical alignment is curved for the central 305 m of the main span with  $R = 10,175$  m, and the tangent for the remainder of the cable-stayed structure on a 1.5 percent grade.

The tender requirements stipulated that the lower carriageways be constructed with a constant 2.5 percent

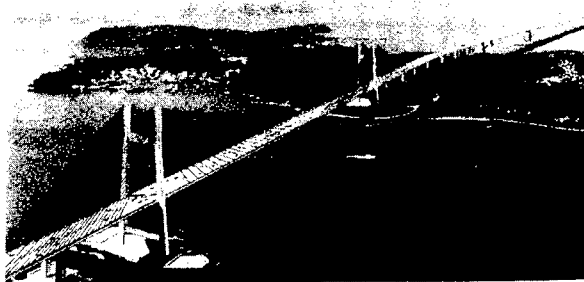


FIGURE 1 Photomontage of Kap Shui Mun Bridge.

cross slope while the upper carriageways maintained the same 2.5 percent cross slope through the tangent sections with a transition to a maximum 2.82 percent superelevation through the curved portion of the alignment. This requirement resulted in an extremely complex geometric criteria for the concrete box sections and greatly complicated the reuse and standardization of the form system. This provision was necessary to ensure that spillage of any hazardous materials on the lower carriageways would not drain into the rail corridor. After the contract award the owner relaxed this requirement, thus allowing both upper and lower carriageways to remain parallel. This concession was granted given that this design maintained a solid concrete web wall between the rail and lower carriageway alignments throughout the superelevated sections, thereby eliminating the concern for contamination of the rail corridor.

### Traffic Requirements

The bridge cross section is a double-deck arrangement, providing six lanes of road traffic on the upper carriageway, two fully enclosed roadway lanes on the lower carriageway, and also two tracks of railway on the lower carriageway. Figure 2 provides an artist's cutaway of the main span deck layout. Under normal operating conditions the upper carriageways are used for roadway traffic and the two lower roadways are used for maintenance or emergency vehicles, or both. Under high wind conditions, roadway traffic is shifted to the lower carriageway. Specifically, operating requirements are as follows:

- Wind speed less than 40 kph: all vehicles use upper deck;
- Wind speed 40 to 65 kph: high-profile vehicles shifted to lower deck;
- Wind speed 65 to 90 kph: all vehicles shifted to lower deck; and

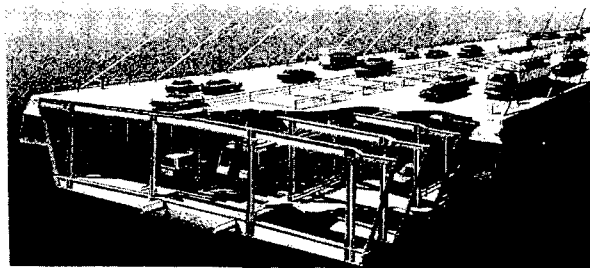


FIGURE 2 Artist's rendering of the deck configuration for the Kap Shui Mun Bridge main span.

- Wind speed over 90 kph: bridge closed to all vehicles except emergency use.

The full enclosure of the lower carriageway necessitated ventilation of the interior of the structure. The main span, which has openings in the central region of the deck (both top and bottom) and small openings along the lower outside edges of the structure, is naturally ventilated. The concrete side spans have top openings in the central region of the deck (above the railway) but a closed bottom soffit (in accordance with a contract requirement to mitigate noise impacts along the Ma Wan corridor). These openings were insufficient for natural ventilation and the side spans are therefore mechanically ventilated with fans.

The upper and lower carriageways are designed for a total of six lanes of live load, positioned between the upper and lower carriageways to produce the most adverse effect. Loading intensities were developed in accordance with the British Design specifications (BS5400) with 45 units of HB loading. The rail load considered was a standard 8-car train, as shown in Figure 3. Also considered was a 10-car train with similar

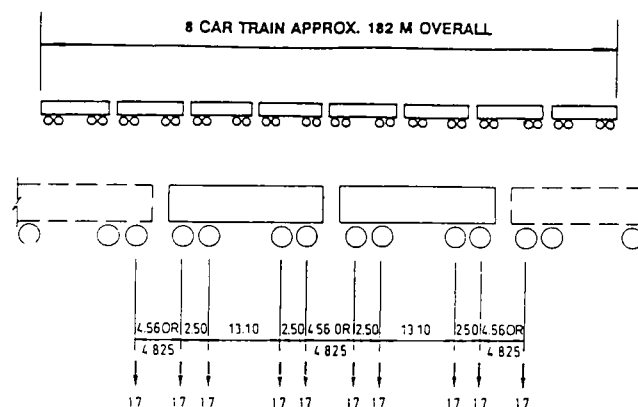


FIGURE 3 Standard railway loading (units are tonnes and meters).

bogie spacing, as shown in Figure 3, but a 13.6-tonne axle load, a check bogie composed of two 24 tonne axles 1.5 m apart, and for fatigue loading, an 8-car train configured as shown in Figure 3 but with a 13-tonne axle load. Stringent dynamic criteria were imposed for both the transverse supporting elements of the rail and the global response of the structure to ensure user comfort. The live load dynamic response criteria were evaluated in a manner consistent with the level of service required for the range of wind speeds explained above.

### Wind Loading Requirements

The Kap Shui Mun Bridge, and Ma Wan Viaduct are located in an exposed site in a region frequented by tropical cyclones. In addition to static load requirements requiring investigation of sustained wind speeds of 80 m/sec, aerodynamic stability also had to be guaranteed for horizontal wind speeds of up to 95 m/sec for the unloaded bridge and up to 50 m/sec for the loaded bridge.

### Aesthetic Requirements

The Kap Shui Mun Bridge and Ma Wan Viaduct were required to meet a specific set of aesthetic goals aimed at ensuring that the Lantau Fixed Crossing Route presented an integrated system from an appearance viewpoint. These aesthetic requirements included the following:

- Provision of a tower compatible with the adjacent Tsing Ma Suspension Bridge, including the overall form as well as the local member details (member rectangular cross section with 1-m radius at corners);
- Provision of intermediate piers similar in form and local member details to the adjacent Tsing Ma Bridge;
- Provision of a mid-depth feature line along the edge of the deck, with the deck edge inclined to reflect the light above and recessed to cast a shadow below the line. (In addition to the mid-depth feature line, an unbroken bottom soffit line was required); and
- Provision of bridge furniture of similar detail to the adjacent projects (barriers, maintenance walkways, sign supports, light poles, and other items not a part of the main structure).

The provision of the unbroken bottom soffit proved to be a challenging aspect of the design. Given that the interior of the section was fully utilized for highway and rail traffic, all pier diaphragms were required to be located around the perimeter of the section. Initial at-

tempts to locally thicken the box section at the piers were rejected by the owner. Ultimately, diaphragms were developed by increasing the level of reinforcing in the webs, without an increase in thickness, combined with a locally thickened bottom slab that is blended with the pier columns.

## KAP SHUI MUN BRIDGE DETAILS

### General Layout

The main structure is a five-span cable-stayed bridge consisting of a 430-m main span and side spans composed of two 80-m spans each, for a total cable-stayed structure of 750 m (Figure 4). The sidespan lengths of 160 m (side span to center span ratio of 0.37) are governed by geometric constraints and are substantially shorter than the ideal length for optimization of a cable-stayed bridge, particularly for one with large live loading. To limit the uplift from this condition, several measures were taken. The side spans were stiffened with an intermediate pier. This pier is also used for erection of the side span superstructure, as will be discussed later. The side span is constructed of prestressed concrete, whereas the central 387 m of main span is steel composite with concrete upper and lower decks, providing a comparatively lighter section than the all-concrete side spans. This heavier section significantly counters the uplift from the relatively short side span and, taken in conjunction with the stiffening provided by the intermediate pier, provides a very stiff side span. This stiff side span further permits all of the side span stays to function as a distributed backstay and avoids the necessity of a concentrated backstay, which is common to cable-stayed bridges.

The deck is supported by two planes of cables in a semifan arrangement. The cables are arranged in a vertical plane, spaced at 8.7 m in the main span and 6.1 m in the side span. The cables are spaced at 1.5 m at the tower head. The fixed end of the stay is at the tower and the stressing end at the deck.

### Side Span Superstructure

The side spans are a concrete box girder arrangement, which is composed of two separate concrete box girder sections representing the northbound and southbound roadways. These box girders are erected by incremental launching, with the northbound and southbound roadways launched separately. On completion of launching, the two sections are joined at the bottom slab level by an inverted T-beam (rail support beam) and solid bottom slab, and at the top slab level by the beams  $300 \times$

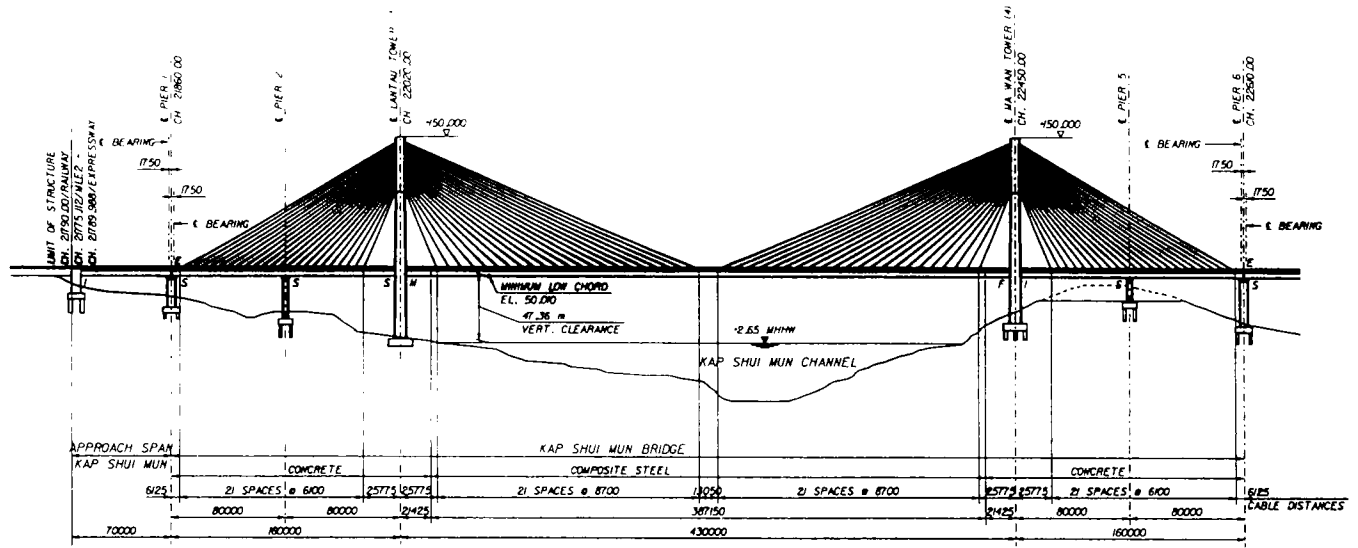


FIGURE 4 Elevation: Kap Shui Mun Bridge.

850 mm at 3-m spacing (Figure 5). This section extends through the entire 160 m of the side span and further extends 21 m into the main span.

The railway is supported by cast-in-place inverted T-beam members. These members are spaced at 3 m to provide support for the trackslabs. The side spans have a continuous closed bottom flange beneath the railway, in response to a contract requirement for a fully closed

bottom soffit for noise abatement. The top slabs are joined by concrete struts, which provide diaphragm action and provide continuity for flow of torsional stresses around the overall cross section.

The side span stays are anchored in a concrete edge beam at the outer edges of the section. Transverse post-tensioning is provided in the webs and bottom slab to resist the local introduction of stay forces. Longitudinal

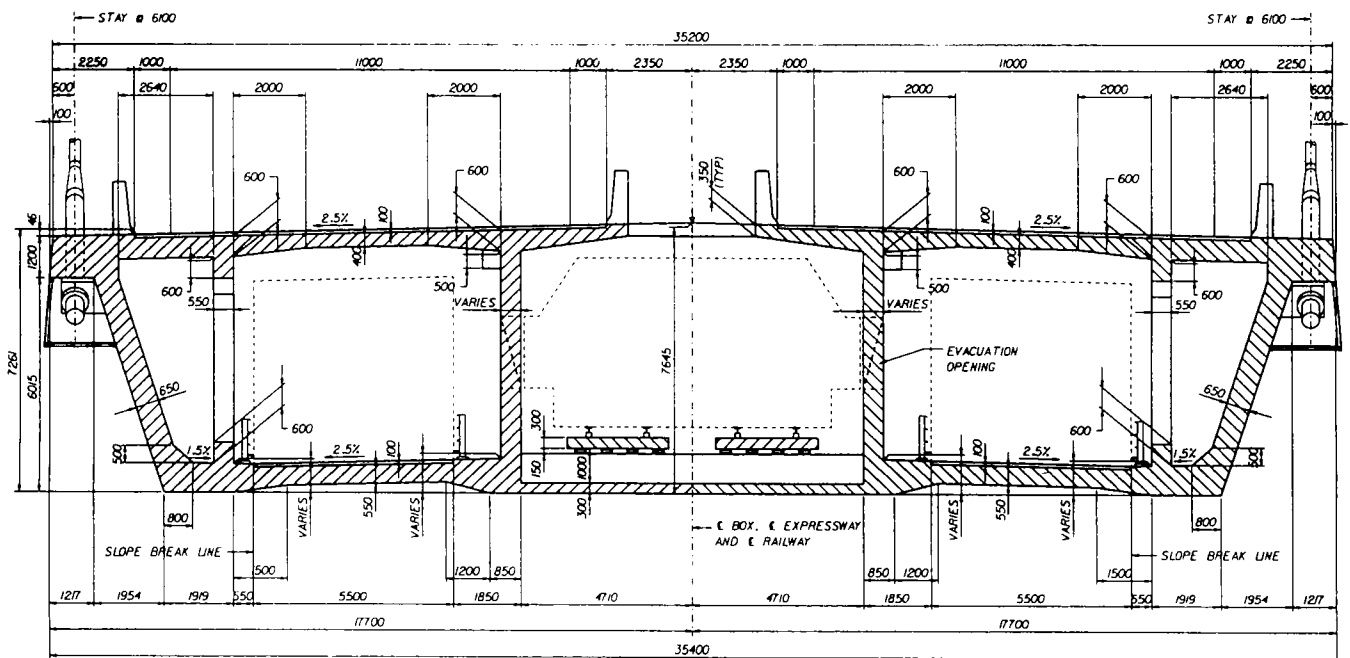


FIGURE 5 Typical section of side span superstructure.

post-tensioning is provided to satisfy the erection and final longitudinal forces.

### Main Span Superstructure

The center 387 m of the 430-m main span is a steel framework with composite concrete carriageway decks (Figure 6). The section is fully composite for both the upper and lower carriageways for both dead loads and live loads. The transverse steel frames are spaced at 4.35-m centers and support a nominal reinforced concrete slab 250 mm thick. The slabs are locally thickened to 500 mm at the edges of the section for local force introduction (stay cable introduction). The depth of the superstructure varies from 7.3 m at the center of the section to 6.8 m at the edges. The transverse frames are designed considering vierendeel truss action. Top lateral bracing is provided in the form of X-bracing in alternate bays. This bracing is provided to increase the overall torsional stiffness of the deck, which was necessary to ensure satisfactory aerodynamic behavior. The top slab chamfer feature was provided as a consequence of the wind-tunnel testing to ensure acceptable aerodynamic behavior.

The main girder longitudinal load-carrying system is composed of the longitudinally stiffened web, a trussed inner "web," and the composite concrete slabs. The outer web is connected to the sloping edge of the cross frames. Only nominal steel flanges are required, as the upper and lower carriageway slabs are fully composite for both dead loads and live loads. The main girder field

sections are 8.7 m long and contain two cross frames. These field sections are fully shop welded and then are joined to adjacent sections by bolted connections.

The railway envelope is located within the center portal and supported by precast prestressed trackslabs seated on the lower chords of the cross frames. An intermediate floor beam is located between cross frames to satisfy a 3-m maximum trackslab span requirement of the project specifications. The stays are anchored in steel anchor boxes, shop welded to the frames at cross-frame locations.

### Launching Nose

The steel launching nose is a unique feature of this structure. This transition element between the normal steel composite main span and the concrete side spans serves a dual purpose as a launching nose for incremental launching of the side span superstructure and then is incorporated into the permanent structure as the transition element. The length of the launching nose taken in conjunction with the portion of the side span superstructure that is launched through the towers was carefully selected to ensure that adequate water depth for erection of the first composite main span sections from a barge was available.

### Stay Cables

The cables are composed of 51 to 102 parallel mono strands, 0.6 in. in diameter, with a tensile strength of

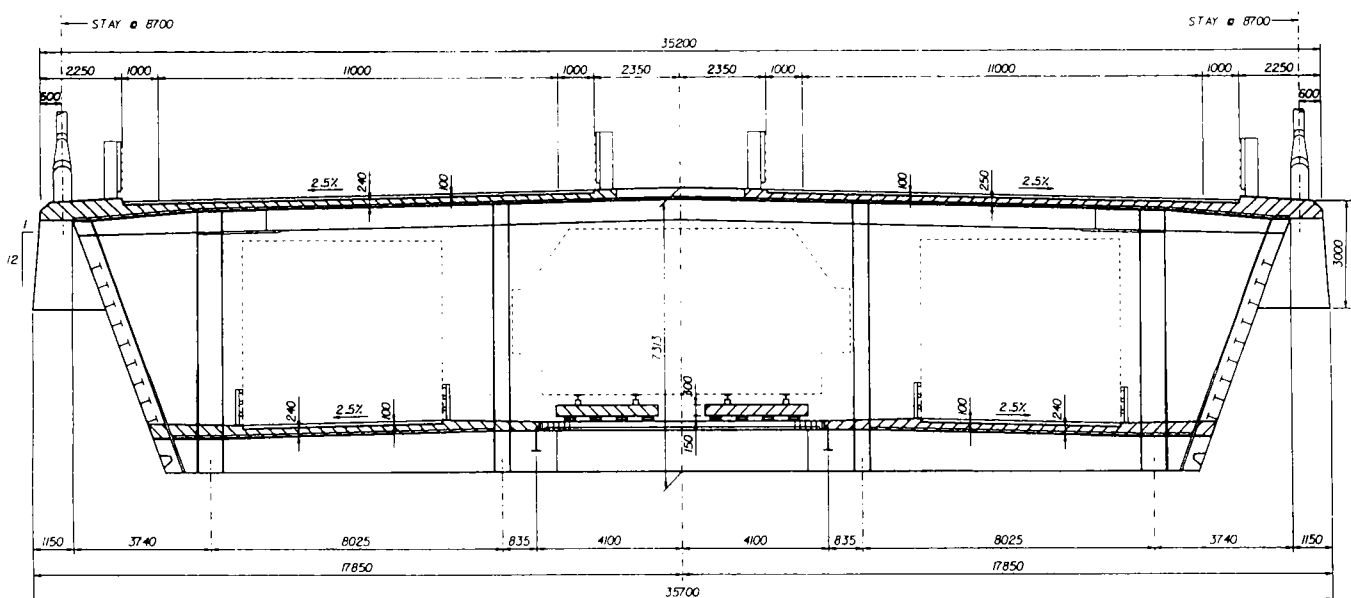


FIGURE 6 Typical section of main span superstructure.

1720 N/mm<sup>2</sup> after galvanizing. The corrosion protection system consists of hot dip galvanizing with 280 g/m<sup>2</sup> corrosion inhibitor grease and a 1-mm polyethylene sheathing around each strand. The entire cable group is further encased in a polyethylene pipe, which remains in its black condition. The strands are anchored in sockets, with permanent loads carried by high fatigue-resistant wedges. Live loads are carried by a combination of these wedges and epoxy bond.

The strands will be individually stressed with mono jacks to the same sag. Subsequently, the entire stay will be stressed with calibrated hydraulic jacks with a maximum capacity of 1500 tonnes. The structure has been designed to allow replacement of individual stays and for the accidental loss of a stay under full live load, ensuring structural stability.

## Bearings

The superstructure is integral to the Ma Wan Tower, so all longitudinal forces are resisted at this location. At the Lantau Tower, vertical forces are resisted by pot bearings on top of the cross girder and laterally by neoprene bearings between the tower legs and the upper and lower deck.

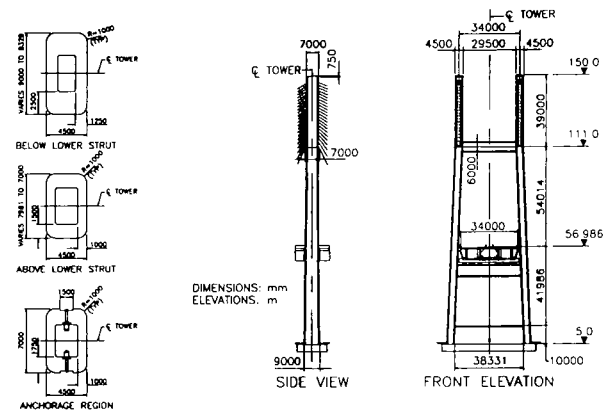
At intermediate piers prestress forces are resisted by pot bearings, and hold-down forces are provided by hold-down cables at the outer webs. These hold downs consist of 3 cables of 68 (or 98, depending on the location) 0.6-in. strands, anchored in the lower portion of the piers. The hold-down cables are sized such that two cables are sufficient for stability to permit future replacement of the cables, one at a time.

The intermediate side span locations are free to translate longitudinally and transversely, and at the end pier locations the deck is free to move longitudinally but restrained laterally. Lateral restraint is provided by steel shear lock assemblies.

## Towers

The towers are H-shaped, as indicated in Figures 7 and 8. The upper region of the towers is vertical, for anchorage of the vertical plane of stay cables. Below the upper strut the tower legs are slightly inclined to clear the superstructure. The tower height is 93 m above the deck, corresponding to a ratio of 0.22 with the main span.

The tower legs are constructed of conventionally reinforced concrete. A horizontal strut is provided just below the lower stay location to resist deviation forces from the change in angle of the tower legs. A second strut is provided below the deck to provide support of



TOWER COLUMN SECTIONS

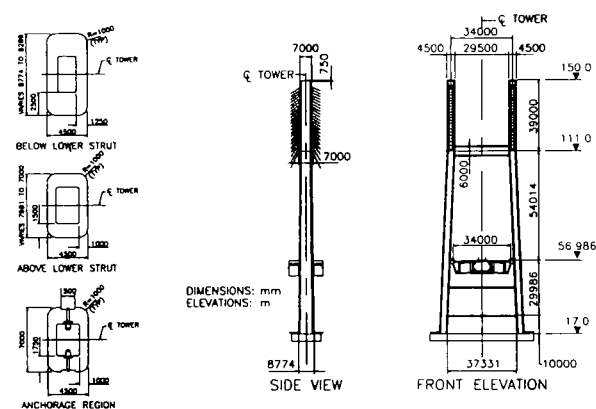
FIGURE 7 Details of Lantau Tower.

the superstructures. Both struts are post-tensioned. The stays are anchored directly in the outer tower walls. Splitting is resisted by loop post-tensioning tendons and short post-tensioning bars.

The Lantau Tower is founded on a spread footing with an allowable bearing pressure of 5.0 MPa. The Ma Wan Tower was originally planned to be founded on hand-dug caissons 4 m in diameter. However, the excavation of the foundation revealed highly variable founding levels that precluded this type of foundation. The final configuration for the Ma Wan Tower was a combined foundation, composed of a spread footing over approximately 80 percent of the footing and two supplemental caissons 4 m in diameter at the southeast corner of the footing.

## Piers

Individual pier shafts support each of the concrete box sections and serve to anchor the side span uplift forces.



TOWER COLUMN SECTIONS

FIGURE 8 Details of Ma Wan Tower.

The piers are constructed of conventionally reinforced hollow concrete box sections. Their mass is engaged through vertical hold-down cables. These cables are anchored near the bottom of the piers to provide sufficient length to minimize cable bending as the superstructure undergoes longitudinal movements. The side span piers are founded on spread footings or hand-dug caissons, depending on location. Bearing pressures range from 4.5 to 7.5 MPa.

## ERECTION

### General

The total construction time is 54 months, commencing on 16 November 1992 and opening to traffic on 18 May 1997. Included in this design period is the preparation of the design, as well as all testing (aerodynamic, ventilation, trackslab, etc.).

### Tower Construction

The towers will be constructed using a jump-forming system with typical lift heights of 3.9 m. The production schedule is based on approximately 5 days per typical lift. The design permits the side span superstructure to be launched across the lower tower strut before completion of the upper portion of the tower to expedite construction.

### Side Span Erection—Incremental Launching

The side spans will be constructed by incremental launching, with segment lengths of approximately 18.30 m. The incremental launching method was selected in response to the inaccessibility of the terrain and for the advantage of the construction schedule so that construction of the towers and sidespan can pro-

ceed simultaneously. The bridge deck is launched in two parts, corresponding to the left and right halves of the superstructure. The cross girders that support the railway are cast in a second step after launching.

Temporary intermediate piers are provided midway between the side span piers to limit the maximum span during launching to 40 m. The Lantau sidespan is launched from a casting bed behind the Lantau abutment. The Ma Wan sidespan is launched from an elevated casting bed within the first 40 m of the side span.

### Main Span Erection—Free Cantilever

The steel composite main span is erected by free cantilevering simultaneously from both towers. The individual elements are lifted together with their precast decks and joined by bolted connections and cast in place slab closures. The erection weight of the individual elements is 500 tonnes. A "purpose-made" erection traveler is used to hoist the superstructure elements. This assembly consists of two main girders and two cross girders and weighs approximately 390 tonnes.

## ACKNOWLEDGMENTS

The owner is the Hong Kong Department of Highways. The engineer for the project is Mott MacDonald, Hong Kong Ltd., with subconsultants Flint & Neill Partnership, London, and Harris & Southerland (Far East) assisting in checking the design of the steel and concrete structures, respectively. The design team was augmented by several specialty consultants: Robert H. Scanlan of the Johns Hopkins University, for wind stability studies; West Wind Laboratory, Carmel, California, for wind tunnel modeling and testing; Laurie Richards, New Zealand, for foundations (rock mechanics); Nick Jones of the Johns Hopkins University, for dynamic studies; and Ashdown Environmental, United Kingdom, for acoustic analyses.



# Implications of Test Results from Full-Scale Fatigue Tests of Stay Cables Composed of Seven-Wire Prestressing Strand

---

Habib Tabatabai, A. T. Ciolko, and T. J. Dickson, *Construction Technology Laboratories, Inc.*

Since 1990 14 full-scale axial and combined axial/flexural fatigue tests of parallel-strand cable specimens representing three recently constructed U.S. cable-stayed bridges have been conducted. Stay cable specimens ranged in size from 17 to 85 strands 15.2 mm (0.6 in.) in diameter with lengths between 4,570 and 14 600 mm (15 and 48 ft) and nominal capacities between 4430 and 22 157 kN (996 and 4,981 kips). The specimens represented the variety of parallel-strand cable anchorage designs in use worldwide, namely, the wedge anchorage, combination wedge/conical socket anchorage, and conical anchorage; they also incorporated uncoated, epoxy-coated, and grit-impregnated epoxy-coated seven-wire strand. The primary goal of each test series was the validation of the as-designed cable system's fatigue performance for each bridge. However, test results indicate that these specification-required tests effectively identified endurance- and durability-impairing features of certain cable components, prompting the system's refinement and validation during test series. The intent of the review is to synthesize test results for a highly diverse sample of stay cable designs, installation procedures, and test criteria, emphasizing fatigue performance enhancements resulting from specific cable configuration refinements. Measured fatigue test data are compared with Post-Tensioning Institute cable testing criteria.

Laboratory structural testing was conducted to evaluate the performance of as-designed stay cable systems when subjected to fatigue and static load conditions. Specimen components were provided and assembled by cable suppliers. The test regimes incorporated axial fatigue and combined axial/flexural fatigue loading, depending on bridge design. Table 1 presents pertinent test data. In general, the stay cable specimens were subjected to 2 million cycles of fatigue loading ranging from 36.5 to 45 percent of guaranteed ultimate tensile strength (GUTS) in accordance with bridge specifications and on the basis of recommendations of the Post-Tensioning Institute (PTI) Committee on Cable-Stayed Bridges (1). The number of wire breaks allowed during fatigue testing was limited to 2 percent. Depending on bridge specification requirements, axial fatigue test specimens were required to withstand a static load of 95 percent of either nominal or actual (determined by tests to failure of representative strands) ultimate tensile strength. All test specimens were dissected after the strength tests to assess the condition and performance of various cable components. Most fatigue tests were performed at an approximate frequency of 2 Hz; some tests were performed at lower frequencies (between 1 and 2 Hz).

TABLE 1 Project-Specific Stay Cable Test Parameters

Test Designation <sup>(1)</sup>	Cable <sup>(4)</sup> Length mm	Cable Nominal Tensile Capacity (GUTS) kN	Fatigue Load Range		Static Proof Load Requirement, kN
			Minimum kN	Maximum kN	
A31	6,183	8,079	2,949	3,636	8,074
A31R <sup>(2)</sup>	6,116	8,079	2,949	3,636	8,065
A49	7,675	12,770	4,661	5,747	12,753
A73	7,879	19,025	6,944	8,561	19,003
B46	5,512	11,989	4,376	5,395	11,387
B37 <sup>(3)</sup>	13,614	9,643	3,519	4,083	N/A
B17	4,877	4,431	1,617	1,994	4,200
B46R	5,487	11,989	4,376	5,395	11,387
C85	5,725	22,153	8,086	9,969	21,520
C79	5,707	20,589	7,515	9,265	19,995
C85R	5,736	22,153	8,086	9,969	21,907
C85U	5,685	22,153	8,086	9,969	21,045
C79U	5,693	20,589	7,515	9,295	19,559
C82U <sup>(5)</sup>	14,595	21,371	7,913	9,275	N/A

(1) Denotes test identifier, including test series (A, B or C), cable size expressed as number of 15.2-mm strand, U denotes uncoated strand cable, R denotes retest.

(2) Ungrouted specimen.

(3) Combined axial/flexural fatigue test incorporated 23 ksi fatigue stress range including 5 ksi flexural stress range. Test geometry incorporated 2,743 mm saddle radius, 23° anchorage angle and 175-mm saddle pipe diameter.

(4) Length between ends of strand anchorages.

(5) Saddle test geometry incorporated 3,505 mm saddle radius, 27° anchorage angle, and 219-mm diameter saddle pipe.

METRIC CONVERSIONS: 1 mm = 0.039 in., 1 kN = 0.2248 kip

## CABLE SYSTEM CONFIGURATIONS

The principal load-carrying elements of the tested stay cables were high-strength steel strands. The function, design, and installation of stay cables are discussed by Podolny (2). A number of seven-wire epoxy-coated or uncoated strands were encased in either high-density polyethylene (HDPE) or steel pipe. The coated strands evaluated in these test series incorporated an epoxy coating that encased the outside periphery of the strand and did not fill the interstitial spaces between wires. Spaces between strands and between strands and pipe were filled with cement grout. The primary function of grout was to protect the strands. Some cable designs also use grout as a structural component of anchorage sockets; grout consisted of cement, water, and admix-

tures. The cables were grouted while they were subjected to a constant load of approximately 39 percent of GUTS. The grout was cured to a specified compressive strength before fatigue testing.

Stay cable anchorage designs vary substantially among bridge projects. In general, strands are splayed outward near anchorages. These strands either terminate in a large socket or are anchored individually with wedges at an anchor plate. In the wedge system, the force in each strand is transferred to the anchorage through a two- or three-piece conical wedge set. Each strand passes through a conical opening in the anchor plate, which constrains the wedges. As the strand force increases, sharp ridges lining the wedge interiors penetrate the surface of the wires and provide a means for transferring force to the anchor plate.

In socket systems, the force transfer occurs over the length of a conical socket. The diameter of the splayed strand bundle decreases with the distance from the anchor plate end of the socket to the location where the nonvariable diameter cable free length begins. Bond between strands and the contents of the socket (epoxy or grout) transfers cable forces to the sockets over their length. Nevertheless, wedges or sewage-type systems are still used at strand ends.

Figure 1 shows the three anchorage systems evaluated in the cable tests discussed here: wedge, socket, and hybrid systems.

Anchorage System A is a prefabricated socket system consisting of a steel socket filled with a mixture of epoxy and steel balls. The strand's epoxy coating is stripped over the strand's length inside the socket and for a relatively short distance adjacent to the socket in the free length of cable. This is done to enhance bond between epoxy-steel ball compound and the strand. A layer of epoxy and a layer of water barrier sealant fill the spaces between strands and HDPE pipe in the area adjacent to the socket. The water barrier sealant was used to prevent penetration of grout bleedwater to unprotected strands. Each strand terminated in a swaged sleeve bearing on a locking plate.

The anchorage used in Test Series B combines features of both the wedge and socket systems. The epoxy coating of the strands is not removed and grout is used to transfer forces from the strands to the socket structure through bond. Unlike the coated strands in Test Series A, the epoxy-coated strands in Series B were manufactured with a grit-impregnated surface to improve bond. All strands pass through a wedge-gripped anchor plate and terminate in a grout cap. To enhance penetration through the epoxy coating, the wedges are manufactured with deeper teeth compared with conventional (uncoated) strand wedges. Since a static load is applied to the cable before grouting, the socket mechanism becomes effective only after grout cure. Therefore, prior to grouting, the entire cable force is carried by the wedges while the subsequent cyclic forces are carried mainly through the socket mechanism.

Anchorage System C relies solely on conical wedges for force transfer between strands and the anchorhead. Steel pipe sheathing was used instead of the HDPE pipe used in the other two systems. The steel transition pipe is bolted to the anchor plate. The strands terminate in a grout cap. This as-designed system used epoxy-coated strands without surface grit. Therefore, bond between strand and grout is comparable to System A.

## TEST FIXTURES

Construction Technology Laboratories (CTL) operates two separate test facilities for axial fatigue and com-

bined axial/flexural fatigue tests of stay cables. In general, axial fatigue tests are incorporated in the test series for all bridges whereas the axial/flexural fatigue tests are performed only for cable-stayed bridge designs incorporating continuous cables through the pylons or towers. In such designs, the cables are not anchored at the pylons but are supported on a curved "saddle" and anchored at the deck level only.

Figures 2 and 3 show the axial and axial/flexural test fixtures, respectively. The test systems are structurally self-reacting and the forces are balanced within the fixtures. The axial test fixture was fabricated of steel, and the axial/flexural fixture is a post-tensioned segmental concrete beam. In the axial/flexural test fixture, the hydraulic ram is placed under the saddle, and cyclic axial and flexural forces are applied through vertical movements of the ram piston. A description of the axial/flexural test fixture and its use was documented by Tabatabai and Pandya (3). A closed-loop servohydraulic system is used to apply cyclic loads to the cables. Both test fixtures incorporate a continuously recording non-destructive wire break detection system for monitoring wire ruptures during cyclic loading.

## TEST RESULTS

The following sections present narrative descriptions of the 14 stay cable fatigue tests, incorporating the authors' discussion of specimen dissections and unique test procedures and cable design features. Fatigue performance data for all tests are presented in Table 2.

### Test Series A

Test Series A consisted of a specified total of three axial tension tests for 31-, 49-, and 73-strand epoxy-coated stay cable specimens. There were no combined axial/flexural fatigue test requirements for this project.

#### *31-Strand Cable Test (Specimen A31)*

During 2 million cycles of fatigue loading on the 31-strand cable, the wire break detection system indicated a total of eight wire breaks, or approximately twice the number of breaks allowed by specification (2 percent of total number of wires, or four wires). The maximum load achieved during the subsequent static load test was 7086 kN (1,593 kips), which was less than the acceptance load level of 8074 kN (1,815 kips).

A number of observations were made during the dissection of the cable. Severe corrosion of strands was noted in the area beneath the epoxy-zinc compound near the bottom cable socket. The corresponding area

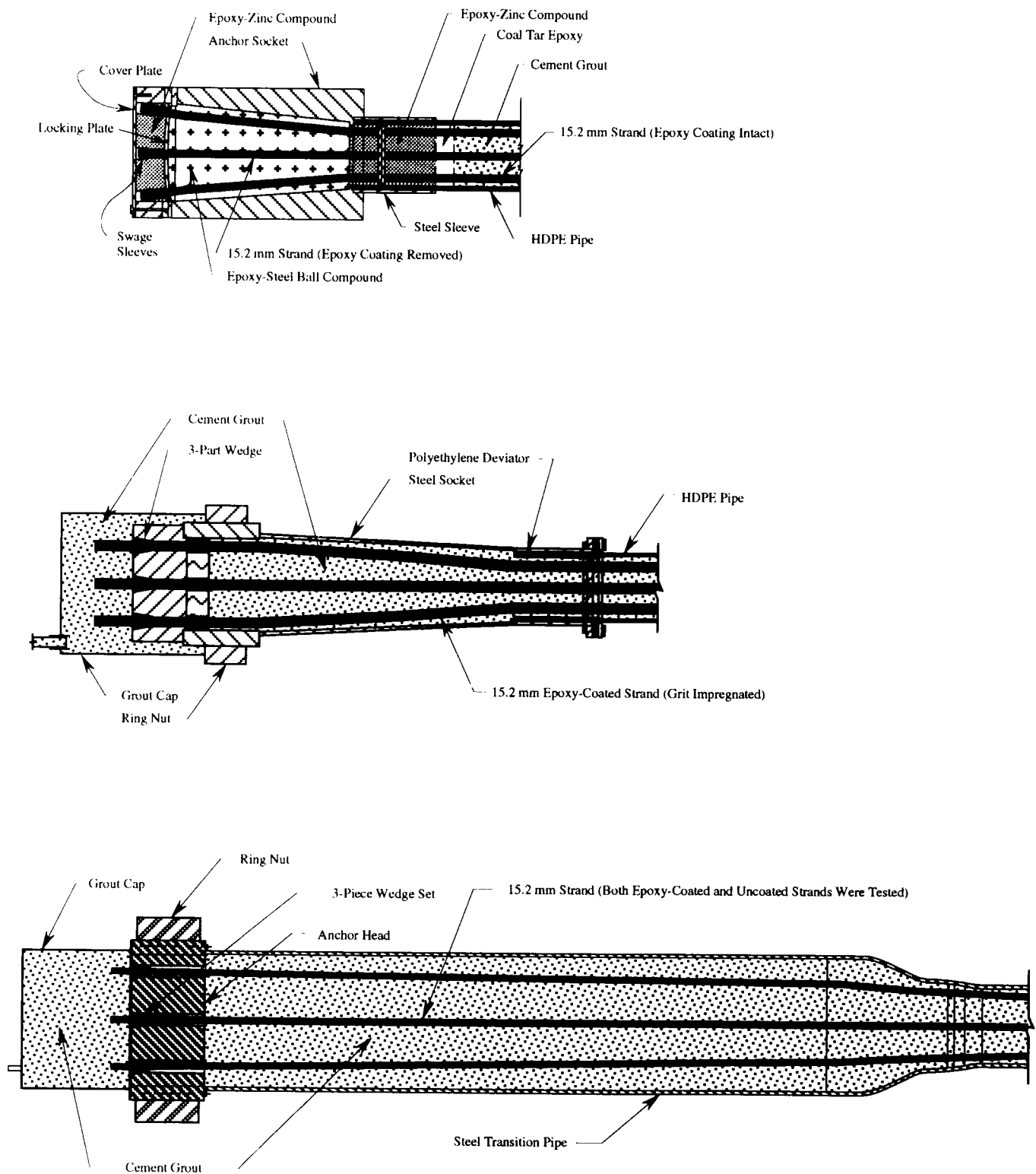


FIGURE 1 Stay cable anchorage systems: *top*, Series A; *middle*, Series B; *bottom*, Series C.

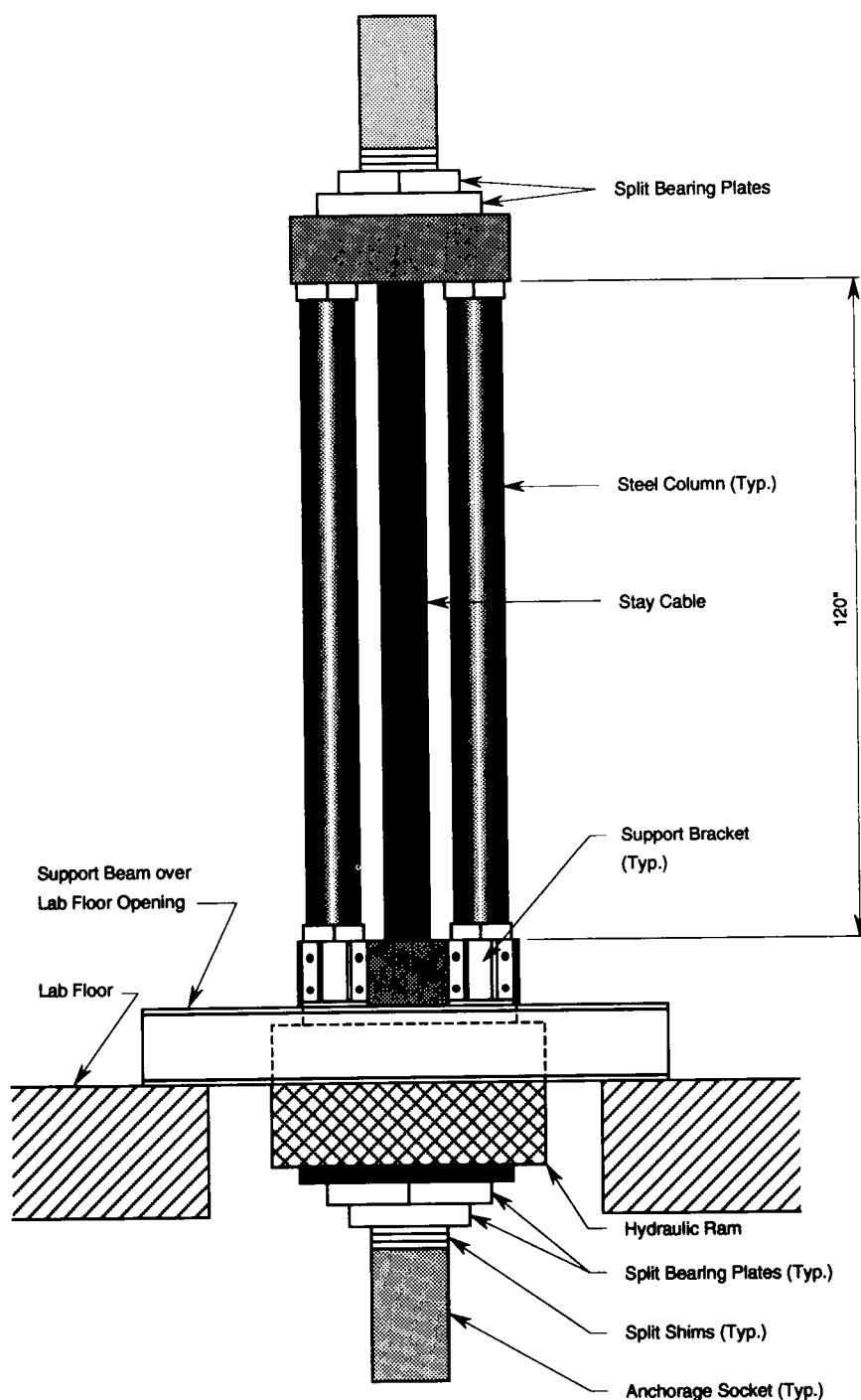


FIGURE 2 Test fixture for axial fatigue testing.

near the top socket was also corroded, but to a lesser degree. It should be noted that the epoxy coating was removed from these regions during assembly of the cable. Although strand areas under the coal tar epoxy had also been stripped bare, these areas were free of corrosion.

Twenty-six broken wires (including three completely severed strands) were found, almost all of which were lo-

cated in the severely corroded area within 190 mm (7½ in.) of the bottom socket. Seventeen wire breaks were considered fatigue fractures, and the rest appeared ductile. It is believed that although eight wire ruptures occurred during fatigue testing, the remaining wire breaks observed in dissection were attributable to static fractures at fatigue damage accumulation sites on the wire.

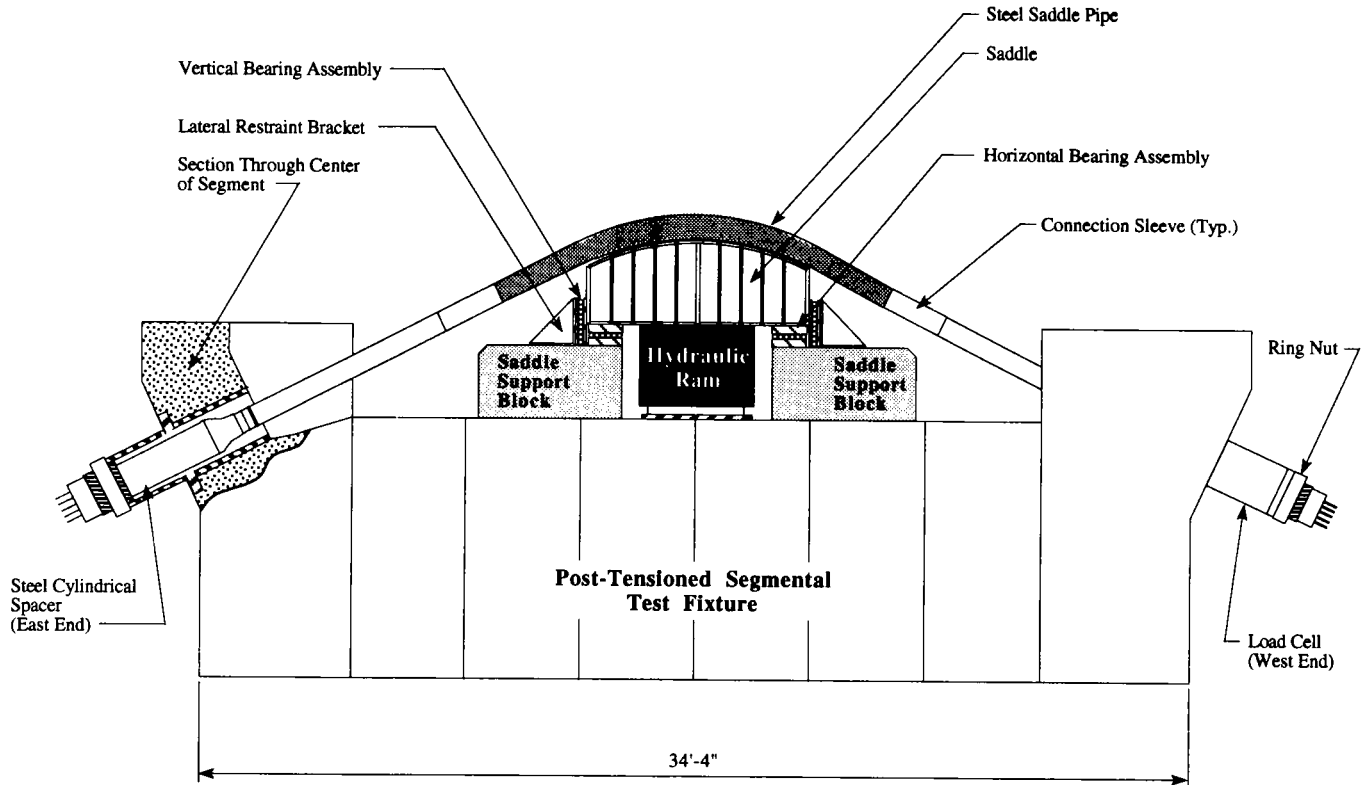


FIGURE 3 Test fixture for combined axial/flexural fatigue testing.

The contents of the bottom socket were forced out in a high-capacity compression testing machine to examine the degree of corrosion inside the socket. Corrosion had extended approximately 178 mm (7 in.) into the epoxy-steel ball compound zone of the bottom socket. It is believed that penetration of grout bleed-water through the boundary between the coal tar epoxy and the HDPE pipe caused the corrosion. The grout bleedwater then reached the bare strands through the closely spaced transverse cracks in the epoxy-zinc compound. The extensive strand corrosion observed occurred during the month between grouting and cable dissection.

### 31-Strand Cable Retest (Specimen A31-R)

A second 31-strand cable was tested. This cable was similar to the first 31-strand cable, except that in accordance with approved test procedure revisions, it was tested ungrouted. During fatigue testing, three wire breaks were detected. Therefore, the allowable number of wire breaks (4) was not exceeded. However, the maximum load of 7037 kN (1,582 kips) achieved during the subsequent static test did not attain the target load level of 8065 kN (1,813 kips). Several wire and strand breaks were heard, and the testing was discontinued.

The cable was then removed from the test fixture and dissected. A total of 22 broken wires, including three completely severed strands, were found. Seven of the wire breaks were considered fatigue fractures, and the rest were ductile. One broken strand was located near the top socket, one near the bottom socket, and the third approximately 1525 mm (60 in.) from the top socket (in the free length). A closer examination of the immediate area of wire fractures in cable free length indicated presence of localized corrosion on several wires. There were no indications of corrosion observed on the bare strands under the coal tar epoxy and the epoxy-zinc compound.

### 49-Strand Cable Test (Specimen A49)

The next stay cable specimen tested in Series A was a grouted 49-strand cable. From the results of the first two tests, the cable manufacturer modified the cable design slightly. Revised anchorage details incorporated a polyurethane material in place of coal tar epoxy. The thickness of the water barrier sealant was also increased, and the strand epoxy coating was left intact at least 127 mm (5 in.) from the socket. The wire break detection system indicated four wire breaks during fatigue tests, which conformed with the acceptable breakage limit of 2 percent, or seven wires.

TABLE 2 Fatigue Test Results

Test Designation <sup>(1)</sup>	Number of Cycles at First Wire Breakage	Number of Broken Wires at 2,000,000 Cycles <sup>(4)</sup>	Number of Fractured Wires Observed After Static Proof Test
A31	1,100,000	8	26
A31R <sup>(2)</sup>	1,029,000	3	22
A49	51,000	4	21
A73	52,000	5	49
B46	600	87	144
B37 <sup>(3)</sup>	N/A	0	N/A <sup>(5)</sup>
B17	N/A	0	0
B46R	1,603,000	4	19
C85	1,370,000	7	7 <sup>(6)</sup>
C79	1,982,000	2	32
C85R	1,490,000	12	60
C85U	N/A <sup>(7)</sup>	0 <sup>(7)</sup>	8
C79U	611,000	10	28
C82U <sup>(3)</sup>	78,000	148 <sup>(8)</sup>	N/A <sup>(5)</sup>

(1) Denotes test identifier, including test series (A, B or C), cable size expressed as number of 15.2-mm strand, U denotes uncoated strand cable, R denotes retest.

(2) Ungrouted specimen.

(3) Combined axial/flexural load regime - see Table 1 for test parameters.

(4) Based on wire break detection system data except for C82U.

(5) Static proof test not required.

(6) Anchorage failure occurred at 57.8% GUTS.

(7) Wire break detection system malfunction noted.

(8) Based on outcome of cable dissection.

The maximum load achieved during the static test was 12 366 kN (2,780 kips), which corresponds to 96.8 percent of GUTS and 92.1 percent of the actual ultimate strength of cable. Several wire and strand breaks were heard during the static test, and the acceptance load level of 12 753 kN (2,867 kips) was not achieved.

Three completely severed strands (21 broken wires) were found inside the cable during dissection. Two strand breaks were near the bottom socket, and one occurred near the top socket. All three breaks occurred on the outside layer of strands. Ten of the broken wires exhibited fatigue fracture features; other breaks were ductile.

### 73-Strand Cable Test (Specimen A73)

The last stay cable specimen tested in Series A was a grouted 73-strand cable. During fatigue testing, five

wire breaks were detected with the wire break detection system. Therefore, the number of breaks conformed with the specification required limit of 2 percent (10 wires). The maximum load achieved during the static test was 17 175 kN (3,861 kips), which corresponded to 90.3 percent of GUTS and 85.9 percent of actual cable strength.

Seven completely severed strands (49 broken wires) were found in the cable during dissection. All breaks were close to the bottom socket and, in general, appeared on the outside layer of strands. Of the total number of broken wires, 36 wires exhibited fatigue fractures and the others were ductile. Two strands showed clear indications of corrosion on the surfaces of the center (king) wire. The surfaces of outside wires in these two strands, which were in contact with the center wire, also showed evidence of corrosion. There was no

evidence of grout bleedwater penetration in the area of these strand fractures.

## Test Series B

Cable Test Series B included axial tests of 17- and 46-strand specimens and one axial/flexural test on a 37-strand cable. The anchorage system for this cable is shown in Figure 1.

### *46-Strand Cable Test (Specimen B46)*

The first stay cable specimen in Series B tests was a 46-strand cable. After placement of individual strands inside the test frame and before placement of grout caps, the cable supplier applied epoxy patches at the ends of each strand protruding beyond the wedge plates. The cable was then statically loaded to 65 percent of GUTS to seat the wedges. The load was reduced to grout load (38.6 percent of GUTS), and the cable was grouted. The grout was allowed to cure for 1 week before the fatigue test was begun.

The wire break detection system recorded 87 wire breaks during the fatigue test. A sharp rise in the number and rate of occurrence of wire breaks occurred after approximately 1,400,000 cycles and continued to increase until the end of the test. It should be noted, however, that the stiffness of the cable and the magnitude of its elongation from minimum to maximum load changed very little as a result of all the wire breaks. The maximum load achieved during the subsequent static proof test was 8452 kN (1,900 kips), or 70.5 percent of GUTS. Several wire and strand breaks were heard during the static test, and the acceptance load level of 11 387 kN (2,560 kips) was not achieved.

After the static test, the cable was removed from the test fixture and dissected. The grout near the area of top socket was wet. Fractured wires were evident beneath the cracked and damaged epoxy coating, and extensive corrosion and moisture were evident near most fractures. Corrosion stains were also apparent on the inside surfaces of epoxy coatings. Strands protruding beyond the bottom wedge plate were sawcut a few inches from the wedge plate. Strands were then numbered and individually sawcut at the inside surfaces of top and bottom wedge plates. As strands were being handled, water (of a yellowish brown color) was observed coming out of a number of strands.

A total of 144 broken wires were found in the cable with multiple successive fractures (up to three) on a number of single wires. Some multiple fractures occurred within a few inches of each other. Only 16 of the 144 fractures were clearly ductile while the balance

exhibited fatigue or brittle fracture features. All wire fractures occurred within 915 to 2000 mm (36 to 79 in.) from the inside face of top wedge plate. This area corresponded to the wet grout zone observed upon removal of HDPE pipe.

It became clear that grout bleedwater found its way into the interstitial spaces between wires under the epoxy coating and remained there throughout the test as free water. It is believed that water may have penetrated through epoxy-patched strand ends and the wedge areas where the epoxy coating is cut with the wedge teeth. It is not clear what role, if any, that possible holidays in the surface of the epoxy coating may have had on the penetration of water or to what extent preexisting corrosion-induced pitting affected fatigue endurance. However, it is also clear that if grout bleedwater can penetrate inside the strand, then severe corrosion of wires can be expected over a short period. On the basis of the observed lack of change in the stiffness of cable after the occurrence of many wire breaks, it is concluded that wires and strands redeveloped relatively large forces a short distance from a break location, possibly because epoxy-coated strands with grit were used. This may also explain why many wires had multiple fractures.

Investigation of the fatigue test failure by the bridge owner (4) revealed that the poor performance was created by preexistent corrosion of the strand used for cable tests. Additionally, the presence of grout water beneath the epoxy was believed to have contributed to fatigue fractures. As a result, strand coils were screened more carefully for the presence of corrosion and grout pressures were reduced to minimize pressure bleed.

### *37-Strand Cable Test (Specimen B37)*

The axial-flexural fatigue test was performed on a 37-strand cable (Figure 3). Before grouting, the cable manufacturer used plastic caps filled with epoxy to cover the ends of strands on both ends of the cable. The epoxy was then allowed to cure. A few hours after grouting, the cable manufacturer removed the grout caps and their grout contents, thereby exposing the strands protruding beyond the wedge plates. The strand ends (including plastic caps) were sawcut a few inches from the wedge plates on both cable ends. Drops of water were observed coming out of some strands. The cable manufacturer subsequently used demisterized and pressurized air to remove moisture from the interstitial spaces between wires in all 37 strands.

Approximately 2 million cycles of fatigue loading were then applied to the cable. The wire break detection system did not indicate any breaks. The acceptance requirements did not specify static proof loading after the fatigue test; therefore, a static test was not performed.



The cable was then removed from the test fixture and dissected after the conclusion of fatigue tests. No wire breaks were found during the dissection.

### **17-Strand Cable Test (Specimen B17)**

Another axial test was performed on a 17-strand cable. Again, prior to grouting, the ends of all strands were covered with plastic caps filled with epoxy and allowed to cure. A few hours after grouting, the grout caps and the grout inside the caps were removed and the strand ends were cut near the wedge plates, thereby removing plastic caps. Water was observed coming out of two strands on the bottom. The cable manufacturer used demoisurized and pressurized air to remove moisture from inside all strands.

After the minimum specified grout strength was achieved, fatigue testing began. The detection system indicated no wire breaks. The acceptance load level of 4200 kN (944 kips) was attained during the static test. No wire fractures were found during dissection of this cable.

### **46-Strand Cable Retest (Specimen B46-R)**

The final test performed in this series was a retest of the 46-strand cable. Before grouting, the cable manufacturer covered the ends of all strands with plastic caps filled with an epoxy. A coating of epoxy was also applied over the plastic caps. Prior to the start of fatigue tests, both top and bottom grout caps were removed and plastic caps on the strand ends were exposed. However, strand ends were not sawcut. Plastic caps on four strands were damaged during removal of grout. A few drops of water were observed coming out of the bottom of one strand with a damaged plastic cap. In addition, yellowish residue was found at the bottom of another strand, which indicated water leakage. During fatigue testing, four wires were broken (fewer than the allowable number of six), as indicated by the wire break detection system.

The acceptance load level of 11 387 kN (2,560 kips) was achieved during the subsequent static test. Before the cable was removed from the test fixture, a plastic cap was removed from the bottom of a strand and water was observed coming out of it.

During dissection, cracked and damaged epoxy coatings indicated the presence of fractured wires. Some corrosion was evident in the vicinity of most fractures on the center wire and along the contact lines between wires. Small amounts of water were observed coming out of five strands. Nineteen broken wires were found in the cable, with four wires having two fracture locations for a total of 23 fractures. All 23 fractures exhibited fatigue features.

## **Test Series C**

Two axial (79- and 85-strand specimens) and one axial/flexural (82-strand specimen) cable tests were originally specified for Series C. When the first manuscript of this paper was submitted for review, three tests of the originally specified epoxy-coated cable and three tests of uncoated strand cable had been completed. The anchorage system for this test series is shown in Figure 1.

### **85-Strand Epoxy-Coated Cable Test (Specimen C85)**

The 85-strand test cable was first statically loaded to 45 percent of GUTS to seat the top wedges. The bottom wedges had been seated to 45 percent of GUTS in the supplier's plant. The load was then reduced to grout load. The strand ends were covered with plastic caps filled with epoxy and the epoxy was allowed to cure. The cable was then grouted. A few hours after grouting, the top and bottom grout caps were removed and the strand ends (both top and bottom) were sawcut to examine whether water had penetrated beneath the epoxy. Water was clearly evident in at least 35 strands. Then, at the direction of the cable supplier, pressurized and demoisurized air was used to remove moisture from inside of all strands.

Very early during cyclic testing, all the bolts 12.7 mm ( $\frac{1}{2}$  in.) in diameter connecting the steel transition pipes to the top and bottom anchor plates failed (six at each anchor plate). Seven wire breaks (1.2 percent) were detected during the fatigue test.

At the conclusion of the fatigue test, the cable was statically loaded with the target of achieving the acceptance load level of 95 percent of the actual cable strength, or 21 520 kN. At a load of 57.8 percent GUTS, or approximately 12 811 kN (2,880 kips), all strands in the top anchor head simultaneously and unexpectedly slipped through their wedges about 70 mm ( $2\frac{3}{4}$  in.). Only the epoxy coating of strands and one broken wire were left standing above the anchor plate.

During dissection of the cable, seven wire fatigue breaks were found. Six breaks occurred on an outer-layer strand approximately 380 mm (15 in.) from the bottom anchor head. Corrosion was observed on this strand in the area of breaks. One wire break occurred on an inner strand approximately 12.7 mm ( $\frac{1}{2}$  in.) below the end of its wedge at the upper anchorhead. Corrosion was also evident on this strand in the fracture area and at random locations on other exposed strands. The teeth of wedges in the top and bottom anchorheads did not show signs of flattening or bending. The penetration of wedges into the wires was not uniform in the top anchorage. However, wherever penetration

was evident, the wire surface was scraped and flattened as a result of strand slippage.

### ***79-Strand Epoxy-Coated Cable Test (Specimen C79)***

The second test in Series C incorporated similar preparations to Test C85's, except that anchorage wedges were seated at a load level corresponding to 70 percent GUTS in order to circumvent the previous anchorage difficulty. Following grouting and at the request of the cable supplier, bleedwater that had penetrated beneath the strand epoxy coating was forced out of each strand with compressed demoisturized air. During fatigue testing, the wire break detection system identified two wire ruptures. After fatigue testing, the cable was loaded statically, withstanding a maximum load of 18 994 kN (4,270 kips). The target load level was 19 995 kN (4,495 kips).

During dissection of the cable, 32 broken wires were noted, along with fractured welds between the transition pipe and its anchorhead attachment flange. Residual moisture, most likely consisting of grout bleedwater, was evident in the specimen. Corrosion with pitting of strand was noted beneath the epoxy coating.

### ***85-Strand Epoxy-Coated Cable Retest (Specimen C85R)***

In preparation for the third test in Series C, the transition pipe-to-anchorhead attachment details were modified. The number of connecting bolts was increased to 12 on each anchorhead, and welding procedures were revised. The cable was grouted, and, at the direction of the cable supplier, strands were dried internally using compressed demoisturized air.

During fatigue testing, 2 percent wire breakage occurred (12 wires); thus this specimen conformed with fatigue test requirements. However, 22 of the 24 transition pipe-to-anchorhead connecting bolts at both anchorheads fractured during fatigue testing. During the static proof test, the specimen attained a maximum load of 20 044 kN (4,506 kips); the target proof load was 21 907 kN (4,925 kips). Subsequent dissection of the specimen revealed 60 fractured wires, with successive multiple fractures on individual wires. Residual moisture, presumably from grout bleedwater, was evident, as was corrosion ranging in severity from light to moderate beneath the epoxy coating.

### ***85-Strand Uncoated Cable Test (Specimen C85U)***

Subsequent to the first three cable tests, the bridge specification was modified to allow an uncoated strand sys-

tem. Revisions included strand anchorage modification and application of a corrosion inhibitor solution to strands before grouting. This latter measure represents an accepted cable installation practice intended to protect uncoated strands from corrosion prior to cable grouting. Further modifications were made in the transition pipe-to-anchorhead bolted connection details to improve performance.

Fatigue testing indicated acceptable performance with respect to wire breakage, and the cable attained the specified static proof load of 95 percent GUTS. Dissection of the specimen revealed eight fractured wires. Difficulties with suitable performance of the transition pipe-to-anchorhead continued, with cracking occurring in the machined transition pipe flange. Strands exhibited evidence of corrosion with surface pitting at locations of transverse cracks in grout.

### ***79-Strand Uncoated Cable Test (Specimen C79U)***

To overcome continuing difficulties in suitable fatigue performance of the steel transition pipe, additional modifications were made to this component. Specimen assembly and grouting procedures were similar to Specimen C85U.

This specimen performed adequately in fatigue, with 10 wire breaks (1.8 percent) occurring through the cyclic load application interval. During static proof loading, the specified maximum load of 19 559 kN (4,397 kips), or 95 percent GUTS, was achieved.

Dissection of the specimen revealed the presence of 28 broken wires in the specimen. Locally severe corrosion was noted at several wire fractures. Areas of corrosion coincided with transverse cracks in the cementitious grout. Weld cracks occurred in the machined flange at the anchorhead end of the transition pipe.

### ***82-Strand Uncoated Cable Test (Specimen C82U)***

A combined axial/flexural fatigue test was conducted on the 82-strand uncoated specimen. Test criteria and specimen geometry data are presented in Table 1. The test specimen was fabricated atop CTL's axial flexural test fixture (Figure 3). Strands were installed and wedges were preseated individually. Grouting load was attained by extending the hydraulic actuator positioned beneath the apex of the saddle pipe.

Two million cycles of fatigue load were applied to the specimen. The repetitive load applied to the cable (measured axially) ranged from 7913 to 9275 kN (1,779 to 2,085 kips). Acceptance criteria required that no more than 12 wires rupture during the fatigue test. No static proof loading of the specimen was required.

From the start of the test, the wire break detection system noted an unusually large number of events that suggested wire breaks. Commencing at approximately 78,000 cycles, a very large number of wire breaks were detected in the cable. Therefore, the specimen did not conform with wire breakage criteria. Subsequent dissection of the specimen revealed 148 fractured wires on 40 individual strands. These fractures were distributed equally between both ends of the saddle (71 and 73 at either end). Ninety-seven percent of the fractures were located in the end regions of the saddle. The remaining four fractures were located in the cable free length. Some corrosion of the specimen was noted at transverse cracks in the grout, and partial penetration weld fatigue fracture was noted at the concentric reducer sections of the transition pipe.

Detailed examination of wire ruptures in the cable indicated that many of the fatigue fractures originated at oval-shaped fretting marks on the wire surface. Brownish staining on fracture faces suggested possible involvement of corrosion in the failure mechanism. The fretting of wire was noted principally at interstrand contact points in high-contact stress regions of the cable over the saddle. Modifications in cable specimen stressing methods, specimen anchorage, and transition pipe details were made in preparation for retest of the specimen, with the intent of improving specimen performance.

## SUMMARY AND CONCLUSIONS

1. Fourteen fatigue tests of full-scale stay cables were performed to fulfill acceptance testing programs for the construction of three U.S. cable-stayed bridges. The cable specimens ranged from 17 to 85 strands 15.2 mm (0.6 in.) in diameter with nominal tensile capacities of 4430 to 22 157 kN (996 to 4,981 kips).

2. Tested cables were composed of seven-wire uncoated and epoxy-coated parallel strands 15.2 mm (0.6 in.) in diameter. Different cable anchorages were used for the three bridges. One test series used epoxy-coated strand with a grit-impregnated surface to improve bond, and the other incorporated epoxy-coated strand with smooth surfaces and uncoated strand. It should be noted that the reported test series did not evaluate cables constructed of the epoxy-encapsulated (filled) strand.

3. Review of fatigue test results indicates that conformance with the current 2 percent limit on wire breakage during cable fatigue testing can be attained. However, it is apparent that design, materials, and fabrication features that have the potential for impairing fatigue resistance of bridge stay cables affect adequate test performance as well. During the three test series, these features resulted in excessive wire breakage during

cyclic load application or wire damage accumulation (transverse cracks) during fatigue testing, which induced wire rupture during static proof loading.

4. Manifestations of wire fatigue fracture during testing occurred principally in cable specimen free length, with few instances of wire fracture in anchorages.

5. Testing revealed that moisture from the cement grouting process can infiltrate the epoxy coating of strands and remain as free water in the cable specimen for the duration of the cable qualification test (1 to 2 months). It is believed that this phenomenon contributed to the premature, corrosion fatigue-related fracture of wires during all three series. Moisture intrusion most likely occurs in the wedge regions where the epoxy coating is breached by wedge teeth. It is possible that holidays in the epoxy coating also promote the penetration of grout bleedwater. It should be noted that grout specification requirements for all three test series contained stringent provisions intended to limit corrosion aggressivity of grout constituents.

6. Test results from an ungrouted cable (A31-R) and investigation of a grouted-cable test failure (B46) indicated that preexistent corrosion of strand beneath the epoxy coating contributed to mechanisms inducing wire fracture during fatigue tests. Preexistent corrosion-induced pitting of strand initiated fatigue cracks.

7. Cement-grouted, uncoated strand cable systems developed localized corrosion activity at transverse grout crack locations during the 1- to 2-month fatigue test duration. These regions near grout cracks acted as sites at which wire fatigue damage accumulated.

8. Extensive fretting-fatigue damage at interstrand contact surfaces within the saddle pipe region was noted during a combined axial/flexural fatigue test of a particularly large cable. Interactions between cable size, saddle radius, saddle pipe diameter, and test methodology were under study at the time this paper was prepared.

9. Cable sheathing consisting of HDPE or steel pipe serves as the primary barrier to passage of deleterious substances to the cable's principal structural element. The sheathing's durability-enhancing function can be disrupted. The sheathing acts compositely (to some extent) with the rest of the cable and is therefore subjected to repetitive stresses and possible failure at connections.

## RECOMMENDATIONS

1. Review of the test results suggests that the presence of free moisture in cement-grouted stay cable specimens contributes to accelerated wire damage during fatigue testing. This phenomenon was observed in both coated and uncoated strand and occurred in the brief

1- to 2-month duration of the affected tests. Although it is unknown to what extent and for what duration grout bleedwater can function as a corrosion medium in an erected, grouted bridge stay cable, even relatively minor surface pitting of cold drawn wire can reduce the fatigue resistance of strand, thereby reducing the potential service life of a cable. For this reason, the authors recommend that methodical development and enforcement of improved grouting procedures be implemented with the goal of minimizing the liberation of free moisture during stay cable cement grouting. From observed cable test performance, this measure would be an effective advance in stay cable durability. Other measures, such as the use of epoxy-encapsulated (filled) strand, may prove to be beneficial should the encapsulating coating resist infiltration of free moisture liberated during pressure grouting.

2. Preexistent corrosion of coated and uncoated strand for stay cable use should be prohibited in specifications for strand procurement. Currently, the PTI recommendations contain no such provisions.

3. Bridge stays incorporating continuous cables over saddles should be designed with caution and evaluated rigorously for the effects of high-contact stress-induced fretting between strands created by cable curvature. Study of this issue on performance of existing uncoated-strand bridge stay cables is warranted.

4. Acceptance testing programs for bridge stay cables should be conducted as early as practical during the process of fabricating and erecting stay cable. This approach allows ample time for implementing cable de-

tail and execution refinements, if proven necessary by test, and limits the impact of testing difficulties on a bridge construction schedule.

#### ACKNOWLEDGMENTS

The information described in this paper was synthesized by the authors from reports furnished in fulfillment of bridge specification-required cable qualification test series for bridge construction programs in the states of Delaware, Illinois, and Iowa. Cable systems for these bridges were furnished by Dywidag Systems International (DSI), Inc. and VSL Corporation. The authors express their appreciation to Johannes Inzenhofer, Ralph Reetz, and Ronald Bonomo of DSI-USA, Inc. and Duncan Lapsley of VSL Corporation for their review comments.

#### REFERENCES

1. *Committee on Cable-Stayed Bridges. Recommendations for Stay Cable Design, Testing and Installation.* Post-Tensioning Institute, Aug. 1993.
2. Podolny, W. *Cable-Stayed Bridge Future Developments.* American Society of Civil Engineers, 1992.
3. Tabatabai, H., and S. Pandya. Test Fixture Design Meets Challenge of Bridge Stay Cable Fatigue Testing. *Test Engineering and Management*, Dec./Jan. 1992-1993.
4. Karshenas, M. Fatigue Strength of Cable Stays for the Clark Bridge at Alton. *Proc., 11th Annual International Bridge Conference*, Pittsburgh, Pa., 1994.

# BRIDGE LOADS AND DYNAMICS

---

# Are Road-Friendly Suspensions Bridge-Friendly? OECD DIVINE

---

Robert J. Heywood, *Queensland University of Technology, Australia*

This paper presents the results of an investigation aimed at developing an understanding of the influence of truck suspensions on the dynamic response of short span bridges. The work forms part of the Organization for Economic Cooperation and Development (OECD) Dynamic Interaction Between Vehicle and Infrastructure Experiment (DIVINE). The hypothesis is based on the assumption that soft, so-called "road friendly" suspensions induce less damage in pavements than stiff suspensions. This paper concentrates on the extension of this hypothesis by discussing its application to short span bridges. Three bridges were instrumented and their dynamic response to the air- or steel-suspended test vehicles was recorded. For two of these bridges, the dynamic wheel forces and the bridge response were acquired simultaneously. The bridges chosen were to have natural frequencies in the range of axle hop frequencies in order to investigate possible resonance effects. The paper details both the vehicle and the bridge responses and the interaction between them. Dynamic increments in excess of 100 percent were recorded. Dynamic coupling between axle hop vibrations and the bridge resulted in up to 10 damage cycles during the passage of a vehicle. The bridge response is shown to be sensitive to the natural frequency of the bridge, the suspension of the vehicle, its speed, and the road roughness. The bridge-friendliness of road-friendly suspensions is discussed in the light of experimental evidence.

The transport industry, vehicle designers, government agencies, and researchers have recognized the reduction in damage afforded to infrastructure and cargo that can be achieved through improved suspension design. The new generation of soft, highly damped "road-friendly" suspensions are rapidly gaining acceptance around the world. In Australia, government authorities are investigating the possibility of increasing axle loads and consequently road transport efficiency in return for fitting road-friendly suspensions.

Future increases in the legal loads will be limited by the strength of an aging infrastructure of bridges in Australia. Hence older short span bridges are the major concern. Seventy-five percent of Australia's bridges have spans less than 15 m, and many of the larger spans have subelements in this range. The possibility of safely carrying heavier loads across short span bridges in return for reduced dynamic loads applied by bridge-friendly suspensions is an attractive option.

The Organization for Economic Cooperation and Development (OECD) has sponsored the international research projects IR2 and IR6 to investigate road-friendly suspensions in a scientific manner. The IR2 project reported its findings in 1992 (1). The IR6 project known as the Dynamic Interaction Between Vehicle and Infrastructure Experiment (DIVINE) is well advanced. This paper is based on research conducted as part of dynamic bridge load research (Element 6) of OECD DIVINE and parallel studies on behalf of the

Roads and Traffic Authority of New South Wales, Vicroads, AUSTRoads, and the Australian National Road Transport Commission.

It is well recognized that the dynamic response of bridges is largest when the natural frequencies of the bridge and the vehicle are equal (2,3). Vehicle vibrations can be organized into two groups: body bounce and axle hop. Body bounce frequencies are in the 1.5- to 2-Hz range for air suspension and 2.5- to 4-Hz range for steel suspensions. Thus dynamic coupling between the body bounce vibrations and bridges will occur for bridges with natural frequencies between 1.5 and 4 Hz corresponding to a span between 80 and 30 m.

Axle hop frequencies (8 to 15 Hz) would be expected to dynamically couple with bridges of similar frequencies (8- to 15-m span). Little research has been undertaken for such short span bridges. An experimental program designed to investigate the influence of axle hop vibrations on the dynamic response of short span bridges and the influence of suspension type is discussed.

The response of medium span bridges with natural frequencies in the range of body bounce is being investigated under the direction of Reto Cantieni of the Swiss Federal Laboratories for Materials Testing and Research (EMPA). The influence of suspension type on this range of spans will be reported as part of OECD DIVINE.

## DESCRIPTION OF BRIDGES

The details of the three short span bridges used during this study are presented in Table 1 and Figure 1. The bridges were selected with a view to investigating possible dynamic coupling with axle hop vibrations. They are representative of short span bridges that are fairly common in Australia.

The Yarriambiack Creek bridge is a three-span, simply supported, cast-in-situ, reinforced concrete T-beam bridge built in 1927 [Figure 1(a)]. Cameron's Creek is

a more modern (1976), four-span, simply supported, prestressed concrete deck unit bridge, the most common short span bridge in Australia [Figure 1(b)]. The three-span semicontinuous timber girder bridge over Cromarty Creek is uniquely Australian [Figure 1(c)]. Timber girder bridges were constructed from a plentiful supply of hardwood logs (450-mm diameter), which were used as girders. Hardwood deck planks (300 × 125 mm) span between the girders. The ends of the girders were made semicontinuous by vertical bolts into corbels, which are in turn supported on timber piers. The 10,000 of these bridges that remain in service present a major management challenge for Australian authorities.

Table 1 summarizes the characteristics of the test bridges. The stiffness was calculated from the measured midspan deflection when the test truck was positioned with its 20-ton triaxle group (tridem) at midspan. The natural frequency and damping attributes of the bridges were derived from the free vibration after the test vehicles left the bridge. The damping has been characterized as low, average, or high in accordance with the limits defined by Cantieni (2).

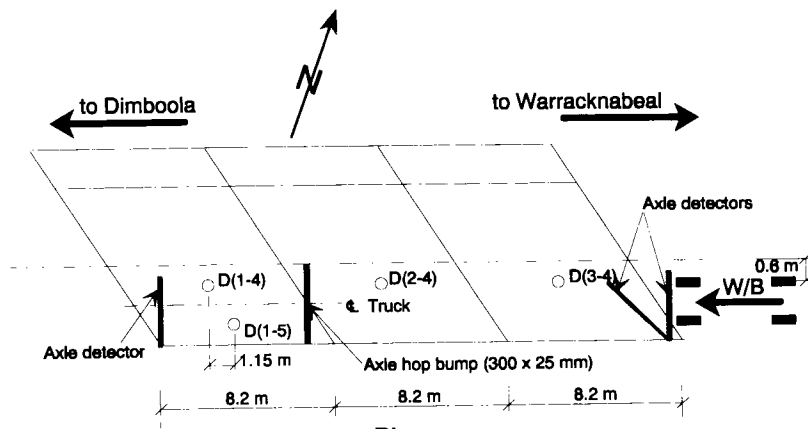
## ROAD PROFILES

The surface profiles for each of the bridges are presented in Figure 2. The surface roughness is consistent with secondary roads rather than high-quality highways. The profiles across Cameron's and Cromarty creeks were measured using the Australian Road Research Board laser profileometer. In the case of the Yarriambiack Creek bridge, the profile was measured using the conventional dumpy level and staff survey.

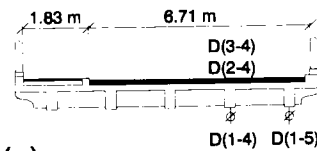
Depressions in the southern approaches to Cameron's and Cromarty creek bridges had been repaired with cold mix asphalt concrete. (Note that Australian traffic travels on the left-hand side of the road.) These repairs are clearly evident on the longitudinal profiles as they exhibit significant short wavelength roughness,

TABLE 1 Characteristics of Test Bridges

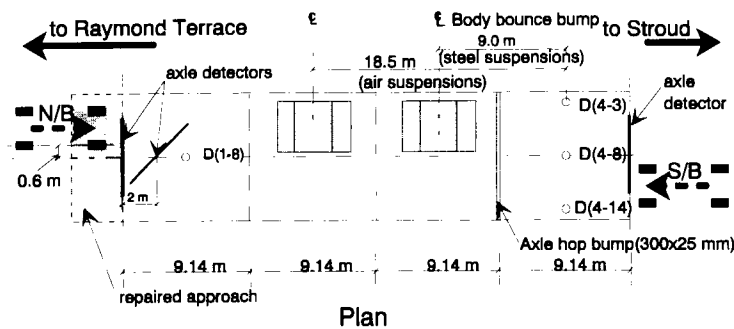
Bridge	Spans (m)	Skew	Mass of span (t)	Stiffness (kN/mm)	Natural frequency (Hz)	Damping coefficient ( $\zeta$ )	Logarithmic decrement ( $\delta$ )
Yarriambiack Creek	3@8.2 Reinforced Concrete	32 deg	85	110	14.1	2.4% (high)	0.15
Cameron's Creek	4@9.14 P/S Concrete	square	110	165	11.3	1.5% (average)	0.509
Cromarty Creek	7.62/9.14/7.62 Timber Girder	25 deg	25	18	8.6 to 9.4	2.6% (high)	0.15



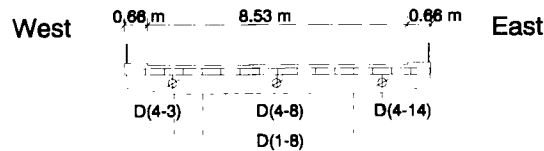
Plan



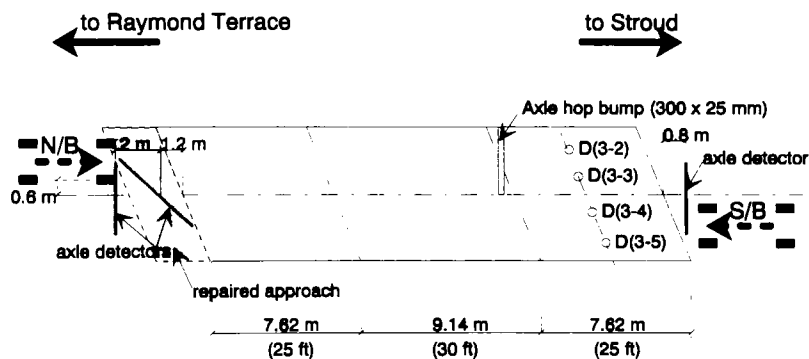
Section



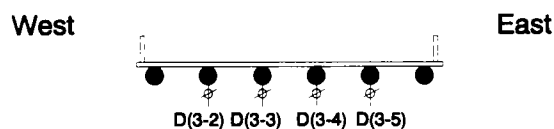
Plan



Section



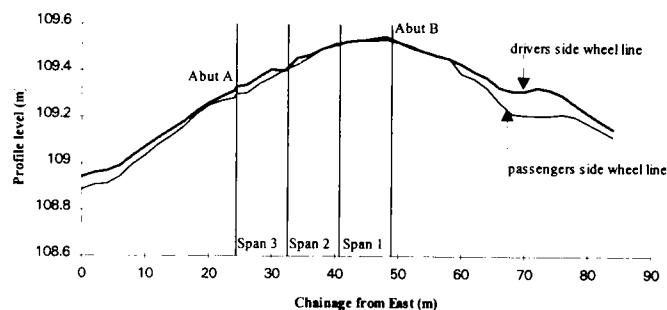
Plan



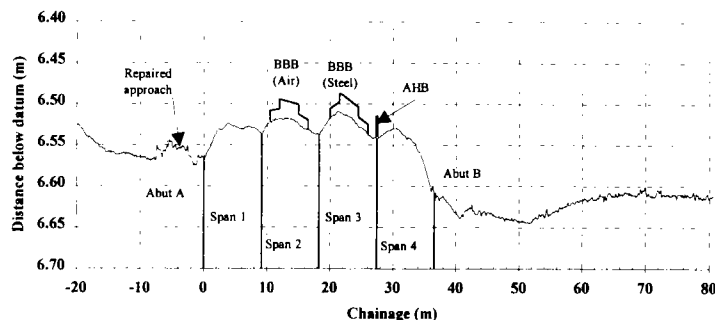
Section

FIGURE 1 Details of test bridges: (a) Yarriambiack Creek bridge, (b) Cameron's Creek bridge, (c) Cromarty Creek bridge.

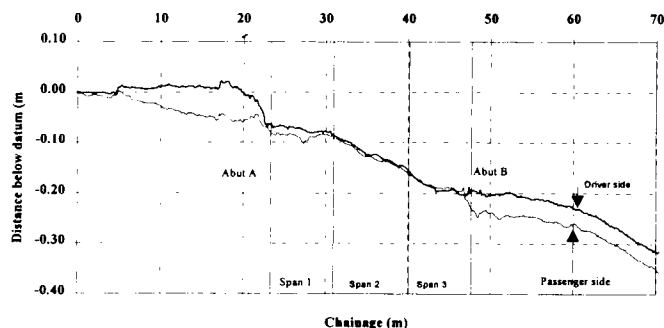




(a) Yarriambiack Creek - Road profile.



(b) Cameron's Creek - Road profile - northbound.



(c) Cromarty Creek Bridge - Road profile - northbound.

FIGURE 2 Road profiles over test bridges.

which proved to be an important factor in the dynamic bridge/vehicle interaction.

The prestressed concrete bridge over Cameron's Creek was designed before partial prestressing was accepted practice. Consequently each span exhibits an upward deflection due to creep (also known as a hog) of approximately 20 mm. Some settlement of the abutments is also evident.

Two bumps were designed to generate axle hop and body bounce behavior. These became known as the axle hop bump (AHB),  $300 \times 25$  mm, and the body bounce bump (BBB),  $6000 \times 24$  mm. Their profiles were added to the longitudinal profile for Cameron's Creek [see Figure 2(b)]. The BBB was positioned approximately one wavelength of body bounce before the center of the instrumented span 3 of Cameron's Creek for vehicles

traveling at 80 km/hr. Since the body bounce frequencies for steel- and air-suspended vehicles are different, the BBB was placed in different positions for the air and steel suspensions. The body bounce wavelength for the steel suspension is approximately one span, whereas for the air suspension it is approximately two spans. This was conceived for flat bridges, but the hogs in Cameron's Creek complicated the profile and thus reduced the value of the BBB in terms of direct comparisons between the steel and the air suspensions.

## TEST VEHICLES

Six-axle articulated gravel trucks were used in the test program. They were loaded to their 42.5-ton legal limit

(steer = 6 tons; tandem = 16.5 tons; tridem = 20 tons). Steel or air suspensions were fitted throughout in order to facilitate a direct comparison of the bridge response to vehicles fitted with air and those fitted with conventional mechanical steel suspension. A description of the prime movers and the suspensions is presented in Table 2.

The suspensions were characterized using the European Community drop test, which defines a road-friendly suspension as one with a natural frequency less than 2.0 Hz and damping greater than 20 percent. The air-suspended vehicle BA 42.5 1.23 satisfied the requirements for road-friendly suspensions; the mechanical suspensions of vehicle BS 42.5 1.23 did not. Thus the research was able to compare the bridge response for geometrically similar vehicles fitted with either road-friendly or non-road-friendly suspensions.

## BRIDGE RESPONSE

### Instrumentation

Midspan deflections were monitored. The locations of the deflection transducers are shown in Figure 1. For

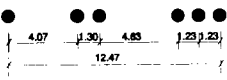
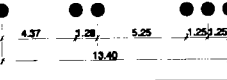
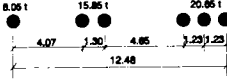
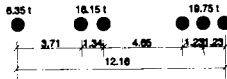
example, at Cromarty Creek, *D*(3-5) refers to the deflection of the fifth girder from the left of the bridge in the third span.

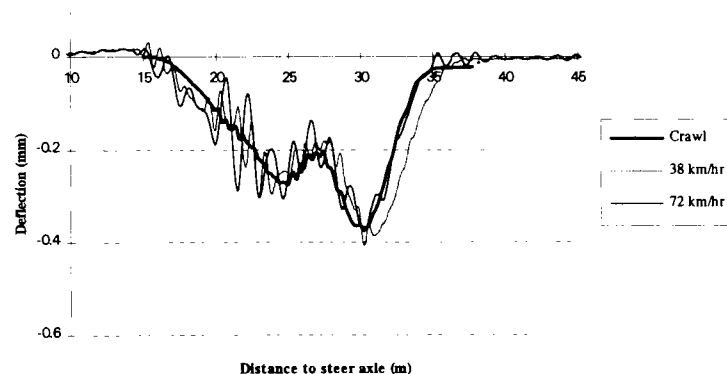
The dynamic deflections of the bridge were measured using an adapted version of the spring and wire system used for many years by EMPA and the Ontario Ministry of Transport (2,4). The system was specifically designed to provide accurate measurements of the dynamic response for frequencies up to the 15 Hz anticipated. The signals were conditioned at the transducer and sampled by a Blastronics data acquisition system after having passed through a 50-Hz low pass filter.

### Time Domain

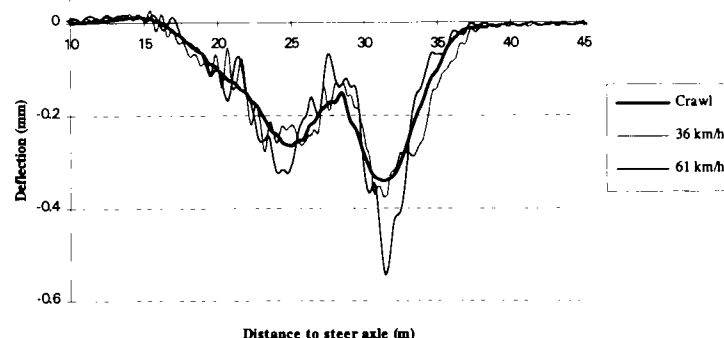
Sample waveforms selected from the hundreds collected are presented in Figures 3, 4, and 5. To facilitate the comparison of multiple waveforms, the time domain responses were converted to the spatial domain. This is achieved by multiplying the elapsed time by the speed of the vehicle. It is clear from Figures 3–5 that speed, roughness, and vehicle suspension are very significant parameters.

TABLE 2 Test Vehicle Suspensions

Prime-mover	Trailer	Gross Laden Mass (t)	Vehicle Code
Freightliner, air suspension	Over the rear axle tri-axle tipper, Evotrac air suspension, 1.23 m spacing 	42.5	FA 42.5 1.23
Mack, Camel back, steel suspension	Over the rear axle tri-axle tipper, York 8 leaf steel suspension, 1.25 m spacing 	42.5	MS 42.5 1.25
Freightliner, air suspension	Over the rear axle tri-axle tipper, BPW air suspension, 1.23 m spacing 	42.5	BA 42.5 1.23
Freightliner, Hendrickson walking beam, steel suspension	Over the rear axle tri-axle tipper, York 8 leaf steel susp'n, 1.23 m spacing 	42.5	BS 42.5 1.23



(a) D(1-4), Truck BA 42.5 1.23, Axle hop bump.



(b) D(1-4), Truck BS 42.5 1.23, Axle hop bump.

FIGURE 3 Yarriambiack Creek: deflection waveforms.

A comparison of the peak deflections showed that the vehicles fitted with air suspensions generally induced deflections at least 10 percent smaller than their steel-suspended counterpart except when axle hop coupled with the bridge. In this case, the peak deflections resulting from air-suspended vehicles were 10 to 20 percent larger than those from the steel-suspended vehicles.

### Dynamic Increment

The dynamic increment ( $DI$ ) has been determined in accordance with the following definition:

$$DI = \frac{(\delta_{\text{dyn}} - \delta_{\text{static}})}{\delta_{\text{static}}} \times 100 \text{ percent} \quad (1)$$

where  $\delta_{\text{dyn}}$  is peak dynamic deflection and  $\delta_{\text{static}}$  is peak static deflection.

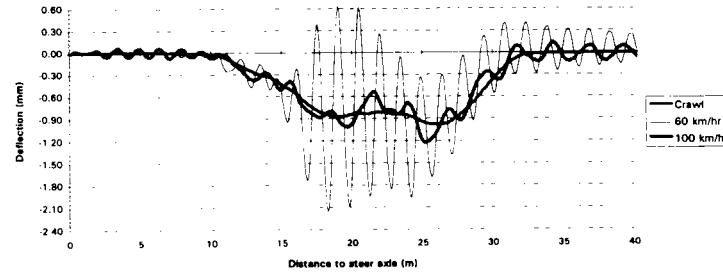
Graphs of  $DI$  versus vehicle velocity are shown in Figures 6, 7, 8, and 9. Positive velocities refer to north-bound traffic and negative velocities correspond to the vehicles traveling south.

Note that the dynamic increment ( $DI$ ) has been calculated only for the deflections that are directly under the zone of influence of the vehicle.

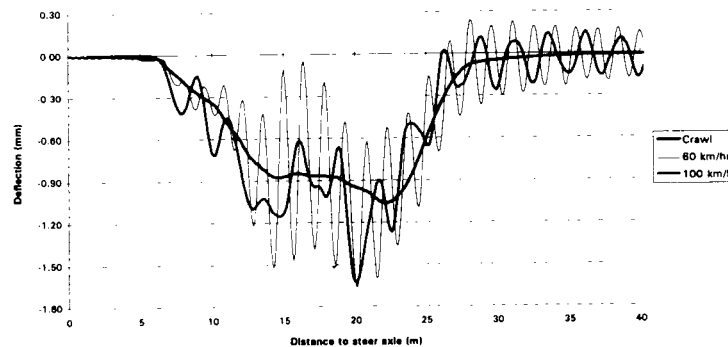
### Discussion

The following observations are made:

1. The dynamic increment ( $DI$ ) is small for speeds less than 40 km/hr.
2.  $DI$ s greater than 50 percent are relatively common.  $DI$ s of 100 percent or more were recorded. The largest  $DI$  recorded was 137 percent for another air-suspended vehicle that was excited by the pavement repair at Cameron's Creek.



(a) D(4-8), Truck BA 42.5 1.23, Axle hop bump.



(b) D(4-8), Truck BS 42.5 1.23, Axle hop bump.

FIGURE 4 Cameron's Creek: deflection waveforms.

3. The relationship between  $DI$  and speed is different for each bridge and each suspension.

4. The  $DI$  from air-suspended vehicles is less than the  $DI$  associated with steel suspensions unless axle hop is excited and coupled dynamically with the bridge. This was strongly evident at Cameron's Creek.

5. The  $DI$  due to steel-suspended vehicles tended to increase with speed.

### BRIDGE DAMAGE ACCUMULATION

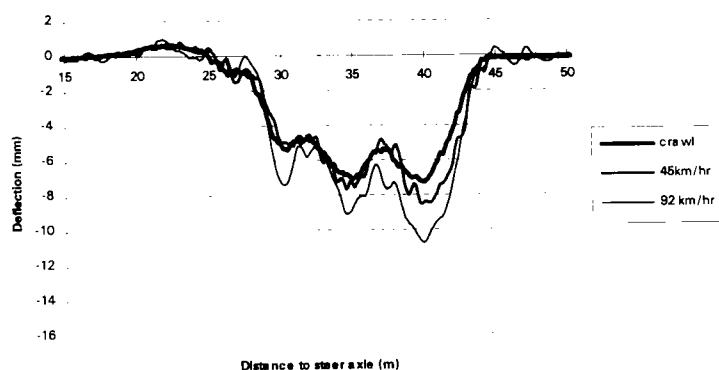
The dynamic coupling between the vehicles fitted with air suspensions and the Cameron's Creek bridge raises questions as to whether comparisons of maximum deflections or stresses are appropriate methods to compare the effects of different vehicle suspensions (see Figure 4).

There seems to be reasonable consensus that the linear Miner's rule is an appropriate model for damage accumulation. Since steel bridges are generally more susceptible to fatigue, a cubic damage accumulation model and a linear Miner's rule were adopted here to provide an approximate comparison of the damage by suspension type and vehicle speed (5-8).

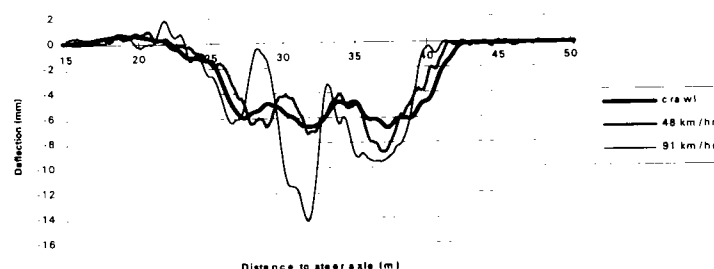
If it is further assumed that the midspan deflections ( $d_{v,il}$ ) are linearly related to stress, the relative total damage induced by a vehicle ( $D_v$ ) can then be compared with that induced by a standard vehicle ( $D_{std}$ ). This comparison can be achieved by using the following equation when the summation is for the  $l$  cycles that occur during the passage of a vehicle:

$$\text{Relative total damage} = \frac{D_v}{D_{std}} \approx \frac{\sum_{i=1}^l d_{v,i}^3}{\sum_{i=1}^l d_{std,i}^3} \quad (2)$$

For the purposes of this study, the standard vehicle was taken as the BS 42.5 1.23 (B series, steel suspension, 42.5 tons and 1.23 m between axles on the tridem) at crawl speed. In this way, the relative damage can be determined for different vehicles and speeds. The endurance limit was assumed to be zero. The number ( $l$ ) and the range of cycles ( $d_{v,i}$ ) while the truck is on the bridge were determined using the rainflow technique (see Figure 10). Using the method detailed above, the



(a) D(3-3), Truck BA 42.5 1.23, No bumps.



(b) D(3-3), Truck BS 42.5 1.23, No bumps.

FIGURE 5 Cromarty Creek: deflection waveforms.

relative damages\* for selected vehicles traveling in a northbound direction are presented in Table 3. When the vehicle fitted with air suspension coupled dynamically with the Cameron's Creek bridge, the damage was approximately six times that for the worst event for a steel-suspended vehicle loaded to 50 tons. Away from these critical speeds, the situation is reversed.

As the damage is speed sensitive, a representative distribution of vehicles and their speeds should be considered before a thorough comparison of accumulated damage can be made. Nevertheless, the strong coupling between this bridge and the vehicles fitted with air suspensions must be understood further and the extent of this coupling for other spans and structural types established.

## VEHICLE RESPONSE

In the tests conducted for Cameron's and Cromarty creek bridges, the triaxle group was instrumented and the dynamic wheel forces measured simultaneously with the bridge response. This was achieved by measuring

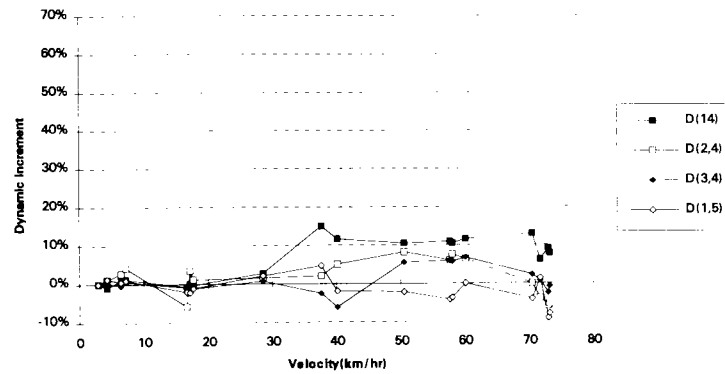
the principal strains induced by the shear in the axle stub and the acceleration of the outboard mass (4).

## Time and Frequency Response

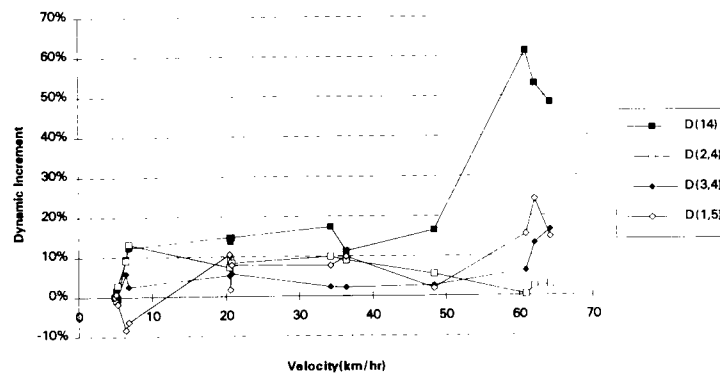
Figure 11 shows the differences between the dynamic wheel forces applied to the bridge by the triaxle group fitted with air or steel suspensions. The dynamic wheel forces applied by the front, central, and rear axles of the tridems are presented along with the total dynamic force applied by the six wheels of the tridem.

The body bounce modes of vibration for the steel suspension exhibit higher frequencies and larger amplitudes than those for the air suspension for these particular waveforms (see Figure 12). This observation is consistent with those at other speeds for soft, highly damped air suspensions versus conventional suspensions. The differences in the frequencies are illustrated in the power spectral densities for individual wheel forces presented in Figure 12.

The power spectral densities highlight the body bounce and axle hop modes. The amplitudes of the axle



(a) Air suspensions - Truck FA 42.5 1.23.



(b) Steel suspensions - Truck MS 42.5 1.25.

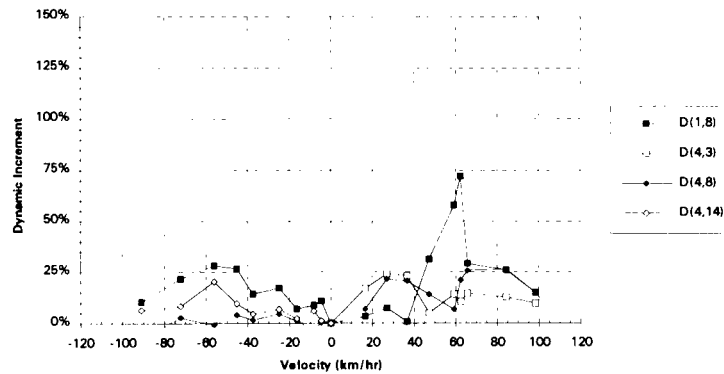
FIGURE 6 Yarriambiack Creek: dynamic increment versus speed, axle hop bump.

hop modes are much smaller than the amplitudes of the dynamic wheel forces associated with the body bounce. However, for short-span bridges with natural frequencies corresponding to those of axle hop, dynamic coupling with these small-amplitude, high-frequency loads can and does occur (Figure 12). Since the frequencies are high, 10 cycles of dynamic load can be applied to a 9-m span bridge during the passage of a tridem at 60 km/hr.

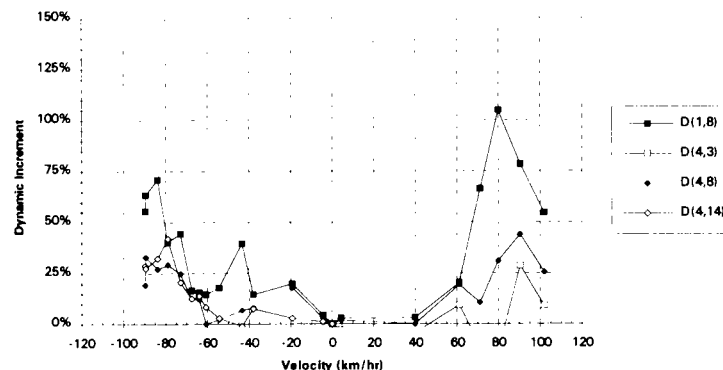
Close inspection of the wheel force waveforms (Figure 11) illustrates the influence of the axle hop bump that was placed between spans 3 and 4. The total force response illustrates that the higher frequencies are very "confused" for the steel suspension, whereas they are evident for the air suspension. Although these differences are relatively subtle, they are important and a consequence of suspension design. The air-bag suspensions are load sharing through pressure equalization. However, under high-frequency dynamic loads, this equalization does not occur. Each axle acts indepen-

dently of the others for dynamic loads. Steel leaf suspensions include a series of rockers that provide the load sharing when the vehicle is stationary but also transmit dynamic forces between axles. Thus when the first axle in a group strikes a bump, a portion of the shock is transmitted to the other axles in a manner that is likely to be out of phase with the first axle. As the axle group continues over the defect, this cross-talk continues, thus diminishing the opportunity for each axle to vibrate independently. A similar argument applies for the steel walking beam suspension fitted to the prime mover.

These differences are further exacerbated by the speed of the vehicle. At a critical speed, the time between each axle's striking an axle hop exciter is equal to the natural period of vibration of each axle. When this occurs, each axle in an air-suspended group vibrates in phase and the effects accumulate. With the steel suspensions used in these tests, the cross-talk diminished this effect. Thus, one would expect speed to be a critical



(a) Air suspensions - BA 42.5 1.23.



(b) Steel suspensions - BS 42.5 1.23.

FIGURE 7 Cameron's Creek: dynamic increment versus speed, no bumps.

issue for air suspensions and that the critical speed ( $v_{crit,ah}$ ) would be approximately the axle hop frequency ( $f_{ah}$ ) times the axle spacing ( $s$ ).

$$v_{crit,ah} \approx s \cdot f_{ah} \quad (3)$$

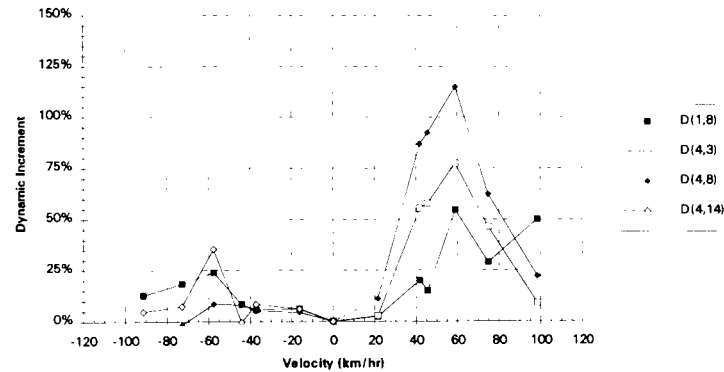
In the case of an axle hop natural frequency of 12 Hz and a spacing of 1.30 m (drive tandem), the critical speed would be  $12 \cdot 1.30 \cdot 3.6 = 56$  km/hr. This is similar to the peak at 60 km/hr evident in the graphs of  $DI$  versus velocity (Figure 8). This response was also observed for another air-suspended test vehicle (4). The peaks associated with the steel suspensions are for higher speeds.

### BRIDGE-VEHICLE INTERACTION

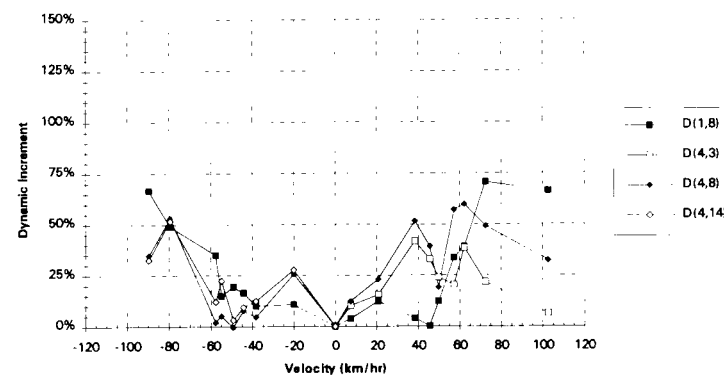
It is informative to consider the forced response of a single-degree-of-freedom system with a natural fre-

quency and damping equivalent to the first flexural mode of vibration measured in the field (see Table 1). The response spectra for the equivalent single-degree-of-freedom systems corresponding to the three bridges are presented in Figure 13. If these are compared with the power spectral densities for the air and steel suspensions (Figure 2), a clearer understanding of the behavior emerges.

The short-span bridge response is influenced by both the axle hop and body bounce modes of the vehicles. For body bounce modes, the frequencies of dynamic wheel forces are typically less than 4 Hz, and any dynamic amplification of the bridge response will be small (see Figure 12). However, for axle hop modes, large dynamic amplification is possible. That is, for the body bounce modes, the magnitude of the bridge response is proportional to the total of the dynamic wheel forces when the axle group is in the critical region of the bridge. As the road-friendly air suspension induced



(a) Air suspensions - BA 42.5 1.23 AHB.



(b) Steel suspensions - BS 42.5 1.23 AHB.

FIGURE 8 Cameron's Creek: dynamic increment versus speed, axle hop bump.

smaller peak dynamic forces, it is expected that the dynamic response induced by the body bounce modes will also be less than those induced by non-road-friendly suspensions. This is consistent with observations. The body bounce forces respond to longer-wavelength ( $\lambda$ ) bumps. The critical speed ( $v_{crit.bb}$ ) is thus dependent on the wavelength ( $\lambda$ ) and the body bounce frequency ( $f_{bb}$ ):

$$v_{crit.bb} \approx \lambda * f_{bb} \quad (4)$$

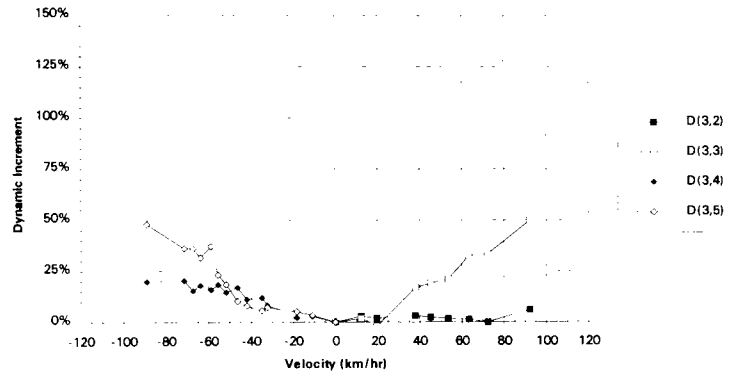
In the case of the bridge over Cameron's Creek that exhibits hogs due to prestress, the critical wavelength is equal to the span length of 9.14 m. Hence for the steel suspension one would expect the critical speed to be of the order of  $9.14 * 3.3 = 30$  m/sec (108 km/hr), whereas for the air suspension  $v_{crit.bb} \approx 1.5 * 9.14 = 14$  m/sec (50 km/hr). Although this is an oversimplification, the maximum dynamic increments for the steel suspension correspond to high speeds (see Figure 2). In the case of the

air suspension, the situation is complicated by the dynamic amplification of the axle hop forces that occurs at similar speeds.

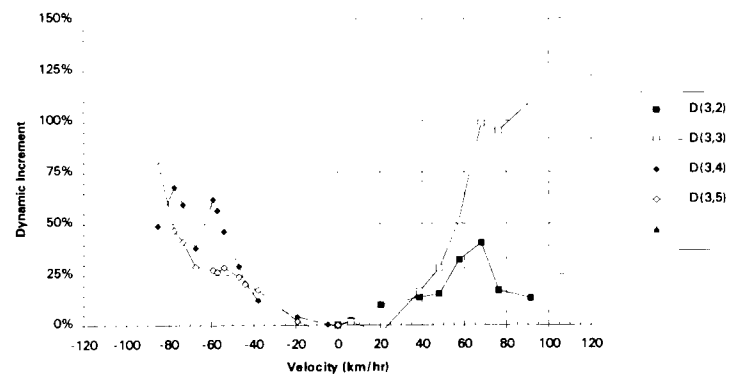
Figure 13 illustrates that for structures with small damping characteristics (such as bridges) the dynamic amplification can be of the order of 20 to 30 should resonance occur. For the range of natural frequencies and damping measured, it is consistent that Cameron's Creek showed the most dynamic coupling with the air suspension at axle hop frequencies. It should be observed that the Cromarty Creek and Yarriambiack Creek bridges are skewed. This immediately puts each wheel of an axle out of phase for a defect such as a poorly aligned deck joint and makes the superstructure mode shapes less sympathetic to resonance with the traveling vehicle.

Hence it is concluded that vehicles fitted with air suspensions will dynamically couple with short span bridges provided that (a) the bridge natural frequency





(a) Air suspensions - BA 42.5 1.23.



(b) Steel suspensions - BS 42.5 1.23.

FIGURE 9 Cromarty Creek: dynamic increment versus speed, no bumps.

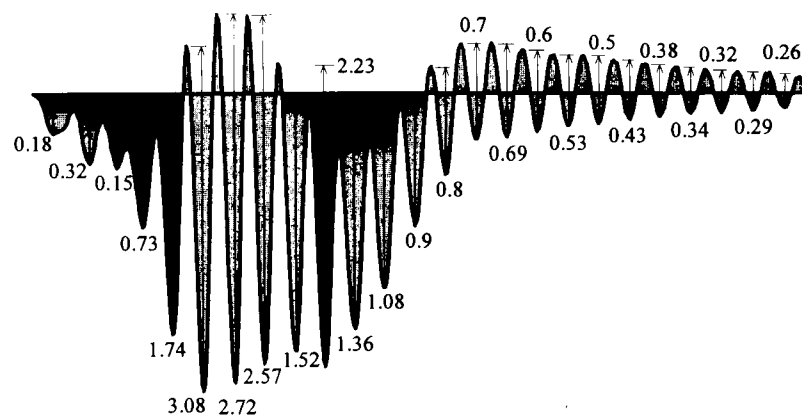
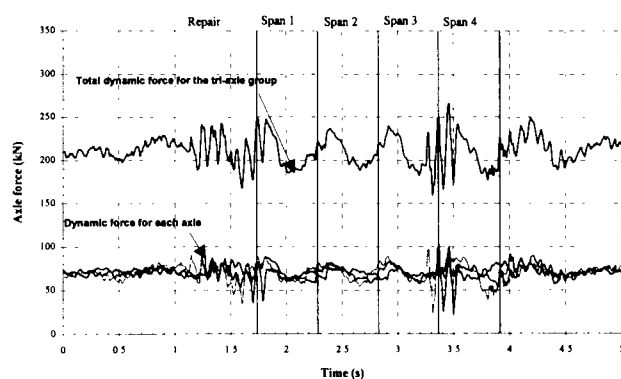


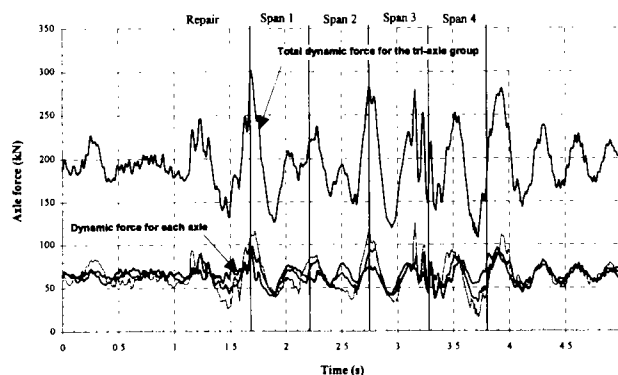
FIGURE 10 Deflection cycles for Cameron's Creek: D(4,8), BS 42.5 1.23 at 59km/hr AHB, northbound.

**TABLE 3 Comparison of Relative Damage Induced in Bridge over Cameron's Creek by Test Vehicles**

Deflection	Vehicle	Speed	Relative Damage
D(1,8)	BS 42.5 1.23	Crawl	1.0
D(1,8)	BS 50.0 1.23	79 km/hr	17.5
D(1,8)	BA 42.5 1.23	Crawl	1.0
D(1,8)	BA 42.5 1.23	60 km/hr	16.5
D(1,8)	BA 42.5 1.23	100 km/hr	4.7
D(4,8)	BS 42.5 1.23	Crawl	1.0
D(4,8)	BS 42.5 1.23 , BBB	81 km/hr	15.1
D(4,8)	BA 42.5 1.23 , AHB	59 km/hr	103

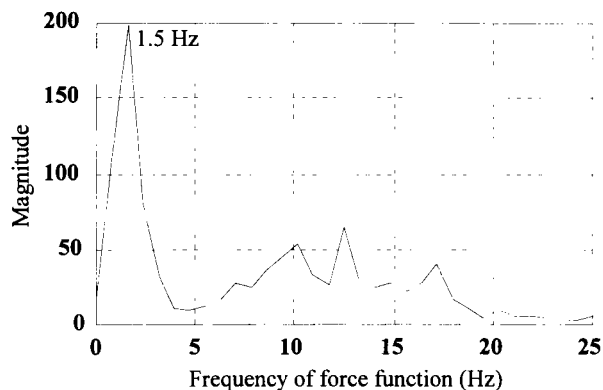


**(a) Air suspensions, 59 km/hr over the axle hop bump (AHB), BA 42.5 1.54.**

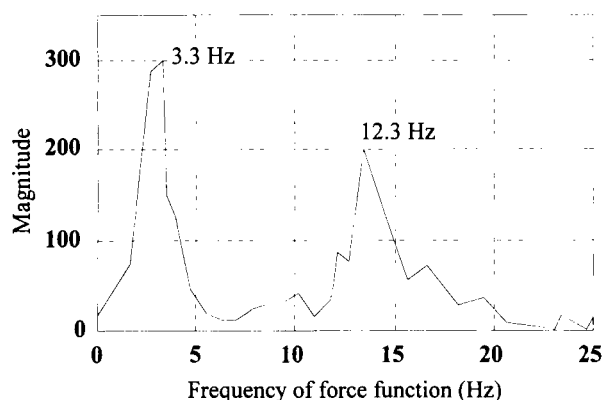


**(b) Steel suspensions, 62 km/hr over the axle hop bump (AHB), BS 42.5 1.23.**

**FIGURE 11 Cameron's Creek: dynamic axle forces for trailer triaxle group.**



(a) Air suspensions, 47 km/hr, Axle hop bump, BA 42.5 1.23.



(b) Steel suspensions, 67 km/hr, Axle hop bump, BS 42.5 1.23.

FIGURE 12 Cameron's Creek: power spectral densities for dynamic wheel force, driver's side center wheel (DC).

is in the range of axle hop frequencies, (b) axle hop is excited by some short-wavelength defect in the road surface, and (c) the vehicle is traveling at a critical speed so that each axle in the group vibrates in phase.

## DISCUSSION OF RESULTS

Canadian and Swiss research has demonstrated increased dynamic amplification for bridges with first flexural frequencies in the range of 2.5 to 4.5 Hz (2,3). Outside of this range the Commentary on the Ontario Highway Bridge Design Code (9) states: "The dynamic response of a component to moving loads results in some additional dynamic load but the frequencies of a longitudinal component with a span less than 22 m are usually sufficiently high that any frequency match between component and vehicle is unlikely." This research has shown that quite severe dynamic coupling can occur

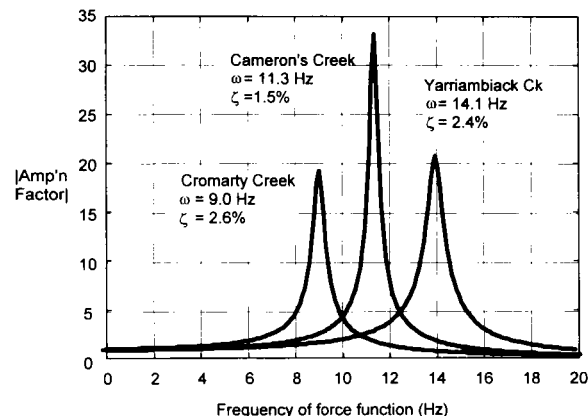


FIGURE 13 Magnification factor versus frequency of force function for single-degree-of-freedom approximation of Cameron's Creek.

for bridges with frequencies in the 10- to 15-Hz range and the new generation of air suspensions.

Analysis of the experimental data shows that a single vehicle registering 100% dynamic increment for the Cameron's Creek bridge induces similar maximum responses as two vehicles plus the AUSTROADS Bridge Design Code (10) dynamic load allowance of 25 percent. Dynamic coupling has also been shown to induce multiple fatigue cycles for the passage of a single vehicle traveling at a critical speed. However, to understand the complete picture, damage should be accumulated over representative speed ranges.

The implications of these findings on bridge design, evaluation, and life prediction must be considered closely. Further testing is necessary to validate the theories presented above and to extend them to the point where recommendations for bridges can be made. Issues associated with multiple presence, speed, and the reduction expected in dynamic increment for grossly overloaded vehicles will reduce the dynamic increment that could be experienced at the strength limit state. However, this is not the case for the fatigue of short span bridges or short span elements within larger structures.

Road-friendly suspensions rely on efficient dampers. These components are subject to wear and must be regularly maintained. A worn damper results in substantial increases in dynamic wheel forces. The consequences for bridges of an air suspension operating with worn dampers has yet to be investigated, but it is expected to be significant.

## CONCLUSIONS

The dynamic responses of three short span bridges to vehicles fitted with air or steel suspensions were mea-

sured experimentally. The air suspensions met the European Community requirements for road-friendly suspensions, whereas the steel suspensions did not. Peak bridge deflections were less for the air-suspended vehicles than for steel-suspended vehicles unless axle hop was excited. When axle hop vibrations were excited, the dynamic response of the bridges was sensitive to vehicle speed and bridge natural frequency. At these critical speeds, multiple fatigue cycles were induced.

The steel-suspended vehicle applied the largest dynamic wheel forces. These forces are associated with truck body bounce modes, which are not amplified by short span bridges.

The maintenance of smooth approaches and profiles across bridges is a very important factor in reducing damage to bridges. This applies to short- and long-wavelength bumps. It has been demonstrated that a cold mix repair to a bridge approach induced axle hop, which coupled dynamically with the bridge.

Road-friendly suspensions are likely to be short span bridge friendly except for those bridges that dynamically couple with axle hop vibrations and provided that suspension dampers are operating efficiently.

#### ACKNOWLEDGMENTS

This research was funded by the Roads and Traffic Authority of New South Wales and Victorian Roads with in-kind contributions from the National Road Transport Commission, Boral Transport (trucks), Transpec Australia (air suspension), BPW Germany (instrumented axles), York Australia (steel suspensions), Hamalex Australia (suspension fabrication), and Mercedes

Benz (video). The contributions of Road User Research, colleagues from OECD DIVINE and QUT, and the Australian Road Research Board are also gratefully acknowledged.

#### REFERENCES

1. Road Transport Research, OECD. *Dynamic Loading of Pavements*. OECD Publications, Paris, 1992.
2. Cantieni, R. I. *Dynamic Behaviour of Highway Bridges Under the Passage of Heavy Load*. EMPA Report No. 220. Dübendorf, 1992.
3. Billing, J. R., and G. Green. *Design Provisions of Dynamic Loading of Highway Bridges*. In *Transportation Research Record 950*, TRB, National Research Council, Washington, D.C., 1984, Vol. 1, pp. 94-102.
4. Heywood, R. J. *Truck Suspensions and the Dynamic Response of the Short Span Bridges over Cameron's Creek and Cromarty Creek*, NSW. Physical Infrastructure Centre Research Report 94-25, 1994.
5. Moses, F., and R. C. Garson. *Probability Theory for Highway Bridge Fatigue Stresses*. Case Western Reserve University, Cleveland, Ohio, 1973, 260 pp.
6. Fisher, J. W. *Fatigue and Fracture in Steel Bridges - Case Studies*. John Wiley & Sons, New York, 1984, 315 pp.
7. British Standards Institution. *Steel, Concrete and Composite Bridges*. BS 5400. London, 1980.
8. Caracostis, C. G. *A Study on the Stress Histories and the Fatigue Life of Highway Bridges*. M.S. thesis. University of Tennessee, 1972, 146 pp.
9. Ministry of Transportation and Communication. *Ontario Highway Bridge Design Code: Commentary*. Highway Engineering Division, Toronto, Canada, 1993.
10. AUSTROADS. *Bridge Design Code*. Sydney, Australia, 1992.

# Analysis and Evaluation of Bridge Behavior Under Static Load Testing Leading to Better Design and Judgment Criteria

---

Munzer Hassan, Olivier Burdet, and Renaud Favre, *Swiss Federal Institute of Technology*

Load testing offers an effective means of investigating the actual behavior of a bridge and detecting a possible abnormal response. A computerized data base of the results of over 200 load tests performed in Switzerland was established to study the behavior of bridges subjected to a load test. This large number of bridges enabled the Institute of Reinforced and Prestressed Concrete of the Swiss Federal Institute of Technology in Lausanne to carry out a comparative statistical study to better understand the behavior of different types of bridges. The main evaluation criteria are the agreement between the measured and calculated deflections and the similarity between the measured and calculated deflected shapes. Although the deflections under loading can be measured precisely, their calculations are difficult because of phenomena usually not taken into account in the design. Statistical analysis of the data base, combined with an analysis of 88 bridges, led to recognition of the contribution to the overall stiffness of nonstructural elements such as reinforced-concrete parapets, asphalt wearing surfaces, and reinforcement. The precise determination of the modulus of elasticity of concrete led to the use of ultrasonic measurements, drilled cores, and molded samples of concrete. The analysis confirmed the correlation between unsatisfactory short-term behavior during the load test and abnormal long-term behavior. Bridges with a low level of prestressing often exhibit unsatisfactory be-

havior, whereas a higher prestressing level seems to prevent abnormal bridge behavior.

Load testing offers an effective means of obtaining a realistic picture of a bridge's response. The results of a load test permit the verification of the serviceability of the bridge and a check on the design calculations. The load test also serves as an essential starting point for monitoring operations. As will be shown, there is a strong correlation between the behavior of the bridge under a load test and its long-term behavior.

The majority of load tests performed in Switzerland are proof tests carried out before the bridge is put in service. Swiss codes recommend a load test for any new bridge with spans exceeding 20 m (1). Since 1973, the Institute of Reinforced and Prestressed Concrete (IBAP) has carried out 210 load tests. The results of these tests, characterizing the static and dynamic behavior of the bridges along with their geometry, were collected in a computerized data base.

Load tests are conducted to determine and quantify the global behavior of a bridge under loading. The load test checks the serviceability of the bridge and identifies

the potential risks of cracking and excessive deflections over the lifetime of the bridge. This is done by studying

- The agreement between the measured and calculated deformations,
- The presence of cracks and how much they open under loading, and
- The magnitude of irreversible or permanent deformations due to the test load.

During the load test, bridges are normally loaded to 80 to 100 percent of the unfactored design load (1.0 DL + 1.0 LL). This level is effective, as it leads to substantial deflections while usually not inducing a large amount of cracking in post-tensioned structures. The proof load on the bridge generally consists of three-axle trucks with an individual weight of 250 kN. The trucks are placed symmetrically with their cumulative center of gravity at midspan (Figure 1). Various other loading patterns are used to test bridge bending, torsion, continuity over the supports, and behavior of side spans. The spans to be tested and the load cases are determined jointly by the testing agency and the design engineer. After the test spans and load cases have been defined, the theoretical deflections are calculated by the engineer before the bridge test.

The measurement techniques used are dependent on the geometry and location of the bridge. The preferred method is to have the deflection gauge at ground level connected to the superstructure by taut wires. Optical and hydrostatic leveling systems are also employed when access to the ground is prevented by the landscape or the traffic under the bridge. To increase the precision of measurements, all loading cases are repeated three times. Temperature changes typically induce deflections that are not negligible, leading to a drift of the position



FIGURE 1 Load test of Daillard bridge in French-speaking Switzerland.

of the unloaded bridge. To improve accuracy, measurements of the unloaded structure are taken about every 15 min after removal of the trucks. These measurements without load are used to correct the reference position and also help track the evolution of the temperature-induced and other permanent deflections of the bridge. For more details on load testing procedure, see the work by Hassan (2) and Markey (3).

## CALCULATION OF DEFLECTIONS

Calculating the exact deflections of a bridge subjected to a load test is not a trivial task. Factors that are often neglected in the design may significantly influence the stiffness of the bridge. An initial evaluation of the data base showed that approximately one out of five bridges (18.5 percent) had measured deflections that exceeded the calculated values by more than 20 percent. This illustrates the complexity of the problem. The two main sources of error in these calculations are uncertainty as to the modulus of elasticity of the concrete and the increase in the moment of inertia caused by nonstructural elements. The level of loading and the amount of prestressing are also important. To achieve reliable results, the following factors need to be considered:

- The actual modulus of elasticity of concrete;
- The effective moment of inertia of the superstructure, including not only the structural members, but also the parapets, asphalt wearing surface, and reinforcement;
- The level of loading during the test and the presence of cracks (state I or state II);
- The level of post-tensioning or prestressing; and
- The method of construction (incremental launching, balanced cantilever method, precast, or cast-in-place).

These points were identified through statistical analysis of the data base and confirmed by a deterministic analysis (2,4–7). Only the main points are presented here.

## Modulus of Elasticity

The modulus of elasticity of concrete should be known precisely for all deflection calculations. The formulas given in national codes usually relate the modulus of elasticity to the compressive strength of concrete, which is rather inaccurate (8). Ideally, the modulus of elasticity of the concrete should be determined on molded samples taken during bridge construction. The value given by the standardized laboratory test has been found to be very reliable and representative of the concrete of an entire bridge. Unfortunately, these results are often un-

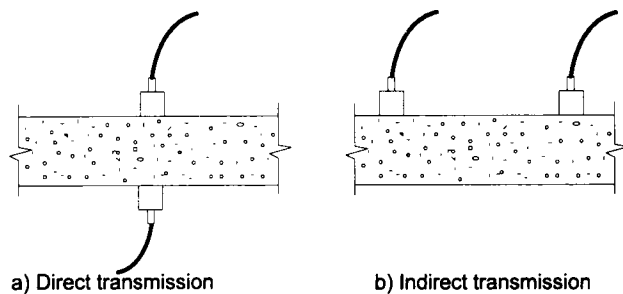


FIGURE 2 Arrangement of transducers for ultrasonic measurements.

available for existing structures. In such cases, ultrasonic measurements offer an efficient method to determine the modulus of elasticity, especially using the direct transmission method (Figure 2).

In the past, this method has often been used to evaluate the compressive strength of concrete. But because there is no physical relationship between the ultrasonic pulse velocity in concrete and concrete strength, this method does not yield accurate results, as illustrated in Figure 3(a), which shows the compressive strength of cores as a function of the measured ultrasonic pulse velocity. However, as Figure 3(b) shows, the dispersion is much smaller for the modulus of elasticity, since there is a direct physical relationship between the speed of sound in a body and the body's modulus of elasticity:

$$E_d = \frac{(1 + \nu)(1 - 2\nu)}{1 - \nu} \gamma v^2 \quad (1)$$

where

$E_d$  = dynamic modulus of elasticity,

$\gamma$  = density of concrete,

$\nu$  = Poisson's ratio, and

$v$  = ultrasonic pulse velocity.

The dynamic modulus of elasticity obtained from the ultrasound pulse velocity can be converted into a static modulus of elasticity. The relationship between the two moduli is empirical and time dependent. Preferably it should be determined experimentally for each geographical area because it depends on the type of aggregate. General formulas giving the modulus of elasticity directly from the ultrasound pulse velocity for all types of concrete and at all times are usually not sufficiently accurate. For the French-speaking part of Switzerland, the following formula (2) gives good results:

$$E_c = kv^2 \quad (2)$$

where

$E_c$  = static modulus of elasticity of concrete (GPa),

$v$  = ultrasonic pulse velocity (km/s), and

$k$  = empirical value ( $k = 1.68$  for  $t \geq 180$  days  
( $t$  in days);  $k = t^{0.1}$  for  $t < 180$  days).

### Effective Moment of Inertia

Analysis of 88 continuous bridges demonstrated significant contributions to the overall stiffness by the parapets, the asphalt wearing surface, and the reinforcement. It

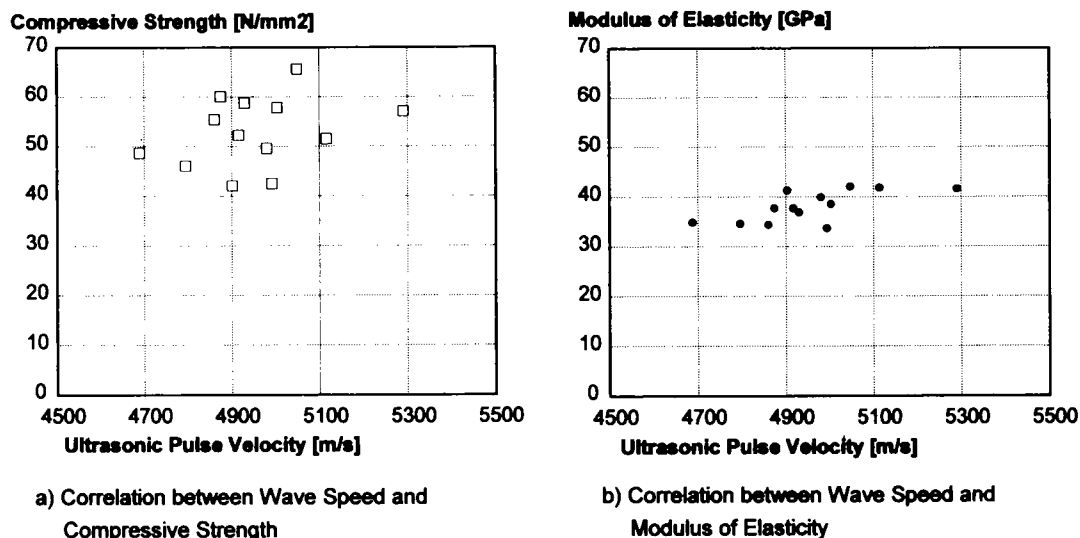


FIGURE 3 Modulus of elasticity and compressive concrete strength versus ultrasonic pulse velocity.

also showed that near the supports, the effective slab width should be taken into account for accurate calculations of deflections.

### Parapets

The contribution of parapets to the overall stiffness of the bridge can be significant, sometimes in excess of 20 percent of the stiffness of the structural concrete. Parapets should therefore be taken into account in calculating the effective moment of inertia of the superstructure. Because of some cracking or microcracking caused by shrinkage, thermal stresses, and external loads, the effectiveness of parapets is slightly lower than if they were designed to be a part of the structural concrete. Also, this study was conducted assuming that the concrete used for the parapets is similar to that used for the structural members. While this is not generally the case, it was considered acceptable because the modulus of elasticity of concrete depends more on the aggregates, which remain the same in a given area, than on the cement paste, which is usually tuned for parapets. The lower effectiveness of the parapets can be accounted for by assigning a lower modulus of elasticity to the parapet concrete. In the positive moment region, the modulus of elasticity of the parapets can be taken as 80 percent of that of the structural concrete. Because the parapets are usually cracked over the supports, the modulus of the parapets should be reduced to 40 percent of the modulus of the structural concrete for a length of 15 percent of the span on either side of the supports, as shown in Figure 4. For smaller parapets, like those supporting metal handrails, the modulus of elasticity needs only to be reduced to 90 percent of its design value over the whole length of the bridge. The metal handrails themselves can be ignored. Some bridges had either partly precast or discontinuous cast-in-place parapets. Overall, the increase in stiffness induced by these parapets is of the same magnitude as if they were monolithically cast and continuous.

### Asphalt Wearing Surface

The asphalt layer increased the moment of inertia of the superstructure by an average of 6 percent for the 88 bridges analyzed. This contribution, which depends on the temperature of the asphalt at the time of the test, can be calculated as shown in Equation 3 (2), which is valid for the type of asphalt used in the French-speaking Switzerland:

$$E_{\text{asphalt}} = 22 - 0.7T \quad (3)$$

where  $E_{\text{asphalt}}$  is the modulus of elasticity of the asphalt wearing surface (GPa) and  $T$  is temperature ( $^{\circ}\text{C}$ ).

Figure 5 shows the average increase of inertia of the superstructure produced by 100 mm of asphaltic wearing surface as a function of temperature for 88 bridges of different cross sections. This thickness is typical of current applications in Switzerland.

### Reinforcement

The reinforcing steel increases the moment of inertia of the superstructure and should be taken into account in calculating the stiffness (transformed section). This increase varies between 2 and 4 percent depending on the type of cross section and the reinforcement ratio.

Grouted post-tensioning cables also increase the moment of inertia slightly, usually by about 2 to 3 percent. For more accurate calculations, the increase of inertia due to the post-tensioning steel can be expressed for box-girder bridges and multigirder bridges as a function of the load balancing level (defined as the fraction of the dead load that is balanced by post-tensioning (3,9) and the span-to-depth ratio of the superstructure as in the following equation (2):

$$\text{Increase of moment of inertia [\%]} = 0.17\beta\lambda \quad (4)$$

where

$\beta = u/g$  = level of load balancing,

$u$  = deviation force (balancing force) due to cable curvature,

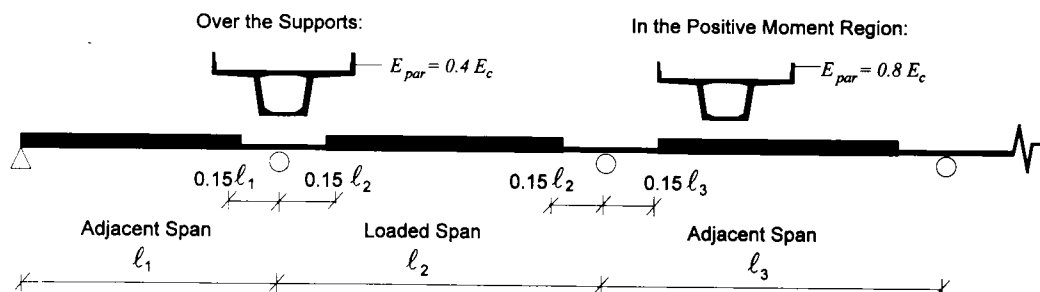


FIGURE 4 Proposed model for taking parapets into account in deflection calculations.



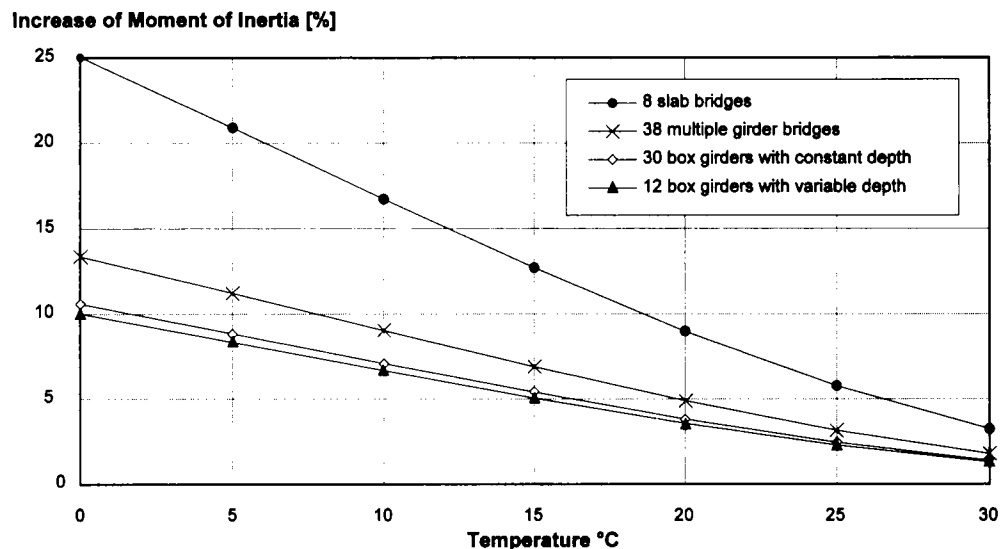


FIGURE 5 Increase in moment of inertia due to 100 mm of asphalt as a function of temperature for 88 bridges of different types.

$g$  = dead weight of the superstructure, and  
 $\lambda = \ell/h$  = span-to-depth ratio of the structure.

The increase of the moment of inertia of slab bridges due to post-tensioning cables is almost negligible (between 0.5 and 1 percent).

### Effective Slab Width

The effective slab width should be used to calculate the effective moment of inertia of the superstructure. It has been shown that the total width of the slab can be taken into account in the span under uniformly distributed loads. Over the supports, however, the full width cannot be used to calculate the effective moment of inertia. The moment of inertia of the cross section at the supports may be reduced by as much as 20 percent because of the effective slab width.

## INTERPRETATION OF RESULTS

The interpretation of the results of a load test is based on the comparison between the measured and calculated deflections, on the similarity between the measured and calculated deflected shapes, and on the presence of cracks or permanent deformations.

The above approach to calculating the deflections results in improved agreement between the measured and calculated deflections. The remaining differences are caused by cracking because of either a high level of loading during the test or a low level of post-tensioning. Bridges with load test deflections higher than those pre-

dicted by calculations typically showed an increase of cracking over time and, in some cases, excessive deflections.

The long-term monitoring of these bridges, along with the detailed analysis below, led to the definition of thresholds beyond which the bridge should be kept under surveillance and inspected more frequently. The proposed thresholds concern two parameters; the first is the difference between the measured and calculated deflection at mid-loaded span, and the second is the lack of similarity, defined as the difference between the ratio of measured to calculated deflections in the loaded span and that in the adjacent spans.

### Alarm Threshold of Deflections Divergence

Three limits have been established as thresholds defining satisfactory behavior; they are shown in Figure 6.

### Tolerance Threshold

Bridges with a ratio  $R$  of measured to calculated deflections exceeding 1.10 are likely to be cracked. These bridges should be examined in more detail by verifying the calculation model and the value of the modulus of elasticity. The tensile stresses should be calculated to check the presence of cracking and a detailed inspection of the bridge should follow. If cracking is observed, the bridge should be inspected more frequently, with special attention paid to the evolution of this cracking. Because of the accuracy of the measurements, the tolerance

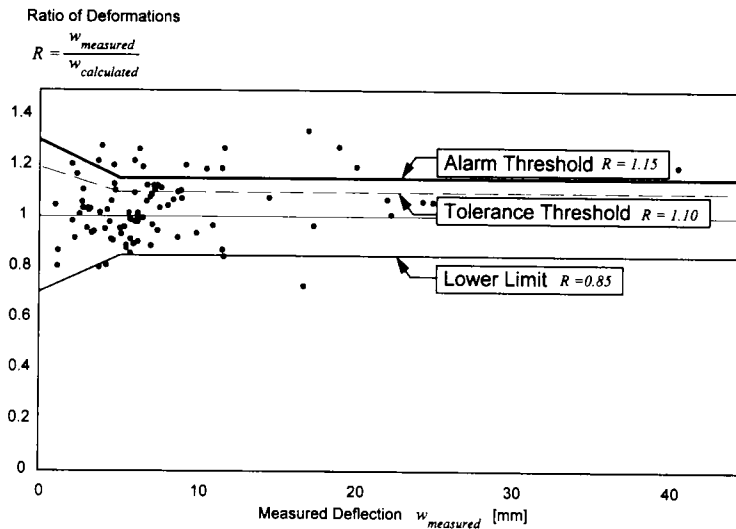


FIGURE 6 Thresholds of tolerance, alarm, and lower limit of ratio of measured to calculated deflections.

threshold for bridges presenting deflections smaller than 5 mm is less severe.

#### **Alarm Threshold**

A ratio of measured to calculated deflections exceeding 1.15 is the signal of cracking that can affect the durability of the bridge. This limit constitutes the alarm threshold for bridge authorities to keep a close eye on the bridge behavior.

#### **Lower Limit**

A measured deflection smaller than the calculated value means that the stiffness is underestimated or that fixities have been neglected in the computational model, which can heavily load some parts of the bridges. To prevent such cases, a lower limit is set at 0.85 for the ratio of measured to calculated deflections, with more tolerance for bridges that have measured deflections less than 5 mm.

#### **Alarm Threshold of Deflections Similarity**

In similar fashion, three limits for the lack of similarity ( $R - R_{adj}$ ), where  $R_{adj}$  is the ratio of measured to calculated deflections in the span adjacent to the loaded span (average of the right and left span for intermediate spans), have been defined as thresholds for satisfactory behavior, as shown in Figure 7.

#### **Tolerance Threshold**

The tolerance threshold for the lack of similarity has been set at 0.10. For bridges exceeding this threshold,

special attention should be paid to checking the presence of cracks. The tolerance threshold for bridges presenting measured deflections smaller than 10 mm is less severe.

#### **Alarm Threshold**

An ( $R - R_{adj}$ ) exceeding 0.15 constitutes the alarm threshold for bridge authorities to increase the frequency of inspection of the bridge. The alarm threshold is less severe for bridges with measured deflections less than 10 mm.

#### **Lower Limit**

A negative ( $R - R_{adj}$ ) should not be less than  $-0.10$ . Such a negative value for the lack of similarity typically results from an inappropriate calculation model. For bridges having measured deflections less than 10 mm, the lower limit is less severe.

#### **Application of Criteria**

The application of criteria led to the establishment of a list of bridges from the data base that need to be more frequently inspected. Eighteen of these bridges violating either of the alarm thresholds are shown in Figure 8. Observations of these bridges showed the presence of cracking. While bridges built by incremental launching showed an irregular pattern of cracking and micro-cracking, cast-in-place bridges showed serious cracking and one of them is currently being investigated for possible reinforcement because of cracking and excessive

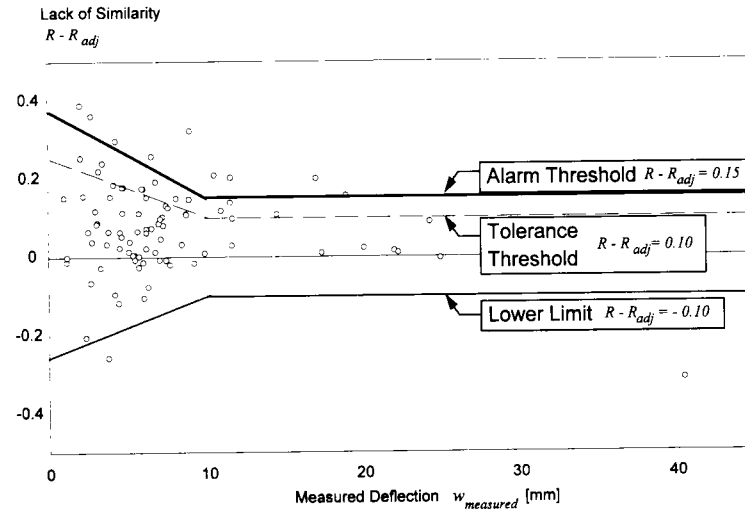


FIGURE 7 Thresholds of tolerance, alarm, and lower limit of lack of similarity.

deformation. This shows that there is a correlation between the short-term behavior and the durability of the structure. Thus, information gathered during the load test can be used for early detection of potential disorders in bridges.

### RECOMMENDED LEVEL OF POST-TENSIONING

A more detailed analysis of 20 bridges showed that the level of post-tensioning plays a prime role in the behavior of the bridge. The variable chosen to characterize the amount of post-tensioning used in a bridge is the level of load balancing, defined as the ratio of the balancing loads induced by the curvature of the tendons (9) to the dead weight of the superstructure. The recommended level of load balancing can be expressed as a function of the performance requirements, which de-

pend on the importance of the bridge and its service conditions. Three broad categories are proposed below.

The high requirement level is recommended when practically no cracking is allowed under the code service loads. This requirement applies to bridges that are important, highly loaded, or in aggressive conditions. In these cases, a load balancing level of 90 percent of permanent loads is necessary to achieve a satisfactory behavior.

The normal requirement level applies to bridges for which limited cracking may be accepted, but should in no case affect the bridge durability. In this case, a load balancing level of 80 percent is recommended.

For bridges with lower loads, of less importance, and in favorable conditions, a low requirement level can be accepted. In these bridges a load balancing level of 70 percent is sufficient. Cracking under service loads will not be prevented but its evolution should remain limited.

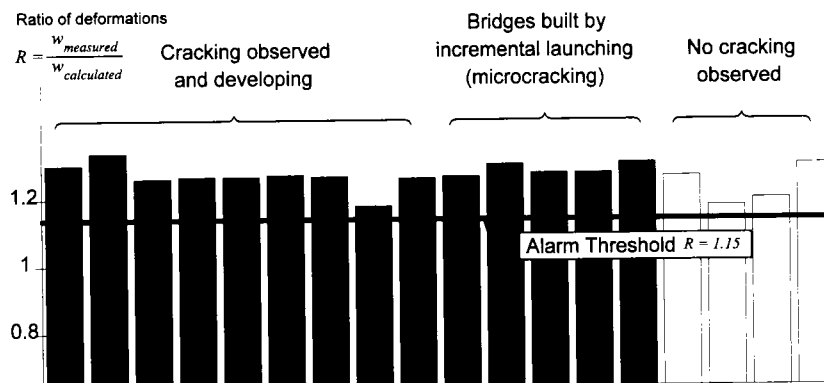


FIGURE 8 Observations on 18 bridges exceeding alarm threshold.

In special cases, a load balancing level of 60 percent or less can be sufficient. Such cases should be appreciated by the owner and the bridge designer. Typical examples are bridges with spans not exceeding 200 m, massive slab bridges, bridges with straight post-tensioning cables, and lightly loaded bridges located in mild environments.

## CONCLUSIONS

Load testing of bridges is an efficient means to obtain qualitative and quantitative information on the actual behavior of the structure; this type of information has also been collected for the dynamic properties of bridges (10). An acceptance load test, performed on a new or recently renovated structure (11), is a necessary reference point for the start of the maintenance of the structure. The methodology proposed above should produce an adequate load test and a proper evaluation of its results.

The importance of elements usually not considered in the design has been shown, since reinforced-concrete parapets or an asphalt wearing surface will contribute to the stiffness of the bridge during the load test. The concrete's modulus of elasticity should be measured on molded samples, on drilled cores, or by ultrasonic measurements. This last method is very cost-effective provided a proper calibration has been made to account for local aggregates.

The thresholds presented above define the acceptable behavior of a bridge under a load test. If these thresholds are exceeded, more attention should be paid to the bridge. A correlation is evident between passing the thresholds and abnormal long-term behavior. As such, a load test not only yields information about the current condition of the structure, but also gives some insight into its future performance. This is a precious tool for maintenance operations, as the more critical structures can be identified at a very early stage.

An adequate level of post-tensioning (or prestressing) has been shown to be instrumental in ensuring proper behavior. A level of load balancing ranging from 70 to

90 percent of the dead weight should ensure proper behavior, depending on the performance requirements.

## REFERENCES

1. SIA 169 (Recommendation). *Maintenance des Ouvrages de Génie Civil*. Société Suisse des Ingénieurs et des Architectes, Zürich, Suisse, 1987.
2. Hassan, M. *Critères pour l'évaluation des ponts en béton et pour le choix de la précontrainte*. Thèse de doctorat. EPFL, Lausanne, 1994.
3. Markey, I. F. *Enseignements Tirés d'Observations des Déformations de Ponts en Béton et d'Analyses Non Linéaires*. Thèse de doctorat N° 1194. EPFL, Lausanne, 1993.
4. Favre, R., M. Hassan and I. Markey. Bridge Behaviour Drawn from Load Tests. In *Proc., Third International Workshop on Bridge Rehabilitation*, Darmstadt, Allemagne, June 1992, pp. 245–257.
5. Hassan M., O. Burdet and R. Favre. Interpretation of 200 Load Tests of Swiss Bridges. In *IABSE Colloquium: Remaining Structural Capacity*, Copenhagen, Denmark, Vol. 67, 1993, pp. 319–326.
6. Hassan, M., O. Burdet and R. Favre. Combination of Ultrasonic Measurements and Load Tests in Bridge Evaluation. Presented at 5th International Conference on Structural Faults and Repair, Edinburgh, Scotland, UK, June, 1993.
7. Favre, R., M. Hassan and O. Burdet. Statistical Data Combined with Linear and Non-Linear Analysis to Interpret Bridge Load Tests. In *Developments in Short and Medium Span Bridge Engineering '94* (A. Mufti et al., eds.), pp. 1197–1208, Halifax, Canada, August 1994.
8. Baalbaki W., P-V. Aïtcin and G. Ballivy. On Predicting Modulus of Elasticity in High-Strength Concrete, *ACI Materials Journal*, Vol. 89, No. 5, 1992, pp. 517–520.
9. Lin, T. Y., and N. Burns. *Design of Prestressed Concrete Structures*, 3rd ed, John Wiley & Sons, New York, 1981.
10. Burdet, O., and S. Corthay. Static and Dynamic Load Testing of Swiss Bridges. Presented at International Bridge Conference Warsaw '94, Poland, June 1994.
11. Favre, R., O. Burdet and H. Charif. *Critères pour le Choix d'une Précontrainte: Application au Cas d'un Renforcement*. Colloque International "Gestion des Ouvrages d'Art: Quelle Stratégie pour Maintenir et Adapter le Patrimoine," 1994, pp. 197–208.

# Experimental Verification of Inelastic Design Procedures for Steel Bridges

---

Michael G. Barker and Bryan A. Hartnagel, *University of Missouri, Columbia*

The first of three composite girder tests is presented from a project with the objectives of validating current inelastic design procedures and developing new inelastic provisions for bridges comprising noncompact girders. The first girder test was a half-scale, three-span composite beam with compact sections. The future tests will be two-span composite girders comprising noncompact sections. The essential components of inelastic design provisions are moment-rotation relations at the critical sections. These relations are necessary to predict inelastic rotations, permanent residual deflections, and redistributed moments in the structure. Along with the design and modeling of the half-scale test, experimental moment-rotation behavior characteristics for moving load inelastic tests and a plastic collapse test are presented. Inelastic behavior in terms of design limits and predicting residual deformations is presented on the basis of the experimental results.

**I**nelastic steel bridge design procedures account for the reserve strength inherent in multiple-span steel girder bridges by allowing redistribution of negative pier region elastic moments to adjacent positive moment regions (1,2). The redistribution causes slight inelastic rotation at the interior pier sections, residual moments in the beam, and some permanent residual deflection. After the redistribution, the structure

achieves shakedown (3,4): deformations stabilize and future loads are resisted elastically.

The AASHTO Alternate Load Factor Design (ALFD) (1) method allows inelastic design for bridges comprising compact sections. ALFD is incorporated into the AASHTO Load and Resistance Factor Design (LRFD) Bridge Design Specification (2). Inelastic design procedures allow the designer flexibility and the possibility of more economical designs by eliminating cover plates and flange transitions at negative moment regions (5). Expanding inelastic designer provisions to include noncompact sections is desirable because of the wide use of plate girders with thin webs.

This paper presents results of a 1/2-scale composite girder test. In all, three composite girders, each approximately 30.5 m (100 ft) long, will be tested. Simulated moving loads in the elastic and inelastic range will be cyclically applied to the test girders. Afterward, the girders will be tested to failure in a static collapse configuration. The first test consists of a three-span, compact, rolled section, whereas the other two will be two-span girders with typical noncompact plate girder sections. The project will verify design limit behavior of current inelastic design provisions for compact bridges and extend the inelastic procedures to include noncompact designs.

The specific objectives of this paper are to (a) present the design and modeling of the test girder, (b) illustrate

the inelastic behavior, and (c) develop critical moment-rotation relations for the first test girder.

### INELASTIC DESIGN OF STEEL GIRDER BRIDGES

ALFD inelastic design procedures (1) specify requirements at service load levels (normal traffic), overload levels (occasional heavy vehicle), and maximum load levels (one-time maximum vehicle). Inelastic LRFD provisions (2) specify these limits as Service I, Service II, and Strength I, respectively. The LRFD procedures also have a separate fatigue limit loading. Following are the LRFD load levels at the respective limits:

$$\text{Fatigue} = D + 0.75L(1 + I), \quad (1a)$$

$$\text{Service I} = D + 1.00L(1 + I), \quad (1b)$$

$$\text{Service II} = D + 1.30L(1 + I), \text{ and} \quad (1c)$$

$$\text{Strength I} = 1.25DC + 1.50DW + 1.75L(1 + I) \quad (1d)$$

where

$D$  = dead load,

$L$  = live load with lateral distribution factor,

$I$  = impact factor (33 percent),

$DC$  = component dead load (slab, beam, and barrier curbs), and

$DW$  = wearing surface.

Fatigue and Service I limits are for fatigue and deflection checks. For inelastic design at the Service II limit state, after interior pier elastic moments are redistributed to adjacent positive moment regions, the design requirement is a limited stress at positive moment regions. At the Strength I level, a mechanism must not form with the application of the factored loads.

### PROTOTYPE BRIDGE DESIGN

The three-span two-lane prototype bridge ( $18.3 \times 23.2 \times 18.3$  m) ( $60 \times 76 \times 60$  ft) was designed according to the fourth draft of the LRFD bridge design specifications using the inelastic design provisions (2). Four  $W30 \times 108$  rolled beam girders with 25.4-mm (1-in.) headed studs at a nominal spacing of 305 mm (12 in.) were selected. A girder spacing of 3.05 m (10 ft) was used to support the roadway that was 11.0 m (36 ft) wide. Yield strength of the steel was 345 MPa (50 ksi). The deck was 203 mm (8 in.) thick with 27.6 MPa (4,000 psi) compressive strength concrete and Grade 60 reinforcing steel. A future wearing surface of 0.57 kN/m<sup>2</sup> (12 psf) [about 25 mm (1 in.) of asphalt] and a barrier rail weighing 4.45 kN/m (305 plf) [a standard 406 mm (16 in.) concrete barrier curb] were considered as composite dead load. The bridge was designed assuming unshored construction. Also, the LRFD HS20 design vehicle and a lane load of 9.34 kN/m (64 plf) was used for determining live load effects. The  $\frac{1}{2}$ -scale experimental test girder models an interior girder from the bridge system. Following is a brief description of the Service II and Strength I limit design procedures (6).

### ELASTIC ANALYSIS TECHNIQUES

A prismatic elastic analysis was used to compute the noncomposite dead load moments, and elastic nonprismatic analyses were used to determine the composite dead load moments and the live load plus impact moment envelopes. LRFD lateral distribution factors were used to approximate the amount of live load applied to a single girder. Figure 1 shows the total live and dead load moment envelopes for the prototype girder including impact and distribution factors.

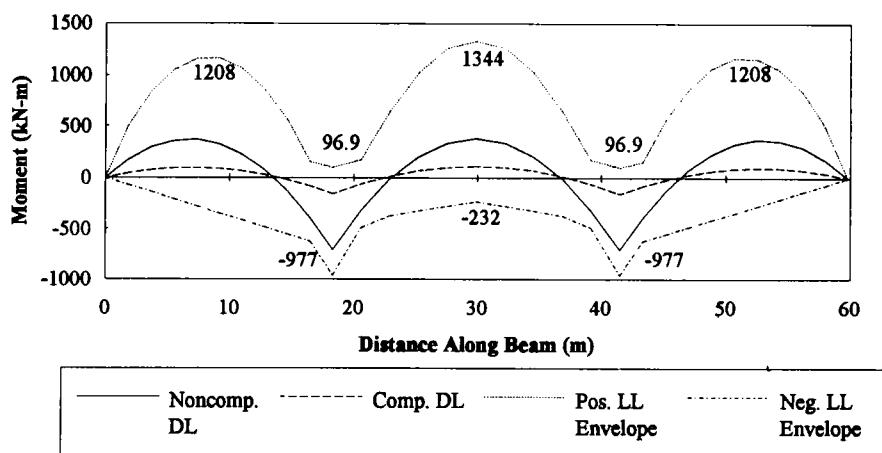


FIGURE 1 Prototype girder moment envelopes.

## DESIGN LIMIT STATES

### Service II Limit State

The Service II check ensures that occasional overload vehicles equal to  $1.30L(1 + I)$  will not cause excessive deformations. Elastic overload moments at the piers are shifted through residual moments,  $M_R$ , that occur at the pier because of inelastic pier rotations,  $\theta_P$ . The residual moment is the difference between the elastic moment and the actual moment at the pier section. Due to inelastic action, the girder develops a residual moment field (self-equilibrating) that is locked in the structure and adds to other applied moments. The pier sections resist bending according to the following relationship (2).

$$M = M_P[0.7 - 60.0(\theta_P)] \leq 1.0 \quad (2)$$

where  $-0.008 \leq \theta_P \leq 0$  radians,

$M$  = actual moment in accordance with continuity and moment-rotation behavior,

$\theta_P$  = plastic rotation at pier in radians (negative), and

$M_P$  = section plastic moment capacity.

For this design, residual moments were related to the pier rotation by an inelastic conjugate beam analysis developed by Dishongh (7). The moments at the piers caused by inelastic rotations at the piers,  $M_a$  and  $M_b$ , and the residual moment,  $M_R$ , are

$$M_a = \frac{\frac{EI\theta_P}{L}}{\left[ \frac{-A}{3} - \frac{1}{2} + \frac{\frac{B}{6} + \frac{1}{4}}{B + 1} \right]} \quad (3a)$$

$$M_b = \frac{-M_a}{2B + 2} \quad (3b)$$

$$M_R = M_a + M_b \quad (3c)$$

where  $A$  and  $B$  are ratios of the two outer-span lengths to the center-span length  $18.3/23.2 = 0.79$ .

At the pier section, the applied Service II moment,  $[D + 1.30L(1 + I)]$  (Equation 1c), plus the residual moment (Equation 3c) is equal to the actual moment defined by the moment rotation relation (Equation 2) for composite pier sections:

$$[D + 1.30 L(1 + I)] + M_R = M_P[0.7 - 60(\theta_P)] \quad (4)$$

Solving Equation 4 for the plastic rotation at the pier section yields  $\theta_P = -0.00083$  radians. The residual moment was found as  $M_R = 46$  kN-m (34 kip-ft) at the two-pier sections and throughout the middle span. The residual moment field is symmetric because of the symmetric bridge design.

For the Service II criteria, center-span, centerline stresses were found to be maximum. LRFD states that the applied stresses must be less than or equal to 0.95 of the flange yield stress,  $F_y$ , for composite, homogeneous sections in positive bending. The maximum Service II stress is determined by superposition of stresses where the live load moment stress component is equal to the elastic moment plus the redistributed residual moment. The total stress was calculated as 330 MPa (47.9 ksi), which is approximately equal to the requirement of  $0.95 F_y = 327$  MPa (47.5 ksi).

### Strength I Limit State

To satisfy the ultimate strength requirement, a plastic collapse mechanism must not form with the application of Strength I factored loads. LRFD inelastic provisions use an effective plastic moment,  $M_{PE}$ , at the negative moment pier hinge sections. The effective plastic moment accounts for moment unloading at large inelastic rotations. The mechanism check was carried out by applying the factored dead loads  $[1.25DC + 1.50DW]$ , moving the factored design truck  $[1.75L(1 + I)]$  over the entire beam in tenth-point increments, and calculating the plastic collapse load factors for all truck positions (5). The critical mechanism, using  $M_{PE}$  at the pier sections, was the maximum positive center span loading configuration. The plastic collapse load factor was found to be 1.38: the structure can withstand 38 percent more factored live loads than caused by the Strength I factored design live loads. Thus, Strength I requirements did not control the design.

### TEST GIRDER MODEL

Structural modeling techniques were employed to determine the theoretical scale factors,  $S$ , for the  $1/2$ -scale fundamental measures of interest. Steel and concrete properties for the prototype and the model were identical; therefore, the independent variables were chosen as elastic modulus,  $E$  ( $S_E = 1$ ), and length,  $L$  ( $S_L = 2$ ). The three-span test girder ( $18.3 \times 23.3 \times 18.3$  m) ( $30 \times 38 \times 30$  ft) was modeled to obtain near-equal width-thickness ratios and stresses. A W14  $\times$  26 rolled shape with headed studs 12.7 mm ( $1/2$  in.) at a nominal spacing of 152 mm (6 in.) was selected. The deck was 102 mm (4 in.) thick and 1.3 m (50.5 in.) wide with No. 3 rebar

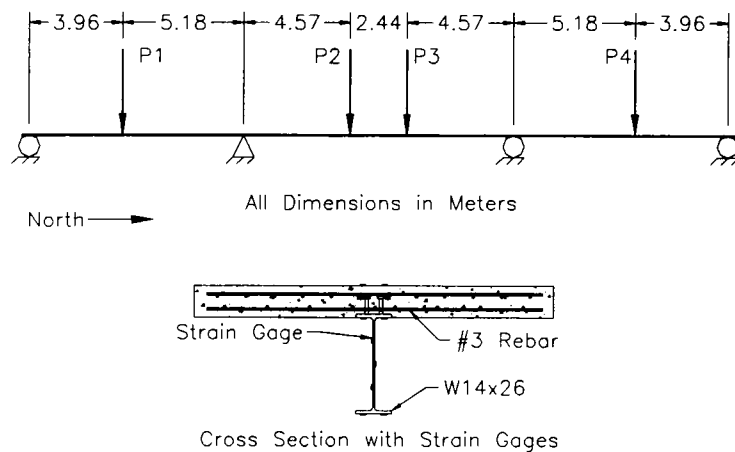


FIGURE 2 Model beam load locations and cross section.

in two layers in each direction. Figure 2 illustrates the test girder configuration.

Loading applied to the model was scaled to simulate equal stresses in the model and the prototype. Although most properties modeled closely, the scale factors for all the section moduli were approximately 8.5 instead of the theoretical 8.0. Therefore, to model equal stresses, all prototype bending moments were factored by  $1/8.5$ .

Compensatory dead load was added to accurately simulate dead load stresses because a half-scale model weighs only one-quarter of the prototype and the proper scale factor is one-half. Ten concrete blocks 8.9 kN (2,000 lb) were hung from the bottom of the W-shape before the concrete deck was placed to compensate for the self-weight lost as a result of scaling. Additional concrete blocks were placed on top of the deck

after it hardened to represent the composite dead loads (wearing surface, guard rails, etc.).

Moving live loads were simulated with four discrete loading points on the test beam, as indicated in Figure 2. Influence lines and linear programming were used to determine the sequence of loads needed to simulate a moving truck. Five individual load stages were developed to represent the moving load sequence. The critical location moments produced by the four discrete loading points are shown in Figure 3 along with the scaled Service I theoretical design truck  $[L(1 + I)]$  moment envelopes. The truck load sequence could be linearly adjusted to represent any percentage of the modeled truck design weight (LL).

Several different measurements were recorded for the test including rotation, deflection, reaction, strain

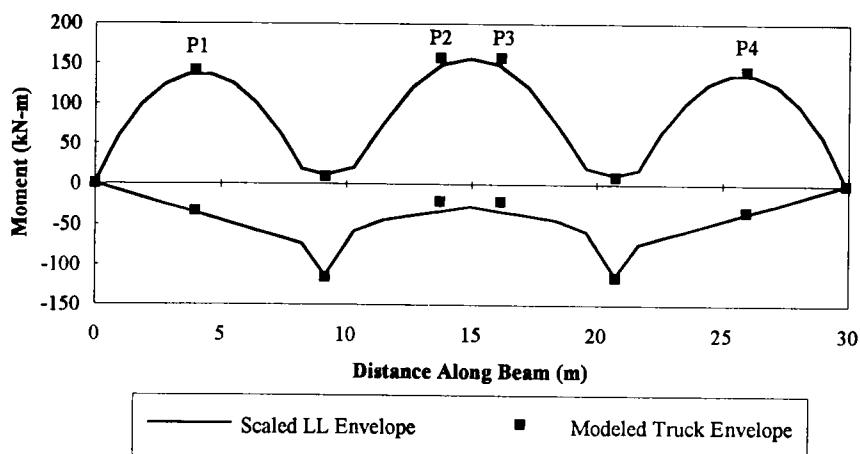


FIGURE 3 Modeled truck moment envelope and scaled prototype moment envelope.



gauge, and deck slip readings. The locations of these measurements are shown in Figure 4.

## TESTING AND DESIGN LIMITS

The modeled live loads were applied to the test beam at various load levels cyclically at slow rates (impact included in static load). The entire loading history of the test is as follows. Elastic low-level tests were carried out at 10, 20, 40, 60, 70, 80, and 90 percent LL where LL is the modeled Service I loading. These provided an opportunity to confirm elastic behavior and instrumentation performance.

Service I level loads (100 percent LL) were applied to validate fatigue (ratioed to 75 percent LL) and deflection requirements of the LRFD provisions. Maximum strains at the fatigue level loading were  $158 \mu\epsilon$ , whereas the LRFD limit is  $200 \mu\epsilon$ . The maximum Service I elastic deflection was 31 mm (1.22 in.), which corresponds to a predicted deflection of 30 mm (1.16 in.). However, there was also a permanent set residual deflection of 3 mm (0.12 in.) at this level because of nonlinear behavior.

Increasing the loads toward the Service II level, loads of 110 and 120 percent LL were applied to examine the behavior in this range of loads. At the Service II level (130 percent LL), the girder experienced significant nonlinear behavior. Design provisions predict this residual deflection and limit stresses in positive moment portions of the structure to  $0.95 F_y$  for composite girders. A maximum strain of  $1450 \mu\epsilon$  occurred at the bridge centerline compared with the allowed strain of  $1638 \mu\epsilon$  for 345 MPa (50 ksi) steel. Therefore, the structure met the Service II limit state criteria. However, at the 130 percent LL level, strain measurements in the negative bending sections were substantially higher than were elastic strains, indicating that some yielding had occurred in accordance with the design provisions. The residual deflection at the bridge centerline was 9.7 mm (0.38 in.) after the 130 percent LL loadings. The design provisions suggest cambering this residual deflection during fabrication.

Cyclic loads were applied at 140, 155, and 166 percent LL to examine the inelastic behavior above the Service II level. The last simulated moving load test was at 175 percent LL plus factored dead loads [ $1.25DC + 1.5DW + 1.75L(1 + I)$ ] (Strength I level). This loading represents the worst possible maximum design load level applied to a bridge. The girder resisted this repeated load three times before some web buckling occurred. The final residual deflection from the moving load tests was 65 mm (2.6 in.).

After the cyclic tests, the girder was tested to failure by monotonically increasing loads proportioned to rep-

resent the theoretical design collapse configuration. This configuration simulated a stationary truck where the center axle of the truck was located at the centerline of the middle span. The additional factored dead load was applied by adding extra simulated loads to the P1 through P4 discrete load locations. Live loads were then applied to P1, P2, and P3 to recreate the prototype mechanism moment diagram. The P1 and P4 loads were set to load control for the duration of the collapse test, whereas the P2 and P3 loads were slowly increased under stroke control until the girder failed by concrete crushing at the bridge centerline. The maximum collapse load was 36 percent above the Strength I design limit. This corresponds to 38 percent excess capacity predicted in the design calculations.

## INELASTIC BEHAVIOR

### Moving Load Tests

Each modeled truck weight percentage loading was repeated until the residual deflections stabilized and the bridge experienced shakedown. Figure 5 shows the permanent set residual deflection at the centerline of the bridge in terms of the percent Service I load level. This shakedown plot shows how the structure suffered increasing permanent set as the live load level increased. The onset of permanent set occurred at 70 percent LL. After the last cycle of loads, the girder had a residual deflection at the centerline of 65 mm (2.6 in.).

Stabilization of residual deflections was obtained with all live load levels except for the factored dead load plus 175 percent LL level (Strength I). Three cycles were carried out at the Strength I load level upon which each cycle resulted in large increases in residual deflection. The cyclic live loading portion of the test concluded at this level because some slight web buckling at the pier sections was detected. At the Strength I load level, the structure may or may not have shaken down. However, it can be concluded that the incremental collapse load, where inelastic deflections continually grow, occurred above the 166 percent LL level.

The moment-inelastic rotation at the negative moment pier section is the determining relation for the inelastic design method. From this behavior, the inelastic rotation, residual moment field, actual moments, and residual deflection are determined.

For the Service II limit, Figure 6 shows the moving load experimental moment-total rotation (elastic + inelastic) and the moment-inelastic rotation for the south pier. Figure 7 shows the same information except with the addition of the plastic collapse test moment-rotation data. Figure 6 includes live load negative moment loadings, whereas Figure 7 includes both dead and live load

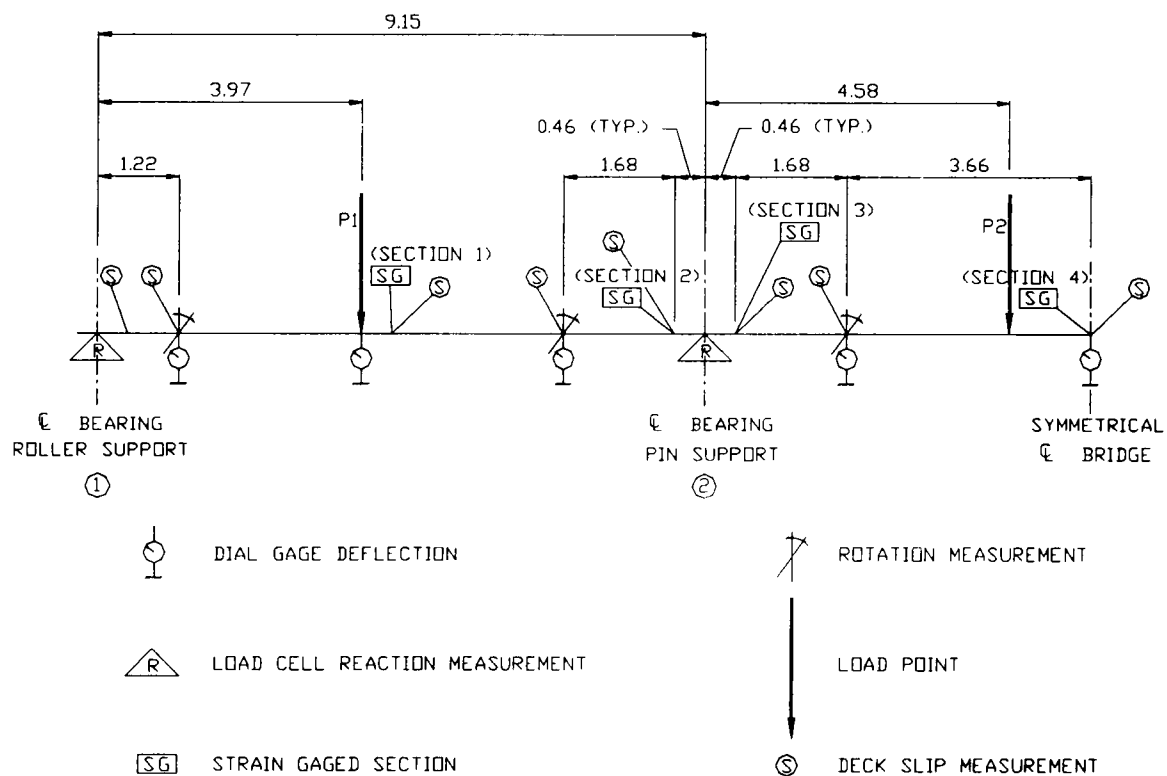


FIGURE 4 Measurement and load locations.

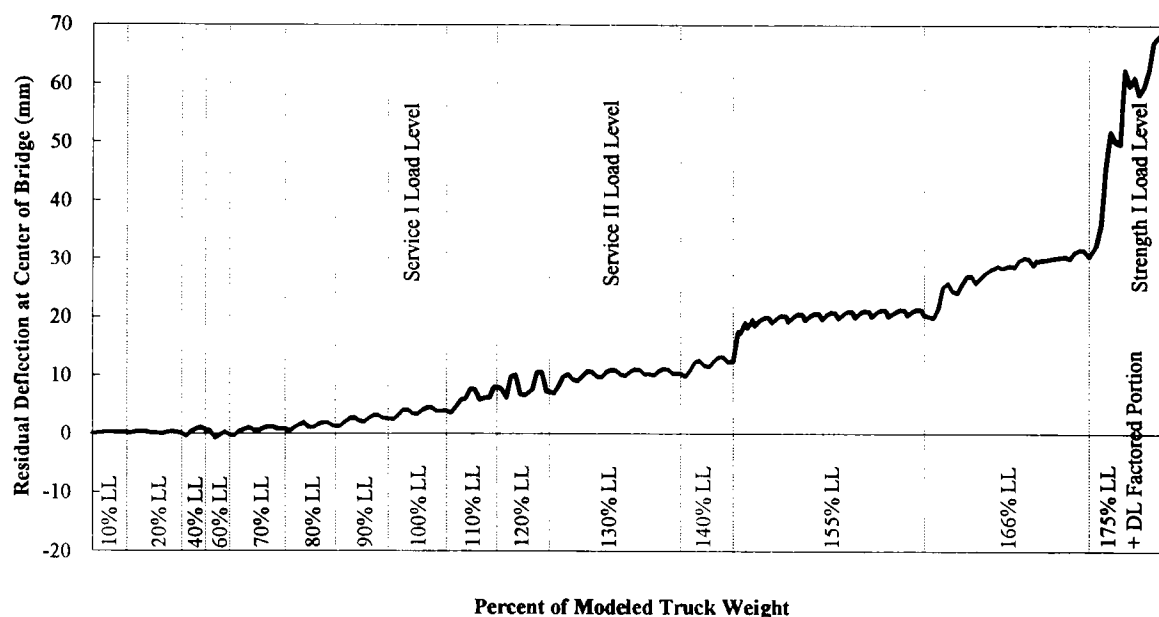


FIGURE 5 Residual deflection versus percent of modeled truck weight.

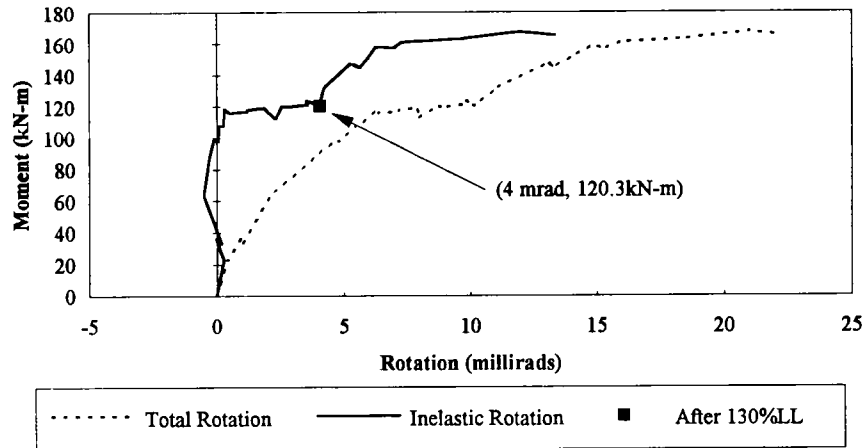


FIGURE 6 Negative moment: rotation for moving load test at pier.

negative moment loadings. From Figure 6, the inelastic rotation at the south pier (and north) is 4 mrad at the Service II level (130 percent LL).

Positive moment regions also show similar moment-rotation behavior, as shown in Figure 8 for the centerline of the girder. At the Service II level, the inelastic rotation is 0.8 mrad. Even though stresses are less than  $0.95 F_y$ , there is some nonlinear behavior. The inelastic design provisions do not explicitly incorporate positive region inelastic rotation; however, although it is small, this inelastic rotation does have an effect on residual moments and deflections.

The residual deflection at 130 percent LL (design limit), based on the actual inelastic rotations at the two piers and at the girder centerline, is calculated in Figure 9. The conjugate beam method, using a length weighted moment of inertia, is employed loaded with an unknown residual moment field and known concentrated inelastic rotations. Figure 9 shows the calculated resid-

ual deflection to be 9.1 mm (0.36 in.), which is very close to the experimental deflection of 9.7 mm (0.38 in.). The determinate residual moment is 22 kN-m (16.2 kip-ft), which also agrees with experimental pier residual moments of 27.4 kN-m (20.2 kip-ft) and 25.9 kN-m (19.1 kip-ft) after the 130 percent LL load cycles.

The residual moment field increases the total moment in positive moment regions by adding to the elastic applied moments. Because this total moment must not cause stresses above  $0.9 F_y$ , it is important to estimate the residual moment accurately. Thus, the pier section moment-rotation relation should represent the true behavior.

Concrete cracking over the pier regions, although important for serviceability, has little effect at Service I or Service II levels, as indicated in Figure 10. At low loads, the concrete is uncracked or partially cracked and the neutral axis is high in the beam. However, at design limit loads, the concrete has cracked sufficiently such

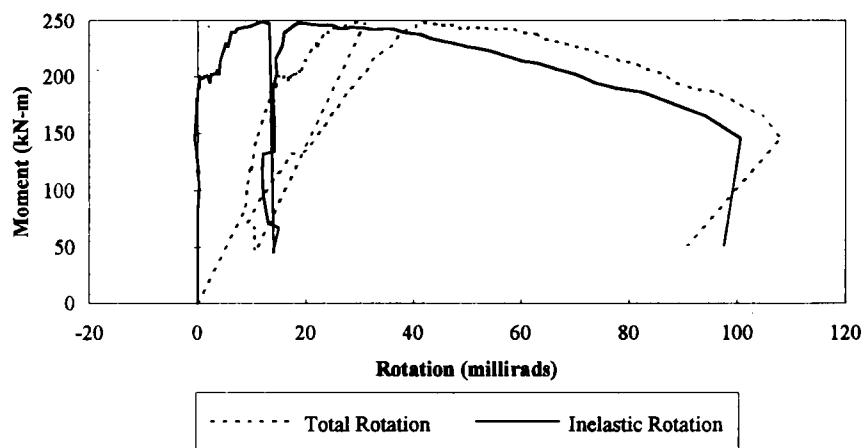


FIGURE 7 Total negative moment: rotation at pier.

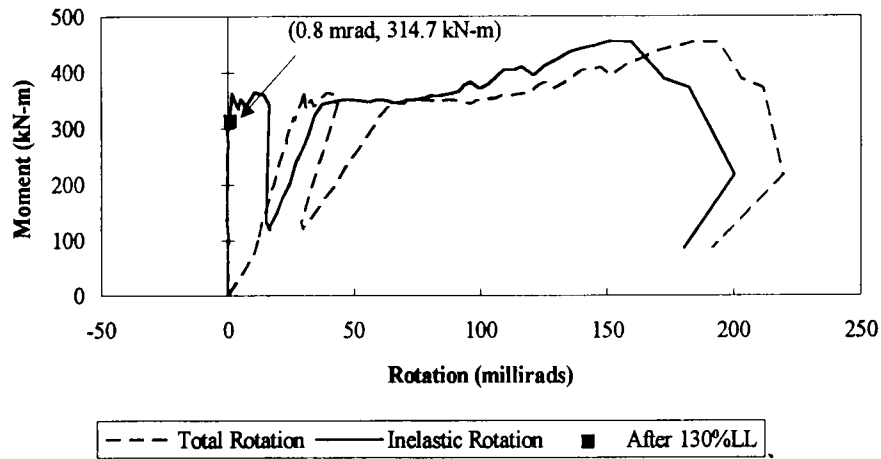


FIGURE 8 Total positive moment: rotation at bridge centerline.

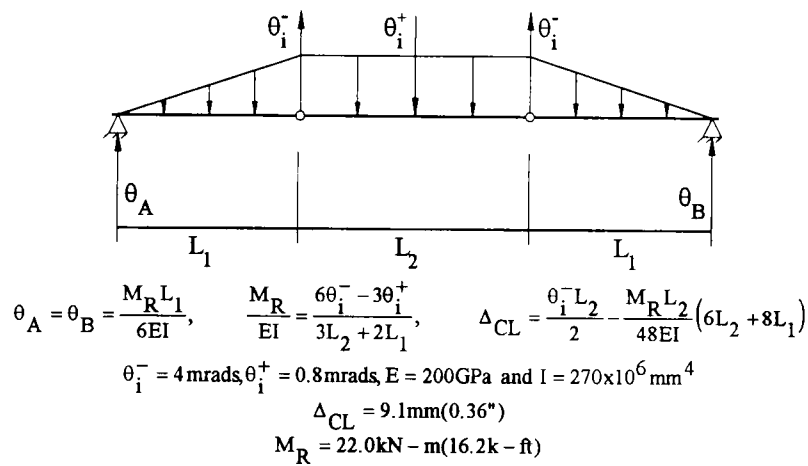


FIGURE 9 Conjugate beam derivation.

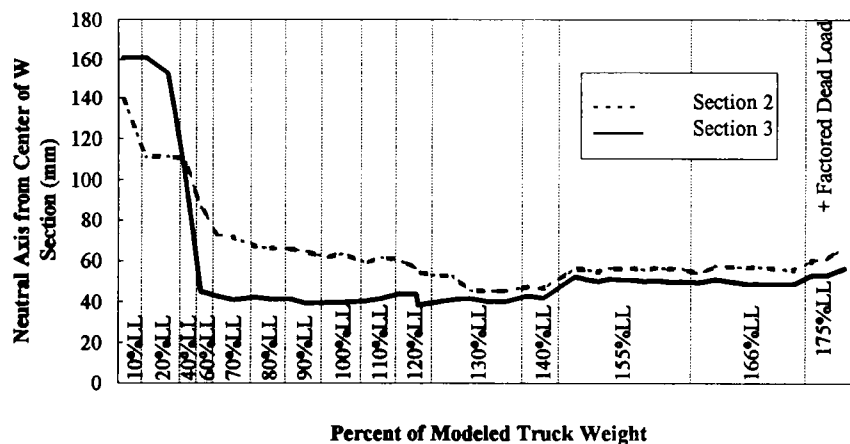


FIGURE 10 Section neutral axis location at pier for moving load test.

that the neutral axis has settled near the design position. At the 175 percent LL, the neutral axis starts to migrate toward the plastic hinge location.

### Plastic Collapse Test

After the moving load tests, the girder was tested to failure by monotonically increasing loads proportioned to represent the theoretical design collapse configuration. The simulated factored portion of the dead load was applied to P1, P2, P3, and P4 and then P1, P2, and P3 were loaded to simulate the truck. Figure 11 is the total load at P2 and P3 ( $P2 + P3$ ) plotted against the deflection at the girder centerline. The figure shows the Strength I factored load level (175 percent LL plus factored dead load) in relation to the load-deflection response. The figure clearly shows that the girder had excess capacity (36 percent) beyond the Strength I loading in accordance with the design calculations. The theoretical plastic collapse load was calculated using the effective plastic moment at the pier sections and the plastic moment capacity of the section at location P2. The actual maximum attained load was within 1 percent of the theoretical collapse load.

After sustaining about 356 mm (14 in.) of deflection at the bridge centerline (in addition to the 65 mm (2.6 in.) from the shakedown tests), the concrete crushed at the bridge centerline. Two aspects of the collapse test are worthy to note. The first is that the girder resisted 350 mm (13.8 in.) of deflection at near maximum loads. This deflection (length/deflection = 33) shows tremendous ductility for this compact girder. The second item is that this ductility behavior was not from an ideal elastic-perfectly plastic mechanism.

In Figure 7 it was seen that the pier sections are unloading moment with increasing rotation throughout

the test. This is primarily caused by flange buckling, web buckling (started during the moving load tests), and lateral buckling. The lateral torsional buckling was very apparent with two distinct sine waves [sweep approximately 25 mm (1 in.)] between the bracing 1.22 m (4 ft) on each side of the pier. The flange and web buckling were visible but seemed to stabilize early in the collapse loading.

Although the pier sections were unloading, the centerline positive moment section was absorbing the redistributed moments as shown in Figure 8. The combination resulted in a very ductile girder.

### SUMMARY AND CONCLUSIONS

More economical steel bridge designs (for compact girders) can be realized using inelastic design provisions. Inelastic design provisions can reduce material and fabrication costs by eliminating flange transitions and cover plates at interior piers (5). Bridge safety is not compromised because, after the structure has experienced several passes of the design limit loads, future loads are resisted elastically. Results from this test validate the LRFD inelastic provisions at all design limit states. Extending provisions to allow inelastic design for bridges comprising noncompact sections would also be beneficial. However, even though the analytical tools exist (6) for developing inelastic design procedures for these girders, large-scale testing is necessary to validate theoretical engineering practice.

The test results reported herein give an overview of the inelastic and plastic behavior of the  $\frac{1}{2}$ -scale three-span composite test beam. The experimental results compared well with theoretical expectations. The test showed that residual deflections stabilize well above current serviceability limits. Also, the accuracy of pre-

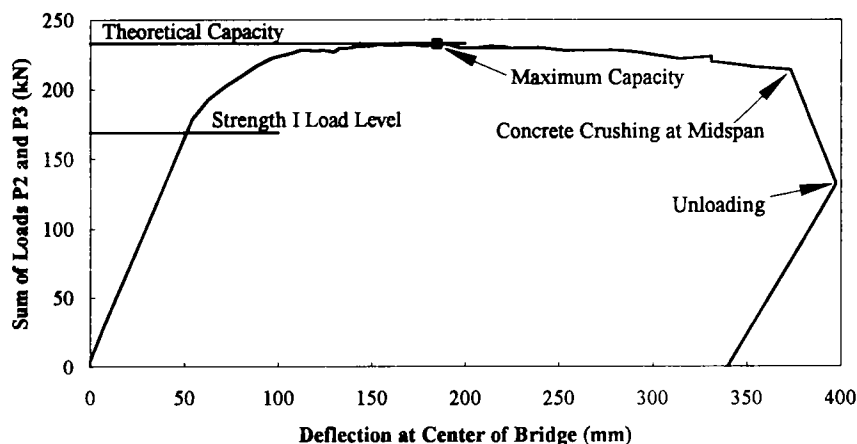


FIGURE 11 Collapse test middle span load: deflection response.

dicting inelastic behavior is dependent on the accuracy of the analytical models.

For inelastic design, estimating inelastic deflections, residual moments, and inelastic rotations is of great importance. The key to accurately predicting the bridge response is in the moment-inelastic rotation relation. This test produced one such relation for the negative pier region. However, it also developed the relation for positive bending. Positive inelastic rotations affect the results and can be easily incorporated into design provisions.

The plastic collapse test illustrated the ductility in compact composite beams. The primary reason that the beam behaved so well is that it is compact, with the flanges being well below the compactness requirements (ultracompact). This will not be the case for the second two girder tests planned for this project. The flanges will still be ultra-compact, but the webs will have typical plate girder width/thickness ratios. However, previous work has shown that, although these girders are not as ductile, the noncompact sections have predictable moment-rotation behavior (6) that can be incorporated into inelastic design provisions. The second two noncompact girder tests from this project will provide vital information for the development of inelastic design provisions for noncompact girders.

#### ACKNOWLEDGMENTS

The authors gratefully acknowledge the sponsors of this work: the National Science Foundation, the American

Iron and Steel Institute, the American Institute for Steel Construction, the Missouri Highway and Transportation Department, Louisiana Transportation Research Center, Bethlehem Steel, Nucor-Yamato Steel, US Steel, St. Louis Screw & Bolt Co., and Stupp Bros. Inc.

#### REFERENCES

1. *Guide Specification for Alternate Load-Factor Design Procedures for Steel Beam Bridges Using Braced Compact Sections*. AASHTO, Washington, D.C., 1986.
2. *NCHRP Project 12-33: Load and Resistance Factor Design Bridge Design Specifications and Commentary*. Fourth Draft Copy. TRB, National Research Council, Washington, D.C., 1993.
3. Neal, B. G. *The Plastic Methods of Structural Analysis*, John Wiley & Sons, New York, 1956.
4. Barker, M. G. and T. V. Galambos, Shakedown Limit State of Compact Steel Girder Bridges, ASCE, *Journal of Structural Engineering*, Vol. 118, No. 4, April 1992, pp. 986–998.
5. Barker, M. G. Inelastic Design and Rating of Steel Girder Bridges. *Proc., 1993 National Symposium on Steel Bridge Construction*, Atlanta, Nov. 1993, pp. 2.1–2.17.
6. Weber, D. C. *Experimental Verification of Inelastic Load and Resistance Factor Design Limits*. Master's thesis. University of Missouri, Columbia, Aug. 1994.
7. Dishongh, B. E. *Residual Damage Analysis: A Method for the Inelastic Rating of Steel Girder Bridges*, Ph.D. thesis. University of Minnesota, Minneapolis, June 1990.

# Load Spectra for Girder Bridges

---

Jeffrey A. Laman, *University of Michigan*

Measurement results of static truck loads and the corresponding response of the girders under normal traffic on six girder bridges located on Interstate highways, state highways, U.S. highways, and surface streets are presented. Truck data are available from highway weigh station logs and citation files and also through the use of weigh-in-motion (WIM) technology. Stationary scales are biased and do not accurately reflect the distribution of truck axle weights and gross vehicle weight caused by avoidance of scales by illegally loaded trucks. Citation data are helpful in understanding the nature and extent of overloaded trucks but cannot present the entire spectra of normal traffic. WIM measurements of trucks can be taken discretely during normal traffic, resulting in unbiased data for a statistically accurate sample of truck traffic traveling a particular highway. The results show that truck loads are strongly site specific. There is a negative correlation between law enforcement effort and occurrence of overloaded trucks. Overloaded trucks are observed on roads not controlled by truck weigh stations. A comparison of the weigh station data, truck citation data, and WIM measurements obtained in this study confirms this observation. Additionally, load spectra for each girder are strongly component specific as demonstrated by this study. This information is useful to focus inspection efforts.

**P**resented are measurement results of truck loads on six bridges. A study of the bridge structures was performed at locations of different average daily truck traffic and proximity to stationary weigh

stations. Measurements were conducted using two systems: a truck weighing system and a strain data acquisition system. The data include approximately 22,000 truck files including axle weight and spacing, speed, and multiple presence and 150 stress spectra records representing 1 week of normal traffic each. The recorded truck data were processed to develop cumulative distribution functions (CDFs) of gross vehicle weight (GVW) for each of six sites. The stress histories are collected at midspan of each girder bottom flange and processed using the rainflow algorithm. These data are then converted to an equivalent (root mean cube) stress as a convenient method of comparison between components.

Also presented are truck data provided by the Michigan State Police Motor Carrier division and the Michigan Department of Transportation (MDOT). These data include both weigh station and 1985 citation data, which serve as a point of reference for the weigh-in-motion (WIM) data.

## MEASUREMENT EQUIPMENT AND BRIDGES

Truck axle weights, gross vehicle weights, and axle spacing were obtained with a bridge WIM system from Bridge Weighing Systems, Inc. using prescribed procedures for setup and calibration. Strain data (stress spectra) were collected using the rainflow algorithm with a data acquisition system from the SoMat Corporation. During 1991, 1992, and 1993 WIM and strain mea-

surements were conducted at six bridge sites (1). These sites are located in southeast Michigan on U.S. Interstate, Michigan, and city roadways. The location and description of the bridges are as follows:

1. The bridge on US-23 over the Huron River (US-23/Huron River) is constructed as a two-lane, five simple span, six steel composite girder structure that carries northbound (NB) traffic.

2. The bridge on US-23 over the Saline River (US-23/Saline River) is constructed as a two-lane, three simple span, ten steel composite girder structure that carries southbound (SB) traffic between the metropolitan Detroit area and Toledo, Ohio. There is no weigh station on the route.

3. The bridge on I-94 over Pierce Road (I-94/Pierce Rd.) is constructed as a three simple span, ten steel composite girder bridge that carries eastbound (EB) traffic between Detroit and Chicago. The site is 6.5 km east of a weigh station.

4. The bridge on I-94 over Jackson Road (I-94/Jackson Rd.) is constructed as a three simple span, nine steel composite girder bridge and carries westbound (WB) traffic between Detroit and Chicago. The weigh station for this route is 40 km west.

5. The bridge on US-23/M-14 over the New York Central Railroad (M14/New York RR) is constructed as a two-lane, three simple span, eight steel composite girder structure and carries EB traffic.

6. The bridge on Wyoming Road over I-94 (Wyoming Rd./I-94) in Detroit is constructed as a four simple span, ten steel composite girder bridge and carries SB surface street traffic in Detroit. The area is heavily industrialized with more truck traffic than is typical for a city street.

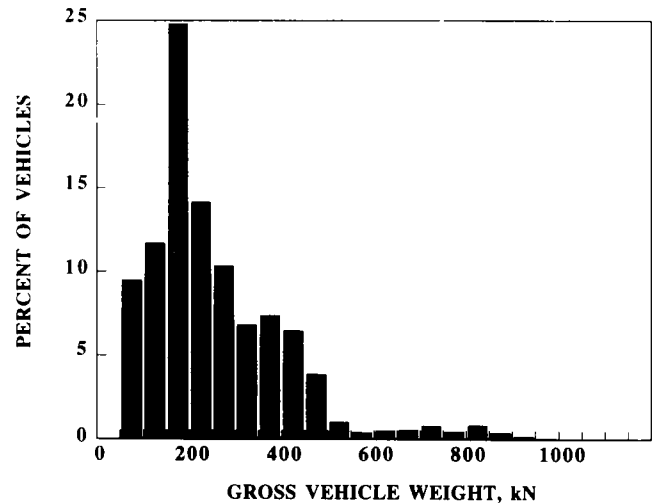


FIGURE 2 Histogram of GVW, US-23/Saline River, 1992.

### TRUCK WEIGHT MEASUREMENTS

Statistical data are presented in the form of histograms and cumulative distribution functions. CDFs are used to present and compare the critical extreme values of the data and are plotted on normal probability paper (2).

Most states allow a maximum GVW of 355 kN; however, Michigan legal limit allows for an 11-axle truck of over 710 kN, depending on axle configuration. From the tables and graphs it can be seen that there were a number of illegally loaded trucks measured during data collection at several of the sites.

Measurement results of GVW taken at US-23/Huron River NB in 1992 (Figure 1) indicate that the extreme values are dominated by 11-axle vehicles. This bridge

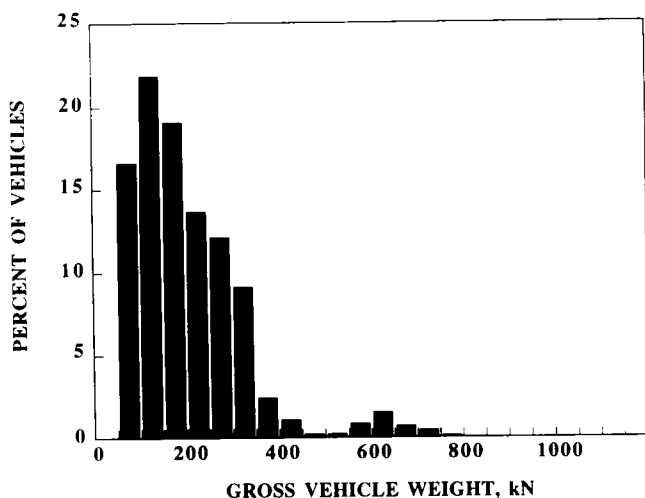


FIGURE 1 Histogram of GVW, US-23/Huron River, 1992.

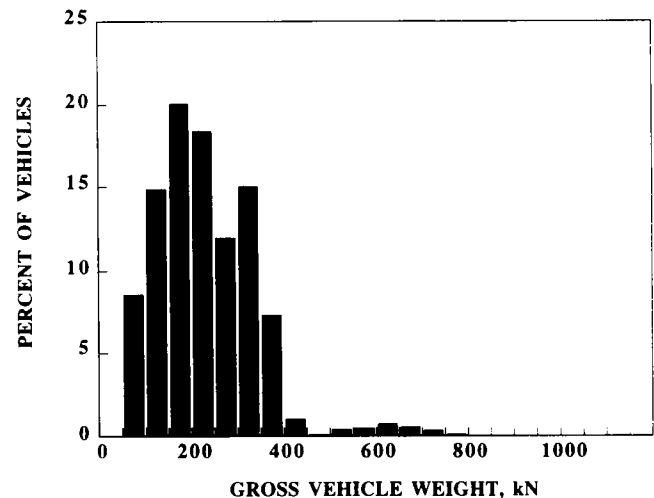


FIGURE 3 Histogram of GVW, I-94/Pierce Rd., EB, 1993.



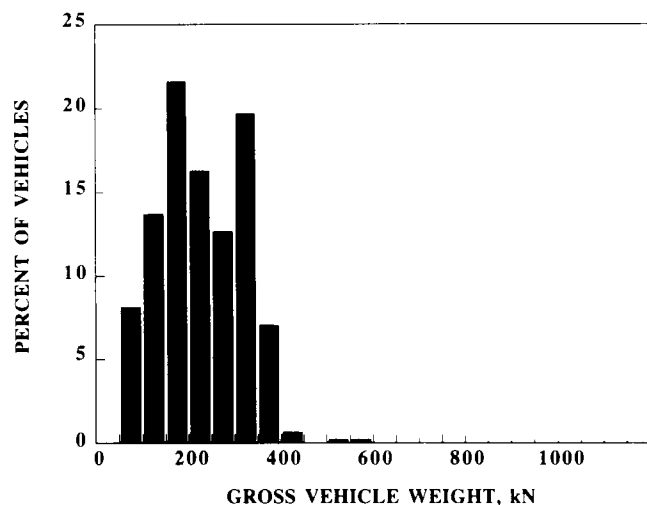


FIGURE 4 Histogram of GVW, I-94/Pierce Rd., EB, 1991.

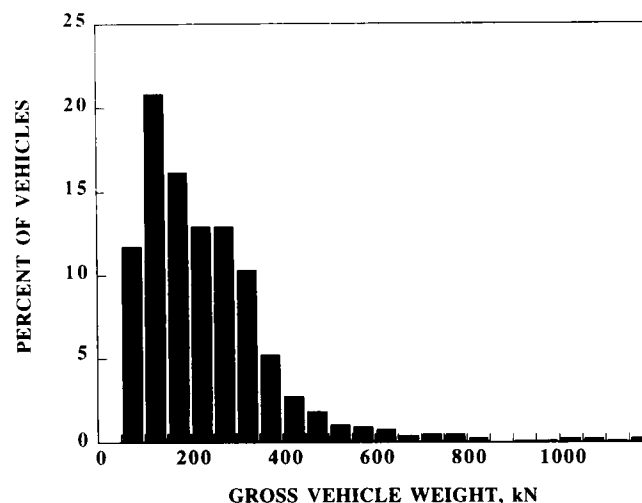


FIGURE 6 Histogram of GVW, M-14/New York Central RR, EB.

is not on a route near or between major industrial areas and the data reflect this because there are almost entirely legally loaded vehicles, despite the absence of a weigh station in the vicinity.

The US-23/Saline River SB bridge site is along a north-south route between the major industrial areas of metropolitan Detroit and Toledo, Ohio, as well as a heavily used route between Chicago and other Ohio cities. A critical factor affecting the use of this route is the absence of a weigh station. It can be expected, as the GVW (Figure 2) data reveal, that heavily and illegally loaded trucks are motivated to travel this route. The heaviest vehicle weighed was a 1100-kN, 11-axle truck. Several vehicles weighed over 900 kN and many exceeded legal limits.

Measurements taken at I-94/Pierce Rd. in 1993 (Figure 3) were conducted when the nearby stationary weigh station was closed for repairs. I-94/Pierce Road is 7 km east of the stationary weigh station on I-94 EB. As a comparison, WIM data were collected in 1991 (Figure 4) with the stationary weigh station in operation. It is suspected that illegally loaded trucks avoid stationary weigh scales causing the data to be biased. The data presented support this as seen from comparing both the GVW and lane moment. A total of 1,031 trucks were weighed in 1991 and a total of 2,951 trucks were weighed in 1993. Trucks weighed in 1991 while the stationary weigh scales were open had much lower GVWs than the trucks weighed in 1993 when the stationary weigh scales were closed, as seen in Figures 3

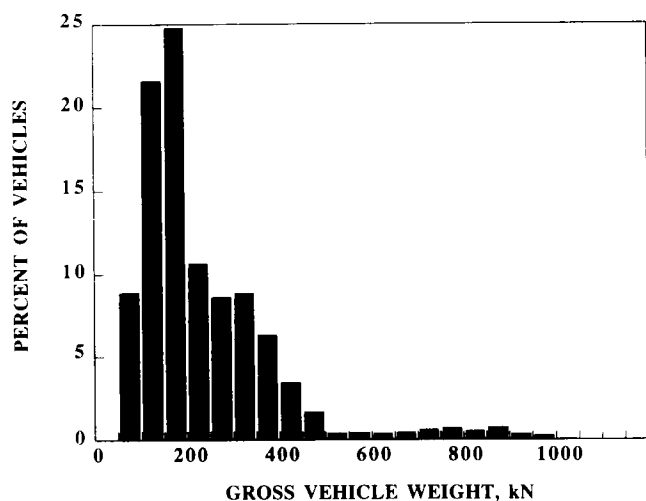


FIGURE 5 Histogram of GVW, I-94/Jackson Rd., WB.

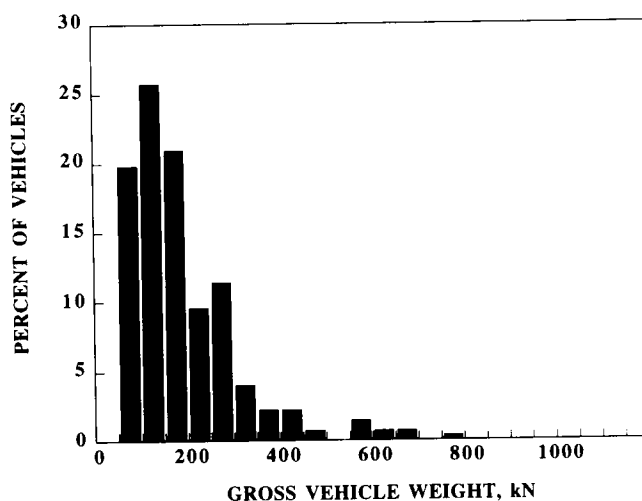


FIGURE 7 Histogram of GVW, Wyoming Rd./I-94, SB.

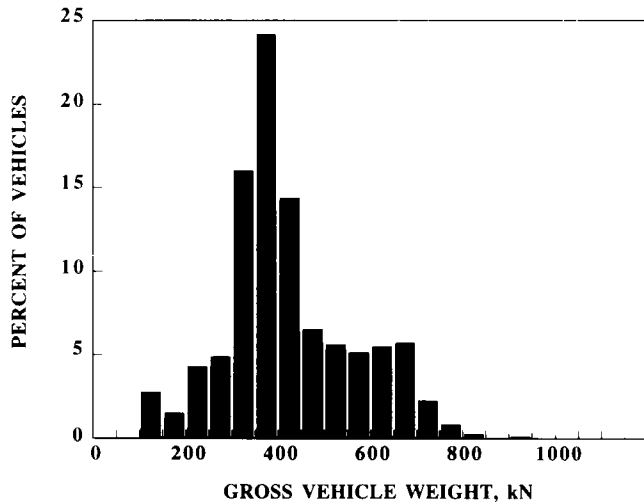


FIGURE 8 Histogram of GVW of Michigan citation data, 1985.

through 9. The 1993 maximum GVW of 807 kN is considerably larger than the 1991 maximum GVW of 593 kN.

GVW measurements collected at I-94/Jackson Rd. WB (Figure 5) indicate very heavy vehicles with the extreme values dominated by 11-axle vehicles. This bridge is on the major route between Detroit and Chicago, which accounts for the very heavy vehicles. The nearest weigh station is approximately 40 km west of the site, also contributing to higher GVWs and illegally loaded vehicles.

GVW measurements collected at M-14/New York RR EB (Figure 6) indicate very heavy vehicles with the extreme values dominated by the 11-axle vehicles. This bridge, although not in an industrial area, is a route used between northern Detroit suburbs and the metropolitan Chicago area, accounting for the very heavy vehicles.

Extreme values of GVW (Figure 7) at Wyoming Rd./I-94 SB reflect very few vehicles exceeding that allowed by the state of Michigan. Although the vicinity of the bridge is heavily industrialized, trucks traveling the surface street may be engaged in shorter local deliveries, reducing the incentive to overload.

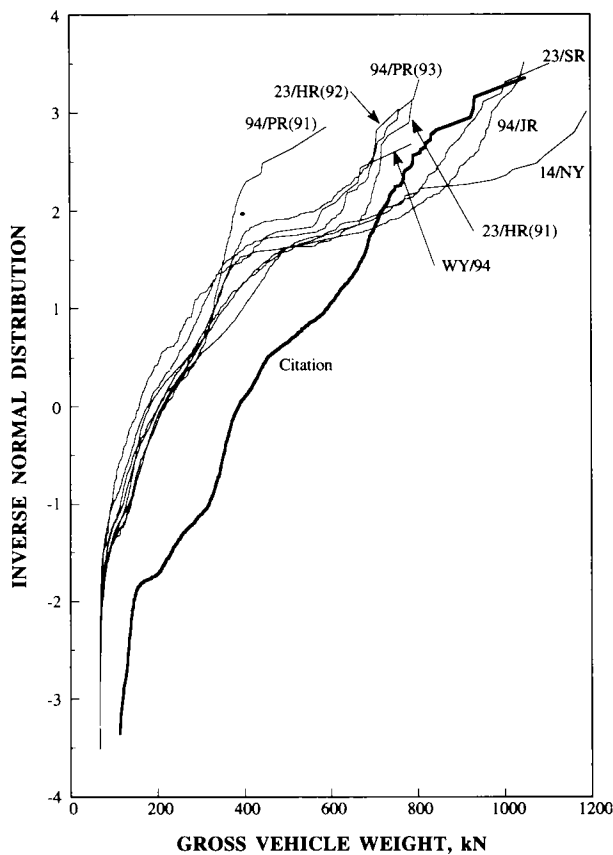


FIGURE 9 Comparison of GVW CDF for all bridges (all vehicles GVW > 67 kN).

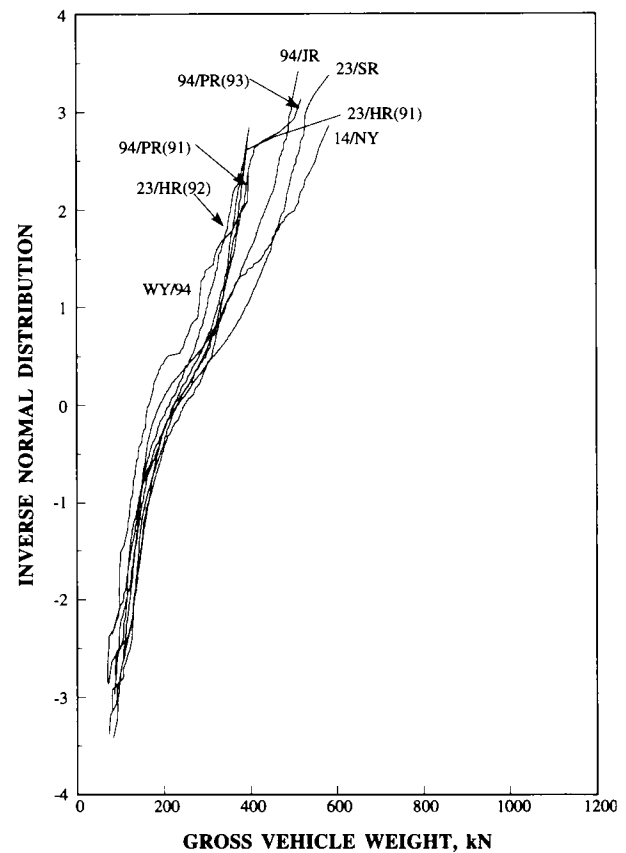


FIGURE 10 Comparison of GVW CDF for five-axle vehicles for all bridges.

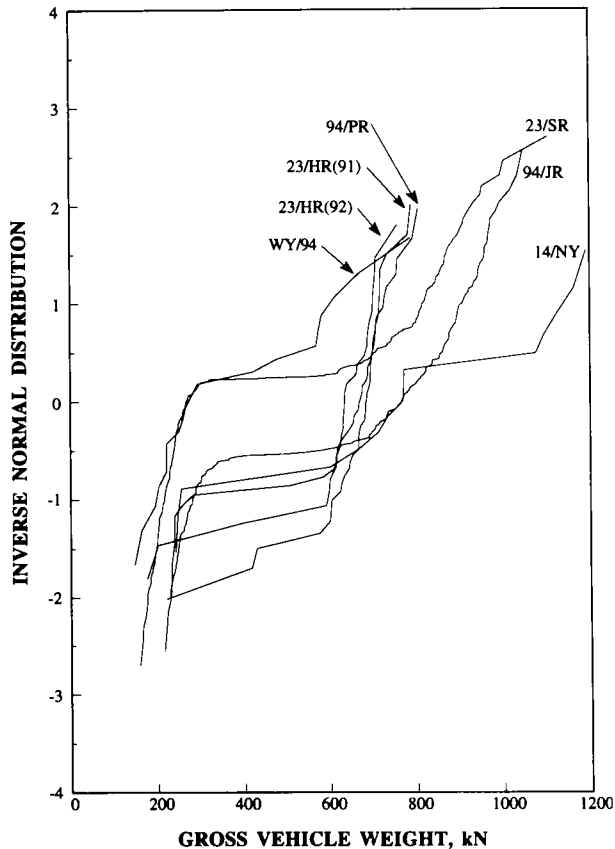


FIGURE 11 Comparison of GVW 11-axle vehicles for all bridges.

For comparison, Figure 8 presents data (approximately 2,500 trucks) obtained for overload citations issued in Michigan for 1985. The maximum GVW was approximately 1070 kN.

Figures 9–11 present the GVW CDF of trucks from each bridge file. Figure 9 indicates the distribution of all vehicles weighed for the particular site weighing greater than 67 kN plotted with the 1985 citation data. Figure 10 indicates the distribution of GVW for five-axle vehicles greater than 67 kN, and Figure 11 indicates that for 11-axle vehicles.

### LANE MOMENT DISTRIBUTIONS

Static lane moment CDFs are presented for simple spans of 9, 18, 27, and 36 m in Figures 12 through 15 for each bridge. The truck files of each bridge site were processed through influence lines to determine maximum lane moments, which are then divided by the HS20 lane moment for that span.

The 9-m lane moments in Figure 12 show a wide variation between bridges. Maximum values of lane moment to HS20 moment vary from 1.4 at I-94/Pierce Rd. (1991) to 3.05 at I-94/Jackson Rd. The CDF for US-23/Huron River for both 1991 and 1992 are somewhat similar, with maximum lane moment to HS20 moment ratios of 2.0 and 2.3, respectively. All sites have a median lane moment between 0.45 and 0.6 times HS20 moment, which corresponds to an inverse normal value of 0.

The 18-m lane moment CDFs in Figure 13 also show wide variation between bridge sites. Maximum values of

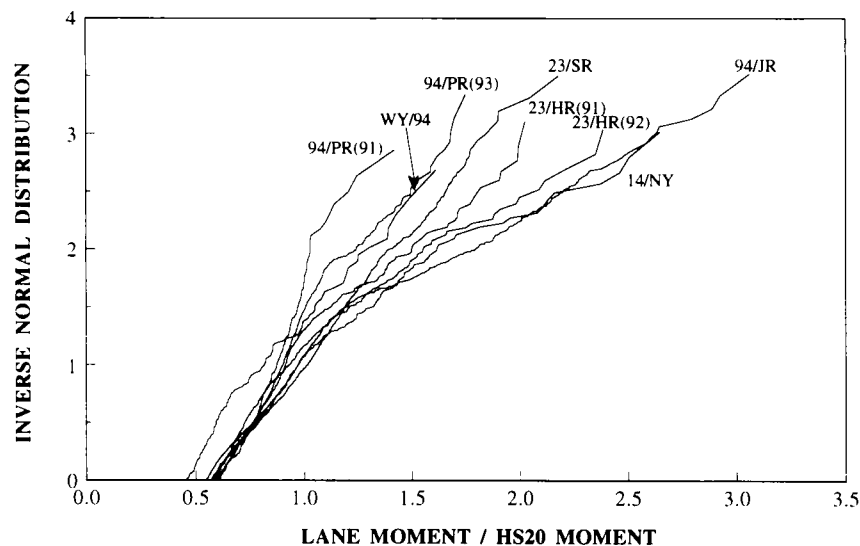


FIGURE 12 Comparison of 9-m static lane moments, all bridges (GVW > 67 kN).

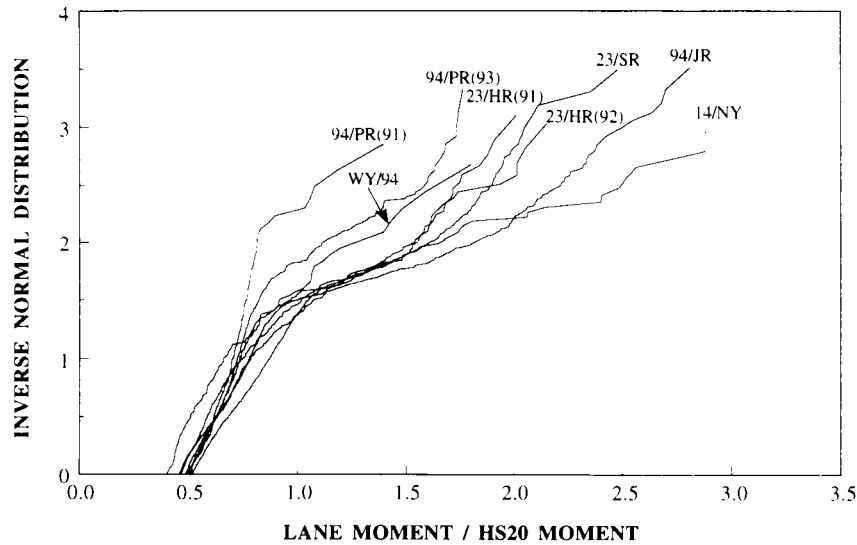


FIGURE 13 Comparison of 18-meter static lane moments, all bridges (GVW > 67 kN).

lane moment to HS20 moment vary from 1.4 at I-94/Pierce Rd. (1991) to 2.9 at 14/NY. The extreme values of all distributions are dominated by US-23/Saline River, M-14/New York Central RR, and I-94/Jackson Rd. where there is little or no control by weigh stations. Again the CDFs for US-23/Huron River during 1991 and 1992 are similar with maximum lane moment to HS20 moment ratios of 2.0 and 2.2, indicating little change from year to year, whereas the 1991 and 1993 CDFs of I-94/Pierce Rd. are considerably different. All sites have a median lane moment between 0.40 and 0.50 times HS20 moment.

The 27- and 36-m lane moment CDFs in Figures 14 and 15 again demonstrate the wide variation between bridge sites of the load spectra. Observations for the 27- and 36-m span are similar to observations of the 18-meter span lane moment CDFs, although the trends are more pronounced. As the span increases, the lane moment is more closely a function of the GVW rather than axle weight, and similarities in the distributions can be observed.

Stationary weigh station scale data were provided by MDOT from stations located on I-75 at Monroe, Michigan, and I-94 at Grass Lake, Michigan (7 km east of

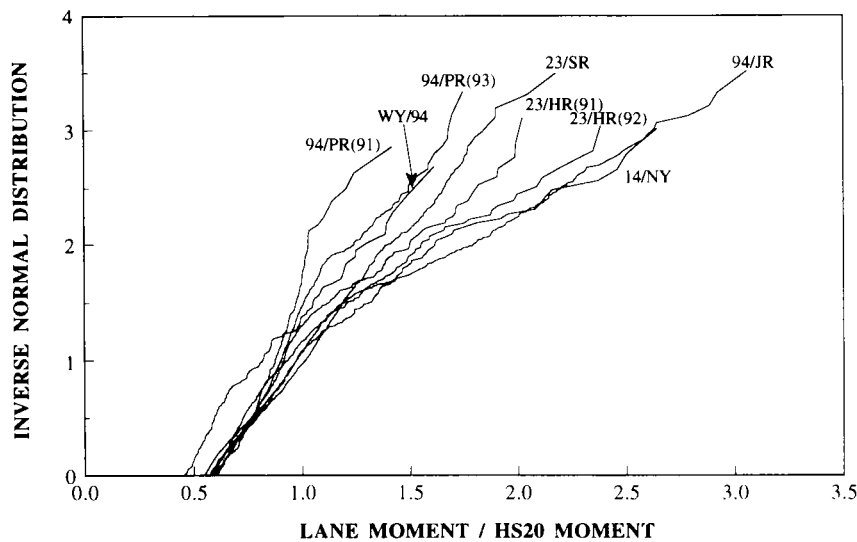


FIGURE 14 Comparison of 27-m static lane moments, all bridges (GVW > 67 kN).

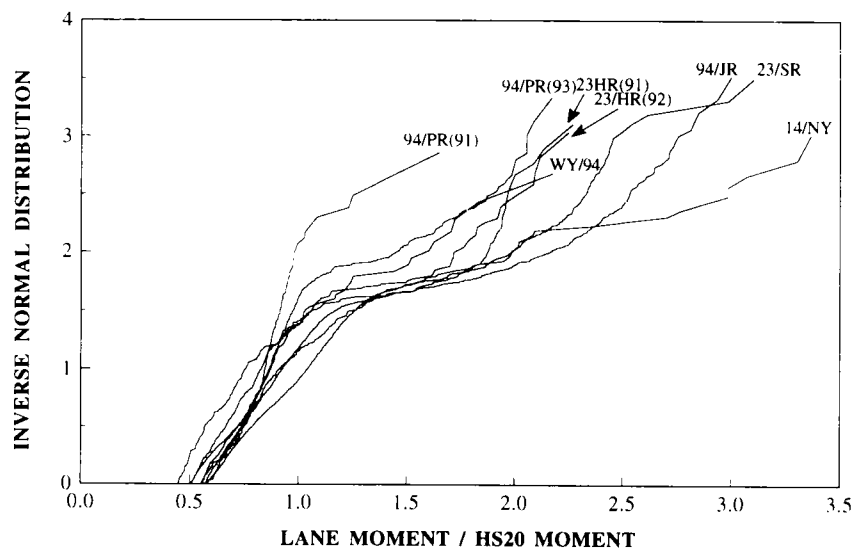


FIGURE 15 Comparison of 36-meter static lane moments, all bridges (GVW > 67 kN).

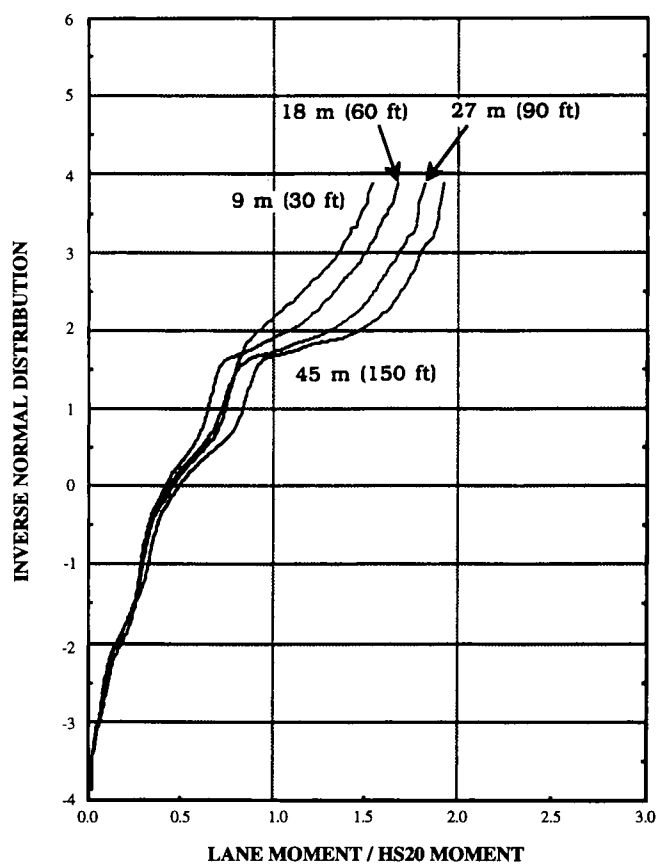


FIGURE 16 CDF of truck static lane moments from stationary weigh station data (4).

the tested bridge I-94/Pierce Rd.). The data presented here in Figure 16 are CDFs of lane moments caused by the trucks passing through the I-94 weigh station. Simple spans of 9, 18, 27, and 36 m were analyzed by Nowak et al. (4). The I-94 EB data are for October and November 1989 and include 19,874 trucks. Lane moment/HS20 moment values for I-94 Pierce Rd. (1993) ranged from 1.7 to 2.2 compared with 1.5 to 1.9 for the weigh station data. Lane moment/HS20 moment

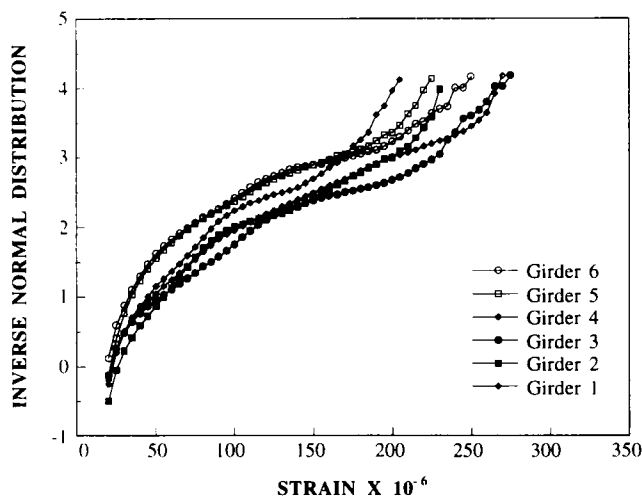


FIGURE 17 US-23/Huron River NB rainflow strain CDFs for G1-G6.

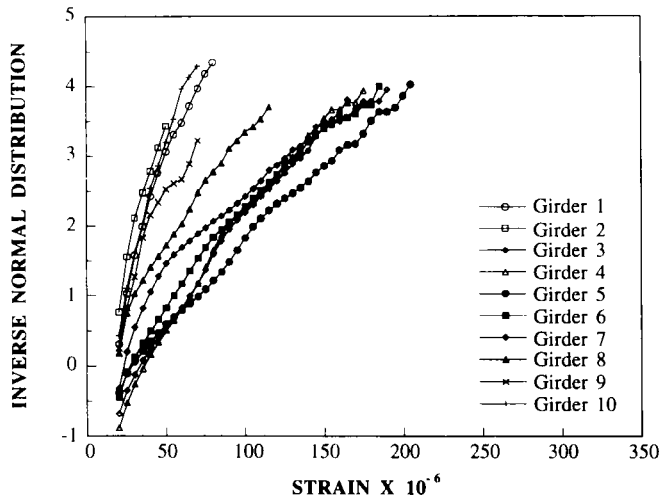


FIGURE 18 US-23/Saline River SB, rainflow strain CDFs for G1-G10.

values for I-94 Pierce Rd. (1991) ranged from 1.4 to 1.7, demonstrating that although the weigh station was open in 1992 the load spectra of WIM and stationary scales were very much the same and increased when the station was closed in 1993.

### STRAIN MEASUREMENTS

All strain measurements were taken at the bridge girder bottom flange at midspan (5). The strain data were collected using the rainflow algorithm enabling long periods of data collection. The data presented in Figures 17

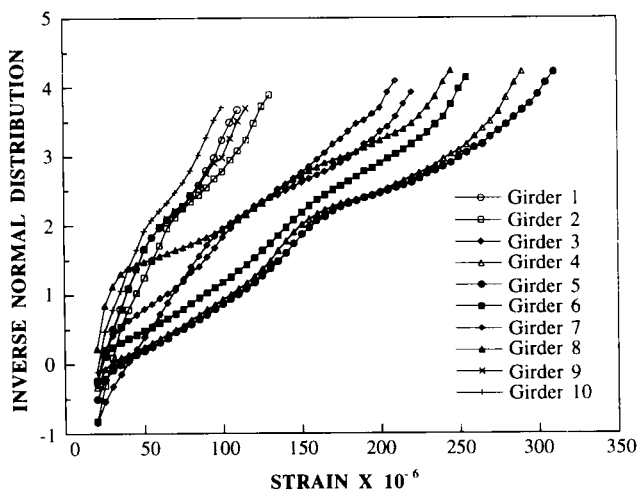


FIGURE 19 I-94/Pierce Rd. EB rainflow strain CDFs for G1-G10.

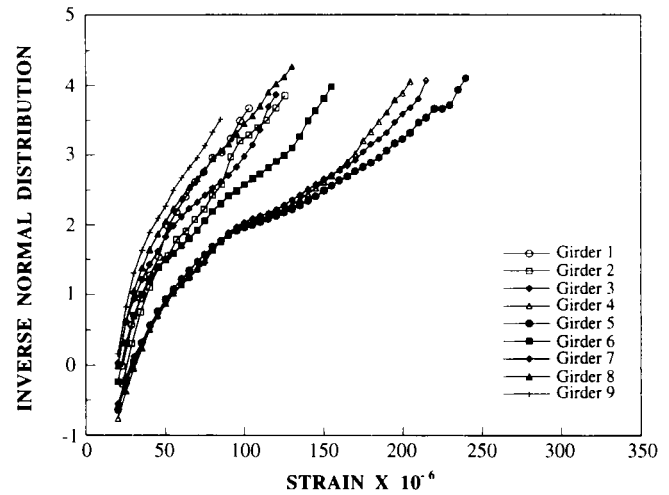


FIGURE 20 I-94/Jackson Rd. WB rainflow strain CDFs for G1-G9.

through 21 are the result of 1 week of continuous data collected at each bridge site. The bridge at Wyoming Rd./I-94 was not instrumented for strain data because of equipment security concerns. Equivalent stress (root mean cube) results of the strain data collection are presented in Figure 22. For orientation, Girder 1 is located at the extreme right of the right lane of the bridge.

The CDFs for US-23/Huron River in Figure 17 show considerable uniformity between girders, as may be expected as a result of the longer span and fewer girders. Girder 4 is the most highly stressed and Girder 6 experiences the lowest stresses, with a difference between the maximums at these girders equal to only 45  $\mu$ strain. The variation becomes more pronounced as the ratio of

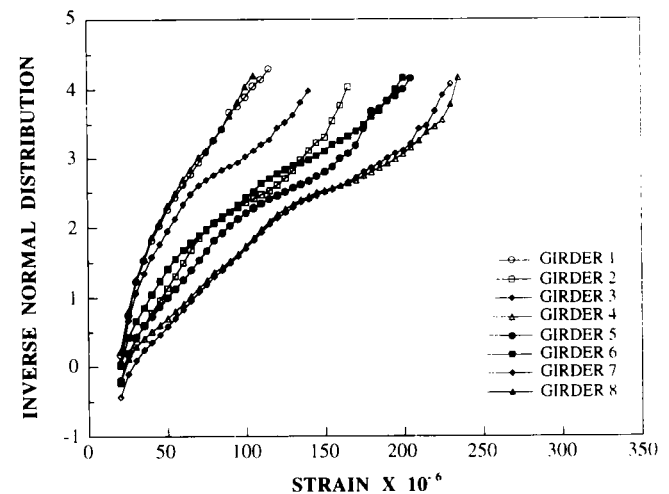


FIGURE 21 M-14/New York City RR EB, rainflow strain CDFs for G1-G8.

width to length of the bridge dimensions increases. Maximum strains measured in the girders of the bridge on US-23/Saline River vary from 50  $\mu$ strain in Girder 2 to 205  $\mu$ strain in Girder 5. Maximum strains measured in the girders of the bridge on I-94/Pierce Rd. vary from 100  $\mu$ strain in Girder 10 to 310  $\mu$ strain in Girder 5. The unusually high strain at this location was investigated and the design of the bridge was compared with others of similar span and girder spacing. The bridge at US-23/Saline River is a shorter span (9.9 m) than I-94/Pierce Rd. (10.5 m), and both bridges have girder spacing of 1.5 m; however the girder size at I-94/Pierce Rd. is substantially smaller (W24 $\times$ 68 versus W27 $\times$ 102). This size differential is likely the cause of the higher stresses.

I-94/Jackson Rd. and M-14/New York Central RR exhibit similar CDFs for girder stresses, as seen in Figures 20 and 21. This may be expected since the load

spectra are somewhat similar and the bridge spans are approximately the same. Both bridges experienced a maximum strain of about 240  $\mu$ strain.

The plots of equivalent (root mean cube) stresses (Figure 22a through e) demonstrate that girders nearest the left wheel of vehicles traveling in the right lane experience the highest stresses. This observation is important for fatigue considerations and inspections.

## CONCLUSIONS

From the presented data of GVW and lane moments, load spectrum is highly site specific and is dependent on a number of factors. These factors include proximity to stationary weigh stations, weigh station hours of operation, proximity to industrial areas, and desirability of the route for traffic between major metropolitan areas.

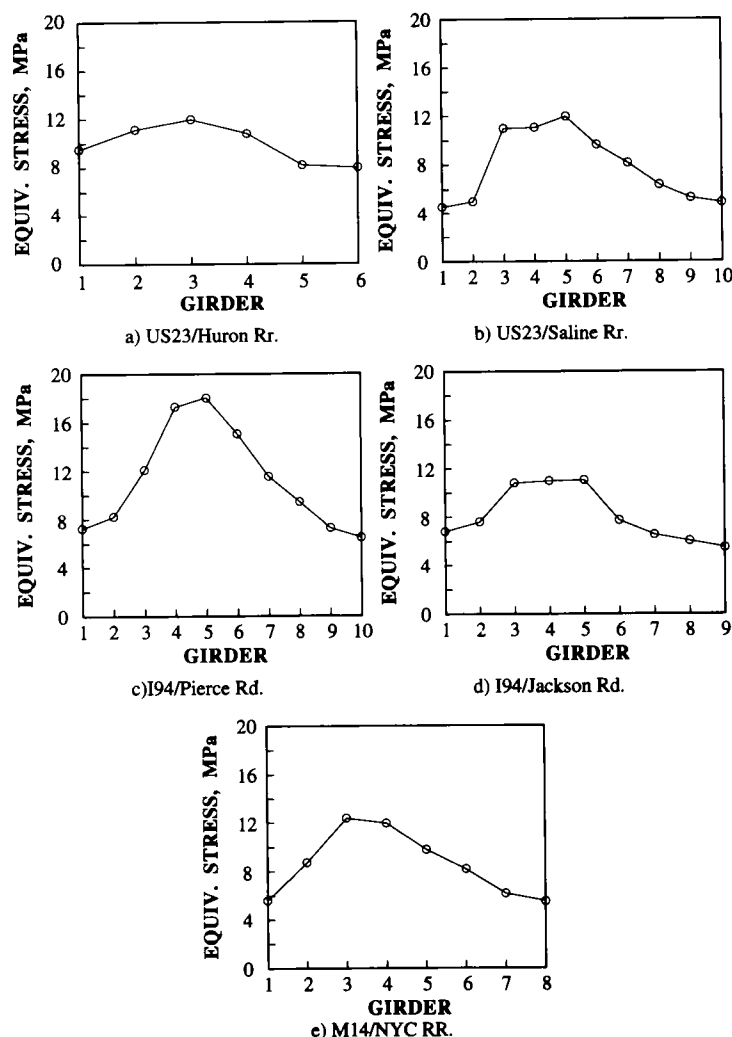


FIGURE 22 Equivalent (root mean cube) stress for each girder of the selected bridges.

The distribution of moments caused by the truck traffic is related to the same factors as GVW. In some locations the level of the lane moments may be exceedingly high.

Michigan State Police citation data confirm that very heavy trucks should be expected when data are collected without observation, which is possible with WIM equipment. Resources devoted to legal load limit enforcement activities can directly affect load levels within a given location and will prevent accelerated deterioration of the transportation systems.

Strain spectrum is component dependent and varies greatly from girder to girder. The tests consistently indicated that girders located nearest the right lane left wheel vehicle track experienced the highest strains, typically Girders 3 to 5. These girders are affected by side-by-side multiple presence of vehicles, in addition to the predominant traffic in the right lane. Girders supporting the left lane experienced moderate strains, and outer girders experienced low levels of strain. Truck traffic in the left lane is significantly lower in volume than that in the right lane, which results in different stress spectra. Exterior girders are a greater distance from the load location and may also benefit from stiffening effects of the concrete barriers.

#### ACKNOWLEDGMENTS

The research presented in this paper was sponsored by the Michigan Department of Transportation and the Great Lakes Center for Truck Transportation Research, which is gratefully acknowledged.

#### REFERENCES

1. Nowak, A. S., and J. A. Laman. *Effect of Truck Loads on Bridges*. Research Report UMCE 94-22. Department of Civil and Environmental Engineering, The University of Michigan, Ann Arbor, Sept. 1994.
2. Benjamin, J. R., and C. A. Cornell. *Probability, Statistics, and Decision for Civil Engineers*. McGraw Hill Book Company, New York, 1970.
3. *Standard Specifications for Highway Bridges*. AASHTO, Washington D.C., 1992.
4. Nowak, A. S., H. Nassif, and L. DeFrain. Effect of Truck Loading on Bridges. *ASCE Transportation Division*, Vol. 119, No. 6, Nov./Dec., 1993.
5. Laman, J. A., and A. S. Nowak. *Fatigue Load Spectra for Steel Girder Bridges*. Report UMCE 92-34. Department of Civil and Environmental Engineering, University of Michigan, Ann Arbor, 1992.



# Simplified Numerical Analysis of Suspension Bridges

---

Diego Cobo del Arco and Angel C. Aparicio, *Technical University of Catalonia, Spain*

Discretization methods are widely used in the analysis and design of suspension bridges. However, the large number of variables involved do not normally allow examination of the influence of different parameters on the behavior of suspension bridges. This paper presents a numerical method of analysis of suspended cables under vertical loads. Both explicit equilibrium and tangent stiffness matrices are derived by the finite element method. The expressions are also presented in dimensionless form, so that parametric studies can be performed. The obtained matrices can be assembled easily in a general structural analysis computer program. The proposed method is applied to the simplified analysis of suspension bridges. Some dimensionless charts are given for a single span suspension bridge. These include displacement and bending moments under the position of a concentrated load, pseudoinfluence line of displacement and bending moments at the quarter of span, and maximum displacements and bending moments for an arbitrarily located distributed load. It is believed that these charts can be useful in the first phase of design of suspension bridges and can contribute to the understanding of suspension bridge behavior.

**S**uspension bridges are flexible structures where geometric nonlinear analysis must be performed in order to include the stiffening effect of the tension in the cable.

Various methods of analysis have been applied to the study of the behavior of suspension bridges. A historical review of the approximate methods that lead to the deflection theory can be found elsewhere (1,2). The well-established deflection theory (2-4) tries to solve the differential equilibrium equation and allows the use of analytical expressions for the solutions. However, explicit analytical solutions are not always possible, and numerical techniques must be used (2,5).

On the other hand, discretization methods have been widely used in the modern design and analysis of suspension bridges, both in the static and the dynamic fields (e.g., 6-9). Normally this leads to problems where the number of unknowns is very large (9). It is difficult, then, to examine the influence of different parameters on the behavior of the suspension bridge.

This paper presents a numerical method of analysis of suspended cables under vertical loads. The finite element method is used to obtain an explicit stiffness matrix, where the different nonlinear terms are readily identified. The equations are also presented in their nondimensional form (5). Parametric studies can then be performed. This stiffness matrix can be assembled in a general computer program.

The proposed method is applied to the analysis of suspension bridges. Two parameters govern the behavior of the single-span suspension bridge. Some dimensionless charts are developed as a function of these two

parameters for a single-span suspended bridge. These charts include displacement and bending moment under the position of a concentrated load, pseudoinfluence lines for displacement and bending moments at the quarter of span, and maximum displacement and bending moments for an arbitrarily located distributed load.

## GOVERNING EQUATIONS

According to Figure 1,  $q_0$  is the load per unit of horizontal length in the reference configuration, and  $H$  is the horizontal force in the cable. The vertical equilibrium equation reads (5)

$$H \frac{d^2 z}{dx^2} = -q_0 \quad z(0) = 0 \quad z(l) = 0 \quad (1)$$

Under the action of additional load  $q(x)$  and rise of temperature  $t$ , the cable deforms from the reference configuration. The differential equations of equilibrium are (5)

$$\left. \begin{aligned} H \frac{d^2 w}{dx^2} + h \left( \frac{d^2 z}{dx^2} + \frac{d^2 w}{dx^2} \right) &= -q \\ V_A &= -(H + h) \left( \frac{dw}{dx} \right)_A - h \left( \frac{dz}{dx} \right)_A \\ V_B &= (H + h) \left( \frac{dw}{dx} \right)_B + h \left( \frac{dz}{dx} \right)_B \end{aligned} \right\} \quad (2)$$

$$\frac{dh}{dx} = 0 \quad F_A = -h_A \quad F_B = h_B \quad (3)$$

$V_A, V_B, F_A, F_B$  are the increment in reaction forces at ends A and B with the signs of Figure 2. Equations 2 and 3 assume that  $du/dx \ll 1$  where  $u(x)$  is the horizontal movement.

The increment in horizontal force  $h$  can be obtained from the compatibility equation. This equation, up to the second order, is given by

$$h = \frac{EA}{L_e} \left[ u_B - u_A + \left( \frac{dz}{dx} \right)_B w_B - \left( \frac{dz}{dx} \right)_A w_A + \frac{q_0}{H} \int_A^B w dx + \frac{1}{2} \int_A^B \left( \frac{dw}{dx} \right)^2 dx \right] - \frac{EA \alpha t L_t}{L_e} \quad (4)$$

where  $E$  is the elastic modulus,  $A$  is the cross-sectional area of the cable,  $\alpha$  is the thermal expansion coefficient, and  $L_e$  and  $L_t$  are defined as

$$L_e = \int_A^B \left( \frac{dS_R}{dx} \right)^3 dx \quad L_t = \int_A^B \left( \frac{dS_R}{dx} \right)^2 dx \quad (5)$$

For the particular case of supports and at the same level, it is commonly accepted that

$$L_e = \left[ 1 + 8 \left( \frac{f}{l} \right)^2 \right] l \quad L_t = \left[ 1 + \frac{16}{3} \left( \frac{f}{l} \right)^2 \right] l \quad (6)$$

$f$  being the sag in the cable (Figure 1). Equations 1 through 6 are valid as long as only vertical loads are applied. These include cases such as Figure 1, but also cases such as Figure 2, where reactions at intermediate points are treated as external vertical forces.

The virtual work principle for the cable can be obtained from Equations 2 and 3. Considering a cable be-

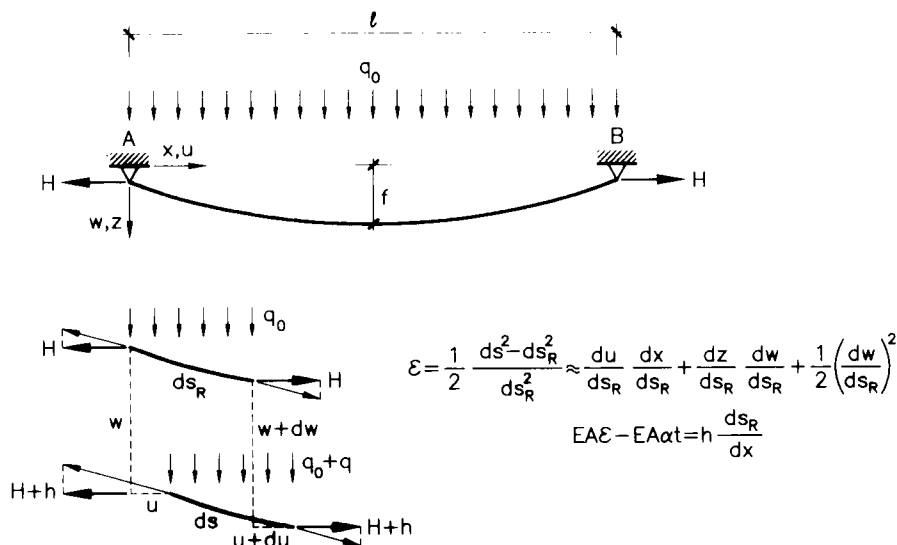


FIGURE 1 Reference and deformed configuration under vertical load.



FIGURE 2 Definition of forces at ends of cable.

tween points A and B, let  $F_A$ ,  $F_B$ ,  $V_A$ ,  $V_B$  be the increments in forces at the ends of the cable (see Figure 2). Let Equation 2 be multiplied by an arbitrary function  $\delta w(x)$  and let Equation 3 be multiplied by an arbitrary function  $\delta u(x)$ . Using Equation 1, integrating the equations and adding them yields (10)

$$\begin{aligned} & H \int_A^B \frac{dw}{dx} \frac{d\delta w}{dx} dx + h \int_A^B \frac{dw}{dx} \frac{d\delta w}{dx} dx + h \\ & \times \left[ \frac{q_0}{H} \int_A^B \delta w dx + \delta u_B - \delta u_A + \left( \frac{dz}{dx} \right)_B \delta w_B \right. \\ & \left. - \left( \frac{dz}{dx} \right)_A \delta w_A \right] = F_A \delta u_A + F_B \delta u_B + V_A \delta w_A \\ & + V_B \delta w_B + \int_A^B q \delta w dx \end{aligned} \quad (7)$$

This is the virtual work principle for the cable. The last term of the right-hand side should include the term  $\sum q_i \delta w_i$  when concentrated vertical loads  $q_i$  are applied.

### FINITE ELEMENT MODEL

A simple finite element model can be obtained from Equations 4 and 7. Let the cable between points A and B be discretized into  $n$  parts, each of horizontal length  $l_i$  (Figure 3).

Linear displacements are assumed between nodes  $i$  and  $i + 1$ . This leads to  $dw/dx$  being discontinuous between nodes, which actually occurs when a concentrated load acts at a particular node. Defining,

$$\mathbf{d}^t = (u_1, w_1, w_2, \dots, w_n, w_{n+1}, u_{n+1}) \quad (8)$$

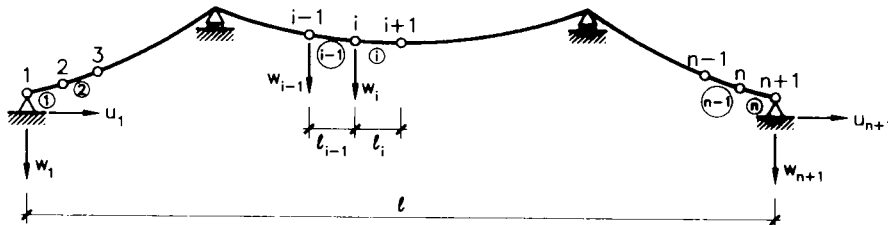


FIGURE 3 Finite element discretization.

$$\delta \mathbf{d}^t = (\delta u_1, \delta w_1, \delta w_2, \dots, \delta w_n, \delta w_{n+1}, \delta u_{n+1}) \quad (9)$$

it is possible to express

$$\int_A^B \frac{dw}{dx} \frac{d\delta w}{dx} dx = \delta \mathbf{d}^t \cdot \underline{\underline{C}} \cdot \mathbf{d} \quad (10)$$

$$\begin{aligned} u_B - u_A + \left( \frac{dz}{dx} \right)_B w_B - \left( \frac{dz}{dx} \right)_A w_A \\ + \frac{q_0}{H} \int_A^B w dx = \mathbf{a}^t \cdot \mathbf{d} \end{aligned} \quad (11)$$

where  $\mathbf{a}$  is a vector whose dimension is  $(n + 3)$  and  $\underline{\underline{C}}$  is a symmetric matrix whose dimension is  $(n + 3) \times (n + 3)$ . The explicit expressions for  $\mathbf{a}$  and  $\underline{\underline{C}}$  can be found in Tables 1 and 2, respectively.

Introducing Equations 10 and 11 in Equation 4, Equation 12 is written

$$h = \frac{EA}{L_e} \left( \mathbf{a}^t \cdot \mathbf{d} + \frac{1}{2} \mathbf{d}^t \cdot \underline{\underline{C}} \cdot \mathbf{d} \right) - EA \alpha t \frac{L_r}{L_e} \quad (12)$$

Introducing Equations 10 and 11 in Equation 7, after manipulations, the virtual work principle is being given by

$$\begin{aligned} \delta \mathbf{d}^t \cdot [H \underline{\underline{C}} \cdot \mathbf{d} + h(\mathbf{a} + \underline{\underline{C}} \cdot \mathbf{d})] \\ = \delta \mathbf{d}^t \cdot (\mathbf{F} + \sum \mathbf{q}_i) \end{aligned} \quad (13)$$

As Equation 13 holds for every virtual displacement  $\delta \mathbf{d}$ , it is possible to write the equation of equilibrium as

$$H \underline{\underline{C}} \cdot \mathbf{d} + h(\mathbf{a} + \underline{\underline{C}} \cdot \mathbf{d}) - \sum \mathbf{q}_i = \mathbf{F} \quad (14)$$

TABLE 1 Expression for Vector  $\mathbf{a}$ 

	$u_i$	$w_i$	$w_2$	...	$w_i$	...	$w_n$	$w_{n+1}$	$u_{n+1}$
$i$	1	2	3		$i+1$		$n+1$	$n+2$	$n+3$
$a_i$	-1	$-Z'_{A+}$ $q_0 l_i / 2H$	$q_0(l_1 + l_2) / 2H$		$q_0(l_i + l_{i+1}) / 2H$		$q_0(l_n + l_{n+1}) / 2H$	$Z'_{B+}$ $q_0 l_n / 2H$	1

Equation 13 is a typical finite element equilibrium equation (11).  $\mathbf{F}$  is the internal force vector at the ends of the element and  $\Sigma \mathbf{q}_i$  is the external force vector, although  $\Sigma \mathbf{q}_i$  could be interpreted as internal forces if the cable is a part of a general structure. Introducing Equation 12 in Equation 14, an equilibrium stiffness matrix (12) can be readily identified:

$$\underline{\underline{K}}_e \cdot \mathbf{d} - EA\alpha t \frac{L_t}{L_e} \mathbf{a} - \Sigma \mathbf{q}_i = \mathbf{F} \quad (15)$$

$$\begin{aligned} \underline{\underline{K}}_e = & \frac{EA}{L_e} \mathbf{a} \cdot \mathbf{a}' + \left( H + \frac{1}{2} b^1 + \frac{1}{3} b^2 - EA\alpha t \frac{L_t}{L_e} \right) \underline{\underline{C}} \\ & + \frac{EA}{L_e} \left[ \frac{1}{2} (\mathbf{a} \cdot \mathbf{d}' \cdot \underline{\underline{C}} + \underline{\underline{C}} \cdot \mathbf{d} \cdot \mathbf{a}') \right. \\ & \left. + \frac{1}{3} \underline{\underline{C}} \cdot \mathbf{d} \cdot \mathbf{d}' \cdot \underline{\underline{C}} \right] \end{aligned} \quad (16)$$

where the increment in horizontal force  $b$  is obtained as the sum of the first-order contribution  $b^1$  and the second-order contribution  $b^2$ , which are given by

$$\left. \begin{aligned} b^1 &= \frac{EA}{L_e} \mathbf{a}' \cdot \mathbf{d} \\ b^2 &= \frac{1}{2} \frac{EA}{L_e} \mathbf{d}' \cdot \underline{\underline{C}} \cdot \mathbf{d} \\ b &= b^1 + b^2 - EA\alpha t \frac{L_t}{L_e} \end{aligned} \right\} \quad (17)$$

Equation 15 gives an explicit equilibrium stiffness matrix for the whole cable under vertical loads. It is of interest to note that the structure of Equation 15 is the same as in a total Lagrangian geometrically nonlinear analysis (12). Thus, differentiating Equation 14, the tangent stiffness matrix for the whole cable is obtained straightforwardly and given by

$$\begin{aligned} \underline{\underline{K}}_t = & \frac{EA}{L_e} \mathbf{a} \cdot \mathbf{a}' + \left( H + b^1 + b^2 - EA\alpha t \frac{L_t}{L_e} \right) \underline{\underline{C}} \\ & + \frac{EA}{L_e} (\mathbf{a} \cdot \mathbf{d}' \cdot \underline{\underline{C}} + \underline{\underline{C}} \cdot \mathbf{d} \cdot \mathbf{a}') \\ & + \underline{\underline{C}} \cdot \mathbf{d} \cdot \mathbf{d}' \cdot \underline{\underline{C}} \end{aligned} \quad (18)$$

The first term of the expression 18 can be regarded as the linear contribution, the second term is the initial stress matrix, and the third term is the initial displacement matrix (12). This tangent stiffness matrix can be used to perform an analysis with a Newton-Raphson scheme (11). The residual vector can be evaluated with either Equation 14 or 15.

### DIMENSIONLESS EQUATIONS

All the equations presented can be put in dimensionless terms, as shown by Irvine (5). Defining the nondimensional variables,

$$\left. \begin{aligned} x' &= \frac{x}{l} & b' &= \frac{b}{H} & \mathbf{d}' &= \frac{H}{q_0 l^2} \mathbf{d} \\ \mathbf{q}' &= \frac{1}{q_0 l} \mathbf{q} & \theta &= \frac{\alpha t L_t}{H L_e} & \lambda^2 &= \left( \frac{q_0 l}{H} \right)^2 \frac{l}{H L_e} \end{aligned} \right\} \quad (19)$$

where  $l$  is a characteristic length of the cable (see, for example, Figure 1 or Figure 3), it is possible to derive

$$\underline{\underline{K}}'_e \cdot \mathbf{d}' - \theta \mathbf{a}' - \Sigma \mathbf{q}' = \mathbf{f}' \quad (20)$$

$$\begin{aligned} \underline{\underline{K}}'_e = & \lambda^2 \mathbf{a}' \cdot \mathbf{a}'' + \left( 1 + \frac{1}{2} b^{1'} + \frac{1}{3} b^{2'} - \theta \right) \underline{\underline{C}}' \\ & + \lambda^2 \left[ \frac{1}{2} (\mathbf{a}' \cdot \mathbf{d}'' \cdot \underline{\underline{C}}' + \underline{\underline{C}}' \cdot \mathbf{d}' \cdot \mathbf{a}'') \right. \\ & \left. + \frac{1}{3} \underline{\underline{C}}' \cdot \mathbf{d}' \cdot \mathbf{d}'' \cdot \underline{\underline{C}}' \right] \end{aligned} \quad (21)$$

$$\begin{aligned} \underline{\underline{K}}'_t = & \lambda^2 \mathbf{a}' \cdot \mathbf{a}'' + (1 + b^{1'} + b^{2'} - \theta) \underline{\underline{C}}' \\ & + \lambda^2 (\mathbf{a}' \cdot \mathbf{d}'' \cdot \underline{\underline{C}}' + \underline{\underline{C}}' \cdot \mathbf{d}' \cdot \mathbf{a}'') \\ & + \underline{\underline{C}}' \cdot \mathbf{d}' \cdot \mathbf{d}'' \cdot \underline{\underline{C}}' \end{aligned} \quad (22)$$

$$\begin{aligned} b^{1'} &= \lambda^2 \mathbf{a}'' \cdot \mathbf{d}' & b^{2'} &= \frac{1}{2} \lambda^2 \mathbf{d}'' \cdot \underline{\underline{C}}' \cdot \mathbf{d}' \\ b' &= b^{1'} + b^{2'} - \theta \end{aligned} \quad (23)$$

TABLE 2 Expression for Matrix  $\underline{\underline{C}}$ 

$\underline{\underline{C}}$		$u_1$	$w_1$	$w_2$	$w_3$	...	$w_{n-1}$	$w_n$	$w_{n+1}$	$u_{n+1}$
		1	2	3	4		n	n+1	n+2	n+3
$u_1$	1	0	0	0	0	0	0	0	0	0
$w_1$	2	0	$1/l_1$	$-1/l_1$	0	0	0	0	0	0
$w_2$	3	0	$-1/l_1$	$1/l_1+1/l_2$	$-1/l_2$	0	0	0	0	0
$w_3$	4	0	0	$-1/l_2$	$1/l_2+1/l_3$	...	0	0	0	0
...	...	0	0	0	...	...	...	0	0	0
$w_{n-1}$	n	0	0	0	0	...	$1/l_{n-2}+1/l_{n-1}$	$-1/l_{n-1}$	0	0
$w_n$	n+1	0	0	0	0	0	$-1/l_{n-1}$	$1/l_{n-1}+1/l_n$	$-1/l_n$	0
$w_{n+1}$	n+2	0	0	0	0	0	0	$-1/l_n$	$1/l_n$	0
$u_{n+1}$	n+3	0	0	0	0	0	0	0	0	0

$$a' = \frac{H}{q_0 l} a \quad \underline{\underline{C'}} = \underline{\underline{IC}} \quad (24)$$

The expressions for  $a'$  and  $\underline{\underline{C'}}$  are extremely simple when the cable is discretized in  $n$  equal parts and can be obtained easily from the values of Tables 1 and 2.

Equations 19 through 23 can be very useful when performing a parametric investigation. The behavior of the cable is uniquely described by  $\lambda^2$  and the values of the nondimensional loads  $q'$ . Parameter  $\lambda^2$  has been interpreted by Irvine (5). It accounts for the relation between geometric and elastic stiffness. It is small for taut flexible cables and it approaches infinity for an inextensible suspended cable. Typical values for  $\lambda^2$  in suspension bridge cables lie in the range 100 to 400 (5). Effectively, for the usual ratio  $f/l = 0.1$  in a steel suspension bridge cable and for a service stress  $\sigma$  about 500 MPa, the value of  $\lambda^2$  is on the order of 250. On the other hand, typical values for nondimensional concentrated loads are on the order of 0.01 in suspension bridges because of the large dead load. As an example,

for the George Washington Bridge, neglecting the side spans,  $\lambda^2 = 255$ , and for a concentrated load of 1000 kN, the value of  $q'$  is as low as 0.0016 [data are taken from Buonopane and Billington (1) for the George Washington Bridge as originally built].

The nondimensional approach can be used to examine the accuracy of the proposed method of analysis. Table 3 shows the vertical displacements in the center of the span of a suspended cable with supports at the same level under a central concentrated load  $q' = 1.0$ . Whereas the values chosen for  $\lambda^2$  are typical of suspension bridge cables, the value chosen for  $q'$  is extremely high. It is seen in Table 3 that even for a small number of discretization points the accuracy obtained is high.

The previously derived formulation can be used directly to obtain the solution for the inextensible cable. From Equation 14, the displacements  $d'$  in dimensionless form are given by

$$d' = \frac{1}{1 + h'} \underline{\underline{C'}}^{-1} \cdot (\Sigma q'_i - h'a') \quad (25)$$

TABLE 3 Accuracy of Proposed Method of Analysis

	$w$ $\lambda^2=100$	$h$ $\lambda^2=100$	$w$ $\lambda^2=200$	$h$ $\lambda^2=200$	$w$ $\lambda^2=400$	$h$ $\lambda^2=400$
n+1=11	0.0371	1.314	0.0280	1.450	0.0226	1.541
n+1=21	0.0374	1.310	0.0284	1.445	0.0230	1.534
n+1=40	0.0374	1.308	0.0285	1.443	0.0231	1.532
Irvine [9]	0.0375	1.308	0.0285	1.443	0.0231	1.532

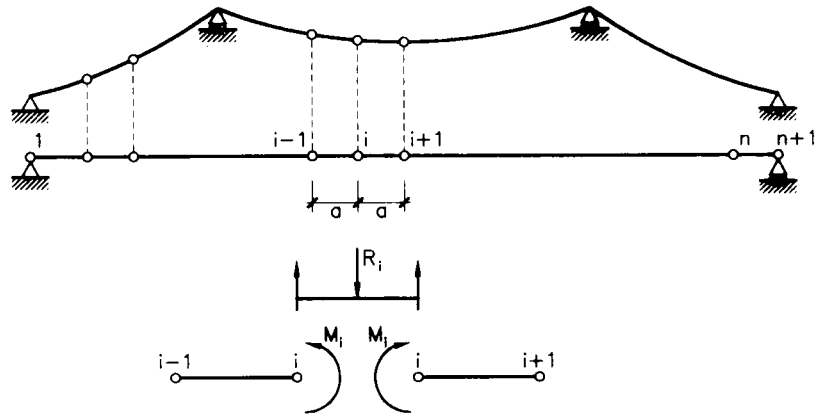


FIGURE 4 Discretization of suspension bridge.

TABLE 4 Expression for Matrix  $\underline{K}_g'$  for Single-Span Bridge

$\underline{K}_g'/n^3$		$w_1$	$w_2$	$w_3$	$w_4$	$w_5$	...	$w_{n-2}$	$w_{n-1}$	$w_n$	$w_{n+1}$
		1	2	3	4	5	...	n-2	n-1	n	n+1
$w_1$	1	$\alpha^2$	$-2\alpha^2$	$\alpha^2$	0	0	0	0	0	0	0
$w_2$	2	$-2\alpha^2$	$5\alpha^2$	$-4\alpha^2$	$\alpha^2$	0	0	0	0	0	0
$w_3$	3	$\alpha^2$	$-4\alpha^2$	$6\alpha^2$	$-4\alpha^2$	$\alpha^2$	0	0	0	0	0
$w_4$	4	0	$\alpha^2$	$-4\alpha^2$	$6\alpha^2$	$-4\alpha^2$	...	0	0	0	0
...	...	0	0	...	...	...	...	...	0	0	0
$w_{n-2}$	n-2	0	0	0	0	0	...	$6\alpha^2$	$-4\alpha^2$	$\alpha^2$	0
$w_{n-1}$	n-1	0	0	0	0	0	...	$-4\alpha^2$	$6\alpha^2$	$-4\alpha^2$	$\alpha^2$
$w_n$	n	0	0	0	0	0	0	$\alpha^2$	$-4\alpha^2$	$5\alpha^2$	$-2\alpha^2$
$w_{n+1}$	n+1	0	0	0	0	0	0	0	$\alpha^2$	$-2\alpha^2$	$\alpha^2$

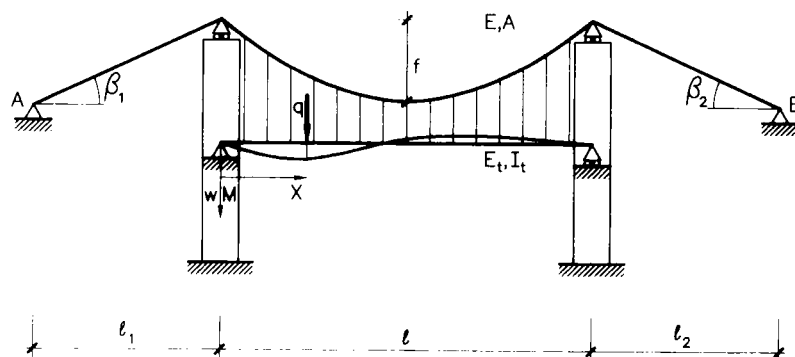


FIGURE 5 Example of single suspended bridge analyzed.

where forces at the ends of the cable have been ignored by assuming that the end displacements are null (matrix  $\underline{C}'$  should be modified accordingly). If in Equation 12 only first-order terms are retained and cable flexibility is neglected,

$$\mathbf{a}'' \cdot \mathbf{d}' = 0 \rightarrow \mathbf{h}' = \frac{\mathbf{a}'' \cdot \underline{C}'^{-1} \cdot \Sigma \mathbf{q}_i'}{\mathbf{a}'' \cdot \underline{C}'^{-1} \cdot \mathbf{a}'} \quad (26)$$

Temperature has not been taken into account in Equation 26. Equations 25 and 26 are the solutions for the inextensible cable. For example, if a load  $q$  is uniformly distributed over the whole span, using Equation

26 and Table 1, it is easily derived that  $\mathbf{h}' = q/q_0$  and  $\mathbf{d}' = 0$ , which are the expected results.

### SIMPLIFIED ANALYSIS OF SUSPENSION BRIDGES

The stiffness matrices given in Equations 16 and 18 can be directly assembled to solve any kind of structure with a parabolic cable. The external constraints or boundary conditions are introduced in the usual way. The analysis will be correct provided that the forces applied to the cable are vertical. This is the only limitation of the equations.

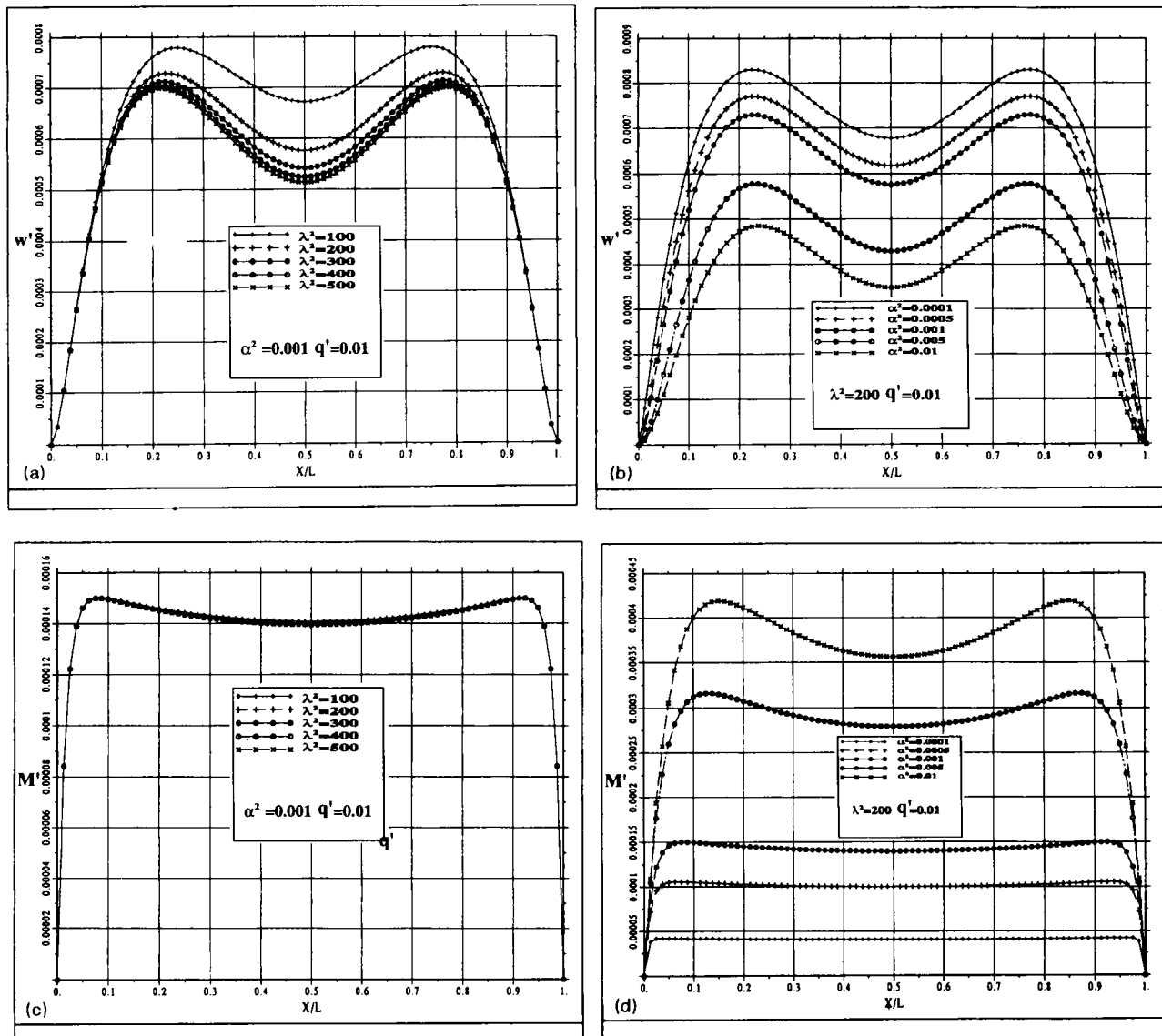


FIGURE 6 Dimensionless displacement under position of concentrated load as a function of (a)  $\lambda^2$ , (b)  $\alpha^2$ ; dimensionless bending moment under position of concentrated load as a function of (c)  $\lambda^2$  and (d)  $\alpha^2$ .

In the case of a suspension bridge with vertical hangers, the problem can be simplified by making the following assumptions:

1. Vertical movements of the cable are the same as those of the beam girder.
2. The hangers remain vertical, so only vertical forces are induced in the cable.
3. The distance between the hangers is assumed to be as small as desired so that vertical interaction forces induced in the cable can be assumed to act at any point of the cable.

These three assumptions are usual in the deflection theory but have also been used in finite element analysis of suspension bridges (6). Referring to Figure 4, a very simple analysis can be made by adding the stiffness matrix of the cable to the stiffness matrix of the beam girder.

Any formulation can be used for the determination of the stiffness matrix of the beam. In order to reduce the number of unknowns, in this work the stiffness matrix of the beam has been determined by finite differences. In this way, only vertical movements are taken into account. With reference to Figure 4, flexural mo-

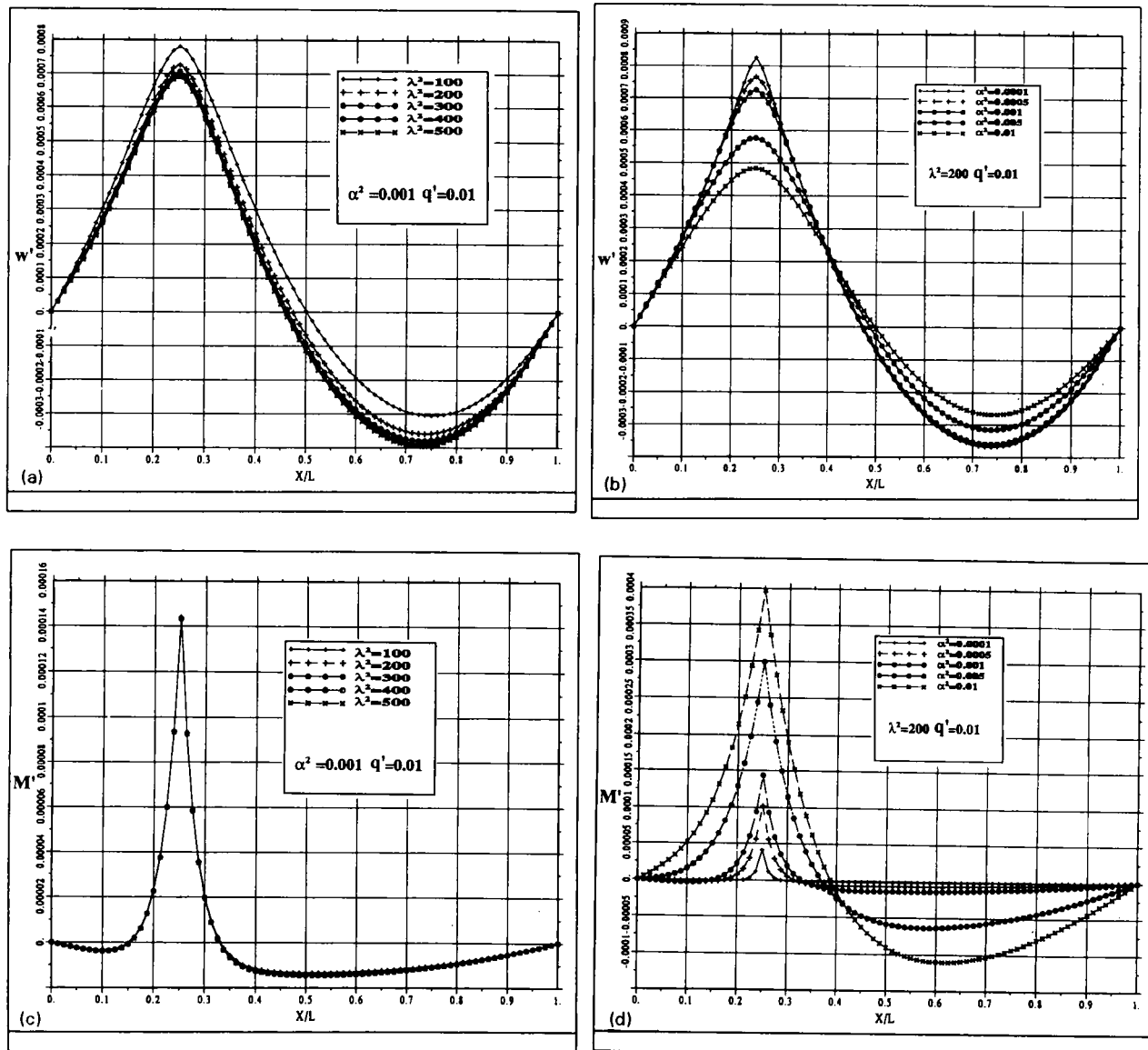


FIGURE 7 Pseudoinfluence line of dimensionless displacement at quarter of span as a function of (a)  $\lambda^2$  and (b)  $\alpha^2$ ; pseudoinfluence line of dimensionless bending moment at quarter of span as a function of (c)  $\lambda^2$  and (d)  $\alpha^2$ .



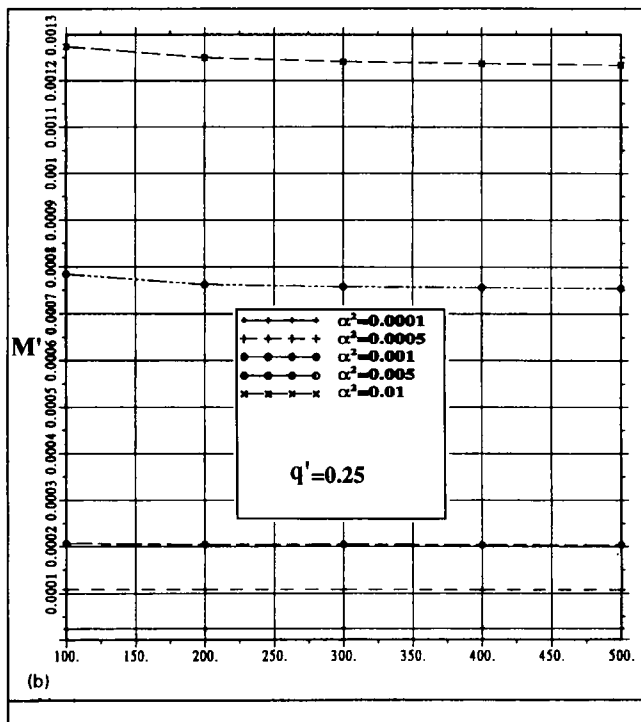
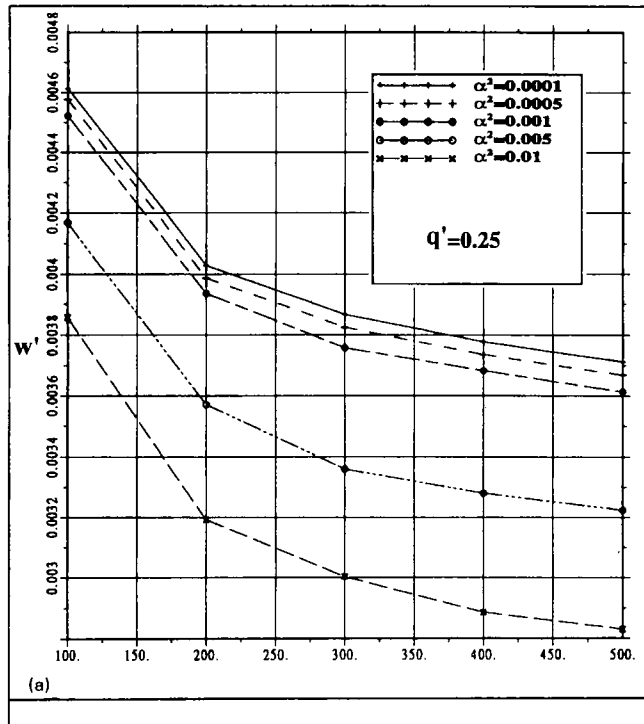


FIGURE 8 (a) Maximum dimensionless displacement and (b) maximum dimensionless bending moment for arbitrarily located distributed load  $q = 0.25q_0$ .

ments are given by the following approximation:

$$\left. \begin{aligned} M_i &= \frac{E_g I_g (w_{i-1} - 2w_i + w_{i+1}))}{a^2} \\ R_i &= 2 \frac{M_i}{a} - \frac{M_{i+1}}{a} - \frac{M_{i-1}}{a} \\ \underline{K}_g \cdot \underline{d} &= \underline{R} \end{aligned} \right\} \quad (27)$$

where  $M_i$  stands for bending moment at node  $i$ ,  $w_i$  for vertical displacement at node  $i$ ,  $E_g I_g$  for the stiffness of the beam, and  $a$  for the spacing between points.  $\underline{R}$  is the external force vector acting on the beam. The linear stiffness matrix  $\underline{K}_g$  for the beam can be easily formulated. Assuming that the sum of external forces in the cable plus the external forces in the beam is a vector  $\underline{P}$  of external forces in the suspension bridge, the assembly of the global stiffness matrix is obtained straightforwardly by adding the flexural contribution of the beam and the contribution of the suspended cables:

$$[\underline{K}_g + \underline{K}_c(\underline{d})] \cdot \underline{d} = \underline{\Sigma P} \quad [\underline{K}_g + \underline{K}_c(\underline{d})] \cdot \underline{\Delta d} = \underline{\Sigma \Delta P} \quad (28)$$

Again, the expressions are simplified when dimensionless variables are used. The new nondimensional variables introduced are

$$M' = \frac{M}{q_0 l^2} \quad \alpha^2 = \frac{E_g I_g}{H l^2} \quad (29)$$

The resultant stiffness matrix  $\underline{K}_g$  for the beam in dimensionless form is given in Table 4. Only vertical displacements are taken into account.

Examining Equations 19 through 24 and 28 and 29 and Tables 1, 2, and 4, it is seen that the behavior of a given suspension bridge is characterized by only two parameters ( $\lambda^2$ ,  $\alpha^2$ ). The variable  $\lambda^2$  has already been explained. Parameter  $\alpha^2$  is Steinman's stiffness factor ( $S^2$ ) (4). It measures the ratio between the elastic stiffness of the beam and the gravity stiffness of the cable (2). In long-span suspension bridges  $\alpha^2 \ll 1$  (5). For example, for the main span of the George Washington Bridge, as originally built (1),  $\alpha^2 = 8.97 \times 10^{-4}$ .

Solutions based on the cable inextensibility could be obtained by adding the flexural stiffness matrix to matrix  $\underline{C}$  in Equations 25 and 26.

Simplified static and dynamic analysis of suspension bridges can be made at a low computational cost with the given expressions. As an example, some dimensionless charts that can be useful in the first phase of design are given below.

#### DIMENSIONLESS CHARTS

As an example application of the proposed formulation, a single span suspended bridge has been analyzed under

different loading conditions. Two parameters ( $\lambda^2$ ,  $\alpha^2$ ) govern the behavior of the bridge. These parameters can be calculated using only the data of Figure 5. The structural model is also shown in Figure 5. To include the contribution of the backstays in the determination of  $L_e$ , Equation 30 should be used:

$$L_e = \left[ 1 + 8 \left( \frac{f}{l} \right)^2 \right] l + \frac{l_1}{(\cos \beta_1)^3} + \frac{l_2}{(\cos \beta_2)^3} \quad (30)$$

Results for the dimensionless displacement and bending moment under the position of a concentrated load ( $q' = 0.01$ ) are shown in Figure 6. The analyses have been performed for a given  $\alpha^2 = 0.001$  as a function of  $\lambda^2$  [see Figure 6(a) for displacement and Figure 6(c) for bending moment], and for a given  $\lambda^2 = 200$  as a function of  $\alpha^2$  [see Figure 6(b) for displacement and Figure 6(d) for bending moment]. These charts are similar to those developed by Jennings (13).

The pseudoinfluence line for the displacement and the bending moment at the quarter of span for a concentrated load  $q' = 0.01$  are given in Figure 7.

Finally, the maximum displacement and the maximum bending moment obtained for an arbitrarily located distributed load ( $0.25q_0$ ) are shown in Figure 8. The length of the loaded zone and the point of maximum displacement and maximum bending moment have been obtained for every pair  $\lambda^2$ ,  $\alpha^2$ , performing similar analyses to those shown in Figures 6 and 7.

Some trends of suspension bridge behavior are readily explained in these charts. In particular, it is clearly seen that, in modern suspension bridges, where typically  $\alpha^2 \ll 1$ , the stiffness of the beam girder does not contribute to the reduction of the displacements. In the past, this observation led to more flexible beam girders and eventually was one of the causes for the Tacoma Narrows Bridge disaster (1).

It is also observed that approximate solutions based in the cable inextensibility ( $\lambda^2 \rightarrow \infty$ ) will underestimate the displacements in practical cases. However, as shown in Figures 6(c), 7(c) and 8(b), bending moments are not dependent on  $\lambda^2$ , so solutions based on the cable inextensibility will give very accurate results. Interpreting a solution due to Jennings (13), the bending moment under the position of a concentrated load  $q'$  could be obtained as follows:

$$M' = q' \frac{\alpha}{2} (1 - 3\alpha) \quad (31)$$

which is approximately correct for every position of the load. As it can be seen, Equation 31 is in close agreement with Figure 6(c) and (d).

## CONCLUSION AND FUTURE WORK

The objective of this paper has been to introduce a simple numerical method for the analysis of suspended cables under vertical loads, which can be easily applied to the study of suspension bridges.

Both explicit equilibrium and tangent stiffness matrices for the cable have been derived. The implementation of these stiffness matrices in a general computer program for the analysis of structures is straightforward. Any planar structure with a parabolic cable can be solved in this manner, provided that the cable is only subjected to vertical loads.

The application of the proposed method to the analysis of suspension bridges is direct and can be simplified using some of the hypotheses of deflection theory (2–4). Although any formulation can be used, the flexural stiffness matrix for the beam in this work has been determined by finite differences. This has been done in order to reduce the number of variables, but will also help for the dynamic analyses.

By using dimensionless variables, parametric studies can be executed easily. The influence of every parameter in the equations is observed directly.

Some charts have been given for a single span suspension bridge, and trends of suspension bridge behavior have been discussed. It is hoped that these charts can be useful in the first phase of design as well as in the understanding of suspension bridge behavior.

## ACKNOWLEDGMENTS

This work was supported by a grant to the first author from the Comissionats per a Investigació i Recerca, Generalitat de Catalunya.

## REFERENCES

1. Buonopane, S. G., and D. P. Billington. Theory and History of Suspension Bridge Design from 1823 to 1940. *Journal of Structural Engineering*, Vol. 119, No. 3, 1993, pp. 954–977.
2. Pugsley, A. *The Theory of Suspension Bridges*. Edward Arnold, 2 ed., 1968.
3. Ulstrup, C. C. Rating and Preliminary Analysis of Suspension Bridges. *Journal of Structural Engineering*. Vol. 119, No. 9, 1993, pp. 2653–2679.
4. Steinman, D. B., *A Practical Treatise on Suspension Bridges*. J. Wiley & Sons, New York, 1953.
5. Irvine, M. *Cable Structures*. M.I.T. Press, Cambridge, Mass., 1981.
6. Abdel-Ghaffar, A. M. Vertical Vibration Analysis of Suspension Bridges. *Journal of the Structural Division*, Vol. 106, No. 10, 1980, pp. 2053–2075.

7. Chaudhury, N. K., and D. M. Brotton. Analysis of Vertical Flexural Oscillations of Suspension Bridges by Digital Computer. *Proc., International Symposium on Suspension Bridges*, Lisbon, 1966.
8. Jennings, A., and J. E. Mairs. Static Analysis of Suspension Bridges. *Journal of the Structural Division*, Vol. 98, No. 11, Nov. 1972, pp. 2433-2455.
9. Arzoumanidis, S. G. and M. P. Bienek. Finite Element Analysis of Suspension Bridges. *Comput. Struct.* Vol. 21, No. 6, 1985, pp. 1237-1256.
10. Cobo del Arco, D. *Static and Dynamic Analysis of Cable Structures*. Doctoral thesis, to be completed in 1996.
11. Crisfield, M. A. *Non-linear Finite Element Analysis of Solids and Structures*, Vol. 1. Wiley, 1991.
12. Wood, R. D., and B. Schrefler. Geometrically Non-Linear Analysis. A Correlation of Finite Element Notations, *International Journal for Numerical Methods in Engineering*, Vol. 12, 1978, pp. 635-642.
13. Jennings, A. Gravity Stiffness of Classical Suspension Bridges, *Journal of Structural Engineering*, Vol. 109, No. 1, Jan. 1983, pp. 16-36.

# FRP COMPOSITES AND OTHER MATERIALS FOR BRIDGES

---

# Shear Strengthening of Concrete Bridge Girders Using Carbon Fiber-Reinforced Plastic Sheets

---

Efrosini Drimoussis, *Buckland and Taylor, Ltd., Canada*

J. J. Roger Cheng, *University of Alberta, Canada*

Many older reinforced or prestressed concrete bridges designed in accordance with now obsolete design codes and for much lighter traffic loads have been found to be shear deficient. It is of great interest to develop rehabilitation techniques that are both structurally efficient and economically competitive. The main objective of the research program was to investigate the feasibility of strengthening concrete bridge girders for shear using carbon fiber-reinforced plastic (CFRP) sheets bonded externally to the webs of the girders. The advantages of such advanced composite materials include their high tensile strength, noncorrosive properties, light weight, and small sectional dimensions, all of which make them competitive with more traditional materials for use in rehabilitation applications. Three precast reinforced concrete bridge girders 9.1 m long, hat-shaped in section, were salvaged from a demolished bridge that had originally been constructed in the late 1950s. CFRP sheets were bonded to the vertical web faces in various arrangements, the members were tested to failure, and the results were compared with those associated with the unstrengthened condition. Shear failure was governed by the strength of the concrete rather than by the CFRP material, and the behavior indicated that anchorage of the sheets is a key consideration. The results showed an increase in shear capacity of between 21 and 55 percent. On the basis of the test results, mechanisms were proposed by which the bonded CFRP sheets contributed to the shear strength of the section, and a method was suggested for calculating this contribution.

There are approximately 14,000 highway bridges in operation in the Province of Alberta, Canada, most of which are reinforced or prestressed concrete structures. Many of these concrete bridges were designed and built more than 30 years ago in accordance with now obsolete standards. In particular, an extensive inspection and assessment program has identified many of these bridges as being shear deficient. Although this problem and its potential solutions are applicable to many types of concrete bridges, the discussion in this paper is limited to the "Type-E" girder, which forms the superstructure of about 50 highway bridges in the province. The Type-E girder is a simply supported precast reinforced concrete member designed in the late 1950s in accordance with AASHO-57 (1) and used in bridge construction for several years. It is hat-shaped in section and varies between 9.1 and 12.8 m in length. Placed side by side, the girders are transversely connected by means of a reinforced grouted shear key. All girders are identical, except that the longer ones have heavier flexural reinforcement. All girders are reinforced identically for shear. Schematic views of the cross section and elevation are shown in Figure 1.

In the years since the original design of the Type-E girder, the situation has changed on both the load and resistance sides of the equation. The design truck loading originally specified was the H20-S16 truck loading,

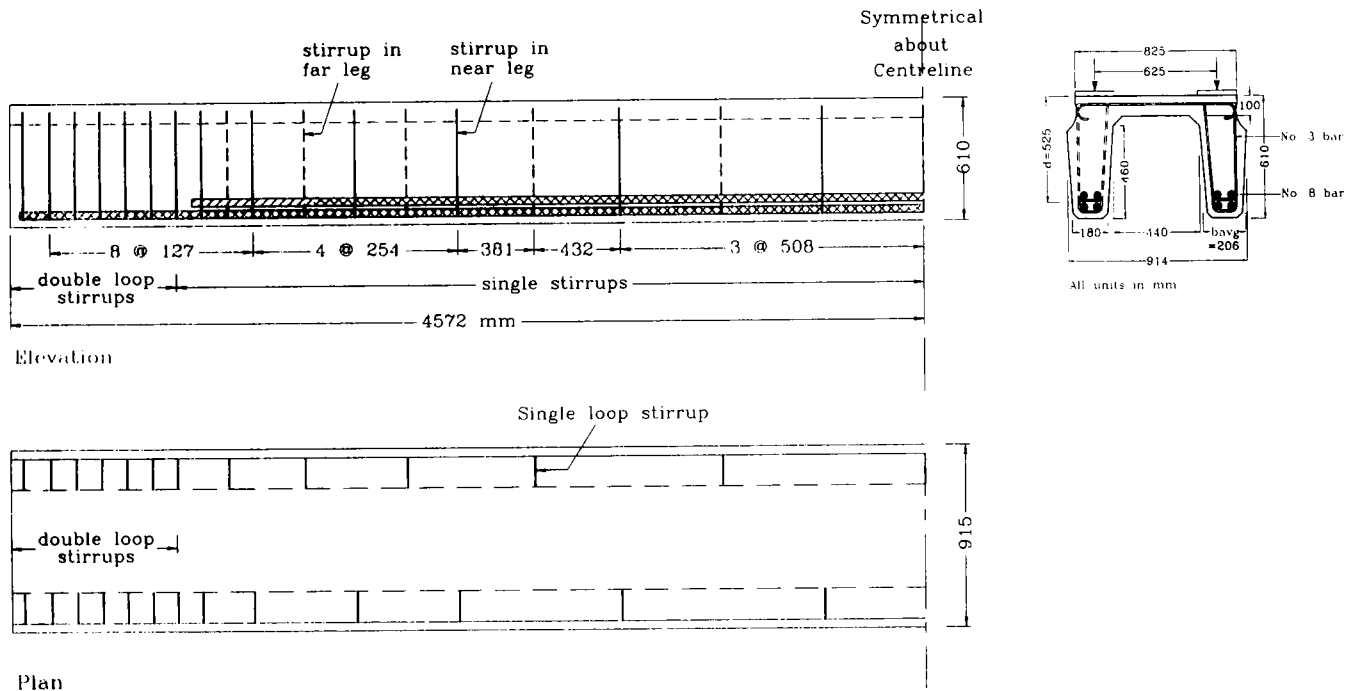


FIGURE 1 Typical elevation, plan and cross section of Type-E girder.

as defined in AASHO-57, with a total weight of  $W = 320$  kN. The maximum standard truck used in Alberta today,  $W = 647$  kN, is more than double the weight of the 1957 truck; in addition, traffic volume has increased significantly. On the resistance side, there are two fundamental differences between the original AASHO-57 shear provisions and those in common use today, such as AASHTO-89 (2). Changes have been made both to the way in which the allowable shear stress in the concrete is calculated and in the requirements for transverse reinforcement.

If, for example,  $f'_c = 20$  MPa, then the two codes give the following permissible shear stresses in the concrete:

$$\text{AASHO-57: } v_c = 0.03f'_c = 0.60 \text{ MPa} \quad (1)$$

$$\text{AASHTO-89: } v_c = 0.078 \sqrt{f'_c} = 0.35 \text{ MPa} \quad (2)$$

or

$$v_c = 0.075 \sqrt{f'_c} + 7.6\rho_w \frac{V_d}{M} = 0.46 \text{ MPa} \quad (3)$$

where  $\rho_w$  is the web reinforcement ratio,  $V$  and  $M$  are the design shear and moment, respectively, at the section being considered, and  $d$  is the effective depth. For this comparison,  $V_d/M$  was set equal to 1.0, which is the maximum permitted, and  $\rho_w$  was taken as 1.7 percent, which is appropriate for the members used in this test program and which is a reasonable value for under-reinforced members.

The second basic change in code shear requirements affects the amount of transverse reinforcement required. In AASHO-57 the spacing limits were as follows:

(a) Where stirrups were required to carry shear:

$$s_{\max} = 1/2 h \quad (4)$$

(b) Where stirrups were not required to carry shear:

$$s_{\max} = 3/4 h \quad (5)$$

where  $h$  is the overall depth of the beam. The current spacing requirements are expressed in terms of the effective depth:

$$s_{\max} = 0.50d \leq 600 \text{ mm} \quad (6)$$

In addition, according to AASHO-57, stirrups did not have to be provided until the allowable unit shearing stress for concrete ( $v_c$ ) was exceeded, with the exception of the webs of T-girders and box sections, which had to be reinforced with stirrups in all cases, in which case Equation 5 applied. In current codes, if one-half the permissible shear resistance provided by the concrete is exceeded, stirrups must be provided such that the following minimum area requirement is satisfied:

$$A_v > \frac{0.35b_w s}{f_y} \quad (7)$$

where

- $A_v$  = the area of shear reinforcement;
- $f_y$  = the specified yield stress of the reinforcement;
- and
- $s \leq s_{max}$ .

This area calculation is equivalent to providing enough web reinforcement to transmit a shear stress of 0.35 MPa (3). There was no such provision in the original code.

Analysis and evaluation of the original design have indicated that, although adequate in flexural capacity, the Type-E girders are, indeed, deficient in shear. Thorough field inspections have been carried out on all Type-E girder bridges and, along with various other problems, diagonal shear cracks have been observed in the webs of more than 60 percent of them, thus supporting the analytical results.

### STRENGTHENING FOR SHEAR DEFICIENCIES

Over the last 30 years various solutions have been implemented to upgrade existing structures for both shear and flexure. Ideally, a good repair technique will possess the following: ease of implementation; minimal disruption to use and service of the bridge during construction; minimal addition of dead weight or loss of clearance or both; efficient labor techniques; rapid installation; minimal disruption to the existing members; and adequate behavior under service conditions (e.g., fatigue, corrosion, fluctuating temperatures, and creep).

One means of increasing the shear capacity is to drill through the deck to install additional steel stirrups embedded within or placed adjacent to the webs (4,5). One disadvantage of such a solution is that installation requires drilling through the deck, which is awkward and labor intensive and disrupts traffic. The use of steel as a retrofit material adds considerable dead weight and may lead to corrosion problems. Alternatively, strengthening can be achieved by bonding steel plates to the exterior of members (6,7). Although this technique eliminates drilling and minimizes traffic disruption, the other disadvantages persist.

Some or all of the disadvantages described in the steel plating method may be eliminated by using advanced composite materials or fiber-reinforced plastics (FRPs) instead of steel plates. Although these FRPs come in a variety of forms and their properties can vary in some ways, they all possess certain advantages over more traditional materials, such as steel, which may make them particularly attractive for use in the rehabilitation of existing bridges. They are extremely strong and lightweight, resulting in a favorable strength-to-weight ratio. Their light weight makes them easy to handle and install and contributes negligibly to the

weight of the structure. They can be easily applied to concrete members and do not require special handling skills. FRPs are noncorrosive and appear to have good durability in exposed environments (8). Tests of externally FRP-bonded concrete beams under fatigue loading and at low temperatures (9) as well as creep tests (10), have shown good results, especially when carbon FRPs have been used.

Extensive research has been carried out in the last 10 years using a variety of uni- or bidirectional FRPs in plate or sheet form to strengthen existing concrete members (8). Primarily, the investigations have involved applying these materials to the tension flanges of beams to increase the flexural capacity. Although various researchers have demonstrated experimentally that this technique improves both the ultimate strength and stiffness of the members, very little consideration has been given to extending the concept to shear strengthening.

The primary objective of the research program described in this paper was to strengthen existing concrete bridge girders using a carbon fiber-reinforced plastic (CFRP) material to increase the shear capacity of the members. Further, the goal was to find a means of repair that could be achieved only from the underside of the bridge, thus avoiding traffic disruption or drilling through the deck, that is, through the top flange of the girders. The remainder of this paper outlines the experimental program undertaken to investigate the behavior and effectiveness of this strengthening technique. On the basis of the test results, a mechanism was proposed to model the behavior of the strengthened girders and to determine the shear capacity contributed by the CFRP sheets.

### EXPERIMENTAL PROGRAM

The experimental program consisted of tests of three precast reinforced concrete Type-E girders salvaged from a demolished highway bridge in Alberta. They were strengthened for shear externally using CFRP sheets bonded to the webs, failed in shear, and the results were compared with those associated with the unstrengthened condition. All girders were tested under symmetrical two-point loading, producing a constant moment region in the center and two equal shear spans (Figure 2). Each shear span of each girder was strengthened in a different manner; after failing one side, the girder was repaired and retested to fail the second. This allowed a total of five shear tests to be carried out.

### Description of Test Specimens

Typical elevation and cross-section details for the 9.1-m Type-E girder are shown in Figure 1. The member is

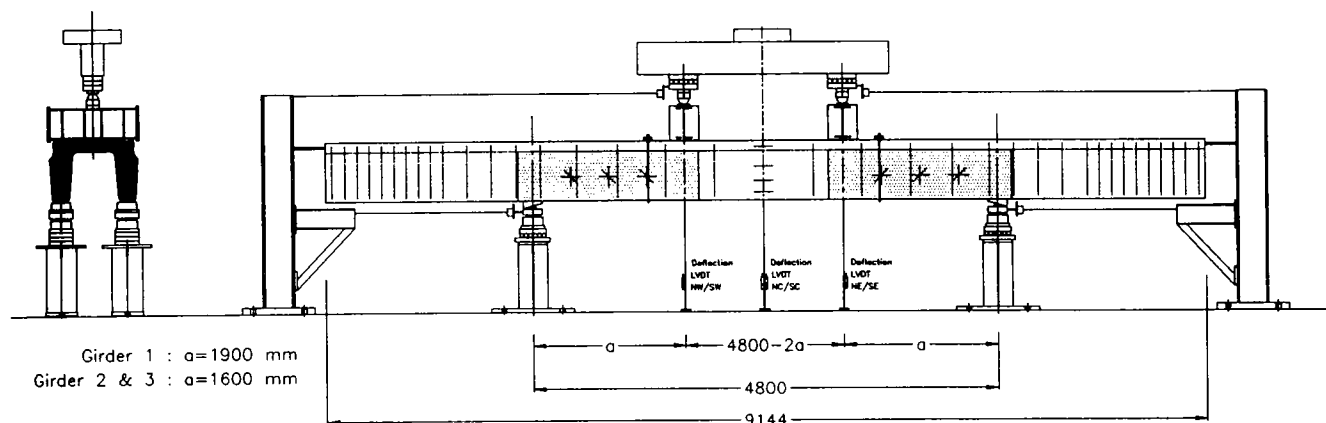


FIGURE 2 Elevation and cross section of 9.1-m girder in test setup.

610 mm deep and 914 mm wide, with eight 25-mm bars as longitudinal reinforcement and 10-mm bars forming looped stirrups. A peculiarity of this girder type is that, over most of the girder's length, the stirrups alternate from leg to leg (single loop stirrups). This means that, although the maximum spacing was specified according to Equation 5, it is actually twice this amount if considering only one leg. The design and geometry details, obtained from original drawings, were confirmed by measurement of the actual members tested, including the use of a rebar detector for locating stirrups and longitudinal bars. The stirrup spacings, per leg, varied from  $0.84$  to  $2.1d$  (440 to 1100 mm).

### Material Properties

The original specified material strengths were 27.6 MPa for concrete and 276 MPa for steel. For the purposes of this test program, twelve cores  $75 \times 150$  mm were removed from each of the specimens after testing. Three cores were removed from each leg, at each end of the girder, from outside the loaded region. The average concrete strength for the three girders was 27.8 MPa, with only a slight variation from girder to girder. On the basis of tensile tests of steel removed from the girders, the average yield stress of the flexural reinforcement was 384 MPa and the average yield stress of the stirrups was 395 MPa. The actual material properties as tested for each girder were used in the analysis.

The CFRP sheets consisted of unidirectional continuous carbon fibers in a pliable sheet form, pre-impregnated with an epoxy resin. The sheets were bonded to the concrete surface with an epoxy resin, which also formed the matrix of the finished composite. The composite has a specified ultimate tensile strength of 2250 MPa and a specified modulus of elasticity of 141 GPa.

In the field, lay up is not as controlled, irregularities may be present (e.g., tiny voids) in the matrix or adhesive, and the material is bonded to a substrate. Perhaps more realistic results would be obtained from samples laid up in a manner similar to that for the practical application. Therefore, rather than perform uniaxial tension tests on CFRP coupons prepared under ideal laboratory conditions, samples were laid up in the same manner as that used on the girder tests; sheets were bonded to two small concrete blocks, which were then pushed apart (Figure 3). Under these conditions, a failure stress of 625 MPa and modulus of elasticity of 114 GPa were obtained. Failure occurred by concrete delamination, a mode similar to that observed in the full-scale girder tests. The discrepancy between the specified and experimental stiffnesses exists because the sheets used in the small block tests were fully cured and therefore had a larger cross section than the coupons normally used for CFRP material testing.

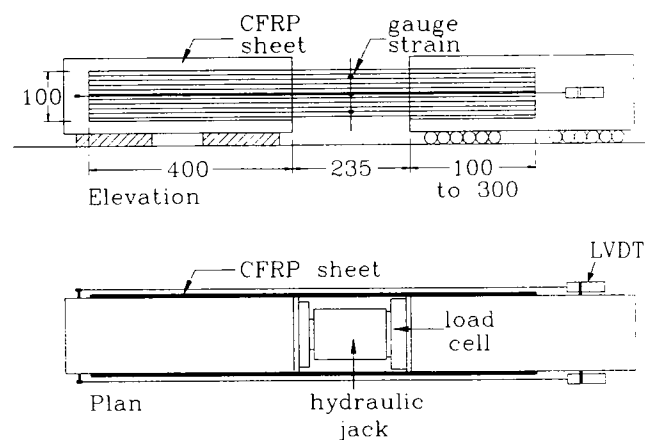


FIGURE 3 Schematic of test setup for small concrete block tests.



## CFRP Strengthening Schemes

For the strengthening technique to be a practical solution for use on this type of bridge, the limited access in the field (i.e., only from beneath the structure) had to be taken into consideration. When the girders are in place in a bridge, the outer faces of the webs are almost flush against each other, with only a small gap between adjacent legs. Therefore, access is available only to the inside web faces and bottom flanges of the girders. The depth of the girder over which sheets can be applied is thus also limited. As much as possible, the vertical bonded length was varied from specimen to specimen.

The sheets were applied continuously throughout the shear span (shaded regions in Figure 2); the variations for each girder are summarized in Figure 4. Either one or two layers of CFRP were bonded to the webs. One layer was always oriented vertically. The second, if used, was oriented horizontally. The east shear span of Girder 1 was left unstrengthened to serve as a control. In the west span, two layers of CFRP sheets were used—the bottom layer oriented vertically and the top one horizontally. The vertical sheets extended between the top and bottom chamfers, 430 mm in length. The horizontal sheet was centered vertically on the inside face of the web leg and was the width of the sheet (300 mm). This strengthening arrangement was repeated on

the east shear span of Girder 2 as the first girder failed prematurely in flexure before failing the west span in shear. The west shear span of Girder 2 was strengthened with one vertical layer only. In this case, the sheet was extended slightly higher, along the chamfer to meet the underside of the top flange. Because the west span of Girder 1 failed prematurely in flexure before failing in shear, three longitudinal layers of CFRP sheets were applied, in addition to shear strengthening, to the bottom flange of Girders 2 and 3 to avoid flexural failure.

In the east span of Girder 3, the two-layer scheme of the west span of Girder 2 was again used, with the difference that the vertical sheet was extended, to wrap right around the bottom of the girder and, at the top, 30 mm onto the underside of the top flange. The west span was strengthened with one vertical layer, which not only wrapped around the bottom of the girder but continued up the outer face of the web leg, as high as possible, given that the concrete was sometimes chipped away where the group key had been. This last method was not practicable as a field application but gave an indication of the improvement that was possible if the member could be strengthened on both sides of both legs—perhaps more feasible on other types of girder cross sections. Note, however, that the bonded length was even shorter on the outer face, and this may affect results more than the advantage gained.

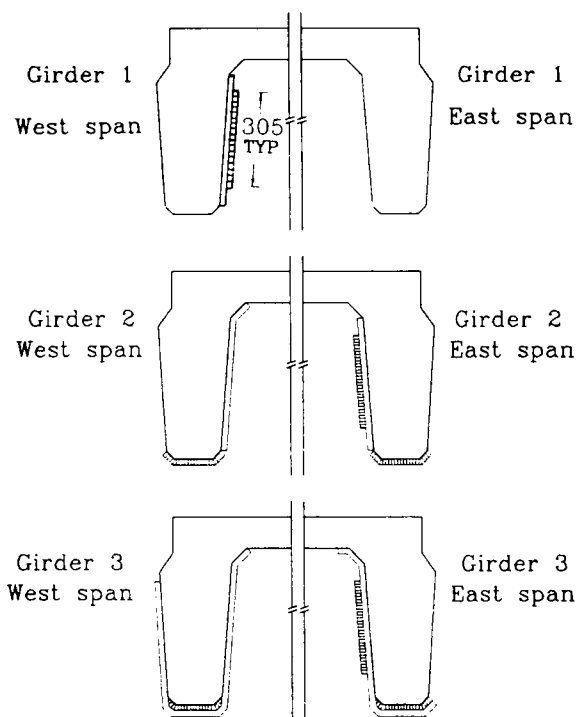


FIGURE 4 Cross sections showing CFRP strengthening schemes.

## Testing

The general test setup is shown in Figure 1. All girders were tested in symmetric four-point bending over a 4.8-m simple span. The objective was to achieve as high a  $V/M$  ratio as possible to avoid failing prematurely in flexure. The shear span/depth ( $a/d$ ) ratio was thus minimized as much as possible while remaining in the beam behavior range and avoiding arching action. Preliminary analysis indicated that  $a/d = 3.6$  would be appropriate. This ratio was further decreased for Girders 2 and 3 after Test 2 of Girder 1 ended with a flexural failure. Shear spans were 1.9, 1.6, and 1.6 m for Girders 1, 2 and 3, respectively.

For two reasons the supports were located as far from the ends of the girder as possible without cracking the top concrete. First, they were located beyond all bar cutoff locations to avoid the complication of bar termination and anchorage problems, and to have consistent moment capacity throughout the tested region. Second, this permitted testing in the region of the girder with fewest stirrups, allowing the potential for most improvement with the strengthening method. It is acknowledged that this is obviously not realistic given that these girders are actually simply supported at the ends, but the primary objective was to test for an in-

crease in shear capacity under the worst-case situation. The load applied by the testing machine was distributed to loading pads centered over the legs—a total of four load points. The girder was supported under each leg; that is, a total of four supports, each of which was monitored by a load cell. Thus, each leg was simply supported and, taking into account the various stirrup arrangements and the locally measured reactions, four shear spans could be analyzed independently.

Vertical deflections were measured with 25-mm linear variable differential transformers (LVDTs) located under both legs, at each of the load points and at mid-span. Strains on the concrete surface on the outer faces of the girder were measured using a 200-mm Demec gauge. Electrical resistance strain gauges with a gauge length of 5 mm were used extensively to obtain a distribution of strains over the strengthened shear span. In both shear spans, 2.5-mm LVDTs mounted between the top and bottom flanges at the location of stirrups measured the overall depth change of the girder as an indirect measure of vertical strain. These measurements, along with the visual aid of surface crack patterns, helped indicate if or when the stirrups were yielding. Because each girder was tested more than once, the first tests were continued only until the load leveled off. The tests were then stopped, and the specimen was unloaded completely. To test both shear spans of each girder, assuming that one side would fail first by a significant margin, some means of repairing the failed span was required. This was achieved by using external stirrups consisting of four threaded tie rods 25 mm in diameter at six locations along the shear span. After the shear span failed, the test was stopped and the specimen was completely unloaded. Holes were drilled through the top flange between the web legs, and rods were in-

stalled, braced with two HSS members ( $75 \times 100$  mm) above and below the member.

## TEST RESULTS

Load-deflection curves are shown for all tests in Figure 5. The overall failure mode of all the shear failures was by diagonal tension. The CFRP sheets affected neither this basic mechanism nor the onset of cracking or the angle of the compression diagonal that formed. The overall cracking pattern development, as observed on the outer faces of the girders, was not noticeably altered by the presence of the bonded sheets but was governed by the distribution of the internal steel stirrups and the concrete strength. The effect of the CFRP sheets was noticed once the cracks began to open up, at which time the sheets began to influence the behavior of the member.

The bond between the CFRP sheets and the concrete substrate was generally excellent. Debonding occurred only in areas in which the concrete surface was very uneven. Although "failure" of the sheets is generally described in the following as "peeling," this refers to the sheet peeling concrete away, such that the failure is in the concrete rather than in the bond line. No disturbance was noted in the CFRP sheets until the tests were quite advanced, typically about 90 percent of the ultimate load. In every case, visible signs were preceded by cracking or crackling noises, which continued until failure. These were not characteristic concrete cracking noises but sounded more like wood cracking. This sound was caused by CFRP sheets peeling away the concrete substrate and, in doing so, not only cracking through the concrete but failing through its own resin

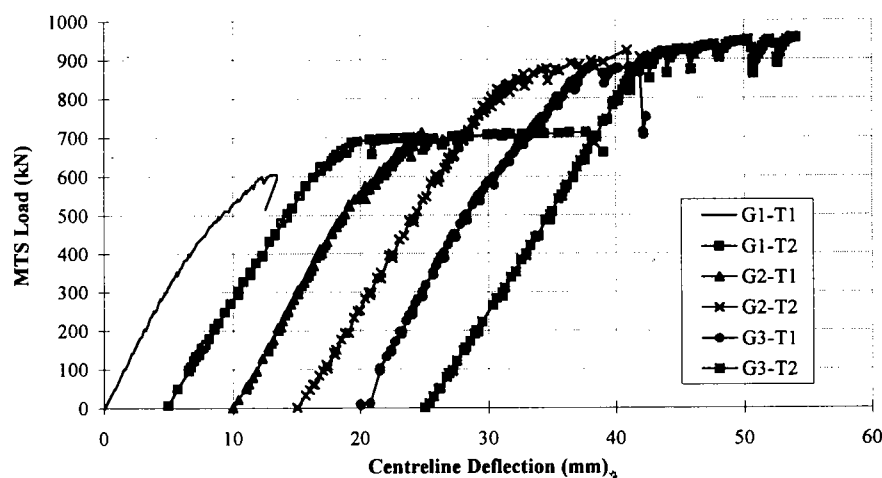


FIGURE 5 Total load versus midspan deflection.

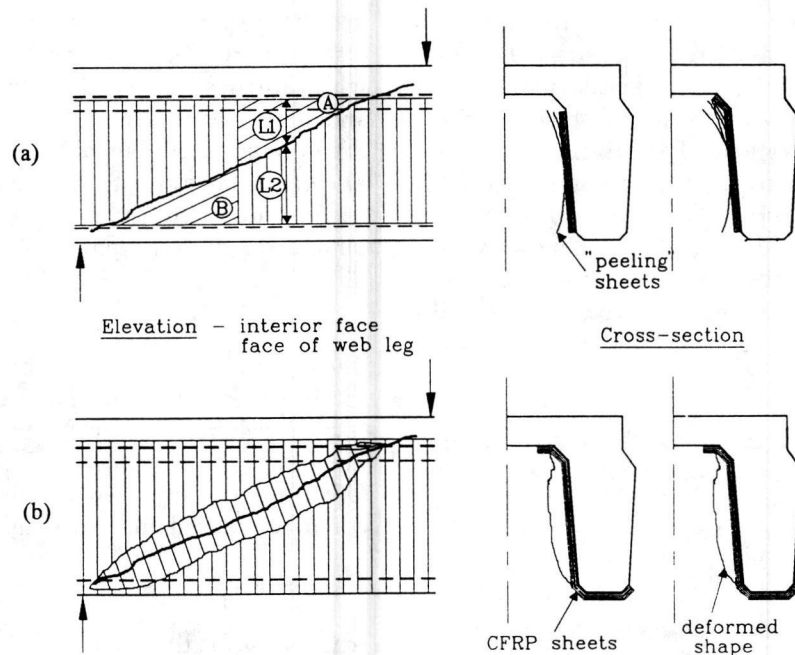


FIGURE 6 Progression of failure of cracked section with bonded CFRP sheets.

matrix once peeled away from the main body. In no cases did the fibers fail in tension. Although they broke in some instances, this was caused by local stress concentrations. The horizontal sheets did not seem to have a significant influence on the behavior of the member; no difference was seen in the load capacity achieved.

Peeling always began near the top or bottom edges of the sheets, but the severity and progression of failure depended a great deal on the detailing and bonded lengths provided. Figure 6 shows failure cracks spanned by the CFRP sheets. The vertical hatching indicates fibers and concrete still intact. The diagonal hatching indicates where the sheets have peeled away the concrete. If the anchorage provided was not adequate, failure progressed as shown in Figure 6a; the first signs of distress were at the top or bottom edges of the sheets. To extend the sheets up the top chamfer, they had to be bent around a relatively abrupt corner, which made it difficult to get as good a bond to the concrete in the corner. Under increasing load, tension in the sheet straightened the bend and the sheet began to "pop off" along this corner, although it remained well bonded above along the chamfer itself and below along the height of the web. This was typical of the first sign of distress seen in cases where the sheet was continued up around this corner of the girder. Once the sheets began peeling away the concrete at the top and bottom (Points A and B), failure continued progressively toward the crack line. The peeling began once the bonded length

L1 or L2 or both, became small enough. During the observed tests, this occurred when L1 or L2 approached about 75 mm. The situation shown schematically in Figure 6a was exhibited by Girders 1 and 2. This can also be seen in Figure 7; delamination of sheet and concrete has occurred from both the top and bottom edges. In Figures 7 and 8, the white lines drawn on the CFRP surface indicate the extent of peeling or bulging.

If the anchorage is good enough at top and bottom, then the progression of failure will be more like that in

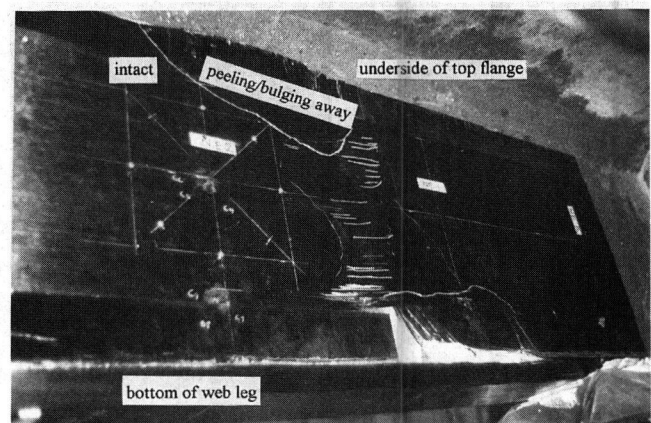


FIGURE 7 Interior face of one web leg, after failure (Girder 2, Test 1).

Figure 6b; the sheets were not peeling away the concrete layer but were bulging away from the substrate. As long as the sheets remain anchored, the tensile strength of the sheet can be developed, despite the bulging, and they can continue to carry load. The details used in the shear spans of Girder 3 resulted in this improved behavior, as can also be seen in Figure 8. Although this bulging continued up to the top flange, almost everywhere the CFRP remained attached to the concrete along the chamfer, and thus the tension in the sheets could continue to be mobilized over the full height of the sheets, unlike the places where the sheets pulled away completely from the bottom flange up. In both spans of Girder 3, the sheets wrapped around the bottom flange, and this kind of bottom-edge peeling did not occur.

### DISCUSSION OF TEST RESULTS

Because each of the girder legs was loaded and supported concentrically, the shear capacity of the section was determined per leg using the load measured by the load cell at the support and based on a cross section consisting of one leg only.

The total shear capacity is given by

$$V_n = V_c + V_s + V_{CFRP} \quad (8)$$

where  $V_c$ ,  $V_s$  and  $V_{CFRP}$  are the shear resistances provided by the concrete, stirrups, and CFRP sheets, respectively.

To account for the force carried by the stirrups, each leg in each span was considered individually. Observations of the crack patterns and measurement of vertical member deformations indicated if a stirrup was mobilized. Because there were only ever one or two stirrups

per shear span, in almost all cases it was clear from crack pattern observations and measured vertical strains which stirrups were yielding. In two cases, observations and measured strains did not warrant neglecting the stirrup completely but did not support yielding either. Therefore, an estimate was made of the force in the stirrup, equivalent to half a stirrup. The stirrup contribution was then calculated as

$$V_s = A_v f_y \quad (9)$$

The control section consisted of the northeast and southeast legs of Girder 1. Both these regions had one stirrup yielding, and this information was used with Equation 9 to calculate the  $V_s$  contribution. Because no CFRP sheets were used in the east span, Equation 8 could be reduced and rearranged as

$$V_{cTEST} = V_{nTEST} - V_{sTEST}$$

where  $V_{nTEST}$  is the average of the two load cell readings at the northeast and southeast reactions, including the shear caused by the girder's own weight.

Table 1 summarizes the shear capacity results for each leg of the shear span.  $V_{nTEST}$  comes directly from the test results and is the maximum shear carried by that leg at failure as measured by the reaction load cell, including the girder's own weight. The concrete contribution was calculated using the actual material properties and the Zsutty formulation (3):

$$v_c = 2.137 (f'_c \rho_w d/a)^{1/3} \quad (10)$$

The shear capacity attributed to the sheets was calculated as:

$$V_{CFRP} = V_{nTEST} - V_c - V_s$$

Table 1 shows the calculated values for  $V_c$ ,  $V_s$ , and  $V_{CFRP}$ . The shear carried by each specimen,  $V_{nTEST}$ , was compared with the shear carried by the control section,  $V_{G1T1}$  (subscript G1T1 denotes Girder 1, Test 1) to determine the increase in shear strength made possible by the use of the bonded CFRP sheets. Because the control section included only one internal steel stirrup per leg, a direct comparison could be made only to other sections with only one stirrup per leg. If the test section had a fewer or greater number of stirrups, the comparison was made possible by adjusting  $V_{G1T1}$  appropriately. Hence, for example, for the southeast leg of G2-T1, the ratio  $V_{nTEST}/V_{G1T1}$  was calculated as the following:

$$\frac{V_{nTEST}}{V_{G1T1}} = \frac{192 \text{ kN}}{169 \text{ kN} - \frac{V_s}{2} = \frac{53.5 \text{ kN}}{2}}$$

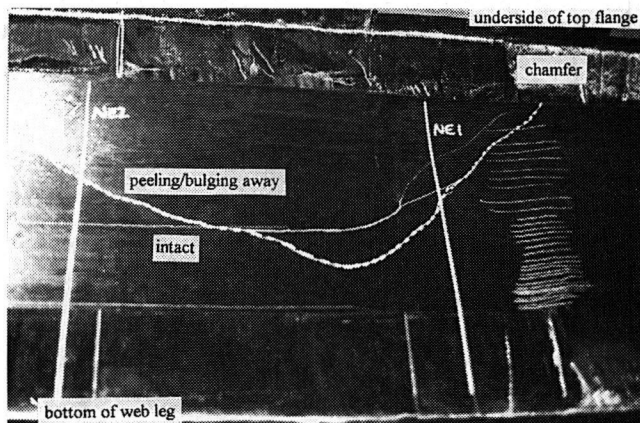


FIGURE 8 Interior face of one web leg, after failure (Girder 3, Test 1).

TABLE 1 Shear Capacity Results of Girder Tests

	Failure Mode	Critical leg	No. of Stirrups Crossed	$V_{nTEST}$ (kN)	$V_c$ (kN)	$V_s$ (kN)	$V_{CFRP}$ (kN)	$\frac{V_{CFRP}}{V_{nTEST}}$	$\frac{V_{nTEST}}{V_{G1T1}}$
<b>Girder 1</b>									
Test 1 (Control)	diagonal	South East <sup>a</sup>	1	168	115.7	53.8	--	--	--
	shear	North East <sup>a</sup>	1	171	115.7	53.8	--	--	--
Test 2	flexure	South West	0.5	184	115.7	26.9	41.4	0.23	1.29
		North West	1	205	115.7	53.8	35.5	0.17	1.21
<b>Girder 2</b>									
Test 1	diagonal	South East	0.5	192	126.9	26.75	38.35	0.20	1.35
	shear	North East <sup>a</sup>	0.5	198	126.9	26.75	44.35	0.22	1.39
Test 2	diagonal	South West <sup>a</sup>	1	229	126.9	53.5	48.6	0.21	1.35
	shear	North West <sup>a</sup>	1.5	263	126.9	80.3	55.8	0.21	1.34
<b>Girder 3</b>									
Test 1	diagonal	South East	1	237	128.1	54.8	54.1	0.23	1.40
	shear	North East <sup>a</sup>	1	235	128.1	54.8	52.1	0.22	1.39
Test 2	diagonal	South West <sup>a</sup>	1	239	128.1	54.8	56.1	0.23	1.41
	shear	North West <sup>a</sup>	1	263	128.1	54.8	80.1	0.30	1.55

<sup>a</sup> Critical leg(s)

As seen in the Table 1, the CFRP-strengthened sections showed an improvement of 21 to 55 percent over G1-T1. Included in Table 1 is the ratio  $V_{CFRP}/V_{nTEST}$ , which indicates the proportion of the shear capacity of the section attributed to the bonded CFRP sheets. This ratio ranged between 0.17 and 0.30. The degree to which the composite sheets improved the shear capacity did not seem to clearly depend on particular parameters. This was most likely because of the interaction of various conditions, such as strength of concrete, effectiveness of the internal stirrups, and effectiveness of the bonded sheets.

It is proposed that the CFRP sheets bonded to the webs of the members contribute to the shear strength of the section by the interaction of two separate mechanisms. The first mechanism is one of crack control, in which the sheets act as "bandages" to prevent or limit cracking. In the second mechanism, the fibers may be modeled as a series of "stirrups" and then analyzed in a manner analogous to that used for the analysis of sections reinforced with internal steel stirrups. Both of these two mechanisms will be discussed and predictions of CFRP contribution to shear strength will be calculated on the basis of the second model.

In the first mechanism, CFRP sheets can be effective in providing crack control when glued to the surface of concrete members. Fibers oriented in any direction can

contribute to this mechanism, although they will be most efficient when oriented perpendicular to the crack line. If cracks are pre-existing, CFRP sheets may easily be applied in the optimum orientation for repair purposes and would be even more effective if the member is first jacked so as to close the cracks before the sheets are applied. By holding the cracked surfaces together, the CFRP sheets can help increase the effective shear strength contribution of the concrete by maintaining or improving interface shear transfer. This effect may significantly improve the shear strength of the section.

In the second mechanism, the CFRP sheets are modeled as a series of discrete stirrups. If the validity of this assumption is accepted, then the contribution of the sheets may be determined by existing methods of analysis used for steel stirrups, such as the truss model analogy. As is the case for internal steel stirrups, the CFRP sheets may be oriented either vertically or inclined to the vertical. For simplicity of design, to deal with stress reversals, and to avoid errors in construction, vertically oriented stirrups are preferable. During testing, the vertical fibers spanned over bulging sections, as long as anchorage at the top and bottom was sufficient, and so continued to carry load over their length for as long as they remained in this condition.

The familiar truss equation for shear was modified so that it could be applied to the use of bonded external

sheets and includes several redefined terms:

$$V_{\text{CFRP}} = \frac{A_{\text{CFRP}} \sigma_{\text{eff}} l_{\text{eff}}}{s} \quad (11)$$

where

- $A_{\text{CFRP}}$  = the cross-sectional area of one stirrup;
- $s$  = the spacing of the stirrups;
- $l_{\text{eff}}$  = the effective length of the sheets; and
- $\sigma_{\text{eff}}$  = the design stress level used.

Figure 9 shows the definition of these terms graphically.  $A_{\text{CFRP}}$  and  $s$  depend on the layout of sheets. If the sheets are applied in strips, then  $A_{\text{CFRP}}$  is simply the product of the width of one strip and the thickness of the sheets. In the case of the girders tested, the sheets were bonded continuously through the shear span. In this case, a tributary width equal to the spacing,  $s$ , must be assumed, as shown in Figure 9. In this analysis,  $s$  was taken as 100 mm. The results do not depend on the tributary width used, although  $s$  should be kept reasonably small. Once  $s$  is set,  $A_{\text{CFRP}}$  may be calculated as before. The thickness of the sheets used was approximately 0.2 mm.

The stress level,  $\sigma_{\text{eff}}$ , is not the specified ultimate strength of the CFRP material, but some reduced value. For this analysis, the results of the CFRP material testing were used. To check the reasonableness of this value, estimated and measured strains were compared. Using the test results for  $\sigma_{\text{eff}}$  (625 MPa) and modulus of elasticity ( $E = 114$  GPa), a maximum strain of  $\epsilon = 5482 \mu\epsilon$  was obtained. The highest strain measured in the direction of the vertically oriented fibers was 5084  $\mu\epsilon$ . This indicated that the stress level used was reasonable.

The final parameter,  $l_{\text{eff}}$ , is the effective length of the fiber sheets. The sheets are not effective over their full length but require some minimum length with which they can be adequately anchored. As described earlier,

if the crackline intercepts the sheets too close to the edge, the sheets will begin to peel away the concrete, leading to failure. The anchorage length required was estimated on the basis of test observations of the minimum length required beyond a crack to avoid peeling. If adequate means of anchorage is provided at the top or bottom or both, it may not be necessary to reduce the total length of sheets applied.

The contribution of the sheets to the shear strength of the section ( $V_{\text{CFRP}}$ ) was calculated using Equation 11, and the results are summarized in Table 2. The concrete and steel stirrup contributions (summarized in Table 1) were added to the predicted  $V_{\text{CFRP}}$  values to obtain a total predicted shear capacity,  $V_{\text{PRED}}$ . When this value was compared with  $V_{\text{TEST}}$ , the agreement was reasonable, except for the west span of Girder 3, which had CFRP sheets bonded to both faces of the web legs. The larger discrepancy may be because the minimum anchorage length used may not have been as appropriate.

Although the results of the analysis seem to predict well the test results, it is important to note that the validity of the approach may not hold when extended to other types of members. The analysis was based on a very particular type of member and must be verified more rigorously for the more general case, especially for the definition of  $l_{\text{eff}}$ .

## SUMMARY AND CONCLUSIONS

Despite the limitations inherent in using pre-existing specimens, and the limited number of tests that were carried out, several conclusions can be drawn from the results of this investigation. The CFRP sheets bonded to the web faces of the girders increased the shear capacity of the sections by 21 to 55 percent. The bonded sheets did not change the fundamental shear failure mode of the specimens, which was always by diagonal tension. The failures of the specimens were ultimately governed by the strength of the concrete, rather than by the strength of the bonded sheets. The bonded length or anchorage, or both, of the sheets was an important parameter. The longer the bonded length provided, the better the performance of the strengthened member. Anchorage may be improved if longer bonded lengths are provided or if physical anchorage is used, for example, wrapping around the member. Further parametric studies performed on carefully designed laboratory specimens will be able to confirm or further develop the method proposed for predicting the shear strength contribution of the bonded CFRP sheets. Because the intention is to use the CFRP material to strengthen existing bridges, further research is still required to investigate long-term effects of environmental exposure, fatigue, and other serviceability and durability issues.

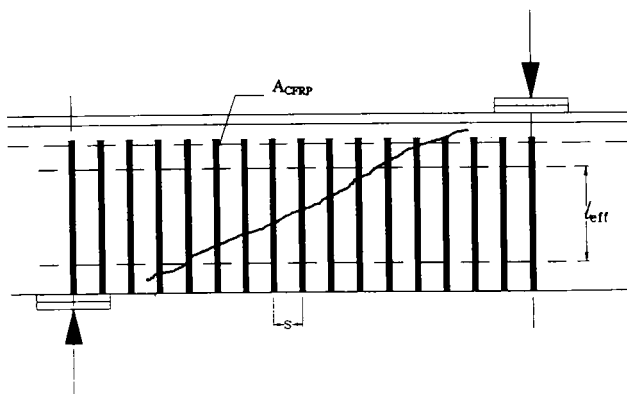


FIGURE 9 Truss equation definitions.



TABLE 2 CFRP Shear Contribution Predictions

Shear Span	Leg	Sheet Pattern	$l_{eff}$ (mm)	Predicted			$V_{PRED} =$		
				$V_{CFRP}$ (kN)	$V_c$ (kN)	$V_s$ (kN)	$V_{CFRP} +$ $V_c + V_s$	$V_{nTEST}$ (kN)	$\frac{V_{nTEST}}{V_{PRED}}$
G1-West	South	(a)	280	35.0	115.7	26.9	177.6 <sup>a</sup>	184.0	1.04
	North				115.7	53.8	204.5	205.0	1.00
G2-East	South	(a)	280	35.0	126.9	26.75	188.7	192.0	1.02
	North				126.9	26.75	153.7	198.0	1.29
G2-West	South	(b)	354	44.2	126.9	53.5	224.6	229.0	1.02
	North				126.9	80.3	251.4	263.0	1.05
G3-East	South	(c)	455	57.3	128.1	54.8	240.2	237.0	0.99
	North				128.1	54.8	240.2	235.0	0.98
G3-West	South	(d)	786 <sup>a</sup>	97.9	128.1	54.8	280.8	239.0	0.85
	North				128.1	54.8	280.8	263.0	0.94

<sup>a</sup> Includes both faces of webs

## ACKNOWLEDGMENTS

Funding for this project was provided by Alberta Transportation and Utilities. The technical assistance of T. Morrison and S. N. Samejima is gratefully acknowledged.

## REFERENCES

1. *Standard Specifications for Highway Bridges*, 7th ed. AASHTO, Washington, D.C., 1957.
2. *Standard Specifications for Highway Bridges*, 14th ed. AASHTO, Washington, D.C., 1989.
3. MacGregor, J. G. *Reinforced Concrete—Mechanics and Design*. Prentice Hall, Englewood Cliffs, N.J., 1992.
4. Klein, G. J., and P. L. Popovic. Shear Strength Evaluation of Existing Concrete Bridges. *Strength Evaluation of Existing Concrete Bridges*. ACI SP-88, 1985, pp. 199–224.
5. Ramsay, B. Evaluation and Strengthening of Concrete T-Girder Bridges for Shear. *Developments in Short and Medium Span Bridge Engineering*, Toronto, Ontario, Canada, 1990, pp. 381–391.
6. Eberline, D. K., F. W. Klaiber, and K. Dunker. Bridge Strengthening with Epoxy-Bonded Steel Plates. In *Transportation Research Record 1180*, TRB, National Research Council, Washington, D.C., 1988, pp. 7–11.
7. Klaiber, F. W., K. F. Dunker, T. J. Wipf, and W. W. Sanders. *NCHRP Report 293: Methods of Strengthening Existing Highway Bridges*. TRB, National Research Council, Washington, D.C., 1987.
8. Mufti, A. A., M. A. Erki, and L. G. Jaeger, eds. *Advanced Composite Materials with Applications to Bridges*. Canadian Society for Civil Engineering, Montreal, Quebec, Canada, 1991.
9. Meier, U., M. Deuring, H. Meier, and G. Schwegler. Strengthening of Structures with CFRP Laminates: Research and Applications in Switzerland. In *Proc., 1st International Conference on Advanced Composite Materials in Bridges and Structures*, Sherbrooke, Quebec, Canada, 1992, pp. 243–251.
10. Plevris, N., and T. C. Triantafillou. Time-Dependent Behavior of RC Members Strengthened with FRP Laminates. *Journal of Structural Engineering*, ASCE, Vol. 120, No. 3, 1994, pp. 1016–1037.

# Advanced Composites for Bridge Infrastructure Renewal

---

Frieder Seible, Gilbert A. Hegemier, and Vistasp Karbhari, *University of California, San Diego*

Applications of advanced composite materials such as glass fibers, aramids, or carbon fibers in polymer matrices are important in extending the life of our nation's bridge infrastructure into the 21st century. The increasing number of deficient bridge structures necessitates the rapid development of new rehabilitation technologies in the form of new materials and applications, with proven structural effectiveness, quality control, durability, and affordability. Advanced composite materials offer unique mechanical and durability characteristics that can affect bridge infrastructure renewal. Recent developments in automated manufacturing and application processes of advanced composite structural components indicate that not only structurally, but also economically, these new materials are becoming very competitive in civil engineering applications. Research at the University of California, San Diego (UCSD), by the Advanced Composites Technology Transfer Consortium (ACTT), shows that, for example, seismically deficient bridge columns can be wrapped with carbon fibers in an automated fashion, reducing current time requirements for equivalent steel jacket installations, and advanced composite replacement bridge decks can be built in one-step manufacturing processes at weight savings by a factor of 10 or more over conventional concrete decks.

Problems with the existing bridge inventory range from wear and environmental deterioration of structural components to increased traffic load demands, and from insufficient detailing at the time of the original design to inadequate maintenance and rehabilitation measures. An estimated 40 percent of all bridges are believed structurally deficient or obsolete, requiring repair, strengthening, widening, or replacement. In addition to increasing or changing traffic demands, common deficiencies include:

1. Deck deterioration due to wear, de-icing salts, temperature and freeze/thaw cycles, chain beating, etc.,
2. Scour at bridge substructures in riverbeds,
3. Corrosion of structural steel members,
4. Corrosion of reinforcement in structural concrete, both mild and post-tensioned,
5. Dynamic response problems under extreme wind or earthquake loads, and
6. Aging of materials.

With the majority of the U.S. bridge inventory built in the fifties and sixties, many bridges are at an age where environmental deterioration, wear, and changing demands require rehabilitation and upgrading measures. Repair, strengthening, and/or retrofitting technologies are still at a state where most applications are empirical, based on experience and trial and error



rather than on a sound scientific basis, without the benefits of large-scale experimental verification or adequate analytical predictive and diagnostic modeling.

The art of rehabilitation needs to be quickly developed into a broad-based science to provide the required technical database for the proper assessment of existing structural condition, materials and application processes, combined structural behavior of existing and added components, durability, and environmental impact. The large volume of rehabilitation work requires the development of new technologies based on new materials, new manufacturing processes and, to the civil construction area, new industries, in order to extend the bridge inventory at current service levels into the 21st century.

Advanced composite materials, primarily developed and used in the defense and aerospace industries, offer unique mechanical and chemical characteristics in terms of strength, stiffness, durability, and adhesion to conventional structural materials, with great potential for a wide variety of infrastructure rehabilitation applications. While past attempts to introduce advanced composite materials such as glass, aramid, or carbon fiber polymer matrix composites to the civil construction area have proven uneconomical, recent advances can make advanced composite materials affordable to a degree, where, in combination with strength, weight, and ease of installation benefits, very competitive rehabilitation systems can be developed.

An Advanced Research Project Agency (ARPA) Technology Reinvestment Project (TRP) program conducted by the Advanced Composites Technology Transfer Consortium (ACTT) at the University of California, San Diego (UCSD), addresses the development and application of advanced composites for bridge infrastructure renewal in the form of automated polymer matrix composite (PMC) manufacturing and retrofit technology development for deficient steel and concrete bridges, concrete deck replacement by all PMC bridge decks, and new all advanced composite bridge systems.

#### OPPORTUNITIES FOR ADVANCED COMPOSITES IN BRIDGE INFRASTRUCTURE RENEWAL

Advanced composites are materials created through the combination of several material phases, one or more serving as the reinforcement and the other as the matrix. The idea of an advanced composite is analogous to that of reinforced concrete. However, advanced composites present immense opportunities for the tailoring of the material to fit the specific requirements of structural elements. Special mechanical and chemical characteristics of advanced composites, as well as their durability in the civil environment, make them attractive for

use in infrastructure rehabilitation. Some of the generic advantages that motivate the investigation for use of advanced composites in bridge repair and renewal are:

1. High strength-to-weight ratio,
2. High stiffness-to-weight ratio,
3. Resistance to chemical attack,
4. Corrosion resistance,
5. Good fatigue resistance,
6. Controllable thermal expansion characteristics, and
7. Unique and controllable damping characteristics.

These advantages, combined with the potential to tailor materials for enhanced performance (such as crash resistance, damping, etc.), have led to increased research into the use of composites in civil infrastructure related applications. For the successful implementation of advanced composites in all of these applications, however, it is essential to understand that design cannot be done following the metals paradigm. Design decisions for composites are coupled to such an extreme degree that decisions made regarding materials, configuration, and processes have intricate connections and interrelations (Figure 1).

A decision made with regard to any one of these has ramifications on the others. For example, if pultrusion were selected as the manufacturing process, fabrication is restricted to constant cross-section products with a large percentage of reinforcement in the axial direction. Similarly, the choice of 3D woven architectures in near-net shape would almost automatically result in the selection of resin transfer molding (RTM) as the manufacturing process. This choice in turn would result in the deselection of matrix material choices to the thermoset family, based on viscosity requirements. The need for cylindrical structural elements presents the opportunity to use a number of fabrication technologies, but the final choice will be determined not only on the basis of shape, but also on the orientation needed. A need for continuous fiber in the hoop direction almost always predicates the selection of a winding type of operation over others because of the intrinsic capability to lay down continuous fibers in tension. In the case of advanced composites, the design process can be thought of as the management of the product realization process (PRP) in the concurrent fashion. A generic materials transformation process for composites is depicted in Figure 2. Within each step, the designer (or design team) faces a number of alternatives (including the possibility of skipping the step). Given the many alternate routes and the implications of early decisions on product competitiveness, the successful completion of the conceptual stage of the PRP, which includes the design of the materials transformation process, is of utmost importance.

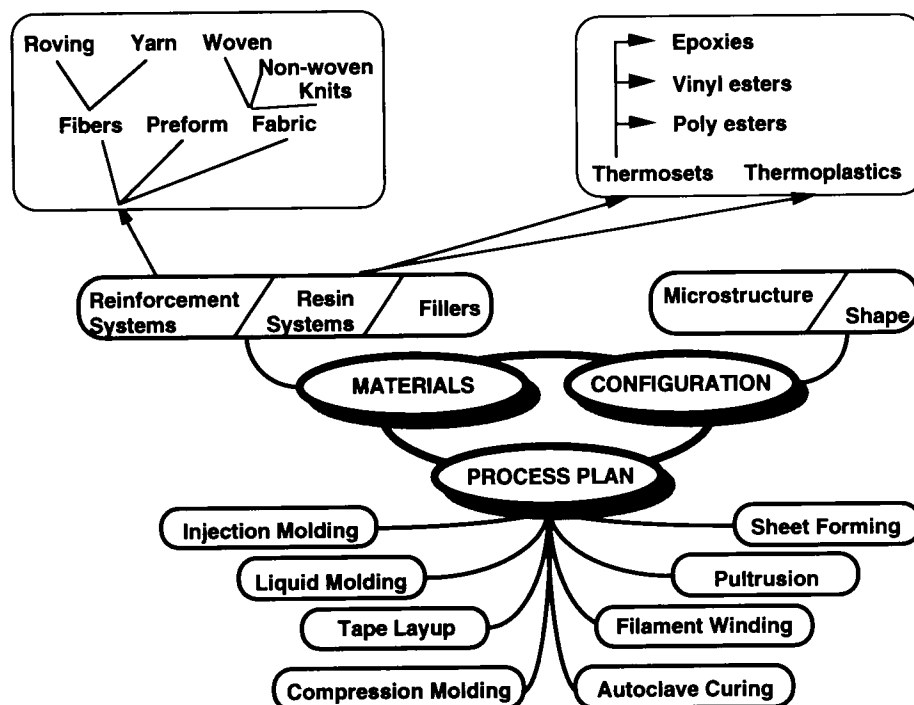


FIGURE 1 Advanced composite materials and manufacturing interactions.

In advanced composites design, the material and structure are very often realized at the same time, thereby complicating the design process. In the case of RTM thermoset systems, the composite material is actually formed at the same time as the structure itself. This important aspect presents both a designer's dream and nightmare at the same time. If armed with the appropriate tools of design and analysis, the designer is able to select the appropriate fabric types the fiber types for each part of a large structure and combine them into one manufacturing operation, such that the structure is tailored to respond appropriately at different points. Advanced composites design, then, is not just the design of an element or structure but essentially the design of the material from which the element is to be fabricated and the design of the fabrication process.

Materials and processes have to be chosen appropriately—glass would be the preferred reinforcement material based on economics, with carbon being used selectively in critical areas. Manufacturing processes such as pultrusion—estimated to give completed profiles and shapes in the \$2 to \$3/lb range, with raw material costs being as high as 80 percent of the overall costs—are obviously preferably to others such as fiber placement, where costs can be hundreds of dollars per pound, with material costs being in the 10 to 30 percent range. Costs dictate that such processes must be used only for very specific applications and are typically not competitive in the civil construction industry. Table 1

shows some representative property ranges of advanced composites for possible civil construction applications.

For any load-carrying structure, shape is often forgotten. For the application of composites to civil engineering, a one-to-one replacement will not be successful. In fact, a major criticism of pultruded sections applied to date has been that the I-beams buckle or fail in overload. The use of such shapes is probably not appropriate for the loading and materials used, and considerable attention needs to be paid to this factor. The concept of the shape factor was introduced as a dimensionless number characterizing the efficiency of a

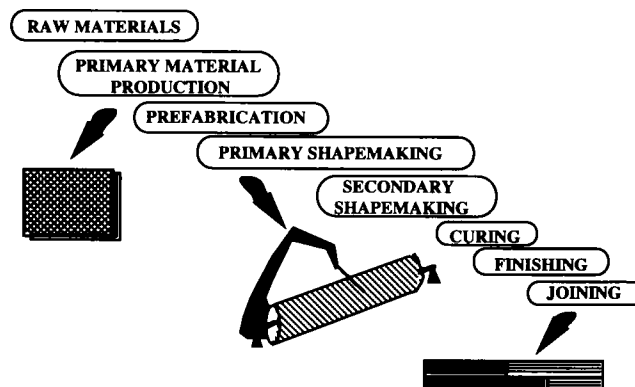


FIGURE 2 Materials transformation process.

TABLE 1 Advanced Composite Material Properties

High Performance Fibers (High Modulus)				
Type	E GPa (Msi)	$f_u$ GPa (ksi)	$\epsilon_u$ (%)	\$/lbs
Carbon	320 - 725 (46 - 110)	1.7 - 5.5 (250 - 800)	1.7 - 2.2	40 - 700
Aramid (Kevlar 49,149)	117 - 186 (17 - 27)	3.4 - 4.1 (500 - 600)	2.0 - 2.8	10 - 25
Glass (S)	89 (12.9)	4.6 (665)	5.4 - 5.7	3 - 5
Low-Medium Performance Fibers (Low-Med Modulus)				
Type	E GPa (Msi)	$f_u$ GPa (ksi)	$\epsilon_u$ (%)	\$/lbs
Carbon	170 - 310 (25 - 45)	1.4 - 6.8 (200 - 1000)	1.3 - 2.0	12 - 40
Aramid (Kevlar 29)	62 - 83 (9 - 12)	2.8 (400)	3.6 - 4.0	8 - 12
Glass	55 - 81 (8 - 12)	2.8 - 4.1 (400 - 600)	3 - 4.8	1 - 3
Polyethylene (Spectra 900)	117 (17)	2.6 (380)	3.5	40
Resin				
Type	E GPa (Msi)	$f_u$ GPa (ksi)	$\epsilon_u$ (%)	\$/lbs
Epoxy	2.0 - 4.5 (0.3 - 0.65)	27.6 - 62.0 (4 - 9)	4.0 - 14.0	1.20 - 3
Vinylester	3.6 (0.49)	80 (12)	4.0	1 - 1.5

specific shape (cylinder, square, I-beam, etc.) for a given mode of loading. Following that approach, it is clear that under tension the best performance (axial load-carrying capacity at the lowest self weight) is given by the combination that results in the highest value of  $E/\rho$ , where  $E$  is the Young's modulus and  $\rho$  is the density. Similarly, in flexure, the higher factor,  $E^{1/2}/\rho$ , indicates the best materials system for flexural shapes. Table 2 gives the results for a number of materials systems

based on these two measures and clearly shows the mechanical advantages that can be derived from advanced composite structural elements and systems.

### SEISMIC RETROFITTING OF BRIDGE COLUMNS

Recent earthquakes in California, such as Whittier 1987, Loma Prieta 1989, and Northridge 1994, have

TABLE 2 Comparison of Axial and Flexural Efficiencies for Different Material Systems

Materials System	Youngs Modulus (GPa) E	Density (g/cm <sup>3</sup> ) $\rho$	Axial Efficiency		Flexural Efficiency	
			$E/\rho$	Ranking	$E^{1/2}/\rho$	Ranking
Mild Steel	200	7.8	25.6	4	1.8	5
Carbon-PEEK	134	1.6	83.8	2	7.2	2
HS Carbon-epoxy	181	1.6	113.1	1	8.4	1
E-glass-epoxy	38.6	1.8	21.4	5	3.5	4
Kevlar-epoxy	76	1.46	52.1	3	6.0	3

shown the vulnerability of bridge columns built before the 1971 San Fernando earthquake.

For example, six of the seven bridge collapses during the recent Northridge earthquake could have been prevented if existing steel jacket column retrofit technology were implemented. Tests on 0.4 scale bridge columns at UCSD (1) have shown that carbon fiber jacket retrofits in a flexural lap-spliced plastic column hinge zone, and for full height shear retrofit, can be just as effective as comparable steel jacket retrofits (2).

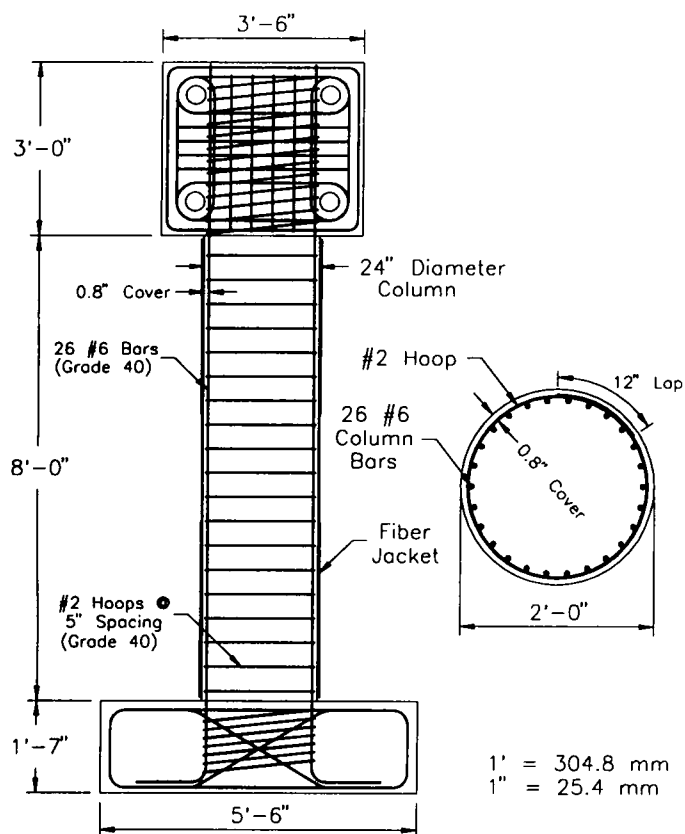
The carbon jackets were installed using an automated winding machine that places six toes of prepreg carbon (12k, AS4) at up to 40 rpm on the column. Advantages of the automated carbon jacket installation are the speed of application, including controlled curing, at approximately one-quarter of the time of installation for comparable steel jackets, and the tailoring of the jacket thickness and fiber orientation, which allow use of the carbon fiber material to the fullest extent.

As an example, the dimensions and reinforcement layout of a shear column test specimen are depicted in Figure 3 together with the variable thickness carbon

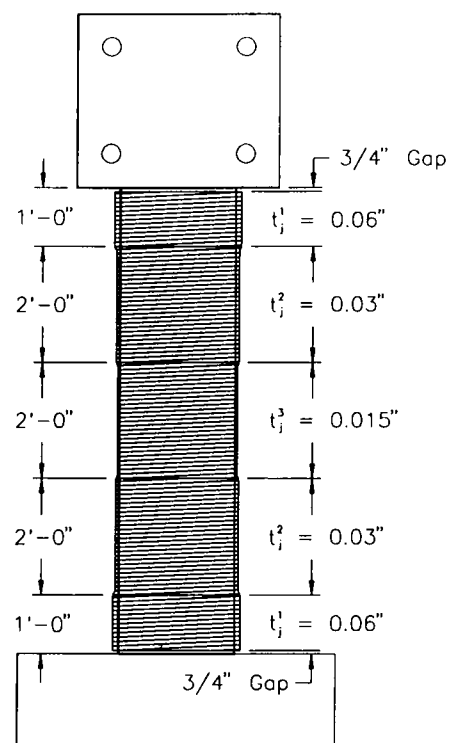
jacket design. A jacket thickness of only 0.4 mm (0.015 in.) of carbon was required over the shear critical center region of the column to prevent brittle shear failure. The schematic shear test setup is depicted in Figure 4 and experimental load-deflection hysteresis loops for the carbon fiber retrofitted shear column are shown in Figure 5. Completely stable hysteresis loops up to a displacement ductility level of  $\mu\Delta = 10.5$  were achieved, at which point the test was terminated due to test setup limitations.

Comparative load-deflection curve envelopes for the unretrofitted or "as-built" shear column, a steel jacket retrofitted column with 5 mm (3/16 in.) jacket thickness, and the carbon fiber retrofitted column are depicted in Figure 6, with a clear improvement of deformation capacity in both steel and carbon retrofitted cases over the "as-built" case, which failed in brittle shear at a displacement ductility of  $\mu\Delta = 2.0$ .

The steel jacket retrofitted column exhibited a slightly higher initial stiffness and a slight increase in lateral load carrying capacity, with increasing displacement levels due to the isotropic nature of the steel



(a)



(b)

FIGURE 3 Carbon fiber jacket shear column test specimen details: (a) specimen dimensions and reinforcement, (b) jacket retrofit design.

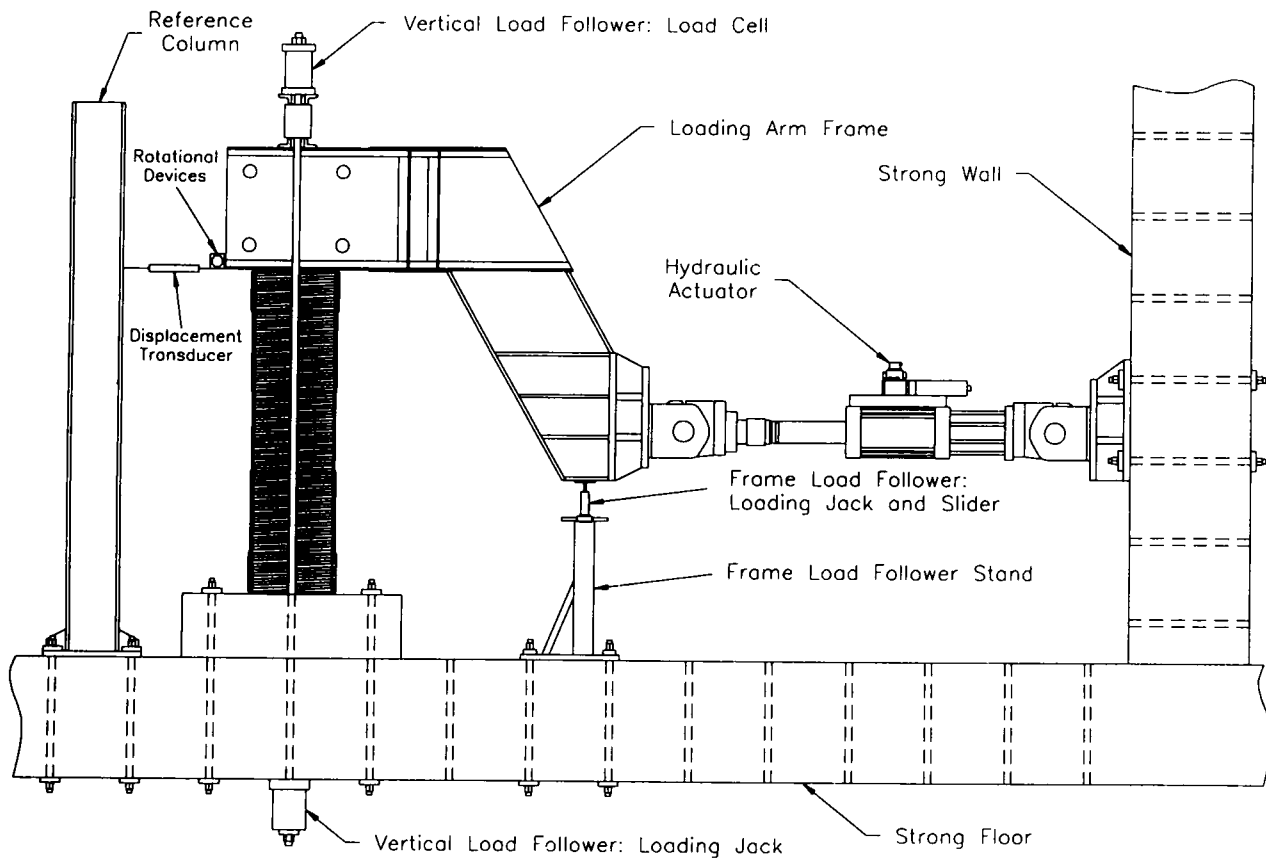


FIGURE 4 Schematic test setup.

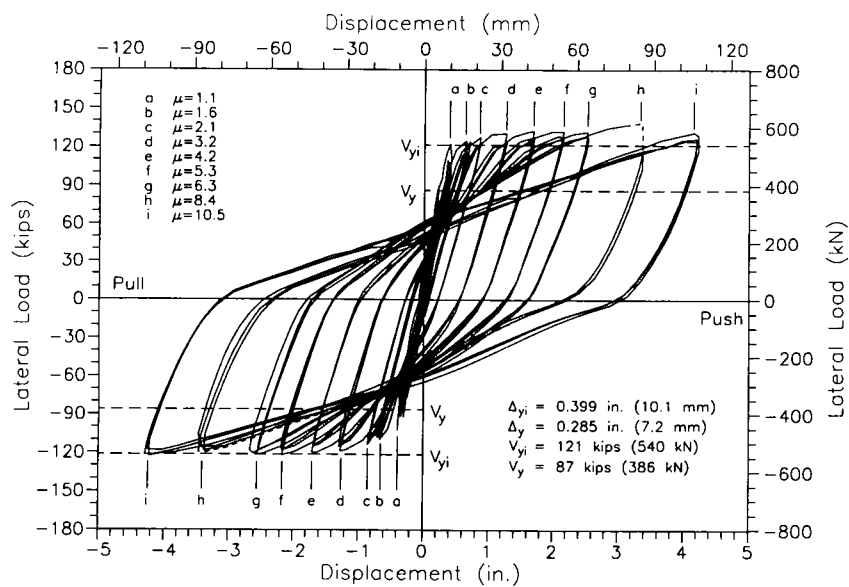


FIGURE 5 "Reduced" horizontal load-displacement curve for fiber retrofitted column.

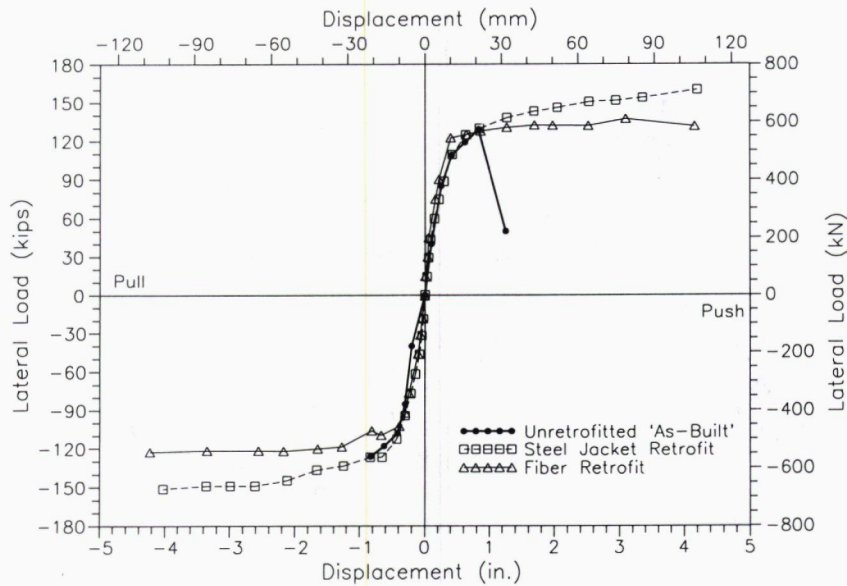


FIGURE 6 Comparison of load-displacement envelopes for "as-built" steel jacket and carbon jacket retrofits.

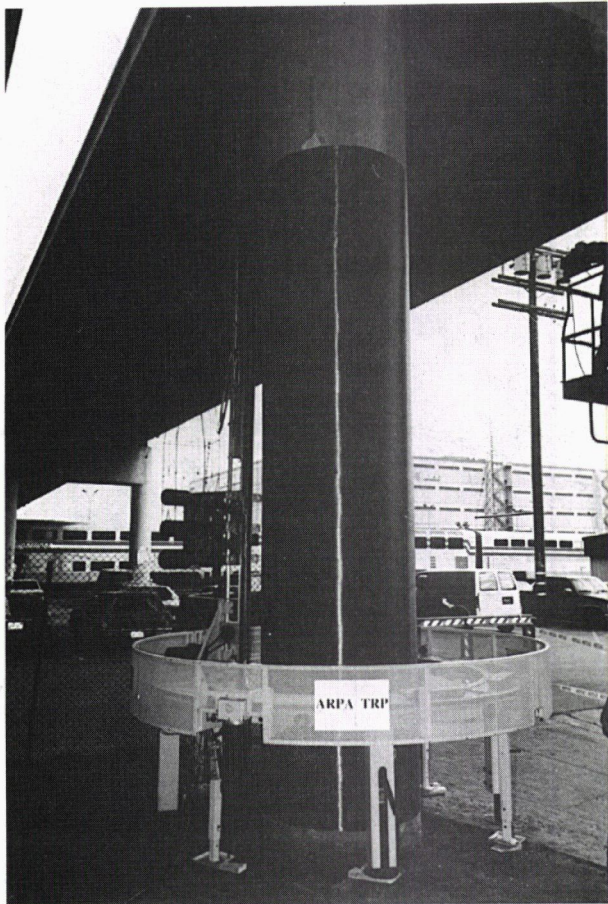


FIGURE 7 Automated carbon jacket installation.

jacket, resulting in a more concentrated plastic hinge and more strain hardening at the column ends. Stiffness and capacity increases are not sought for in bridge column retrofits, since typically higher seismic force levels are transmitted to adjacent structural elements. Thus, the carbon jacket with only horizontal or hoop directional strength and stiffness can accommodate the requirement for no stiffness or strength increase even better than a steel jacket, as in Figure 6. With the automated fiber lay-up, which can also be employed for rectangular columns (Figure 7), carbon fiber jackets can be competitive with steel jacket retrofits without even considering premiums for reduced lane closure requirement or early completion incentives.

In addition to automated carbon fiber jacketing systems, developments on in-situ applications of advanced composite hybrid jackets to columns using a resin infusion molding process are currently in progress at UCSD.

### BRIDGE DECK REPLACEMENT

Due to their light weight, corrosion resistance, environmental durability, and high stiffness-to-weight and strength-to-weight ratios, advanced composites have potential for use in bridge decks. It should be remembered that a major factor leading to the deterioration of our infrastructure, including bridges, is the deterioration of steel by corrosion, due to both moisture ingress and the use of de-icing salts. The use of composites



readily addresses this concern. Although lighter weight may not initially appear to be a major factor beyond reduced seismic demands, it does play an important role. Reduction in dead weight of bridge decks translates to increased live load capacity. In terms of rehabilitation, this could mean that if heavy decks were to be replaced (even partially) with lighter composite construction, the load rating could conceivably be increased. Lighter weight of sections also means a reduced need for specialized equipment such as huge cranes, resulting in lower overall project costs. Transportation costs are also reduced, enabling the designer to consider the use of large sections prefabricated under controlled factory conditions. However, the main impetus would be the significant reduction in life-cycle costs. Despite these advantages, the application of advanced composites to bridges, and in fact to all civil engineering structures, will depend on two major factors: the development of cost-competitive materials and technology, and the deployment of appropriate technology.

A number of manufacturing techniques lend themselves to the efficient fabrication of large structures such as bridge decks. The resin infusion molding process allows for the lay-up of fabric around cores and mandrels (which can later be removed, leaving gaps similar to those in hollow box girders) with specific tailoring of the reinforcement architecture for complex loading conditions. It does not require expensive tooling and, due to the ease of fabrication, can be conducted with relatively low capital expense. Figure 8 shows an example of a full-scale deck section fabricated in a single manufacturing step using the resin infusion molding process. The flexibility of the process lends itself to a true blending of form and function in the same element. The deck section in Figure 8, manufactured and tested by ACTT at UCSD, showed twice the capacity of a comparable

concrete deck at one-tenth of the weight. Pultrusion is, as mentioned above, perhaps the most cost-efficient composites fabrication process. It is capable of fabricating large elements of constant cross-section that can then be combined using mechanical or adhesive means for joining. This enables the use of standard type elements so as to fabricate large structures using a building block approach. The Aberfeldy bridge (3) is one example of this technology. Perhaps the best option is a combination of pultrusion and VARTM, with the building blocks (in the form of triangular and/or trapezoidal sections) being fabricated using pultrusion and then being connected using the VARTM process. In this case, additional fabric would be used between the pultruded cores, with resin then infused into the fabric. This technology would depend on the formulation of suitable resin systems and control of cure mechanisms to allow good secondary bonds between the pultruded parts and the infusing resin system. Such a method could open new avenues for rapid bridge deck construction, with the last stages even being conducted on site.

Cost-effectiveness of the manufacturing process will be a major factor in the selection and use of a fabrication process. Costs are not only related to those of the constituent materials (resin and fiber) but also to the tooling (molds and dies), quality control, and processing steps. Methods that are automated and use prefabricated elements will obviously have a higher degree of robustness and hence efficiency. It is feasible that in the near future composite components will be available, analogous to prefabricated and precast concrete or steel girders. Concurrent cost modeling with advanced composite replacement decks to date shows that even on a first cost basis, advanced composite decks can be competitive with conventional reinforced concrete or orthotropic steel bridge decks.

## NEW BRIDGE SYSTEMS

Developments at UCSD through ACTT and in cooperation with Caltrans and the Federal Highway Administration are demonstrating both the technical and economical feasibility of using advanced composite materials for complete new bridge systems (4).

One demonstration project is focusing on a cable-stayed traffic bridge at Gilman Drive across Interstate 5 in La Jolla, where all components, including deck, superstructure, pylon, and cables (Figure 9), are manufactured using advanced composite materials and automated manufacturing technology.

Overall geometry and dimensions are depicted in Figure 10, which shows a cable-stayed bridge solution using conventional materials such as reinforced concrete for the superstructure and steel for pylon and cables. Direct

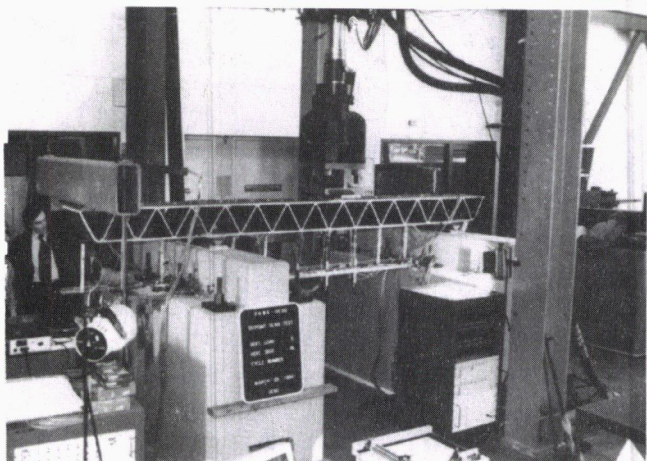


FIGURE 8 Advanced composite bridge deck test.



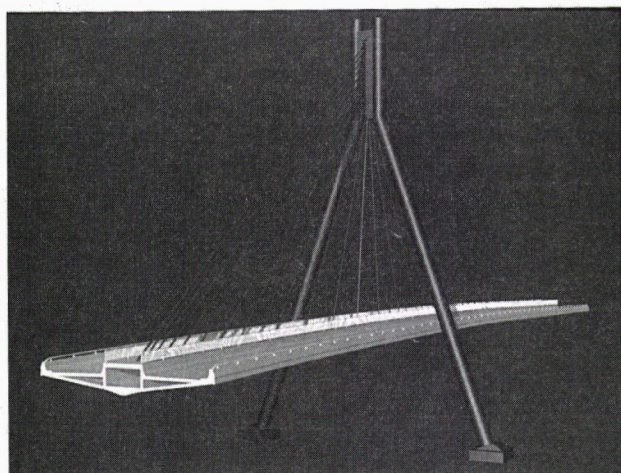


FIGURE 9 Schematic of Gilman/I-5 cable-stayed bridge.

cost comparisons are made by means of detailed cost modeling, even during the preliminary design phase, to ensure the development of an affordable and competitive product. The design development to date focuses on two alternate composite bridge types in which design alternative A is considering mass-manufactured, erector set-type composite components assembled by adhesive joining in the field with predominantly longitudinal construction joints. Design alternative B is examining

segmental construction with transverse joints or continuous in-situ resin transfer molding technology.

In terms of materials and manufacturing processes, alternative A is investigating the use of standardized pultruded fiberglass sections, which are preassembled to modular deck or soffit panel units prior to field assembly. On the other hand, alternative B is studying the Resin Infusion Molding process, currently used primarily in the ship industry.

In addition to the Gilman/I-5 cable-stayed bridge demonstration project, these new materials seem to be especially advantageous for the construction and erection of smaller modular bridge systems in regions where heavy lifting equipment is not available or access is restricted. Studies for single span vehicular bridges or pedestrian bridges similar to applications in China (5) and Europe (3) are currently under way at several research organizations throughout the United States. A major impact on bridge renewal with advanced composite bridge systems can be expected.

## CONCLUSIONS

Aging and deterioration of the U.S. bridge inventory require the rapid development of new rehabilitation technologies. The large volume of bridge infrastructure renewal work necessitates exploration of materials and

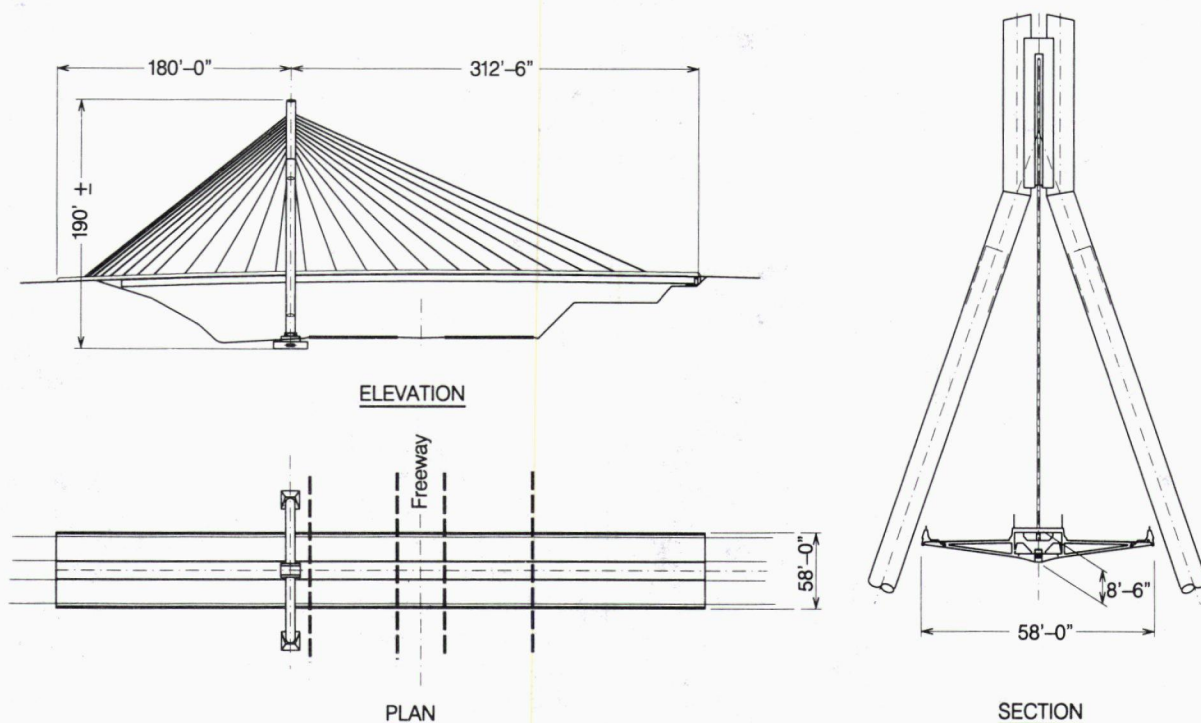


FIGURE 10 Geometry and dimensions of Gilman/I-5 bridge.



manufacturing processes that are new to the civil construction industry.

Promising infrastructure renewal technologies based on polymer matrix composites, primarily developed and used in the defense industry, are under development by ACTT. Specific developments and applications to date consist of advanced composite carbon jackets for the seismic retrofit of bridge columns, bridge decks for the complete replacement of existing concrete decks, and design developments for new all-advanced-composite bridge systems.

Research indicates that advanced composite jackets for the seismic retrofit of bridge columns can be just as effective structurally as the current steel jacketing technology. Advanced composite bridge decks, without corrosion or spalling problems, developed and tested show weight and savings over conventional concrete decks by factors of 5 to 10. Furthermore, developments with advanced composites for bridge infrastructure renewal have shown that as soon as automated manufacturing and installation processes can be developed, advanced composite rehabilitation and renewal components can be deployed at full cost-competitiveness with conventional construction materials, even at relatively high current costs for the advanced fibers and resin systems. Combined with excellent mechanical and durability characteristics, even complete advanced composite

bridge systems are likely to play a major role in the nation's bridge infrastructure renewal program.

#### REFERENCES

1. Seible, F. S., G. Hegemier, M. J. N. Priestley, D. Innamorato, J. Weeks, and F. Policelli. *Carbon Fiber Jacket Retrofit of Circular Shear Bridge Column*, CRC-2. Advanced Composites Technology Transfer Consortium, Report No. ACTT-94/02, Structural Engineering, University of California, San Diego, La Jolla, September 1994, 54 pp.
2. Priestley, M. J. N., F. Seible, and Y. H. Chai. *Design Guidelines for Assessment Retrofit and Repair of Bridges for Seismic Performance*. Structural Systems Research Project Report No. SSRP-92/01, University of California, San Diego, August 1992, 266 pp.
3. Seible, R., G. A. Hegemier, and G. Nagy. *The Aberfeldy Glass Fiber Composite Pedestrian Bridge*. Advanced Composites Technology Transfer Consortium, Report No. ACTT-94/01, Structural Engineering, University of California, San Diego, La Jolla, January 1994, 52 pp.
4. Seible, F., and R. Burgueño. *Advanced Composites in Cable-Stayed Bridges*. Seminar on Cable-Stayed Bridges, Miami, Florida, October 1994.
5. Seible, F., S. Zunling, and G. Ma. *Glass Fiber Composite Bridges in China*. Advanced Composites Technology Transfer Consortium, Report No. ACTT-93/01, Structural Engineering, University of California, San Diego, La Jolla, April 1993, 36 pp.

# Modern Brickwork Highway Structures

---

S. W. Garrity, *University of Bradford, England*

Clay brickwork is set to reemerge as a major structural material with the growing emphasis on designing aesthetically pleasing highway structures with low maintenance costs. This paper addresses the use of clay brickwork construction for new highway structures such as earth retaining walls, short-span arch bridges and bridge abutments, piers, parapets, and wingwalls. The performance of existing masonry structures is appraised, the principal design requirements for new brickwork structures are identified, and recent research and development is summarized. Two recently completed bridges with major elements of structural clay brickwork construction are described in brief.

**M**any of the canal and railway structures built in Britain during the eighteenth and nineteenth centuries, such as earth retaining walls, viaducts, arch bridges, and tunnel linings, were of unreinforced clay brickwork construction. Although most of these structures have been under very severe exposure conditions for long periods, many are still in service. They have needed comparatively little maintenance, in part due to the inherent durability of many types of well-fired clay brick. Although clay brickwork and other forms of masonry such as dressed stone and concrete bricks and blocks now tend to be used merely as cladding, a number of structurally efficient, cost-effective forms of masonry construction developed in the last 30 years are likely to be suitable for new highway structures.

The aim of this paper, therefore, is to investigate the viability of clay brickwork construction for new high-

way structures such as earth retaining walls, short-span arch bridges and bridge abutments, piers, parapets, and wingwalls. The following aspects of brickwork construction are considered:

1. Critical review of existing brickwork highway structures,
2. Design requirements for new brickwork highway structures,
3. Plain or unreinforced brickwork,
4. Reinforced brickwork,
5. Prestressed brickwork, and
6. Case studies of Foxcovert Road Bridge and Kimbolton Butts Bridge.

## EXISTING BRICKWORK HIGHWAY STRUCTURES

If highway and bridge engineers are to consider clay brickwork for use as a structural material, they must develop modern designs that retain the benefits of old forms of brickwork construction but overcome the limitations. Some understanding of the limitations may come from a critical review of the construction and performance of existing arch bridges such as the one shown in Figure 1, which is typical of nineteenth century construction in the United Kingdom. Different aspects of the performance of such bridges are reviewed.

## Materials

Most brick arch bridges were built using weak hydraulic or semi-hydraulic lime mortar, with little or no at-

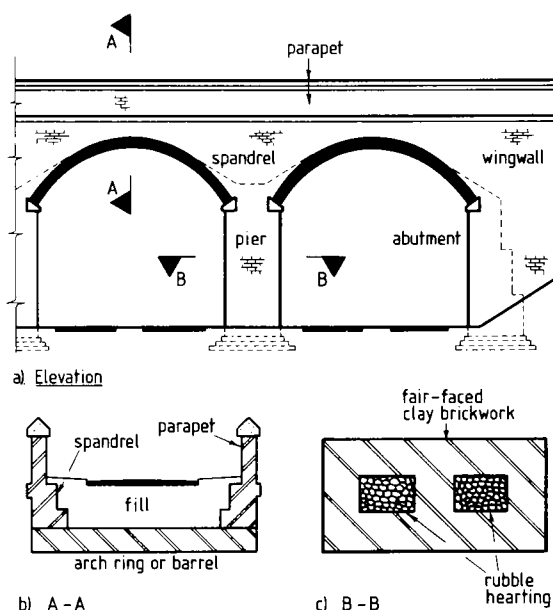


FIGURE 1 Typical brickwork arch bridge details: (a) elevation, (b) A-A, (c) B-B.

tempt to protect the joints from rainwater leaching through the fill material from the carriageway above. Although such mortars are capable of accommodating movements due to changes in the ambient conditions and small amounts of differential settlement, they are prone to deteriorate from the effects of frost, and lime can leach out of the mortar, leaving unsightly calcium carbonate deposits on the exposed faces of the brickwork. As a result, the bricks have tended to become debonded from the mortar, causing a severe reduction in the tensile strength. Furthermore, the aesthetic quality of some structures has been reduced considerably by lime staining and fungal growths on damp patches of brickwork. Other less common causes of deterioration include abrasion from wind and water, salt crystallisation damage, and the effects of the expansive reaction between cements and sulfates in groundwater or polluted air.

As far as clay bricks are concerned, there have been relatively few problems. The main form of deterioration has been the progressive degradation of the exposed faces of some bricks due to freeze-thaw action, although this has not occurred where the bricks have remained relatively dry or where well-fired, low porosity engineering bricks have been used.

## The Arch

The inherent strength of the voussoir arch ring or barrel is well known (1); where distress has occurred it has

often been due to failure of the abutments or piers resulting either from scour or from the excessive settlement typical of shallow, inadequate foundations (2). There can be little doubt that most arch bridges built today would not suffer from such problems because of the vast improvements both in ground investigation techniques and in foundation design and construction.

Although the curved profile of the arch undoubtedly contributes to its aesthetic appeal, the low headroom close to the supporting abutments or piers of highway overbridges can result in "bridge bashing," that is, damage from tall vehicles. In addition, flooding can occur where arch bridges span watercourses, because the bridge creates an increasingly greater obstruction to flow as the water level rises.

As many of the proposals for new brickwork highway structures are for vertical elements of construction, it is appropriate to consider the wingwalls, parapets, spandrels, abutments, and piers of arch bridges in more detail.

## Wingwalls and Spandrel Walls

These walls are subjected to horizontal earth pressure from the fill material placed at the ends and over the top or extrados of the arch ring. In addition, the spandrel walls and, to a lesser extent, the wingwalls stiffen the outer edges of the arch ring. The combined effects of lateral pressure and the central portion of the arch ring deforming under the action of live loading can lead to cracking and eventually partial collapse, as the wingwalls and spandrel walls become separated from the rest of the structure (3,4). This behavior is, again, indicative of brickwork's low tensile strength and is often exacerbated by rainwater leaching through the fill material into the mortar joints (5), as described above.

The craftsmen of the past were certainly aware of brickwork's very low and sometimes unreliable tensile strength. To overcome this, they usually built very thick wingwalls and spandrel walls, the aim being to provide sufficient dead weight to counteract any flexural tension caused by the lateral earth pressure. As this philosophy was also used when designing and building masonry earth retaining walls, it is not surprising that some of the solid brickwork walls built by Victorian railway engineers to support the sides of deep cuttings were well over 2 m thick in places.

## Parapet Walls

The principal function of the parapets of any highway bridge is to contain a vehicle collision in as safe a manner as possible. In the case of masonry parapets, it is

very difficult to quantify the impact resistance because of the very complex behavior of unreinforced masonry when subjected to high rates of loading from a non-rigid body such as a vehicle. In order to assess the behavior and strength of masonry parapets when subjected to vehicle impact the County Surveyor's Society of the United Kingdom recently funded a research program that included a series of full-scale vehicle impact tests on masonry parapets at the Motor Industry Research Association in Nuneaton, England (6); all the tests were carried out in accordance with Appendix E of BS 6779 (7). Although most of the tested masonry parapets adequately confined the test vehicle, the research indicated that some existing walls may need to be modified to minimize the safety hazard caused by the masonry projectiles produced immediately after impact.

### Piers and Abutments

Although usually of solid masonry, some piers and abutments were built with an outer skin of fair-faced stone or clay brick masonry with a low cost rubble infill or hearting (8).

As the compressive stress due to the vertical loads acting on a pier or an abutment of an arch bridge tends to be greater than the flexural tensile stress produced by the lateral forces, the masonry is generally in a net state of vertical compression throughout. Therefore, provided that the compressive stress is small, the piers and abutments can remain in an uncracked and stable condition for many years. As with the wingwalls and spandrel walls, piers and abutments were usually of massive construction to ensure sufficient dead weight to maintain the masonry in a net state of compression.

Lime mortars were used extensively in brickwork construction. The compressive strength of such mortar was invariably an order of magnitude lower than that of the bricks. Hence, it is very likely that the compressive stresses in the bricks of existing structures are very low, which may explain why there have been very few collapses resulting from compression failures. Where piers and abutments have failed, it has usually been as a result of tensile stresses or instability caused either by scour, excessive ground movements, or the effects of severe overloading produced by modern traffic.

### Construction

The arch rings of masonry bridges were constructed in-situ on temporary centering. This was usually of timber construction and often consisted of an elaborate array of interconnected diagonal members, which was necessary to provide a stiff platform on which to build the

arch. Invariably the installation of centering was very time consuming and often fraught with delays arising from the combination of inclement weather and the complexity of construction.

As noted previously, most vertical structural elements of arch bridges were of massive construction to provide stability. As a result, arch bridge construction was very slow and very labor intensive, sometimes involving huge numbers of bricks: the 544-m-long, 27-arch Victorian railway viaduct in Stockport, England (9), is thought to consist of some 22 million bricks.

Taking into account the slow, labor-intensive construction methods and the difficulties experienced with the construction of centering, it is not difficult to appreciate why there was a decline in the use of masonry as stronger alternative materials such as cast iron, wrought iron, structural steels, and reinforced concrete were developed.

### Workmanship

Judging by the results of many highway schemes that have involved the use of brick clad reinforced concrete it is clear that, with adequate supervision, very high quality brickwork can be achieved.

An advantage of brickwork is that the main construction defect, namely poorly filled mortar joints, can be detected by visual inspection. With reinforced concrete construction, durability depends on ensuring that the permeability of the surface zones of concrete is reduced as much as possible in order to provide the maximum protection to the steel reinforcement. This is achieved by using well compacted concrete with a relatively high cement content and a low water:cement ratio; surface porosity is further reduced by good curing. In practice, however, it is difficult to check the porosity and permeability of the concrete because the capillary pores in the cement paste, which permit the ingress of chloride ions and other deleterious substances, are microscopic. Hence, although the finished concrete may appear satisfactory to the naked eye, there is no way of easily checking that the quality of the cover concrete is adequate without carrying out in-situ permeability measurements. In short, it is not possible to visually inspect the concrete for quality. The water:cement ratio of the mortar in brickwork construction, however, does not have the same influence on durability, and only very inaccurate batching and poor mixing of the mortar constituents is likely to cause major problems in the future.

### DESIGN REQUIREMENTS FOR NEW BRICKWORK HIGHWAY STRUCTURES

All structures must be strong, stable, robust and safe. Taking into account the points raised in the critical re-

view and the experience gained from the deterioration of some reinforced concrete structures, the additional requirements of new brickwork highway structures are summarized below.

### Construction Methods

Construction methods must be simpler and quicker than in the past and must involve less labor and materials. Mortars in which the principal binding agent is ordinary portland cement rather than lime should also be used, as the rate of strength gain is conducive to ensuring the rapid construction times required by most clients.

### Structural Form

Judging from the problems that occur with old arch bridges, it appears that major improvements need to be made to the laterally loaded structural elements, namely the parapets, spandrels, and wingwalls. To improve structural performance and reduce construction times and cost, it is necessary to adopt more efficient forms of construction that make optimum use of brickwork's relatively high compressive strength but overcome its inherently low tensile strength. It is therefore suggested that reinforced or prestressed forms of brickwork construction be used as alternatives to the massive forms of construction used in the past.

### Compressive Stresses

Although modern cement-based mortars are much stronger than lime mortars, in order to reduce the risk of overstressing the bricks, a low compressive stress limit should be used when designing new brickwork structures.

### Durability

New brickwork structures must be durable and easy to maintain. In particular, where any steel is used in construction, it is necessary to minimize the risk of corrosion caused by chloride attack from deicing salts and other sources. More durable mortars are preferable to the lime-based mortars of old, which were very prone to weathering and erosion.

A durable combination of bricks and mortar that is resistant to frost and chemical attack therefore must be specified. The guidance given in BS 5628: part 3 (10) recommends the use of frost resistant clay bricks with

a low soluble salt content; such bricks are defined as "durability designation FL" in BS 3921 (11). In addition, brick specifications should include a maximum water absorption of about 10 to 12 percent and a minimum compressive strength of about 50 MPa. Where the brickwork is likely to remain saturated for long periods, the use of bricks with a lower water absorption may be necessary.

The most appropriate mortar mix for highway structures will generally be a weigh batched 1:1/4:3 OPC:lime:sand mix (ASTM type M). Some engineers recommend the use of a styrene butadiene rubber (SBR) latex additive in the proportion of 6 litres of SBR per 50 kg of OPC. The SBR acts as a bonding and waterproofing agent, and may help reduce lime staining of the mortar joints and facilitate the removal of graffiti. New brickwork highway structures must be adequately waterproofed and drained to reduce the risk of deterioration from freeze-thaw action.

### Aesthetics

Brickwork highway structures must be aesthetically pleasing. In addition to providing adequate waterproofing and drainage to prevent the occurrence of damp patches and the growth of unsightly fungi, measures must also be taken to minimize the risk of efflorescence and lime staining.

### Movement

Cement mortars, which often contain a non-hydraulic lime plasticizer, are used exclusively in new construction; such mortars are much more brittle than their hydraulic lime-based predecessors. As a result, with modern brickwork construction it is essential to provide joints capable of accommodating movements due to moisture and thermal effects.

### Cost

Brickwork structures must be cheaper to construct than brick faced concrete structures. Many engineers are familiar with reinforced concrete design and construction and are, perhaps, reluctant to use alternatives. Although some engineers may accept that clay brickwork structures can have very low whole-life costs, the prospect of initial cost savings is probably necessary to motivate most to consider brickwork as an alternative to structural concrete. New forms of plain, reinforced, and prestressed brickwork have been developed, which may

satisfy some or all of the above criteria and are therefore worth further consideration.

### PLAIN OR UNREINFORCED BRICKWORK

Plain brickwork is commonly used for the stems of low-rise earth-retaining walls. To provide the necessary stability against overturning, walls up to 1 m high may need to be up to 665 mm (three bricks) thick. In the last 30 years, more structurally efficient alternatives to the solid brickwork wall have been developed, as discussed below.

### The Cellular or Diaphragm Wall

Although the diaphragm wall was originally developed as an alternative to the brick-clad steel or concrete frame for tall single story buildings (12), it has also been used for earth retaining walls (13). It consists of two wythes or flanges of brickwork linked by brickwork webs to form a series of interconnected I-sections. Separation of the leaves of brickwork by the webs considerably increases the second moment of area of the wall, with a very small increase in the amount of brickwork; hence the cellular wall is much more structurally efficient than the solid wall. The cellular spaces in the brickwork can be filled with selected fill material or lean mix concrete to increase stability, and a pleasing effect can be created by topping the fill with plants.

### Brickwork-Faced Reinforced Soil

This is a form of reinforced earth where the soil reinforcement is built into the bed joints of a brickwork wall. As with other forms of reinforced earth, the facing material, in this case the brickwork, is likely to be very lowly stressed. Indeed, its principal role is that of a durable protective cladding that also retains the edges of the soil mass. It must also be capable of resisting any localized earth pressures created during the compaction of the fill material.

This form of construction was probably first used in the United Kingdom by highway engineers from West Yorkshire County Council, England, following trials in 1977. Later, research using "Terram" geotextile at the University of Leeds (14,15) and "Tensar" geogrid at the University of New Brunswick, Canada (16,17), confirmed that the effective strength of small earth retaining walls could be substantially increased with the addition of soil reinforcement with a very small increase in cost. This technique seems to be particularly suitable for repairing and strengthening existing masonry earth re-

taining walls; as far as the author is aware, it is rarely used for new construction in the United Kingdom.

### NEW BRICKWORK ARCH BRIDGES

The improvements in ground investigation techniques and the design and construction of foundations referred to earlier, coupled with the development of lightweight, easy-to-install falsework suitable for centering, may make the brickwork arch an economically viable form of new construction for small span bridges. Furthermore, experience in the United Kingdom has shown that the maintenance costs for masonry arch bridges can be on the order of 30 percent less than those for other forms of bridge construction (18). The aesthetic appeal of the unreinforced brick or stone masonry arch and the anticipated savings in whole-life costs have prompted many bridge owners in the United Kingdom, such as the Department of Transport, the Scottish Office (19), and some local regional Highway Authorities (18,20), to recommend the use of the masonry arch form of construction for new short span bridges. One of these, Kimbolton Butts Bridge, is described below.

Judging from the above, many engineers recognize the potential advantages of brick and stone masonry arch bridges. However, few bridges of this type are likely to be built until a lower cost, more rapid method of arch construction is developed; such a technique, which involves the use of prefabricated brickwork arch rings, is currently at the very early stages of development at the University of Bradford (21). In addition, the critical review has identified the need to adopt forms of construction that can overcome the aforementioned problems with the spandrel walls, wingwalls, and parapets of arch bridges. Reinforced or prestressed brickwork can be used for such structural elements and others subjected to large magnitude lateral loading, such as bridge piers, abutments, and earth retaining walls; these are considered in more detail below.

### REINFORCED BRICKWORK

As noted previously, a major limitation of plain brickwork is its low flexural tensile strength. However, as with other low tensile strength materials such as concrete, the flexural strength of brickwork can be increased considerably with steel reinforcement. This concept is not new; indeed, Brunel is reported to have used a form of reinforced brickwork for the construction of the Wapping to Rotherhithe Thames tunnel caissons in London in 1825 (22). In a design guide published in the United States in 1953 (23), the use of reinforced brickwork is cited for several types of structure, including

earth retaining walls, bridges, and culverts built in India and Japan during the period 1919–1930. A highway bridge, built in Ohio in 1934 with reinforced brickwork parapets, abutments, and piers, is also described. More recently, the use of reinforced brickwork for the construction of earth retaining walls (24,25) has been reported.

Cost studies by independent quantity surveyors (26, 27,28) have shown that, in the case of retaining walls, reinforced brickwork construction may be a cheaper alternative to brick clad reinforced concrete. Similar economies may also be possible for other structures where an exposed brickwork finish is required. Although some small earth retaining walls were built in London in the 1960s and in Dartford, Kent in the mid-1970s (29), there has been comparatively little use of reinforced brickwork construction in the United Kingdom. There is, however, considerable knowledge of the behavior of reinforced brickwork earth retaining walls. Research was conducted at the Building Research Establishment (30), at Edinburgh University (31,32), and at the British Ceramic Research Association (33,34) during the 1970s and early 1980s. More recently Redland Brick Limited and the Brick Development Association have sponsored a program of full-scale testing at British Ceramic Research Limited (35). As well as funding research, various U.K. brick manufacturers have built trial walls, notably George Armitage and Sons (now Marshalls Clay Products) (36) and Butterley Brick Limited, who investigated the feasibility of using prefabricated retaining wall panels (37). As a result of this research and development, two main forms of reinforced brickwork have emerged for the construction of laterally loaded walls, namely, the reinforced grouted cavity wall and the reinforced pocket-type wall; more recently the reinforced cellular or diaphragm wall has been suggested as an additional form of reinforced brickwork construction (38).

The most likely uses of reinforced brickwork are for laterally loaded structures such as noise barriers, earth retaining walls, wingwalls, small bridge abutments, and bridge parapets. A more detailed review of reinforced brickwork for highway structures, including a comparison of the different forms of construction and case study details, is given in the references (39); reinforced grouted cavity and reinforced pocket-type walling were also used for the case study bridges described in this paper.

## PRESTRESSED BRICKWORK

It is likely that prestressed brickwork will be more economical than reinforced brickwork for the construction of most bridge piers, abutments, and tall earth

retaining walls. The development of prestressed brickwork is still at a relatively early stage; most uses have been in building construction where vertical walls must resist a large horizontal thrust from a sloping roof or surge effects from crane girders. Prestressing has also been used to improve the resistance of brickwork walls to the effects of settlement and seismic activity. As far as highway structures are concerned, laboratory-based full-scale tests of prestressed brickwork retaining walls (40,41) and a bridge abutment (42,43) have been reported. Design guidance is given in part 2 of BS 5628 (44) and elsewhere (45,46,47). The aforementioned tests have shown that the design shear strength recommendations of BS 5628: part 2 are conservative when applied to sections suitable for highway structures; a new design method proposed for revision of BS 5628: part 2 and the proposed Eurocode for masonry, EC6, based on recent research (48), should lead to greater economy.

The main aim of prestressing brickwork is to produce sufficient vertical compressive stress to counteract any tensile stresses that would otherwise have been caused by lateral loading. Even when subjected to design ultimate loads, the maximum compressive stress in the brickwork due to combined prestress and flexural compression is unlikely to be greater than 6 or 7 MPa, hence the brickwork stresses are relatively low.

As bridge piers and abutments are subject to a vertical compressive force from the bridge deck that they support and to reversible horizontal forces caused by traction, skidding, wind, and temperature changes, the most appropriate form of brickwork construction is likely to be symmetrical, such as the cellular or diaphragm wall.

In many respects the prestressed brickwork diaphragm wall is the modern equivalent of the cellular masonry piers and abutments built well over 100 years ago; both forms of construction are hollow or cellular and in both cases the masonry is always in a state of vertical compression. Details of a typical abutment are given in Case Study 1, below.

## CASE STUDY 1: FOXCOVERT ROAD BRIDGE

This bridge carries the Glington-Northborough bypass over a minor road that links the villages of Glington and Werrington to the north of Peterborough, England. It was designed by the engineers of the Transportation Department of Cambridgeshire County Council, who required all structures on the scheme to have an exposed brickwork finish to ensure visual harmony with existing and proposed brick-clad housing near the site. The 7.2-km-long scheme was opened to traffic in 1989.

The designers chose structural brickwork for the abutments and wingwalls rather than brick-clad rein-



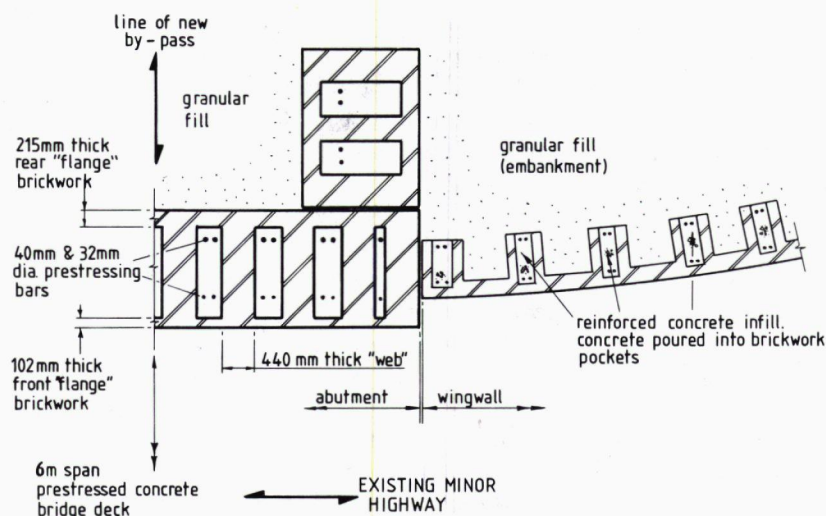


FIGURE 2 Foxcovert Road Bridge: horizontal section through end support showing prestressed brickwork diaphragm wall abutment and reinforced pocket-type wingwall.

forced concrete because of the lower anticipated long-term maintenance costs. The 6m span square bridge deck, consisting of precast prestressed concrete inverted T-beams with in situ concrete infill, is supported on prestressed brickwork diaphragm wall abutments. The wingwalls are of reinforced brickwork pocket-type construction.

The exposed brickwork consists of FL quality clay bricks, with a minimum compressive strength of 56 MPa and a maximum water absorption of 10 percent, laid in 1:1/4:3 cement:lime:sand mortar containing an SBR additive. Class B engineering bricks were used for the buried faces of the abutments and wingwalls. Details of the prestressed brickwork abutment and the curves reinforced pocket-type wingwall are given in Figures 2 and 3.

### Prestressed Brickwork Abutments

The abutments are 1.565 m thick and measure approximately 6.5 m high from the top of carriageway down to the top of the reinforced concrete (r.c.) foundation. The front and rear flanges of the diaphragm wall are 102.5 mm (one-half brick) and 215 mm (one brick) thick, respectively, and are connected by 440-mm (two-brick) thick webs spaced at 787-mm centers.

Corrosion protected 40- and 32-mm-diameter high tensile steel Macalloy bars, initially stressed to 70 percent of their characteristic load using hydraulic jacks, provide the prestress. The lower and upper end anchorages were provided by the r.c. foundation and the r.c. bearing shelf. After prestressing, the annular spaces

between the tendons and the ducts cast into the r.c. anchorages were filled with a cementitious grout. A 20 percent loss of prestress was assumed in design to take account of the effects of stress relaxation, temperature change, and creep.

Corrosion protection of the Macalloy bars consisted of hot dip galvanizing followed by a covering of grease and two layers of waterproof tape. Small plastic tubes were also built into the exposed faces of the brickwork to permit inspection of the bars and the voids or cells of the diaphragm walls using a borescope. Unfortunately, out of the 184 bars used on the scheme, 9 failed between 2 and 3 days after stressing as a result of hydrogen embrittlement caused during galvanizing; for-



FIGURE 3 Foxcovert Road Bridge under construction.



tunately it was possible to replace the defective bars. In future, the use of lowly stressed, ungalvanized bars with waterproof coatings or stainless steel bars is recommended.

An 18-m span rail bridge with prestressed diaphragm wall abutments (49) was also part of the Glington-Northborough bypass scheme; outline design calculations for these abutments have been published by the Brick Development Association (50).

### Reinforced Brickwork Wingwalls

These are curved in plan and vary in height from about 5.5 m adjacent to the abutments to about 0.9 m on the foot of the bypass embankment. They are of counterfort reinforced brickwork pocket-type construction with 215-mm-thick front face brickwork and 787-mm-deep pockets spaced at 1125-mm centers.

### CASE STUDY 2: KIMBOLTON BUTTS BRIDGE

Cambridgeshire County Council also designed Kimbolton Butts Bridge, which is thought to be the first new brick arch bridge built in the United Kingdom for almost 100 years. The bridge carries the B660 highway over the River Kym in Huntingdon, near Cambridge, and was opened to traffic on December 16, 1992; details of the bridge are shown in Figure 4. The original structure, which was not strong enough to carry modern highway loading, was of composite steel beam/concrete deck construction. At the early stages of the design of the replacement bridge, a conventional structure with

a precast prestressed concrete beam deck was compared with the design eventually adopted; each bridge was estimated to cost approximately £100,000 (18). The arch bridge was selected because it was judged to have the greatest aesthetic appeal for its rural location, it was much preferred by the representatives of the local Parish Council, and the anticipated maintenance costs were less than that for the concrete alternative.

The design of the arch ring was based on the Department of Transport's guidelines for the strength assessment of masonry arches (4). The problem of spreading spandrels and wingwalls and the need to contain the damaged masonry resulting from vehicle collision with the parapets were addressed by using prestressed brickwork diaphragm walls for the wingwalls and reinforced grouted cavity brickwork for the parapets. The comparatively small spandrel walls were of mass brickwork construction. Although the vertical settlement of the abutments was estimated to be on the order of 15 mm, because a masonry arch is known to be capable of accommodating small movements, spread footings rather than piled foundations were judged to be adequate. Clay bricks and mortar with a similar specification to those in the Foxcovert Road Bridge were used for this project.

The arch ring was built on centering consisting of plywood sheet decking nailed onto timber members, which were fastened to curved, rolled steel universal column sections spanning across the river between the reinforced concrete foundations of the bridge. The top surface of the arch and the inner faces of the wingwalls and spandrel walls were waterproofed with a spray applied, two-coat acrylic membrane. It is interesting to note that, to date, the Cambridgeshire engineers have

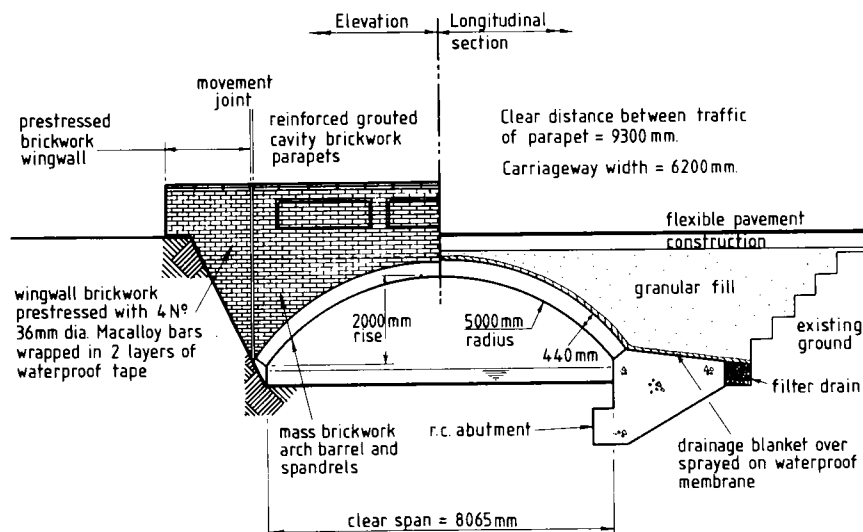


FIGURE 4 Kimbolton Butts Bridge: general details.

not experienced any difficulty in finding bricklayers with skills adequate to cope with the construction of arches, reinforced brickwork, or prestressed brickwork.

## CONCLUDING REMARKS

Judging from the excellent long-term performance of many of the existing brickwork structures that were built well over 100 years ago in the United Kingdom, clay brickwork has proved that it can withstand the severe exposure conditions experienced by most highway structures. Following over 30 years of research, a number of cost-effective, structurally efficient forms of plain, reinforced, and prestressed brickwork have been developed. Recently, these forms of construction have been successfully used for new highway structures such as short span arch bridges, earth retaining walls, bridge abutments, wingwalls, and parapets. These projects have demonstrated that structural brickwork is worthy of serious consideration as a viable structural medium for new highway works.

## ACKNOWLEDGMENTS

The author would like to thank S. E. Bell, Technical Director of Marshalls Clay Products, Wakefield, England, and R. Halsall, Chief Structural Engineer of Cambridgeshire County Council, England, for their help in preparing this paper. Thanks are also due to R. M. Galloway and W. G. Middleton of Parkman Consulting Engineers, Manchester, England, for the information on the masonry parapet research project.

## REFERENCES

- Heyman, J. *The Masonry Arch*. Ellis Horwood, Chichester, England, 1982.
- Jones, C. J. F. P. In *The Maintenance of Brick and Stone Masonry Structures* (A. M. Sowden, ed.), E. & F. N. Spon, London, 1991, Chap. 9, pp. 141–156.
- Sowden, A. M., and C. J. F. P. Jones. In *The Maintenance of Brick and Stone Masonry Structures* (A. M. Sowden, ed.), E. & F. N. Spon, London, 1991, Chap. 10, pp. 157–182.
- Department of Transport. BA 16/93—*The Assessment of Highway Bridges and Structures*. Department of the Environment/Department of Transport Publication Sales Unit, London, 1993.
- Powell, J. In *The Maintenance of Brick and Stone Masonry Structures* (A. M. Sowden, ed.), E. & F. N. Spon, London, 1991, Chap. 11, pp. 183–195.
- Galloway, R. M. *Research Projects into the Upgrading of Unreinforced Masonry Parapets*. Proceedings of the Centenary Year Bridge Conference, University of Wales, Cardiff, 1994 (accepted for publication).
- BS 6779—*Highway Parapets for Bridges and Other Structures. Part 1. Specification for Vehicle Containment Parapets of Metal Construction*. British Standards Institution, London, 1992.
- Ruddock, T. *Arch Bridges and Their Builders, 1735–1835*. Cambridge University Press, Cambridge, England, 1979.
- Hayward, D. *Manpower over the Mersey*. New Civil Engineer, Thomas Telford Limited, 28 July 1988, pp. 21–23.
- BS 5628—*British Standard Code of Practice for Use of Masonry. Part 3. Materials and Components, Design and Workmanship*. British Standards Institution, London, 1985.
- BS 3921—*British Standard Specification for Clay Bricks*. British Standards Institution, London, 1985.
- Curtin, W. G. Brick Diaphragm Walls—Development, Application, Design, and Future Development. *The Structural Engineer*, Vol. 58A, No. 2, Feb. 1980, pp. 41–48.
- Sharpe, W. Refurbishment of Retaining Walls using Cellular Wall Construction. In *Proc., Eighth International Brick/Block Masonry Conference* (J. W. de Courcy, ed.), Elsevier Applied Science, London, 1988, pp. 1824–1835.
- Cousens, T. W., D. C. Dalton, and J. Walsh. The Behaviour of Composite Brick and Geotextile Earth Retaining Walls. In *Proc., Fourth Canadian Masonry Symposium*, New Brunswick, Canada, 1986, pp. 946–959.
- Cousens, T. W., D. C. Dalton, and J. Walsh. *The Behaviour of Brick Retaining Walls with and without Geotextile Reinforcement*. Paper 21, Institution of Civil Engineers Symposium on the Practical Design of Masonry Structures, Thomas Telford Limited, London, 1986, pp. 307–317.
- Dawe, J. L., A. J. Valsangkar, and Y. Gonzalez. The Effect of Inclusion of Geogrid on the Behaviour of Masonry Joints. In *Proc., Fifth Canadian Masonry Symposium*, University of British Columbia, Vancouver, 5–7 June 1989, pp. 839–848.
- Valsangkar, A. J., J. L. Dawe, and S. Tekle. Geogrid Anchored Masonry Retaining Walls. In *Proc., Fifth Canadian Masonry Symposium*, University of British Columbia, Vancouver, 5–7 June 1989, pp. 848–855.
- Halsall, R. and R. Cox. Aesthetics of Masonry Arches. *Highways and Transportation*, Vol. 41, No. 7, July 1994, pp. 26–28.
- The Scottish Office. *Roads, Bridges and Traffic in the Countryside. A Review for Discussion*. The Scottish Office Roads Directorate, Edinburgh, 1992.
- Harvey, W. J., J. W. S. Maxwell, and F. W. Smith. Arch Bridges Are Economic. In *Proc., Eighth International Brick/Block Masonry Conference* (J. W. de Courcy, ed.), Elsevier Applied Science, London, 1988, pp. 1302–1310.
- Short, T. *Prefabricated Masonry Arch Bridges*. B. Eng (Honours) Thesis, Department of Civil Engineering, University of Bradford, Bradford, 1993.
- Roberts, J. J., G. J. Edgell, and A. J. Rathbone. *The Development of Reinforced and Prestressed Masonry*. Hand-

- book to BS 5628: Part 2. Palladian Publications, London, 1986.
23. Plummer, H. C., and J. A. Blume. *Reinforced Brick Masonry and Lateral Force Design*. Structural Clay Products Institute, Washington D.C., 1953, pp. 1–26.
  24. Cochran, M. R. Retaining Wall for North Carolina's Death Valley. In *Designing, Engineering and Constructing with Masonry Products*. (F. B. Johnson, ed.), Gulf Publishing Company, Houston, Texas, 1969, pp. 393–395.
  25. Abel, C. R., and M. R. Cochran. A Reinforced Brick Masonry Retaining Wall with Reinforcement in Pockets. In *Proc., Second International Brick Masonry Conference*, Stoke-on-Trent, England, 1970, pp. 295–298.
  26. Maurenbrecher, A. H. P., A. B. Bird, R. J. M. Sutherland, and D. Foster. *Reinforced Brickwork: Vertical Cantilevers I*. Publication No. SCP 10, Structural Clay Products Limited, St. Neots, England, 1976.
  27. Haseltine, B. A., and J. N. Tutt. *The Design of Brickwork Retaining Walls*. Design Guide No. 2, The Brick Development Association, Winkfield, England, Sept. 1991.
  28. Garrity, S. W., and R. D. Nicholl. Reinforced and Prestressed Masonry Earth Retaining Walls—A Cost Study. In *Proc., 10th International Brick/Block Masonry Conference*, Calgary, 5–7 July 1994, pp. 431–440.
  29. Sutherland, R. J. M. Reinforced Masonry Cantilever Construction. In *Reinforced and Prestressed Masonry: Proceedings of an ICE Conference*, Thomas Telford Ltd., London, 1982, pp. 31–42.
  30. Maurenbrecher, A. H. P., A. B. Bird, R. J. M. Sutherland, and D. Foster. *Reinforced Brickwork: Vertical Cantilevers II*. Publication No. SCP 11, Structural Clay Products Limited, St. Neots, England, 1976.
  31. Sinha, B. P. *Reinforced Brickwork: Grouted Cavity Shear Tests*. Publication No. SCP 16, Structural Clay Products Limited, St. Neots, England, 1979.
  32. Sinha, B. P., and D. Foster. *Reinforced Brickwork: Retaining Walls—Long Term Tests*. Publication No. SCP 14, Structural Clay Products Limited, St. Neots, England, 1979.
  33. Tellett, J., G. J. Edgell, and H. W. H. West. *Research into the Behaviour of Pocket-type Retaining Walls*. Technical Note 329, British Ceramic Research Association, Stoke-on-Trent, England, 1982.
  34. Tellett, J., and G. J. Edgell. *The Structural Behaviour of Reinforced Brickwork Pocket-type Retaining Walls*. Technical Note 353, British Ceramic Research Association, Stoke-on-Trent, England, 1983.
  35. Fisher, K., B. A. Haseltine, and P. Watt. Structural Testing of Brick Pocket-type Retaining Walls. In *Proc., 10th International Brick/Block Masonry Conference*, Calgary, 5–7 July 1994, pp. 441–448.
  36. Maurenbrecher, A. H. P. *Reinforced Brickwork: Pocket Type Retaining Wall*. Publication No. SCP 13, Structural Clay Products Limited, St. Neots, England, 1977.
  37. Sutherland, R. J. M. Brick and Block Masonry in Engineering. In *Proc., Institution of Civil Engineers*, Part 1, Vol. 70, London, Feb. 1981, pp. 31–63.
  38. Garrity, S. W. Reinforced Clay Brickwork Highway Structures. In *Proc., Sixth Canadian Masonry Symposium*, University of Saskatchewan, Saskatoon, 15–17 June 1992, pp. 735–749.
  39. Garrity, S. W. Clay Brickwork—An Alternative Material for New Highway Structures. *Masonry Society Journal*, Vol. 11, No. 2, Feb. 1993, pp. 53–65.
  40. Curtin, W. G., and J. Howard. Research on Prestressed Cantilever Diaphragm Walls. *The Structural Engineer*, Vol. 69, No. 6, 19 March 1991, pp. 105–112.
  41. Ambrose, R. J., R. Hulse, and S. Mohajery. Cantilevered Prestressed Diaphragm Walling Subjected to Lateral Loading. In *Proc., Eighth International Brick/Block Masonry Conference*, Dublin, 1988, pp. 583–594.
  42. Garrity, S. W., and T. G. Garwood. The Construction and Testing of a Full-scale Prestressed Clay Brickwork Diaphragm Wall Bridge Abutment. In *Proc., British Masonry Society*, Stoke-on-Trent, No. 4, July 1990, pp. 24–29.
  43. Garrity, S. W., and T. G. Garwood. Further Testing of a Prestressed Brickwork Bridge Abutment. In *Proc., Sixth North American Masonry Conference*, The Masonry Society, Boulder, Colorado, 6–9 June 1993, pp. 633–644.
  44. BS 5628—*British Standard Code of Practice for Use of Masonry. Part 2. Structural Use of Reinforced and Prestressed Masonry*. British Standards Institution, London, 1985.
  45. Curtin, W. G., G. Shaw, and J. K. Beck. *Design of Reinforced and Prestressed Masonry*. Thomas Telford Publishers, London, 1988.
  46. Curtin, W. G., G. Shaw, J. K. Beck, and J. Howard. *Design of Post-Tensioned Brickwork*. The Brick Development Association, Winkfield, England, 1989.
  47. Phipps, M. E. Prestressed Masonry Walls. In *Reinforced and Prestressed Masonry* (A. W. Hendry, ed.), Longman Scientific and Technical, England, 1991, Chap. 6, pp. 125–159.
  48. Phipps, M. E. The Codification of Prestressed Masonry Design. In *Proc., Sixth Canadian Masonry Symposium*, University of Saskatchewan, Saskatoon, 15–17 June 1992, pp. 561–572.
  49. Garrity, S. W., S. E. Bell, and D. J. Cox. Prestressed Clay Brickwork Bridge Abutments—Research, Design and Construction. In *Bridge Management 2—Inspection, Maintenance, Assessment and Repair* (J. E. Harding, G. A. R. Parke, and M. J. Ryall, eds.), Thomas Telford Limited, London, 1993, pp. 180–189.
  50. Halsall, R. *Post Tensioned Brickwork Abutments of Glington By Pass*. Engineers File Note No. 12, The Brick Development Association, Winkfield, England, September 1991.

# Large Deformation Cyclic Tests on Stainless Steel Reinforcing Bars for Reinforced-Concrete Structures in Seismic Regions

---

Roberto Gori, *University of Padua, Italy*

Enzo Siviero and Salvatore Russo, *Istituto Universitario de Architettura, Italy*

Stainless steel reinforcing bars, proposed for use in reinforced-concrete (r/c) structures, are available with the same lengths and current diameters of conventional carbon steel bars. They present advantages as regards durability, and anti-oxidability, and mechanical properties. These may make them economically competitive with conventional steel bars, and therefore suitable for use in bridge decks in severe environments. Recent earthquakes have further emphasized the need for metal reinforcements capable of resisting considerable and often repeated deformations. The problem is particularly acute in the case of continuous-beam viaducts, since severe strain comes to bear on the integral joints between the deck and the piers. A solution is the use of stainless steel bars because of their intrinsic stress-strain features. R/c seismic-resistant structures may benefit from stainless steel bars as reinforcement for their higher ductility and toughness. These mechanical properties are particularly suitable for critical regions of r/c continuous beams or frames, as the capability of energy dissipation as well as the ductile elongation are greater than for conventional carbon steel. In addition, the anti-oxidability property of reinforcing bars affects the durability of the structure and its serviceability. Comparative experimental static monotonic and cyclic large deformation uniaxial tests have

been carried out until failure on stainless steel AISI 304L bars with different strain rates, in order to reproduce the actual behavior of steel for r/c structures. Cumulative plastic damage has been also analysed. Initial results reveal a significant dependence of fatigue parameters on the strain rate, particularly for relatively small plastic strain ranges.

Stainless steels are ferrochromium or ferrochromium-nickel alloys with a high corrosion resistance, even at high temperatures, because of their high content of chromium (more than 12 percent) and nickel, which promotes the formation of a passive layer with a considerable chemical inertia in certain ambient conditions. According to the microstructure of the matrix, these steels can be grouped into three major categories: martensitic, ferritic, and austenitic stainless steels.

Martensitic stainless steels have a carbon content of 0.10 to 1.10 percent and have excellent mechanical features in terms of tensile strength and a fair corrosion resistance. Heat treatments can be performed on these alloys as on ordinary steels for hardening and tempering.

Ferritic stainless steels are ferrochromium alloys with lower carbon content and a higher percentage of chro-

mium (17 to 26 percent). They are unsuitable for hardening treatment.

The austenitic steels are the most valuable and most studied of the stainless alloys, as they are best suited to resisting humid corrosive phenomena. They are used in a variety of sectors because of their well-demonstrated corrosion resistance and very high ductility, in addition to the high yield strength they can achieve with work hardening. For these properties, this type of steel can be used successfully in the form of ribbed bars for reinforced concrete structures. In civil works, the carbon steel reinforcement in standard and prestressed reinforced concrete is prone to chemical and electrochemical oxidation, with a consequent progressive reduction in the load-bearing capacity of the structure as a whole (1). Therefore corrosion-resistant steel has been recommended (2) especially for use in conditions in which the risk of pollution from chlorides is high, such as in sections of road where salt is used to prevent freezing, in reinforced concrete structures in seaside areas, or in environments with problems of aggressive smog.

The stainless steel used as reinforcing bars in concrete can be of three types:

1. AISI 304 (or AISI 304L if welded joints are required) for polluted environments,
2. AISI 316 (or AISI 316L if welded joints are required) for environments containing considerable proportions of chlorides; or
3. AISI 329 biphasic for strongly aggressive ambient conditions involving considerable tensile stresses and high working temperatures.

The use of stainless steel reinforcement is all the more advisable in the case of reinforced concrete structural elements in seismic areas, because it combines the advantages of corrosion resistance (3,4) with high ductility and tensile strength (5) and, above all, it has a greater dissipating capacity in the plastic deformation range when repeated cycles occur (6,7).

Stainless steel bars have already been cyclically tested by others; for example, Ciampoli and Mele (6) increased the strain range, where the high slenderness of the specimens, for small diameters, characterized the behavior in compression fields, due to buckling of bars. The aim of this work was to test the tenacity and the cyclic behavior to collapse of stainless steel bars (AISI 304L) in large deformation ranges, and to investigate their dependence on the strain rates, especially regarding strength deterioration.

In the present research, the authors used the experience reached in other cyclic tests with large strains (7-9). Cyclic axial loads were applied, imposing for each test prescribed symmetric strain excursions in the plastic range (up to 16 percent) with constant strain rates, cor-

responding to vibration natural frequencies typical of reinforced concrete bridges. Particular attention was devoted to avoiding the buckling of specimens.

In a previous paper by the authors (10), resilience tests were performed to evaluate very good localized behavior in the case of impact. In the same paper, monotonic tests were carried out on stainless steel and conventional carbon steel bars. Again, bond characteristics have already been tested. They do not differ substantially from conventional carbon steel bars.

## NOTATION

- $\delta_i$  = plastic excursion of each cycle  $i$ ,
- $\delta_{u,mon}$  = monotonic test plastic excursion,
- $\epsilon$  = deformation of steel,
- $\epsilon_u$  = uniform elongation,
- $\epsilon_y$  = deformation at yield,
- $\epsilon_{r5\phi}$  = deformation at the collapse on five diameter length,
- $\phi$  = diameter of steel specimen,
- $\mu_i$  = ductility of each cycle  $i$ ,
- $\mu_{u,mon}$  = monotonic test ductility,
- $A, b$  = cumulative damage structural constants,
- $D_F$  = damage functional,
- $f_t$  = tensile strength of steel,
- $f_y$  = tensile stress at yield of steel,
- $n$  = total number of plastic cycles,
- $N_i$  = number of symmetric cycles to failure with the same plastic excursions  $\delta_i$ .

## INELASTIC CYCLIC BEHAVIOR OF METALS

Several theories describe the inelastic cyclic behavior of metals, among them the isotropic hardening theory of Hill (11); the kinematic hardening theory of Prager, modified by Shield and Ziegler (12,13); and the theories of Mroz (14,15) and those of Peterson-Popov (16,17).

For strain-hardening materials, the yield function changes progressively, whereas for an elastic-perfectly-plastic material, it is constant after yield. A hardening rule is needed to describe how the yield function changes. In stress space, a change of the yield function corresponds to a variation of size, shape, and position of the yield surface. The isotropic hardening rule corresponds to an expansion of the yield surface without any change of shape and of the origin in 3D principal stress space. The kinematic hardening rule corresponds to a translation of the yield surface without any change of size or shape. Both rules do not agree exactly with experimental tests. In particular, the isotropic rule is inexact in predicting elastic behavior for constant stress cycles, while the kinematic rule is generally incorrect in

describing stable hysteresis cycles. Thus, for cyclic behavior, a combination of the isotropic and kinematic hardening rules must be employed with the yield surface allowed to expand and to translate.

A number of formulations have been developed. A very general formulation (16,17) distinguishes two limiting material states: a virgin state (strength and hardening defined in the first half cycle of loading), and a fully cycled state. The transition from the virgin state to the fully cycled state is controlled by a weighting function based on accumulated strain. A model based on the principles of this theory and extending the Mroz model to cyclic phenomena was developed (18) with combined isotropic and kinematic hardening. However, to give an engineering answer to the problem of finding a general definition of plastic collapse under cyclic loadings, it has been proposed to use normalized damage functionals (19), varying from 0 (no plastic damage) to 1 (failure).

Some methods use the hysteresis energy as the damage parameter (20): collapse occurs when the structure dissipates an energy equal to a limit value. Other methods are based only on the measure of ductility, neglecting cycle history. More advanced methods (21) take into account energy and ductility. A method that considers the actual distribution of plastic cycles and generalizes the linear cumulative law of plastic fatigue (22) was developed by Cosenza et al. (19). In the present paper, an application of this method was carried out for cyclic uniaxial tests on stainless steel bars for different strain rates.

## EXPERIMENTAL PROCEDURES

Monotonic and cyclic tests were carried out by using a universal Dartec actuator (1200 kN, working pressure 207 bar) with two hydraulic grips with variable high 150 to 1050 mm. The lateral compression on specimens was 200 bar.

Monotonic tensile tests were performed according to ISO 6892 (1984), using different rates for elastic and plastic phases. Cyclic tests were carried out using strain control with three different constant strain rates of 6500, 13 000, and 26 000  $\mu\epsilon/\text{sec}$ , which correspond to

**TABLE 2 Mechanical Characteristics of Stainless Steel Specimens**

	$f_y$ (MPa)	$f_t$ (MPa)	$f_t/f_y$	$\epsilon_y$ (%)	$\epsilon_u$ (%)	$\epsilon_{r5\phi}$ (%)
$\phi$ 10	723.60	850.32	1.18	1.89	11.26	21.05
$\phi$ 12	716.20	849.36	1.18	1.68	10.02	21.05

relative displacement rates of the grips of 0.25, 0.50, and 1.00 mm/sec.

These tests were carried out on specimens with diameters of 10 and 12 mm in the central part obtained from 32-mm-diameter bars of stainless steel (AISI 304L), the chemical composition of which is shown in Table 1. Specimen length was 140 mm, with a base for measures of 38 mm, and 26-mm-diameter threaded heads (in order to allow the reversal of loading) (7).

## Monotonic Tests

Results of monotonic tensile tests for the two specimens are shown in Table 2. Even if only a small number of tests was carried out, the results present very good characteristics as regards ductility requirements (23). In particular, the excellent values of  $\epsilon_u$ , together with the high values of  $f_t/f_y$ , make them respect class S (seismic) of the CEB-FIP code ( $\epsilon_u > 6$  percent and  $f_t/f_y > 1.15$ ) (24) and class H (high ductility) of the EC2 code ( $\epsilon_u > 5$  percent and  $f_t/f_y > 1.08$ ) (25). The very high value of  $\epsilon_{r5\phi}$  must be stressed, which could make them respect the lower limits (6, 9, 12 percent) of the EC8 code (26), even if stress ratio requirements are slightly higher. In stainless steel, the specific deformation energy prior to necking is significantly high, about twice that of the conventional carbon steel FeB44k, which confirms the results of previous tests (10).

## Cyclic Tests

All cyclic tests were carried out as constant strain cycling by imposing the upper and lower symmetric limits for plastic strain, with constant strain rates, as specified above, of 6500, 13 000, and 26 000  $\mu\epsilon/\text{sec}$  (relative displacement rates of the grips of 0.25, 0.50, and 1.00 mm/sec). All the tests were performed until collapse of the specimens. Plastic strain ranges considered, for both diameters  $\phi$ 10 and  $\phi$ 12, were +2.5 to -2.5 percent;

**TABLE 1 Chemical Composition (%) of Tested Steel**

C	Si	Mn	P	S	Cr	Ni	Mo	Cu
0.034	0.48	1.48	0.032	0.025	18.46	8.56	0.56	0.45

**TABLE 3** Number of Cycles to Failure for Symmetric Large Deformation Uniaxial Tests on Stainless Steel Bars, AISI 304L

plastic range		+2.5%-2.5%	+5%-5%	+7%-7%	+8%-8%
strain rate ( $\mu\text{E/s}$ )					
$\phi$ 10	6500	34	11	5	4
	13000	46	8, 10	5, 8	4
	26000	58	17, 9	6	4
$\phi$ 12	6500	24	13	8	5
	13000	112, 64, 65	22, 14, 19	9	7
	26000	99, 74, 90	12, 11, 13	9	7

+5 to -5 percent; +7 to -7 percent; +8 to -8 percent (7). The number of symmetric cycles to failure is shown in Table 3.

The shapes of the stress-strain curves seem to follow with good agreement the isotropic hardening rules.

The total plastic excursions versus the number of cycles to failure were reported in logarithmic scales for the three different strain rates in Figure 1 (for specimens  $\phi$ 10) and in Figure 2 (for specimens  $\phi$ 12), obtaining bilogarithmic diagrams of plastic fatigue.

As an example of the cyclic strength deterioration, Figures 3 and 4 report the ratios between the stress peaks at reversal (compression stress or tensile stress) versus the number of hysteresis cycles for  $\phi$ 10-mm specimens in symmetric cyclic tests with axial plastic strain ranges +2.5 to -2.5 percent (Figure 3) and for  $\phi$ 12-mm specimens in symmetric cyclic tests with axial plastic strain ranges +5 to -5 percent (Figure 4) for two strain rates 13 000 and 26 000  $\mu\text{E/sec}$  (displacement rates 0.50 and 1.00 mm/sec).

## ANALYSIS OF RESULTS

From results of the above monotonic and cyclic tests, it has been possible to evaluate for different strain rates, the two parameters that characterize the linear cumulative law of plastic fatigue.

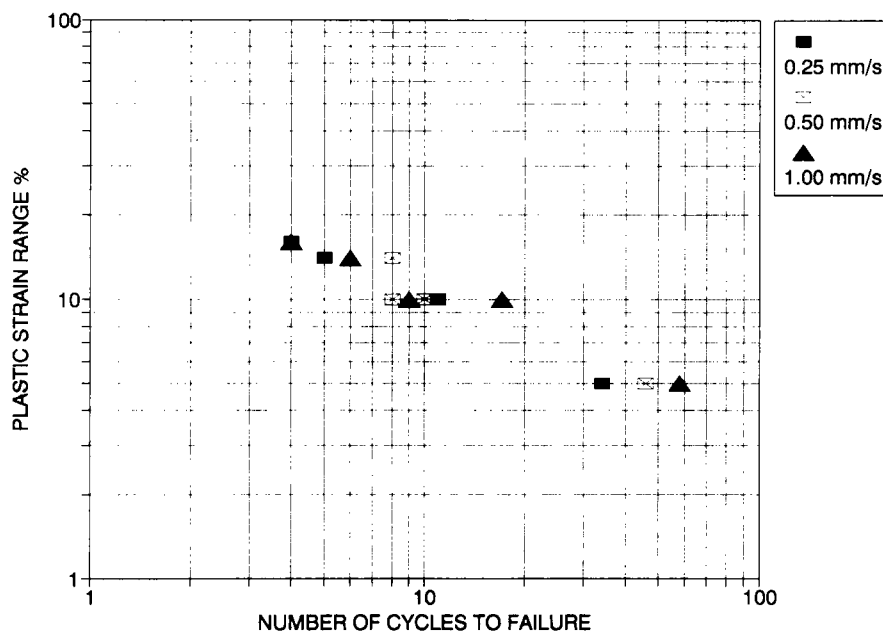


**FIGURE 1** Symmetric uniaxial cyclic tests on AISI 304L stainless steel specimens  $\phi$ 10 mm in diameter; plastic strain range versus number of cycles to failure for constant strain rates of 6500, 13 000, and 26 000  $\mu\text{E/sec}$  (relative displacement rates of the grips of 0.25, 0.50, and 1.00 mm/sec).

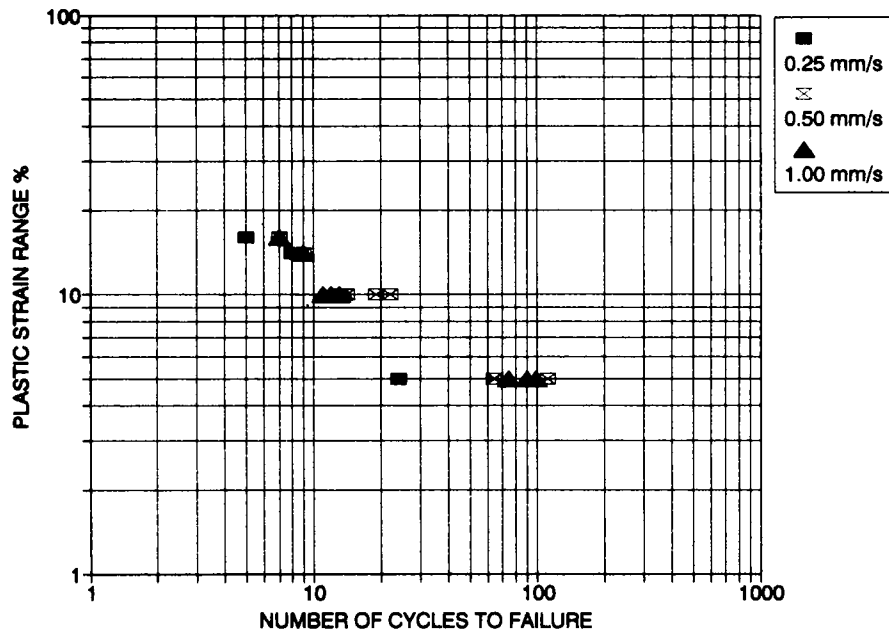


FIGURE 2 Symmetric uniaxial cyclic tests on AISI 304L stainless steel specimens  $\phi 12$  mm in diameter; plastic strain range versus number of cycles to failure for constant strain rates of 6500, 13 000, and 26 000  $\mu\epsilon/\text{sec}$  (relative displacement rates of the grips of 0.25, 0.50, and 1.00 mm/sec).

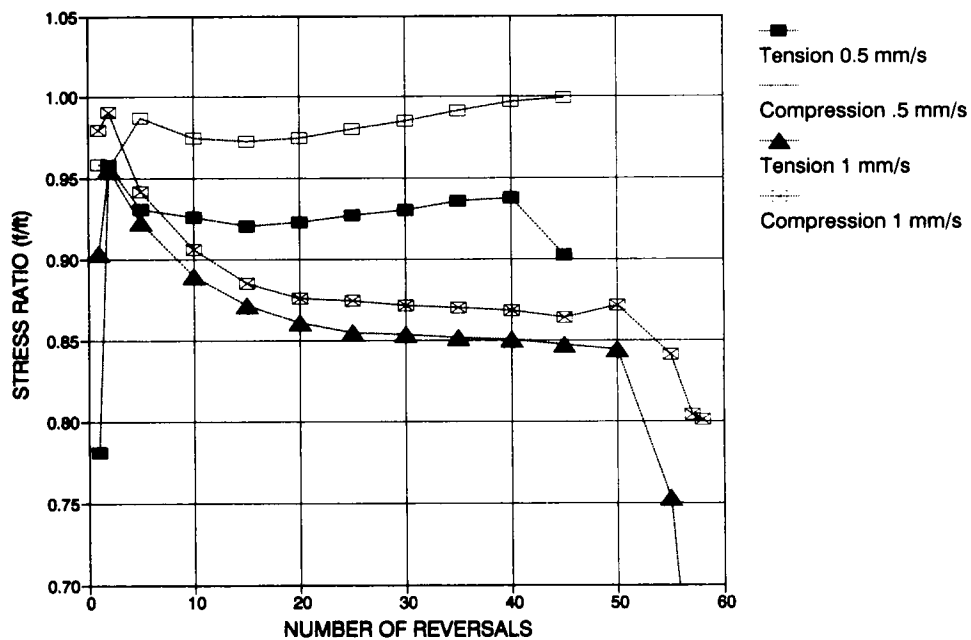


FIGURE 3 Stress ratio for peaks versus number of reversals for two AISI 304L stainless steel specimens,  $\phi 10$  mm in diameter, for symmetric cyclic tests with axial plastic strains between 2.5 and  $-2.5$  percent, for constant strain rates of 13 000 and 26 000  $\mu\epsilon/\text{sec}$  (relative displacement rates of the grips of 0.50 and 1.00 mm/sec).



The damage functional  $D_F$ , which takes into account the different amount of plastic displacement, can be obtained by using the law of cumulative damage (22,27), generalizing the Coffin and Mason and Miner laws:

$$D_F = A \sum_{i=1}^n (\mu_i - 1)^b \quad (1)$$

where  $A$  and  $b$  are structural constants to be determined by means of experimental tests,  $n$  is the total number of plastic cycles, and  $\mu_i$  is the ductility (kinematic or cyclic) corresponding to the generic plastic displacement (19).

The parameter  $A$  can be evaluated by means of a monotonic test carried through to failure (28):

$$A = (\mu_{u,mon} - 1)^{-b} = (\delta_{u,mon})^{-b} \quad (2)$$

where  $\delta_{u,mon}$  is the corresponding plastic excursion.

Parameter  $b$  can be evaluated as the angular coefficient of the line that describes, in logarithmic scales, the equation

$$\log(A) + \log(N_i) + b \log(\delta_i) = 0 \quad (3)$$

which represents the linear damage cumulative law for a test with  $N_i$  cycles with the same plastic excursions  $\delta_i$ , carried through failure (28):

$$D_F = A \cdot N_i \cdot (\delta_i)^b = 1 \quad (4)$$

Even if the number of tests was very small for this first campaign,  $b$  was evaluated for each strain rate by means of Equation 3 as the mean slope of lines in the two bilogarithmic diagrams of plastic fatigue in Figure 1 (for  $\phi 10$  mm) and in Figure 2 (for  $\phi 12$  mm). Then, using Equation 2 or measuring the  $y$  coordinate for  $\log(N_i) = 0$  in the bilogarithmic diagrams, the parameter  $A$  can be evaluated. It must be noted that the former requires knowledge of the monotonic tests for the different strain rates.

Values of  $b$  and  $A$  had been already found in a previous paper by the authors (7) for a small number of specimens with diameters of  $\phi 10$  mm and  $\phi 12$  mm, respectively, for a constant strain rate of 13 000  $\mu\epsilon/\text{sec}$  (displacement rate 0.50 mm/sec). These results were substantially confirmed in this second campaign; for tests with that strain rate, average values  $b = 2.05$  to 2.06 and  $A = 11.41$  to 6.28 were found for specimens with diameters of  $\phi 10$  mm and  $\phi 12$  mm, respectively.

Tests with the other strain rates furnished the following results. For a constant strain rate of 6500  $\mu\epsilon/\text{sec}$  (displacement rate 0.25 mm/sec), average values of  $b = 1.83$  to 1.73 and  $A = 8.05$  to 4.31, and for a constant strain rate of 26 000  $\mu\epsilon/\text{sec}$  (displacement rate 1.00 mm/sec), average values of  $b = 2.24$  to 2.20 and  $A = 14.83$  to 8.40 were found for specimens with diameters of  $\phi 10$  mm and  $\phi 12$  mm, respectively.

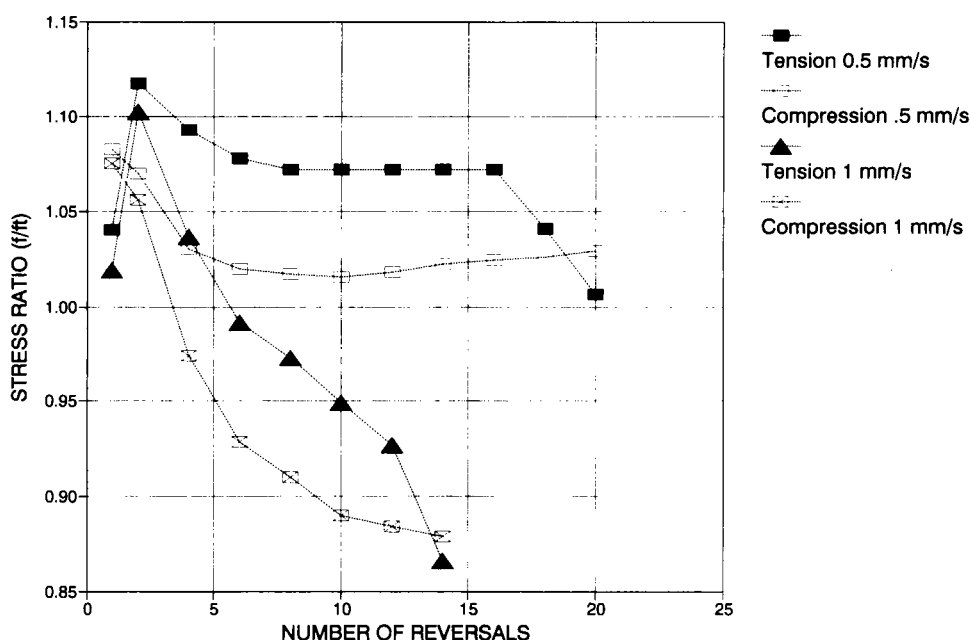


FIGURE 4 Stress ratio for peaks versus number of reversals for two AISI 304L stainless steel specimens,  $\phi 12$  mm in diameter, for symmetric cyclic tests with axial plastic strains between 5 and -5 percent, for constant strain rates of 13 000 and 26 000  $\mu\epsilon/\text{sec}$  (relative displacement rates of the grips of 0.50 and 1.00 mm/sec).

The different slenderness of the specimens and the nonhomogeneous composition of the core of the original bar are probably responsible for the different behavior of the two specimens.

## CONCLUSIONS

The bars for reinforced-concrete seismic-resistant bridges can be used in stainless steel alloys with very good results for their high toughness and ductility, as well as for their great capability of energy dissipation and good performances as regards resilience. Furthermore, the well-known antioxidability property of these bars plays a very important role as regards the durability of the structure and the serviceability limit state. At present the site cost of stainless steel bars is about five times that of high resistant steel. This cost can be reduced in case of large market conditions.

The campaign of experimental monotonic and cyclic tests was carried out on stainless steel bars, and parameters that characterize the linear cumulative law of plastic fatigue were evaluated for uniaxial cyclic tests for different strain rates. Even if only a small number of tests was carried out, the results were good from the mechanical point of view. At this point of the research, the following conclusions can be drawn:

- Stainless steel has a high tensile strength as a result of work hardening;
- The total ductility of stainless steel is considerable and generally very regular;
- Stainless steel specimens present very good characteristics as regards ductility and strength requirements: the excellent values of  $\epsilon_u$ , together with the high values of  $f_t/f_y$ , make them respect class S (seismic) of the CEB-FIP code and class H of the EC2 code;
- This type of lattice, with its larger number of sliding systems, is also responsible for the constantly ductile behavior of stainless steels whatever the conditions of load (even pulsing) and temperature, this feature marking an important difference with respect to conventional carbon steels;
- In stainless steel, the specific deformation energy prior to necking is significantly high (about two that of the conventional carbon steel) which confirms its considerable dissipating features; and
- The strain rate seems to influence the plastic fatigue parameters: constant  $b$  increases in a significant way, while constant  $A$  decreases, in a minor way, when strain rate increases.

Future steps in the research will deal with the influence of strain rates on cyclic behavior of more ductile stain-

less steel bars and the comparison with conventional carbon steel bars.

## ACKNOWLEDGMENT

The research discussed in this paper was supported by Italian Ministero dell'Università e della Ricerca Scientifica e Tecnologica.

## REFERENCES

1. Mele, M., and E. Siviero. Considerazioni generali sulla durabilità delle strutture in c.a. e c.a.p. In *Problemi avanzati per la costruzione di ponti*, CISM, Udine, 1991.
2. Siviero, E. Durability of Reinforced Concrete Structures and Use of Stainless Steel. *Proc., Steel '90*, Genova, May 1990.
3. Flint, G. N., and R. N. Cox. The Resistance of Stainless Steel Partly Embedded in Concrete to Corrosion by Sea Water. *Magazine of Concrete Research*, No. 40, 1988.
4. Kulussa, G. Stainless Steel Reinforcement for Concrete. *Betonwerke + Fertigteil - Technik*, Marz 1988.
5. Paolucci, G. M., E. Siviero, S. Rasera, and G. Barba. Ductility of Stainless Steel Rebars. *CEB Bulletin d'information*, No. 218, 1993.
6. Ciampoli, M., and M. Mele. Comportamento ciclico di barre di acciaio inossidabile per c.a. *Proc. Giornate AICAP '91*. Spoleto, 1991.
7. Gori, R., E. Siviero, and S. Russo. Cyclic Tests on Stainless Steel Reinforcing Bars for r.c. Bridges in Seismic Regions. In *Proc., 2nd International Conference on New Dimensions in Bridge and Flyovers*, Ipoh, Malaysia, October 1994, pp. 75-80.
8. Gori, R., and L. Briseghella. Comportamento ciclico di barre di acciaio ad alta duttilità per calcestruzzo armato in campi di deformazione post-elastici contenuti. *CEB Italia Notizie*, No. 5, Venezia, Maggio 1993.
9. Gori, R. Indagini sperimentali sul comportamento ciclico a compressione di calcestruzzi confinati con spirali di acciaio. *Studi e Ricerche*. No. 14, Scuola di specializzazione in Costruzioni in C.A. e C.A.P., 1993.
10. Paolucci, G. M., R. Gori, E. Siviero, and G. Barba. The Use of Stainless Steel Bars as Reinforcement of R/C Structures in Seismic Regions. In *Proc., 5th U.S. National Conference on Earthquake Engineering*, Chicago, 1994, pp. II 795-805.
11. Hill, R. *The Mathematical Theory of Plasticity*. Oxford University Press, Oxford, England, 1950.
12. Shield, R. T., and H. Ziegler. On Prager's hardening rule. *ZAMP* 9a. 1958, pp. 260-276.
13. Ziegler, H. A Modification of Prager's Hardening Rule. *Quarterly Journal of Applied Mathematics*, Vol. 17, 1959, p. 55.
14. Mroz, Z. An Attempt to Describe the Behaviour of Metals, Under Cyclic Loads Using a More General Work-hardening Model. *Acta Mechanica*, Vol. 7, Nos. 2-3, 1969, pp. 199-212.

15. Kujawski, D., and Z. Mroz. A Viscoplastic Material Model and Its Application to Cyclic Loading. *Acta Mechanica*, Vol. 36, 1980, pp. 213–230.
16. Peterson, H., and E. P. Popov. Constitutive Relations for Generalised Loadings. *Journal of the Engineering Mechanics Division*, ASCE, Vol. 103, No. EM4, August 1977, pp. 611–627.
17. Popov, E. P., and H. Peterson. Cyclic Metal Plasticity: Experiments and Theory. *Journal of the Engineering Mechanics Division*, ASCE, Vol. 104, December 1978, pp. 1371–1388.
18. Mosaddad, B., and G. H. Powell. *Computational Models for Cyclic Plasticity, Rate Dependence, and Creep in Finite Element Analysis*. Earthquake Engineering Research Center Report UCB/EERC-82/26, Berkeley, California, 1982.
19. Cosenza, E., G. Manfredi, and R. Ramasco. The Use of Damage Functionals in Earthquake Engineering: A Comparison Between Different Methods. *Earthquake Engineering and Structural Dynamics*, Vol. 22, 1993, pp. 855–868.
20. Briseghella, L., and R. Gori. Indicatori di Danno del Comportamento Sismico di Materiali Soggetti ad Azioni Normali e Taglianti. In *Proc., II Conv. L'ingegneria Sismica in Italia*. Rapallo, Giugno 1984.
21. Park, Y. J., and A. H. S. Ang. Mechanistic Seismic Damage Model for Reinforced Concrete. *Journal of Structural Engineering*, ASCE, Vol. 111, No. 4, April 1985, pp. 722–739.
22. Krawinkler, H., and M. Zohrei. Cumulative Damage in Steel Structures Subjected to Earthquake Ground Motions. *Computers and Structures*, 1983, pp. 531–541.
23. Siviero, E., and S. Russo. Ductility Requirements for Reinforcement Steel. *CEB Bulletin d'information*, No. 218, 1993.
24. CEB-FIP Model Code 1990. *CEB Bulletin d'information* No., 213/214, T. Telford Ed., 1993.
25. *EUROCODE 2, Design of concrete structures*. Final Draft, 1990.
26. *EUROCODE 8, Strutture in zona sismica. Progetto*, Parte I, 1988.
27. Powell, G. H., and R. Allahabadi. Seismic Damage Prediction by Deterministic Methods: Concepts and Procedures. *Earthquake Engineering and Structural Dynamics*, Vol. 16, 1988, pp. 719–734.
28. Cosenza, E., G. Manfredi, and R. Ramasco. La fatica plastica in ingegneria sismica. *Ingegneria sismica*, Anno X, No. 2, 1993.

The **Transportation Research Board** is a unit of the National Research Council, which serves the National Academy of Sciences and the National Academy of Engineering. The Board's purpose is to stimulate research concerning the nature and performance of transportation systems, to disseminate the information produced by the research, and to encourage the application of appropriate research findings. The Board's program is carried out by more than 330 committees, task forces, and panels composed of more than 3,900 administrators, engineers, social scientists, attorneys, educators, and others concerned with transportation; they serve without compensation. The program is supported by state transportation and highway departments, the modal administrations of the U.S. Department of Transportation, and other organizations and individuals interested in the development of transportation.

The National Academy of Sciences is a private, nonprofit, self-perpetuating society of distinguished scholars engaged in scientific and engineering research, dedicated to the furtherance of science and technology and to their use for the general welfare. Upon the authority of the charter granted to it by the Congress in 1863, the Academy has a mandate that requires it to advise the federal government on scientific and technical matters. Dr. Bruce M. Alberts is president of the National Academy of Sciences.

The National Academy of Engineering was established in 1964, under the charter of the National Academy of Sciences, as a parallel organization of outstanding engineers. It is autonomous in its administration and in the selection of its members, sharing with the National Academy of Sciences the responsibility for advising the federal government. The National Academy of Engineering also sponsors engineering programs aimed at meeting national needs, encourages education and research, and recognizes the superior achievements of engineers. Dr. Harold Liebowitz is president of the National Academy of Engineering.

The Institute of Medicine was established in 1970 by the National Academy of Sciences to secure the services of eminent members of appropriate professions in the examination of policy matters pertaining to the health of the public. The Institute acts under the responsibility given to the National Academy of Sciences by its congressional charter to be an adviser to the federal government and, upon its own initiative, to identify issues of medical care, research, and education. Dr. Kenneth I. Shine is president of the Institute of Medicine.

The National Research Council was organized by the National Academy of Sciences in 1916 to associate the broad community of science and technology with the Academy's purpose of furthering knowledge and advising the federal government. Functioning in accordance with general policies determined by the Academy, the Council has become the principal operating agency of both the National Academy of Sciences and the National Academy of Engineering in providing services to the government, the public, and the scientific and engineering communities. The Council is administered jointly by both the Academies and the Institute of Medicine. Dr. Bruce M. Alberts and Dr. Harold Liebowitz are chairman and vice chairman, respectively, of the National Research Council.

---

Abbreviations used without definitions in TRB publications:

AASHO	American Association of State Highway Officials
AASHTO	American Association of State Highway and Transportation Officials
ASCE	American Society of Civil Engineers
ASME	American Society of Mechanical Engineers
ASTM	American Society for Testing and Materials
FAA	Federal Aviation Administration
FHWA	Federal Highway Administration
FRA	Federal Railroad Administration
FTA	Federal Transit Administration
IEEE	Institute of Electrical and Electronics Engineers
ITE	Institute of Transportation Engineers
NCHRP	National Cooperative Highway Research Program
NCTRP	National Cooperative Transit Research and Development Program
NHTSA	National Highway Traffic Safety Administration
SAE	Society of Automotive Engineers
TRB	Transportation Research Board





NATIONAL ACADEMY PRESS  
ISBN 0-309-06109-1